Targeting PD-L1/ PD-1-mediated inhibitory signaling with BTK inhibitors in Chronic Lymphocytic Leukemia (CLL)

Mark-Alexander Schwarzbich

A thesis submitted in partial fulfillment of the requirements
of the Degree of Doctor of Philosophy
Queen Mary University of London

April 2019

Centre for Haemato-Oncology

Barts Cancer Institute

Statement of Originality

I, Mark-Alexander Schwarzbich, confirm that the research included within this thesis is my own work or that where it has been carried out in collaboration with, or supported by others, that this is duly acknowledged below and my contribution indicated. Previously published material is also acknowledged below.

I attest that I have exercised reasonable care to ensure that the work is original, and does not to the best of my knowledge break any UK law, infringe any third party's copyright or other Intellectual Property Right, or contain any confidential material.

I accept that the College has the right to use plagiarism detection software to check the electronic version of the thesis.

I confirm that this thesis has not been previously submitted for the award of a degree by this or any other university.

The copyright of this thesis rests with the author and no quotation from it or information derived from it may be published without the prior written consent of the author.

Signature: Mark-Alexander Schwarzbich

Date:16/10/19

Details of collaboration and publications:

Animal maintance was performed with support of lab member Arantxa Romero-Toledo. Selected animal interventions were performed by the BCI Animal Technician Service (ATS) or by the Biological Services Unit (BSU) Charterhouse Square staff member Mr. Arif Mustafa. All procedures and interventions were performed under my direction and following experimental procedures, plans and standard operation procedures that I have established. For BTK occupancy testing, treatment of animals and preparation of samples was performed by me while the assay was performed by our collaborators at Acerta pharma.

Publications:

Schwarzbich MA, Romero-Toledo A, Frigault M, Gribben JG. Modulation of T-Cell Function in the Microenvironment of Emu-TCL1 CLL Bearing Mice By Btki Appears Independent of ITK. Blood. 2018;132(Suppl 1):3139-.

Schwarzbich MA, Romero-Toledo A, Gribben JG. Modulation of T-Cell Function and Immune Phenotype in the Microenvironment of Emu-TCL1 CLL Bearing Mice By Ibrutinib. Blood. 2018;132(Suppl 1):3138-.

Romero-Toledo A, **Schwarzbich MA**, Sanderson R, Gribben JG. Monocytic but not granulocytic MDSCs increase with Ibrutinib but not Acalabrutinib treatment in Eμ-TCL1 mice with CLL, suggesting a role for ITK inhibition in monocytic MDSCs. EHA Library. Romero-Toledo A. Jun 15, 2019; 266752; PS1135.

Abstract

Chronic lymphocytic leukemia (CLL) is the most frequent leukemia in adults in the West. An unmet need for equally curative and tolerable treatment approaches exists. Our group has previously shown that the PD-1/PD-L1 immune checkpoint pathway is pivotal in mediating CLL-associated T-cell dysfunction. Bruton's tyrosine kinase inhibitors such as Ibrutinib have been shown to be able to modulate the function of T-cells and myeloid cells. Using the Eµ-TCL1 mouse model of CLL, we have aimed to analyse the effect of BTK inhibitors on expression of immune checkpoint molecules, immune phenotype and T-cell function as well as develop a combination approach of BTK inhibitors and anti-PD-L1 immune checkpoint blockade. We detected a modest increase in PD-L1 expression among CLL B-cells and a decrease among myelomonocytic cells with both Ibrutinib and Acalabrutinib treatment. We have demonstrated an amelioration of the exhaustion phenotype of CD4+ and CD8+ T-cells with BTK-inhibitor treatment with downregulation of CD69, PD-1, LAG-3 and KLRG-1. We also found downregulation of inhibitory receptor 2B4, LAG-3 and KLRG-1 on NK cells. On myeloid cells we observed downregulation of PD-1 and 2B4 as well as a differential effect on expression of TIM-3 with upregulation among myelomonocytic cells and downregulation among classical dendritic cells. Immunophenotypes of BTK inhibitor and BTK inhibitor/anti-PD-L1 combination treated animals were similar with a slightly higher expression level of PD-1 among combination treated animals. Both substances improved helper cell cytokine profiles, degranulation capacity of cytotoxic T-cells and T-cell synapse formation to a similar extent. The combination of BTK inhibitor treatment and PD-L1 blockade failed to achieve improved correction of CLL-associated T-cell exhaustion phenotype and Ibrutinib/anti-PD-L1 combination treatment achieved only a very modest improvement of T-cell function over single agent treatments. Suprisingly, the combination of Acalabrutinib and anti-PD-L1 immune checkpoint blockade was detrimental regarding both helper cell and cytotoxic T-cell function. These findings would caution against the use of Acalabrutinib/anti-PD1 or anti-PD-L1 combinations in the clinical setting.

Table of Contents

List of Figures

List of Tables

Abbreviations

ABVD	Doxorubicin, bleomycin, vinblastine, dacarbazine
ADAP	Adhesion- and Degranulation-promoting Adapter Protein
ADCC	antibody dependent cellular cytoxicity
ADF	actin-depolymerization factor
ADP	adenosine dinucleotide phosphate
Ag	Antigen
AIHA	Autoimmune haemolytic anaemia
ALK	anaplastic lymphoma kinase
AMC	absolute monocyte count
AML	Acute Myeloid Leukemia
AMPK	AMP-activated protein kinase
APC	antigen presenting cell
APRIL	A proliferation-inducing ligand
Arp	actin-related protein
ARPC1B	Actin-related protein 2/3 complex subunit 1B
ASH	American Society of Hematology
ATM	ataxia telangiectasia mutated
ATP	adenosine triphosphate
BAD	Bcl-2-associated death promoter
BAFF	B-cell activating factor
BAK	Bcl-2 homologous antagonist killer
BAT3	HLA-B-Associated Transcript 3
BAX	Bcl-2-associated X protein
BCL-w	B-cell lymphoma w
BCK-XL	B-cell lymphoma-XL
BCL1	murine B cell lymphoma
BCL-2	B-cell lymphoma 2
BCR	B-cell receptor
BH3	BCL-2 homology 3
BID	BH3 domain-only death agonist protein
BIM	Bcl-2 Interacting Mediator of cell death
BIRC3	Baculoviral IAP repeat-containing protein 3
Blk	B lymphocyte kinase
BLAST-1	B-lymphocyte activation marker 1
BM	bone marrow
BLNK	B-cell linker protein
BNX	beige/nude/Xid
BR	Bendamustin, Rituximab
Breg	regulatory B-cells

BSA	bovine serum albumin
BSU	biological services unit
BTK	Bruton's Tyrosine Kinase
BTKi	BTK inhibitor
BTLA	B- and T-lymphocyte attenuator (BTLA)
CK2	casein kinase 2
CCL	C-C motif ligand
CCR	C-C motif receptor
CD	Cluster of differentiation
CDR	complementary determing region
CDR3	complementarity determining region 3
CDC	complement dependent cytotoxicity
Cdc42	Cell division control protein 42 homolog
CDC42EP3	Cdc42 effector protein 3
CDK	Cyclin-dependent kinase
CEACAM1	carcinoembryonic antigen cell adhesion molecule 1
CIA	Collagen-induced arthritis
CIITA	MHC class II transactivator class II, major histocompatibility complex, transactivator
CITRUS	cluster identification, characterization, and regression
CLL	Chronic lymphocytic leukemia
CLL-IPI	CLL international prognostic index
CMAC	7-Amino-4-Chlormethylcumarin
CMML	Chronic myelomonocytic leukemia
CMV	Cytomegalie Virus
CNS	central nervous system
CnA	Calcineurin
CpG-ODN	CpG oligodeoxynucleotide
CR	Complete Response
CRAC	Calcium-release activated channels
CRC	CLL Research Consortium
CSF-1	Colony stimulating factor 1 (CSF-1)
CSF1R	Colony stimulating factor 1 receptor
Csk	C-terminal Src kinase
c-SMAC	central SMAC
CTLA-4	cytotoxic T-lymphocyte-associated protein 4
CXCL	CXC Motif Ligand
CXCR	CXC Motif Receptor
C481	cysteine resiude 481
C481S	mutation of cysteine to serine in position 481

DAG	Diacylglycerol
DAMP	damage associate molecular pattern
DAPI	4′,6-diamidino-2-phenylindole
Del 11(q)	Deletion on the long arm of chromosome 11
Del13(q)	Deletion on the long arm of chromosome 13
Del(17p)	Deletion on the short arm of chromosome 17
DLBCL	diffuse large B-cell lymphoma
DLEU2	deleted in lymphocytic leukemia 2
Dlg1	Discs large homolog 1
DMSO	dimethyl sulfoxide
DNA	Deoxyribonucleic acid
DNAM-1	DNAX accessory molecule-1 (DNAM-1)
Dnmt	DNA methyltransferase
dnRAG1	dominant-negative recombination activating gene 1
d-SMAC	distal SMAC
EAE	experimental autoimmune encephalitis
EAT-2	EWS-Fli1-activated transcript-2
EBMT	European Society for Bone Marrow Transplantation
ECOG	Eastern Cooperative Oncology Group
EDTA	Ethylenediaminetetraacetic acid
EdU	5-ethynyl-2´-deoxyuridine
EFS	Event Free Survival
EGFR	Epidermal growth factor receptor
eNAMPT	extracellular nicotinamide phosphoribosyltransferase
ERIC	European Research Initiative on CLL
ERK	extracellular signal–regulated kinase
ERM family	ezrin, moesin and radixin family
ERT	EAT-2-related transducer
ESCCA	European Society for Clinical Cell analysis
FACS	Fluorescence-activated cell sorting
FAK	focal adhesion kinase
Fas	first apoptosis signal
FasL	Fas ligand
Fc	crystallisable fragment
FCR	Fludarabine, cyclophosphamide, rituximab
FCRγ	fragment, crystallizable region receptor γ
FCS	fetal calf serum
FCγRIII	Low affinity immunoglobulin gamma Fc region receptor III
FDA	food and drug adminstration
FGL1	fibrinogen-like protein 1

FISH	fluorescence in situ hybridisation
FL	follicular lymphoma
Flt3	FMS-like tyrosine kinase 3 Receptor
FMO	fluorescence minus one
FOXD3	Forkhead box D3
FOXP3	forkhead box P3
FRET	fluorescence resonance energy transfer
Fyn	Fgr/Yes novel tyrosine kinase
Fzd6	Frizzled-6
GCLLSG	German CLL Study Group
GEF	Guanine nucleotide exchange factor
GITR	glucocorticoid-induced TNFR-related protein
GM-CSF	Granulocyte-macrophage colony-stimulating factor
GPI anchor	glycophosphatidylinositol anchor
GPVI	Glycoprotein VI
GPIb	Glycoprotein Ib
GSK3	Glycogen synthase kinase 3
GvHD	graft versus host disease
GvL	graft-versus-leukaemia effect
HAVCR2	hepatitis A virus cellular receptor 2
HCDR3	heavy chain third complimentary determining region
HL	Hodgkin lymphoma
HLA	human leukocyte antigen
HPBCD	Hydroxypropyl-β-cyclodextrin
Hpf	high power field
Hs1	Hematopoietic-Specific Protein 1
HSCT	haematopoetic stem cell transplantation
HVEM	herpes virus entry mediator
ICAM-1	Intercellular Adhesion Molecule 1
ICAM-3	Intercellular adhesion molecule 3
ICOS	Inducible T-cell costimulator
IDO	indoleamine 2,3-dioxygenase
ID4	inhibitor of DNA binding 4
IFN	Interferon
IFNGR1	Interferon gamma receptor 1
Ig	Immunoglobulin
IgC	Ig constant
IgG1	immunoglobulin G1
IgHD	immunoglobin heavy diversity and
IgHJ	immunoglobulin heavy joining

IgI	Ig intermediate
IgV	Ig variable
Igκ	Immunoglobulin light chain kappa
Igλ	Immunoglobulin light chain lambda
IgVH	immunoglobulin heavy chain variable region
IKFZ1	Ikaros family zinc finger protein 1
IKFZ3	Ikaros family zinc finger protein 3
IKK	IκB kinase
IL	Interleukin
iMID	immunomodulatory drug
IMS	industrial methylated spirit
iNKT	Invariant Natural Killer T
IP$_3$	inositol 1,4,5-trisphosphate
irAE	Immune-related adverse event
IRAK1	Interleukin-1 receptor-associated kinase 1
IRF4	Interferon regulatory factor 4
IS	Immunological synapse
ITAM	Immunoreceptor-based activation motifs
ITIM	immune receptor tyrosine-based inhibitory motif
ITK	IL-2-inducible T-cell kinase
ITP	Immune thrombocytopenia
ITSM	immunoreceptor tyrosine-based switch motif
ITT	Ig tail-tyrosine
iwCLL	International Workshop on CLL
JAK	Janus kinase
JNK	c-Jun N-terminal kinase
KIR	killer cell Ig-like receptors
KLRG-1	Killer cell lectin-like receptor subfamily G member
LAG-3	lymphocyte activation gene 3
LcK	lymphocyte-specific protein tyrosine kinase
LDT	lymphocyte doubling time
LFA-1	lymphocyte function-associated antigen 1
LFA-3	lymphocyte function-associated antigen 3
LIGHT	lymphotoxin-like, exhibits inducible expression, and competes with herpes simplex virus glycoprotein D for HVEM
LMP2A	latent membrane protein 2A
LN	peripheral lymph nodes (LN)
LSECtin	lymph node sinusoidal endothelial cell C-type lectin
LTα	lymphotoxin α
Lyn	Lck/Yes novel tyrosine kinase

MACS	magnetic activated cell sorting
MAPK	mitogen activated protein kinases
MBG	Mouse beta globulin
MBL	monoclonal B lymphocytosis
MCL	Mantel Cell Lymphoma
MCL-1	Myeloid Cell Leukemia 1
MDS	Myelodysplastic Syndrome
MDSC	myeloid derived suppressor cell
MEK	MAPK/Erk kinase
MIF	macrophage migration inhibitory factor
MM	Multiple Myeloma
MP1	HL matrix protein 1 (MP1)
Myc	myelocytomatosis viral oncogene homolog
NCR	natural cytotoxicity trigerring receptor
NHL	non-Hodgkin lymphoma
NK	natural killer
NKT	Natural killer T
NLC	nurse-like cell
NOD	Non-Obese Diabetic
NPM	nucleophosmin
NSG	NOD SCID gamma
mDIA1	mammalian homolog of Drosophila diaphanous 1
MHC	major histocompatibility complex
miR	microRNA
MMP9	Matrix Metalloproteinase 9
MTOC	microtubule organiying centre
mTOR	mammalian target of rapamycin
MYD88	Myeloid differentiation primary response 88
N_{BH}	neutrophil B-helper cells
Necl5	Nectin-like protein 5
NFAT	Nuclear factor of activated T-cells
NIH	National Institute of Heaααh
NKG2D	natural killer group 2 member D
NMII	non-muscle myosin II
NOD	nucleotide oligomerization domain
NZB	New Zealand Black
ORR	Overall Response Rate
OS	Overall Survival
PAMP	pathogen-associated-molecular patterns
PAR complex	partitioning defective polarity complex

PB	peripheral blood (PB)
PBS	phosphate buffered saline
PCNSL	primary CNS lymphoma
PCR	Polymerase chain reaction
PDAC	pancreatic ductal adenocarcinoma
PES	Polyethersulfone
PDK1	3-phosphoinositide-dependent protein kinase-1
PD-L1	programmed death ligand 1
PD-1	programmed cell death protein 1
PFS	Progression free survival
PIP2	Phosphatidylinositol 4,5-bisphosphate
PIP3	Phosphatidylinositol 3,4,5-trisphosphate
PI3K	Phosphoinositide 3-kinase
PKC	Protein kinasen C
PLCγ-1	Phospholipase C gamma 1
PLCγ-2	Phospholipase C gamma 2
PLL	Prolymphocytic leukemia
PMA	Phorbol 12-Myristate 13-Acetate
PMBL	primary mediastinal B-cell lymphoma
PMT	photomultiplier tube
PND	paraneoplastic neurologic degeneration
PPA2	protein phosphatase 2
PP2c	protein phosphatase 2C
PRR	pattern recognition receptor
p-SMAC	peripheral SMAC
PTCL	peripheral T-cell lymphoma
PtdSer	Phosphatidyl serin
PTEN	Phosphatase and Tensin homolog
PTGR2	Prostaglandin Reductase 2
PTL	primary testicular lymphoma
PVRL2	Poliovirus receptor-related 2
PVR	Poliovirus receptor
qTOF	quadrupole-time-of-flight instrument. time of flight (TOF)
RAB35	Ras-related protein 35
Rac1	Ras-related C3 botulinum toxin substrate 1
RAG	recombinase activating gene
Rb	Retinoblastoma protein
Rap1	Ras-related protein 1
RAP1GAP	Rap1 GTPase-activating protein
RAS	Rat sarcoma

RasGRP1	RAS guanyl nucleotide-releasing protein 1
R-CHOP	Rituximab, cyclophosphamide, doxorubicin, vincristine and prednisolone
RDX	radixin
RGMb	Repulsive guidance molecule b
RhoaA	Ras homolog gene family member A
RhoH	Ras homolog gene family member H
RIAM	Rap1-GTP-interacting adapter molecule
RIG-I	retinoic acid inducible gene-I
RING	Really Interesting New Gene
ROR1	Receptor tyrosine kinase–like orphan receptor 1
RPMI 1640	Roswell Park Memorial Institute medium 1640
RS	Richter syndrome
SAP	signaling lymphocytic activation molecule-associated protein
SCF complex	Skp, Cullin, F-box containing complex
scFv	Single chain variable fragment
SCID	Severe combined immunodeficiency
SDF-1	stromal derived factor 1
SDS	sodium dodecyl sulfate
SEA	staphylococcus enterotoxin A
SEB	staphylococcus enterotoxin B
SEREX	serological expression cloning technique
SF3B1	Splicing factor 3B subunit 1
SHIP-1	Src homology 2 domain containing inositol polyphosphate 5-phosphatase 1
SHP-1	Src homology 2-containing protein tyrosine phosphatase-1
SHP-2	Src homology 2-containing protein tyrosine phosphatase-2
Sh-RNA	short hairpin RNA
SH2	Src homology 2 domain
SKAP	Src kinase-associated phosphoprotein
Skp2	S-phase kinase-associated protein 2
SLAMF2	Lymphocyte Activation Molecule Family 2
SLAMF4	Signalling Lymphocyte Activation Molecule Family 4
SLE	systemic lupus erythematodes
SLL	Small lymphocytic lymphoma
SMAC	supramolecular activation cluster
SMAD3	Mothers against decapentaplegic homolog 3
Sp1	specificity protein 1
Src	sarcoma
STAT	Signal transducer and activator of transcription
SV40	simian virus 40
Syk	Spleen tyrosine kinase

TACTILE	T cell activation, increased late expression
TAM	tumour associated macrophage
TAN	tumour associated neutrophils
TCL1	T-cell leukemia/lymphoma protein 1
tBregs	Tumour associated regulatory B-cells
TCRBV	T-cell receptor B variable
T_{EM}	effector memory T-cells
T_{EMRA}	CD45RA+ effector memory cells
TGF	transforming growth factor
Th1	T helper 1
Th17	IL17 producing helper cells
Th2	T helper 2
Tie-2	tyrosine kinase that contains immunoglobulin-like loops and epidermal-growth-factor-similar domains 2
TIGIT	T-cell immunoreceptor with immunoglobulin and ITIM domains
TIL	tumour infiltrating lymphocyte
TIM-3	T-cell immunoglobulin and mucin-domain containing-3
TLR	toll-like receptor
TLS	tumour lysis syndrome
TNF	Tumour necrosis factor
TNFRSF14	TNFR superfamily 14
TOF	time of flight
TP53	Tumor Protein p53
TRAF	TNF receptor associated factor
TRAIL	TNF-related apoptosis-inducing ligand
TRAMP	transgenic adenocarcinoma of the mouse prostate
Treg	regulatory T-cell
TRIS	tris(hydroxymethyl)aminomethane
TTT	time to treatment
ULBP	UL16-binding protein
VCX	Venetoclax
VEGF	vascular endothelial growth factor
VR	Venetoclax and Rituximab
WASp	Wiskott–Aldrich Syndrome protein
WAVE	WASP family Verprolin-homologous protein
Wnt	wingless-related integration site
XBP1	X-box binding protein 1
XID	X-linked Immune Defect
ZAP-70	Zeta-chain-associated protein kinase 70

1   Introduction

1.1   Chronic lymphocytic leukaemia

1.1.1   Epidemiology, clinical features and diagnosis of the disease

Chronic lymphocytic leukemia (CLL) is the most frequently occurring form of leukemia in adults in the West. The incidence rate is about 4 in 100,000 per year (1-3). In contrast, the incidence rate is about 5-10 times lower among East Asians and those of Asian descent (4-6). The disease has a median age of onset of 70 and thus largely affects an elderly patient population. The risk is slightly higher among men compared to women with a male to female ratio of 1.5 (3, 7). Internationally there are an estimated 191,000 cases and 61,000 deaths per year due to CLL and the related non-leukaemic lymphoma *Small lymphocytic lymphoma* (SLL) (8).

The hallmark of CLL is the gradual amassment of mature B-lymphocytes within *peripheral blood* (PB), spleen, *bone marrow* (BM) and *peripheral lymph nodes* (LN). The clinical presentation and course of the disease are highly variable. The condition is typically initially asymptomatic. However, subgroups of patients with a swifter disease onset and more aggressive course exist. Advanced CLL presents with constitutional symptoms including fatigue, fevers, weight loss and night sweats. Peripheral lymphadenopathy, hepatosplenomegaly and more rarely extranodal manifestations can occur as well. As the disease progresses signs of BM insufficiency occur. Other frequently observed phenomena are immune deficiency, manifested by chronic and recurring infections, as well as a reduced response to vaccinations. Autoimmune effects including *autoimmune haemolytic anaemia* (AIHA) and *immune thrombocytopenia* (ITP) occur relatively frequently (9).

The diagnosis of CLL is made following the criteria of the *International Workshop on CLL* (iwCLL) from 2018. The diagnostic assessment is made according to lymphocyte morphology and immunophenotype (10). On blood smears, CLL cells appear as mature lymphocytes characterized by a slim rim of cytoplasm and a dense nucleus without nucleoli or partial chromatin aggregations. Cellular debris known as Gumprecht nuclear shadows are often associated with CLL. Prolymphocytes can occasionally be found among the mature appearing morphologically typical CLL B-cells. A percentage of prolymphoctes equal to or exceeding 10% has been linked to a more aggressive course of CLL. However, a proportion of ≥55% of prolymphocytes would suggest a diagnosis of *prolymphocytic leukemia* (PLL) (11).

The classical CLL immune phenotype has been described as *Cluster of Differentiation* (CD)5+/CD19+/CD20+/CD23+/Immunoglobulin(Ig)M+/IgD+. The expression levels of markers CD20 and CD79b are typically very low compared to physiological B-cells. Clonality of the CLL B-cells can be confirmed by demonstrating light chain restriction with exclusive expression of either Immunoglobulin light chain kappa (Igκ) or Immunoglobulin light chain lambda (Igλ). Expression of CD5 on B-cells is also observed in other lymphoid malignancies such as *Mantel Cell Lymphoma* (MCL). A harmonization project by the *European Research Initiative on CLL* (ERIC) and the *European Society for Clinical Cell analysis* (ESCCA) has recently described a panel of CD19, CD5, CD20, CD23, Igκ, and Igλ to be satisfactory for diagnosing the disease. Additional markers such as CD43, CD79b, CD81, CD200, CD10 or *Receptor tyrosine kinase–like orphan receptor 1* (ROR1) may be of use in establishing the diagnosis in more atypical cases (12).

The diagnosis of CLL is made when >5×10^9/l B-cells with confirmed light chain restriction are observed in the peripheral blood for at least 3 month (10). The presence of lymphadenopathy with the typical histopathological finding and typical immune phenotype but with a number of B-cells in the peripheral blood of <5×10^9/l is indicative of SLL (10). An absolute count of < 5×10^9/l B-cells with typical immune phenotype of CLL in the absence of hepatosplenomegaly, cytopenia or disease related symptoms is defined as *monoclonal B lymphocytosis* (MBL) (13). The condition can be found in over 5% of those over 60 years of age. MBL, while indolent and not causing symptoms by itself, can progress to CLL requiring treatment. Those with low clonal B-cell counts (≤0.5×10^9/l) progress rarely. Among high count MBL patients (>0.5×10^9/l clonal B-cells), however, 1-2% of patients progress per year (14-16).

1.1.2 Clinical staging and risk stratification

Various staging systems have been developed to assess the prognosis of CLL patients – the most common and widely used of which are the Binet and Rai staging systems. (17, 18). Both use a combination of clinical parameters and standard laboratory tests to stratify patients (Table 1).

Rai Staging System	
Stage	*Clinical Features*
0	lymphocytosis (>15x10^9/l) only
I	lymphocytosis + lymphadenopathy
II	lymphocytosis + splenomegaly/ hepatomegaly
III	lymphocytosis + anaemia (haemoglobin <11g/dl)
IV	lymphocytosis + thrombocytopenia (platelets <100x10^9/l)
Binet Staging System	
Stage	*Clinical Features*
A	< 3 affected lymph node areas, no anaemia or thrombocytopenia
B	≥ 3 affected lymph node areas, no anaemia or thrombocytopenia
C	haemoglobin <10g/dl and/or platelets <100x10^9/l ± lymphadenopathy/ organomegaly

Table 2: Staging systems for CLL.

In addition to the staging systems according to Rai and Binet a large number of prognostic markers have been suggested. Among these prognostic parameters characteristics like age, comorbidities, performance status as well as biomarkers related to the disease are featured. Very few of these markers have been validated in prospective studies including *immunoglobulin heavy chain variable region* (IgVH) mutation status (19, 20), CD38 expression, (19) *Zeta-chain-associated protein kinase 7*0 (ZAP-70) expression (21), serum markers like β2-microglobulin (22, 23) as well as cytogenetic aberrations which can be visualized using *fluorescence in situ hybridisation* (FISH) (24).

CLL cells use *IgVH* genes that can be very similar to their germline variants or may have undergone somatic mutation (25-27). If CLL cells harbour an IgVH sequence that shows at least 98% sequence homology to the nearest germ line gene, this is defined as umutated IgVH. Patients that suffer from CLL with unmutated IgVH have inferior prognosis to those with mutated IgVH (19, 20). Presence of mutated IgVH, especially when found alongside other prognostic factors such as a favourable cytogenetic profile and achievement of *minimal residual disease* (MRD) negativity defines a subgroup of patients with very favourable outcome when treated with a chemoimmunotherapy composed of fludarabine, cyclophosphamide and Rituximab (28-30).

Expression of CD38 and ZAP-70 among CLL B-cells correlates with unmutated IgVH and can be associated with poor prognosis. However, exceptions exist which are found more frequently among patients with high risk cytogenetics (19, 21, 31-35).

Several serum markers such as β_2-microglobulin, thymidine kinase and soluble CD23 have been reported to be associated with poor overall survival and progression-free survival among CLL patients (22, 23, 36-39). β_2-microglobulin is used in several multiparameter scores including the *CLL international prognostic index* (CLL-IPI) (40).

Cytogenetic aberrations are identified in >80% of CLL cases (24). The most common alteration is *deletion on the long arm of chromosome 13* (del(13q)) (55% of cases). Other frequently occurring chromosome aberations are *deletions on the long arm of chromosome 11* (del(11q)) (18% of cases), *trisomy of chromosome 12* (16% of cases) and *deletions on the short arm of chromosome 17* (del(17p)) (6% of cases) (24). Of these cytogenetic changes del(17p) is of particular prognostic significance. Patients suffering from CLL carrying del(17p) usually are in need of therapy within 12 months of disease detection and have a median *overall survival* (OS) of a mere 32 months, largely as a result of very limited responsiveness to standard chemoimmunotherapy (24). Only very few patients with del(17p) demonstrate an indolent course of disease (41). Trisomy 12 and del(11q) are associated with a decreased median survival as well (114 and 79 months respectively) while del 13(q) as the sole cytogentic aberration is associated with a favourable outcome (median overall survival (OS) 133 months).

The reason for poor chemo-sensitivity of CLL cases carrying del (17p) is the lack of the tumour suppressor *Tumor Protein p53* (*TP53*) which can be found on the short arm of chromosome 17 (42). Del(17p) often occurs in the setting of additional loss of function mutations of the second allele of *TP53* which result in a complete loss of tumour suppressor function (43, 44). Critical genes associated with other commonly affected chromosome regions include *Notch1* which is found on chromosome 9 but is frequently associated wit trisomy 12 (45), *radixin* (RDX) and ataxia *telangiectasia mutated* (ATM) for del(11q) (46) and *deleted in lymphocytic leukemia 2* (DLEU2)/*microRNA*(miR)-15a/miR-16 for del13(q) (47). Other genes that have been demonstrated to be commonly mutated in CLL B-cells include *Myeloid differentiation primary response 88* (*MYD88*), *Baculoviral IAP repeat-containing protein 3* (*BIRC3*) and *Splicing factor 3B subunit 1* (*SF3B1*) (48-50), all of which have been linked to high-risk CLL and poor response to conventional chemoimmunotherapy (51-53).

Several new stratification systems taking novel prognostic markers into account have been developed (36, 40). Using a multivariate cox regression model Pflug et al. identified 8 factors idenpendently associated with inferior survival in a cohort of CLL patients enrolled in phase III trials of the *German CLL Study Group* (GCLLSG): del17p, del11q, elevated serum thymidine kinase, β_2 microglobulin, unmutated *IgVH, Eastern Cooperative Oncology Group* (ECOG) performance status greater than 0, male gender and age over 60 years. Based on these, they developed a prognostic index stratifying patients in 4 risk categories with a 5-year OS between 18.7% to 95.2% and a C-statistic of 0.75 (36). The CLL-IPI is based on an analysis of 3472 treatment naïve CLL patients from various international clinical trials and uses a weighted score including clinical stage, age, IGVH mutational status, $\beta2$ microglobulin and del17p. The score divides four diagnostic subgroups with a 5-year OS ranging from 23.3%-93.2% and a C-statistic of 0.723 (40).

Richter Syndrome (RS) denotes the transformation of CLL into an aggressive lymphoma, usually *diffuse large B-cell lymphoma* (DLBCL) and, more rarely, Hodgkin lymphoma (HL). Approximately 2-10% of CLL patients will develop Richter syndrome during their lifetime, the incidence rate is 0.5% per year of observation (54). In CLL cases with NOTCH1 mutations and TP53 abnormalities Richter transformation has been described to occur more commonly (55-57) as well as in those expressing certain stereotyped immungloblins, particularly those with IgVH4-39 and *heavy chain third complimentary determining region* (HCDR3) encoded by genes *immunoglobin heavy diversity* (IgHD) 6-13 and *immunoglobulin heavy joining* (IgHJ) 5 (HDCR3 subset 8) (58). Patients with Richter syndrome have an especially poor prognosis (59). In DLBCL type RS the prognosis is dependent on the clonal relationship between CLL and DLBCL clones: While those DLBCL cases with an unrelated clone have a median survival comparable to that of de novo DLBCL, the survival of patients with DLBCL of clonality related to the underlying CLL is significantly shorter (60). Tsimberidou et al. have developed a prognosis score for RS based on ECOG performance status, serum LDH, platelet count and number of prior therapies for CLL distinguishing 4 risk strata with an overall survival ranging from 1.1 years to 0.1 years (59).

Our increasing understanding of molecular and cytogenetic aberrations in CLL continues to reshape risk stratification in CLL. In the era of chemoimmunotherapy "high risk" patients have not been defined along the lines of the classical staging systems anymore but as those being refractory to purine analog–based therapy, those with a short time to progression after therapy and those with high risk cytogenetic features such as *deletions*

on the short arm of chromosome 17 (del(17p)). A newer definition in the age of novel molecularly targeted therapies has distinguished a "high-risk I" category for those patients with TP53 abnormalities resistant to chemoimmunotherapy but responsive to a first line pathway inhibitor (inhibitors of *Bruton's Tyrosine Kinase* (BTK) or BCL2) and a "high risk II" category for patients who have independent of TP53 status failed both chemoimmunotherapy and a firt line pathway inhibitor (61).

1.1.3   Indications for treatment, treatment options and unmet needs

In the absence of reliable and tolerable curative treatment approaches for CLL the treatment decision is made according to the onset of symptoms and the activity of the disease. Patients with asymptomatic early stage disease (Rai stage 0, Binet stage A) are usually observed closely without treatment initiation unless there is evidence of rapidly progressive disease (10). Treatment of these early stage patients has been demonstrated to not result in a survival benefit (62-64). In intermediate stage patients (Rai stage I and II, Binet stage B) treatment is initiated when signs of symptomatic or rapidly progressing disease are found. These include progressive marrow failure (haemoglobin <10 g/dl, thrombocytes <100x10^9/l), very prominent (≥ 6 cm below costal arch) or rapidly progressing or symptomatic splenomegaly, very prominent (≥10 cm in longest diameter) or rapidly progressing or symptomatic lymphadenopathy, progressive lymohocytosis (≥50% increase over a time of two months or lymphocyte doubling time (LDT) <6 months), the presence of autoimmune complications (AIHA or ITP) which do not respond to steroid treatment well, symptomatic extranodal manifestations and symptomatic disease (unintentional weight loss ≥10% within 6 months, fatigue, ECOG performance scale 2 or worse, fevers ≥38.0°C lasting at least 2 weeks in the absence of infection, night sweats ≥1 month in the absence of infecftion). Patients with a high stage of disease (Rai stage III and IV, Binet stage C) already have signs of BM failure and should be treated immediately (10).

Leukostasis does not occur in CLL patients - elevation of the absolute lymphocyte count by itself is therefore not a treatment indication. Moreover, hypogammaglobulinema or paraproteinemia are not considered indications for treatment (10). Asymptomatic disease relapse alone is not considered a treatment indication. Rather initiation of second- or subsequent lines of treatment should follow the same indications as the initial treatment decision (10).

The treatment recommendations for CLL are rapidly changing at the moment. For patients <65 years of age without significant comorbidities and no evidence of del(17p) or TP53 until very recently a chemoimmuntherapy with *fludarabine, cyclophosphamide*

and the anti-CD20 monoclonal antibody Rituximab (FCR) has been used exclusively (65, 66). The CLL08 study reported an ORR of 90%, a PFS of 51.8 months and a 3-year OS of 87% in a cohort of treatment naïve physically fit CLL patients with this combination (66). However, this approach is increasingly being supplanted by monotherapy with the small molecule BTK inhibitor Ibrutinib based on the findings of the E1912 study presented at the annual meeting of the *American Society of Hematology* (ASH) in 2018. Here a significant improvement of progression free survival (PFS) as well as OS with single agent Ibrutinib over FCR was reported in patient <70 years of age (67). This, however, is an interim analysis with a still relatively short follow-up period of only 33.4 months. Hence, the previous standard treatment is still commonly used as well.

Chemoimmunotherapy with FCR, while leading to high OS and PFS, may not be tolerable for those with significant comorbidities or beyond 65 years of age (68). For these patients chlorambucil in combined with an anti-CD20 antibody can be used. Traditionally the combination of Chlorambucil and Rituximab was used, which is generally well tolerated and has been shown to have improved OR and PFS compared to fludarabine or chlorambucil alone (66).

Novel CD20 targeting antibodies are now available as combination partners. The humanized monoclonal antibody Ofatumomab interacts with a different epitope of the CD20 molecule than Rituximab (69) and has been reported to result in a more efficient *complement dependent cytotoxicity* (CDC) than Rituximab (69). Ofatumomab has been demonstrated to have high efficacy in both previously untreated and relapsed or refractory CLL patients. Efficacy has been demonstrated even for patients having received prior Rituximab containing treatment (70-72). Another CD20 targeting monoclonal antibody is the glycoengineered type II antibody Obinutuzumab. A direct comparison of Obinutuzumab, Rituximab and Ofatumomab in a xenograft mouse model as well as in vitro experiments has demonstrated improved direct cell death and *antibody dependent cellular cytoxicity* (ADCC) with Obinutuzumab compared to both Rituximab and Ofatumomab but 10 to 10 000 times reduced portency in induction of CDC. Obinutuzumab also showed slower internalization and improved in vivo efficacy (73). The novel glycoengineered anti-CD20 antibody Ublituximab has been designed to have high affinitiy of *Low affinity immunoglobulin gamma Fc region receptor III* (FCγRIII) and improved ADCC compared to Rituximab (74). The agent is currently being tested in combination trials with *Phosphoinositide 3-kinase* (PI3K) inhibitor Umbralisib (NCT02612311), *BTK inhibitor* (BTKi) Ibrutinib (NCT02013128) and *B-cell lymphoma 2* (BCL-2) antagonist Venetoclax (NCT03379051).

The CLL11 trial evaluated chlorambucil/Rituximab and chlorambucil/Obinutuzumab against Chlorambucil alone and found a significantly longer median PFS for chlorambucil/Obinutuzumab compared to chlorambucil/Rituximab (26.7 months vs. 16.3 months) (75). The COMPLEMENT1 trial has successfully confirmed the superiority of chlorambucil/Ofatumomab over single agent chlorambucil (76).

Another option is combination treatment with Rituximab and Bendamustine (BR) which has been shown to result in an *Overall Response Rate* (ORR) of 88% and an *event free survival* (EFS) of 34 month while causing only moderate toxicities (77). Bendamustine treatment has also been assessed in combination with Obinutuzumab in a phase Ib trial with promising outcomes (78). FCR and BR treatment were directly compared in a phase III randomized open-label trial conducted by GCLLSG. This trial demonstrated a higher rate of *complete response* (CR) and CR without evidence of MRD and higher PFS with FCR in comparison to BR. However, the patients in the BR arm were significantly older and had a higher proportion of case with unmutated IgVH. Also, patients in the FCR arm had higher rates of neutropenia and infectious complications (79). The MABLE study found a significantly prolonged PFS but not OS with BR compared to Chlorambucil/Rituximab (80). BR has thus been preferred over Chlorambucil combinations for the physically fit patients beyond 65 years of age.

As with FCR therapy, a shift away from classical immunochemotherapeutic approaches towards monotherapy with Ibrutinib for elderly and physically unfit CLL patients is occurring. The recently published ALLIANCE study reported an improved PFS but not OS with single agent Ibrutinib compared to BR in patients >65 years of age who had not received prior treatments. The combination of Ibrutinib-Rituximab had no added benefit over Ibrutinib monotherapy in this study (81). Moreover, the combination of Ibrutinib and Obinutuzumab was recently tested against Chlorambucil/Obinutuzumab in patients >65 years of age or those younger than 65 with comorbidities in the iLLUMINATE study. The Ibrutinib combination was reported to lead to significantly prolonged PFS (82). Given the high efficacy of Ibrutinib as a single agent most experts interpret this as a recommendation for the use of Ibrutinib monotherapy as with the above findings (81). Results from both the ALLIANCE and iLLUMINATE study still relate to a relatively short follow-up period so that chemo-immuntherapy continues to be used by many haematologists as of early 2019.

Patients with del(17p) or TP53 mutation have significantly lower ORR and shorter PFS with standard immunochemotherapy (83-85). In vitro studies have demonstrated reduced chemosensitivity in CLL cells harbouring aberrant TP53 (86). Combinations of

the CD52 targeting antibody Alemtuzumab with chlorambucil, Rituximab, FCR or high dose methylprednisolone have been reported to be able to overcome this lack of chemo-sensitivity in CLL with del(17p) (87-90). However, Alemtuzumab is associated with severe haematological adverse effects and infectious complications and is thus usually not tolerable in CLL patients. The approach has largely been abandoned in the wake of novel molecularly targeted treatment approaches. The standard first-line treatment in these patients now is Ibrutinib monotherapy which has been reported to achieve excellent ORR, PFS and OS despite the presence of del(17p)/TP53 mutation (91, 92).

The choice of treatment in relapsed/refractory CLL patients depends on the primary line of treatment, presence of del(17p) and patient characteristics like age and comorbidities. Patients who have been refractory to chemo-immunotherapy or have achieved only a short-lived response (<24 months) as well as those who relapse with del(17p) or TP53 mutations have a particularly poor outcome with a median OS of only 1-2 years prior to introduction of novel molecularly targeted therapies (93). The RESONATE-1 and HELIOS trials have established Ibrutinib therapy in relapsed/refractory CLL patients showing improved outcomes compared to Ofatumomab monotherapy and BR respectively (94, 95). The BCL-2 inhibitor Venetoclax has been shown to have superior PFS and OS compared to BR (96). This treatment option can be used as an alternative to Ibrutinib treatment in those who are unable to tolerate Ibrutinib or in those with progression after Ibrutinib treatment. Importantly, Venetoclax has been shown to be efficacious in patients with del(17p) who progressed while on Ibrutinib (97). Direct head to head comparisons between Ibrutinib and Venetoclax in the setting of a relapse have not been conducted so far. The PI3K inhibitor Idealisib in combination with Rituximab can be used in relapsed/refractory patients as well. However, while having been shown to lead to superior PFS and OS compared to Rituximab monotherapy (98) and Ofatumomab monotherapy (99), it is used less commonly and usually restricted to further lines of treatment due to an unfavourable toxicity profile with high rates of immune-related hepatotoxicity, colitis and pneumonitis as well as opportunistic infections such as Pneumocystis jiroveci (99-102). In patients with long-lasting remissions of at least 2-3 years after chemoimmunotherapy additional cycles of chemoimmuntherapy can be considered as an alternative to novel treatment approaches as well.

Treatment for RS is particularly challenging. The mainstay in DLBCL type RS is chemoimmunotherapy with *Rituximab, cyclophosphamide, doxorubicin, vincristine and prednisolone* (R-CHOP). While the prognosis of clonally unrelated RS is comparable to de novo DLBCL with a median survival of 65 months those with clonally related disease

only fair poorly with a median survival of 12 months (103) . In the former group stem cell transplantation would be reserved to those failing to achieve remission or relapsing. In the latter group consolidation either with reduced-intensity conditioned allogeneic stem cell transplantation or autologous stem cell transplantation depending on donor availability should be offered (104, 105). In addition, several novel agents have been evaluated for treatment in RS. Transient activity of Ibrutinib in RS patients has been reported in a small cases series achieving response in 3 out of 4 patients with a median duration of response of 6 months (106). In the phase I/II ACE-CL-001 trial Acalabrutinib was reported to achieve an ORR of 38% and a PFS of 3 months (107). In the M12-175 phase I trial a small number of DLBCL type RS patients were treated with Venetoclax achieving an ORR of 43% (107). The *programmed cell death protein 1* (PD-1) targeting antibody Pembrolizumab achieved response in 4 of 9 patients with DLBCL-type RS (108). In a phase II trial combining the immune checkpoint PD-1 blocking antibody Nivolumab and Ibrutinib showed promising signals with 3 out of 5 patients achieving response (109). HL-type RS is very rare compared to DLBCL type. All information on treatment efficacy regarding this subtype comes from small retrospective analyses. The standard treatment is chemotherapy with D*oxorubicin, bleomycin, vinblastine and dacarbazine* (ABVD). Among HL type RS an ORR of 40-60% and median OS of 4 years has been reported with this strategy (110-112). As outcomes are better than in those patients with DLBCL type RS consolidation stem cell transplantation is less commonly used in these patients (104).

The only established treatment option for CLL offering a potential cure continues to be allogeneic *haematopoetic stem cell transplantation* (HSCT). The treatment modality is based on the *graft-versus-leukaemia* (GvL) effect which is caused by transplanted lymphocytes, which are able to induce an anti-tumour immune response with the possibility of clinical remission lasting for a long time (113). In approximately 50% of high risk CLL patients treated with HSCT MRD negativity and long-term survival are achieved irrespective of genomic risk factors such as del(17p) (114, 115). However, given its high toxicity, HSCT is only applicable in a minority of young and physically fit CLL patients. The treatment approach is associated with significant mortality and morbidity, which is mainly due to *graft versus host disease* (GvHD) (116) and is therefore usually reserved for those patients with high risk CLL (*i.e.* those with del(17p) or TP53 mutations or a complex karyotype. With the advent of novel molecular targeted treatment options, patients with high risk CLL now typically receive BTK inhibitors or BCL-2 antagonists before considering HSCT. ERIC and the *European Society for Bone Marrow Transplantation* (EBMT) have recently published revised indication criteria,

distinguishing between high risk CLL resistant to chemoimmunotherapy but amenable to BCR pathway inhibitors or BCL-2 antagonists and CLL resistant to both avenues of treatment. While in the first group consolidation HSCT should only be considered in patients with explicitly low risk of transplantation-associated mortality and morbidity (well-matched donor, no comorbidities, <65 years of age) in the latter group HSCT should universally be considered. Also patients with Richter transformation should be offered HSCT provided the patient fitness is deemed sufficient (61). HSCT always needs to be carefully weighed against novel non-curative but significantly less toxic treatment approaches and treatment decisions need to be made on a patient-by-patient basis (117).

1.1.4   BCR pathway inhibitors and BH3 mimetics

A breakthrough in CLL therapy has been achieved with new classes of drugs targeting the B-cell receptor (BCR) pathway. Both antigen dependent and independent BCR stimulation is pivotal for proliferation and survival of CLL B-cells (118). The BCR is a complex consisting of a membrane bound Ig coupled with heterodimers of the transmembrane proteins CD79a (Igalpha) and CD79b (Igbeta) joined together by disulphide bridges. Physiologically, engagement of the Ig by antigen results in receptor aggregation, which subsequently activates the *sarcoma* (Src) family kinases *Lck/Yes novel tyrosine kinase* (Lyn), *B lymphocyte kinase* (Blk), *Fgr/Yes novel tyrosine kinase* (Fyn), *Spleen tyrosine kinase* (Syk) and BTK. Phosphorylation of these kinases, as well as phosphorylation of the *immunoreceptor-based activation motifs* (ITAMs) found in the cytoplasmic tail of CD79a/b occurs (119).The phosphorylated BCR binds to either the Syk or Lyn protein tyrosine kinase, which consequently activate downstream signaling cascades. The *B-cell linker protein* (BLNK) acts as a scaffold for *Phospholipase C gamma 2* (PLCγ-2), *Phosphoinositide 3-kinase* (PI3K) and BTK to form a microsignalosome that initiates downstream signaling. Hydrolysis of membrane *Phosphatidylinositol 4,5-bisphosphate* (PIP$_2$) by PLCγ-2 occurs which leads to the production of *inositol 1,4,5-trisphosphate* (IP$_3$) and *Diacylglycerol* (DAG). IP$_3$ activates the corresponding IP$_3$ receptors leading to efflux of calcium from the endoplasmic reticulum (120, 121). This promotes the influx of more Ca^{2+} through *calcium-release activated channels* (CRAC). Free calcium in the cytosol binds to and activates the proteinphosphatase *Calcineurin* (CnA) which then dephosphorylates and activates the transcription factor *Nuclear factor of activated T-cells* (NFAT). DAG binds to and activates the calcium dependent protein kinase C (PKC) β which subsequently phosphorylates and therby activates various *mitogen activated protein kinases* (MAPK) including *extracellular signal–regulated kinase* (ERK), *c-Jun N-terminal kinase* (JNK) and

p38. Moreover, *IκB kinase* (IKK) is activated by PKCβ leading to phosphorylation and subsequent ubiquination and thus degradation of the IκB. This activates the transcription factor NFκB which is normally bound and inactivated by IκB (122, 123). PI3K catalyzes the phosphorylation of PIP_2 to *Phosphatidylinositol (3,4,5)-trisphosphate* (PIP_3). The latter triggers phosphorylation and activation of AKT which mediates IKK activation and thus degradation of IκB via *mammalian target of rapamycin* (mTOR) (124). These pathways can be also be activated and enhanced through integrin signaling via *focal adhesion kinase* (FAK) (125) or chemokine receptor signaling (126, 127). In their sum, these various pathways achieve continuation of the cell cycle, as well as increased transcriptional activity, proliferation and survival through BCR signalling (128, 129) (Figure 1).
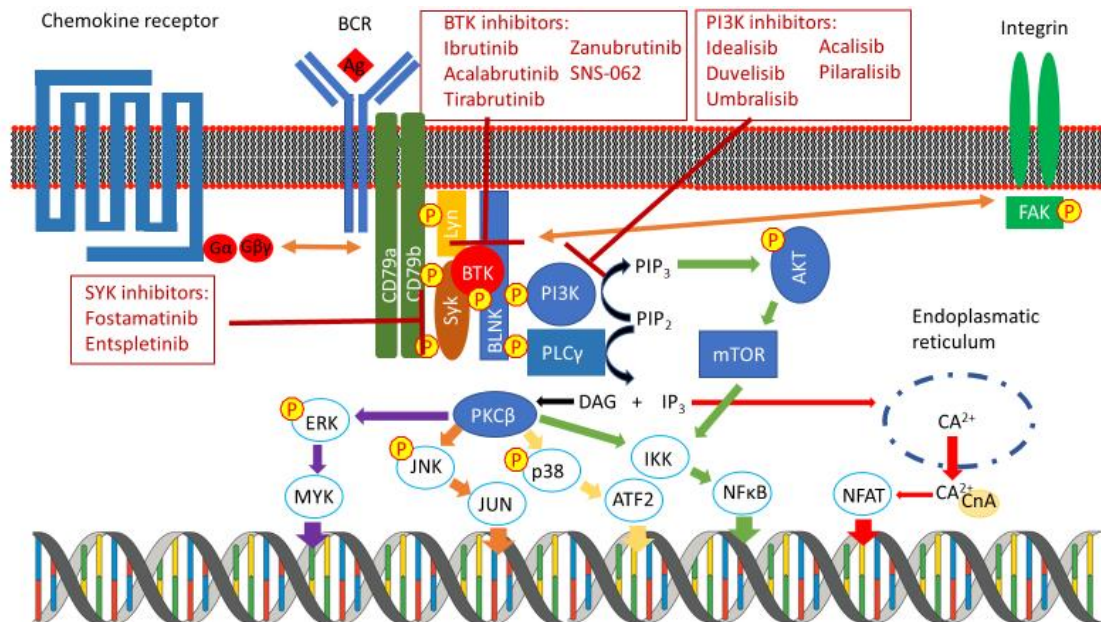
Figure 2: BCR signalling pathway and targets for molecular inhibitors: Exposure of the BCR to antigen (Ag) causes phosphorylation of ITAMs at the cytoplasmatic portion of the complex through tyrosine kinase Lyn. Subsequently the tyrosine kinase Syk is recruited. When Syk is activated it forms a membrane-associated signalosome with other tyrosine kinases including Lyn and BTK. The complex is supported by scaffolding molecules like B-cell linker protein (BLNK). The resulting signalosome activates downstream signalling pathways such as PLCγ and PI3K. PLCγ mediates the release of calcium in the cytoplasm which results in activation of PKCβ. PI3K generates the second messenger PIP_3 which activates the Akt signalling cascade. These events lead to activation of MAPKs including p38, JNK and ERK as well as activation of transcription factors NFκB and NFAT. These cascades can be activated and enhanced via chemokine receptor signalling and integrin binding.

The most clinically successful and widely used BCR pathway inhibitor is the the small molecule Ibrutinib. The *BTK inhibitor* (BTKi) binds covalently and irreversible to *cysteine residue 481* (C481) within the *adenosine triphosphate* (ATP) binding domain of BTK thus

rendering the tyrosine kinase inactive (130). The inhibitor has demonstrated efficacy in those suffering from relapsed or refractory CLL following standard immunochemotherapy. Due to its favourable toxicity profile and high efficacy it has revolutionized the treatment of the elderly or less physically fit CLL patients. Moreover, the efficacy of the substance is not reduced by the presence of del(17p) or TP53 mutations.

In a phase I/II study of Ibrutinib monotherapy in a cohort of heavily pretreated patients with relapsed/refractory CLL an ORR of 71%, an OS of 83% and a PFS of 75% were achieved at 26 months follow-up (131). Long-term follow-up data on this trial was reported in 2015 showing an ORR of 89% and an impressive median progression free survival (PFS) of 52 months (132). These results have since been confirmed in the phase III RESONATE trial where 391 relapsed/refractory CLL patients were treated with either Ibrutinib or ofatumumab. Ibrutinib treatment resulted in a significantly improved ORR (90% vs. 25%) as well as prolongede median PFS (median not reached vs. 8.1 months) and 18-month OS (85% vs. 78%). Ibrutinib treated patients demonstrated no differences in PFS regardless of the presence of del(17p) (94, 133). Moreover, the phase III HELIOS trial compared Ibrutinib or placebo in combination with BR. The Ibrutinib group achieved a significantly improved ORR (86% vs. 69%) and 18-months PFS (79% vs. 24%) (95). The RESONATE-2 trial has established the efficacy of first line Ibrutinib in CLL/SLL patients ≥ 65 years of age (134). 269 patients were randomized to either single—agent Ibrutinib until disease progression or unacceptable adverse events or bi-weekly Chlorambucil up to 12 months. The median follow-up was 18.4 months. An ORR of 86% in the Ibrutinib cohort and 35% in the Chlorambucil cohort were reported. Moreover, Ibrutinib significantly increased 18-months PFS from just 52% in the Chlorambucil cohort to 90% in the Ibrutinib cohort. Long-term follow-up data was presented at the ASH meeting in 2016: With a median follow-up of 28.6 months the 24-month PFS was 89% in the Ibrutinib group vs. only 34% in the Chlorambucil group while the 24 month OS was 95% vs. 84% respectively(135). In a single arm phase II study conducted by the *National Institute of Health* (NIH) the question of Ibrutinib efficacy in CLL with del(17p)/TP53 mutation has be addressed specifically (91). 51 CLL patients with del(17p) or TP53 mutation, 35 of whom were treatment naïve, were treated with single agent Ibrutinib. An ORR of 97% was achieved in the treatment naïve cohort and 80% in the R/R CLL cohort. The estimated 24-month PFS was 82%. An updated reported on the extend 36 months follow-up found the ORR not to differ significantly compared to a cohort of patients without del(17p) and TP 53 mutation (n=35) (136). In addition to these findings, O'Brien et al. reported outcomes of the phase II RESONATE-17 trial. 144 patients with del(17p)

relapsed/refractory CLL were treated using single agent Ibrutinib. The estimated PFS was 63% and the median follow-up 27.6 months (92). As mentioned above, single agent Ibrutinib is increasingly supplanting standard immunochemotherapy as the treatment of choice as a first line treatment even in younger a physically fit CLL patients. The E1912 trial has demonstrated improved PFS and OS with single agent Ibrutinib over FCR in patient <70 years of age (67). The ALLIANCE study and iLLuminate study have shown superiority of Ibrutinib to Chlorambucil/Obinutuzumab and Bendamustine/Rituximab respectively (81, 82).

Ibrutinib treatment in CLL is associated with a phase of lymphocytosis in the first weeks of treatment that is not due to disease progression but rather redistribution of CLL B-cells to the blood stream (137). Several studies have tried to elucidate the mechanism of this phenomenon. De Rooij et al. demonstrated inhibition of chemotaxis by CLL cells as well as of CLL cell adhesion mediated by Intergrins in the setting of Ibrutinib treatment (137, 138). Ponader et al. showed reduced migration toward chemokines *CXC Motif Ligand* (CXCL)12 and CXCL13. Ibrutinib was also shown to downregulate secretion of BCR-dependent chemokines (*C-C motif ligand* (CCL)3, CCL4) by CLL cells (139). A study on patient CLL cells after Ibrutinib treatment showed rapidly reduced capability of CLL cells to adhere to fibronectin, a moderate reduction of migration towards cytokines as well as a reduction of adhesion surface molecules CD49d, CD29, and CD44 (140). In addition, Chen et al. showed reduced expression of *CXC Motif Receptor* (CXCR)4, CXCR5, CD49d and other homing/adhesion related surface molecules in a mouse model of CLL after Ibrutinib treatment (141). As the direct cytotoxic effect of Ibrutinib against CLL B-cells in vitro is rather modest (142) it has been speculated that this egress of malignant B-cells from their protective microenvironment rather than its direct effects on B-cell survival and apoptosis may be responsible for the high clinical efficacy of the substance. A study by Wodarz et al. sought to correlate serial lymphocyte counts of CLL patients after Ibrutinib treatment with CT based volumetric assessment of lymph node and spleen size to address this question. However, it was estimated that only 23.3% +/- 17% of total CLL load in the peripheral tissues was redistributed to the peripheral blood suggesting that CLL cell death rather egress from nodal compartments is responsible for the clinical efficacy of the substance (143). Further support for these findings comes from a study by Burger et al. using isotopic labelling of CLL B-cells with deuterated water to directly measure the effects of Ibrutinib in 30 CLL patients. The CLL proliferation rate was reduced from 0.39% of the clone per day to 0.05% per day with treatment while death rates of CLL cells increased from 0.18% per day prior to treatment to 1.5% per day (144).

Ibrutinib is generally very well-tolerated. Adverse events include nausea, fatigue, myalgias and muscle spasms, as well as pyrexia, skin rashes, diarrhea and headaches. The majority of these untoward effects are grade 1 or 2 adverse events and they are usually self-limiting. Importantly, Ibrutinib is not associated with significant myelosuppression and in some cases has been shown to promote marrow restoration (145). Major adverse effects include treatment induced hypertension (145, 146) and atrial fibrillation (133, 147). Infection is another common adverse event during Ibrutinib treatment. A recent retrospective analysis on 200 patients receiving Ibrutinib for various hematologic malignancies found that 52% developed infection with pneumonia (30%) and upper airway infection (26%) being the leading courses (148). The majority of these infectious complications are self-limiting and are commonly observed early in the course of Ibrutinib treatment (94, 149-152). However, cases of severe opportunistic infections like invasive aspergillosis (153) and disseminated cryptococcal infection (154) have recently emerged. Moreover, BTK is present on platelets and is known to play a role in *Glycoprotein VI* (GPVI)- and *Glycoprotein Ib* (GPIb)-mediated platelet aggregation and adhesion on von Willebrand factor. Treatment associated bleeding is a common adverse event of Ibrutinib therapy and is mainly attributed to the drug's off-target effects, including TEC kinase inhibition (155-158).

Second generation BTK inhibitors with higher binding specificity have been developed. Acalabrutinib (ACP-196), like Ibrutinib, is an irreversible inhibitor of BTK. However, the substance has higher specificity and thus potentially less off-target effects. Unlike Ibrutinib, Acalabrutinib does not inhibit *Epidermal growth factor receptor* (EGFR), *IL-2-inducible T-cell kinase* (ITK) or Tec kinases (159). Common adverse effects of Acalabrutinib treatment include hypertension, fatigue, headache, diarrhea, nausea, upper respiratory tract infections, diarrhea, petechiae and atrial fibrillation (159, 160). Whether the different pharmacological properties of Acalabrutinib will really translate into clinical differences in toxicity and efficacy in CLL patients will be determined by the outcome of the randomized Elevate CLL R / R trial comparing Ibrutinib and Acalabrutinib monotherapy head to head (NCT02477696). Results of a phase I/II multicentre study of Acalabrutinib monotherapy in relapsed/refractory CLL showed an ORR of 85%, comparable to outcomes with Ibrutinib monotherapy (159). Approval of Acalabrutinib for the treatment of CLL will depend on the results of several ongoing trials: The Elevate CLL TN study comparing Obinutuzumab/Chlorambucil, Acalabrutinib/Chlorambucil and single agent Acalabrutinib in CLL patients > 65 years of age who haven't received any prior treatments (NCT02475681), the aforementioned Elevate CLL R/R study comparing single agent Ibrutinib and single agent Acalabrutinib

in patients with relapsed/refractory CLL (NCT02477696) and a trial of Acalabrutinib monotherapy compared to Idealisib/Rituximab or BR in patients with CLL who have relapse after or are refractory to prior treatments (NCT02970318).

Tirabrutinib is another irreversible BTK inihibitor with higher binding specificity compared to Ibrutinib. In a phase I study Tirabrutinib achieved an ORR of 96% among 25 relapsed/refractory CLL patients with the typical reduction of lymphadenopathy and redistribution of lymphocytes to PB (161). The substance is evaluated for CLL in active clinical trials in combination with Entospletinib and Idelalisib with and without Obinutuzumab (NCT02983617 and NCT02968563).

Another second generation BTK inhibitor with higher specificity is Zanubrutinib. In a phase I-II trial of single agent Zanubrutinib in 45 relapsed/refractory CLL/SLL patients an ORR of 90% was achieved with a median follow-up of 7.5 months. Adverse effects included atrial fibrillation and petechiae (162). A phase III trial comparing single agent Zanubrutinib with BR in patients with previously untreated CLL is ongoing (NCT03336333).

An acquired mutation of *cysteine to serine in position 481* (C481S) of BTK has been described as one of the main mechanisms leading to Ibrutinib resistance (163). A number of novel non-covalent BTK-inhibitors have been developed to overcome this resistance mechanism. One of these novel agents is Vecabrutinib (SNS-062). Results from an in vitro study support activity of the agent in the setting of BTK^{C481S} (164). Clinically the substance has only been tested in a phase Ia trial in healthy volunteers with promising signals regarding safety, pharmacodynamics and pharmacokinetics (165). A Phase 1b/2, open-label dose-escalation study evaluating safety, pharmacokinetics, pharmacodynamics, and antitumor activity of Vecabrutinib is currently ongoing (NCT03037645). Another non-covalent reversible BTK inhibitor designed to overcome C481S mutation, LOXO-305, is currently evaluated as a single agent for previously treated CLL/SLL patients in a phase I/II study (NCT03740529). ARQ-531 is a non-covalent reversible inhibitor of BTK as well. Intermin results from an ongoing phase I dose escalation trial of ARQ-531 for various hematologic malignancies (NCT03162536) were presented at the ASH 2018 annual meeting. 3/12 heavily pre-treated CLL patients were reported to have achieved stable disease (166).

Idelalisib is a reversible inhibitor of PI3K regulatory subunit p110δ. The enzyme is involved in CLL cell survival and proliferation as well as retention in secondary lymphoid organs (167, 168). Similar to the BTK inhibitors, it causes redistribution of CLL B-cells to

the PB (169). However, as opposed to the BTK inhibitors, the resulting lymphocytosis does not abate over time – combinations with Rituximab to target the CLL B-cells in the blood stream have thus been used in subsequent trials (98). In a phase I trial of single agent Idelalisib doses from 50-350 mg once or twice daily were tested in 54 relapsed/refractory CLL patients. An ORR of 72% was achieved. The overall median PFS was 15.8 months. The median PFS was increased to 32 months in patients receiving doses of 150 mg twice daily or above. This dosage was thus carried forward in subsequent trials (169). A phase III trial in 220 patients with relapsed/refractory CLL receiving Idelalisib/Rituximab or placebo/Rituximab was interrupted after the first interim analysis due to a markedly improved ORR (81% vs. 13%). The primary adverse effects were reported to be neutropenia, diarrhea and transaminitis (98). Idelalisib in combination with Rituximab has also been evaluated as an initial treatment in CLL patients >65 years of age. An ORR of 97% overall and 100% in patients with del(17p) was reported. The 36-months PFS was 83% (170). Idelalisib was also tested in a phase II trial involving 24 treatment naïve patients (median age 67, range 58 to 85) as upfront single agent treatment for 2 months followed by 6 months of Idelalisib/Ofatumomab. In this trial frequent immune-mediated hepatotoxicity was observed. 79% of patients experienced ≥ grade 1 transaminitis, 54% ≥ grade 3 transaminitis (102). Several subsequent combinations trials have since confirmed significant toxicities including hepatotoxicity, rashes, opportunistic infections, colitis and pneumonitis (99-101). Pneumonitis, colitis and hepatitis are considered to be immune-mediated due to their responsiveness to corticosteroids and T-cell infiltration in affected organs (102). Moreover, preclinical trials have demonstrated hat PI3Kδ blockade in regulatory T-cells leads to induction of cytotoxic T-cell responses (171). Given its unfavourable toxicity profile the combination of Idelalisib/Rituximab is usually only utilized in patients that cannot tolerate both Ibrutinib and the BCL-2 inhibitor Venetoclax or who have progressed while on these treatments.

The PI3K inhibitor Duvelisib has dual activity against both PI3Kδ and PI3Kγ. A phase Ib trial evaluating Duvelisib monotherapy for various hematologic malignancies revealed an ORR of 56% in relapsed/refractory CLL patients and 83% in the treatment naïve CLL patients. Adverse events included febrile neutropenia, pneumonia and hepatotoxicity which was observed in about 30% of patients. Of note, more patients discontinued the treatment due to toxicity than due to disease progression (31% vs 24%) (171). The phase III DUO trial compared single agent Duvelisib to Ofatumomab monotherapy in 319 relapsed/refractory CLL patients. The PFS was significantly improved with Duvelisib compared to Ofatumomab (13.3 months vs. 9.9 months). Moreover, the ORR was

improved significantly as well (74% vs. 54%). Severe immune related toxicities were reported in 21% of patients (colitis 12%, transaminits 6%, pneumonitis 3%) and were managed with dose interruptions and steroid therapy. Infectious complications occurred in 69% of patients including 3 cases of Pneumocystis jiroveci infection (172). Duvelisib has also been tested in combination with either Rituximab, Bendamustin or BR in relapsed/refractory CLL and indolent *non-Hodgkin lymphoma* (NHL) patients. At a median follow-up of 16.3 months an ORR of 92 % was reported for CLL patients (173). The combination of Duvelisib and FCR was reported to lead to MRD negativity in the bone marrow in 89% of 30 treatment naïve CLL patients <65 years of age (174).

Umbralisib is a second generation PI3Kδ inhibitor which differs in its chemical structure from Idelalisib and Duvelisib. The agent appears to have a more favourable toxicity profile with less frequent hepatic toxicity and colitis. In a phase I dose escalation trial an ORR among CLL patients of 85% was achieved (175). An ongoing phase III trial evaluates Umbralisib/Ublituximab vs. Umbralisib or Ublituximab monotherapy vs. chlorambucil/Obinutuzumab (NCT02612311).

Two additional novel PI3k inhibitors, Acalisib and Pilaralisib, are currently in clinical development. Acalisib was tested for various relapsed/refractory hematologic malignancies in a phase Ib study. For CLL patients an ORR of 53.3% and a median PFS of 16.6 months was observed (176). Pilaralisib was evaluated in patients with CLL or relapsed/refractory lymphoma in a phase I trial. In CLL patients an ORR of 50% and a 6-months PFS of 70% were reported (177).

Fostamatinib is an inhibitor of the tyrosine kinase SYK which is of central importance in the B-cell receptor pathway. Early preclinical data suggested that inhibition of Syk could lead to proliferation arrest and apoptosis in CLL B-cells (178). Fostamatinib has been evaluated for treatment of NHL and CLL in a phase I/II trial. Only a modest ORR rate of 55% were achieved (179). The manufacturer has since shifted their clinical development strategy away from B-cell malignancies to rheumatoid arthritis and hence no follow-up studies have been conducted.

Entospletinib is a SYK inhibitor with greater selectivity than Fostamatinib (180). In a phase II trial enrolling patients with various B-cell malignancies the agent achieved an ORR of 61% and a PFS of 14 months. Common adverse events included febrile neutropenia, pneumonia and transient transaminitis (180).

BH3 mimetics are a novel class of substances with the ability to induce apoptosis in CLL B-cells. Apoptosis is regulated by a balance of anti-apototic (*e.g.* BCL-2, *B-cell*

lymphoma w (BCL-w), *B-cell lymphoma-XL* (BCL-XL) , *Myeloid Cell Leukemia 1* (MCL-1)) and pro-apoptotic (*e.g. Bcl-2-associated death promoter* (BAD), *Bcl-2-associated X protein* (BAX), *Bcl-2 homologous antagonist killer* (BAK), *Bcl-2 Interacting Mediator of cell death* (BIM), *BH3 domain-only death agonist protein* (BID)) members of the BCL-2 family of proteins (181). Anti-apoptotic proteins act by sequestering pro-apoptotic initiator proteins such as BIM or BID preventing them from interacting and thus activating effector pro-apoptotic proteins such as BAX or BAK. Interaction of BCL-2 family proteins occurs via a shared domain known as *BCL-2 homology 3* (BH3) (181, 182). BH3 mimetics such as Venetoclax act by displacing initiator pro-apoptotic proteins from BCL-2 thus leading to activation of effector pro-apoptotic proteins. When activated, effector pro-apoptotic proteins form an oligomeric pore in the *outer mitochondrial membrane* (OMM) leading to permeabilization and thus allowing for efflux of cytochrome c. In the cytosol cytochrome c induces caspase activation and subsequently apoptosis (183) (Figure 2). BCL-2 has been shown to be overexpressed in CLL – expression correlates with chemo-resistance and poor survival (184).
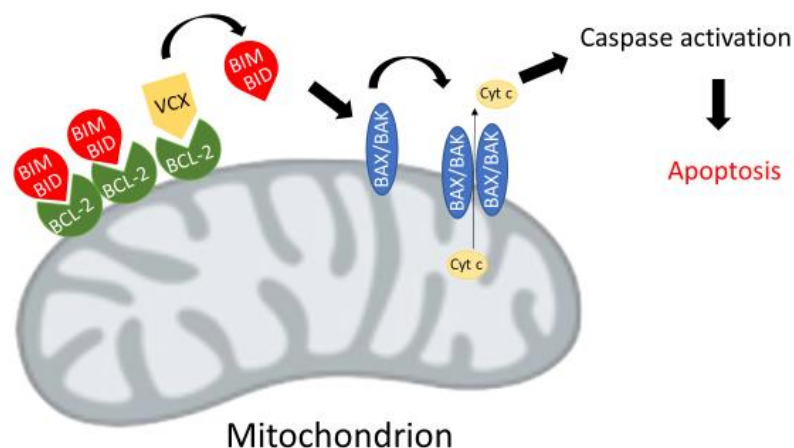
Figure 2: Venetoclax (VCX) mode of action: Anti-apoptotic BCL-2 prevents apoptosis in an apoptotically primed cell by sequestering pro-apoptotic molecules like BIM or BID. Binding of VCX to BCL-2 displaces BIM/BID and allows interaction with pro-apoptotic proteins BAX and BAK. BAX/BAK form an oligomeric pore which allows release of cyctochrome c (cyt c). In the cytosol cyt c activates caspases leading to apoptosis.

The BH3 mimetic Navitoclax was tested in 25 patients with relapsed/refractory CLL in a phase I trial. The median PFS was 25 months, a >50% reduction of lymphocytosis was achieved in 19/21 patients with baseline lmyphocytosis. 9 patients (36%) achieved a partial response. Unfortunately, the agent was found to induce severe thrombocytopenia which was deemed dose-limiting. The clinical development was thus stopped (185). It is

believed that Navitoclax-induced thrombocytopenia is due to an on-target effect on BCL-X, which is important for survival of platelets (186).

Given the haemato-toxicity of Navitoclax, significant effort was directed at developing a BH3 mimetic with binding specificity to BCL-2. This resulted in the synthesis of Venetoclax (186). In the first in-human trial of the agent 3/56 relapsed/refractory CLL patients developed clinical tumour lysis syndrome. Two of these patients died and one developed acute renal failure and eventually needed dialysis treatment. Due to this initial experience a slow weekly increase of doses to a recommended dose of 400mg qd was utilized in the expansion cohort of the subsequent phase I/II trial. Here, an ORR of 79% including a *complete remissions* (CR) rate of 20% were achieved. The estimate 15-month PFS was 69% (187). In a phase II study of 107 patients with relapsed/refractory CLL with del(17p) an ORR of 77% and a 24-month PFS of 54% were achieved (97). The combination of *Venetoclax/Rituximab* (VR) was well tolerated in a phase Ib trial and resulted in an improved CR rate of 41% and a rate of MRD negativity of 75% in those patients (188). In the phase III MURANO trial of VR compared to BR in relapsed refractory CLL a significantly improved estimated 2-year PFS (84.9% vs. 36.3%) and 2-year OS (91.9% and 86.6) was achieved. Importantly, the outcome was similar among patients with del(17p). The rate of *tumour lysis syndrome* (TLS) was a mere 3.1% in the VR group (96). Finally, a phase II trial has evaluated Venetoclax in patients with relapsed/refractory CLL that had progressed on Ibrutinib or Idealisib therapy. An ORR of 65% and a median PFS of 24.7 month were achieved (189).Venetoclax is currently approved for use in patients with del(17p) CLL who have progressed after at least one prior line of treatment. The substance is frequently used in patients who have experienced disease progression on therapy with Ibrutinib or Idealisib.

1.1.5   Other emerging treatment modalities

Following the success of monoclonal antibodies targeting CD20 in CLL and other B-cell malignancies several therapeutic antibodies targeting different surface antigens have been developed.

CLL cells, unlike physiological B-cells, express ROR-1, a transmembrane protein normally only found during embryogenesis (190). Functional studies have indicated that ROR-1 serves as a receptor for lipid modified glycoprotein *wingless-related integration site* (Wnt) 5a and promotes CLL survival and cancer stem-cell self-renewal through non-canonical Wnt signalling (191). Cirmtuzumab (UC-961) is a humanized monoclonal antibody targeting ROR-1. The agent effectively inhibited Wnt signalling in CLL cells in vitro and showed synergistic effects when combined with Ibrutinib in a mouse model of

CLL (192). In a phase I trial the substance was well tolerated in patients with relapse/refractory CLL. Transcriptome analysis showed that the treatment inhibited CLL stemness gene expression profiles in those patients (193). A phase Ib/II trial evaluating the combination of Cirmtuzumab and Ibrutinib is currently ongoing (NCT03088878).

MOR208 is a novel *crystallisable fragment* (Fc)-engineered humanized monoclonal antibody targeting CD19. In a phase I trial for relapsed/refractory CLL the agent demonstrated safety and preliminary efficacy with an ORR of 66.7% (194). A phase II multicentre open label trial of MOR208 combined with either Idelalisib or Venetoclax in relapsed/refractory CLL pre-treated with Ibrutinib is currently ongoing (NCT02639910).

Ortlertuzumab is a humanized anti-CD37 *single chain variable fragment* (scFv)-based *immunoglobulin G1* (IgG1) antibody construct. In a phase I trial single agent Ortlertuzumab was observed to achieve an objective response in 23% of treated CLL patients (195). A randomized phase II trial has evaluated the combination of Ortlertuzumab and Bendamustin versus bendamustin only in patients with relapsed CLL. The combination significantly increased the ORR (69% vs. 39%) and PFS (15.9 months vs. 10.2 months) (196). A phase Ib trial evaluating Ortlertuzumab in combination with Rituximab or Rituximab/idelalisib or Obinutuzumab or Ibrutinib in CLL patients is being conducted (NCT01644253).

Daratumumab is a CD38 targeting humanized monoclonal antibody approved for the use in multiple myeloma (197). A phase Ib trial currently evaluates the agent in combination with Ibrutinib in symptomatic CLL (NCT03447808).

The humanized monoclonal anti-CD44 antibody RG7356 has been demonstrated to be directly cytotoxic to CLL B-cells as well as being able to induce apoptosis mediated by caspases in ZAP-70 positive leukemia cells (198). However, no clinical development for this agent in CLL is currently being pursued.

REGN1979 is a bispecific antibody binding both CD20 and CD3 and thus crosslinking B-cells and T-cells leading to T-cell activation and local cytolytic activity independent of T-cell receptor mediated recognition. In an intermin analysis of an ongoing phase I study in various CD20+ B-cell malignancies 2 of 5 CLL patients achieved stable disease. The agent was reported to result in frequent cytokine release syndrome but no notable *central nervous system* (CNS) toxicity was observed (199).

MCl-1 is an anti-apoptotic protein of the BCL-2 family. Similar to BCL-2 it acts by sequestering pro-apoptotic initiator proteins (181). *Cyclin-dependent kinases* (CDK) are a family of small protein kinases. CDKs bind to regulatory proteins called cyclins. The resulting CDK/cyclin complexes are involved in cell cycle regulation and transcription

regulation (200). MCL-1 expression has been demonstrated to be enhanced through the CDK9/cyclin T complex (201). CDK9 inhibition can thus induce apoptosis in CLL B-cells. Importantly, this mechanism is independent of the presence of del17(p)/TP53 mutations.

Flavopiridol is a flavonoid alkaloid derived from the tree *Aphanamixis polystachya* native to south Asia. The alkaloid has natural CDK9 blocking ability. Flavopiridol has been demonstrated to have clinical activity in high-risk CLL by several studies (202, 203). However, these early phase trials were complicated by hyper-acute TLS as a dose-limiting toxicity occurring in 46% of patients with 19% requiring dialysis (204). In a phase I trial combining Flavopiridol with prior cytoreductive treatment with cyclophosphamide and Rituximab better tolerability and no dose-limiting toxicities were observed (205). However, concerns regarding Flavopiridol toxicity remain and further clinical development seems unlikely.

CYC065 is a novel synthetic CDK2/9 inhibitor. The combination of CYC065 and venetoclax has shown synergistic effects in vitro (206). The combination is currently assessed in a phase I trial in relapsed/refractory CLL (NCT03739554). Moreover, the CDK9 inhibitor Voruciclib has been demonstrated to induce apoptosis in CLL cells in vitro (207). A phase I trial study in several hematologic malignancies including CLL is currently being conducted (NCT03547115).

MiR-155 has been reported to be overexpressed in aggressive forms of CLL (208). The micro-RNA is believed to promote CLL B-cell proliferation and survival through suppression of its predicted target *Src homology 2 domain containing inositol polyphosphate 5-phosphatase 1* (SHIP-1), a protein phosphatase that acts in opposition to kinases involved in BCR signalling (209). Cobomarsen (MRG-106) is an oligonucleotide inhibitor of miR-155. The agent is being evaluated in a phase 1 trial in Mycosis fungoides, CLL, DLBCL and adult T-cell leukemia/lymphoma (NCT02580552).

Lenalidomide is a thalidomide derivate. This class of drugs has been dubbed *immunomodulatory drugs* (iMID). The mechanism of action of this substance is still not understood entirely. Lenalidomide has been reported to bind to cereblon. The protein is responsible for target protein recognition and binding in a multi-protein E3 ubiquitin ligase complex. Interaction with Lenalidomide enhances binding of cereblon to transcription factors *Ikaros family zinc finger protein 1* (IKZF1) and *Ikaros family zinc finger protein 3* (IKZF3) resulting in ubiquination and degradation (210, 211). This leads to suppression of malignant B-cell proliferation through an increase in expression of p21 (212). However, the direct cytotoxic potential of Lenalidomide against CLL B-cells is small and the drug

seems to exert its effects primarily through enhancing anti-tumour immune responses. Various effects on immune cells have been described including an increase in *Interleukin* (IL)-2 production by T-cells (213), an increase in dendritic cell cross-priming of CD8+ T-cells (214), a repair of CLL induced T-cell synapse defect (215, 216) and a repair of impaired T-cell mobility by normalization of signalling G-proteins *Ras-related C3 botulinum toxin substrate 1* (Rac1), *Ras homolog gene family member A* (RhoA), and *Cell division control protein 42 homolog* (Cdc42) (217). While several trials have reported activity of Lenalidomide in both treatment-naïve and relapsed/refractory CLL patients including those with del17(p) its use in the clinical setting is impeded by dose-limiting toxicities including myelosuppression, tumour flare reactions and tumour lysis syndrome (218-226). Avadomide (CC-122) is a novel cereblon targeting agent that is currently in clinical development. The phase I/II ENHANCE trial evaluates Avadomide in combination with Ibrutinib and Obinutuzumab in CLL/SLL patients (NCT02406742).

1.2   CLL and the immune system

1.2.1   Remodelling of the microenvironment, disruption of immune function and T-cell exhaustion in CLL

Disruption of normal immune function is one of the hallmark characteristics of CLL. Immune dysfunction in the setting of CLL is the most common feature (227). Clinically this can manifest in the form of hypogammaglobulinema, recurrent infection and poor response to vaccination (228). Infections are one of the major factors influencing morbidity and mortality in CLL patients being responsible for approximately 50% of CLL-related deaths (229-231). Both the underlying disease as well as sequela of the treatment may be responsible. Immunochemotherapy for CLL is indeed a major contributor to disease related immunodeficiency with the number of prior lines of chemotherapy being an important risk factor for infections in CLL patients. (232, 233). Autoimmune reactions directed against haematopoetic cells are also common in CLL. Such autoimmune phenomena occur in 10-25% of patients at some point during the course of the disease and usually manifest as either AIHA or ITP (234).

A series of qualitative and quantitative defects of the innate immune system relating to CLL have been described. Several authors have reported alterations in the complement system. Schlesinger et al. found decreased levels of serum complement proteins of both the classic and alternate pathway in CLL patients compared to healthy controls. Complements defects correlated with disease stage (235). Füst et al. described decreased levels of complement factors C1 and C4 in CLL. The resulting impairment in recruiting of C3b to the surface of bacterial pathogens may contribute to the increased

risk of infection in CLL (236). Deficiencies of classical pathway complement proteins have been confirmed by other authors and have been shown to predict poor survival in CLL patients (237, 238). Michelis et al. reported increased levels of terminal complement complex soluble C5b-9 and complement factor C5a in the sera of CLL patients while the activation of the classical pathway via aggregated IgG and specifically the activity of the classical pathway C5 convertase were decreased (239).

Moreover, a range of deficits of the cellular compartment of the innate immune system has been reported. Kontoyiannis et al. have described a decreased ability of neutrophil granulocytes to phagocytose non-opsonised bacteria and a reduction of C5a induced chemotaxis (240). In another study significant impairment of random migration, C5a induced chemotaxis and chemiluminescence response in neutrophils from CLL patients with a history of infection were found (241). A deficiency in lysozyme and myeloperoxidase was observed among CLL patient derived neutrophils (242). Podaza et al. reported an increase in CD16^{high} CD62L^{dim} neutrophils in the peripheral blood of CLL patients, a subset that has been reported to have immunosuppressive properties (243). In a mouse model of CLL splenic neutrophils were reported to exhibit a gene expression profile reminiscent of tumour-promoting N2 differentiation of *tumour associated neutrophils* (TAN). These cells had increased expression of cytokines that promote CLL B-cell survival like *B-cell activating factor* (BAFF) *and A proliferation-inducing ligand* (APRIL) as well as functional similarities to *neutrophil B-helper cells* (N$_{BH}$) promoting function and differentiation of B-cells under physiological conditions. Ablation of neutrophils resulted in delayed leukemia development in this model (244).

The absolute monocyte count is increased in the peripheral blood of CLL patients by more than 60%. In a study by Herishanu et al. the *absolute monocyte count* (AMC) was found to stratify CLL patients into 3 distinct groups: Those with high and low absolute monocyte count had shorter time to treatment compared to those with intermediate counts. Moreover, low counts were also associated with increased mortality due to infection (245). Friedman et al. reported elevated AMC to correlated with reduced *time to treatment* (TTT) and poor OS in a retrospective analysis of 1168 CLL patients (246). Monocytes in the peripheral blood of CLL patient have been reported to have a non-classical CD14+CD16++ immunephenotype and express the angiopoetin receptor *tyrosine kinase that contains immunoglobulin-like loops and epidermal-growth-factor-similar domains 2* (Tie-2), a feature known to disrupt T-cells activation and promote *regulatory T-cells* (Treg). Gene expression profiles demonstrated an upregulation of *Rap1 GTPase-activating protein* (RAP1GAP) and downregulation of *Cdc42 effector protein 3* (CDC42EP3) and tubulins which would indicate impaired phagocytotic

properties. In addition, down-regulation of *Prostaglandin Reductase 2* (PTGR2), a reductase with the ability to inactivate prostaglandin E2 and thus suppress inflammatory reactions, was observed. In coculture experiments T-cells showed reduced proliferation when brought in contact to monocytes derived from patients compared to those from healthy controls. Healthy monocytes upregulated CD16, RAP1GAP, IL10, IL8 and *Matrix Metalloproteinase 9* (MMP9) and down-regulate PTGR2 when brought in contact with leukemic cells or leukemic-cell-conditioned media (247). In a study by Gustafason et al. monocytes in the peripheral blood of CLL patients were found to have a decrease in expression of surface protein *human leukocyte antigen* (HLA)-DR and CD86 which are important for antigen presentation and activation of T-cells. Higher numbers of HLA-DR[low]monocytes correlated with shorter time to disease progression (248). Lapuc et al. reported that the number of classical CD14++CD16- monocytes in the peripheral blood of CLL patients negatively correlated with lymphocytosis and was markedly decreased in those requiring immediate therapy. Immunochemotherapy with FCR reduced the number of non-classical CD14+CD16++ monocytes in these patients as well as the surface expression of CD163 and the levels of soluble CD163, a marker that has been linked to the tumour promoting M2 polarization of macrophages (249). Patient derived monocytes were demonstrated to exhibit features of endotoxin tolerance. These include reduced cytokine production and poor expression of HLA-DR and DQ when challenged with *lipopolysaccharide* (LPS). This has been linked to a miR-146a mediated suppression of *Interleukin-1 receptor-associated kinase 1* (IRAK1) and *TNF receptor associated factor* (TRAF)6 (250). Deficiences in beta-glucoronidase and myeloperoxidase were reported among monocytes derived from CLL patients (242). Jitschin et al. reported an increased frequency of CD14+HLA-DR[low]cells in the peripheral blood of CLL patients as well. These cells were shown to suppress proliferation of autolougs T-cells in vitro and were also demonstrated to express CD11c, CD13, CD33, CD11b, CD62L, CD120b, CD115, CD124, CD163 and HLA-G, thus likening them functionally and phenotypically to *myeloid derived suppressor cells* (MDSCs), a heterogenous population of aberrant myeloid cells with the ability to suppress T-cell function. Expression of immune checkpoint protein *programmed death ligand 1* (PD-L1) but not of co-stimulatory proteins CD80 or CD86 were found. MDSCs generated in vitro by coculturing of monocytes from healthy donors with CLL B-cells were able to induce Tregs and suppress T-cell proliferation by an *indoleamine 2,3-dioxygenase* (IDO) dependent mechanism (251). MDSC induction by CLL B-cells has been reported to be mediated by exosomal transfer of miR-155 (252) and non-coding y RNA hY4 via *toll-like receptor* (TLR)-7 signalling (253).

A further line of evidence for the tumour promoting role of myelomonocytic cells comes from reports that monocytes from the peripheral blood of CLL patients can be differentiated into *nurse-like cells* (NLC) ex vivo. NLC attract CLL cells by secretion of stromal derived factor 1 (SDF-1) (254) and CXCL13 (255) and thus retain them in their supporting microenvironment. NLC also promote survival of CLL B-cells through direct cell-cell contact mechanism such as LFA-3/CD2 (256) and CD100/plexin-B1 (257) interaction as well as soluble factors such as *stromal derived factor 1* (SDF-1) (254), BAFF and APRIL (258) or indirectly via stimulation of release of CCL3 and CCL4 (259) or CXCL2 and CCL2 (260) from B-cells*. C-C motif receptor (*CCR)1-mediated upregulation of MCL-1 in CLL B-cells by NLCs has been demonstrated (261). Indeed, ablation of NLC by either liposomale clodronate or monoclonal antibody mediated inhibition of *Colony stimulating factor 1 receptor* (CSF1R) signalling reduced leukemia load in a mouse model of CLL (262). Moreover, NLC were found to confere resistance to chlorambucil and dexamethasone induced apoptosis in CLL B-cells in an in vitro co-culture system (263). NLCs correspond to *tumour associated macrophages* (TAM) in solid malignancy. Like TAM, NLC exhibit an M2 polarization with expression of CD14, CD11b, CD68, *major histocompatibility complex* (MHC) type II, CD163, CD206 and IL10 but not IL12 (264-267). As an in vivo correlate to in vitro generated NLCs, a population of CD68+CD14+ cells with similarity to TAMs has been described in proliferation centres of secondary lymphoid organs (266). NLCs have been demonstrated to suppress T-cell proliferation and promote Treg expansion which can be prevented by anti-IL10 or anti-*transforming growth factor* (TGF)-β antibodies as well as IDO inhibitors (268). Several mechanism driving the polarization of NLCs in CLL have been suggested including secretion of immunoregulatory chemokine *macrophage migration inhibitory factor* (MIF) (269) and *Colony stimulating factor 1* (CSF-1) (270), production of *extracellular nicotinamide phosphoribosyltransferase* (eNAMPT), which has a cytokine-like function independent of its enzymatic activity (271), as well as interaction of secreted hepatocyte growth factor with receptor c-MET on nurse like cells and monocytes (268).

The role of dendritic cells is to process antigens and present them to resting T-lymphocytes in order to activate them. As such they function as intermediaries between the innate and adaptive immune system (272). Orsini et al. have reported significant alterations in function and phenotype in circulating dendritic cells derived from CLL patients. The cells lacked CD83 and the costimulatory molecule CD80. Moreover, they could not induce significant levels of proliferation in allo-mixed lymphocyte reactions, released lower levels of interleukin 12 and had reduced capacity to induce Th1 immune responses (273). In addition, dendritic cells derived from monocytes from the peripheral

of CLL patients with active disease were shown to have lower CD1a expression as well as reduced expression of costimulatory molecules CD40 and CD80. Moreover, these cells retained expression of CD14, which signifies a lack of maturation. Functionally, they had signifcantly reduced allostimulatory capacity as well. Dendritic cells generated ex-vivo in the presence of allogeneic CLL B-cells showed similar phenotypic and functional impairment (274). The cytokine profile of monocyte derived dendritic cells from CLL patients has been reported to be altered with a decrease of interferon gamma production and increase in IL10 production (275, 276). Plasmacytoid dendritic cells, a subtype pivotal in supporting T-cell reactions against viral infections and anti-tumour immunity, have been reported to be decreased in numbers and functionally deficient with reduced production of *Interferon* (IFN)-α. This was shown to be secondary to decreased expression of *FMS-like tyrosine kinase 3 receptor* (Flt3) and TLR9 (277).

Qualitative and quantitative defects have also been observed among *natural killer* (NK) cells. Decreased capacity of patient-derived NK cells to induce lysis of CLL B-cells has been reported early on (278, 279). The functional deficit of NK cells from CLL patients has been associated with a lack of cytoplasmatic granules (279). Kay et al. showed that impaired CLL associated NK-cell activity could be restored by IL2 (280). NK cells derived from CLL patients have been reported to have low expression of activating receptor *natural killer group 2 member D* (NKG2D) and high expression of CD27, indicating a lack of maturation. In addition, lower numbers and decreased viability of NK cells with expression of the inhibitory *killer cell Ig-like receptors* (KIR)2DL1 and KIR3DL1 have been noted. This suggests an activation-induced apoptosis of mature NK cells (281). A decrease of NKG2D expression on NK cells in the peripheral blood of CLL patients was also described by Huergo-Zapico et al. This downregulation of NKG2D was most pronounced in patients with advanced and progressive disease (282). A recent study by Hadadi et al. noted an increased expression of inhibitory factor *mucin domain-containing molecule-3* (Tim-3) as well as a downregulation of the NKp30 activating receptor on the surface of Nk cells from CLL patients (283). In a xenograft-model of CLL reduced NK-cell activating receptor expression including NKG2D, *DNAX accessory molecule-1* (DNAM-1) and various *natural cytotoxicity triggering receptors* (NCR) was demonstrated. This was associated with transcriptional downregulation of cytotoxic pathway genes, including adhesion molecules, cytotoxic molecules and intracellular signalling molecules (284). Induction of impaired NK-cell function has been suggested to be mediated by soluble factors such as *HLA-B-Associated Transcript 3* (BAT3) (285) as well as surface expression of tolerogenic factor HLA-G (286) and 4-1BB ligand (287) on the surface of CLL B-cells. Moreover, pronounced expression of the *glucocorticoid-induced TNFR-*

related protein (GITR) ligand on CLL B-cells was described. Upon interaction with GITR on the surface of NK cells the release of IL6, IL8 and TNF, which act as pro-survival factors for CLL cells, was observed. GITR/GITR ligand interaction also impaired Rituximab induced degranulation of NK cells as well as cytotoxicity and interferon gamma production (288). The clinical relevance of impaired NK-cell function in CLL was demonstrated by a series of studies. In patients with low disease stages and those with mutated IgVH, higher NK-cell numbers in the peripheral blood were reported. A higher NK/CLL ratio predicted a longer TTT (289). This was confirmed in a study by Wang et al. which found higher NK-cell numbers in early stage disease patients, those with <20% ZAP-70 expression and those with normal serum albumin and β2-Mikroglobulin levels. Those patients with lower NK-cell counts had significantly shorter OS (290).

CLL associated humoral and cellular immune defects are not limited to the innate immune system but also affect the function of the adaptive immune system. One of the major clinical parameters known to correlate with risk of infection in CLL is hypogammaglobulinema (230, 291). Despite the low tumour load in early disease stage, levels of immunoglobulins tend to be decreased early on in both CLL and SLL. The severity of hypogammagloblinemia increases over time and with progression of the disease and can involve all types of immunoglobulins (IgA, IgG, IgD) (292, 293). In a study of 1485 newly diagnosed, treatment naïve CLL patients, 26% were reported to have hypogammaglobulinemia. Patients with hypogammaglobulinema were more likely to have advanced Rai stage and had shorter median TTT (294). Patients with Ig levels <700 mg/dl have been shown to have shortened survival in a study by Rozman et al. In the subgroup analysis reduced levels of IgG and IgA were of particular prognostic significance with the IgA levels being of prognostic value independent of clinical stage in multivariate analysis (292). A decrease in IgA level was confirmed to be an independent risk factor prediciting infection in one study while among IgG only subclasses IgG2 and IgG4 were reported to be predictive of an increased risk (295). Copson et al. showed significantly decreased levels of IgG3 and IgG4 among CLL patients (296). The frequently observed decrease in IgA levels among CLL patients may potentially explain the high rate of sinopulmonary infections among these patients. In addition, low levels of pneumococcal antibodies were reported to be more frequent among CLL patients and observed more often among patients with recurrent or severe infections (297). The mechanism of induction of hypogammaglobulinema by CLL cells is only partially understood. The CLL associated hypogammaglobulinema cannot simply be due to a dilution of physiological B-cells by defective CLL B-cells as the phenomenon can occur in early stage disease. It has been suggested that impaired T-helper cell activity (298) is

to blame, possibly due to a downregulation of surface CD40L expression leading to impaired CD40/CD40L mediated antibody class switching (299). Cerutti et al. have demonstrate that T-helper cells upregulate surface expression of CD30 in an OX40 and IL4 dependent manner when activated in the presence of CLL B-cells. Interaction of CD30 with CD30L on the surface of CLL B-cells has been demonstrated to downregulate the CD3-induced expression of CD40L. Moreover, CD30/CD30L interaction interfered with CD40 induced TRAF signalling in non-malignant B-cells leading to impaired *Deoxyribonucleic acid* (DNA) class-switch recombination (300). Interaction of CD70 which is constitutively expressed on the surface of a subset of CLL B-cells has been reported to interact with CD27 on the surface of T-cells leading to PI3K and *MAPK/Erk kinase* (MEK) mediated reduction of immunoglobulin secretion (301). CLL cells have also been shown to be able to directly induce apoptosis of autologous plasma cells via *first apoptosis signal* (Fas)/*Fas ligand* (FasL) interaction (302).

Antibody responses to vaccinations are often inefficient even in early stages of CLL (303, 304). Vaccinations have been shown to be most effective in patients with preserved immunoglobulin levels and when conjugated vaccines are used (305). Still only 58% of CLL patients have been reported to respond to a 13-valent conjugated pneumococcal vaccine compared to 100% of healthy controls in a 2014 trial (306). It is recommended for standard vaccinations to be performed before treatment for CLL is initiated. Immunization against seasonal influenza is recommended (10). Live vaccines are generally contraindicated in CLL patients – severe complications, sometimes even leading to death, have been observed (307). Several randomized studies have been conducted addressing the use of intravenous immunoglobulin substitution as a prophylactic treatment in CLL patients in the 1980s and 1990s. While immunoglobulin substitution reduced the risk of severe infection, it had no appreciable effect on mortality (307, 308). Hence, immunoglobulin substitution is only recommended in patients with hypogammaglobulinemia suffering from repeated infections (10).

CLL B-cells themselves may negatively impact immune reactions. It has been suggested that decreased T-cell function observed among CLL patients is due to a decreased ability of CLL B-cells to present antigens (309, 310), in part due to decreased levels of expression of costimulatory molecules CD86 and CD80 (311). The propensity of CLL B-cells and T-cells to form activating immune synpases has been reported to be severely impaired (215). Surface expression of immunoinhibitory molecules including CD200 (312, 313), PD-L1, B7-H3 and CD270 (216) has been described and is linked to disruption of CLL-associated immune responses. The immune suppressive surface molecule *cytotoxic T-lymphocyte-associated protein 4* (CTLA-4), which is known to be

expressed on the surface of regulatory T-cells, can also be found on CLL B-cells and has been implicated in suppression of costimulation of T-cells (314). Moreover, CLL B-cells have been described to share phenotypic and functional features with *regulatory B-cells* (Breg) (315). Bregs are a subset of physiological B-cells that regulate immune responses through soluble factors, primarily IL10 (316). The anti-inflammatory cytokine IL10 is known to regulate immune function primarily via effects on myeloid derived antigen presenting cells and CD4+ helper cells. In antigen presenting cells IL10 decreases secretion of inflammatory cytokines such as *Tumour necrosis facto*r (TNF), IL-1α and β, IL6 (317, 318) and reduces the surface expression of MHC type II, costimulatory molecules and adhesion molecules (319-321). IL10 has been described to directly inhibit proliferation and cytokine secretion by both *T helper 1* (Th1) *and T helper 2* (Th2) cells (322, 323). Bregs have been described to have regulatory functions in various animal models of autoimmune disease including *experimental autoimmune encephalitis* (EAE) (324), *collagen-induced arthritis* (CIA) (325) and the MRL/lpr model of *systemic lupus erythematodes* (SLE) (326). *Tumour associated regulatory B-cells* (tBregs) that promote tumour growth and suppress anti-cancer immunity have been described in various solid cancers (327-329). In analogy to tBregs, CLL B-cells share phenotypic and functional characteristics with Bregs. Like Bregs derived from the blood of healthy donors, CLL cells show a CD24^{high}CD27+ immune phenotype (315). Another shared phenotypic feature is the surface expression of CD38, an ectoenzyme that promotes B-cell cytokine production and migratory capacity though production of second messenger cyclic *adenosine dinucleotide phosphate* (ADP)-ribose (330). As mentioned under 1.1.2, CD38 can also be used as a prognostic marker in CLL (19). Granzyme B is a serin protease involved in cytotoxic T-cell mediated cell death. However, it also has a secondary function in regulation of immune homeostasis through contact mediated inhibition of activated T-cells by regulatory T-cells (331) and plasmacytoid dendritic cells (332). In B-cells from the peripheral blood of patients with solid cancers an IL21 induced outgrowth of granzyme B expressing CD19+CD38+CD1d+IgM+CD147+ B-cells that were able to inhibit T-cell proliferation by a granzyme B dependent reduction of T-cell receptor ζ-chain has been observed (329). Similarly, CLL B-cells have been described to express CD1d and granzyme B after activation with IL21 (333). Like Bregs CLL B-cells have been reported to be able to secrete large amounts of IL10 (315). IL10 serum levels have been reported to be increased in CLL patients compared to healthy controls (334). CD5 has been described to control IL10 production in CLL B-cells through a *Signal transducer and activator of transcription* (STAT)3 and NFAT2 mediated mechanism (335). Similar to the situation in Bregs, BAFF stimulation of CLL B-cells promoted production of IL10 in a mouse model (336). Both granzyme B and IL10 production could

be enhanced via TLR9 stimulation with *CpG oligodeoxynucleotides* (CpG-ODN) (337, 338). In a mouse model CLL cell growth was significantly reduced in IL10 receptor -/- mice, in which immune cells are unresponsive to IL10, compared to wild type animals. Moreover, IL10 was reported to reduce generation of effector CD4 and CD8 cells in responsive vs. unresponsive animals. The production of IL10 was reported to be regulated by BCR signalling through the Syk/MAPK pathway mediated by the transcription factor *specificity protein 1* (Sp1) (339).

CLL has been described to have a profound impact on phenotype and function of T-cells as well as T-cell numbers and composition of the T-cell compartment. Despite a reduction in relative numbers of CD3+ T-cells early studies have described an expansion of the entire T-cell compartment in terms of absolute numbers in the setting of CLL (340-342). While both the numbers of CD4+ helper cells and CD8+ cytotoxic T-cells in the peripheral bloods seems to be increased, a more pronounced expansion of CD8 T-cells relative to CD4 T-cells with an inversion of the CD4:CD8 ratio has been described (341, 343, 344). It has been hypothesized that this shift in CD4:CD8 ratio in the peripheral blood may be the result of a preferential migration of CD4+ T-cells into CLL bearing lymphoid organs. This notion is supported by reports that CD4+ cells are the predominant T-cell subset in the bone marrow of CLL patients (345). It has been suggested that attraction of activated CD40L+CD4+ T-cells to focal points of CLL cell accumulation in the tissue is mediated by the cytokine CCL22, which is secreted abundantly by CLL B-cells (346). Several authors have demonstrated a clinical significance of the inverted CD4:CD8 ratio. Early studies have shown the CD4:CD8 ratio inversion to be associated with disease stage (343, 344) and development of CLL associated hypogammaglobulinemia (341). Guarini et al. have reported the presence of a CD4:CD8 ratio >1 to be predictive of disease stability (347). These findings have been supported by two studies among treatment naïve early stage CLL patients that have linked inverted CD4:CD8 ratios to shorter TTT(348) and shorter TTT and OS (349), respectively.

Among CLL patient derived T-cells a shift away from naïve subsets towards more antigen experience T effector memory (T_{EM}) and terminally differentiated CD45RA+ effector memory cells (T_{EMRA}) has been described (348, 350-355). This phenotype mimics replicative senescence in the sense of an accelerated ageing of the immune system (356). The loss of costimulatory receptors such as CD27 and CD28, the reduced cell proliferation and increased susceptibility to apoptosis are likely to contribute to CLL associated T-cell deficiency. Reported phenotypic changes also include an increased expression of CD57 (357-359). The CD3+CD57+ T-cells appear to be largely comprised of a select few clones with identical *T-cell receptor B variable* (TCRBV) gene usage and

complementarity determining region 3 (CDR3) size distribution, possibly as a result of chronic activation of T-cells (358, 360-362). A similar activation induced clonal expansion and accumulation of antigen-experienced T-cells has been described in the setting of chronic viral infections such as *Cytomegalo Virus* (CMV) (363). Indeed, several reports have linked the CLL associated expansion of effector memory T-cells to CMV infection (364-366). However, CMV positive T-cells make up a relatively small proportion of the overall T-cell pool in most patients and CLL associated T-cell expansion and senescences still occurs in CMV-seronegative individuals (364). Moreover, the impact of T-cell expansion and inverted CD4:CD8 ratio on TTT and OS appears to be independent of the presence of CMV infection (367). Analysis of the T-cell receptor repertoire in CLL patients revealed shared clonotypes between patients that appear to be CLL-specific. This suggests that antigen drive by CLL B-cells themselves may underlie the CLL-associated T-cell expansion (368). Several authors have stressed the role of specific T-cell subsets in the CLL microenvironment. Regulatory T-cells (Tregs) are CD4+CD25+ *forkhead box P3* (FOXP3)+ T-cells that serve to limit excessive immune reactions, maintain tolerance to self and prevent autoimmune diseases (369). In solid malignancies Tregs have been reported to be enriched in the tumour microenvironment and to interfere with anti-tumour immune responses (370). Similarly, increased frequencies of regulatory T-cells in the peripheral blood of CLL patients have been noted in various studies and have been shown to correlate with more advanced disease stages and shorter TTT (371-380). In addition, in a study by Weerdt et al. increased frequencies of Tregs in lymph node biopsies from CLL patients were described (381). Another helper cell subset of interest is *IL17 producing helper cells* (Th17). Their role in the tumour microenvironment is controversial with potential for both tumour promoting and tumour suppressing properties (382). In the setting of CLL higher numbers of Th17 and serum levels of Il17A have been linked to less advanced clinical stage of the disease and have been shown to inversely correlated with Treg numbers. (383, 384). *Natural killer T* (NKT) cells are a heterogenous group of T-cells that also express NK-cell markers. They only make up approximately 0.1% of peripheral blood T-cells. These cells serve an intermediary role between the innate and adaptive immune system. Many of these cells recognize lipids and glycolipids presented by the surface molecule CD1d found on various antigen-presenting cells (385). CD1d has been demonstrated to be expressed on the surface of CLL B-cells, particularly those with unmutated IgVH, and has been shown to be able to present synthetic lipid alpha-galactosylceramide to NKT cells resulting in cell death (386). In a mouse model of CLL NK1.1+ T-cells were found to be overrepresented. Moreover, CD1d expression on B-cells was demonstrated to be decreased in disease bearing animals and CLL patient samples compared to controls. CD1d -/- mice were

demonstrated to have accelerated leukemia development and decreased survival (387). In a study by Bojarska-Junak et al. reduced numbers of CD3+CD16+CD56+ NKT cells were associated with disease progression and a higher mortality (388). Similarly, Jadidi-Niaragh et al. showed numbers of NKT cells to be significantly reduced in patients with progressive CLL compared to those with indolent disease and healthy controls. Interestingly, NKT cells numbers were inversely correlated with those of Tregs suggesting a Treg modulated downregulation of protective NKT cells in those patients (389). *Invariant Natural Killer T-* (iNKT) cells, a subtype of NK cells, have been demonstrated to significantly delay disease onset in a mouse model of CLL but ultimately to become functionally impaired upon disease progression. In patient samples disease progression correlated with impaired iNKT function. In vitro iNKT cells were shown to hinder CLL survival by restraining CD1d expressing NLCs (390).The ratio of Infγ+ iNKT : IL4+ iNKT was reported to be decreased in CLL patients and shown to correlated with disease progression (391). Another uncommon subtype of T-cells with an intermediary function between innate and adaptive immune system are γδ T-cells. In addition to the γδT-cell receptor they also express natural killer receptors such as NKG2D. They are able to respond to many different types of antigens including peptides, sulfo- and phospholipids independent of MHC molecules (392). In the peripheral blood of CLL patients γδ T-cells expressing Vδ1 and Vδ3 gene segments were shown to be significantly expanded. Both subsets were found significantly more frequently among patients with advanced stages of CLL. Moreover, a large proportion of γδ T-cells from CLL patients expressed Vγ9, indicating an oligoclonal expansion of certain subsets similar to the situation in classical T-cells (393). In another study an expansion of Vδ1 + T cells with increasing expression of granzyme B was noted. This phenomenon was most pronounced among those patients with advanced stages of disease (394). CLL patients with low numbers of Vδ1 T-cells and no detectable expression of *UL16-binding protein* (ULBP) 3, an important ligand for NKG2D, were more likely to progress then those with high numbers of Vδ1 T-cells and detectable or inducible ULBP3 expression on B-cells (395). Coscia et al. have evaluated the responsiveness of Vγ9Vδ2 T cells derived from CLL patients to stimulation by zolendronic acid. Low responder patients had higher baseline counts of Vγ9Vδ2 T cells and a more pronounced shift to effector memory and terminally differentiated effector memory phenotypes. IgVH was more frequently unmutated in low responder patients and higher numbers of circulating Tregs were detected in those patients. Low responders Vγ9Vδ2 status correlated with shorter TTT (396). Given the complexity of T-cells subsets in CLL and their complex and incompletely understood interplay, attempts have been made to summarize abundancy of these various subsets in a unified prognostic score. Rissiek et al. have analysed 24 circulating

T-cell subsets by multiparametric flow cytometry in a cohort of MBL and CLL patients of various stages. Multidimensional scaling analysis was applied to globally assess the composition of the T-cell compartment and develop a T-cell score reflecting its integrity. The resulting T-cell score was able to distinguish MBL as well as different stages of CLL development and changes were detected during disease progression and after chemoimmunotherapy. T-cell scores could also be utilized as a prognostic tool. Patients with higher scores had significantly shorter TTT. The scores also correlated with already established markers of prognosis inculding IgVH mutational status and cytogenetic abnormalities. Changes in the score were shown to be mainly due to changes in numbers of Tregs, NKT cells, $\gamma\delta$ T cells and terminally differentiated T_{EMRA} CD8+ subsets (376).

The development of CLL is associated with severe functional defects of T-cells in several areas. T-helper cell function has been described to be defective in the setting of CLL early on (298, 397). It has been suggested that this is due to an acquired deficiency in CD40L surface expression (299). Severely impaired cytotoxic T-cell function against CLL B-cells has been described as well (398-401). Moreover, similar to NLCs, CD4+ T-cells seem to be critical in boosting of growth and survival of CLL B-cells in vivo as demonstrated by Bagnara et al. in a xeno-transplant model of CLL (402).

The T-helper cell polarity has been reported to be shifted away from a cellular immunity promoting Th1 phenotype towards a more humoral immunity and B-cell growth promoting Th2 phenotype in CLL (334, 403) with a decreased production of classical Th1 cytokines such as IL2 (353, 404) and increased expression of Th2 cytokines such as IL4, IL5 and IL10 (334, 353, 405, 406). IL4 has been observed to promote proliferation of CLL B-cells and to shield CLL cells from apotosis by increasing expression of BCL-2 (407) as well as increased STAT6 phosphorylation and resulting NK-κB activation (408). Similarly, IL10 has been reported to have anti-apoptotic properties towards CLL B-cells in vitro (409). CLL B-cell-secreted IL6 has been shown to promote IL4 production by T-cells and thus further support the skewing of the helper cell polarity towards Th2 (410). Both IL6 and IL10 have been described to be increased in the serum of CLL patients and correlate with poor survival (411, 412). Interestingly, there is significant evidence that secretion of classical Th1 cytokines IFN-γ and TNF-α is increased rather than decreased in CLL T cells and this has been shown to correlate with disease stage (405, 406, 413-415). Both cytokines have also been demonstrated to promote survival and proliferation of CLL B-cells (416, 417). Serum levels of TNF-α have been shown to be elevated in CLL patients and correlate with poor survival (418). This indicates that the model of Th1/Th2 polarity may be insufficient to describe the complexity of cytokine profiles of T-cells in the setting of CLL. Rather than acting against single targets, cytokines and chemokines are likely to

exert their functions in a dynamic network. In order to address this level of complexity Yan et al. attempted to assess the prognostic significance of the serum levels of 23 different cytokines in a cohort of 84 CLL patients and 49 age matched controls by applying unsupervised hierarchical cluster analysis. 3 clusters of differentially expressed cytokines were identified: Cluster 1 (CXCL9, CXCL10, CXCL11, CCL3, CCL4, CCL19, IL5, IL12 and INF-γ), cluster 2 (TNF-α, IL6, IL8 and *Granulocyte-macrophage colony-stimulating factor* (GM-CSF)), cluster 3 (IL1β, IL2, IL4, IL15, IL17 and INF-α). Combination scores of intergrated clusters 1/2 and clusters 1/3 strongly correlated with TTT and OS, respectively (419).

The formation of immunological synapses between both CD4+ and CD8+ CLL patient derived T-cells and superantigen pulsed CLL B-cells was shown to be severely impaired. Importantly, this was found to be due to defects of both the CLL B-cells and T-cells. Moreover, CLL B-cells have been shown to be able to induce the same functional defect in healthy allogeneic T-cells. The underlying mechanism was described to be a dysregulation of actin remodelling and impaired recruitment of key cytoskeletal signalling molecules such as *lymphocyte-specific protein tyrosine kinase* (LcK), Cdc42, *Wiskott–Aldrich Syndrome protein* (WASp), filamin-A and dynamin-2 (215). CLL cells have also been shown to induce impaired *lymphocyte function-associated antigen 1* (LFA-1) mediated motility of T-cells by downregulating Rho GTPases RhoA and Rac1 and upregulating CdC42 (217). Our own group has studied the molecular mechanisms of CLL induced T-cell dysfunction in detail by analysing the gene expression profile of CLL patient derived T-cells. CD4+ and CD8+ T-cells from CLL patients showed numerous genes with differential expression patterns when compared to those derived from healthy controls. Dysregulated genes were mainly involved in processes such as T-cell proliferation and differentiation, vesicle trafficking and actin cytoskeleton remodelling including CdC42, *Ras-related protein 35* (RAB35) and *Actin-related protein 2/3 complex subunit 1B* (ARPC1B). In analogy to the findings in T-cell synapse assays, these profiles of gene expression could also be induced in T-cells derived from healthy donors in a cell-contact depended fashion by co-culturing with allogeneic CLL B-cells (420). These findings have since been confirmed in a study by Di Ianni et al. who reported a similar pattern of dysregulated genes involved in cell differentiation and proliferation, survival, apoptosis, cystoskeleton remodelling, vesicle trafficking and T-cell activation in CLL patients (421). The functional defects in actin remodelling and consequently synapse formation and T-cell migratory activity described above have been shown by our group to be directly induced by CLL B-cells via inhibitory surface receptors CD200, PD-L1, B7-H3 and CD270 by modulating RhoA, Rac1, and Cdc42 Rho-GTPases (216).

As the studies referenced above demonstrate, development of CLL is association with a chronic activation induced functional deficit of both helper and cytotoxic T-cells. A similar state of T-cells dysfunction has been described to occur in chronic viral infections and has been dubbed "T-cell exhaustion". This condition is caused by persistent exposure of T-cells to antigen-stimulation or inflammatory stimuli leading to progressive loss of effector CD8+ and CD4+ T-cell function. The condition has been attributed to overexpression of co-inhibitory immune checkpoint molecules such as PD-1, *lymphocyte activation gene 3* (LAG-3), *T-cell immunoglobulin and mucin-domain containing-3* (TIM-3), 2B4, CD160, *Killer cell lectin-like receptor subfamily G member 1* (KLRG1), CTLA4 and *T-cell immunoreceptor with immunoglobulin and ITIM domains* (TIGIT) (422, 423). We have been able to demonstrate that, similar to the situation in chronic viral infection, the functional T-cell impairment induced by CLL coincidences with an overexpression of immune checkpoint molecules such as 2B4, CD160 and PD-1. This condition is similar to chronic viral infection induced T-cell exhaustion in many ways such as impaired capacity for proliferation and cytotoxic activity of CD8+ T-cells but also differs significantly in some regards such as increased rather than decreased production of cytokines TNF-α and INF-γ. Hence, this functional state has been referred to as "pseudo T-cell exhaustion". Importantly, this has been shown to be independent of CMV sero-status (424). Overexpression of other known immune checkpoint molecules on CD8+ T-cells in the setting of CLL such as LAG-3 and KLRG-1 have been described (352, 425). The development of CLL has been linked to decreased DNA methylation and hence potential for increased expression in gene loci coding for PD-1 and KLRG-1 among CD8 T-cells (349). In the realm of CD4+ T-cells the presence of an exhaustion phenotype with overexpression of TIM-3 and PD-1 has also been documented (426). Catakovic et al. reported an increase of TIGIT expressing CD4+ T-cells in CLL patients correlating with the disease stage. Depleting CD4+TIGIT+ cells or blockade of TIGIT- *poliovirus receptor* (PVR)/CD226 interaction by TIGIT-Fc fusion protein decreased CLL cell viability in vitro, indicating an additional role in promoting CLL cell survival (427). Overexpression of CTLA4 has been demonstrated on both patient derived CD4+ and CD8+ T-cells (372). It has been suggested that PD-L1 expression in CLL cells and PD-1 expression in CLL associated T-cells and thus the exhaustion phenotype is promoted by direct cell-cell interaction via CD84 (428).

1.2.2 T-cell receptor signaling, Co-stimulation, Immune synapse and Immune Checkpoints

Figure 3 summarizes T-cell receptor signaling, co-stimulation and mechanisms of inhibtion by immune checkpoint molecules CTLA-4 and PD-1.
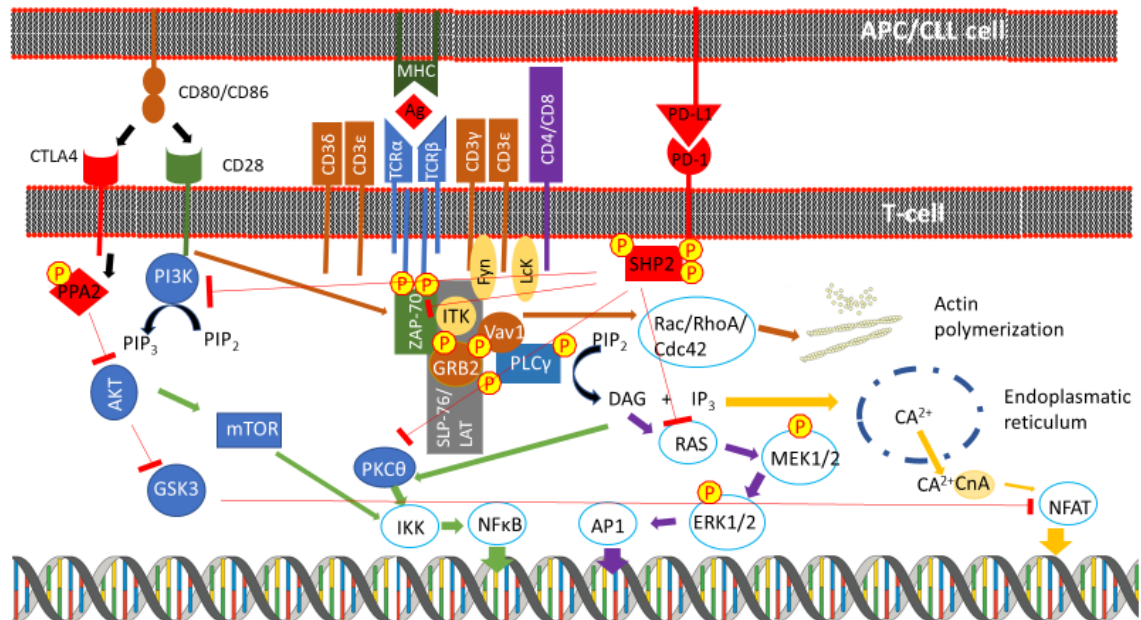
Figure 3: T-cell receptor signaling, co-stimulation and mechanism of inhibtion by immune checkpoint molecules CTLA-4 and PD-1: The T-cell receptor complex is an octomeric complex of TCR α/β, CD3 δ/ε, CD3 γ/ε and CD247ζ/ζ. Engagement of the TCR complex together with co-receptor CD4/CD8 by the specific peptide antigen presented by MHC leads to T-cell receptor signalling. Lck/Fyn phosphorylate and activate ζ chain bound ZAP-70 which phosphorylates and activates adaptor proteins LAT and SLP-76. They serve as a scaffold for further effector molecules such as ITK, GRB2, Vav1 and PLCγ. Vav1 mediates remodelling of the actin cytoskeleton via small GTPases Rac, RhoA and Cdc42. PLCγ activates the downstream IP_3-Ca^{+2}-NFAT, PKCθ-IKK-NFκB and Ras-Erk1/2-AP1 pathways. Costimulation via CD28/CD80/CD86 is necessary for T-cell activation. CD28 activates the PI3K/AKT pathway and directly activates effectors of the TCR signalling complex such as GRB2, Vav1 and Lck. CTLA-4 mediates negative signals by competitive binding and sequestering of CD80/CD86 and inhibits AKT signalling via PPA2. PD-1 inhibts T-cell activation via SHP-2 mediate inhibition of PI3K, ZAP-70, RAS and PKCθ.

The primary signal necessary for T-cell activation is transmitted though the T-cell receptor complex which recognizes specific peptides presented by MHC molecules on the surface of *antigen presenting cells* (APC) or target cells. The T-cell receptor is a disulfide-bond-linked membrane-anchored heterodimer of two highly variable proteins. In human beings 95% of T-cells contain T-cell receptors consisting of an α and β chain whereas 5% of T-cell contain T-cell receptors made up of a γ and δ chain (392, 429). Each chain is composed of two immunoglobulin superfamily domains, the variable and constant region. The variable region contains three hypervariable or *complementary determing regions* (CDR) of which CDR3 has been demonstrated to be the main region

responsible for recognition of processed antigen (430). The T-cell receptor is associated via a network of polar ineractions with three adjunct dimeric signaling molecules forming the T-cell receptor complex: CD3 δ/ε, CD3 γ/ε and CD247 ζ/ζ (431). The cytosolic domains of CD3 and CD247 contain ITAMs which are responsible for transmitting the TCR signal (432). The T-cell receptor complex signal is further promoted by binding of MHC molecules by their respective co-receptor: CD4 on helper T-cells interacts with MHC class II on APCs while CD8 on cytotoxic T-cells interacts with MHC class I on target cells (433). Antigen engagement by the T-cell receptor leads to phopsphorylation of CD3 ITAMs by several Src-family protein kinases such as Lck (434) and Fyn (435). Activation of Lck is promoted by dephorsphorylation via tyrosine phosphatase CD45 (436). The phosphorylation of ITAMs at the ζ chain leads to binding of ZAP-70 via its *Src homology 2* (SH2) domains and phosphorylation of ZAP-70 by LcK (437, 438). ZAP-70 in turn phorphorylates and activates adaptor proteins such as transmembrane protein *Linker for the activation of T cells* (LAT) and cytosolic protein *SH2 containing leukocyte phosphoprotein of 76 kDa* (SLP-76) which act as a scaffold for recruitment of various downstream effector proteins (439, 440). Binding of Vav1 to SLP-76 via its SH2 domain leads to activation of Rho-family GTPases inculding Rac1, RhoA and Cdc42 promoting actin cytoskeleton reorganization (441). Similarly, LAT interacts with GRB2 via its SH2 domain (442). Activated GRB2 promotes *Rat sarcoma* (RAS) activation by binding of *Guanine nucleotide exchange factor* (GEF) *son of sevenless* (SOS) via its Src homology 3 (SH3) domain (443, 444). GRB2 has also been shown to bind to and promote function of Vav1 via SH3 (445). A key event in the signalling cascade is binding and activation of *Phospholipase C gamma 1* (PLCγ-1) by both LAT and SLP-76. Activated PLCγ-1 hydrolyzes membrane-bound PIP_2 into second messengers IP_3 and DAG linking the proximal T-cell receptor signalling complex to various downstream signalling cascades such as the IP_3-Ca^{+2}-NFAT pathway, the PKCθ-IKK-NFκB pathway and the the Ras-Erk1/2-AP1 pathway (446, 447). Both reorganization of the actin cytoskeleton and PLCγ-1 activation as well as downstream signalling have been shown to be dependent on the tyrosine kinase ITK (448-450).

IP_3 generated by PLCγ-1 binds to its receptor on the endoplasmatic reticulum leading to efflux of Calcium in the cytoplasm. This triggers further calcium influx through CRAC (451, 452). Calcium activates the protein phosphatase calcineurin which leads to dephosphorylation and subsequent transport of transcription factor NFAT to the nucleus (453). PLCγ-1 derived DAG triggers PKCθ signalling. This leads to activation of IKK which in turns phosphorylates IκB leading to its ubiquination and degradation. This results in the release of NF-κB which is subsequently transported into the nucleus (454).

In addition to SOS another GEF called *RAS guanyl nucleotide-releasing protein 1* (RasGRP1) is known to induce RAS activation. RasGRP1 binds DAG leading to its membrane translocation and activation (455). GDP bound RAS is inactive. GEFs modulate release of GDP and replacement with GTP. Activated RAS-GTP triggers a cascade of phosphorylating protein kinases including Raf, Mek1/2 and Erk 1/2 leading to formation of transcription factor AP-1, a dimeric complex of JUN/FOS that is pivotal in regulating activation induced modulation of gene expression in T-cells (456, 457).

Initial immunological models postulated that the adaptive immune system was working via a simple distinction between self and non-self (458). In 1989 Charles Janeway introduced a new concept, the infectious non-self model (459). He postulated that APCs are *activated by pathogen-associated-molecular patterns* (PAMPs) through *pattern recognition receptors* (PRRs) which thus can distinguish infectious non-self from non-infectious self. In 1994 a novel model was conceived by Poly Matzinger, the so called danger model, which would supplanted these earlier conceptions. Martzinger proposed that the immune system does not function by discerning between self and non-self but by detecting states of safety or danger through sensing of the presence of pathogens or alarm signals from injured or stressed cells (460). "Danger signals", the so called alarmins, include PAMPs but also *damage associated molecular patterns* (DAMPs) such as heat shock proteins, DNA, hyaluronic acid, RNA, uric acid, serum amyloid A protein, ATP and cytokines like IFN-α and IL-1β (461). Alarmins are recognized by APCs through PPRs such as TLRs, *nucleotide oligomerization domain*(NOD)-like receptors, *retinoic acid inducible gene-I* (RIG-I)-like receptors and c-type lectins (462-465). Stimulation of APCs through PPRs leads to activation of the molecular machinery to process and present antigen but also to expression of secondary, "co-stimulatory" molecules necessary for T-cell activation. This co-stimulatory signal is primarily mediated via CD28, which is constitutively expressed on the surface of T-cells, in interaction with its ligands CD80 (B7.1) and CD86 (B7.2) on the surface of APCs and B-cells (466). Other costimulatory pathways include *Inducible T-cell costimulator* (ICOS)/ICOS ligand (467), CD70/CD27 (468), 4-1BB/4-1BB ligand and OX40/OX40 ligand (469). After binding of CD28 to its ligands it is able to interact with various downstream signalling cascades through interaction of immunotyrosine motifs with SH2 or proline rich regions with SH3 domains. Activated CD28 binds to and activates PI3K in an SH2 dependent manner (470). PI3K derived PIP$_3$ triggers phosphorylation and activation of AKT which promotes NFκB signaling via mTOR (124). Moreover, AKT mediated phosphorylation inhibits *Glycogen synthase kinase 3* (GSK3) (471). At steady state GSK3 prevents nuclear translocation of NFAT which is thus promoted by AKT signaling (472). In addition to PI3k

mediated signalling CD28 is also able to directly bind to and activate adaptor proteins of the proximal signalisome of the T-cell receptor. Ras signaling has been shown to be promoted by interaction with GRB2/SOS (473). CD28 also promotes actin cytoskeleton remodeling in a Vav1/SLP-76 dependent fashion (474). Lck binding and activation has been shown to mediate PKCθ phosphorylation and thus enhance downstream NFκB signaling (475, 476).

The interface area between T-cell and APC or target cell is referred to as the *immunological synapse* (IS). Within the area of contact the distribution of receptor surface molecules as well as intracellular signaling molecules is not random. Rather, the immune synapse is organized in concentric rings containing segregated cluster of proteins, the *supramolecular activation clusters* (SMACs). At the centre of the synapse is the *central SMAC* (c-SMAC) containing the components of the T-cell receptor complex such as TCR and CD3 (477) as well as co-receptors CD4, CD8 and CD28 (478), components of the proximal signalosome such as LcK, Fyn, ZAP-70 and PKCθ (479, 480) and cell adhesion molecule CD2 (481). The c-SMAC is surrounded by the *peripheral SMAC* (p-SMAC) within which the cell adhesion molecule LFA-1 and the cytoskeletal protein talin are clustered (477). This is followed by the *distal SMAC* (d-SMAC) which is enriched in adjunctive transmembrane proteins CD43 and CD45 as well as polymerized F-actin (482-484). However, aberrations from this model pattern do exist. In DC/T-cell interaction a multifocal pattern of separate but partially overlapping TCR/CD3 and LFA1 containing clusters resembling the microcluster architecture of the nascent IS has been reported (485-487). The formation of the IS is a complex multi-step process. An initial phase of exploratory contact is mediated by low affinity protein/protein interactions between LFA-1 and *Intercellular adhesion molecule 3* (ICAM-3) (488) as well as *lymphocyte function-associated antigen 3* (LFA-3) and CD2 (489). If successful interaction between the TCR complex and a peptide loaded MHC molecule is established, processes are initiated that overcome opposing charge dependent repulsive glycocalyx interactions (490) and galectin mediated TCR inhibition (491). Moreover, TCR engagement has been demonstrated to halt motility of migrating T-cells to allow for synapse formation (492). After successful engagement and crosslinking, TCRs are immobilized and clustered in the area of contact (478). Electron-microscopic imaging revealed that this initial phase of contact is via actin rich lamellopodia extending from the surface of the T-cell and penetrating deep into the opposing cell. With consolidation of the synapse the area of contact is flattened and smoothed out (493-495). TCR-containing microclusters/lipid rafts are continually produced in the periphery of the contact site and coalesce to the centre to form the c-SMAC (487). The mechanism of coalescence is

incompletey understood but appears to depend on continuous TCR ligation and F-actin flow (496) as well as on dynein driven microtuble movement (497). As mentioned above, signaling through the T-cell receptor complex leads to phosphorylation and activation of scaffolding proteins such as SLP-76 which in turn associates with Vav1 through SH2 interaction leading to activation of downstream GTPases (441). The small GTPase RhoA activates the protein *mammalian homolog of Drosophila diaphanous 1* (mDIA1), a member of the formin family which mediates the nucleation and unbranched extension of actin filaments (498). The *actin-related protein* (Arp)2/3 complex mediates nucleation and branched actin filament extension. In order to function it needs to associated with nucleation-promoting factors from the Wiskott-Aldrich syndrome family of proteins (499). Interaction of small GTPase Cdc42 with WASp discloses its binding site for the *Arp2/3* complex (500). *WASP family Verprolin-homologous protein* (WAVE) is activated by Rac1 in association with *non-catalytic region of tyrosine kinase adaptor protein* (Nck) and subsequently associates with the Arp2/3 complex (501). The Arp2/3 complex works together with filamins, large multidomain proteins which mediate actin crosslinking, to build the actin structure. Filamin-A has been shown to directly interact with CD28 and be recruited to the IS following CD28 ligation. Knockdown of filamin-A resulted in impaired Cdc42 activitiy and CD28 mediated lipid raft accumulation (502). The large GTPase dynamin-2 has also been shown to be required for actin polymerization at the IS (503). Dynamin-2 interacts directly with Vav1. While it has been shown to interact with several actin-binding proteins, its mechanism of action is not understood (504). Actin depolymerization occurs passively but is promoted by *actin-depolymerization factor* (ADF) and cofilin (505). In T-cells co-stimulation via CD2, CD4, CD8 and CD28 but not TCR-signalling itself has been shown to promote cofilin phosphorylation and activation (506). The TCR signal mediates LFA-1 trans-activation, leading to conformational extension and binding to *Intercellular Adhesion Molecule 1* (ICAM-1), which is the basis for the formation of the p-SMAC ring (507). *Ras-related protein 1* (Rap1), a small RAS-like GTPase is activated by TCR signalling through GEFs. It activates *Rap1-GTP-interacting adapter molecule* (RIAM) which targets talin, a protein linking the actin-cytoskeleton to integrins, to the plasma membrane leading to LFA-1 transactivation (508). A complex consisting of SLP-76, *Adhesion- and Degranulation-promoting Adapter Protein* (ADAP) and *Src kinase-associated phosphoprotein* (SKAP) links RIAM to the TCR complex and Rap1, thus participating in the delivery of talin to LFA-1(509). Transactivation of LFA-1 is further promoted by Kindlin-3 (510). TCR- and integrin signaling promote redistribution of the *microtubule organizing centre* (MTOC), golgi apparatus and microvesicles within the T-cell towards the contact area with the APC or target cell (511, 512). T-cell polarization has been shown to be dependent on

components of the proximal TCR receptor signaling complex such as Lck, ZAP-70, SLP-76 and LAT (513, 514). Further downstream, DAG produced by PLCγ (515) and cascades of various PKC isoenzymes (516) have been shown to be essential for MTOC polarization. PKCθ has been demonstrated to mediate accumulation of motor protein dynein in the area of the IS, which pulls the MTOC forward, and of *non-muscle myosin II* (NMII) at the opposing pole of the cell, which pushes the MTOC towards the synapse (517). PKCζ, another TCR activated but DAG independent PKC isoform, which forms part of the *partitioning defective polarity complex* (PAR complex) has also been described to modulate T-cell polarity (518). Interestingly, formins like mDIA1 have also been implicated in microtuble network organization and MTOC polarization (519). Ezrin, a member of the *ezrin, moesin and radixin family* (ERM family) of proteins, is able to bind F-actin via its c-terminal domain and plasma membrane proteins via its n-terminal domain (520). Ezrin has been described to interact with microtubules via *Discs large homolog 1* (Dlg1) and integrate regulation of the various components of the cytoskeleton and the TCR signaling cascade (521). In cytotoxic T-cells the final step is a clearance of a part of the central actin accumulation forming a secretory domain. The mechanisms mediating this process are poorly understood (522). Formation of the secretory domain allows for target cell killing via secretion of granzymes, perforin and granulysin or direct Fas/FasL interaction. T helper cells, on the other hand, create an activating microenvironment for other immune cells by paracrine secretion of cytokines.

Increasing evidence suggests that T-cell anergy and tolerance to self are not simply due to the absence of co-stimulatory signals but rather actively induced by a series of "co-inhibitory" surface molecules, the so-called "immune-checkpoints". The two immune checkpoint pathways that are most prominent and best understood are CTLA-4 and PD-1. Both PD-1 and CTLA-4 delivery co-inhibitory signals to T-cells. However, they exert their functions at different stages of the induction of the T-cell response. While CTLA-4 exerts its function early on during T-cell priming within lymphoid organs and has a more generalized impact on the immune system, PD-1 suppresses T-cell function in the peripheral tissues containing the target cells (523). This fact is also illustrated by the differential effects of immune checkpoint knockout in mouse models. CTLA-4 -/- mice suffer from early onset autoimmune multiorgan tissue destruction mediated by uncontrolled CD4+ costimulation-dependent lymphoproliferation that is lethal at 3-4 weeks of age (524-526). In contrast, PD-1 deficient animals develop more organ specific symptoms with a more protracted onset. C57BL/6 PD-1 -/- mice have been shown to develop lupus-like autoimmune phenomena such as proliferative arthritis and glomerulonephritis and exhibited increased T-cell receptor mediated proliferation of

CD8+ T-cells in response to stimulation with specific antigen presenting cells (527). Similarly, spontaneous development of auto-immune induced dilatative cardiomyopathy was reported with PD-1 knockout in BALB/c mice (528).

CTLA-4 was the first immune-checkpoint to be discovered by Brunet et al. in 1987 (529). It is a protein encoded by the CTLA-4 gene on chromosome 2q33.2. Just like CD28, CD80 and CD86 it belongs to the immunoglobulin superfamily of proteins. In resting naïve T-cells CTLA-4 is primarily found in the cytoplasm. Surface expression is detected 1 to 2 days following T-cell activation (530). More rapid induction and longer lasting surface expression is found in memory T-cells (531). The protein is constitutively expressed by Tregs (532). CTLA-4 transmits an inhibitory signal to T-cells. This is illustrated by the fact that antibody blockade of CTLA-4 increases T-cell proliferation in allogeneic mixed lymphocyte reactions (533) as well as with anti-CD3/anti-CD28 induced T-cell proliferation in vitro (534). CTLA-4 ligation has also been demonstrated to block IL2 production, IL2 receptor expression and cell cycle progression in T-cells in vitro (535). Moreover, CTLA-4 has been shown to promote T-cell motility and disrupt synapse formation with APCs by overriding the TCR mediated stop-signal (536). CTLA-4 has been demonstrated to induce a polarized morphology typical of more mobile T-cells (537). The reverse-stop effect on T-cells appears to be limited to conventional T-cells while regulatory T-cells are unaffected (538). In addition, increased T-cell motility secondary to CTLA-4 induced upregulation of chemokine receptors CCR5 and CCR7 as well as increased sensitivity for signaling though CCL4, CXCL12, CCL19 and CXCL9 has been described (539). CD28 and CTLA-4 exhibit a large degree of homology: both share the MYPPPY motif for ligand binding and are able to interact with both CD80 and CD86 (540). However, CTLA-4 binds both ligands with greater affinity than CD28 and thus can outcompete the co-stimulatory molecule for its binding partners (534). Moreover, it has been demonstrated that CTLA-4 is able to capture CD80 and CD86 molecules from the surface of the opposing cell through trans-endocytosis, thus removing them as binding partners for CD28 (541). Unlike other immune checkpoint molecules, the cytoplasmatic tail of CTLA-4 does not contain an *immune receptor tyrosine-based inhibitory motif* (ITIM) and does not have catalytic activity of its own. CTLA-4 has been shown to bind *protein phosphatase 2* (PPA2) at baseline rendering CTLA-4 inactive. Upon receptor co-ligation PPA2 is phosphorylated and dissociates from CTLA-4. PPA2 inhibits PI3k signaling via inhibition of AKT (542). A potential interaction of CTLA-4 with protein tyrosine phosphatase *Src homology 2-containing protein tyrosine phosphatase-1* (SHP-1) (543) and *Src homology 2-containing protein tyrosine phosphatase-2* (SHP-2) (544) has been suggested but remains controversial.

Subsequent studies have failed to demonstrate direct interaction of CTLA-4 with either SHP-1 or SHP-2 (545, 546).

Another member of the immunoglobulin superfamily is PD-1 (CD279). PD-1 was first discovered by Ishida et al. in 1992 in search of genes inducing apoptosis (547). In human beings the PD-1 gene is located on chromosome 2q37.3. It codes for a type I transmembrane protein of 288 amino acids that is comprised of an immunoglobulin V set domain, a transmembrane domain and an intracellular domain that contains an ITIM as well as an *immunoreceptor tyrosine-based switch motif* (ITSM) (548, 549). Expression of PD-1 is found on effector T-cells, Tregs, naïve and activated B-cells, NK cells, myeloid dendritic cells and activated monocytes. Resting T-cells do not express PD-1 but expression can be induced by T-cell activation within 24 hours (550).

PD-1 binds two ligands, PD-L1 and PD-L2. The first ligand to be discovered was PD-L1. The protein is encoded by the CD274 gene on chromosome 9p24.1. The ligand was first discovered under the name of B7-H1 in 1999 by Dong et al. The group identified the protein as a novel member of the B7 family but was at first unaware of its role as a ligand for PD-1 (551). Later Freeman et al. demonstrated that B7-H1 acts as a ligand for PD-1 and coined the term PD-L1. They were able to show that PD-1/PD-L1 interaction inhibits CD3-mediated T-cell proliferation. In these experiments the effect of PD-1/PD-L1 interaction depended on the intensity of both the T-cell receptor signal as well as the strength of the CD28 costimulation signal. Suboptimal T-cell receptor stimulation by CD3 beads in the presence of PD-L1 resulted in 80% reduction of proliferation that could only be rescued with maximal CD28 stimulation. However, when maximum T-cell receptor stimulation was achieved, PD-L1 mediated inhibition of T-cell proliferation was only reported when no CD28 mediated costimulation was present. This indicates that PD-1 mediated T-cell suppression can be overcome by an appropriate degree of co-stimulation (552). PD-L1/PD-1 interaction has also been shown to attenuated secretion of IL2 by T-cells (553). Similar to CTLA-4, PD-L1/PD-1 interaction has also been shown to disrupt synapse formation by blocking the TCR-induced stop signal for T-cell motility (554). PD-L1 expression is found ubiquitously in many tissues. On the mRNA level constitutive PD-L1 expression could be detected in non-lymphoid organs. Inducible mRNA expression in peripheral blood CD14+ monocytes, dendritic cells, activated B-cells and on CD3+ T-cells themselves could be demonstrated (551, 552). On the protein level PD-L1 expression has been described in a small subset of splenic T and B-cells, in most pre-B-cells and myeloid cells in the BM as well as on a subset of thymocytes. Moreover, a larger proportion of immature linage marker negative and c-Kit positive bone

marrow cells were found positive for PD-L1 (555). Expression of PD-L1 has been shown to be primarily promoted and regulated by IFN γ through *Janus kinase* (JAK)1/JAK2-STAT1/STAT2/STAT3 via interaction of *Interferon regulatory factor 1* (IRF-1) with its response element in the PD-L1 promotor region (556, 557). In the mouse constitutive PD-L1 expression on splenic T- and B-cells, macrophages and dendritic cells was confirmed. Expression on T-cells was shown to be upregulated by anti-CD3 stimulation, expression on macrophages by LPS, IFN-γ, GM-CSF and IL4 and expression on dendric cells by IFN-γ, GM-CSF and IL4 (558). In PD-L1 -/- mice an accumulation of CD8+ T-cells but not CD4+ T-cells could be observed that was spontaneously occuring. This was shown to lead to accelerated hepatocyte damage with induction of experimental autoimmune hepatitis (559). In another study both CD4+ and CD8+ T-cell responses were shown to be enhanced in PD-L1 -/- mice in vitro and in vivo. Moreover, PD-L1 deficiency was reported to lead to greater susceptibility to EAE (560).

PD-L2 (CD273, B7-DC) is the second ligand known to interact with PD-1. In humans it is encoded by the PDCD1LG2 gene found in close proximity to the CD274 gene on chromosome 9p24.1. It was first discovered in 2001 independently by Latchman et al. (561) as well as Tseng et al. (562). PD-L2/PD-1 interaction, similarly to engagement of PD-1 by PD-L1, has been demonstrated to inhibit T-cell receptor mediated proliferation of and cytokine production by CD4+ T-cells. The effect was shown to be dependent on antigen dose. Previously activated CD4+ T-cells derived from D011.10 mice expressing a transgenic TCR specific for ovalbumin were re-stimulated. At low ovalbumin concentrations PD-L2/PD-1 interaction led to pronounced cell cycle arrest while at higher ovalbumin concentrations PD-L2/PD-1 interaction inhibited cytokine production but not T-cell proliferation. This may indicate a role in preferentially attenuating weaker immune responses (561, 563). In comparison to PD-L1, PD-L2 is expressed on a much more limited number of cell types. Expression has only been observed in activated CD4+ and CD8+ T-cell subsets, myeloid dendritic cells, macrophages, monocytes, endothelial cells and syncytiotrophoblasts of the placenta (564). One study has even suggested no PD-L2 expression at all among lymphohaematopoetic cells (555). Among mouse splenocytes expression of PD-L2 was not detect among resting B- and T-cell and could only marginally be induced with T-cell- but not B-cell-stimulation. On macrophages and dendritic cells expression could be induced by stimulation with IFN-γ, GM-CSF or IL-4 (558). Experiments with mice lacking PD-L1, PD-L2 or a combination of both have demonstrated that both PD-1 ligands have very similar functions in inhibiting IL2 and INF-γ production following T-cell activation. However, PD-L1 expression on parenchymal as opposed to haematopoetic cells appeared to be of greater importance in promoting

tolerance to self and preventing autoimmune disease such as autoimmune diabetes (565).

Paradoxically, both PD-L1 and PD-L2 have been demonstrated to be able to transmit co-stimulatory rather than co-inhibitory signals under certain conditions (562, 566-568). Several studies suggest that costimulatory capacity of PD-L1 and PD-L2 is mediated via a second yet undiscovered receptor. A structure-based mutational analysis of PD-L1 and PD-L2 revelead PD-1 binding residues that, when mutated, resulted in molecules without PD-1 binding capacity but retained potential for co-stimulation (569). In a separate study dendritic cells from PD-L2 -/- animals were shown to have diminished capacity to stimulate CD4+ T-cells. Immobilized PD-L2 was shown to be able to stimulate IL-2 and INF-γ production in T-cells, even when derived from PD-1 -/- animals (570). Butte et al. have demonstrated that PD-L1 is also able to interact with CD80 but not CD86 with an affinity greater than that of CD28 but less than that of CTLA-4 (571). However, the functional relevance of this interaction remains controversial. While some studies indicate that T-cell/APC PD-L1/CD80 interaction may transmit a negative signal limiting T-cell expansion and promoting T-cell anergy (572, 573) newer studies suggest that cis-interaction of PD-L1 and CD80 on the same cell surface may interfere with PD-1/PD-L1 mediated T-cell inhibition (574, 575). The complex nature of the functional properties of PD-L1 and PD-L2 becomes especially apparent in animal models of allergic asthma. A shift of helper cell polarity away from Th1 towards Th2 has been suggested to be involved in the pathogenesis of asthma (576). In PD-L2 -/- animals airway hyperreactivity and IL4 production by iNKT cells are increased compared to wildtype animals after experimental induction of asthma while PD-L1 -/- animals show decreased airway hyperreactivity and increased INF-γ production by iNKT cells. This may indicate that PD-L2 preferentially promotes Th1 responses and has protective properties in the pathogenesis of asthma (577). *Repulsive guidance molecule b* (RGMb) has recently been described to be a novel bindings partner of PD-L2 and mediator of Th1 promoting co-stimulation and amelioration of airway hyperreactivity in animal models of asthma (578).

Several studies have shed light on the molecular mechanism leading to PD-1 mediate T-cell inhibition. Ligand-bound PD-1 interacts with SHP-2 via its ITSM and ITIM domain leading to SHP-2 phosphorylation. Mutational studies have shown that SHP-2 binding to PD-1 is primarily mediated though the ITSM domain (579). While both SHP-1or SHP-2 could associated with PD-1 when artificially moved to T-cell receptor microclusters, live cell-imaging confirmed that only SHP-2 will interact with the immune checkpoint molecule under physiological conditions (580). PD-1 has been shown to suppress ZAP-70 and

PKCθ phosphorylation through a SHP-2 dependent mechanism (581). PD-1 has also been shown to facilitate inhibitory phosphorylation of LcK by *C-terminal Src kinase* (Csk) though SHP-2 (582). In addition, PD-1 has been shown to interfere with PI3K signaling. This is mediated through increased phosphatase activity of *Phosphatase and Tensin homolog* (PTEN) which antagonizes PI3K. PD-1 was shown to inhibit *casein kinase 2* (CK2) which under physiological conditions phosphorylates PTEN leading to decreased phosphatase activity (583). In addition, Patsoukis et al. have shown an inhibition of the RAS/MEK/ERK pathway by PD-1 (584). Both PI3K/AKT and RAS/MEK/ERK inhibition were shown to lead to cell cycle arrest. This was demonstrated to be due to transcriptional down regulation of *S-phase kinase-associated protein 2* (Skp2). The enzyme acts as the substrate recognition factor of the ubiquitin E3 ligase complex *Skp, Cullin, F-box containing complex* (SCF complex). PD-1 mediated down-regulation of Skp2 hinders ubiquitination and thus degradation of Cyclin-dependent kinase inhibitor 1B (p27^{kip1}) which prevents activation of cyclinE-CDK2 and cyclin D-CDK4 complexes and thus interferes with cell cycle progression. This was shown to lead to impaired phosphorylation of two important CDK2 substrates, *Retinoblastoma protein* (Rb) and transcription factor *Mothers against decapentaplegic homolog 3* (SMAD3). Supression of E2F target genes but increased transactivation of SMAD3 has been demonstrated. In consequence, increased expression of G1 phase cell cycle inhibitor p15^{INK4B} and decreased expression of CDK-acitvating phosphatase Cdc25A leading to further disruption of CDK2, CDK4 and CDK6 dependent cell cycle progression was observed (584). PD-1 mediated PI3K inhibition was also described to result in repression of anti-apototic BCL2 family member BCL-XL (585). Moreover, CD8+ T-cells derived from PD-L1 -/- mice were shown to have lower levels of pro-apoptotic protein Bim. Binding of activated CD8+ T-cells to plate-bound PD-L1 led to increased Bim expression and cell death. These findings may indicated that a PD1/PD-L1 mediated disruption of the balance of pro- and anti-apoptotic proteins could result in the depletion of CD8+ effector T-cells (586). PD-L1/PD-1 interaction has also been shown to increase TCR-downregulation by internalization via increased expression of E3 ubiquitin-protein ligase *Casitas B-lineage Lymphoma b* (Cbl-b) (587). In a planar bilayer the translocation of PD-1 to TCR microclusters upon PD-L1 ligation and subsequent SHP-2 mediated TCR signalling inhibition could be demonstrated (580).

PD-1 appears to mediate T-cell inhibition not only directly but also indirectly via Tregs. Fransciso et al. have demonstrated that PD-L1 is able to transform naïve CD4+ T-cells in vitro to CD4+FOXP3+ regulatory T-cells. In vivo, the conversion of CD4+T-cells to Tregs was inhibited and a swiftly progressing inflammation could be observed in PD-L1

-/- PD-L2 -/- Rag -/- aimals when transplanted with naïve CD4 T-cells. PD-L1 induced Treg development was shown to be mediated through down-regulation of phosphor-AKT, mTOR, ribosomal protein S6 and ERK2 as well as upregulation of PTEN (588).

1.2.3   Other Immune Checkpoint Pathways

Following the clinical success of CTLA-4 and PD-1/PD-L1 immune checkpoint inhibitors other co-inhibitors pathways have received increasing attention. LAG-3 was discovered by Triebel et al. in 1990 (589). The protein is a member of the immunoglobulin superfamily. It is encoded for by the LAG-3 gene on chromosome 12p13.31 and has structural homology to CD4. The extracellular region contains 4 Ig-like domains. The intracellular region contains the KIEELE motif, which has been shown to be essential for LAG-3 mediated T-cell inhibition (590). However, the precise mechanism of action is not understood to this point. Expression of LAG-3 has been observed on activated T-cells, NK-cells, activated B-cells and plamacytoid dendritic cells (589, 591, 592). LAG-3 primarily binds to MHC type II with greater affinity than CD4 (593). Other ligands have been reported to be *lymph node sinusoidal endothelial cell C-type lectin* (LSECtin) expressed on melanoma cells (594) as well as *fibrinogen-like protein 1* (FGL1), a liver secreted protein also found in hepato-cellular carcinoma and gastric cancer (595). LAG-3 negatively regulates activation, proliferation, effector functions and homeostasis of both CD4+ and CD8+ T-cells (590, 596-600). LAG-3 is also constitutively expressed on a subset of Tregs and has been implicated in their suppressive functions (601-603). LAG-3 has been linked to maturation processes of dendritic cells (604). Co-expression of LAG-3 and PD-1 has been noted on *tumour infiltrating lymphocytes* (TILs) from both patient samples and mouse models indicating a similar role of both (605, 606).

TIM-3, also known as *hepatitis A virus cellular receptor 2* (HAVCR2), was first discovered in 2002 by Monney et al. (607). The HAVCR2 gene is located on chromosome 5q33.3. The encoded protein is a type I transmembrane protein consisting of an Ig domain and glycosylated mucin domain in the extracellular region, a single transmembrane domain and an intracellular region containing five conserved tyrosine residues that have been shown to interact with multiple components of the TCR complex (608, 609). Expression of TIM-3 has been described on CD4+ Th1 (607) and Th17 cells (610), Tregs (611), NK cells (612), DCs (613), monocytes and macrophages (614). Expression on CD8+ T-cells has been described in the setting of T-cell exhaustion in the tumour microenvironment and with chronic viral infections (615-617). Similar to LAG-3, co-expression with PD-1 was described in CD8+ TILs (616, 618). Some of the functions of TIM-3 relate to phagocytic cells like macrophages and DCs. *Phosphatidyl serin* (PtdSer) is enriched on

the surface of apoptotic cells. Interaction of TIM-3 with PtdSer has been shown to promote phagocytosis of apoptotic cells and cross-presentation of antigens by CD8+ DCs (619). Chiba et al. have shown that TIM-3 in tumour infiltrating dendritic cells suppresses recognition of nucleic acids by TLRs through interaction with h*igh mobility group protein 1* (HMGB1), which attenuated recruitment of DNA into DC endosomes (620). The TIM-3 ligand for modulation of T-cell function has been shown to be *Galectin-9* (Gal-9) (621). The available data on T-cell function has been conflicting - both positive and negative effects have been reported. It has been suggested that upon binding of TIM-3 to Gal-9 members of the Src family of kinases such as LcK, Fyn and ITK are able to bind to a phosphorylate tyrosine residues in the cytoplasmic tail of TIM-3. This has been shown to result in recruitment of adaptor protein p85 and subsequent activation of PI3K (608, 609). On the other hand, a plethora of data suggest a negative regulation of T-cell function by TIM-3. Binding of TIM-3 to Gal-9 has been shown to increase the apoptotic potential of INF-γ secreting murine Th1 but not Th2 cells. TIM-3/Gal-9 interaction thus leads to suppression of Th1 immune responses (621). Moreover, TIM-3 has been shown to suppress secretion of IFN-γ, IL17, IL2 and IL6 by T-cells (610). In another study, TIM-3 has been demonstrated to suppress CD3/CD28 induced NFκB/NFAT activation, CD69 expression and IL2 secretion in both Jurkat cells and primary human CD8+ T-cells (622). TIM-3 was found within lipid rafts at the IS of primary human CD8+ T-cells and antibody blockade of TIM-3 led to a significant increase in synapse formation and stability between CD8+ T-cells and target cells. The same study showed that Tim-3 co-localizes with both CD45, which promotes TCR-signalling through dephosphorylation and activation of Lck, and CD148, a protein tyrosine phosphatase that negatively regulates T-cell receptor signalling though dephosphorylation of effector molecules such as PLCγ and LAT. The interaction with both phosphatases was increased by Gal-9 binding (623). In mouse models, blockade of TIM-3 with antibody or TIM-3-Ig fusion protein was shown to enhance EAE (607), autoimmune diabetes (624, 625) and transplant rejection (625, 626). In a mouse model of GvHD, Tim-3 blockade by TIM-3-Ig or transplantation of T-cells from a Tim-3 -/- donor increased T-cell proliferation and resulted in higher mortality from GvHD. Paradoxically, in the absence of Tregs, TIM-3 inhibition resulted in decreased GvHD (627). It has been suggested that Tim-3 mediated T-cell inhibition is dependent on co-expression of *carcinoembryonic antigen cell adhesion molecule 1* (CEACAM1). TIM-3 has been shown to bind to CEACAM1 through both cis- and trans interactions which has been shown to enable TIM-3 mediated T-cell inhibition and increase TIM-3 expression (628). BAT3 has been shown to bind to and repress function of TIM-3, protecting Th1 cells from apoptosis and promoting

proliferation and proinflammatory cytokine production (629). The precise mechanism of action of TIM-3 remains to be elucidated.

KLRG-1 is a homodimeric member of the killer cell lectin-like family, a group of transmembrane proteins preferentially expressed in NK-cells. It is a C-type lectin inhibitory receptor with an ITIM in its cytoplasmic tail (630). The KLRG-1 gene is found on chromosome 12p13.31. Expression has been reported on NK-cells, antigen experienced T-cells and a subset of γδ T-cells (631-633). In young adults, KLRG-1 is expressed in approximately 40% of CD8+ T-cells and 20% of CD4+ T-cells. The expression increases strongly with age. Greater than 90% of CD8+ T-cells have been reported to express KLRG-1 in individuals greater than 65 years of age – as such KRLG-1 is being considered a marker of T-cell senescence (634). Expression not only increases with age but also with increased levels of antigen experience. The highest levels of expression have been observed in memory and terminally differentiated effector T-cells (632). Like other immune checkpoint molecules, KLRG-1 has been implicated in T-cell exhaustion related to malignancy and chronic viral infection(635, 636). KLRG-1 has been demonstrated to be a receptor for E-, N- and R-cadherin (637-639). Cadherins are class of transmembrane glycoproteins. Their function is the mediation of Ca^{2+}dependent cell-cell adhesion. They consist of an extracellular domain subdivided into 5 repetitive subdomains, which mediate Ca2+ dependent cell adhesion, a transmembrane domain and a C-terminal cytoplasmic domain. While expression of N- and R- cadherin is limited to the nervous system, expression of E-cadherin is found on epithelial cells (640). In addition, E-cadherin expression has been observed on classical APCs such as monocytes, macrophages, dendritic cells and Langerhans cells (641). Mutational studies have shown the first and second extracellular domain of E-cadherin to be essential for interaction with KLRG-1 (642). KLRG-1 has been demonstrated to have an inhibitory role in NK cells. Antibody mediated cross-linking of KLRG-1 on mouse NK-cells resulted in a decreased cytolytic activity and INF-γ production (643). Similarly, antibody mediated blockade of KLRG-1 increased cytolytic activity in human NK-cells and ligation with E-cadherin inhibited degranulation and INF-γ production of polyclonal human KLRG-1+ NK-cells (639). It has been suggested that KLRG-1 inhibits NK cell function through activation of metabolic sensor *AMP-activated protein kinase* (AMPK) by prevention of its inhibitory dephosphorylation by *protein phosphatase 2C* (PP2C) (644). In activated murine T-cells, the cross-linking of KLRG-1 by plate bound antibodies significantly lowered Ca^{2+} flux and IL2 production (645, 646). In vitro, ectopic expression of E-cadherin by B16.BL6 melanoma cells was shown to inhibit the proliferation of KLRG-1 transgenic murine CD8+ T-cells (637). In a CD4+T-cell hybridoma line

transduced with KLRG-1 co-engagement of KLRG-1 and CD3/TCR was shown to inhibit NFAT signalling and Fas/FasL mediated lysis (642). Disruption of KLRG-1/cadherin-E interaction by anti-cadherin-E antibodies resulted in increased T-cell receptor mediated AKT phosphorylation and proliferation in human CD8+ T-cells (647). KLRG1+ T-cell were found to be enriched in the peripheral blood of cancer patients. Those T-cells were shown to have decreased proliferative activity. Moreover, KLRG1+ CD4+ T-cell showed reduced production of IL17 while KLRG1+ CD8 T-cells showed decreased production of IFN-γ, granzyme B and TNF-α (648). KLRG-1 mediates its downstream effects through association of its ITIM motif with phosphatases SHIP-1 and SHP-2 and downstream inhibiton of PI3K/AKT signalling (646, 647, 649). KLRG-1 exists in both a monomeric and dimeric form with a substantial fraction of molecules on the cell surface found as disulphide-bond- linked trimeric or tetrameric complexes. KLRG-1 monomers compared to tetrameric complexes show little binding potential for E-cadherin, suggesting that KLRG-1 binding occurs with relatively low affinity. Multimerisation appears to increase avidity and the associated potential for inhibition (642).

2B4, also known as CD244 or *Signalling Lymphocyte Activation Molecule Family 4* (SLAMF4), was first described as an activating receptor on NK cells (650). Later on, expression has also been described on monocytes, basophils, eosinophils, γδT-cells and a subpopulation of CD8+ T-cells (651-654). In mice, expression has been shown on NK-cells, γδT-cells, monocytes, mast cells and a subset of memory CD8+ T-cells (655-657). The 2B4 gene is found on chromosome1q23.3. The resulting gene product is a type I transmembrane protein. Like with other members of the SLAM family, the extracellular domain of 2B4 is made up of one *Ig variable* (IgV) and one *Ig constant* (IgC) domain while the intracellular domain contains 4 ITSMs (658). In both humans and mice 2B4 binds to another member of the SLAM family - CD48, also known as *Signalling Lymphocyte Activation Molecule Family 2* (SLAMF2) and *B-lymphocyte activation marker 1* (BLAST-1) (659, 660). CD48 is ubiquitously expressed on haematopoetic cells (661-663). The CD48 gene is found on chromosome 1q23.3, in close proximity to 2B4. The CD48 protein, like other members of the SLAM family, contains an IgV and IgC domain. However, it does not have a transmembrane domain but is anchored in the plasma membrane through a *glycophosphatidylinositol anchor* (GPI anchor). As with other GPI-anchored proteins, a membrane bound and a soluble form exist (658). The interaction of 2B4 and CD48 can induce both activating and inhibitory signals. 2B4 mediated activation of NK cells has been suggested by various studies (664-666). Another study by Mooney et al. has shown 2B4 mediated NK-cell inhibition (667). Moreover, experiments in 2B4 -/- mice indicate that the cytotoxic and secretory function

of NK cells are increased when NK cells lack 2B4 or their target cells lack CD48 (668, 669). Similarly, some studies suggest an activating role of 2B4 on T-cells (657, 666, 670) while others provide evidence for an inhibitory role (671, 672). The dual function of 2B4 in mice is further complicated by the presence of two splice variants – the full length protein that contains all 4 ITSMs and a truncated version that contains only 1 ITSM (673). While overexpression of the full-length form was shown to inhibit NK-cell function, overexpression of the truncated splice variant was shown to promote target cell lysis (674). 2B4 mediated signal transduction remains incompletely understood. NK cell activation through 2B4 leads to phosphorylation of the cytoplasmatic ITIMs and recruitment of Fyn and *signalling lymphocytic activation molecule-associated protein* (SAP) (675, 676). Patients suffering from X-linked lymphoproliferative disease, a severe inherited immune deficiency characterized by inability to mount a sufficient immune response to EBV infection, carry a mutation of SAP rendering the protein dysfunctional. In these patients, cross-linking of 2B4 instead of inducing NK-cell activation inhibits NK-cell mediated cytotoxicity (677). This indicates that SAP is essential in determining activating or inhibitory function of 2B4. The third ITSM of the 2B4 cytoplasmatic tail is also able to recruit SHP-1, SHP-2, SHIP-1 and Csk. Binding of these inhibitory phosphatases or SAP have been shown to be mutually exclusive (676). The related adaptor proteins *EWS-Fli1-activated transcript-2* (EAT-2) and *EAT-2-related transducer* (ERT) appear to serve comparable functions to SAP (678). Recruitment of 2B4 to lipid rafts has been shown to be essential for downstream signaling (679). In lipid rafts 2B4 becomes associated with LAT and this appears to be essential for its activating function (680). Similar to other immune checkpoint receptors, 2B4 has been implicated in chronic viral infection and malignancy associated T-cell exhaustion (681, 682).

TIGIT is a member of the PVR/nectin family, a subset of the Ig superfamily. It was first discovered in 2009 in a genomic search for genes specifically expressed in T-cells that had protein structures indicative of a potential inhibitory role (683). The TIGIT gene is found on chromosome 3q13.31. The protein has an extracellular IgV domain, a transmembrane domain and a cytoplasmatic tail containing an ITIM and an *Ig tail-tyrosine* (ITT)-like motif (684). CD96, also known as *T cell activation, increased late expression* (TACTILE), is a similar protein that also belongs to the PVR/nectin family and was first described in 1992 (685). The associated gene is found on chromosome 3q13.13 in close proximity to TIGIT. Compared to TIGIT, the CD96 extracellular domain is more complex with three Ig-like domains linked by conserved cysteines and a membrane-proximal stalk domain rich in serine, threonine and proline. Exon 4 is alternatively spliced, generating two isoforms that differ in the second Ig domain. The more abundant variant

1 contains an *Ig intermediate* (IgI) domain, the less abundant variant 2 contains an IgV domain (686). The cytoplasmic domain of CD96 contains an ITIM motif and, similar to CD28, a YXXM motif with the ability to interact with SH2 domains (685). TIGIT, CD96 and CD226, also known as DNAM-1, form a system similar to CD28/CTLA-4. CD226 has been shown to mediate co-stimulation via interaction with its ligands CD155 (PVR, *Nectin-like protein* 5(necl5)) and CD112 (*Poliovirus receptor-related 2* (PVRL2), nectin-2) (687, 688). Similar to CTLA-4, TIGIT has been shown to bind both CD155 and CD112. Binding of CD155 occurs with much higher affinity than that of CD266 while affinity for CD112 is comparably low. Human CD96 binds selectively to CD155 with an intermediary affinity between that of TIGIT and CD226 (683). Murine CD96 has also been reported to interact with CD111 (nectin-1) (689). TIGIT is expressed on conventional T-cells upon activation (684), on memory T-cells, regulatory T-cells, follicular helper T-cells and NKT cells and NK cells (683, 684, 690-692). Expression of CD96 is found on conventional T-cells, γδ T-cells, NK-cells and NKT-cells (685). CD155 and CD112 are expressed on DCs, T-cells and tumour cells (693-695). TIGIT has been shown to function as an inhibitor of NK-cells. The cytotoxic activity of the human YTS NK-cell line transfected with TIGIT was inhibited by CD155 (691). TIGIT/ CD155 interaction inhibited cell killing by both human and mouse primary NK-cells (691, 696). In human NK-cells, TIGIT expression was inversely correlated with INF-γ production, degranulation and cytotoxic potential (697). MDSC mediated suppression of NK-cell function was shown to be dependent on CD155/TIGIT interaction (697). The data on influence of CD96 on NK-cell function is somewhat conflicting with positive effects reported in human NK-cells (698) and negative effects in mouse NK-cells (695). Among T-cells, TIGIT has been shown to mediate inhibitory functions, especially in the setting of malignancy. TIGIT expression has been shown to be enriched in CD8+ TILs derived from various solid malignancies (694, 699). Among CD8+ TILs, TIGIT+ cells were found to be especially poor producers of TNF-α and IL2. Moreover, they were found to have decreased cytotoxic capacity compared to TIGIT- cells. CD8+ TILs from TIGIT -/- mice were shown to have increased proliferative and cytotoxic capacity (700). Knockdown of TIGIT in CD8+ T-cells derived from the peripheral blood of *acute myeloid leukemia* (AML) patients resulted in a reversal of the functional deficits associated with the development of AML (701). TIGIT expression was found to be upregulated on Tregs in the tumour microenvironment. Expression of immomodulatory effector molecules such as IL10, perforin and TGF-β was increased in TIGIT+ Tregs. Deletion of TIGIT in Tregs alone was found to be sufficient to delay tumour growth and promote IFN-γ, TNF-α and IL2 production by CD8+ TILs in this study (700). Several mechanisms of action have been proposed for TIGIT. As it binds CD115 with higher affinity than CD226, it could potentially outcompete CD226 for its

binding partner, therby disrupting co-stimulation (683). Experiments using *fluorescence resonance energy transfer* (FRET) have suggest that TIGIT is able to interfere with cis-homodimerization of CD226. However, it remains unclear how this affects CD226 signaling (699). Engagement of TIGIT on T-cells by CD155 on dendritic cells resulted in phorsphorylation of CD155 and downstream MAPKs ERK and p38. This resulted in increased production of IL10 and decreased production of pro-inflammatory cytokines such as IL12, which could affect T-cells indirectly via a cell-extrinsic mechanism (683). In NK-cells TIGIT/CD155 interaction was shown to lead to recruitment of GRB2 and β-Arrestin-2 via its TTT motif, leading to activation of SHIP-1 and SHP-2 and subsequent inhibition of PI3K and NFκB signalling (702, 703). Cell-intrinsic signalling of TIGIT in T-cells remains poorly understood.

Another receptor/ligand system with dual stimulatory/inhibitory role is the *herpes virus entry mediator* (HVEM) network. HVEM, also known as *TNFR superfamily 14* (TNFRSF14), was first identified as a molecule that is used by herpes viruses to facilitate viral entry into the cell (704). In humans the HVEM gene is located on chromosome 1p36.32. Expression has been reported on T-cells, B-cells, NK-cells, dendritic cells and other myeloid cell subsets (705-708). HVEM is a type I transmembrane protein containing 4 pseudo-repeats of cysteine-rich domains in its extracellular domain. The cytoplasmatic tail contains a TRAF binding site. Engagement of HVEM by two different ligands, *lymphotoxin-like, exhibits inducible expression, and competes with herpes simplex virus glycoprotein D for HVEM* (LIGHT) and *lymphotoxin α* (LTα), has been shown to mediate a co-stimulatory signal (709-711). Two other ligands, *B- and T-lymphocyte attenuator* (BTLA) and CD160 have been shown to mediate a co-inhibitory signal. The BTLA gene is found on chromosome 3q13.2. The resulting protein is a type I transmembrane protein. Binding of BTLA to HVEM occurs through interaction with an extended β-strand in the membrane-distal region of a cysteine rich domain forming an intramolecular anti-parallel β-sheet with the extracellular domain of BTLA (712). The cytoplasmatic tail contains two ITIMs and a GRB2 recognition site (713). BTLA is expressed in naïve T-cells, both naïve and activated B-cells, DCs, macrophages, NK-cells and NKT-cells (714-716). Several lines of evidence show an inhibitory role of BTLA/HVEM interaction. BTLA deficient mice have been demonstrated to have enhanced T-cell proliferation in response to mitogenic stimulation or activation with anti-CD3 antibodies (714, 715). These animals also show increased propensity to develop autoimmune diseases like EAE (714). Stimulatory antibodies to BTLA inhibit T-cell proliferation and production of IL2, IL4, IL10 and IFN-γ(717, 718). It has been suggested that co-inhibition by BTLA is mediated through recruitment of SHP-1 and SHP-2 to the

cytoplasmatic tail (719). The CD160 gene is located on chromosome 1q21.1. The protein contains a single IgV domain and is bound to the plasma membrane through a GPI anchor (720). Like BTLA, CD160 binds HVEM through interaction with its cysteine rich domain (721). The CD160 expression pattern is highly restricted to NK-cells, T-cells and NKT-cells (720, 722, 723). Cross-linking of CD160 with stimulatory antibodies has shown a strong inhibition of CD3/CD28 induced T-cell activation(724). A soluble form has also been shown to inhibit NK-cell cytotoxicity (725). How CD160 mediates T- and NK-cell inhibition remains unclear. It has only been shown that cross-linking of CD160 interferes with ζ-chain phosphorylation (724). As LTα and LIGHT bind to different HVEM cysteine rich domains compared to CD160 and BTLA, competitive inhibition seems unlikely as a mechanism of action (724, 726). CD160 has been implicated in T-cell exhaustion due to chronic viral infection or malignancy (727, 728).

1.2.4   Cancer Immunosurveillance, Cancer Immunoediting and Adaptive Immune Resistance

The concept, that the immune system has the capacity to identify and eliminate primary developing malignancy and thus protect the body from malignant diseases was first suggest by Ehrlich in 1909 (729). This notion could not be experimentally tested at the time, though. More than 50 years later, on the background of an emerging understanding of transplant and cancer immunity, the concept was formally introduced as the "cancer immunosurveillance hypothesis" by Sir Frank Macfarlane Burnet and Lewis Thomas (730, 731). They had speculated that healthy lymphocytes would eliminating constantly forming newly transformed malignant cells. When this hypothesis was put to the test in a series of experiments in nude mice, the most immundeficient mouse model available at the time, by Strutman in the 1970s no evidence of such a process could be obtained (732-734). However, in hindsight the nude mice have been recognized as an inexact model of immunodeficiency. These animals do produce functional T-cells, albeit in very low numbers, (735) and also normal numbers of fully functional NK-cells (736). The profound influence of the innate immune system on the adaptive immune system had not been understood at the time (459). Moreover, the CBA/H strain of mice used by Stutman et al. expressed a highly active isoform of the enzyme aryl hydroxylase, which is required for activation of 3-methylcholanthrene, thus making chemical carcinogensis overly effective and potentially masking protective effects of the immune system (737). Still, at the time the experiments of Strutman et al. were deemed so convincing that the cancer immunosurveillance hypothesis was largely abandonded until the early 1990s, when interest in the concept was reignited by mouse experiments demonstrating that

endogenous INF-γ can protect the host against transplanted, chemically induced and spontaneous tumours (738-741). Similarly, mice lacking perforin were shown to have a higher susceptibility to chemically induced and spontaneous tumour development (740-744). Definitive evidence of a lymphocyte dependent mechanism of cancer immunosurveillance was finally provided by experiments with mice deficient for *recombinase activating gene* (RAG)-2. The gene is essential for the process of V(D)J recombination underlying the formation of the highly diverse repertoire of immunoglobulins and T-cell receptors. RAG-2 -/- mice thus lack T-, B- and NKT-cells. This transgenic mouse was found to be the ideal model to study the effects of the immune system on development and elimination of cancer since the expression of RAG-2 is only found in cells of the immune system and its absence does not result in impaired DNA repair in non-lymphoid tissues unlike with other models of immunodeficiency (745). Application of 3-methylcholanthrene resulted in a higher frequency and more rapid development of sarcoma in RAG-2 -/- animals compared to wild-type mice (746). Moreover, a similar effect was observed in RAG-1 -/- animals (747). The connection of IFN-γ dependent and lymphocyte dependent tumour suppressor mechanisms was illustrated by experiments with mice lacking IFN-γ responsiveness (*Interferon gamma receptor 1* (IFNGR1) -/- or STAT1 -/-), lymphocytes (RAG-2 -/-) or both (RAG-2 -/- X STAT1 -/-). Each of these strains were approximately 3 times more likely to develop chemically induced tumours compared to syngenic wild-type mice. Since no significant differences were detected between these strains the IFN-γ and lymphocyte dependent mechanisms of tumour suppression were concluded to be overlapping (746). Other effector and recognition pathways that have been shown to be critical in cancer immunosurveillance are type I Interferons (748, 749), *TNF-related apoptosis-inducing ligand* (TRAIL) (750-752), IL12 (753), TNF-α (754), Fas/FasL (755) and DNAM-1 (756). Interestingly, the treatment of wild-type mice with antibodies blocking receptor NKG2D, an activating receptor on CD8+ T-cells but also γδ T-cells and NK-cells, was also reported to increase chemically induced sarcoma development (757). Moreover, mice deficient of NKG2D are more susceptible to Eγ-*myelocytomatosis viral oncogene homolog* (myc) driven B-cell lymphomas. In the same study, *transgenic adenocarcinoma of the mouse prostate* (TRAMP) mice developed more aggressive tumours in NKG2D deficient animals compared to wild type animals (757). In terms of cellular components, several studies have found that mice lacking either αβ- or γδ-T-cells have increased susceptibility to tumour induction, indicating that both lymohocyte populations are critical for cancer immunosurveillance (758, 759). In addition, innate-like lymphocyte subsets have been shown to be critical in elimination of transformed cells. Mice lacking NKT-cells were shown to be more susceptible to chemically induced sarcoma development (760,

761). Similarly, mice depleted of NK-cells display an increased tumour incidence of chemically induced sarcoma (747). In a mouse model of liver carcinoma, NK cell were demonstrated to be able to kill senescent tumour cells via a NKG2D mediate mechanism in a manner dependent on TP53 (762).

Several lines of evidence suggest that a mechanism of cancer immunosurveillance similar to that observed in mouse models does exist in human beings as well. Analysis of patients with either congential or acquired immunodeficiency has shown a highly increased rate of virally induced malignancies such as Kaposi's sarcoma, NHL or urogenital cancer like cervical cancer (763-765). The study of the incidence of tumours of non-viral origin in these patients has proven to be more challenging. Still, a role of the immune system in control of these malignancies is illustrated by several observations. First of all, an increased rate of a broad range of tumours of non-viral origin has been observed in patients on immunosuppressive therapy due to organ transplantation (766-769). In addition, substantial evidence supports the notion that cancer patients can develop responses of the adaptive immune system against tumour antigens. Starting in the 1970s the approach of autologous typing allowed for the discovery of patients who bear antibodies or T-cells that recognize autologous tumour antigens (770, 771). The identification of molecular targets recognized by CD8+ T-cells has been achieved by application of the gene cloning and expression systems developed by Thierry Boon's lab (772). Michael Pfreundschuh's lab has developed the *serological expression cloning technique* (SEREX), a similar approach to identify antibody-recognized tumour antigens (773). A large number of human tumour antigens with the potential to elicit adaptive immune response has since been identified (774-777). The presence of cancer specific adaptive immune responses is also suggested by the phenomenon of *paraneoplastic neurologic degenerations* (PNDs), a class of rare autoimmune diseases arising in cancer patients caused by autoantibodies or cytotoxic T-cells cross-reacting with antigens expressed in both nervous tissue and cancer (778, 779). The sporadically occurring spontaneous regression of melanoma lesions in the setting of a clonal expansion of T-cells is one of the most prominent pieces of evidence for cancer immunosurveillance in human beings (780, 781). Another line of evidence comes from studies showing that the presence of TILs in the tumour microenvironment predicts an improved clinical outcome. The first studies suggesting this correlation have been conducted in malignant melanoma patients and dates to the 1990s (782, 783). Similar correlations have since been shown in other entities including ovarian cancer (784), colorectal cancer (785) and esophageal cancer (786). Similar positive correlations have also been demonstrated between NK-cell infiltration and patient survival in various types of malignancy (787-789).

Despite strong evidence for the presence of cancer immunosurveillance malignancy does still occur, even in the setting of the immunocompetent host. Evidence points to an immune mediated mechanism that allows the outgrowth of tumours that are less immunogenic or have developed mechanism to evade immune rejection by the host. This idea is epitomized by studies showing that a large number of sarcomas derived from RAG-2 -/- mice are rejected when transplanted into wild type animals. On the other hand, sarcomas derived from wild type mice grow readily when transplanted into either wild type or RAG-2 -/- animals (746). Genomic analysis of sarcoma cell lines derived from 3-methylcholanthrene treated RAG2 -/- animals showed a point mutation in Spectin-$\beta2$ as a highly immunogenic neo-epitope. Enforced expression of this epitope in sarcoma cell lines was shown to be sufficient for rejection in wild type animals, suggesting that T-cell dependent immunoselection results in an outgrowth of less immunogenic sarcoma cells in these animals (790). Similar results were obtained in a separate study that used both immunocompetent and immunodeficient mice expressing an oncogenic form of K-RAS to induce sarcomagenesis. Intramuscular injection of lentiviral vectors transferring strong class I model epitopes (SIINFEKL and SIYRYYGL) led to development of sarcomas expressing these epitopes in immunodeficient mice. However, in immunocompetent animals the occurrence of sarcomas was delayed and when they did occur, they lacked the model antigens. This suggests a mechanism of T-cell dependent immunoselection (791). These and other studies demonstrated that the classical concept of cancer immunosurveillance is insufficient to describe the complex interaction between a nascent malignancy and the host immune system. Robert Schreiber and colleagues have thus suggest a new model of cancer immunology known as "cancer immunoediting" (792). The process has been suggested to be comprised of three phases known as the "three Es of cancer immunoediting": Elimination, Equilibrium and Escape.

The elimination phase is represented by the classical model of cancer immunosurveillance. The anti-tumour immune response is launched when the innate immune system becomes alarmed by local stromal remodeling, neo-angiogenesis and tissue invasive growth (793) resulting in formation of alarmins signalling a source of local "danger"(460). NK-cells, NKT-cells, γδ T-cells, macrophages and dendritic cells are recruited to the tumour mass. Contact of macrophages with extracellular matrix components results in their activation. They can then cross-activate NK-cells through secretion of cytokines such as IL12 and CD40/CD40L interaction (794-796). Similarly, DCs can cross-activate innate lymphocytes through IL12 and CD40/CD40L (797, 798). INF-γ release and CD40/CD40L interaction by innate lymphoctes in turn promotes differentiation and activation of DCs and macrophages forming a positive feedback loop

(799, 800). Engagement of NK-cell receptors with their respective ligands on tumour cells further promotes INF-γ secretion (801). The cytokine mediates killing of tumour cells through direct anti-proliferative, pro-apoptotic and angiostatic effects (802-804) as well as indirectly through reactive oxygen and nitrogen species secreted by activated macrophages (805) and via NK cells through TRAIL- (806) and perforin-dependent mechanisms (807). Tumour antigens released in this process are taken up, processed and presented by dendritic cells. Immature dendritic cells become activated by the cytokine cocktail released by the innate immune response or via direct interaction with NK or NKT cells (808). Activated mature antigen bearing DCs move to the draining lymph nodes where they induce naïve tumour specific CD4+ Th1 cells which subsequently promote the development of tumour specific CD8+ cytotoxic T-cells though cross-presentation of antigens on DC MHC type I molecules (809-811). Th1 cells secret, among other cytokines, IL2 which helps to maintain CD8 T-cell function and IFN-γ to perpetuate the immune reaction (812). CD8+ T-cells kill tumour cells by release of cytotoxins like perforin, granzyme and granulysin but also secret cytokines such as IFN-γ and TNF-α (813).

The elimination phase is followed by the equilibrium phase, which is probably the longest phase and can last many years in human beings. A small but heterogenous and genetically unstable fraction of tumour cells may survive elimination by the immune system and remain in the tumour bed. These cells, however, are kept in constant check by the ongoing immune response. It has been suggested that the associated genetic instability may be the driving force that eventually allows the tumour to evade the host immune rejection (814). The molecular mechanisms driving the immune-mediated tumour dormancy are only partially understood as they are difficult in model in mice. Early experiments using transfer of *murine B cell lymphoma* (BCL1) into animals immunized against BCL1 to create dormancy have shown a role of IFNγ and CD8+ T-cells to maintain dormancy (815). It has been suggested that a balance between elimination promoting IL12 and persistence promoting IL23 is key in maintain tumours in equilibrium (816). Another study of mouse sarcoma found that tumours in equilibrium versus those who esacape are characterized by high relative numbers of CD8+ T-cells, NK-cells, γδ T-cells and low relative numbers of NKT-cells, Tregs and MDSCs (817). In a mouse model of experimentally induced pancreatic cancer, antigen specific T-cells were shown to arrest tumour growth via concomitant action of cytokines IFN-γ and TNF. In the absence of TNF receptor or IFN-γ the very same T-cells led to increased angiogenesis and carcinogenesis (818). In a mouse model *Simian virus 40 large T antigen* (Tag) expressed under the control of the rat insulin promoter was used to induce

neoplasma trough the resulting suppression TP53- and Rb-mediated cell cycle control. In this model, the combination of IFN-γ and TNF was shown to drive tumours into growth arrest through activation of p16INK4a, a cyclin-dependent kinase Inhibitor, and downstream hypophosphorylation of Rb (819). In human beings the presence of the equilibrium phase may be evidenced by cases of transmission of malignancies from organ donor to recipients. Here, organs that a macroscopically normal and free of malignancy at the time of harvest lead to donor derived malignancy in the recipient years later (820).

In the escape phase, tumour cells that have acquired the ability to circumvent host immune defence emerge as a progressively growing and clinically detectable tumour. Many different mechanisms of cancer immune evasion have been described. These include modes of reduced immune recognition such as loss of powerful tumour antigens, loss of MHC type I or costimulatory molecules, increased tumour cell survival such as overexpression of STAT3 or BCL-2 and formation of an immunosuppressives niches in the microenvironment through cytokines such as IL10, TGF-β, *vascular endothelial growth factor* (VEGF) or expression of immunosuppressive molecules such as IDO and immune checkpoints such as PD-1/PD-L1 (821). Overexpression of the immune checkpoint molecule PD-L1 is now recognized as one of the major mechanisms of cancer immune evasion. Expression of PD-L1 has been observed on tumour cells from various solid malignancies (822-825). Aberrant PD-L1 expression is also used as a means of immune escape by hematologic malignancies. Our group has previously shown upregulation in primary tumour cells of CLL, *follicular lymphoma* (FL) and DLBCL patients (216). Aberrant expression has also been described in MCL (826), *primary mediastinal B-cell lymphoma* (PMBL) (827), HL (828) and Multiple Myeloma (MM) (829) as well as on CD34+ blasts from patients with *Myelodysplastic Syndrome* (MDS) (830), *Chronic myelomonocytic leukemia* (CMML) and AML (831). PD-L1 is not only found on tumour cells themselves but also on myeloid cells in the tumour microenvironment of various malignancies including CLL (832-835). The first piece of evidence supporting a functional role of PD-L1 in toumour microenvironment comes from a study that showed that cancer associated PD-L1 increases the apotosis of antigen-specific T-cells in vitro (823). Moreover, in vivo experiments have demonstrated that PD-L1 deficient mice have increased rates of proliferation of CD8+ T-cells and more protracted patterns of T-cell expansion when immunized. In these animals a CD8+ T-cells clone with the ability to reject metastatic tumour foci could be demonstrated (586). Similar results were obtained with regards to hematologic malignancies. In a PMBL cell line overexpression of wildtype PD-L1 as well as a fusion protein of *MHC class II transactivator class II, major*

histocompatibility complex, transactivator (CIITA) and PD-L1 were able to suppress Jurkat T-cell activation (827). In MCL cell lines both antibody blockade of PD-L1 and knockdown of PD-L1 by *short hairpin RNA* (sh-RNA) was shown to increase the proliferation of cocultured allogeneic T-cells (826). As described above, our own group has reported a functional relevance of PD-L1 in CLL associated T-cell dysfunction (216). Moreover, in a mouse model of CLL we were able to show that PD-L1 blockade results in prevention of T-cell dysfunction and leukemia growth (836).

Studies on tumour cell lines have greatly helped to advance our understanding of the molecular mechanisms involved in controlling PD-L1 mediated immune evasion. In some malignancies, overexpression of PD-L1 has been shown to be driven by constitutive oncogenic signalling pathways in the tumour cell itself – a mechanism described by the term "innate immune resistance". For example, in human glioma PD-L1 expression is increased by loss of the tumour suppressor PTEN which increases translation of the PD-L1 gene (837). Both PMBL and HL frequently have cytogenetic aberrations of chrosome 9p, which contains the genes for PD-L1 and PD-L2 as well as JAK2 which promotes PD-L1 expression. Indeed, one study has shown increased expression of PD-L1 and PD-L2 to be a very common in PMBL cases with 9p aberrations (838). In cell lines derived from nodular sclerosing HL PD-L1 and PD-L2 were demonstrated to be increased as a result of an amplification of 9p24.1 (839). In EBV positive HL *matrix protein 1* (MP1) and *latent membrane protein 2A* (LMP2A) were shown to increase transcription of PD-L1 indicating a latent virus infection mediated upregulation of the immune checkpoint (828). In T-cell lymphoma, a regulation by the oncogenic chimeric *nucleophosmin* (NPM)/ *anaplastic lymphoma kinase* (ALK) has been described. NPM/ALK+ T-cell lymphoma was shown to increase expression of PD-L1 in a STAT3 dependent manner (840). Disruptions of the 3' untranslated region leading to overexpression of a truncated form of PD-L1 have been reported in DLBCL and T-cell lymphomas (841). An alternative mechanism of increased PD-L1 expression is "adaptive immune resistance". Here the upregulation reflects an adaption of the immune system to endogenous tumour specific immune responses, primarily via secretion of IFN-γ by T-cells themselves – i.e. the tumour abuses mechanisms in place to prevent immune-mediated tissue damage from continous unabated local T-cell activation to protect itself form immunosurveillance. Such an IFN-γ dependent upregulation of PD-L1 expression was first described by Taube et al. in the setting of malignant melanoma (842). Similar IFN-γ driven upregulation of PD-L1 expression has also been described in hematologic malignancies such as MCL (826), multiple myeloma (829), AML(843) and MDS blasts (830). PD-L1 upregulation has also

been observed in response to IL10 in MCL (826) and TLR ligands in MM and AML (829, 843).

1.2.5   Immune checkpoint blockade in hematologic malignancies and CLL

The concept of immune checkpoint blockade was conceived following the discovery and increasing understanding of the role of immune checkpoint molecules in immunoregulation and maintenance of the immune homeostasis. We now have recognized the role of immune checkpoint molecules in cancer immune evasion and their potential as therapeutic targets. The first monoclonal antibody blocking an immune checkpoint molecule to be developed was Ipilimumab, which targets CTLA-4 (844). The substance was shown to lead to greatly improved survival in patients with metastatic melanoma and was approved by the *food and drug adminstration* (FDA) in 2011 as the first ever immune checkpoint inhibitor (845). Development of novel immune checkpoint inhibitors has focused on the PD-1/PD-L1 pathway yielding the PD-1 blockers Nivolumab and Pembrolizumab and the PD-L1 blockers Durvalumab and Atezolizumab. Immune checkpoint blockade is now used as a treatment strategy in a plethora of solid malignancies (846-852).

 A first attempt to implement immune checkpoint blockade in the treatment of hematologic malignancies was made in 2009 in a phase I study of Ipilimumab in 18 patients with relapsed /refractory B-cell NHL including cases of FL, DLBCL and MCL. The ORR was disappointing at only 11% (853). Inspired by the concept of Ipilimumab/Nivolumab combination treatment in malignant melanoma the combination was investigated in a phase I/Ib trial in patients with various lymphatic and myeloid hematologic malignancies who had relapsed following allogeneic stem cell transplantation. In patients receiving a dose of 10 mg/kg an ORR of 32% with a CR rate of 23% and a PR rate of 9% were achieved. With a median follow-up of 15 months the 1-year OS rate was 49% (854). Preliminary data on a phase I study of Ipilimumab/Nivolumab in relapsed refractory lymphoma was reported in 2016. ORRs of 74%, 20% and 9% were observed among HL, B-cell lymphomas and T-cell lymphoma patients, respectively. The study also involved 7 patients with relapsed/refractory MM. While a single patient achieved stable disease, four others died from disease progression (855). In a phase I study Ipilimumab was evaluated in 29 MDS patients who were refractory to hypomethylating agents. 1 patient achieved CR, prolonged stable disease was seen in 7 patients (24%) (856). In 2015 a phase Ib study demonstrated an acceptable safety profile and significant clinical activitiy of Nivolumab in relapsed/refractory HL (857). These results were confirmed in a subsequent phase II

study (CheckMate 205) showing an ORR of 69% with a median follow-up of 18 months. Overall, the median duration of response was 16.6 months and the median PFS was 14.7 months (858, 859). In 2016 Nivolumab was approved by the FDA for treatment of HL. The substance has also been tested in various relapsed/refractory B- and T-cell lymphomas in a phase Ib study. With a median follow-up of 66.6 weeks an ORR of 40%, 36%, 15% and 40% was reported for FL, DLBCL, mycosis fungoides and *peripheral T-cell lymphoma* (PTCL), respectively. The study also included 27 patients with MM. Stable disease was achieved in 63% of these patients lasting a median of 11.4 weeks (860). A pilot study of nivolumab single agent in 5 patients with relapsed/refractory *primary CNS lymphoma* (PCNSL) and *primary testicular lymphoma* (PTL) found objective response in all patients with four CRs and 1 PR (861). A single centre phase Ib/II study of Nivolumab/azacytidine in patients with relapsed AML showed superior survival compared to a historical cohort of relpased AML patients treated with azacytidine based salvage therapy (862). Preliminary results were reported on a phase II study in MDS patients involving various combinations of Nivolumab, Ipilimumab and azacytidine. In treatment naïve patients an ORR 0f 69% was achieved with Nivolumab/azacytidine. In MDS patients refractory to hypomethylating agents Ipilumumab showed some activity with an ORR of 22% while Nivolumab single agent showed no response (863). Similar to Nivolumab, Pembrolizumab has shown safety and activity in HL in a phase I trial (KEYNOTE-013) (864). Its activity was confirmed in a phase II study (KEYNOTE-087): The ORR was 69% with a CR rate of 22% in all cohorts (865). The FDA approved the substance for treatment of HL in 2017. The KEYNOTE-013 trial also enrolled 19 patients with relapsed/refractory PMBL in an independent cohort. The median follow-up of these patients was 11.3 months. An ORR of 50% was achieved (866). In MDS patients refractory to hypomethylating agents participating in the KEYNOTE-013 trial an ORR of 4% was reported (867). In a phase I trial of Pembrolizumab in combination with Lenalidomide and low-dose dexamethasone in patients with relapsed/refractory MM 20/40 patients (50%) achieved an objective response (868). Similarly, in a phase II trial of Pembrolizumab, Pomalidomide and dexamethasone in 48 patients with relapsed/refractory MM an ORR of 56% was achieved (869). A similar phase III study with less participants found comparable results (870). The combination of Ateolizumab and Obinutuzumab was evaluated in a phase Ib trial in patients with relapsed/refractory DLBCL and FL. Preliminary results reported the combination to be very well tolerable and yielded promising signs of clinical efficacy (871).

Despite clear evidence of efficacy in other hematologic malignancies and promising pre-clinical studies (836) attempts to utilize immune checkpoint blockade in CLL have been

disappointing. In 2017 results of a phase II trial on Pembrolizumab in relapsed CLL and RT have been reported. While objective responses were described in 4/9 RT patients (44%) none of the 16 CLL patients were reported to respond to the treatment (108). Single agent Durvalumab is currently being assessed in NHL and CLL patients (NCT02733042). Interestingly, pre-clinical data has shown impressive results with combinations of Ibrutinib inhibitors and PD-1/PD-L1 immune checkpoint blockade in the A20 mouse model of lymphoma, which is normally insensitive to Ibrutinib (872). Indeed, a phase I/IIa study of Nivolumab/Ibrutinib in patients with relapse NHL and CLL/SLL recently showed an ORR of 61% of high risk CLL/SLL patients and 65% in RT patients enrolled (873). Several clinical trials evaluating various combinations of BTK inhibitors and PD-1/PD-L1 immune checkpoint blockade are currently ongoing (NCT03204188, NCT03153202, NCT03514017, NCT02362035, NCT02846623).

Immune checkpoint blockade, like any other mode of treatment, is associated with sometimes serious adverse effects. *Immune-related adverse events* (irAEs) are a spectrum of immune-mediated phenomena involving endocrine, gastrointestinal, hepatic and dermatologic events. Patients with irAEs of grade 3 or higher are usually treated with systemic glucocorticoids (intravenous methylprednisolone 1-2 mg/kg/day or equivalent). Treatment with Infliximab 5mg/kg or mycofenolate mofetil in case of immune mediated hepatitis should be considered if symptoms persist beyond 3 days. Infliximab treatment should be repeated after 2 weeks should symptoms persist further (874). IrAEs related to anti-CTLA-4 therapy are generally more common than those related to PD-1/PD-L1 blockade. In a study involving 298 melanoma patients treated with Ipilimumab irAEs of any grade occurred in 85% of patients. IrAEs grade 3 or higher were seen in 38% of patients (875). In contrast, in an analysis involving 576 melanoma patients treated with Nivolumab, 71% of patients were reported to expierence irAEs of any grade with irAEs of grade 3 or higher in a mere 10% (876).

1.2.6 Immune modulation using novel agents

It has been suggested that modulation of T-cell and myeloid cell function by Ibrutinib contributes to increased malignant cell death after Ibrutinib treatment. Indeed, Dubovsky et al. were able to demonstrate that Ibrutinib has the potential to shift T-helper cell polarity away from Th2 towards Th1 by targeting ITK and could thereby correct malignancy associated T-cell defects (877). Moreover, Kondo et al. have reported downregulation of PD-L1 on the surface of CLL B-cells in the peripheral blood of Ibrutinib treated CLL patients as well as downregulation of expression of PD-1 on the surface of CD4+ and CD8+ T-cells, both in a STAT3 dependent manner (878). Stiff et al. demonstrated

expression of BTK in both human and murine MDSCs and showed that Ibrutinib treatment is able to decrease BTK phosphorylation resulting in impaired nitrous oxide production, cell migration, expression of IDO as well as impaired in vitro generation of human MDSCs. Ibrutinib treatment led to a decrease in numbers of MDSCs in both spleen and tumours of mouse models of mammary cancer and melanoma (879). A study by Ping et al. demonstrated decreased production of CXCL12, CXCL13, CCL19 and VEGF by human macrophages after Ibrutinib treatment. Moreover, adhesion, migration and invasion of co-cultured lymphoid cells was significantly impaired (880). Finally, Gunderson et al. reported that tumour growth in a model of *pancreatic ductal adenocarcinoma* (PDAC) was dependent on a cross-talk between B-cells and *fragment, crystallizable region receptor γ* (FcRγ) + tumour associated macrophages resulting in a Th2-permissive macrophage phenotype via BTK activation in a PI3Kγ dependent manner. Ibrutinib treatment result in a shift towards a more Th1-permissive macrophage phenotype and fostered CD8+ T-cell cytotoxicity (881).

Idelalisib was described to modulate cytokine production by T-cells. T-cells derived from CLL patients were shown to have decreased production of IL10, IL6 and IL4 when treated with Idelalisib. Similarly, NK cells treated with Idelalisib showed a modest but significant decrease in IFN-γ production (882). PI3Kδ deficient Tregs were shown to produce lower levels of IL10 and expressed lower levels of CD38 correlating to defective immunsuppressive function (883). Disruption of Treg function was shown to significantly contribute to anti-tumour effects of PI3Kδ inactivation. However, PI3Kδ inactivation was also demonstrated to interfere with the anti-tumour effects of cancer vaccines and immune checkpoint blockade (884). In a mouse model of CLL, genetic inactivation of PI3Kδ was shown to impair Treg expansion with associated disease clearance but also result in rectal prolapse resembling colitis observed in human Idelalisib patients (885). In human Tregs, PI3Kδ inactivation by Idelalisib was shown to inhibit proliferation, alter the immune phenotype and impair the suppressive function towards CD4+ and CD8+ effector T-cells (886). Idelalisib was also shown to promote an undifferentiated phenotype in mouse CD8+ T-cells. These Idelalisib treated T-cells had improved engraftment and persisted longer after transfer into tumour bearing animals. They also showed an increased anti-tumour immunity compared to traditionally expanded T-cells (887). In another study using a CLL mouse model, pharmacological inhibition of PI3Kδ was shown to decrease Treg numbers and their proliferation and activation status but did not result in improved CD8+ T-cell function due to concomitant inhibition of CD8+ effector T-cell differentiation, activation and effector function (888).

1.3   Murine models of CLL

1.3.1   The Eµ-TCL1 mouse model

Today the Eµ-TCL1 mouse model is the most commonly used animal model of human CLL. The *T-cell leukemia/lymphoma protein 1* (TCL1) locus consists of two genes, TCL1A and TCL1B, located on chromosome 14q32.1 (889, 890). TCL1 was first discovered as the oncogene which causes T-prolymphocytic leukemia (T-PLL). In this disease, overexpression of TCL1 has been reported in almost 100% of cases due to t(14;14)(q11;q32) translocation or an inv(14)(q11;q32) inversion (891). Physiological functions of TCL1 related to embryonic development, B-cell maturation and stem cell regulation (892-894). In adults, expression is limited to early stage CD4-/CD8- double negative thymocytes, pre-B-cells, surface IgM expressing virgin B-cells, mantle cells and germinal center B-cells under physiological conditions (891). TCL1 is also expressed in nearly 100% of CLL cases. Here, high protein levels have been shown to correlate with markers of poor prognosis such as unmutated IgVH, ZAP-70 expression and del(11q) (895). TCL1 is a low molecular weight protein that functions by activating the PI3K cascade through direct interaction with AKT1/2 (896). TCL1 also interacts with other signaling proteins, the most important of which for their role in CLL are ROR1, transcription factor p300, components JUN and FOS of transcription factor AP1, IκB, transcription factor *X-box binding protein 1* (XBP1) and *DNA methyltransferase* (Dnmt)3A and Dnmt3B (897-900). In 2002 the Eµ-TCL1 mouse model was created in Carlo M. Croce's lab by expressing the entire human TCL1 locus under control of the VH-promoter-IgH-Eµ-enhancer resulting in expression of human TCL1 in both mature and immature murine B-cells (901). In these initial experiments, transgenic mice were shown to develop a B220low/IgM+ clonal B-cell population coexpressing CD5 in the peripheral blood at around 6 monhs of age. This population could also be detected in the peritoneal cavity, bone marrow and spleen and was shown to expanded in an exponential fashion over time. (Table 2).

	% IgM+CD5+ B cells		
Eμ-TCL1, age	bone marrow	spleen	peritoneal cavity
2 months	1	4	45
4 months	2	9	46
8 months	43	68	74
Wild type, age			
4 months	1	1	20

Table 2: **Progressive accumulation of an IgM+CD5+ B-cell population in various organs of Eμ-TCL1 mice.** Adapted from *Bichi et al. Proceedings of the National Academy of Sciences. 2002;99(10):6955-60.* (901).

All transgenic mice around the age of 13 to 18 months became visibly ill presenting with hepatosplenomegaly, peripheral lymphadenopathy and markedly increased WBC counts. This indicates a phenotype similarity to human CLL. Transgenic mice reaching the endpoint had spleen weights ranging from 1.5 – 2.3 g compared to 0.07g ± 0.01g among wildtype animals and a mean WBC count of 180.0×10^6 /ml compared to 2.8×10^6 among wild type mice. The penetrance of leukemia development was described to be 100% (901). The long latency to development of TCL-1 driven B-cell leukemia in these animals is a major obstacle to their use as platforms for the study of the biology of CLL and for drug development. Adoptive transfer of B-cells derived from leukemia bearing Eμ-TCL1 mice into syngeneic animals has been shown to lead to development of leukemia over the course of several weeks and can thus overcome this hinderance (902-904).

Numerous studies have demonstrated that the Eμ-TCL1 mouse model accurately depicts the biology of human CLL. Yan et al. have shown that the model replicates the B-cell receptor V-region characteristic of aggressive, unmutated human CLL. The study demonstrated minimal Ig heavy chain and light chain somatic mutation, use of stereotyped $V_H D J_H$ and $V_L J_L$ rearrangements resulting in equally stereotyped CDR3 characteristics and BCR usage. Immunoglobulins used by CLL bearing animals were shown to be very similar to auto-antibodies and antibodies to microbial antigens. This may by a sign of an antigen driven stimulation of the BCR signalling cascade in Eμ-TCL1, similar to human CLL patients (905). Moreover, a study by Chen et. al. was able to demonstrate that the Eμ-TCL1 mouse model recapitulates the epigenetic changes observed in human CLL patients, e.g. methylation of promoter sequences with binding sites for transcription factor *Forkhead box D3* (FOXD3) (906). CLL B-cells derived from

Eµ-TCL1 mice were also shown to resemble IL10 producing Bregs phenotypically and functionally similar to human CLL (315). Hofbauer et al. have shown that development of leukaemia in Eµ-TCL1 mice results in skewing of T-cell subsets from naïve to more antigen-experienced, similar to findings in human CLL. Adoptive transfer of CLL B-cells could reproduce these alterations in recipients. In both spontaneously developing leukemia and adoptively transferred CLL a loss of T-cell receptor diversity with development of clonal T-cell populations was observed (903). Our group has previously demonstrated that the Eµ-TCL1 mouse model recapitulates the T-cell defects observed in human CLL patients. T-cell derived from CLL bearing Eµ-TCL1 mice showed various functional defects such as reduced gp33 antigen-specific T-cell activation, decreased mitogen induced T-cell proliferation and and impaired induction of idiotype-specific CD8 T-cells capable of killing CLL cells. Moreover, T-cell from leukemic mice had dysfunctional cytokine production with increased levels of IL1, IL4 and IL6 but decreased levels of IL2, INF-γ and IL12-β (907). Gene expression profiles from CD4+ and CD8+ T-cells from tumour bearing animals revealed alterations in gene expression that became more pronounced with increasing tumour load and correlated with findings in human CLL patients. Comparative anlysis of gene- expression profiles of human CLL patients and leukemic mice detected 45 overlapping differentially expressed genes in CD8+ T-cells and 50 overlapping genes in CD4+ T-cells which were primarily involved in pathways of cell activation and proliferation, vesicle formation and trafficking as well as cytoskeleton formation. Similar to findings in human CLL, development of leukemia in animals resulted in defects of T-cell synapse formation that could be repaired with lenalidomide treatment. When adoptively transferring CLL B-cells from leukemic mice into young transgenic animals without disease, gene-expression profiles comparable to those from ageing CLL bearing Eµ-TCL1 animals developed within 8 days (907). We have also demonstrated the importance of myeloid cells in the microenvironment of CLL bearing Eµ-TCL1 mice in promoting B-cell survival and shaping an immunosuppressive niche in analogy to human NLCs (908) and have demonstrated that the role of the PD-L1/PD-1-axis in induction of CLL-associated T-cell defects is replicate in both ageing Eµ-TCL1 mice as well as following adoptive transfer of CLL B-cells (904).

Several studies have validated the Eµ-TCL1 model as a platform for the preclinical testing of new modes of treatment for CLL. Johnson et al. have demonstrated that transformed B-cells derived from Eµ-TCL1 mice express important therapeutic targets such as DNMT1, MCL-1, BCL-2, AKT and *3-phosphoinositide-dependent protein kinase-1* (PDK1). The TP53 status has been reported to be wild type. Treatment with low dose fludarabine was shown to lead to a survival advantage and reduce lymphocytosis in the

animals. However, fludarabine resistance developed eventually (909). Other studies have shown Eµ-TCL1 mice to be amenable to novel substances such as inhibitors of the BCR signalling cascade including Ibrutinib and Acalabrutinib (910, 911) as well as agents targeting other pathways (912-915).

1.3.2   Other genetically engineered mouse models of CLL

A number of other genetically engineered mouse models of CLL has been developed. These include mouse models mimicking commonly occurring genetic lesion as well as animals overexpressing oncogenes or having targeted deletions of tumour suppressors. Del(13q) is the most common cytogenetic lesion found in CLL and is associated with a favourable prognosis. Transgenic mouse models with targeted deletions on murine chromosome 14qC3 mimicking those of the del(13q) minimal deleted region including DLEU2 and miR-15a/16-1 (916) and the del(13q) common deleted region (917) have been developed. Both models manifest a range of B-cell malignancies including MBL, CLL and CD5- NHL. In both minimal deleted region and common deleted region animals clonal B-cell populations first develop at around 6-18 months of age with clinically manifest disease at around 12-18 months, similar to the Eµ-TCL1 model. The ratio of CLL-like disease compared to other B-cell malignancies dependent on the type of the deletion with approximately 50% of common deleted region animals developing a CLL-like clonal B-cell expansion compared to only 22% of minimal deleted region animals. The targeted deletion of the miR-15a/16-1 locus led to a CLL like disease with a longer latency (12-18 months) and a penetrance of only 20% compared to minimal deleted region animals. (916). The importance of the miR-15a/16-1 locus is also illustrated by the inbred *New Zealand Black* (NZB) strain of mice which are primarily used for the study of autoimmune diseases such as SLE but also develop sporadic late onset CLL-like B-cell proliferations due to a naturally occurring point mutation in the miR16-1 sequence (918-920). Another model used miR-29a overexpression to obtain a model of CLL a latency of 12-24 months but a penetrance of only 20% (921). Other genetically engineered mouse models of CLL include double transgenic animals for a TRAF2 mutatant lacking the N-terminal *Really Interesting New Gene* (RING)- and zinc finger domains (TRAF2DN) and BCL2 (922) which develop CLL-like B-cell proliferations at around 9-15 months of age with a penetrace of approximately 80%, animals transgenic for APRIL (923) which develop CLL-like disease at around 9 months of age with a penetrance of 40% and animals double transgenic for myc and BAFF who develop CLL like disease at around 3 months of age in 78% of male animals but only 3% of female animals (924). A model using overexpression of ROR1 has been reported to display

CLL-like B-cell proliferations but only a very poor penetrance of 5% (897). All of the above models are inferior to Eµ-TCL-1 mice in terms of disease penetrance. This has been attributed to the strong oncogenic functions of TCL1 in numerous singnalling pathways. Two other models approaching a 100% disease penetrance have been described: *Interferon regulatory factor 4* (IRF4) knock-out immunoglobulin heavy chain V_h11 knock-in animals (925) and *simian virus 40* (SV40) T antigen transgenic mice (926). However, both models have highly skewed IgVH repertoires and thus mimicking human CLL poorly in terms of phenotype. Moreover, IRF4 deficiency in itself leads to severe immunodeficiency due to its critical function in various types of immune cells and the IRF4-/-/V_h11 mice thus are not suitable to model CLL induced alterations of the immune microenvironment.

1.3.3   Eµ-TCL1 model-based crosses with other murine models

In order to study the role of specific molecules involved in cell signaling, cytoskeleton formation and cell trafficking, proliferation and cell survival as well as microenvironmental interactions in the pathobiology of CLL Eµ-TCL1 mice have been crossed with a number of other genetically engineered mouse models yielding unique mouse strains. Table 3 gives an overview of these models and the resulting characteristics.

Model	Characterisitcs
Signaling	
Eμ- TCL1 *x* xbp1 ^{fl/fl} CD19-Cre (927)	Delayed progession, compromised BCR signalling
Eμ- TCL1 *x Toll/IL-1R 8* (TIR8)-/- (928)	Faster disease progression, prolymphocytoid transformation
Eμ- TCL1 *x* pkcβ-/- or pkcβ+/- (929)	pkcβ+/-: Delayed onset pkcβ-/-: Disease prevention
Eμ- TCL1 *x X-linked Immune Defect* (XID) (930)	Delayed onset, 18% T-cell leukemia
Eμ- TCL1 *x dominant-negative recombination activating gene 1* (dnRAG1) tg (931)	Early onset, more aggressive course
Cytoskeleton and cell trafficking	
Eμ- TCL1 *x Hematopoietic-Specific Protein 1 (*hs1) -/- (932)	Early onset
Eμ- TCL1 *x Ras homolog gene family, member H* (RhoH) -/-(933)	Delayed onset, reduced bone marrow homing
Proliferation and cell survival	
Eμ- TCL1 *x inhibitor of DNA binding 4 (*ID4) -/- (934)	Early onset, more aggressive course
Eμ- TCL1 *x* TP53-/- (935)	Early onset, more aggressive course
Eμ- TCL1 *x* miR29a/b-tg (921)	Disease acceleration
Microenvironmental interactions	
Eμ- TCL1 *x Frizzled-6 (*fzd6) -/- (936)	Delayed onset, reduced expression of β-catenin
Eμ- TCL1 *x* CD44-/-(937)	Reduced tumour load, prolonged survival, increased apoptosis
Eμ- TCL1 *x* MIF-/- (269)	Delayed onset, reduced number of TAMs, increased apoptosis
Eμ- TCL1 *x* ROR1 tg (897)	Early onset, increased proliferation and reduced apoptosis of leukemic cells
Eμ- TCL1 *x* APRIL tg (938)	Early onset, increased survival of leukemic cells
Eμ- TCL1 *x* BAFF tg (939)	Early onset, more aggressive course

Table 3: Characterisitcs of genetically engineered mouse models crossed with Eμ TCL1 mice. Adapted from Simonetti *et al. Blood. 2014.*(940). Abbreviations: tg – transgenic.

1.3.4 Xenograft models of CLL

Several xenograft models using transplantation of human CLL cells into mice have been described (941). The generation of xenograft models for CLL is obstructed by the fact that these cells are rejected when implanted into immunocompetent animals. Use of immunocompromised animals such as *Severe combined immunodeficiency* (SCID) mice on the other hand does not allow for the study of CLL-immune cell interactions. Moreover, these animals can develop CD5- EBV driven B-cell malignancies not related to human CLL limiting the utility of the model (942, 943).

Initial studies used intraperitoneal injection of CLL cells into BALB/c or *beige/nude/Xid* (BNX) mice which had been lethally irradiated and transplanted with bone marrow from *Non-Obese Diabetic* (NOD)/SCID mice (944, 945). These protocols were later optimized by use of concomitant intravenous and intraperitoneal injections of CLL cells resulting in improved engraftment (946, 947). Interestingly, the engraftment of CLL cells appears to be dependent on the presence of T-cells. Bagnara et al. used *NOD SCID gamma (*NSG) mice (NOD/SCID x IL2Rγ-/-) and reported that engraftment of CLL cells in these animals was only feasible when co-tranferred with autologous T-cells while in vivo elimination of CD3+ or CD4+ cells abrogated CLL cell survival and proliferation. However, the transplanted CLL B-cells could not be observed after 3 months time. Around the same time a severe GvHD reaction mediated by transplanted human T-cell occurred. Thus T-cells had both CLL promoting and anti-tumour properties in this model (948). Kikushige et al. injected immature CD34+CD38- stem cells derived from the bone marrow of CLL patients into newborn NSG mice. The cells were shown to develop into clonal CLL-like B-cells with a clonality independent of the original CLL clone. It could thus be speculated that the potential to generate clonal B-cell proliferations may already be present on the level of stem cells in the pathogenesis of CLL (949). The NSG xenograft model of CLL has been utilized in preclinical studies of Ibrutinib efficacy and maybe useful as a platform for testing of other substances as well *(950).*

Xenograft models, while being adequate to study the genetic basis and evolution of CLL as well as being useful platforms for drug testing, cannot mirror the complex interactions between CLL cells and the surrounding immune microenvironment. The Eµ-TCL1 with its 100% penetrance and ability model the biology of human CLL as well as CLL associated remodelling of the microenvironment and CLL mediated immune evasion thus remains the most useful model to study potential immunotherapeutic strategies.

1.4   Summary

CLL is a very common form of hematologic malignancy primarily affecting the elderly. The disease remains incurable using standard immunochemotherapy as well as novel treatment strategies targeting the B-cell receptor pathway or anti-apoptotic mechanisms. The only established potentially curative treatment approach remains allogeneic stem cell transplantation which can only be applied in a small subset of the patient population. Its high toxicity is often prohibitive in elderly patients suffering from relevant comorbidities. A significant unmet need for equally curative and tolerable treatment strategies remains. CLL is associated with a pronounced immunodefiency which is a result of a combination of various humoural and cellular immune defects. Resulting infections are a major source of morbidity and mortality in CLL. Moreover, CLL associated immunodeficiency also is a reflection of immune evasion mechanisms. CLL cells are now understood to be closely interacting with their microenvironment which promotes CLL B-cell survival and provides immunosuppressive niches. Correction of immune evasion mechanism could, according to the cancer immunoediting hypothesis, provide a potentially curative approach. Overexpression of immune checkpoint molecules has been established as a major mechanism of cancer immune evasion in recent years. PD-1 and its ligand PD-L1 have been demonstrated to be pivotal in mediating CLL associated T-cell deficiency. Despite promising pre-clinical data and successful application in other malignancies including Hodgkin lymphoma, attempts at establishing PD-1/PD-L1 immune checkpoint blockade as a treatment modality in CLL have been disappointing so far. Interestingly, BTK inhibitors such as Ibrutinib and Acalabrutinib have also been shown to have the ability to modulate T-cell function and partially correct CLL associated immune defects. Recent pre-clinical data suggests a potential synergistic effect in combining BTK inhibition and immune checkpoint blockade. Today the Eµ-TCL1 mouse model is the most commonly used animal model of human CLL. Its hallmark characteristics are a high penetrance and a faithful replication of phenotype and biology of human CLL including remodelling of the microenvironment and CLL induced immune defects. Eµ-TCL1 mice also mirror the role of PD1/PD-L1 in mediating CLL associated T-cell defects and the effects of BTK inhibitor treatment. The model is thus suitable to assess the effects of BTK-inhibition on T-cell function and as platform to develop combination approaches of immune checkpoint blockade and BTK inhibition.

1.5   Hypothesis and Aims

Based on the available literature and preliminary data of our group we hypothesize that the clinical efficacy of BTK-inhibitors is based on a synergism between direct anti-tumour effects and correction of CLL-associated functional T-cell defects. We have previously shown that PD-1/PD-L1 is pivotal in mediating CLL-associated T-cell exhaustion (216). We speculate that repair of CLL associated T-cell defects is achieved by a modulation of expression of PD-1 and its ligands. Due to their differences in selectivity these effects may be differential between Ibrutinib and second generation BTK inhibitors like Acalbrutinib. We hypothesize that combinations of anti-PD-L1 immune checkpoint blockade and BTK inhibitors may have synergistic effects towards improved T-cell function.

Aim (1)

We hypothesize that PD-L1 expression on CLL B-cells is driven by B-cell receptor signalling. We would therefore like to investigate whether treatment with either Ibrutinib or Acalabrutinib leads to downregulation of PD-L1 expression among CLL B-cells. We further speculate that treatment with either agent could lead to downregulation of PD-1 and other exhaustion associated immune checkpoint molecules among T-cells subsets. Given the well-known expression of BTK among myeloid cell subsets and Ibrutinib ability to modulate myeloid derived suppressor cell function in other forms of malignancy we would further like to investigate whether an influence of either Ibrutinib or Acalabrutinib on phenotype and immune checkpoint expression of myeloid cell subsets exists. (879)

Aim (2)

We speculate that BTK inhibitors have the potential to repair CLL associated T-cell defects and would therefore like to investigate the influence of Ibrutinib and Acalabrutinib on T-helper cell function, cytotoxic T-cell function and capability of T-cell synpase formation in the splenic microenvironment of CLL bearing animals.

Aim (3)

We would like to investigate whether combinations of Ibrutinib or Acalabrutinib with anti-PD-L1 immune checkpoint blockade have syngestic effects towards repair of CLL-associated T-cell dysfunction. As we have previously shown a reversal of exhaustion-phenotype of T-cells with anti-PD-L1 treatment in the splenic microenvironment of CLL bearing TCL-1 mice (836) we would further like to investigate whether BTK-inhibitor/anti-PD-L1 combinations have synergistic effects in correcting the exhaustion phenotype of CLL-associated T-cells.

2 Materials and Methods

2.1 Mice and animal procedures

2.1.1 Ethical considerations

The principles of the "Three Rs" – replacement, reduction and refinement – first described by W.M.S Russel and R.L Burch in 1959 have been designed as a guidance framework for scientific research using animals (951).The goal of these guiding principles is to make sure that animals are used only afer thorough ethical consideration, to protect the welfare of the animals used and to improve the quality of research. The principle of replacement asks for the use of non-animal-based procedures over animal testing wherever possible to achieve the scientific goal. Reduction refers to the obligation of the researcher to use the smallest number of animals possible to achieve valid results in order to answer the research question at hand. Finally, refinement refers to the use of methods that mitigate or minimize pain and distress of research animals. In the EU and USA this framework of principles has been written into laws and guidelines governing animal-based research.

The research project at hand was conducted closely following the principles of the "Three Rs". CLL cell lines or in vitro model systems are unable to mirror the complex interactions between CLL cells and their surrounding microenvironment and are thus unsuitable to answer questions regarding the reciprocal effects of CLL treatment and immune function (replacement). The number of animals used in this project was reduced as far as possible by only applying therapeutic interventions that have been proven effective ex vivo. For each experiment the number of animals needed to obtain at least 80% power in detecting a 1.25 standard deviation difference in a Fisher exact test performed at the one-sided 0.05 significance level was calculated (reduction). Physical signs of disease activity such as lymphocytosis, lymphadenopathy and organomegaly arising with the onset of CLL in mice usually do not cause pain or suffering. Adverse effects such as dyspnoea or restricted movement which negatively affect the wellbeing of the animals are rare. The substances and application routes used in this project are usually well tolerated and only result in minimal and short-term discomfort. Mice were inspected daily and monitored for signs of poor health such as piloerection, squatting posture, sunken eyes, reduced activity, reduced grip strength and weight loss. Physical examination and assessment of disease status and CLL load was conducted regularly and strict endpoint criteria (spleen size >3cm in diameter, WBC count in blood smear >100 WBC/*high power field* (hpf) (40x objective), >90% of lymphocytes CD19+CD5+ cells) applied to minimize suffering from leukemia or interventions (*refinement*).

2.1.2 Breeding and maintenance of mice

Four breeding pairs of Eμ-TCL1 mice on the C3H/Hej genetic background were obtained from Dr. Carlo Croce, Ohio State University, Columbus Ohio, USA via our collaboration within the *CLL Research Consortium* (CRC) and then backcrossed on the C57BL/6 background. Wild type C57BL/6 animals for the purpose of breeding or for the use in experiments were purchased from Charles River laboratories, Margate, UK. The animals were housed using a barrier system in the *biological services unit* (BSU) at Charterhouse Square, London, UK. All in vivo procedures were conducted under sterile conditions in special procedure rooms within the BSU. Breeding of Eμ-TCL1 mice was achieved by pairing transgenic males with 2 syngeneic C57BL/6 wild type females. Pairing of the breeders occurred at the age of 6 to 8 weeks and breeding was conducted for as long as 10 months or when no more new litters had been produced for at least 2 months. Weaning of the litters was performed at 3 to 4 weeks of age. The animals were ear-notched, genotyped and subsequently housed with a maxium of 5 littermates in the same cage. Animals were monitored once a day for signs of poor health. The status and activity of CLL was assessed by physical examination of spleen size as well as by blood smears and immunophenotyping of peripheral blood. The animals were culled when signs of poor health were observed or when they fulfilled one of the following endpoint criteria: spleen size >3cm in diameter, WBC count in blood smear >100 WBC/hpf (40x objective), >90% of lymphocytes CD19+CD5+ CLL cells. Animals were euthanized using cervical dislocation.

2.1.3 Genotyping of mouse litters

Animals were ear notched for identification and to obtain material for genotyping. The material was digested at 55 °C overnight in „tail buffer" (50mM *tris(hydroxymethyl)aminomethane* (TRIS) pH 8.0 (Sigma, UK), 25mM *Ethylenediaminetetraacetic acid* (EDTA) disodium salt pH 8.0 (Sigma, UK), 100mM NaCl (Fisher Scientific, UK), 1% *sodium dodecyl sulfate* (SDS) (Sigma,UK) and Proteinase K 20mg/ml (Roche Diagnostics, UK)). DNA was extracted using alcohol precipitation. *Polymerase chain reactions* (PCRs) were performed using the TCL1 primers (5'-3') GCCGAGTGCCCGACACTC (TCL1 Forward) and CATCTGGCAGCAGCTCGA (TCL1 Reverse). The *Mouse beta globulin* (MBG) gene was used as an internal positive control (5'-3') CAGCTCCTGGGCAATATGAT (MBG Forward) and TTGTTCACAGGCAAGAGCAG (MBG Reverse). A negative control not containing DNA was also utilized. 1μl of DNA, 2μl of TCL1 Forward and Reverse and 2μl of MBG Forward

and Reverse each were filled up with megamix blue PCR mix (Clent Life Science, UK) to a total volume of 25µl. The following PCR conditions were used for both reactions: Activation at 95°C (5 min), denaturation at 95°C (30 sec), annealing at 58°C (30 sec) and extension at 72°C (30 sec) for 35 cycles followed by final extension at 72°C (5 min). The obtained products, the corresponding controls and a 100bp DNA ladder (Life Technologies, UK) were applied on a 2% agarose gel containing 1x gel red at 80 V for 45 minutes for separation.

2.1.4   Haematology testing

In ageing Eµ-TCL1 mice haematology testing was routinely initiated at the age of 6 months and conducted monthly to biweekly. Experimental animals were tested weekly from the day of adoptive transfer of CLL B-cells. The animals were heated under a heat lamp and put in a restrainer. To obtain blood, a 19G needle (BD, UK) was used to puncture the lateral tail vein. Approximately 100µl of peripheral blood were collected in a 0,5 ml microcentrifuge tube (VWR, UK) containing 10 µL of 0.5 M EDTA (Sigma, UK). For preparation of blood smears 10 µl of peripheral blood were pipetted on a microscope slide (VWR, UK) and smeared using an additional slide. Slides were fixed in methanol (Fisher scientific, UK) for 30s, then stained in modified Wright stain (Sigma, UK) for 40s and washed in deionized water (Milipore, Merck, UK) for 45s. Slides were rinsed in deionized water (Milipore, Merck, UK) and allowed to air dry. For hematologic assessment the WBC count was estimated by counting 5- 10 hpf using a 40x objective of a bright field microscope (Zeiss, UK). For flow cytometry-based analysis 20µl of peripheral blood were filled up with *fluorescence activated cell sorting* (FACS) buffer (*phosphate buffered saline* (PBS) (Sigma, UK) with 2% *fetal calf serum* (FCS) (Gibco, UK)) to 100µl in 15 ml centrifuge tube (VWR, UK). The following flurochrome-labelled antibodies were added at a ratio of 1:100: Anti mouse CD45 APC (clone 30-F11, eBioscience, UK), anti-mouse CD19 FITC (clone 1D3, ebioscience, UK) and anti-mouse CD5 PE-Cy7 (clone 53-7.3, biolegend, UK). Cells were incubated for 30 minutes at 4°C. 1ml of FACS buffer was added and cells were centrifuged at 300g for 10 minutes at 4°C. The supernatant was decanted and the washing step repeated. Erythrocytes were then lysed in 5ml 1X ammonium-chloride-based RBC lysis buffer (NH_4CL 8.3g/l (Sigma, UK), $KHCO_3$ 1g/l (Sigma, UK), EDTA 0.037g/l (Sigma, UK)). After 7 minutes incubation, 10 ml of PBS were added and centrifuged at 300g for 10 minutes at 4°C, resuspended in 300µl FACS buffer containing 1:1000 *4',6-diamidino-2-phenylindole* (DAPI) (ebioscience, UK) and transferred to 5 ml polypropylene round bottom tubes (Corning, UK). Cellular events

were then recorded on a BD LSR Fortessa flow cytometer (BD Biosciences, UK). The analysis was conducted using Cytobank (Cytobank Inc, USA).

2.1.5 Processing of mouse spleens into a single cell suspension

Mouse spleens were removed immediately after euthanizing the animals by cervical dislocation. The removal of the organ was performed under sterile conditions in a BSU procedure room. Spleens were transported in PBS (Sigma, UK) containing 20% FCS (Gibco, UK) and kept on ice. The GentleMACS tissue dissociator (Miltenyi, UK) was utilized for preparation of single suspension according to the manufacturer's recommendations for mouse spleen processing without enzymatic treatment. Subsequently the lysis of erythrocytes with an ammonium-chloride-based RBC lysis buffer (NH4CL 8.3g/l (Sigma, UK), KHCO3 1g/l (Sigma, UK), EDTA 0.037g/l (Sigma, UK)) was performed. Centrifugation of cell suspensions was generally performed at 300g for 10 minutes at 4°C. The cells in the obtained single cell solutions were quantified using a Luna fl automated cell counter (Logos bioysstems, USA) after dilution of a 10µl aliquot with an equal amount of 0.4% Tryphan blue (Sigma, UK). Splenocytes were then cryopreserved at a maximum density of 200×10^6 cells/ml in FCS (Gibco, UK) containing 10% *dimethyl sulfoxide* (DMSO) (Fisher Scientific, UK) and kept in a suitable liquid nitrogen storage tank.

2.1.6 Adoptive transfer of CLL B-cells

4×10^7 syngeneic mouse CLL B-cells derived from cryopreservation were injected by tail vein injection in accordance to standard procedures (952). Prior to the injection the content of CD19+CD5+ CLL B-cells in the splenocytes suspensions was measure using flow-cytometry. A maximum volume of 5ml/kg was injected per animal. We used C57BL/6 wild type animals 2.5 months of age as recipients Following the adoptive transfer procedure, animals were closely monitored by inspection and physical examination. The CLL disease status was quantified weekly using peripheral blood smears and flow cytometry. The animals where culled once they showed sign of poor health or fulfilled one of the following endpoint criteria: spleen size >3cm in diameter, WBC count in blood smear >100 WBC/hpf (40x objective), >90% of lymphocytes CD19+CD5+ CLL cells. Euthanization was performed using cervical dislocation.

2.1.7   Application of experimental substances by water bottle preparation or i.p. injection

Ibrutinib (kindly provided by Janssen pharmaceuticals) and Acalabrutinib (kindly provided by Acerta pharma) were applied via water bottle preparation at a concentration of 0.15mg/ml in 2% *Hydroxypropyl-β-cyclodextrin* (HPBCD) (Sigma, UK). Water bottle preparations were prepared under sterile conditions and sterile filtered through a 0.2 µm *Polyethersulfone* (PES) filter top (Thermofisher scientific, UK) before application. Anti mouse PD-L1 clone 80 mIgG1 D265A (equivalent to Durvalumab, kindly provided by Astra-Zeneca) or isotype control NIP228 mIgG1 D265A (kindly provided by Astra-Zeneca) were applied by i.p. injection at a dose of 10mg/kg every 3 days. A maximum volume of 10 ml/kg was used for i.p. injections. Prior to i.p. injections aqueous stock solutions of antibodies were obtained by dissolving the antibody in sterile PBS and under sterile conditions. During the treatment periods the animals were assessed daily by physical examination and culled at predefined endpoints.

2.2   Manipulation of mouse splenocyte single cell suspensions

2.2.1   Cell thawing procedure

Thawing of cryopreserved splenocyte samples was performed in a water bath at 37°C. To avoid contamination the vials were disinfected using 70% *industrial methylated spirit* (IMS) (Fisher Scientific, UK) and subsequently opened in a class II biosafety cabinet. The cell suspension was pipetted into 10ml *Roswell Park Memorial Institute medium 1640* (RPMI 1640) (Gibco, UK) supplemented with 10% FCS (Gibco, UK), 1% Penicillin-Streptomycin (Sigma, UK) at a temperature of 37°C. Subsequently the suspension was centrifuged at 300 x g for 10 minutes at room temperature and resuspended in a volume suitable for number of cells contained in the pellet. Automated cell counting was conducted on a Luna fl automated cell counter (Logos bioystems, USA) after dilution of a 10µl aliquot with an equal amount of 0.4% Tryphan blue (Sigma, UK).

2.2.2   Negative selection of CLL and B cells

CLL and B cells where isolated from splenocytes suspensions using the pan-B-cell isolation kit (Miltenyi, UK) which uses *magnetic activated cell sorting* (MACS). The suspension were centrifuged at 300 x g for 10 minutes at 4°C, the supernatant completely aspirated and the pellet resuspendend in 40 µL of ice-cold MACS buffer (PBS (Sigma, UK) pH 7.2, 0.5% *bovine serum albumin* (BSA) (Sigma, UK), 2mM EDTA (Sigma, UK)) per 10^7 total cells. 10 µL of Pan B Cell Biotin-Antibody Cocktail (Miltenyi,

UK) per 10^7 total cells were added. The cells were well mixed and incubated for 5 minutes at 4°C. A further 30 µL of ice-cold MACS buffer per 10^7 total cells and 20 µL of Anti-Biotin MicroBeads (Miltenyi, UK) per 10^7 cells were added. Cells were mixed well and incubated for another 10 minutes at 4°C. Finally, the volume was adjusted to 500µl per 10^8 cells (minimum 500µl). For separation, a LD column (Miltenyi, UK) was placed in the magnetic field of a MACS separator (Miltenyi, UK) and primed with 2 ml of MACS buffer. The cell suspension was applied to the column and flushed through by applying 1ml MACS buffer twice. The effluent, which was collected in a 15 ml centrifuge tube (VWR, UK), contained the unlabelled pan-B-cell fraction.

2.2.3 Negative selection of T cells

T-cells where isolated from splenocytes suspensions using the pan-T-cell isolation kit II (Miltenyi, UK) which uses MACS. The suspension were centrifuged at 300 x g for 10 minutes at 4°C, the supernatant completely aspirated and the pellet resuspendend in 40 µL of ice-cold MACS buffer (PBS (Sigma, UK) pH 7.2, 0.5% BSA (Sigma, UK), 2mM EDTA (Sigma, UK)) per 10^7 total cells. 10 µL of Pan T Cell Biotin-Antibody Cocktail (Miltenyi, UK) per 10^7 total cells were added. The cells were well mixed and incubated for 5 minutes at 4°C. A further 30 µL of ice-cold MACS buffer per 10^7 total cells and 20 µL of Anti-Biotin MicroBeads (Miltenyi, UK) per 10^7 cells were added. Cells were mixed well and incubated for another 10 minutes at 4°C. Finally, the volume was adjusted to 500µl per 10^8 cells (minimum 500µl). For separation, a LD column (Miltenyi, UK) was placed in the magnetic field of a MACS separator (Miltenyi, UK) and primed with 2 ml of MACS buffer. The cell suspension was applied to the column and flushed through by applying 1ml MACS buffer twice. The effluent, which was collected in a 15 ml centrifuge tube (VWR, UK), contained the unlabelled pan-T-cell fraction.

2.3 BTK occupancy assays

96 well microplates (PerkinElmer, UK) were coated overnight at 4°C with 125 ng/well anti-BTK antibody (Clone 53/BTK, BD Biosciences) and blocked with BSA (Gibco, UK) the following day for 2 to 3 hours at room temperature. Lysis buffer containing protease inhibitor cocktail (Sigma, UK) was used to lyse frozen splenocyte cell pellets. Lysates were incubated for 1 hour on ice in the presence or absence of a saturating concentration of Ibrutinib or Acalabrutinib (10^{-6} mol/L) followed by an incubation of a biotinylated derivate (ACP-4016; 10^{-7} mol/L) serving as a probe. The equivalent of 5×10^5 cells of lysate/well, in replicates of three, were added to the coated OptiPlates and incubated for 2 hours. After a 1-hour incubation with streptavidin–*horse radish peroxidase* (HRP)

(Invitrogen, UK; ELISA grade; 120 ng/mL), a SuperSignal ELISA Femto Substrate (Thermo Fisher Scientific, UK) was added, and chemiluminescence was measured on a multiplate reader (PerkinElmer, UK). The percentage of BTK occupancy for the drug-treated mice was calculated relative to the average signal from the vehicle control group. The samples without exogenous Ibrutinib or Acalabrutinib represented 100% free BTK (or 0% occupied BTK), and the samples with exogenous BTK inhibitor represented 0% free BTK (or 100% occupied BTK).

2.4   Flow cytometry based functional T-cell assays

2.4.1   EdU incorporation

Incorporation of 5-*ethynyl-2´-deoxyuridine* (EdU) was used for assessment of in vivo proliferation of T-cells subsets. The substance is utilized during DNA synthesis in lieu of physiological nucleosides. It can subsequently be visualized by convalent binding to an azide coupled to a flurochrome via an alkyne moiety. The reaction is catalysed by copper (953, 954). The EdU assay can be used alongside traditional flow cytometry staining for both surface and intracellular markers. EdU (Life Technologies, UK) was applied to experimental annimals by i.p. injection at a dose of 100µg/g body weight 20 hours before being culled. Priot to the injection an EDU stock solution was prepared by dissolving the substance in sterile PBS (Sigma, UK) under sterile conditions.

2.4.2   Cell stimulation

$1x10^6$ splenocytes were incubated in 250µl RPMI 1640 with 10% FCS (Gibco, UK), 1% Penicillin/Streptomycin (Life Technologies, UK) in round-bottom 96-well-plates (VWR, UK). 5µg/ml CD107a per well (Clone 1D4B biolegend, UK) was added. The splenocytes were stimulated with *Phorbol 12-Myristate 13-Acetate* (PMA)/ionomycin/brefeldin A/monensin cell stimulation cocktail (eBioscience, UK) for 6 hours at 37ºC/5% CO2. Controls were treated with transport inhibitor cocktail brefeldin A/monensin (eBioscience), but no cell stimulation cocktail.

2.4.3   Surface, intracellular and intranuclear flow cytometry staining

$1x10^6$ PMA/ionomycin/brefeldin A/monensin stimulated splenocytes, $1x10^6$ unstimulated splenocytes and their corresponding controls were used per animal and transferred into 5ml polystyrene round-bottom tubes (Corning, UK). All staining steps were performed at a temperature of 2-8°C to avoid internalisation or capping of the antibodies. Unstimulated cells were split for intracellular EDU stain and intranuclear ki67 stains. Cells were

resuspended in 100 µl of FACS buffer containing viability stain (fixable viability efluor 506, ebioscience, UK) at a concentration of 1:1000. Surface antibodies (CD3e APC/CY 7, clone 145-2C11, biolegend, UK; CD8a BV605, clone 53-6.7, biolegend, UK; CD44 AF700, clone IM7, ebioscience, UK) were added at a dilution of 1:100 and cells incubated at 4 ºC for 30 minutes. Fixation using IC fixation buffer (ebioscience,UK) and permeabilisation using permeabilisation buffer (ebioscience,UK) for intracellular stains or FOXP3 fixation/permeabilisation buffer (ebioscience,UK) and permeabilisation buffer (ebioscience,UK) for intranuclear stains were performed according to the manufacturer's recommendations. Cells were stained with intracellular antibodies (Interferon gamma AF488, clone XMG1.2, biolegend, UK; IL2 PE/Cy7, clone JES6-5H4, biolegend, UK; IL4 PerCPefluor 710, clone 11B11, ebioscience, UK) and intranuclear antibodies (Ki67 PE/Cy7, clone 16A8, biolegend, UK) for 1h at 4ºC at a 1:100 dilution. Compensation controls consisted of ABC total compensation beads (Thermo fisher scientific, UK). In order to obtain compensation controls one drop each of both negative control beads and positive antibody binding beads were added to 80µl FACS buffer in a 5ml polystyrene round-bottom tube (Corning, UK). One tube per flurochrome included in the panel was prepared. Subsequently a dose appropriate for one test of pre-conjugated flow cytometry antibody was added and the sample incubated at 4°C for 30 minutes in the dark. The solution was then washed in 2ml FACS buffer twice and resuspended in 300µl PBS ready for acquisition. Beads could not be used for compensation control of the viability stain-here single-stained cells were used. For EDU staining, cells were fixed in 100µl of "Click it" fixative (life technologies,UK) for 15 minutes at room temperature in the dark. After 2 washes with FACS buffer cells were resuspended in 100µl of 1x "Click it" permeabilization buffer (life technologies,UK) and incubated for an additional 15 minutes at room temperature in the dark. 500 µl of reaction cocktail (2% CUSO4, 0.5% Alexa Fluor 488 azide, 10% 1x "Click it" reaction buffer additive in PBS, all life technologies, UK) were added and cells thoroughly mixed. For the *fluorescence minus one* (FMO) control the cocktail was prepared without fluorescent dye azide. After incubation for 30 minutes at room temperature in the dark cells were washed twice in permeabilization buffer and carried forward for acquisition. Acquisiton was performed on a BD LSR

Fortessa flow cytometer (BD, UK). The recorded .FCS files were analysed using Cytobank (Cytobank Inc., USA).

2.5   Immune synapse formation assay

2.5.1   Synapse formation and actin staining

$1x10E^6$ B-cells are resuspended in serum free RPMI 1640 (Gibco, UK) with 1% Penicillin/Streptomycin (Life Technologies, UK), and labelled using *7-Amino-4-Chlormethylcumarin* (CMAC) (Thermofisher, UK) at a concentration of 2µg/ml for 30 minutes at 37 °C 5%CO_2. B-cells were activated using 2ug/ml *staphylococcus enterotoxin A* (SEA)/ *staphylococcus enterotoxin B* (SEB) (Sigma, UK) for 30 minutes at 37 °C 5%CO_2 in RPMI 1640 (Gibco, UK) with 10% FCS (Gibco, UK), 1% Penicillin/Streptomycin (Life Technologies). $1x10E^6$ T-cells were added in serum free medium and allowed to conjugate to B-cells pelleted for 20 minutes at 37 °C 5%CO_2. Cells were transferred into a 3 well-cell concentrator and plated on a Poly-l-lysine coated microscope slide (VWR, UK) using a Cytofuge (Beckman Coulter, UK) at 1000 rpm for 6 minutes. Cells were preserved in 3% methanol-free formaldehyde/PBS (TAAB laboratories, UK) for 15 minutes, permeabilized in 0.3% Tritonx100/PBS (Sigma, UK) for 5 minutes and stained using Rhodamine phalloidin (Thermo Fisher, UK) in 5% Goat Serum Buffer (Sigma, UK) at a dilution of 1:40. Slides were mounted using H-1500 Hard set mounting medium for fluorescence (Vectashield, UK).

2.5.2   Confocal microscopy and image analysis

A Zeiss 710 confocal laser-scanning microscope with a 63x/1.40 oil objective and Version 2.6 Zen imaging software (Zeiss, UK) was used in order to record confocal microscopy images. Per condition assessed al least 10 images were recorded. The resulting .LSM files were analysed using Zen lite analysis software (Zeiss, UK). The synapse area was defined using the Zen outline tool by marking the edges of the actin accumulation between T cells and B cells. The area of T-cell F-actin immune synapse (µm^2) was used as the readout. A minimum of 100 randomly chosen synapses per condition were analysed.

2.6   Immune phenotyping by mass cytometry

2.6.1   Mass cytometry staining

Mass cytometry is a method of "single cell technology" that allows for the parallel assessment of at least 40 markers. This approach utilises stable isotopes of non-

biological rare earth metals (usually lanthanides) tagged to monoclonal antibodies. $3x10^6$ splenocytes from single cell preparations were carried forward for staining. All staining steps are performed in 5 ml polypropylene round bottom tubes (Corning, UK). Cell were resuspended in "Cell-ID" Cisplatin (Fluidigm, UK) in PBS (Sigma, UK) at a concentration of 5µM and incubate for 5 minutes at room temperature. The reaction was quenched with 5x the volume of "Maxpar" cell staining buffer (Fluidigm, UK) and the samples centrifuged. Cells were resuspended in 50µl of "Maxpar" cell staining buffer containing 1 µl of anti-mouse CD16/CD32 monoclonal antibody (clone 93, ebioscience, UK) and incubated for 10 minutes. The volume was then filled up to 100 µl with "Maxpar" cell staining buffer (Fluidigm, UK) containing mass cytometry antibodies for a final concentration of 1:100. Cell were incubated for 30 minutes at room temperature and then washed 2x in "Maxpar" cell staining buffer (Fluidigm, UK). The samples were then resuspended in 1ml of "Maxpar" Fix and Perm buffer (Fluidigm, UK) containing "Cell-ID" Intercalator-Ir (Fluidigm, UK) at a concentration of 125 nM and incubated over night at 4°C. Cells were washed 2x in "Maxpar" Cell staining buffer (Fluidigim, UK) and 1x in "Maxpar" water (Fluidigm, UK). Cells were left dry-pelleted at 4°C until immediately prior to acquisition on a "cytof 2" mass cytometer (Fluidigm, UK). For a list of mass cytometry antibodies used please refer to table 4.

2.6.2   Acquisition and analysis of mass cytometry data

A "cytof 2" mass cytometer (Fluidigm, UK) was used for acquisition of mass cytometry data. The suspension of stained cells was nebulized in order to create single cell droplets and was subsequently exposed to a high temperature plasma. This breaks the molecular bonds and ionizes the atoms. The resulting charged atomic ion clouds are transferred into the mass spectrometer. The mass cytometer is configured as a *quadrupole-time-of-flight* (qTOF) instrument. The two radiofrequency quadrupoles are tuned to filter out naturally occuring low mass ions. The enriched higher mass reporter ions are quantitated by *time of flight* (TOF) mass analysis. Normalization of the recorded data is achieved via a standardized bead solution containing known concentrations of the metal isotopes 140/142Ce, 151/153Eu, 165Ho, and 175/176Lu. A correction algorithm in the software of the mass cytometer normalizes the recorded data to correct for signal variation that may occur over protracted periods of use.

2.6.3   Citrus analysis of high dimensional single cell immune phenotypic data

For analysis of mass cytometry data, the algorithm *cluster identification, characterization, and regression* (CITRUS) was used. The algorithm was designed to detect statistically

significant differences between experimental groups in highly dimensional data sets. CITRUS performs multiple sequential steps in order to achieve this. First, unsupervised hierarchical clustering of cellular events across multiple samples by phenotypic similarity along the lines of a defined set of markers is performed. Then biologically relevant features within these clusters of cellular events are calculated on a per file basis and the resulting tree of clusters annotated with this information. CITRUS then interrogates this dataset as to whether these clusters differ on a statistically significant level in terms of median expression of a defined set of markers different from the subset used to create the tree of clusters. This is achieved by the use of a correlative linearized regression model, significance analysis of microarrays. The analysis uses non-parametric statistics to test differences along the lines of user defined experimental groups. Repeated permutations of the data are used to determine whether the expression of any of these markers is significantly related to any of the experimental groups (955). The result is reported not by use of classical p-values but by utilizing false discovery rate. This approach is chosen because due to the multiple testing problem an adjustment of p-values is necessary. The use of more traditional techniques such as Bonferroni-correction reduces the number of false positives at the cost of also reducing the number of correctly identified true positive differences. The calculation of a false discovery rate thus has a higher power to detect truly significant differences. After excluding debris and B-cell subsets by manual gating 10000 events per individual were clustered. A minimum cluster size of 1% was chosen. To avoid the detection of false positives only differences with a false discovery rate <1% were reported. The medians were subsequently exported and analysed with the more classical Kruskal-Wallis test with Dunn's post test and correction for multiplicity.

2.7 Statistical considerations

Normality testing of the obtained data was performed using the D'Agostino-Pearson k^2 omnibus test. When a data was deemed to be normally distributed a one-way ANOVA with Turkey's post test and correction for multiplicity was used. In data sets not showing normal distribution the Kruskal-Wallis test with Dunn's post test and correction for multiplicity was used. A p value cutoff of less the .05 was used to define statistically significant findings. Prism Version 7.04 software (GraphPad, USA) was used for all statistical analyses

Target	Clone	Lanthanide Tag
F4/80	BM8	146Nd
Ly6G	1A8	141Pr
Ly6C	HK1.4	150Nd
CD11c	N418	142Nd
CD69	H1.2F3	145Nd
CD45	30-F11	89Y
CD11b	M1/70	147Sm
CD19	6D5	166 Er
CD25	3C7	151Eu
CD3e	145-2C11	165Ho
CTLA4	UC10-4B9	154Sm
CD62L	MEL14	160Gd
CD8a	53-6.7	168Er
TCRb	H57597	169Tm
NK1.1	PK136	170Er
CD44	IM7	171Yb
CD4	RM4-5	172Yb
B220	RA3-6B2	144 Nd
PD-1	J43	159Tb
PD-L1	10F.9G2	153Eu
LAG-3	C9B73	174Yb
Tim-3	RMT3-23	162Dy
Nkp46	29A1.4	167Er
KLRG-1	2F1	176Yb
PD-L2	122	156Gd
2B4	eBio244F4	149Sm
NKG2D	MI6	175Lu

Table 4: List of anti-mouse mass cytometry antibodies used.

.

3 Breeding and maintenance of TCL1 mice, BTK occupancy achieved by water bottle treatment with Ibrutinib or Acalabrutinib, induction of disease by adoptive transfer

3.1 Specific introduction

The Eµ-TCL1 model is the most commonly used mouse model of human CLL. The model is characterized by a penetrance of 100% (901). Eµ-TCL1 mice closely mirror the biology, microenvironment interactions, CLL associated T-cell dysfunction and role of PD-1/PD-L1 in induction of CLL associated T-cell deficiency (903-905, 907, 908). Moreover, Eµ-TCL1 mice have been shown to be a suitable platform to study the effects of BTK-inhibitors such as Ibrutinib and Acalabrutinib in the setting of CLL (910, 911). Transgenic animals generally develop full blown leukemia after 12 to 16 months making the use of ageing Eµ-TCL1 animals very time-consuming and costly. It is therefore very important to identify transgenic mice early on to avoid ageing false positive animals and to accurately assess disease load to avoid sacrificing animals prematurely. Adoptive transfer of CLL B-cells from a pool of ageing Eµ-TCL1 animals into syngeneic wildtype animals has been shown to be a reproducible platform to study the pathobiology of CLL and test novel treatment strategies (903, 907, 909, 956).

3.2 Goals and objectives

Our goal was to obtain a suitable pool of CLL-B-cells from ageing Eµ-TCL1 mice to be adoptively transferred into syngeneic wildtype animals. These animals were subsequently used to test the influence of Ibrutinib and Acalabrutinib treatment on T-cell function and assess the immunophenotype of the CLL microenvironment and develop a combination strategy of BTK inhibitor treatment and anti-PD-L1 immune checkpoint blockade with the goal of achieving optimal T-cell function in the microenvironment. We were aiming to demonstrate that by continuously applying either Ibrutinib or Acalabrutinib by water bottle at a concentration of 0.15 mg/ml in 2% HPBCD full occupancy of BTK could be achieved and this route of application was thus suitable to study the effects of these BTK inhibitors in vivo.

3.3 Specific methods

3.3.1 Genotyping

Animals were ear notched for identification and to obtain material for genotyping. The material was digested at 55 °C overnight in „tail buffer" (50mM TRIS pH 8.0 (Sigma, UK), 25mM EDTA disodium salt pH 8.0 (Sigma, UK), 100mM NaCl (Fisher Scientific, UK), 1%

sodium dodecyl sulfate (SDS) (Sigma,UK) and Proteinase K 20mg/ml (Roche Diagnostics, UK)). DNA was extracted using alcohol precipitation. Polymerase chain reactions (PCRs) were performed using the TCL1 primers (5'-3') GCCGAGTGCCCGACACTC (TCL1 Forward) and CATCTGGCAGCAGCTCGA (TCL1 Reverse). The Mouse beta globulin (MBG) gene was used as an internal positive control (5'-3') CAGCTCCTGGGCAATATGAT (MBG Forward) and TTGTTCACAGGCAAGAGCAG (MBG Reverse). A negative control not containing DNA was also utilized. 1µl of DNA, 2µl of TCL1 Forward and Reverse and 2µl of MBG Forward and Reverse each were filled up with megamix blue PCR mix (Clent Life Science, UK) to a total volume of 25µl. The following PCR conditions were used for both reactions: Activation at 95°C (5 min), denaturation at 95°C (30 sec), annealing at 58°C (30 sec) and extension at 72°C (30 sec) for 35 cycles followed by final extension at 72°C (5 min). The obtained products, the corresponding controls and a 100bp DNA ladder (Life Technologies, UK) were applied on a 2% agarose gel containing 1x gel red at 80 V for 45 minutes for separation.

3.3.2 Haematology testing

In ageing Eµ-TCL1 mice haematology testing was routinely initiated at the age of 6 months and conducted monthly to biweekly. Experimental animals were tested weekly from the day of adoptive transfer of CLL B-cells. The animals were heated under a heat lamp and put in a restrainer. To obtain blood, a 19G needle (BD, UK) was used to puncture the lateral tail vein. Approximately 100µl of peripheral blood were collected in a 0,5 ml microcentrifuge tube (VWR, UK) containing 10 µL of 0.5 M EDTA (Sigma, UK). For preparation of blood smears 10 µl of peripheral blood were pipetted on a microscope slide (VWR, UK) and smeared using an additional slide. Slides were preserved in methanol (Fisher scientific, UK) for 30s, then stained in modified Wright stain (Sigma, UK) for 40s and washed in deionized water (Milipore, Merck, UK) for 45s. Slides were rinsed in deionized water (Milipore, Merck, UK) and allowed to air dry. For hematologic assessment the WBC count was estimated by counting 5- 10 hpf using a 40x objective of a bright field microscope (Zeiss, UK). For flow cytometry-based analysis 20µl of peripheral blood were filled up with FACS buffer (PBS (Sigma, UK) with 2% FCS (Gibco, UK)) to 100µl in 15 ml centrifuge tube (VWR, UK). The following flurochrome-labelled antibodies were added at a ratio of 1:100: Anti mouse CD45 APC (clone 30-F11, eBioscience, UK), anti-mouse CD19 FITC (clone 1D3, ebioscience, UK) and anti-mouse CD5 PE-Cy7 (clone 53-7.3, biolegend, UK). Cells were incubated for 30 minutes at 4°C. 1ml of FACS buffer was added and cells were centrifuged at 300g for 10 minutes at 4°C.

The supernatant was decanted and the washing step repeated. Erythrocytes were then lysed in 5ml 1X ammonium-chloride-based RBC lysis buffer (NH4CL 8.3g/l (Sigma, UK), KHCO3 1g/l (Sigma, UK), EDTA 0.037g/l (Sigma, UK)). After 7 minutes incubation, 10 ml of PBS were added and centrifuged at 300g for 10 minutes at 4°C, resuspended in 300µl FACS buffer containing 1:1000 DAPI (ebioscience, UK) and transferred to 5 ml polypropylene round bottom tubes (Corning, UK). Cellular events were then recorded on a BD LSR Fortessa flow cytometer (BD Biosciences, UK). The analysis was conducted using Cytobank (Cytobank Inc, USA).

3.3.3   Processing of mouse spleens into a single cell suspension

Mouse spleens were removed immediately after euthanizing the animals by cervical dislocation. The removal of the organ was performed under sterile conditions in a BSU procedure room. Spleens were transported in PBS (Sigma, UK) containing 20% FCS (Gibco, UK) and kept on ice. The GentleMACS tissue dissociator (Miltenyi, UK) was utilized for preparation of single suspension according to the manufacturer's recommendations for mouse spleen processing without enzymatic treatment. Subsequently the lysis of erythrocytes with an ammonium-chloride-based RBC lysis buffer (NH4CL 8.3g/l (Sigma, UK), KHCO3 1g/l (Sigma, UK), EDTA 0.037g/l (Sigma, UK)) was performed. Centrifugation of cell suspensuions was generally performed at 300g for 10 minutes at 4°C. The cells in the obtained single cell solutions were quantified using a Luna fl automated cell counter (Logos bioyssstems, USA) after dilution of a 10µl aliquot with an equal amount of 0.4% Tryphan blue (Sigma, UK). Splenocytes were then cryopreserved at a maximum density of 200×10^6 cells/ml in FCS (Gibco, UK) containing 10% dimethyl sulfoxide (DMSO) (Fisher Scientific, UK) and kept in a suitable liquid nitrogen storage tank.

3.3.4   Cell thawing procedure

Thawing of cryopreserved splenocyte samples was performed in a water bath at 37°C. To avoid contamination the vials were disinfected using 70% industrial methylated spirit (IMS) (Fisher Scientific, UK) and subsequently opend in a class II biosafety cabinet. The cell suspension was pipetted into 10ml RPMI 1640 (Gibco, UK) supplemented with 10% FCS (Gibco, UK), 1% Penicillin-Streptomycin (Sigma, UK) at 37°C. Subsequently the suspension was centrifuged at 300 x g for 10 minutes at room temperature and resuspended in a volume suitable for number of cells contained in the pellet. Automated cell counting was conducted on a Luna fl automated cell counter (Logos bioystems, USA) after dilution of a 10µl aliquot with an equal amount of 0.4% Tryphan blue (Sigma, UK).

3.3.5   Negative selection of CLL and B cells

T-cells where isolated from splenocytes suspensions using the pan-B-cell isolation kit II (Miltenyi, UK) which uses MACS. The suspension were centrifuged at 300 x g for 10 minutes at 4°C, the supernatant completely aspirated and the pellet resuspendend in 40 µL of ice-cold MACS buffer (PBS (Sigma, UK) pH 7.2, 0.5% BSA (Sigma, UK), 2mM EDTA (Sigma, UK)) per 10^7 total cells. 10 µL of Pan B Cell Biotin-Antibody Cocktail (Miltenyi, UK) per 10^7 total cells were added. The cells were well mixed and incubated for 5 minutes at 4°C. A further 30 µL of ice-cold MACS buffer per 10^7 total cells and 20 µL of Anti-Biotin MicroBeads (Miltenyi, UK) per 10^7 cells were added. Cells were mixed well and incubated for another 10 minutes at 4°C. Finally, the volume was adjusted to 500µl per 10^8 cells (minimum 500µl). For separation, a LD column (Miltenyi, UK) was placed in the magnetic field of a MACS separator (Miltenyi, UK) and primed with 2 ml of MACS buffer. The cell suspension was applied to the column and flushed through by applying 1ml MACS buffer twice. The effluent, which was collected in a 15 ml centrifuge tube (VWR, UK), contained the unlabelled pan-T-cell fraction..

3.3.6   Adoptive transfer of CLL B-cells

$4x10^7$ syngeneic mouse CLL B-cells derived from cryopreservation were injected by tail vein injection in accordance to standard procedures (952). Prior to the injection the content of CD19+CD5+ CLL B-cells in the splenocytes suspensions was measure using flow-cytometry. A maximum volume of 5ml/kg was injected per animal. We used C57BL/6 wild type animals 2.5 months of age as recipients Following the adoptive transfer procedure animals were closely monitored by inspection and physical examination. The CLL disease status was quantified weekly using peripheral blood smears and flow cytometry. The animals where culled once the showed sign of poor health or fulfilled one of the following endpoint criteria: spleen size >3cm in diameter, WBC count in blood smear >100 WBC/hpf (40x objective), >90% of lymphocytes CD19+CD5+ CLL cells. Euthanization was performed using cervical dislocation.

3.3.7   Application of experimental substances by water bottle preparation or i.p. injection

Ibrutinib (kindly provided by Janssen pharmaceuticals) and Acalabrutinib (kindly provided by Acerta pharma) were applied via water bottle preparation at a concentration of 0.15mg/ml in 2% HPBCD (Sigma, UK). Water bottle preparations were prepared under sterile conditions and sterile filtered through a 0.2 µm PES filter top (Thermofisher scientific, UK) before application. Anti mouse PD-L1 clone 80 mIgG1 D265A (equivalent

to Durvalumab, kindly provided by Astra-Zeneca) or isotype control NIP228 mIgG1 D265A (kindly provided by Astra-Zeneca) were applied by i.p. injection at a dose of 10mg/kg every 3 days. A maximum volume of 10 ml/kg was used for i.p. injections. Prior to i.p. injections aqueous stock solutions of antibodies were obtained by dissolving the antibody in sterile PBS and under sterile conditions. During the treatment periods the animals were assessed daily by physical examination and culled at predefined endpoints.

3.3.8   BTK occupancy assays

96 well microplates (PerkinElmer, UK) were coated overnight at 4°C with 125 ng/well anti-BTK antibody (Clone 53/BTK, BD Biosciences) and blocked with BSA (Gibco, UK) the following day for 2 to 3 hours at room temperature. Lysis buffer containing protease inhibitor cocktail (Sigma, UK) was used to lyse frozen splenocyte cell pellets. Lysates were incubated for 1 hour on ice in the presence or absence of a saturating concentration of Ibrutinib or Acalabrutinib (10^{-6} mol/L) followed by an incubation of a biotinylated derivate (ACP-4016; 10^{-7} mol/L) serving as a probe. The equivalent of 5×10^5 cells of lysate/well, in replicates of three, were added to the coated OptiPlates and incubated for 2 hours. After a 1-hour incubation with HRP (Invitrogen, UK; ELISA grade; 120 ng/mL), a SuperSignal ELISA Femto Substrate (Thermo Fisher Scientific, UK) was added, and chemiluminescence was measured on a multiplate reader (PerkinElmer, UK). The percentage of BTK occupancy for the drug-treated mice was calculated relative to the average signal from the vehicle control group. The samples without exogenous Ibrutinib or Acalabrutinib represented 100% free BTK (or 0% occupied BTK), and the samples with exogenous BTK inhibitor represented 0% free BTK (or 100% occupied BTK).

3.4   Results

3.4.1   Breeding of Eμ-TCL1 animals and genotyping of mouse litters

All animals resulting from the breeding of Eμ-TCL1 animals were genotyped to identify transgenic animals early on. Figure 4 shows an example of genomic PCR results from 9 different littermates. The housekeeping gene MBG was utilized to confirmed the quality of the extracted genomic DNA. MBG is visualized as a 194 bp band in gel electrophoresis. The bands at 350 bp illustrate the presence or absence of the TCL1 trangene. Eμ-TCL1 transgenic males were bred with a harem of 2 C57BL/6 transgenic females. Pairing of the breeders occurred at 6-8 weeks of age and breeding was continued for a maximum of 10 months or until no new litters were born for at least 2 months. The mouse littes were weaned when reaching 3-4 weeks of age, ear notched

and genotyped. The animals were housed in groups of a maximum of 5 littermates. Pairing a transgenic Eµ-TCL-1 male with syngeneic wildtype females usually yielded approximately 50% transgenic pups. Theoretically Eµ-TCL1 mice could also be bred with each other as transgene homozygosity is not fatal. We did, however, refrain from this strategy as to prevent the occurance of sub-strains over time and and ascertain control of TCL1 lines derived from specific index animals as suggested by the good practise guidelines on the maintenance of transgenic mouse strains (957). Wildtype littermates were culled after obtaining genotyping results while transgenic animals were allowed to age and closely monitored for the development of CLL. Animals were culled when found to be fully leukemic at around 12-16 months of age, the spleens harvested, processed to single cell suspensions and cryopreserved in liquid nitrogen for subsequent adoptive transfer experiments.
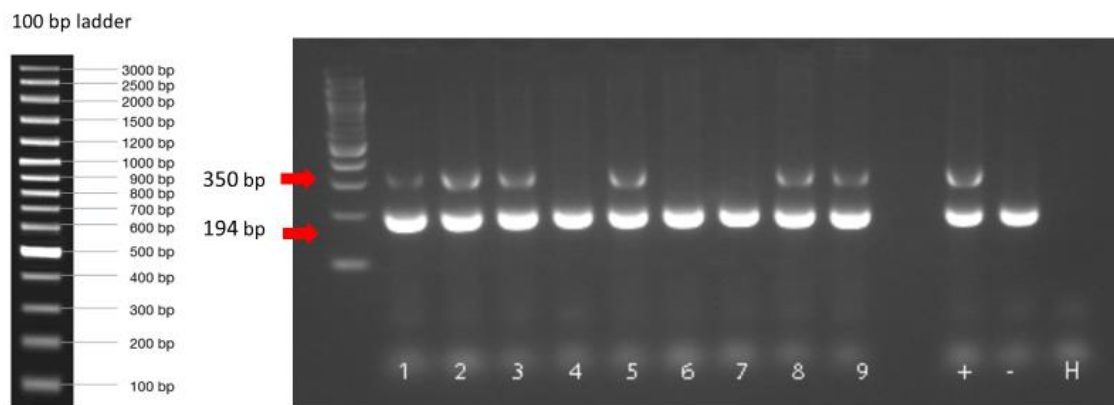
Figure 4: Genotyping procedure to maintain the Eµ-TCL1 colony. Genomic DNA was expanded with TCL1 and MBG primers. MBG bands at 194 bp demonstrate the quality of the extracted DNA, TCL1 bands at 350 bp demonstrated the presence of the Eµ-TCL1 transgene. A positive control with known presence (+) and a negative control with known absence (-) of the transgene as well as a no-template control containing only water (H) were included.

3.4.2 BTK occupancy achieved by water bottle treatment with Ibrutinib and Acalabrutinib

We aimed to determine whether treatment of mice with Ibrutinib and Acalabrutinib by water bottle preparation would yield adequate occupancy of BTK for further experiments. The animal experiment conducted is summarized in Figure 5. Briefly, 4 C57BL/6 wildtype animals (2 males, 2 females) per group with an age of 2.5 months were treated with Ibrutinib or Acalabrutinib by water bottle preparation at a concentration of 0.15 mg/ml in 2% Hydroxpropyl beta-cyclodextrin or vehicle control only for 5 days. Animals were then sacrificed, spleens harvested and single cell splenocyte preparations obtained.
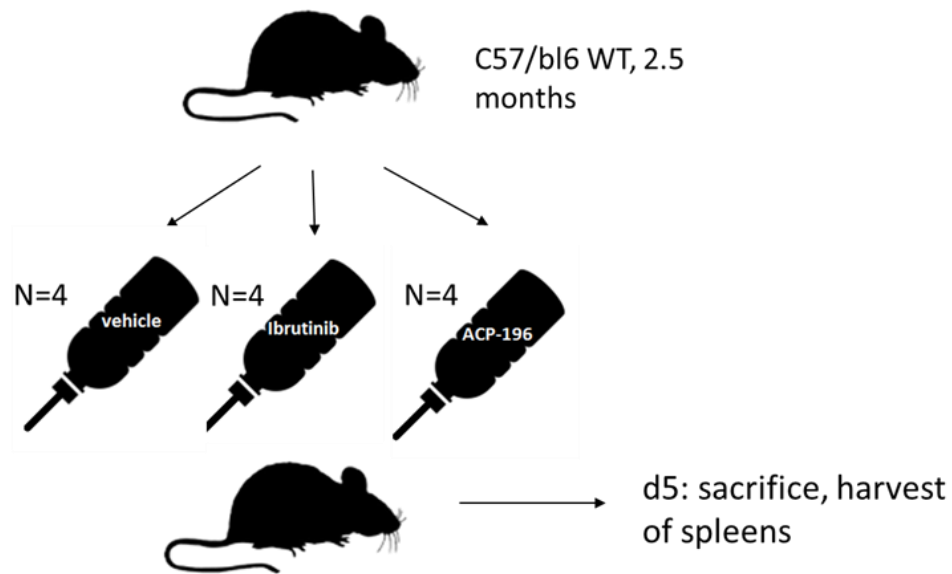
Figure 5: Animals experiment for measurement of BTK occupancy using water bottle preparations of Ibrutinib and Acalabrutinib. 4 animals per group 2.5 months of age were treated with 0.15 mg/ml Ibrutinib in 2% HPBCD, Acalabrutinib (ACP-196) in 2% HPBCD or 2% HPBCD (vehicle) only for 5 days. *Abbreviations: WT- wild type.*

The single cell splenocyte preparations were subsequently subjugated to the BTK occupancy assay described under 3.3.8. Figure 6 illustrates the BTK occupancy achieved with Ibrutinib or Acalabrutinib treatment by water bottle preparation. The readout of the assay is % of free BTK. The percentage of BTK occupancy was calculated relative to the average signal from the vehicle control group. The samples without exogenous Ibrutinib or Acalabrutinib represent 100% free BTK (or 0% occupied BTK), and the samples with exogenous Ibrutinib or Acalabrutinib represent 0% free BTK (or 100% occupied BTK). A BTK occupancy of 90% and 95.9% respectively were reached after 5 days of treatment with Ibrutinib and Acalabrutinib. ≥90% of occupancy of available target is generally considered full occupancy of the receptor (958).

Group	% Occupied BTK	SD
Vehicle	0%	18.3562
Ibrutinib	90.0%	2.6862
Acalabrutinib	95.9%	0.9381
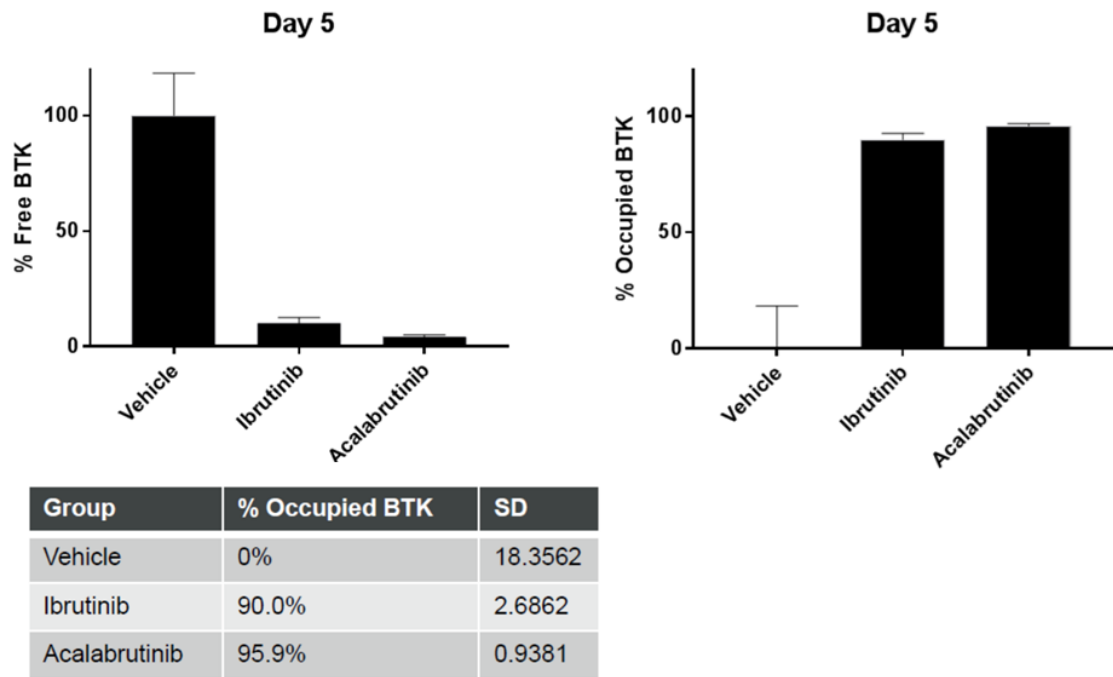
Figure 6: BTK occupancy after 5 days of Ibrutinib or Acalabrutinib treatment by water bottle preparation. The readout of the assay is % of free BTK. The percentage of BTK occupancy was calculated relative to the average signal from the vehicle control group. 3 groups n=4 each. *Abbreviations: SD – standard deviation.*

3.4.3 Adoptive transfer experiments for assessment of influence of Ibrutinib and Acalabrutinib on T-cell function and immunephenotype

Animal experiments in order to obtain samples for subsequent immunophenoypic and functional analysis were conducted as summarized in Figure 7. In short C57BL/6 wildtype animals 2.5 months of age were injected with 4×10^7 syngeneic CLL B-cells from the same donor pool of syngeneic CLL B-cells purified from Eμ-TCL1 transgenic spleens of CLL bearing ageing individuals. Groups were equally split into male and female individuals. Peripheral blood was analysed by blood smears for estimation of the WBC and flowcytometry once weekly. Peripheral blood load of CD5+CD19+ CLL cells exceeded 10% after 2 weeks. At this point animals were randomized to 3 treatment groups consisting of 17 animals each: vehicle treatment (2% HPBCD), Ibrutinib treatment (0.15 mg/ml Ibrutinib in 2% HPBCD) or Acalabrutinib (0.15 mg/ml ACP-196 in 2% HPBCD). Animals were sacrificed after 3 weeks of treatment and spleens harvested.
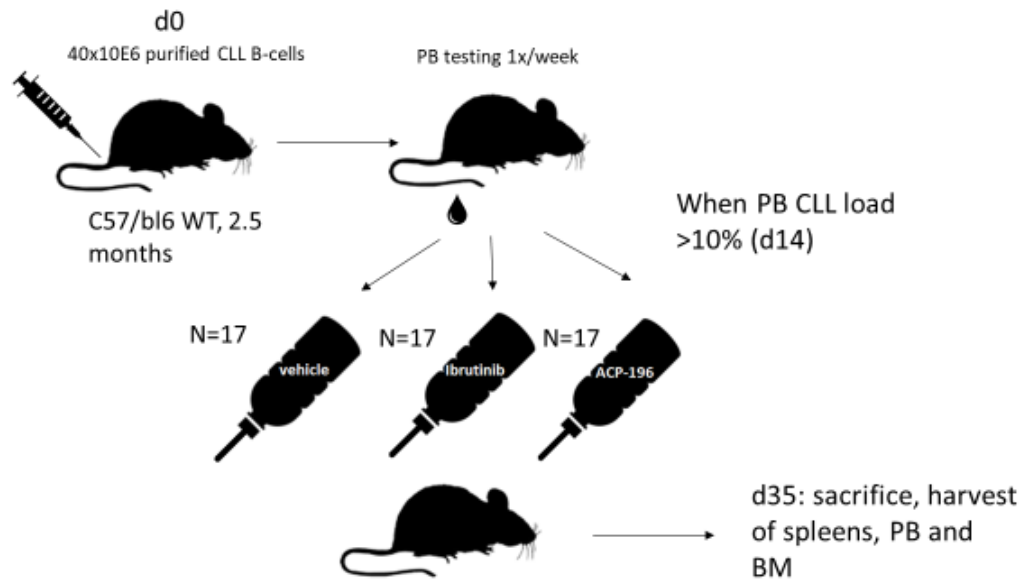
Figure 7: Adoptive transfer experiments for assessment of influence of Ibrutinib and Acalabrutinib on T-cell function and immunephenotype. C57BL/6 wildtype animals 2.5 months of age were adoptively transferred with 4x107 CLL B-cells. Peripheral blood CLL B-cell load was assessed weekly by flow cytometry. When peripheral blood CLL load exceeded 10% (day14) animals were randomized to 3 groups (17 animals each): 0.15 mg/ml Ibrutinib in 2% HPBCD, Acalabrutinib (ACP-196) in 2% HPBCD or 2% HPBCD (vehicle) for 3 weeks. *Abbreviations: wt- wild type, PB – peripheral blood.*

Figure 8A illustrates the flowcytometry assessment of peripheral blood CLL load. CD5+CD19+ events constitute the CLL B-cell population. CLL B-cell load exceeded 10% 14 days after adoptive transfer. Figure 8 B is depicting the load of CD5+CD19+ CLL cells in the peripheral blood from animals of all 3 treatment groups on day 14. Peripheral blood CLL loads were comparable in all 3 groups (no statistically significant differences detected, p=0.5218) demonstrating an equal disease burden at treatment initiation.

Blood smears from CLL bearing adoptively transferred animals showed elevated numbers of mature appearing, enlarged lymphocytes with dense nuclear chromatin structure. Similar to blood smears in human CLL patients, smudge cells were seen as an artefact of the smear preparation (Figure 9A). Figure 9B demonstrates the course of peripheral blood WBC in all 3 treatment groups. Intially an exponential increase in WBC in the peripheral blood occured. This continued unabated in the vehicle treated animals while in both Ibrutinib and Acalabrutinib treated animals a plateau around 20/hpf was reached after 1 week of treatment corresponding to approximately 25000-35000 WBC/µl. On day 28 of the experiment a statiscally significant difference was reached between vehicle treated and Ibrutinib/Acalabrutinib treated animals (p<0.0001).
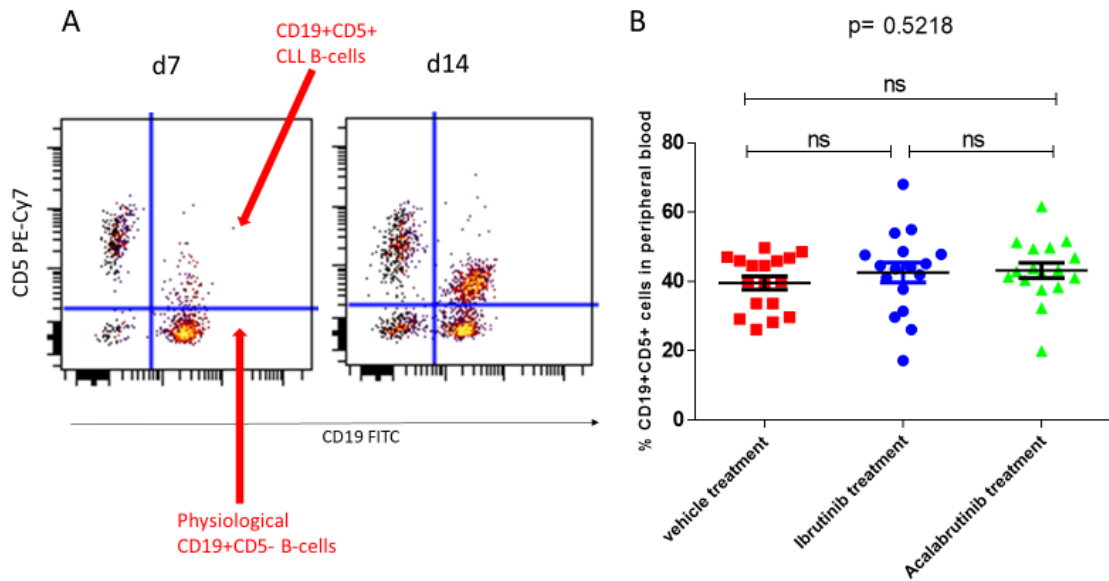
Figure 8: Disease burden in all 3 treatment groups on the day of treatment initiation (d14) assessed by flow cytometry. (A) Example of flow cytometry graphs in peripheral blood C57BL/6 mice adoptively transferred with syngeneic CLL B-cells. Whole blood was stained with anti-CD45, anti-CD19, anti-CD5 and DAPI. Cells were gated on CD45+ viable lymphocytes **(B)** CD19+CD5+ CLL B-cell load at day 15 following adoptive transfer. No statistically significant differencens were detected between treatment groups (p=0.5218). Statistical analysis by 1way Anova. 3 groups n=17 each. *Abbreviations: Ns – not significant, p > 0.05; * - p ≤ 0.05; ** - p ≤ 0.01; *** - p ≤ 0.001; **** - p≤ 0.0001.*
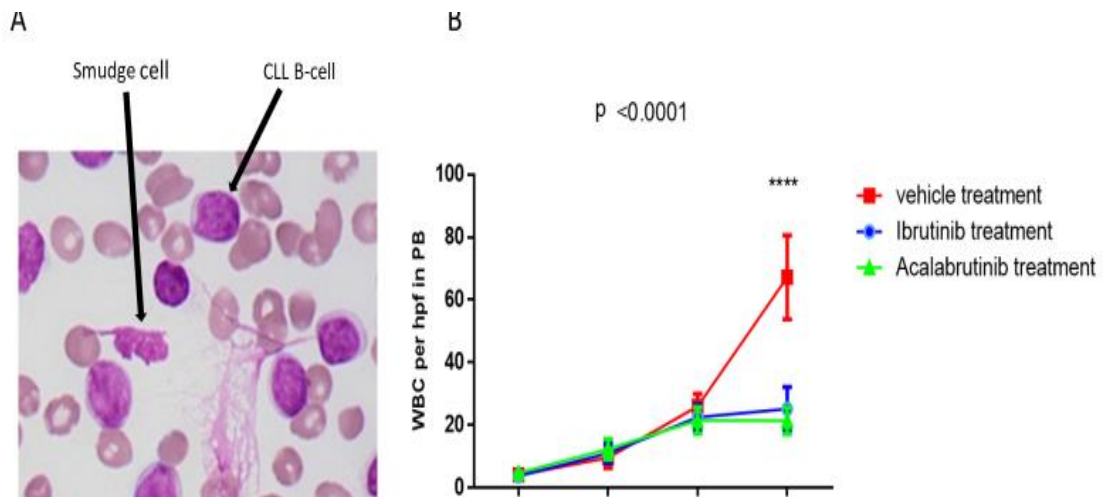
Figure 9: Course of WBC in peripheral blood of vehicle treated, Ibrutinib treated and Acalabrutinib treated animals. (A) Peripheral blood smear of a CLL bearing animal. Smears were stained with a modified Wright stain and leukocytes were counted using a bright field microscope in 5-10 hpf of a 40x objective in a suitable portion of the smear. CLL B-cells were characterized by large size and dense cluttered chromatin structure. Smudge cells could be found. **(B)** Illustration of the course of peripheral blood WBC in all 3 treatment groups. In vehicle treated animals exponential increase of WBC continues unabated. In Ibrutinib and Acalabrutinib treated animals a plateau ~ 20/hps is reached. (p<0.0001). Statistical analysis by Kruskal-Wallis test. 3 groups n=17 each. *Abbreviations: Ns – not significant, p > 0.05; * - p ≤ 0.05; ** - p ≤ 0.01; *** - p ≤ 0.001; **** - p≤ 0.0001; PB – peripheral blood.*

The morphology of the abdominal situs of untreated mice with fully developed CLL following adoptive transfer on day 35 is depicted in Figure 10A. Similar to human CLL patients marked hepatosplenomegaly was observed. Figure 10 B demonstrates spleen weight and spleen size on day 35 after adoptive transfer when animals were sacrificed. Both Ibrutinib and Acalabrutinib treatment reduced spleen size and spleen weight to a similar extent following 3 weeks of treatment compared to vehicle treated animals. The detected differences were statistically significant (p<0.0001).
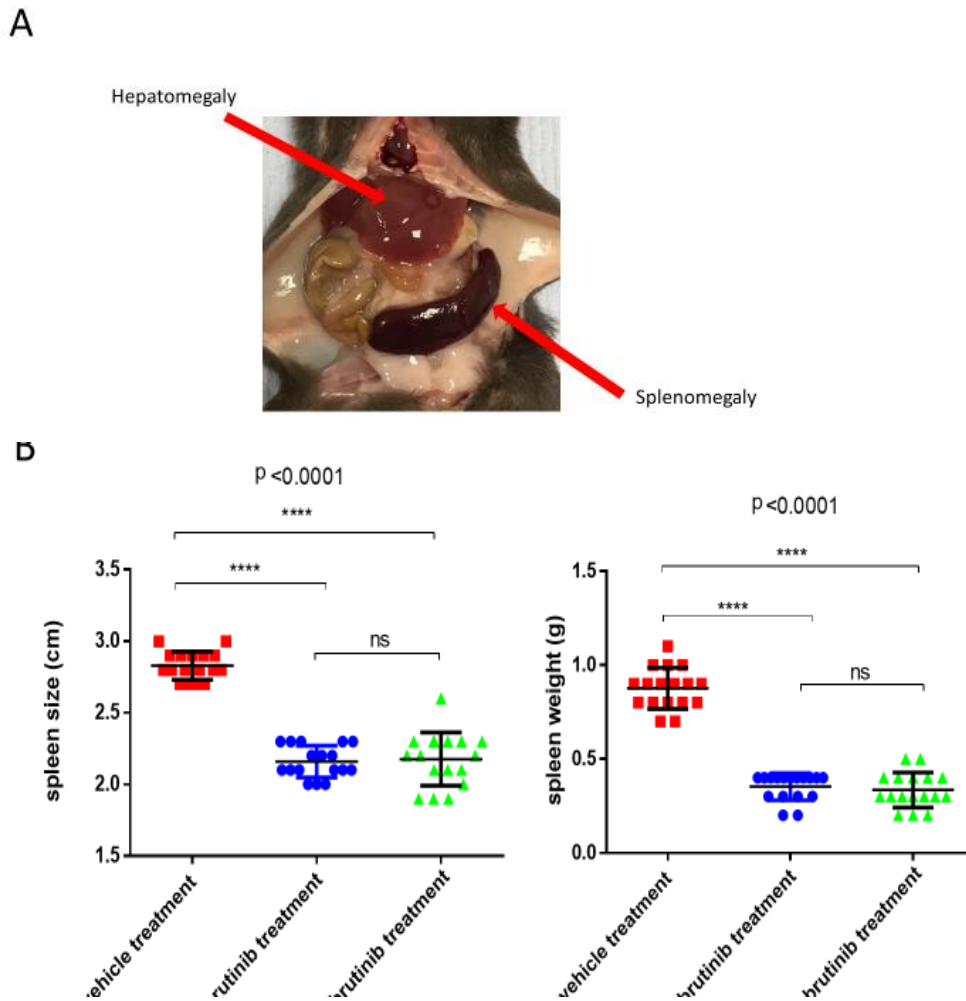
Figure 10: Spleen size and spleen weight at d 35 in vehicle treated and BTK inhibtor treated animals. (A) Mice developed hepatomegaly and splenomegaly with the onset of CLL **(B)** Spleen size and spleen weight on day 35 after adoptive transfer in all 3 treatment groups. Both Ibrutinib and Acalabrutinib treatment decreases spleen size and weight to a similar extent compared to vehicle treated animals. The findings were statiscally significant (p < 0.0001). Statistical analysis by 1way Anova.3 groups n=17 each. *Abbreviations: Ns – not significant, p > 0.05; * - p ≤ 0.05; ** - p ≤ 0.01; *** - p ≤ 0.001; **** - p≤ 0.0001.*

3.4.4 Adoptive transfer experiments for development of a BTK inhibitor anti-PD-L1 combination strategy

In a second adoptive transfer experiment we aimed to obtain splenocyte samples to assess the effect of BTK inhibitor and anti-PD-L1 immune checkpoint blockade on T-cell function and immune phenotype of the CLL microenvironment. The experiment is summarized in Figure 11. In short, C57BL/6 wildtype animals 2.5 months of age were injected with 4×10^7 syngeneic CLL B-cells from the same donor source of syngeneic CLL B-cells derived from ageing Eµ-TCL1 animals. Haematology testing of peripheral blood was conducted once weekly. Peripheral blood load of CD5+CD19+ CLL cells assessed by flow cytometry exceeded 10% after 2 weeks – animals were randomized to 6 treatment groups consisting of 17 animals each: vehicle treatment (2% Hydropropyl beta-cyclodextrin) Ibrutinib treatment (0.15 mg/ml Ibrutinib) or Acalabrutinib (0.15mg/ml) in combination with either antibody isotype control (NIP228 mIgG1 D265A) or anti-PDL1 antibody (anti mouse PD-L1 clone 80 mIgG1 D265A) at a dose of 10 mg/kg *every 3 days* (q3d) i.p. Animals were sacrificed after 3 weeks of treatment and spleens harvested.
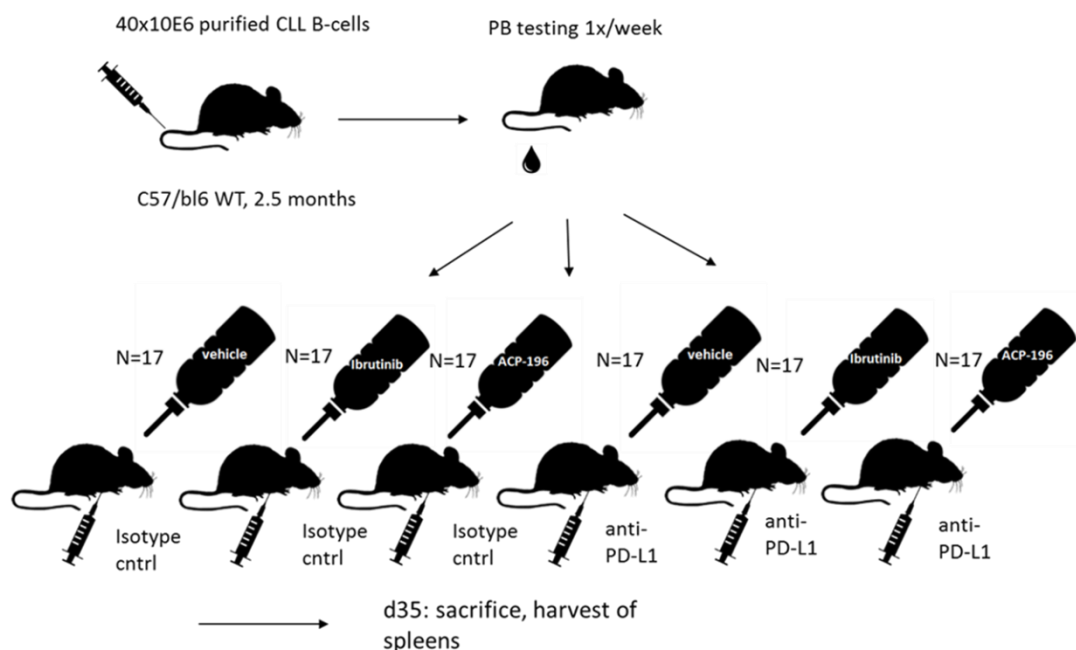
Figure 11: Adoptive transfer experiments for development of a BTK inhibitor anti-PD-L1 combination strategy. C57BL/6 wildtype animals 2.5 months of age were adoptively transferred with 4x107 CLL B-cells. Peripheral blood CLL B-cell load was assessed weekly by flow cytometry. When peripheral blood CLL load exceeded 10% (day14) animals were randomized to 6 groups (17 animals each): 2% HPBCD (vehicle) + NIP228 mIgG1 D265A 10mg/kg q3d, 0.15 mg/ml Ibrutinib in 2% HPBCD + NIP228 mIgG1 D265A 10mg/kg q3d, Acalabrutinib (ACP-196) in 2% HPBCD + NIP228 mIgG1 D265A 10mg/kg q3d, 2% HPBCD (vehicle) + anti mouse PD-L1 clone 80 mIgG1 D265A 10 mg/kg q3d, 0.15 mg/ml Ibrutinib in 2% HPBCD + anti mouse PD-L1 clone 80 mIgG1 D265A 10 mg/kg q3d, Acalabrutinib (ACP-196) in 2% HPBCD + anti mouse PD-L1 clone 80 mIgG1 D265A 10 mg/kg q3d for 3 weeks. *Abbreviations: wt- wild type, PB – peripheral blood.*

Figure 12 shows the peripheral blood CLL B-cell load as assessed by flow cytometry on day 15 following adoptive transfer, right before treatment initiation. No statistically significant differences between treatment groups were detected at this point in time, indicating an equal disease burden before treatment initiation.
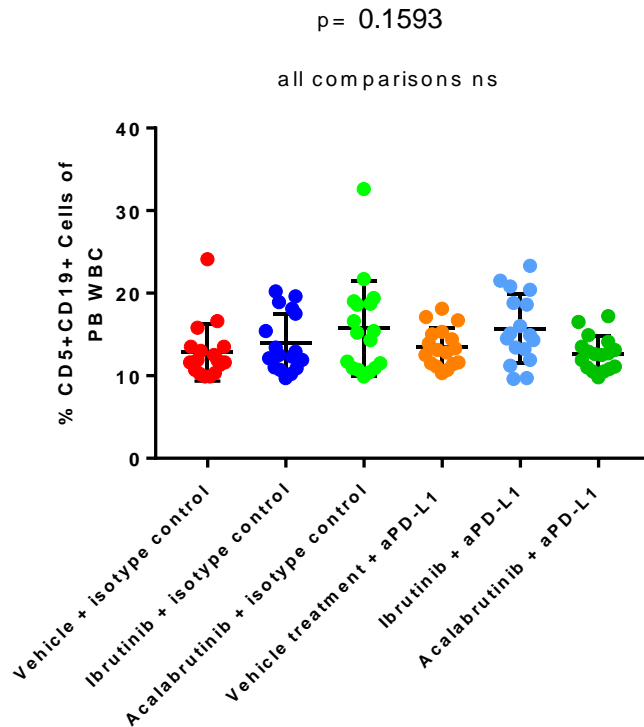
Figure 12: Disease burden in all 6 treatment groups on the day of treatment initiation (d14) assessed by flow cytometry. CD19+CD5+ CLL B-cell load at day 15 following adoptive transfer. Statistical analysis by Kruskal-Wallis-test. 6 groups n=17 each. No statistically significant differencens were detected between treatment groups (p=0.1593). *Abbreviations: Ns – not significant, p > 0.05; * - p ≤ 0.05; ** - p ≤ 0.01; *** - p ≤ 0.001; **** - p≤ 0.0001; PB – peripheral blood; aPD-L1 – anti PD-L1.*

Figure 13 shows the development of WBC in the peripheral blood of adoptively transferred animals in all 6 treatment groups. As with the initial experiment, in vehicle treated animals the exponential increase of WBC continued unbated while in Ibrutinib and Acalabrutinib treated animals a plateau around 20/hpf (corresponding to 25000-35000 WBC/µl) was reached. In animals treated with single agent anti-PD-L1 immune checkpoint blockade, an exponential increase with a slightly lower slope compared to vehicle treated animals was observed. Mice treated with combinations of Ibrutinib or Acalabrutinib and anti-PD-L1 antibodies did not differ from those treated with single agent BTK inhibitors in terms of the course of peripheral blood WBC. All differences reached statistical significance on day 28 following adoptive transfer (p<0.0001).

.

p <0.0001
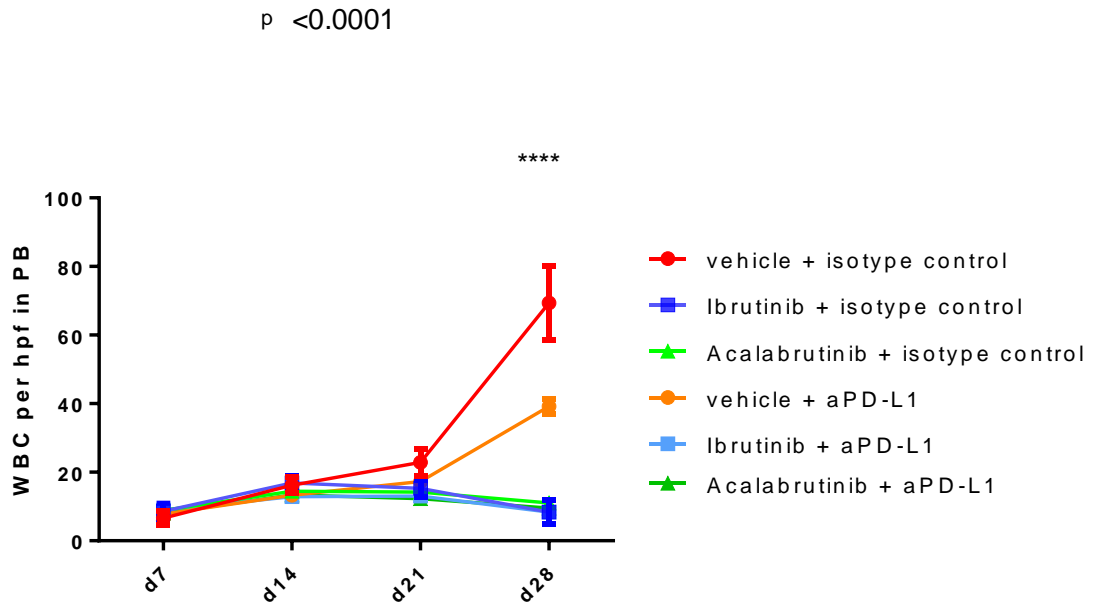
Figure 13: Course of WBC in peripheral blood of BTK inhibitor/anti-PD-L1 combination treated animals. Illustration of the course of peripheral blood WBC in all 6 treatment groups. In vehicle/isotype control treated animals expontenial increase of WBC continues unabated. In Ibrutinib and Acalabrutinib treated animals a plateau ~ 20/hps is reached. In single agent anti-PD-L1 treated animals the slope of the increase is decreased. Combinations of BTK inhibitor and anti-PD-L1 do not differ from single agent BTK inhibitor (p<0.0001). Statistical analysis by Kruskal wallis test. 6 groups n=17 each. *Abbreviations: Ns – not significant, p > 0.05; * - p ≤ 0.05; ** - p ≤ 0.01; *** - p ≤ 0.001; **** - p≤ 0.0001; PB – peripheral blood.*

Spleen weights and sizes have been documented in all animals after being sacrificed on day 35 following adoptive transfer. Results are visualized in Figure 14 A and B. Single agent anti-PD-L1 treatment did not significantly affect spleen size or spleen weight compared to vehicle/isotype control treatment. Ibrutinib and Acalabrutinib decreased spleen size and weight to similar extent. The combinations of Ibrutinib or Acalabrutinib and anti-PD-L1 antibody did not result in a further reduction of spleen size and weight (p < 0.0001). However, it should be noted that disease control with single agent Ibrutinib or Acalabrutinib was already quite far reaching with spleen weight and size approaching those of wild type animals in this experiment. A further clinically appreciable effects may thus be difficult to obtain with the treatment combinations.
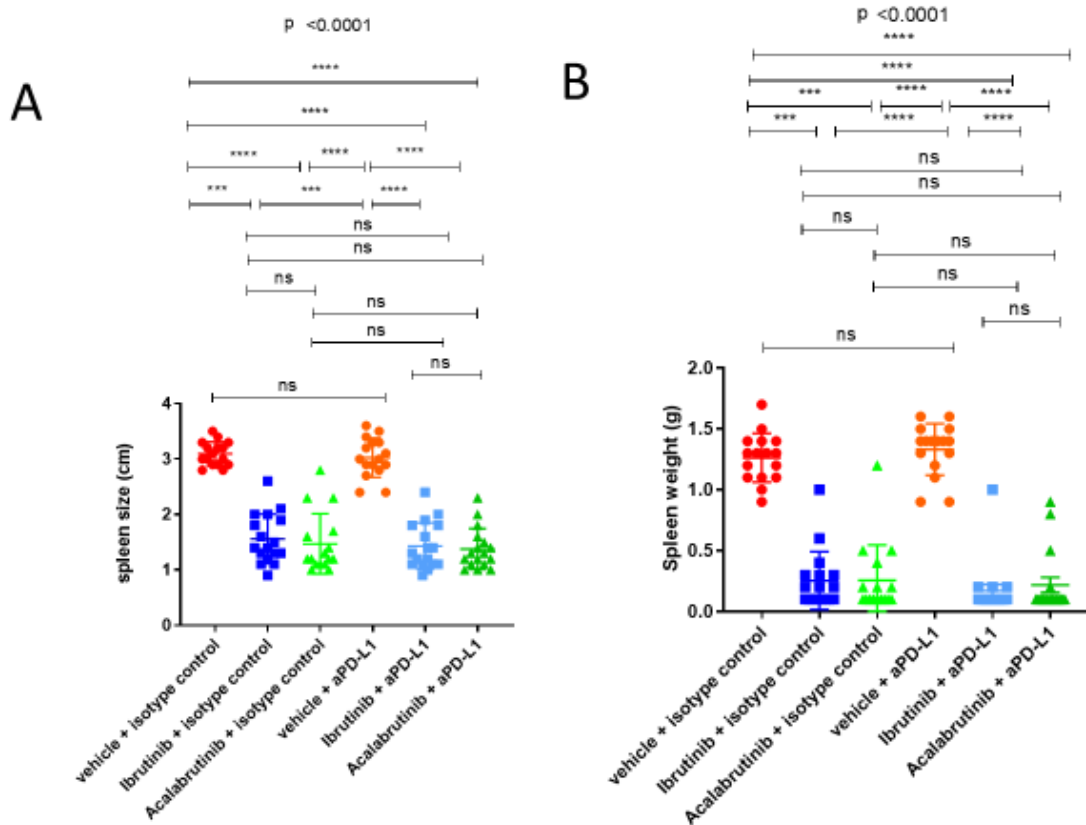
Figure 14: Spleen size and spleen weight at d 35 in BTK inhibitor/anti-PD-L1 combination treated animals. **(A)** Illustration of spleen sizes of animals in all 6 treatment groups. Single agent anti-PD-L1 does not affect spleen size significantly. Single agent Ibrutinib or Acalabrutinib as well as BTK inhibitor/anti-PD-L1 combinations decrease spleen size to a similar extent (p < 0.0001) **(B)** Illustration of spleen weights of animals in all 6 treatment groups. Single agent anti-PD-L1 does not affect spleen size significantly. Single agent Ibrutinib or Acalabrutinib as well as BTK inhibitor/anti-PD-L1 combinations decrease spleen weights to a similar extent (p < 0.0001). Statistical analysis by Kruskal-Wallis test. 6 groups n=17 each. *Abbreviations: Ns – not significant, p > 0.05; * - p ≤ 0.05; ** - p ≤ 0.01; *** - p ≤ 0.001; **** - p≤ 0.0001.*

3.5   Discussion

Our efficient colony of ageing Eµ-TCL1 transgenic mice as well as our well-established procedures for genotyping, hematology assessment of animals and splenocyte manipulation allowed us to quickly obtain a sufficiently large pool of splenocytes from CLL bearing transgenic individuals for the adoptive transfer experiments planned. Before initiation of these pre-clinical intervention trials we sought to confirm that oral administration of Ibrutinib and Acalabrutinib by water bottle would lead to sufficient BTK blockade in vivo. Our BTK occupancy experiments in C57BL/6 wildtype animal showed a BTK occupancy of 95.9% and 90% respectively for water bottle treatment with Ibrutinib and Acalabrutinib at a concentration of 0.15 mg/ml. The average occupancy measured was somewhat higher for Acalabrutinib compared to Ibrutinib treatment, however. Indeed, in the literature higher first past metabolism and lower oral bioavailability has

been described for Ibrutinib compared to Acalabrutinib (959, 960). This may explain the slightly lower BTK occupancy observed for Ibrutinib treatment in these experiments. Still, as ≥90% of occupancy of available target is generally considered full occupancy of the receptor we have confirmed adequate BTK blockade for oral administration of both substances by water bottle at the reported dose (958).

We have previously established optimized and standardized adoptive transfer procedures that reliably replicate the CLL disease phenotype in previously disease-free syngeneic wildtype animals. By using a cell dose of $4x10^7$ CLL B-cells injected intravenously via the tail vein we have achieved a latency of disease development of approximately 2 weeks while fully developed leukemia is observed at approximately 7 weeks after adoptive transfer. This leaves a suitable window to study the influence of novel CLL treatments on the immune microenvironment. Animals 2.5 months of age were chosen to avoid ageing related changes of T-cell phenotype and function which could interfere with the outcome of the subsequent functional and phenotypic assessment. In a first adoptive transfer experiment animals were treated with either Ibrutinib or Acalabrutinib at a concentration of 0.15 mg/ml via water bottle treatment. Both BTK inhibitors showed similar potential to control peripheral blood as well as spleen CLL load in these experiments. In a second round of adoptive transfer experiments animals were treated with single agent Ibrutinib, Acalabrutinib or anti-PD-L1 immune checkpoint blockade as well as combinations of the BTK inhibitors and anti-PD-L1 antibodies. Similar to the initial experiments both Ibrutinib and Acalabrutinib showed efficacy in controlling the peripheral blood and spleen CLL load. Single agent anti-PD-L1 antibody demonstrated no effects on spleen sizes and weights and only a modest effect on peripheral blood CLL B-cell load. This is in contrast to our previous study showing a complete blockade of CLL development in the Eµ-TCL1 adoptive transfer model with anti-PD-L1 immune checkpoint blockade (836). However, it should be noted that anti-PD-L1 immune checkpoint blockade was applied from the day of adoptive transfer in this earlier study. The observed effect was thus a prevention of CLL implantation following adoptive transfer rather than resulting from treatment of established disease. The applicability of these results to the clinical situation in human CLL patients where the disease is usually discovered at more advanced stages and treatment is only initiated in symptomatic patients is thus questionable. The modest effect in the current experiments where treatment was initiated only after established disease could be detected much more closely mirrors the lack of efficacy of single agent Pembrolizumab in CLL patients in early clinical trials (108). Combinations of either Ibrutinib or Acalabrutinib and anti-PD-L1 immune checkpoint blockade have failed to show improved CLL clearance in the

adoptive transfer experiments at hand. However, it should be noted the the current study was neither powered to detect differences in clinical outcomes in these animals nor was the treatment period long enough to appreciate potentially subtle and protracted changes in CLL load with immunotherapy. Moreover, disease control with single agent Ibrutinib or Acalabrutinib was already quite far reaching with spleen weight and size approaching those of wild type animals in this experiment. A further clinically appreciable effect may thus be difficult to obtain with the treatment combinations. The lack of short-term clinical effects does thus not preclude improved disease control in the long run should improved T-cell function be achieved with the combination treatment.

4 Design of a mass cytometry panel for assessment of immune phenotype and immune checkpoint expression in the splenic microenvironment of CLL bearing TCL-1 mice

4.1 Specific introduction

As described in 1.2.1 development of CLL is associated with a pronounced remodeling of the microenvironment to support growth and survival of the CLL B-cells as well as provide an immunosuppressive niche to allow for immune evasion. Overexpression of immune checkpoint molecules such as PD-1/PD-L1, LAG-3, TIM-3 and CTLA-4 contribute to this immunosuppression (216, 352, 372, 425, 426). The BTK inhibitor Ibrutinib has been described to be able to modulate the function of CLL associated T-cells (877, 878). In order to improve the understanding of the underlying mechanisms we sought to detail the influence of BTK inhibitors Ibrutinib and Acalabrutinib on the composition of the CLL microenvironment and the expression of important immune checkpoint molecules. Over the past decades, studies of complex cellular networks have relied on flow cytometry. However, this method is limited by spectral overlap (961). Given the complexity of CLL microenvironment interactions we chose to use mass cytometry for the analysis of the immune phenotype of the CLL microenvironment of the Eµ-TCL1 adoptive transfer model.

Mass cytometry is a method of "single cell technology" that allows for the parallel assessment of at least 40 markers. Mass Cytometry has been developed as a combination of flow cytometry and mass spectrometry. This approach utilises stable isotopes of non-biological rare earth metals (usually lanthanides) tagged to monoclonal antibodies (962). Cells are stained with antibodies labelled with lanthanide metal ions (963, 964) and iridium-conjugated DNA intercalators (965). Chemical labelling with chelated metals such as Cisplatin (966-968) can be used as a viability measure. Single cell droplets are created by nebulization and brought into contact with a high temperature (~7000 K) plasma. This breaks the molecular bonds and ionizes the atoms. This results in clouds of charged ions which can then be analysed using mass spectrometry. The mass cytometer is configured as a qTOF instrument (969). The two radiofrequency quadrupoles are tuned to filter out naturally occurring low mass ions. The enriched higher mass reporter ions are quantitated by time of flight mass analysis (Figure 15).

In order to quantify the amount of each target protein the antibody panel used in mass cytometry must provide sufficient sensitivity (the ratio of signal derived from the target and background signal derived from undesired sources). Although mass cytometry eliminates the issues arising from spectral overlap of fluorochromes in classical flow

cytometry the possibility of interference as a result of of impurities of the mass tags used as well as from oxidation of the reporter ions exists (970). Moreover, small variations in initial position and velocity of ions result in broadening of the apparent mass peak resulting in some signal being measurable in adjacent channels (less than 0.3%) (971). A careful design of mass cytometry panels along the lines of known percent signal overlap, target signal intensity and spillover tolerance using the Maxpar Panel Designer (Fluidigim, UK) should be used to avoid issues with data quality. The Panel Designer assigns a signal and tolerance value to each target based on an included database. Signal is the expected 75th percentile dual count value of the population expressing the highest amount of a given target. The Maxpar Panel Designer calculates the background (in counts) derived from signal overlap expected in all channels of the panel using the following formula:

Signal Overlap = Signal x (percent overlap/100)

The tolerance value is 20% of the 75th percentile for the population expressing the lowest amount of a given target. This value is compared to the cumulative signal overlap within the channel to gauge the appropriateness of the channel for the target.
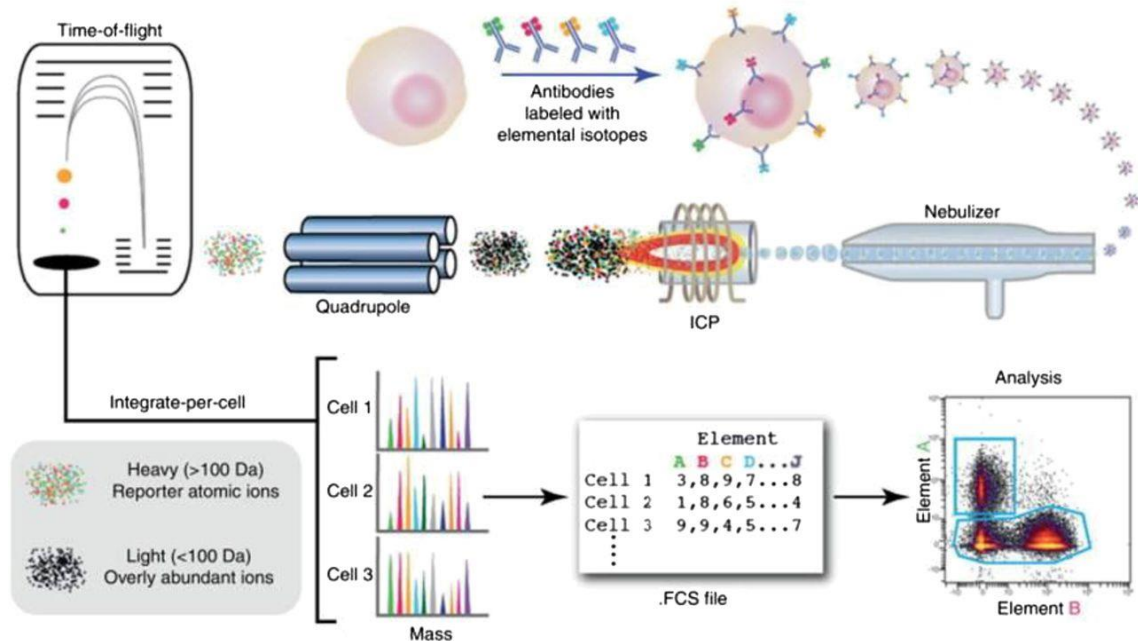
Figure 15: Work-flow summary of mass cytometry analysis. Staining is performed with antibodies attached to heavy metal ion reporters. Single-cell droplets are created by nebulization, and an elemental mass spectrum is acquired on a single cell basis. The integrated signals can then be analysed by traditional gating approaches as well as using advanced analysis algorithms such as tree plots. This Figure was repoduced from Trends in Immunology, A deep profiler's guide to cytometry, 323-32, Bendall SC, Nolan GP, Roederer M, Chattopadhyay PK, copyright Elsevier (2012) (972).

4.2   Goals and objectives

Our goal was to develop a mass cytometry panel that allows for identification of important immune cell subsets in the CLL microenvironment as well as expression of immune checkpoint molecules, PD-1, PD-L1, PD-L2, LAG-3, TIM-3, KLRG-1 and 2B4.

4.3   Specific methods

4.3.1   Antibody labelling for mass cytometry

The following Maxpar X8 antibody labelling kits (Fluidigm, UK) were used: 175Lu, 149Sm, 156Gd, 176Yb, 147Sm. The following antibodies have been labelled: anti-mouse NKG2D mIgG2a clone MI6 (ebioscience, UK), anti-mouse PD-L2 mIgG2a clone 122 (ebioscience, UK), anti-mouse 2B4 mIgG2a clone ebio244F4 (ebioscience, UK), anti-mouse KLRG-1 mIgG2a clone 2F1 (BD biosciences, UK), anti-mouse CD11b mIgG2a clone M1/70 (biolegend, UK). For polymer metal loading Maxpar polymer (Fluidigm, UK) was resuspended in 95 µl of L-Buffer (Fluidigm, UK). 5µl of the appropriate Lathanide metal solution (Fluidigm, UK) were added and the mixture was incubated at 37°C for 40 minutes. 200 µl of L-Buffer (Fluidigm, UK) and the metal-loaded polymer mixture were added to a 3 kDA Amicon Ultra-500 µl V bottom filter unit (Merck, UK) and centrifuged at 12000g for 25 minutes at room temperature. For antibody buffer exchange 300 µl of R-Buffer (Fluidigm, UK) and 100 µg of the appropriate antibody were added to a 50 kDA Amicon Ultra-500 µl V bottom filter unit (Merck, UK) and centrifuged at 12000g for 10 minutes at room temperature. 100 µl of R-buffer containing 4mM *Tris(2-carboxyethyl)phosphine hydrochloride* (TCEP) (Sigma, UK) were added to the 50 kDA filter and incubated at 37°C for 30 minutes to allow for partial reduction of the antibody. The polymer was purified by adding 300µl of C-Buffer (Fluidigm, UK) to the 3kDA filter ant centrifuging at 12000g for 30 minutes at room temperature. Similarly, the partially reduced antibody was purified by adding 300µl of C-Buffer (Fluidigim, UK) to the 50 kDA filter and centrifuging at 12000g for 10 minutes at RT. This purification step was repeated with another 400 µl of C-Buffer (Fluidigm, UK). The lanthanide-loaded polymer was resuspended in 60µl of C-Buffer (Fluidigm, UK) and transferred to the corresponding partially reduced antibody in the 50 kDA filter. The antibody-polymer mix was incubated at 37°C for 90 minutes. Subsequently the metal-conjugated antibody was washed by adding 400 µl of W-Buffer (Fluidigm, UK) and centrifuging at 12000g for 8 minutes. A total of 6 washes were performed. Finally, the metal-conjugated antibody was recovered by adding 50µl of W-Buffer (Fluidigm, UK) and spinning the inverted filter unit over a fresh collection tube at 1000g for 2 minutes twice. The antibody concetration was

measured with a Nanodrop 2000 spectrophotometer at 280 nm against a W-Buffer blank. The antibodies were stored at a concentration of 0.5 mg/ml in PBS based antibody stabilizer (Candor Bioscience, Germany) supplemented with 0.05% sodium azide (Sigma, UK).

4.3.2   Mass cytometry staining

3×10^6 splenocytes from single cell preparations were carried forward for staining. All staining steps are performed in 5 ml polypropylene round bottom tubes (Corning, UK). Cell were resuspended in "Cell-ID" Cisplatin (Fluidigm, UK) in PBS (Sigma, UK) at a concentration of 5µM and incubate for 5 minutes at room temperature. The reaction was quenched with 5x the volume of "Maxpar" cell staining buffer (Fluidigm, UK) and the samples centrifuged. Cells were resuspended in 50µl of "Maxpar" cell staining buffer containing 1 µl of anti-mouse CD16/CD32 monoclonal antibody (clone 93, ebioscience, UK) and incubated for 10 minutes. The volume was then filled up to 100 µl with "Maxpar" cell staining buffer (Fluidigm, UK) containing mass cytometry antibodies at various concentrations. Cells were incubated for 30 minutes at room temperature and then washed 2x in "Maxpar" cell staining buffer (Fluidigm, UK). The samples were then resuspended in 1ml of "Maxpar" Fix and Perm buffer (Fluidigm, UK) containing "Cell-ID" Intercalator-Ir (Fluidigm, UK) at a concentration of 125 nM and incubated over night at 4°C. Cells were washed 2x in "Maxpar" Cell staining buffer (Fluidigim, UK) and 1x in "Maxpar" water (Fluidigm, UK). Cells were left dry-pelleted at 4°C until immediately prior to acquisition on a "cytof 2" mass cytometer (Fluidigm, UK).

4.3.3   Acquisition and analysis of mass cytometry data

A "cytof 2" mass cytometer (Fluidigm, UK) was used for acquisition of mass cytometry data. The suspension of stained cells was nebulized in order to create single cell droplets and was subsequently exposed to a high temperature plasma. This breaks the molecular bonds and ionizes the atoms. The resulting charged atomic ion clouds are transferred into the mass spectrometer. The mass cytometer is configured as a qTOF instrument. The two radiofrequency quadrupoles are tuned to filter out naturally occuring low mass ions. The enriched higher mass reporter ions are quantitated by TOF mass analysis. Normalization of the recorded data is achieved via a standardized bead solution containing known concentrations of the metal isotopes 140/142Ce, 151/153Eu, 165Ho, and 175/176Lu. A correction algorithm in the software of the mass cytometer normalizes the recorded data to correct for signal variation that may occur over protracted periods of use.

4.4   Results

4.4.1   Design of a mass cytometry panel and optimization of tagged metals using the Maxpar Panel Designer

We designed to use the following 27 targets in our mass cytometry panel in order to delineate important immune cell populations of the microenvironment and analyse expression of immune checkpoint molecules: CD45 (identification of leukocytes); CD19, CD45R (B220) (identification in B-cells, differentiation of physiological B-cells and CLL B-cells); TCRb, CD3e, CD4, CD8a, CD25 (IL-2R) (identification of T-cell subsets); CD69 (T-cell activation, BTK inhibitor efficacy); CD62L (L-selectin), CD44 (antigen experience of T-cells); CD161 (NK1.1), NKG2D, CD335 (Nkp46) (identification of NK cells, functional status of NK cells); CD11b (Mac-1), Ly-6C, Ly6G, CD11c, F4/80 (identification of monocytes, macrophages, dendritic cells and granulocytes); CD244.2 (2B4), PD-L2, KLRG-1, CD366 (Tim-3), CD223 (LAG-3), CD274 (PD-L1), CD279 (PD-1), CD152 (CTLA-4) (immune checkpoint molecules). We aimed to utilise commercially available pre-conjugated mass cytometry antibodies where possible and minimize the number of custom conjugated antibodies in the panel. Table 5 gives on overview of targets, optimized mass tag as suggested by the Maxpar Panel designer and assigned signal and tolerance values.

Table 6 summarizes the signal overlap in the utilized mass channels from the various lanthanide tags used in the mass cytometry panel. The cumulative signal overlap is compared to the anticipated tolerance of the target antigen. In general, the calculated signal overlap is well below the tolerance values. Only in the 167 mass channel corresponding to NKp46 167Er the maximum tolerance is reached.

Label	Target	Signal	Tolerance
175Lu*	NKG2D	30	6
149Sm*	CD244.2 (2B4)	55	11
156Gd*	PD-L2	120	20
176Yb*	KLRG-1	15	3
167Er	CD335 (Nkp46)	30	6
162Dy	CD366 (Tim-3)	16	3
174Yb	CD223 (LAG-3)	13	3
153Eu	CD274 (PD-L1)	125	25
159Tb	CD279 (PD-1)	10	3
144Nd	CD45R (B220)	30	6
172Yb	CD4	133	27
171Yb	CD44	333	67
170Er	CD161 (NK1.1)	20	4
169Tm	TCRb	30	6
168Er	CD8a	333	67
160Gd	CD62L (L-selectin)	10	2
154Sm	CD152 (CTLA-4)	39	2
165Ho	CD3e	210	42
151Eu	CD25 (IL-2R)	600	12
166Er	CD19	160	32
147Sm*	CD11b (Mac-1)	500	100
89Y	CD45	736	147
145Nd	CD69	33	2
150Nd	Ly-6C	333	14
142Nd	CD11c	15	3
146Nd	F4/80	50	10
141Pr	Ly-6G	200	40

Table 5: Overview of targets, selected mass tag and assigned signal and tolerance values for mass cytometry panel. Signal and tolerance values derived from Maxpar Panel designer data bank. * - custom conjugated antibodies.

channels	89	141	142	144	145	146	147	149	150	151	153	154	156	159	160	162	165	166	167	168	169	170	171	172	174	175	176
146Nd	0	0	0.25	0.35	0.40		0.15	0	0.05	0	0	0	0	0	0	1	0	0	0	0	0	0	0	0	0	0	0
141Pr	0		0.60	0	0	0	0	0	0	0	0	0	0	0	0	0	0	0	0	0	0	0	0	0	0	0	0
150Nd	0	0	1.67	2.33	0.67	1.67	0	1.00		1.00	0	0	0	0	0	0	0	6.66	0.33	0	0	0	0	0	0	0	0
142Nd	0	0.04		0.04	0	0.01	0	0	0	0	0	0	0	0	0.01	0	0	0	0	0	0	0	0	0	0	0	0
145Nd	0	0	0.10	0.49		1.39	0	0	0	0	0	0	0	0	0	0.03	0	0	0	0	0	0	0	0	0	0	0
89Y		0	0	0	0	0	0	0	0	0	0	0	0	0	0	0	0	0	0	0	0	0	0	0	0	0	0
147Sm	0	0	0	0	0	1.50		2.50	1	0	0	1	0	0	0	0	0	0	0	0	0	0	0	0	0	0	0
166Er	0	0	0	0	0	0	0	0	0	0	0	0	0	0	0	0	0.48		2.72	0.80	0	0	0	0	0	0	0
151Eu	0	0	0	0	0	0	0	0	1.80		4.80	0	0	0	0	0	0	0	0	0	0	0	0	0	0	0	0
165Ho	0	0	0	0	0	0	0	0	0	0	0	0	0	0	0	0		0.63	0	0	0	0	0	0	0	0	0
154Sm	0	0	0	0	0	0	0	0.08	0	0	0.12		0	0	0	0	0	0	0	0	0	0.16	0	0	0	0	0
160Gd	0	0	0	0	0	0	0	0	0	0	0	0	0.02	0.03		0	0	0	0	0	0	0	0	0	0	0	0.13
168Er	0	0	0	0	0	0	0	0	0	0	0	0	0	0	0	0	0	1.00	3.33		1.00	1.67	0	0	0	0	0
169Tm	0	0	0	0	0	0	0	0	0	0	0	0	0	0	0	0	0	0	0	0.09		0.09	0	0	0	0	0
170Er	0	0	0	0	0	0	0	0	0	0	0	0	0	0	0	0	0	0.12	0.10	0.16	0.06		0.06	0	0	0	0
171Yb	0	0	0	0	0	0	0	0	0	0	0	0	0	0	0	0	0	0	0	0	0	1.00		13.65	1.33	0	0
172Yb	0	0	0	0	0	0	0	0	0	0	0	0	0	0	0	0	0	0	0	0	0	0	0.67		0.67	0	0
144Nd	0	0	0.06		0.27	0.09	0	0	0	0	0	0	0	0	0.90	0	0	0	0	0	0	0	0	0	0	0	0
159Tb	0	0	0	0	0	0	0	0	0	0	0	0	0		0.03	0	0	0	0	0	0	0	0	0	0	0.12	0
153Eu	0	0	0	0	0	0	0	0	0	1		0.38	0	0	0	0	0	0	0	0	0	0	0	0	0	0	0
174Yb	0	0	0	0	0	0	0	0	0	0	0	0	0	0	0	0	0	0	0	0	0	0	0	0		0.04	0.04
162Dy	0	0	0	0	0	0	0	0	0	0	0	0	0	0	0		0	0	0	0	0	0	0	0	0	0	0
167Er	0	0	0	0	0	0	0	0	0	0	0	0	0	0	0	0	0	0.45		1.05	0	0.06	0	0	0	0	0
176Yb	0	0	0	0	0	0	0	0	0	0	0	0	0	0	0	0	0	0	0	0	0	0	0	0	0.04	0.04	
156Gd	0	0	0	0	0	0	0	0	0	0	0	0		0	0.24	0	0	0	0	0	0	0	0	1.56	0	0	0
149Sm	0	0	0	0	0	0	0.11		0.94	0	0	0.11	0	0	0	0	0.22	0	0	0	0	0	0	0	0	0	0
175Lu	0	0	0	0	0	0	0	0	0	0	0	0	0	0	0	0	0	0	0	0	0	0	0	0	0.09		0.15
Cumulative Signal Overlap	0.00	0.04	2.68	3.21	1.34	4.66	0.26	3.58	3.79	2.00	4.92	1.49	0.02	0.04	1.17	1.03	0.70	8.86	6.48	2.10	1.06	2.98	0.73	15.21	2.13	0.20	0.32

HEAT MAP
(% of tolerance)

0   100

Table 6: Comparison of signal overlap from lanthanide mass tags and maximum tolerance anticipated for target. Overlap calculated by Maxpar Panel designer software.

4.4.2   Custom conjugation of antibodies with lanthanide metal tag and titration of mass cytometry antibodies

Anti-KLRG-1 176Yb, anti-2B4 149Sm, anti-NKG2D 175Lu, anti-CD11b 147Sm and anti-PD-L2 156Gd mass cytometry antibodies were custom conjugated as described in 4.3.1. Wildtype C57/BL6 splenocytes were stained with anti CD45 89Y as recommended by the manufacturer and the custom conjugated antibodies in dilutions of 1:400, 1:200, 1:150, 1:100 and 1:50. Median signal intensity of positive and negative leukocyte populations were recorded for each dilution. Figures 16 – 20 illustrate the titration curves obtained for each antibody. The maximum separation of positive and negative populations was generally achieved at a dilution of 1:100 with the exception of CD11b 147Sm were separation could be further improved with higher concentrations. However, at a dilution of 1:100 CD11b+ and CD11b- separation was already deemed excellent.

A

	KLRG-1-	KLRG-1+
1:50	2.25	38.18
1:100	0.56	40.94
1:150	0.46	40.02
1:200	0.0	37.87
1:400	0.46	34.24

Calculated Raw values of
Medians using X-Axis
channel(s): KLRG-1

B
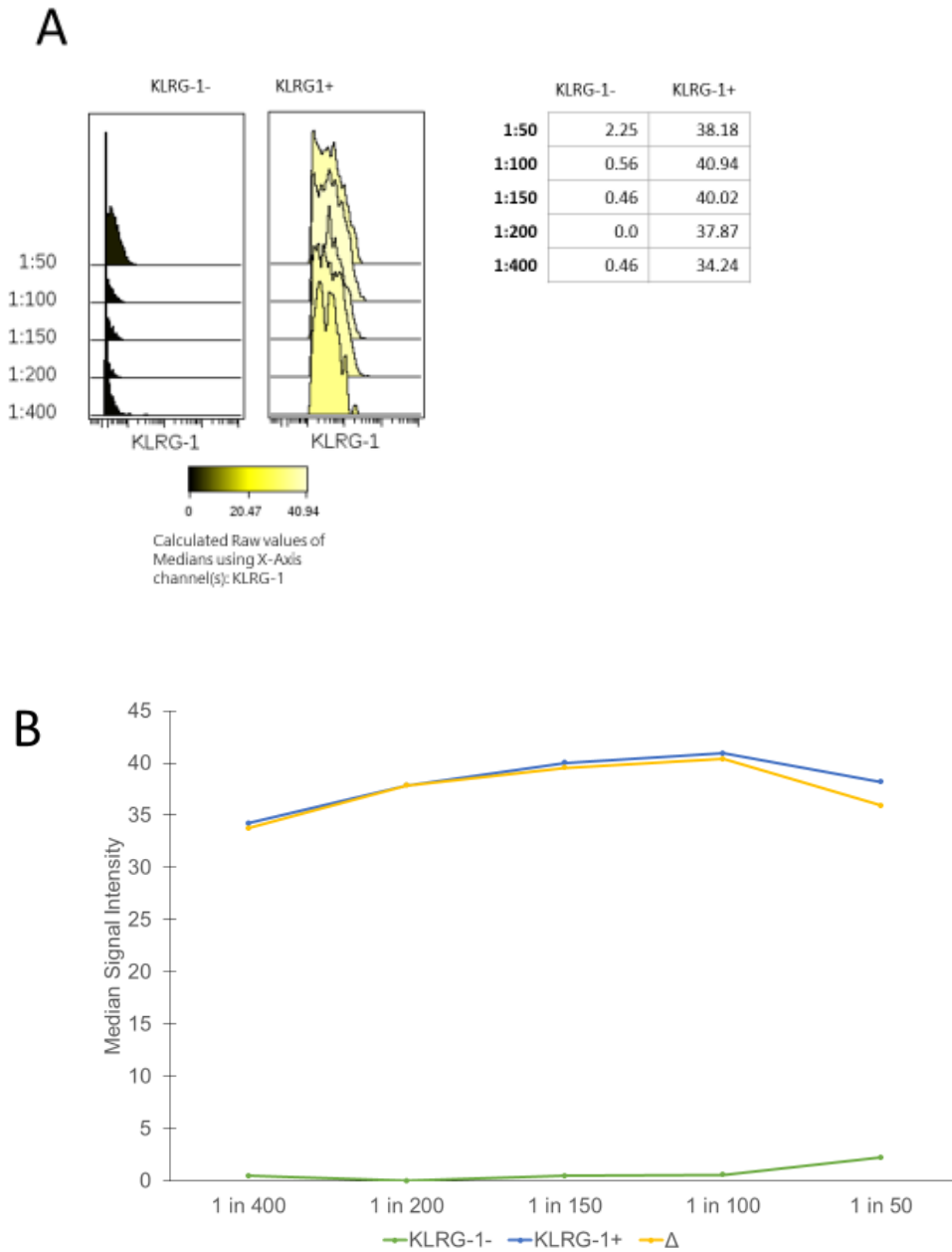
Figure 16: Titration of anti-KLRG-1 176Yb. (A) Median signal intensity measured with various concentration of anti-KLRG-1 176Yb in positive and negative populations (B) Illustration of titration curves.

A

	2B4-	2B4+
1:50	5.68	23.2
1:100	2.06	21.12
1:150	2.28	18.18
1:200	1.12	12.27
1:400	0.75	6.46

0.75   11.98   23.2

Calculated Raw values of
Medians using X-Axis
channel(s): 2B4

B
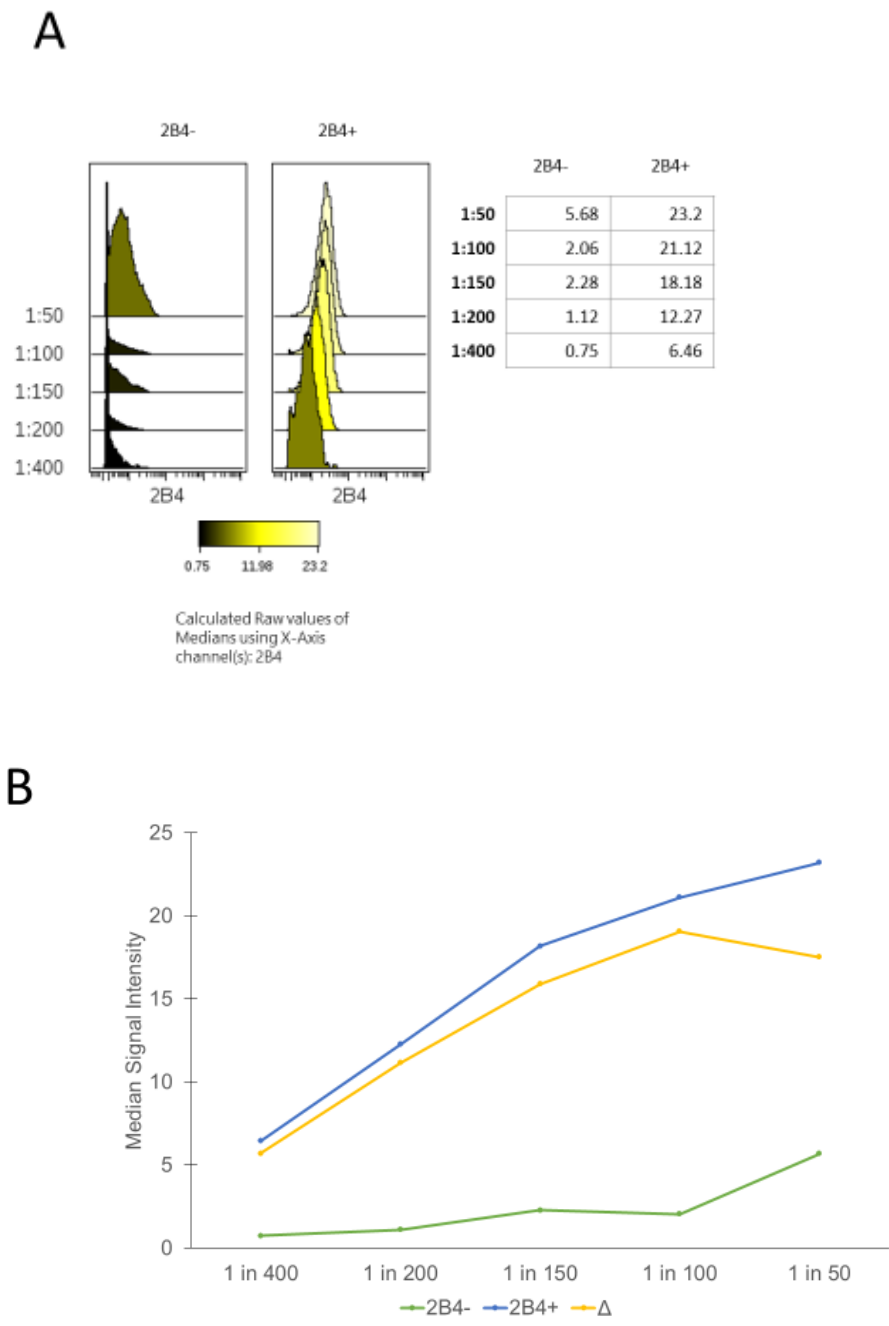
Figure 17: Titration of anti-2B4 149Sm. (A) Median signal intensity measured with various concentration of anti-2B4 149Sm in positive and negative populations (B) Illustration of titration curves.

A

	NKG2D-	NKG2D+
1:50	2.76	13.38
1:100	0.08	10.03
1:150	0.52	9.58
1:200	0.0	8.31
1:400	0.0	7.46

Calculated Raw values of
Medians using X-Axis
channel(s): NKG2d_EQBead
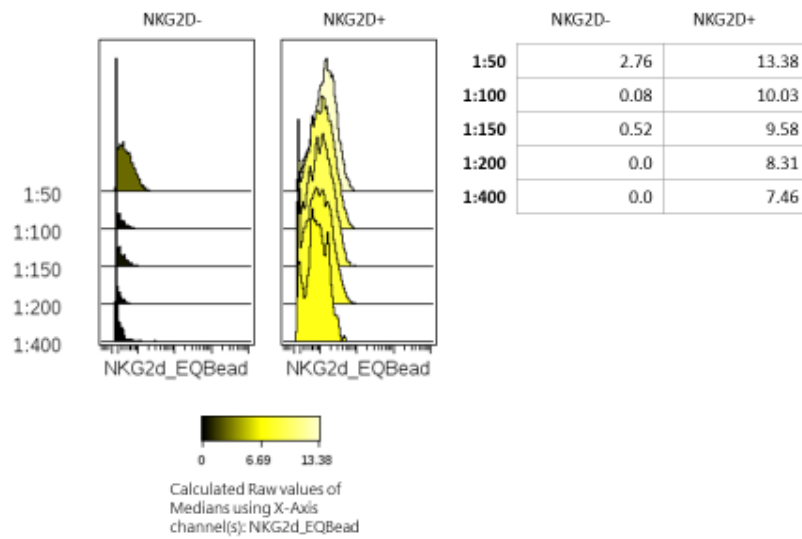
B
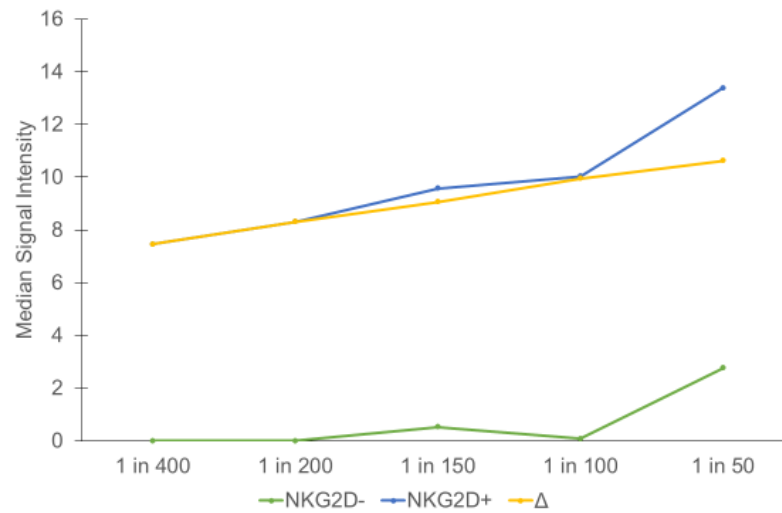
Figure 18: Titration of anti-NKG2D 175Lu. (A) Median signal intensity measured with various concentration of anti-NKG2D 175Lu in positive and negative populations (B) Illustration of titration curves.

	CD11b+	CD11b-
1:50	119.01	0.79
1:100	92.37	0.38
1:150	82.28	2.11
1:200	84.46	0.23
1:400	59.57	0.91
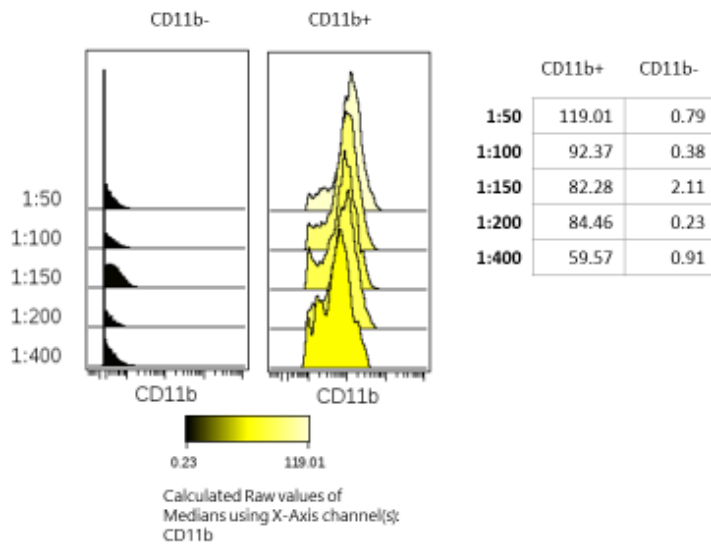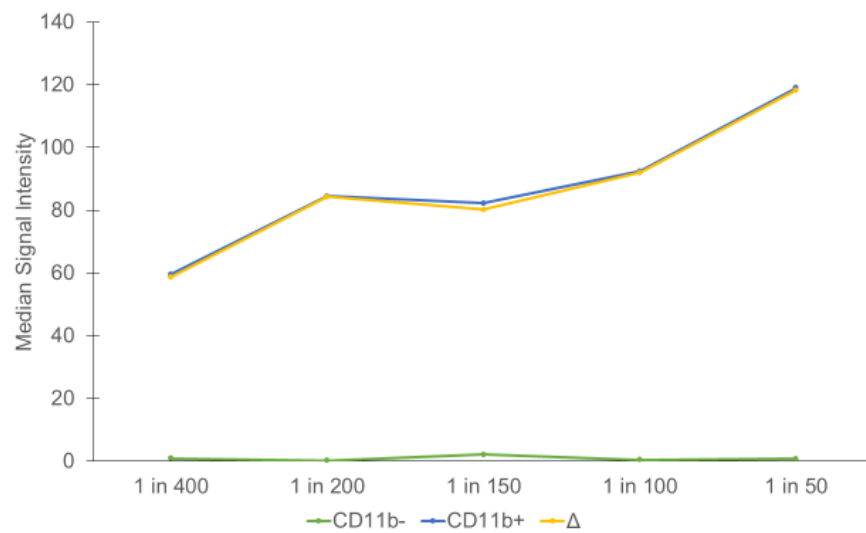
Figure 19: Titration of anti-CD11b 147Sm. (A) Median signal intensity measured with various concentration of anti-CD11b 147Sm in positive and negative populations (B) Illustration of titration curves.

	PD-L2-	PD-L2+
1:50	2.21	17.39
1:100	0	16.14
1:150	2.05	16.58
1:200	0	15.25
1:400	0.31	14.62
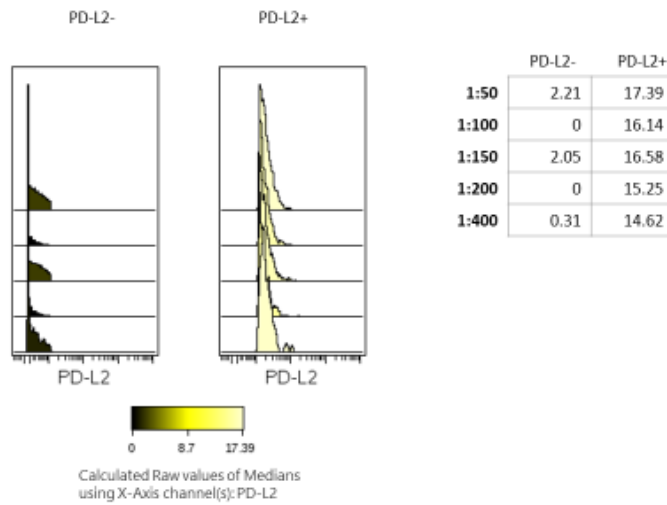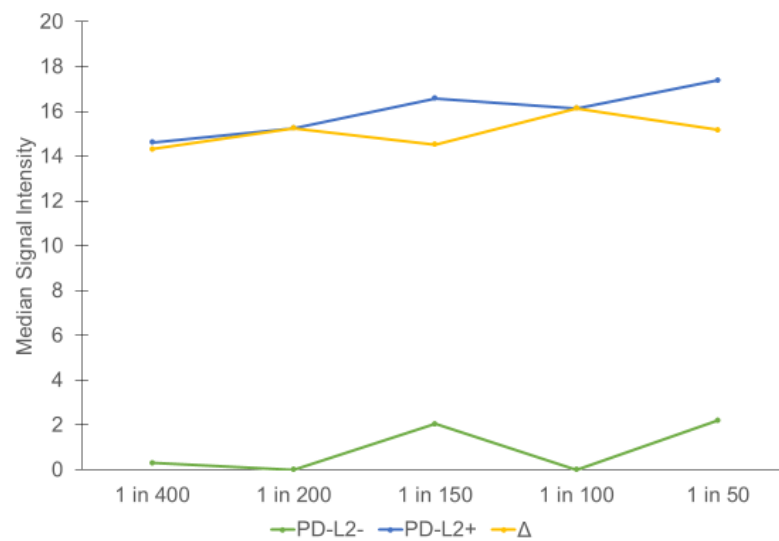
Figure 20: Titration of anti-PD-L2 156Gd. (A) Median signal intensity measured with various concentration of anti-PD-L2 156Gd in positive and negative populations (B) Illustration of titration curves.

4.4.3   Application of the mass cytometry panel on splenocyte samples from wild type and CLL bearing animals

In order to confirm the suitability of the developed mass cytometry panel to identify important immune cell populations among mouse splenocytes and assess the expression of immune checkpoint pathways, we applied the panel to a splenocyte sample of a CLL bearing Eµ-TCL1 transgenic animal and an age matched C57BL/6 wildtype animal. Figure 21 illustrates the gating strategy and identification of physiological B-cell, CLL B-cell and non-B-cell populations. Cellular events were separated from calibration beads by gating on 191Ir DNA-intercalator and excluding Ce140 signal only found on the calibration beads. From the population of cellular events single cells as opposed to cell doublets were isolated by gating on 191Ir and 193Ir DNA intercalator and by excluding events with high event lengths, which tend to be cell doublets or high order multiplets .From the purified population of single cell events viable leukocytes were identified by expression of CD45 and low cisplatin incorporation. The population of viable leukocytes was then further subdivided into CD19+B220+ physiological B-cells, CD19+B220 low CLL cells and CD19-B220- non- B-cells. In the sample derived from the CLL beraing animal a highly abundant population of CD19+B220low CLL B-cells was apparent compared to the wild type sample.
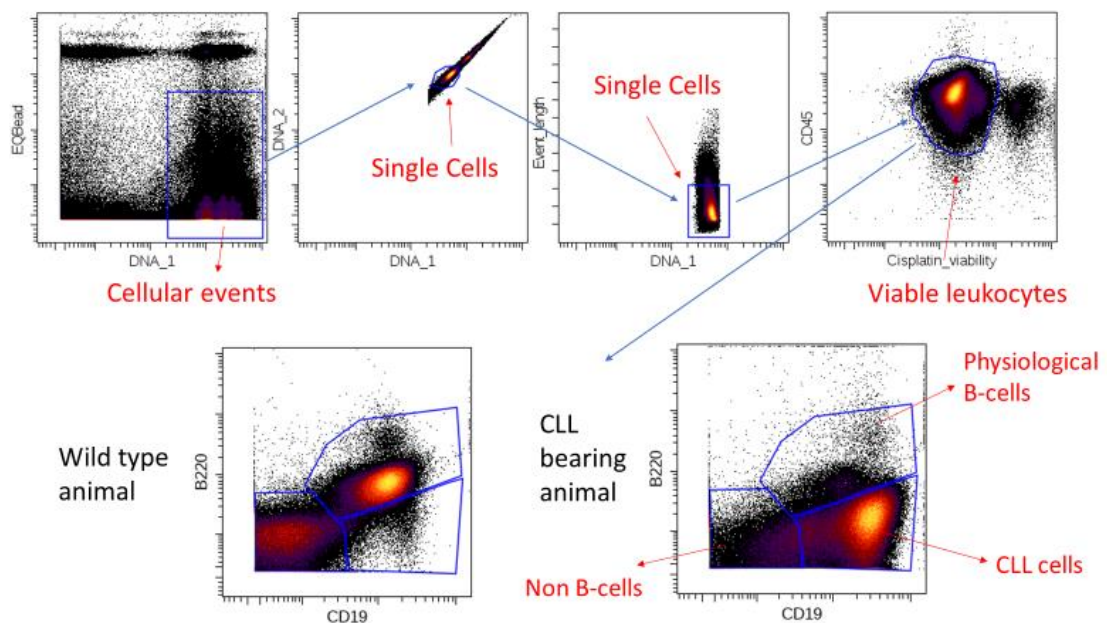
Figure 21: Gating strategy and identification of B-cell subsets: Cellular events were separated from calibration beads by gating on 191Ir DNA-intercalator and excluding Ce140 signal, cell doublets were excluded by gating on 191Ir and 193Ir DNA intercalator and by exluding events with high event lengths, viable leukocytes were identified by expression of CD45 and low cisplatin incorportation. B-cells were separated into CD19+B220+ physiological B-cells and CD19+B220- CLL B-cells. N=2.

Figure 22 illustrates the separation of CD19-B220- non-B-cells from figure 21 into immune cell subsets. CD3 and TCR beta expression identified T-cells. From the T-cell population T helper cells and cytotoxic T-cells can be differentiated through expression of CD4 and CD8. From the CD4+ T-cell population the CD4+CD25+ T- regulatory subset can be differentiated. Among non-T-cells NK1.1 expression was used to identify NK-cells. The Non-T-NK-cell subset was then further subdivided into CD11c high classical dendritic cells and non-T-NK-DCs. In the latter population Ly6G expression denotes the granulocyte subset. The remaining non-T-NK-DC-granulocytes can then be classified according to CD11b and F4/80 expression into CD11b low/- F4/80 high red pulp macrophages and CD11b+ F4/80 intermediate white pulp myelomonocytic cells as illustrated in figure 23. Ly6C expression separates the white pulp myelomonocytic cells into Ly6C high inflammatory monocytes, Ly6C intermediate monocytes and Ly6C low patrolling monocyte/macrophage like cells. The composition of the white pulp myelomonocytic cells is shifted towards the Ly6C low population with the development of CLL. Figure 24 shows the identification of the degree of antigen experience among the T-cell subset from figure 22. Naïve, central memory and effector/effector memory T-cell can be identified via expression of CD44 and CD62L. With the onset of CLL the T-cell compartment is shifted towards a more antigen experienced phenotype.
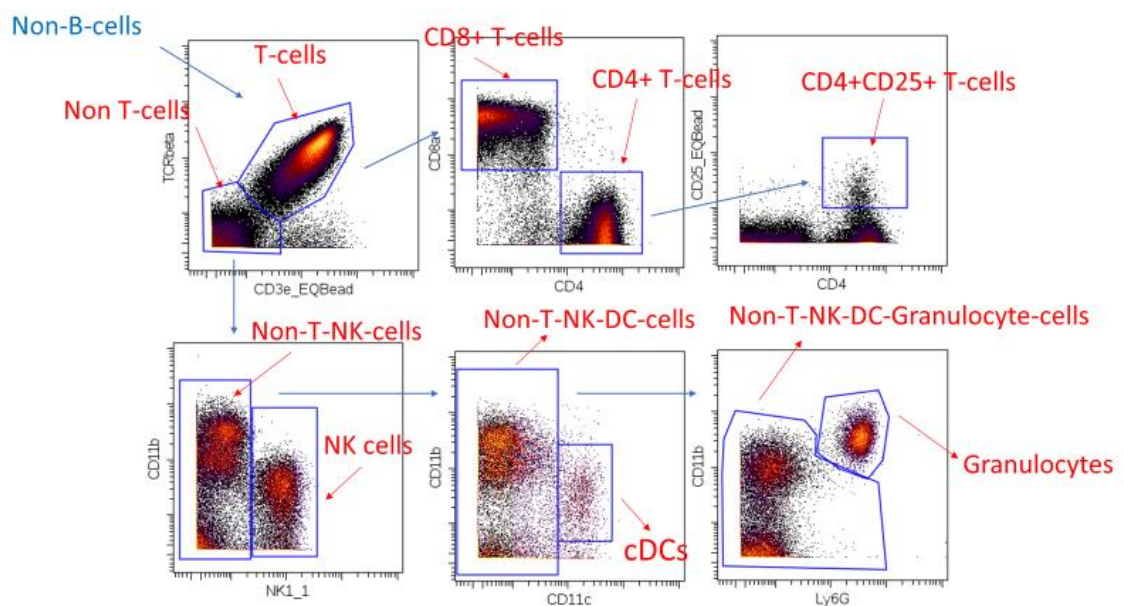
Figure 22: Gating strategy for identification of immune cell subsets. CD3 and TCRbeta expression identifies T-cells. T helper cells and cytotoxic T-cells are identified via expression of

CD4/CD8, CD4+CD25+ expression identifies regulatory T-cells, NK1.1 expression identifies NK-cells, CD11c high cells denote the classical dendritic cells and Ly6G expression the granulocyte subset. N=2.
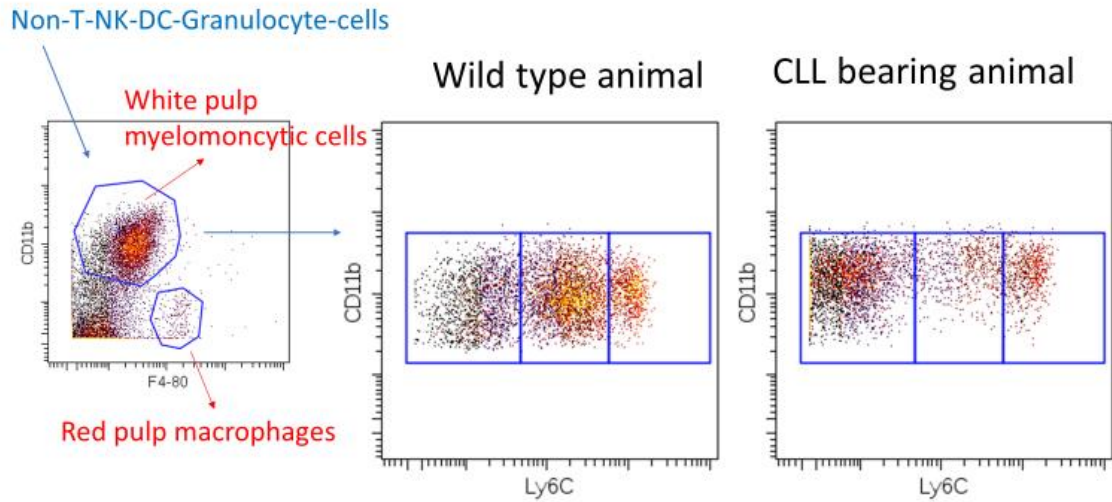
Figure 23: Idenfication of myelomonocytic immune cell populations. CD11b and F4/80 expression classifies myelomonocytic cells into CD11b low/- F4/80 high red pulp macrophages and CD11b+ F4/80 intermediate white pulp myelomonocytic cells. Ly6C expression separates the white pulp myelomonocytic cells into Ly6C high inflammatory monocytes, Ly6C intermediate monocytes and Ly6C low patrolling monocyte/macrophage-like cells. White pulp myelomonocytic cells are shifted towards the Ly6C low population with the development of CLL. N=2
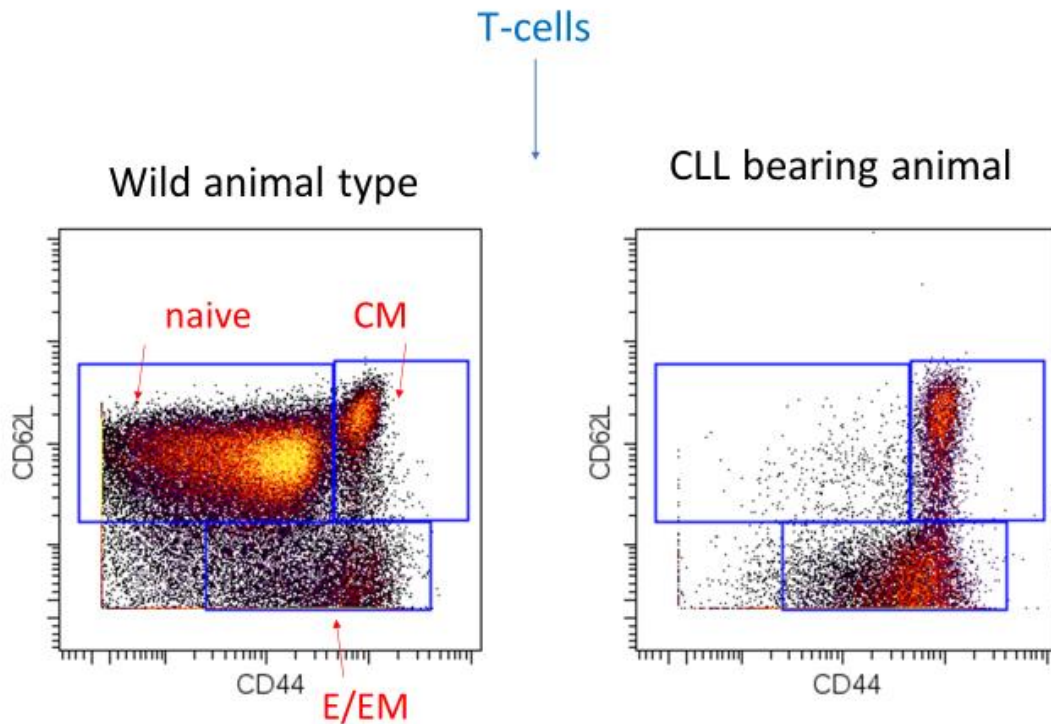
Figure 24: Identification of the degree of antigen experience of T-cells in the splenic microenvironment. CD44 and CD62L expression is used to identify the degree of antigen-experience of T-cells in the splenic microenvironment. With development of CLL T-cell are shifted towards a more antigen-experience phenotype. *Abbreviations: CM – central memory, E/EM – effector/effector memory. N=2*

Figures 25 compares the expression of immune checkpoint receptors PD-1, TIM-3, KLRG-1, LAG-3 and 2B4 on T-cells derived from spleens of CLL bearing and a wildtype animal. Expression of PD-1, LAG-3, 2B4 and KLRG-1 was markedly increased on T-cells from CLL bearing animals compared to wildtype animals. We also found a modest increase in expression of TIM-3 on T-cells from spleen of CLL bearing Eµ-TCL1 animals. This was more pronounced among CD4+ T-cells.
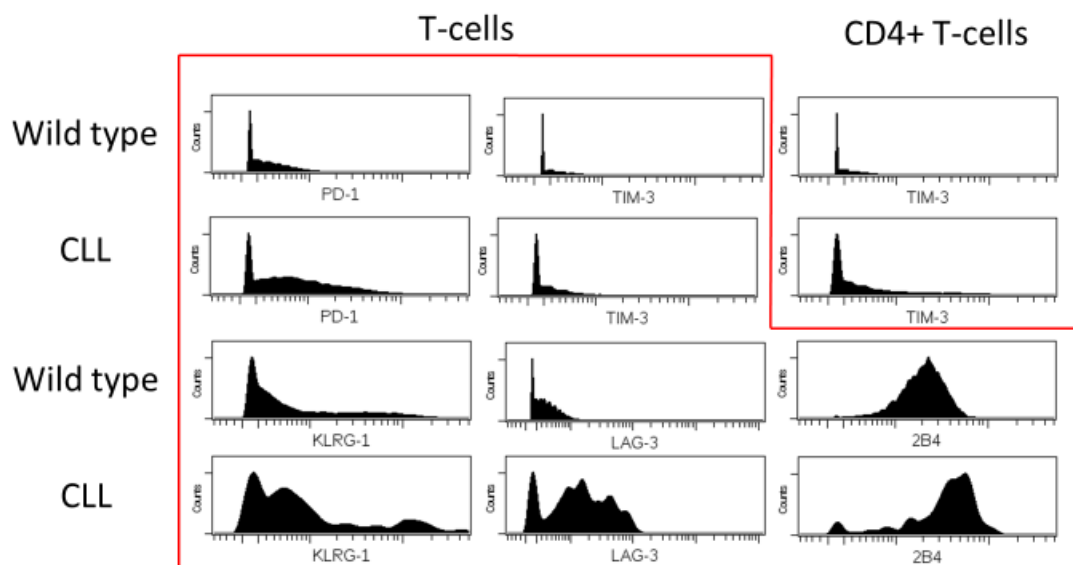
Figure 25: Expression of immune checkpoint molecules on T-cells in CLL bearing and wild type animals. N=2.

Figure 26 illustrates expression of activating and inhibitory NK-cells receptors on NK1.1+ cells derived from spleens of wildtype and CLL bearing animals. More NKp46 low NK-cells were found among splenocytes of CLL bearing animals compared to wild type animal while the expression of NKG2D remained largely unchanged. Expression of dual function receptor 2B4 was found to be increased on NK-cells from CLL bearing animals. Similarly, expression of inhibitory receptor LAG-3 and KLRG-1 was found to be increased in CLL bearing animals compared to wild type animals. Figure 27 illustrates the expression of immune checkpoint molecule PD-L1, PD-L2 and PD-1 among B-cells and white pulp myelomonocytic cells from wild type and CLL bearing animals. On B-cells expression of PD-L1, PD-L2 and PD-1 was found to be increased in the setting of CLL. Among white pulp myelomonocytic cells PD-L1 expression was markedly increased in CLL bearing animals while PD-L2 expression remained largely unchanged.
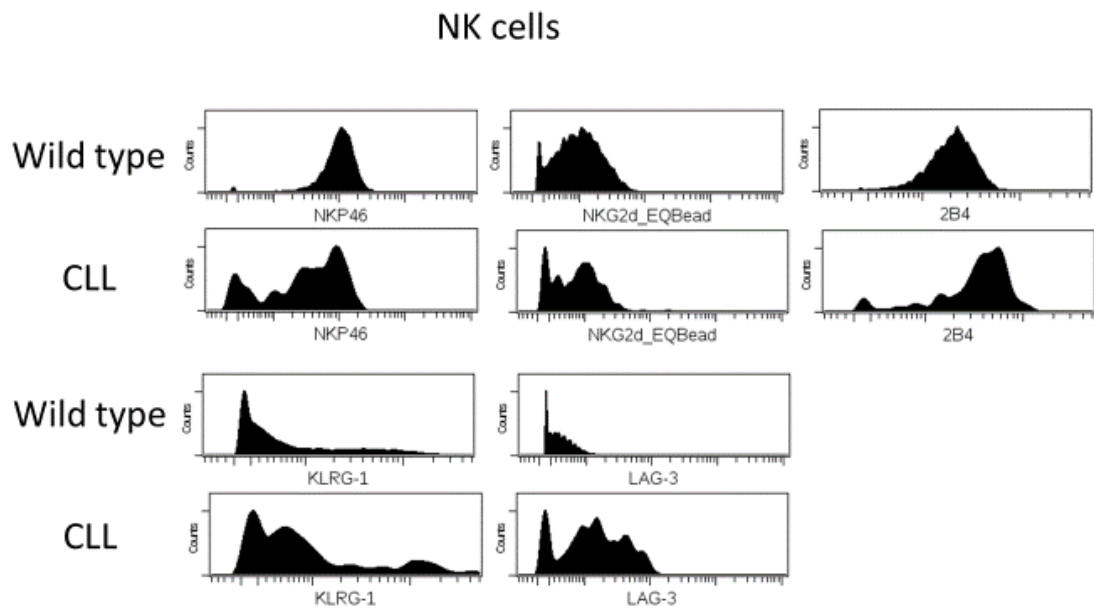
NK cells

Figure 26: Expression of activating and inhibitory receptors on NK-cells in CLL bearing and wild type animals. N=2

B cells

White pulp myelomoncytic cells
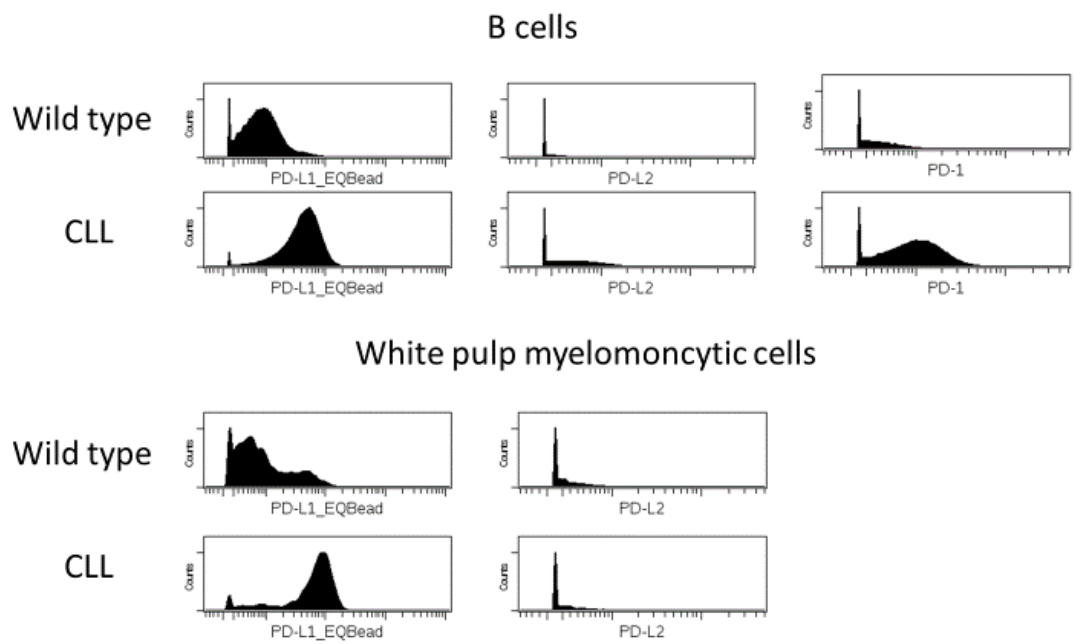
Figure 27: Expression of PD-L1, PD-L2 and PD-1 on B-cells and white pulp myelomonocytic cells in CLL bearing and wildtype animals. N=2.

4.5   Discussion

We optimized a mass cytometry panel to analyse the most important immune cell populations and expression of immune checkpoint receptors in splenocyte samples from experimental animals using the MAXPAR panel designer taking into account expected signal intensity and tolerance for signal overlap for prospective targets. A panel of 27 markers was carried forward. Calculated signal overlap was well below the expected tolerance threshold for all of the markers included in the panel except for the 167 mass channel corresponding to NKp46 167Er where the maximum tolerance was reached. These preliminary calculations suggested that the selected mass cytometry panel was adequate to study changes in immunophenotype and immune checkpoint molecule expression in the splenic microenvironment of CLL bearing animals and the influence of BTK inhibitors on the factors.

When designing the panel, we sought to use commercially available tested pre-conjugated mass cytometry antibodies wherever available and limit the need for custom conjugated antibodies as far as possible. With the panel at hand custom conjugation of 5 antibodies for use in mass cytometry was necessary: Anti-KLRG-1 176Yb, anti-2B4 149Sm, anti-NKG2D 175Lu, anti-CD11b 147Sm and anti-PD-L2 156Gd. Commercially available pre-conjugated antibodies were used as recommended by the manufacturer. For custom conjugated antibodies titration curves were recorded in order to identify the optimal dilution for use of immune phenotypic analysis of mouse splenocytes. For anti-KLRG-1 176Yb, anti-2B4 149Sm, anti-NKG2D 175Lu anti-PD-L2 156Gd the maximum separation of positive and negative populations was found at a concentration of 1:100. For anti-CD11b 147Sm the separation further improved beyond concentration of 1:100. However, separation was already deemed excellent at a concentration of 1:100 – this dilution was therefore chosen for finally application in the mass cytometry panel. A validation of this panel by flow cytometry is necessary and currently ongoing.

In order to confirm the appropriateness of the panel to identify important immune cell populations in the microenvironment and assess expression of immune checkpoint pathways the panel for applied to splenocytes from ageing CLL bearing Eμ-TCL1 mice and age matched C57BL/6 wild type animals. We were able to demonstrate that the panel is capable of identify the major immune cell populations in the splenocyte samples. Moreover, the panel was able to identify changes in antigen experience of T-cell subsets and changes in expression of immune checkpoint receptors and NK-cell receptors in the setting of CLL.

As opposed to the situation in human beings where only 1-2% of CD4+CD25+ T-cell with very high expression of CD25 expression consistently show suppressive function and FOXP3 is necessary for reliable identification of regulatory T-cells (973-975) in mice CD4+CD25+ T-cells are a homogenous population of cells with regulatory function and FOXP3 staining is thus not strictly necessary for identification of Tregs (976, 977). However, moderate suppressive function has been shown for some subsets of CD4+CD25- T-cells (978, 979). The panel at hand thus is limited in its ability to completely identify the mouse regulatory T-cell subsets. Nevertheless, we chose to use the panel in its present form as CD4+CD25+ is a good approximate for identification of the regulatory T-cell subset and a more complete identification would have made the use of intranuclear marker and thus permeabilization of the splenocyte samples necessary. We were reluctant to utilize permeabilization as this is known to disrupt surface staining and thus interfere with staining for immune checkpoint molecules which is major objective of this study.

One potential limitation of the panel is its inability to fully distinguish between white pulp monocyte and macrophages in the splenic microenvironment. In earlier studies using flow cytometry myelomonocytic cells of wild type animals were segregated into two populations based on expression of CD11b and F4/80: CD11b high F4/80- monocytes and CD11b intermediate F4/80 macrophages (908). Our mass cytometry panel on the other hand delineated a small CD11b- F4/80 high population and a larger CD11b+ F4/80 intermediate population of about 10fold magnitude. Rose et al. have previously suggested that F4/80 expression does not reliably separate spleen monocytes and macrophages (980). It has been suggested that this is due to steric hinderance between F4/80 and GR-1 (Ly6C/G) binding antibodies. However, neither strategies of sequential incubation with F4/80 and Ly6C/G binding anbtibodies nor completely leaving out Ly6C/G binding antibodies from the panel improved separation of white pulp monocytes and macrophages. We attempted to expanded the panel with CD115 binding antibodies to allow for separation of white pulp myelomonocytic cell populations. However, neither commercially available CD115 antibodies nor custom conjugated CD115 antibodies showed any staining among splenocyte samples. It has been suggested that CD115 expression among monocytes may be too ephemeral to be reliably detected (981). Attempts to expanded the panel with MHC type II Bi209 antibodies to improve identification of myelomonocytic cell subsets failed due to unexpected spillover of signal into all Yb channels. In depth literature search revealed that the findings of our mass cytometry panel are in reality in line with the natural heterogeneity of spleen myelomonocytic cells: CD11b-/F4/80++ red pulp macrophages, CD11b+ F4/80

intermediate monocytes, monocyte derived white pulp macrophages and marginal zone macrophages that cannot be separate based on staining with these markers, calling into question the findings of previous flow cytometry based studies that have claimed to accurately delineate the populations based on the staining of these markers (982, 983). Separation could still have been achieved by use of primarily intracellular markers such as CD68. However, we were reluctant to apply permeabilization on splenocyte samples out of fear of interference with surface staining for immune checkpoint molecules as stated above. Staining of white pulp myelomonocytic cells with Ly6C still allows for a limited separation into Ly6C high inflammatory monocytes and Ly6C low patrolling monocytes and monocytic phagocytes/macrophages-like cells. Given the above issues and considerations we chose to utilize the panel in its present form and forgo precise separation of white pulp myelomonocytic cell populations.

5   Influence of BTK inhibition on immune phenotype and immune checkpoint expression in the splenic microenvironment of CLL bearing animals

5.1   Specific introduction

The onset of CLL is association with the development of a chronic activation induced functional impairment of both helper and cytotoxic T-cells. A similar state of chronic activation induced T-cell dysfunction has been observed in chronic viral infections and has been called "T-cell exhaustion". The condition is caused by persistent exposure of T-cells to antigen-stimulation or inflammatory stimuli leading to progressive loss of effector CD8+ and CD4+ T-cell function. Overexpression of co-inhibitory immune checkpoint molecules has been implicated in the pathogenesis of this secondary immune deficiency (422, 423).

We have been able to demonstrate that, similar to the situation in chronic viral infection, the functional T-cell impairment induced by CLL coincidences with an overexpression of immune checkpoint molecules such as 2B4, CD160 and PD-1 (401). Overexpression of other known immune checkpoint molecules on CD8+ T-cells in the setting of CLL such as LAG-3 and KLRG-1 have been described (352, 425). In CD4+ T-cells the presence of an exhaustion phenotype with overexpression of TIM-3 and PD-1 has also been documented (426). Catakovic et al. described an increase of TIGIT expressing CD4+ T-cells in CLL patients (427). Overexpression of CTLA4 has been demonstrated on both patient derived CD4+ and CD8+ T-cells (372). We have previously demonstrated that CLL associated T-cell defects can be directly induced by CLL B-cells via inhibitory surface receptors CD200, CD274 (PD-L1), CD276 (B7-H3) and CD270. The PD-1/PD-L1 axis has been demonstrated to be of particular importance in inducing CLL associated T-cell defects (216). Moreover, the CLL microenvironment has been shown to be rich in PD-L1 expressing myeloid-derived cells that have been demonstrated to suppress T-cell effector function and promote T reg mediated immunosuppression (835). In a mouse model of CLL we were able to shown that PD-L1 blockade resulted in prevention of T-cell dysfunction and leukemia growth (836).

A correction of CLL associated T-cell defects could, according to the "cancer immunoediting" hypothesis, help to obtain durable remissions and may offer a path to a cure of the disease (792). Various studies have obtained evidence suggesting that the BTK inhibitor Ibrutinib has the potential to modulate function of T-cells and myeloid cells in the tumour microenvironment. In T-cells derived from the peripheral blood of CLL patients, Ibrutinib has been shown to have the potential to shift T-helper cell polarity

away from Th2 towards Th1 by targeting ITK (877). In a separate study the agent has been reported to downregulate expression of PD-L1 on the surface of patient derived CLL B-cells and expression of PD-1 on the surface of patient derived CD4+ and CD8+ T-cells (878). Stiff et al. have demonstrate expression of BTK in both human and murine MDSCs and showed that Ibrutinib treatment has the ability to suppress BTK phosphorylation in MDSCs resulting in impaired nitrous oxide production, cell migration, expression of IDO as well as impaired in vitro generation of human MDSCs. Ibrutinib treatment resulted in reduced numbers of MDSCs in both spleen and tumours of mouse models of mammary cancer and melanoma (879). Moreover, Ibrutinib treatment has been shown decreased production of CXCL12, CXCL13, CCL19 and VEGF in human macrophages after Ibrutinib treatment resulting in impaired adhesion, migration and invasion of co-cultured lymphoid cells (880). In a mouse model of PDAC, Ibrutinib treatment has been shown to shift the immunophenotype of macrophages towards a more Th-1 permissive state resulting in increased CD8+ T-cell cytotoxicity (881).

5.2   Goals and objectives

We speculate that PD-L1 expression by CLL B-cells is driven by B-cell receptor signalling as has recently been demonstrated in DLBCL (984). BTK inhibitor treatment may therefore decrease PD-1/PD-L1 expression. Using the Eµ TCL-1 mouse model we sought to demonstrate that BTK inhibitor treatment using both Ibrutinib and Acalabrutinib is able to modulate expression of PD-1 and its ligand PD-L1 in the splenic microenvironment of CLL bearing animals

5.3   Specific methods

5.3.1   Cell thawing procedure

Thwaing of cryopreserved splenocyte samples was performed in a water bath at 37°C. To avoid contamination the vials were disinfected using 70% IMS (Fisher Scientific, UK) and subsequently opend in a class II biosafety cabinet. The cell suspension was pipetted into 10ml RPMI 1640 (Gibco, UK) supplemented with 10% FCS (Gibco, UK), 1% Penicillin-Streptomycin (Sigma, UK) at 37°C. Subsequently the suspension was centrifuged at 300 x g for 10 minutes at room temperature and resuspended in a volume suitable for number of cells contained in the pellet. Automated cell counting was conducted on a Luna fl automated cell counter (Logos bioysstems, USA) after dilution of a 10µl aliquot with an equal amount of 0.4% Tryphan blue (Sigma, UK).

5.3.2 Mass cytometry staining

3×10^6 splenocytes from single cell preparations were carried forward for staining. All staining steps are performed in 5 ml polypropylene round bottom tubes (Corning, UK). Cell were resuspended in "Cell-ID" Cisplatin (Fluidigm, UK) in PBS (Sigma, UK) at a concentration of 5µM and incubate for 5 minutes at room temperature. The reaction was quenched with 5x the volume of "Maxpar" cell staining buffer (Fluidigm, UK) and the samples centrifuged. Cells were resuspended in 50µl of "Maxpar" cell staining buffer containing 1 µl of anti-mouse CD16/CD32 monoclonal antibody (clone 93, ebioscience, UK) and incubated for 10 minutes. The volume was then filled up to 100 µl with "Maxpar" cell staining buffer (Fluidigm, UK) containing mass cytometry antibodies for a final concentration of 1:100. Cells were incubated for 30 minutes at room temperature and then washed 2x in "Maxpar" cell staining buffer (Fluidigm, UK). The samples were then resuspended in 1ml of "Maxpar" Fix and Perm buffer (Fluidigm, UK) containing "Cell-ID" Intercalator-Ir (Fluidigm, UK) at a concentration of 125 nM and incubated over night at 4°C. Cells were washed 2x in "Maxpar" Cell staining buffer (Fluidigim, UK) and 1x in "Maxpar" water (Fluidigm, UK). Cells were left dry-pelleted at 4°C until immediately prior to acquisition on a "cytof 2" mass cytometer (Fluidigm, UK). For a list of mass cytometry antibodies used please refer to table 4.

5.3.3 Acquisition and analysis of mass cytometry data

A "cytof 2" mass cytometer (Fluidigm, UK) was used for acquisition of mass cytometry data. The suspension of stained cells was nebulized in order to create single cell droplets and was subsequently exposed to a high temperature plasma. This breaks the molecular bonds and ionizes the atoms. The resulting charged atomic ion clouds are transferred into the mass spectrometer. The mass cytometer is configured as a qTOF instrument. The two radiofrequency quadrupoles are tuned to filter out naturally occuring low mass ions. The enriched higher mass reporter ions are quantitated by TOF mass analysis. Normalization of the recorded data is achieved via a standardized bead solution containing known concentrations of the metal isotopes 140/142Ce, 151/153Eu, 165Ho, and 175/176Lu. A correction algorithm in the software of the mass cytometer normalizes the recorded data to correct for signal variation that may occur over protracted periods of use.

5.3.4   CITRUS analysis of high dimensional single cell immune phenotypic data

For analysis of mass cytometry data, the algorithm *cluster identification, characterization, and regression* (CITRUS) was used. The algorithm was designed to detect statistically significant differences between experimental groups in highly dimensional data sets. CITRUS performs multiple sequential steps in order to achieve this. First, unsupervised hierarchical clustering of cellular events across multiple samples by phenotypic similarity along the lines of a defined set of markers is performed. Then biologically relevant features within these clusters of cellular events are calculated on a per file basis and the resulting tree of clusters annotated with this information. CITRUS then interrogates this dataset as to whether these clusters differ on a statistically significant level in terms of median expression of a defined set of markers different from the subset used to create the tree of clusters. This is achieved by the use of a correlative linearized regression model, significance analysis of microarrays. The analysis uses non-parametric statistics to test differences along the lines of user defined experimental groups. Repeated permutations of the data are used to determine whether the expression of any of these markers is significantly related to any of the experimental groups (955). The result is reported not by use of classical p-values but by utilizing false discovery rate. This approach is chosen because due to the multiple testing problem an adjustment of p-values is necessary. The use of more traditional techniques such as Bonferroni-correction reduces the number of false positives at the cost of also reducing the number of correctly identified true positive differences. The calculation of a false discovery rate thus has a higher power to detect truly significant differences. After excluding debris and B-cell subsets by manual gating 10000 events per individual were clustered. A minimum cluster size of 1% was chosen. To avoid the detection of false positives only differences with a false discovery rate <1% were reported. The medians were subsequently exported and analysed with the more classical Kruskal-Wallis test with Dunn's post test and correction for multiplicity.

5.4   Results

Using our custom 27 marker mass cytometry panel described in chapter 4 we analysed immune checkpoint expression on various immune cell subsets in the splenic CLL microenvironment. The generation of samples for analysis of immune checkpoint expression in vehicle, Ibrutinib and Acalabrutinib treated CLL bearing animals is described in 3.4.3. Figure 28 gives an overview of the gating strategy applied. In short, calibration beads were excluded by gating on Ir191 containing DNA intercalator and Ce140, which is contained in the calibration beads only. Doublets were then excluded

by gating on Ir191 and Ir193 DNA intercalators and event lengths. Viable leukocytes are identified by CD45 staining and cisplatin signal, which enriches in dead cells. Finally, cells are sub-setted into physiological B-cells, CLL-B-cells and other immune cells of the microenvironment based on CD19 and B220 staining.
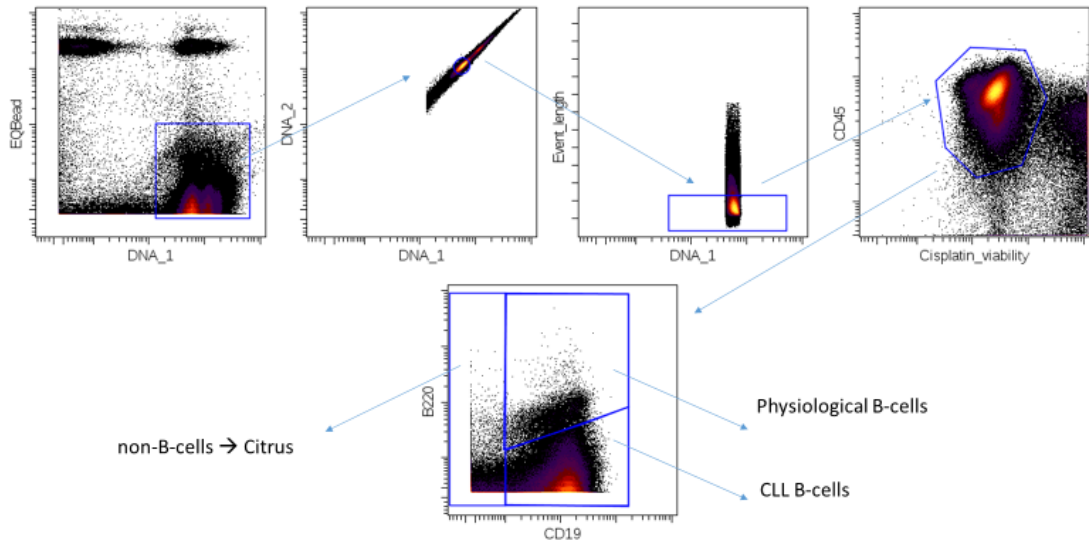
Figure 28: Gating strategy for elimination of cell doublets and dead cells, defining physiological B-cell and CLL-B-cell subsets and other immune cells of the splenic microenvironment.

Figure 29 demonstrates the median PD-L1 153Eu signal intensity on CLL B-cells and physiological B-cells from these samples. We found a statistically significant increase in PD-L1 marker expression on CLL-B-cells in the splenic microenvironment of these animals. Expression on physiological B-cells remained unaltered.
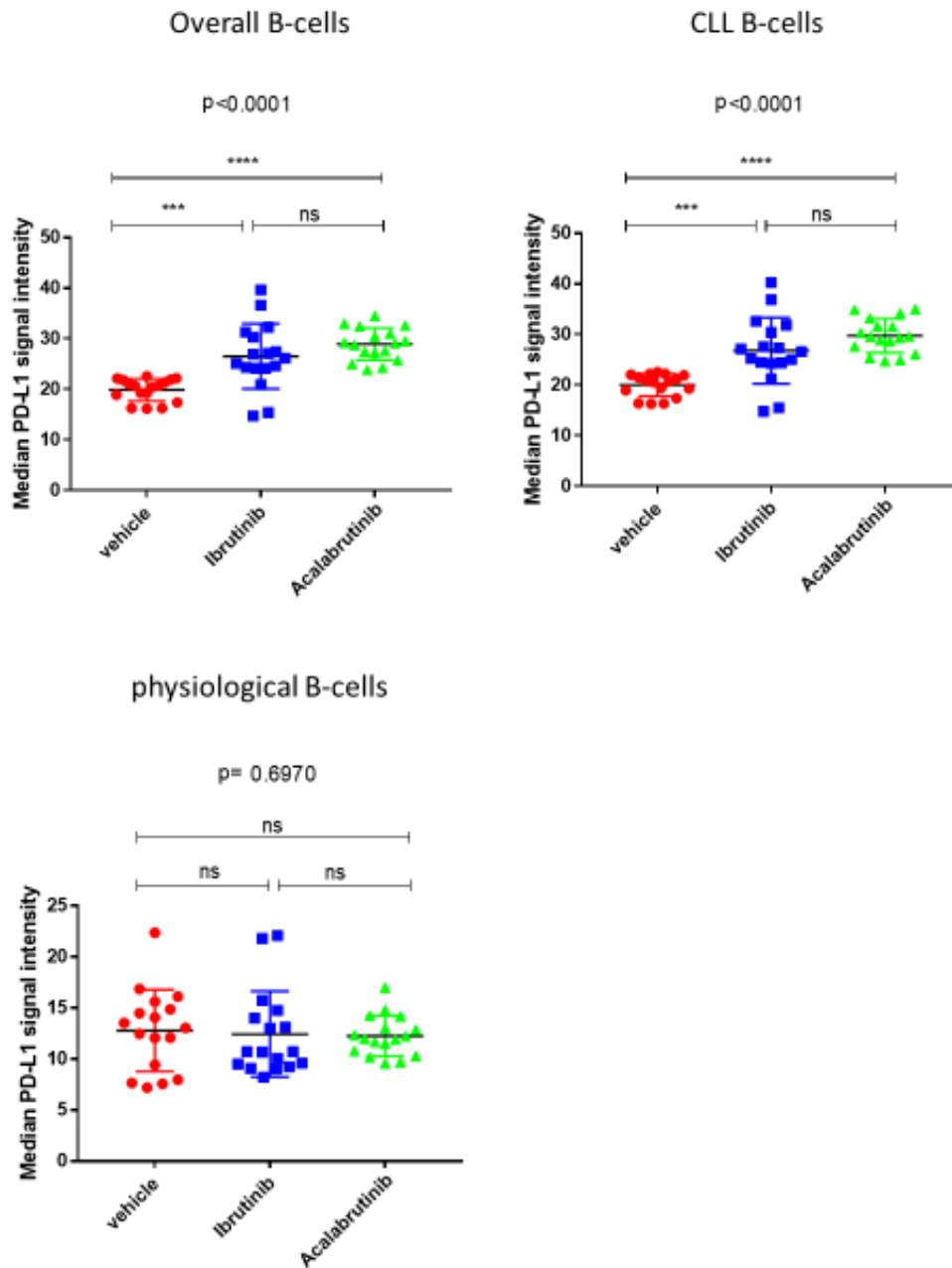
Figure 29: Median PD-L1 153Eu Signal intensity on CLL-B-cells and physiological B-cells of the splenic microenvironment with and without BTKi treatment. Statistical analysis by 1way Anova, 3 groups n=17 each. Abbreviations Ns p > 0.05; *p ≤ 0.05; ** p ≤ 0.01; *** p ≤ 0.001; **** p≤ 0.0001.

Cellular events in the gate comprising the non-B-cell populations were subsequently subjugated to analysis by the CITRUS algorithm as described above. Figures 31-35 display the tree of citrus clusters and demonstrate the identification of major immune cell populations. There were still residual CD19 low B-cells present in this gate, as they are difficult to completely exclude by manual gating due to their sheer abundance.

Figure 30 illustrates the tree of clusters produced by the algorithm. The CITRUS tree will be displayed multiple times and represents all the cellular events from all experimental groups clustered together. Each time the CITRUS tree is displayed the clusters are coloured by different channels to illustrate which clusters are positive for certain markers and allow for the identification of cellular subpopulations. The colour scale indicates the intensity of marker expression per cluster. The size of the clusters represents the relative abundancy of cellular events in that cluster. Each cluster is marked with an ascension number. This number can be used to access the median feature plots generated by the algorithm and the raw median values used for the calculation. The tree structure is reduant. The analysis starts with the central cluster, the largest cluster which has no parent and contains all the cellular events in the analysis. Each cluster has two and sometimes only one daughter cluster. All the cellular events in daughter clusters are also contained in the parent cluster. The following markers were chosen to create the cluster tree: F4/80 146Nd, Ly6G 141Pr, Ly6C 150Nd, CD11c 142Nd, CD11b 147Sm, CD19 166 Er, CD25 151Eu, CD3e 165Ho, CD62L 160Gd, CD8a 168Er, TCRb 169Tm, NK1.1 170Er, CD44 171Yb, CD4 172Yb, B220 144 Nd. The median expression of the following markers was compared within the clusters: CD69 145Nd, CTLA4 154Sm, PD-1 159Tb, PD-L1 153Eu, LAG-3 174Yb, Tim-3 162Dy, Nkp46 167Er, KLRG-1 176Yb, PD-L2 156Gd, 2B4 149Sm, NKG2D 175Lu. Medians of clusters of interest were subsequently exported and anlyzed using a more classical Kruskal-Wallis test with Dunn's post test and correction for multiplicity.
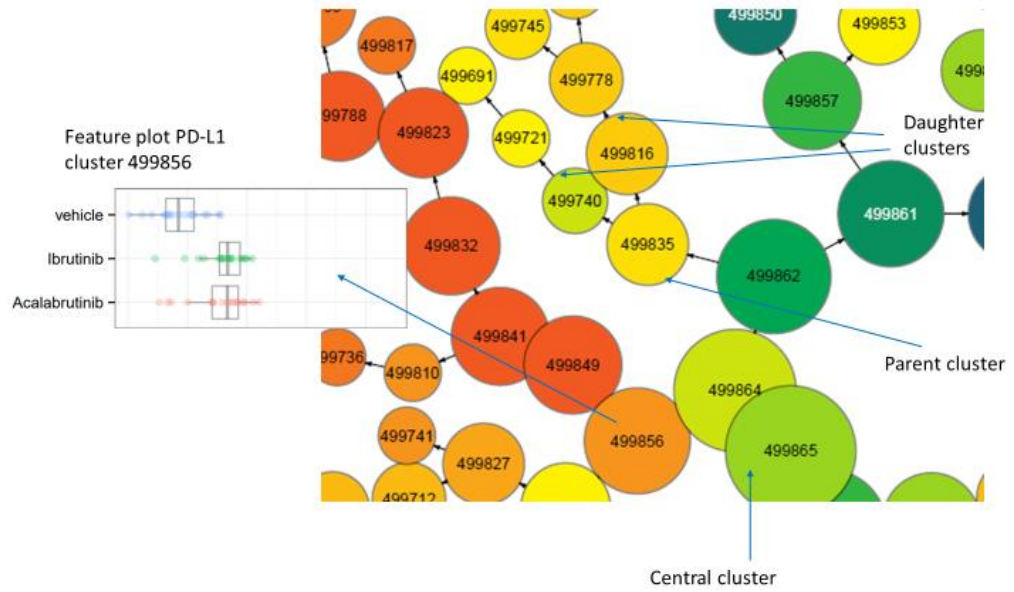
Figure 30: Illustration of citrus cluster tree structre, ascension number, indication of marker expression by colour scale and feature plots.
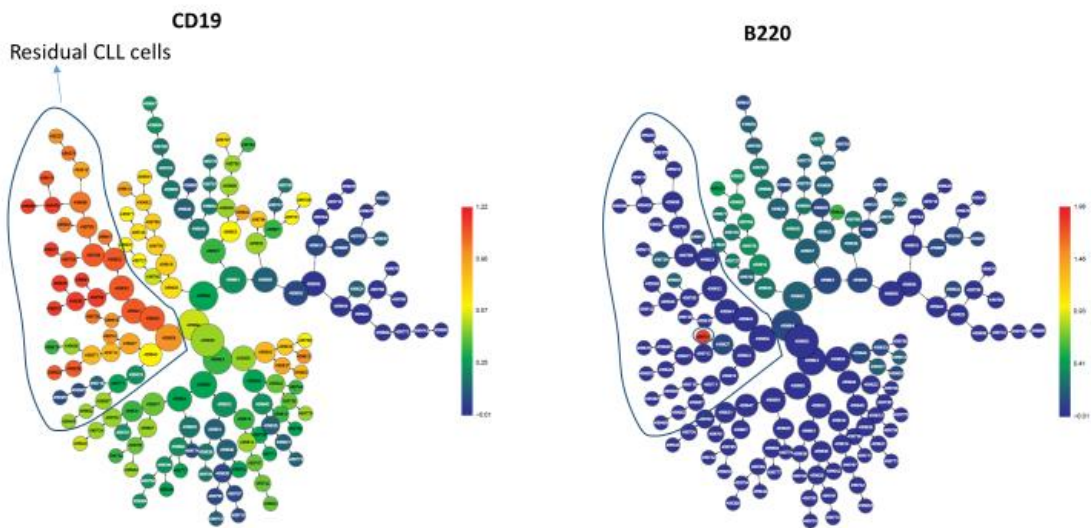
Figure 31: CITRUS cluster tree and identification of residual B-cells. Phenotypically similar events are grouped together in clusters. The distance of clusters is thus a measure of their similarity. The Size of the circles denotes the abundance of cells in the cluster, the colour scale the median marker intensity (red-high expression, blue-low expression). The tree structure is redundant with proximal parent clusters in the centre of the plot containing all events of distal children clusters.
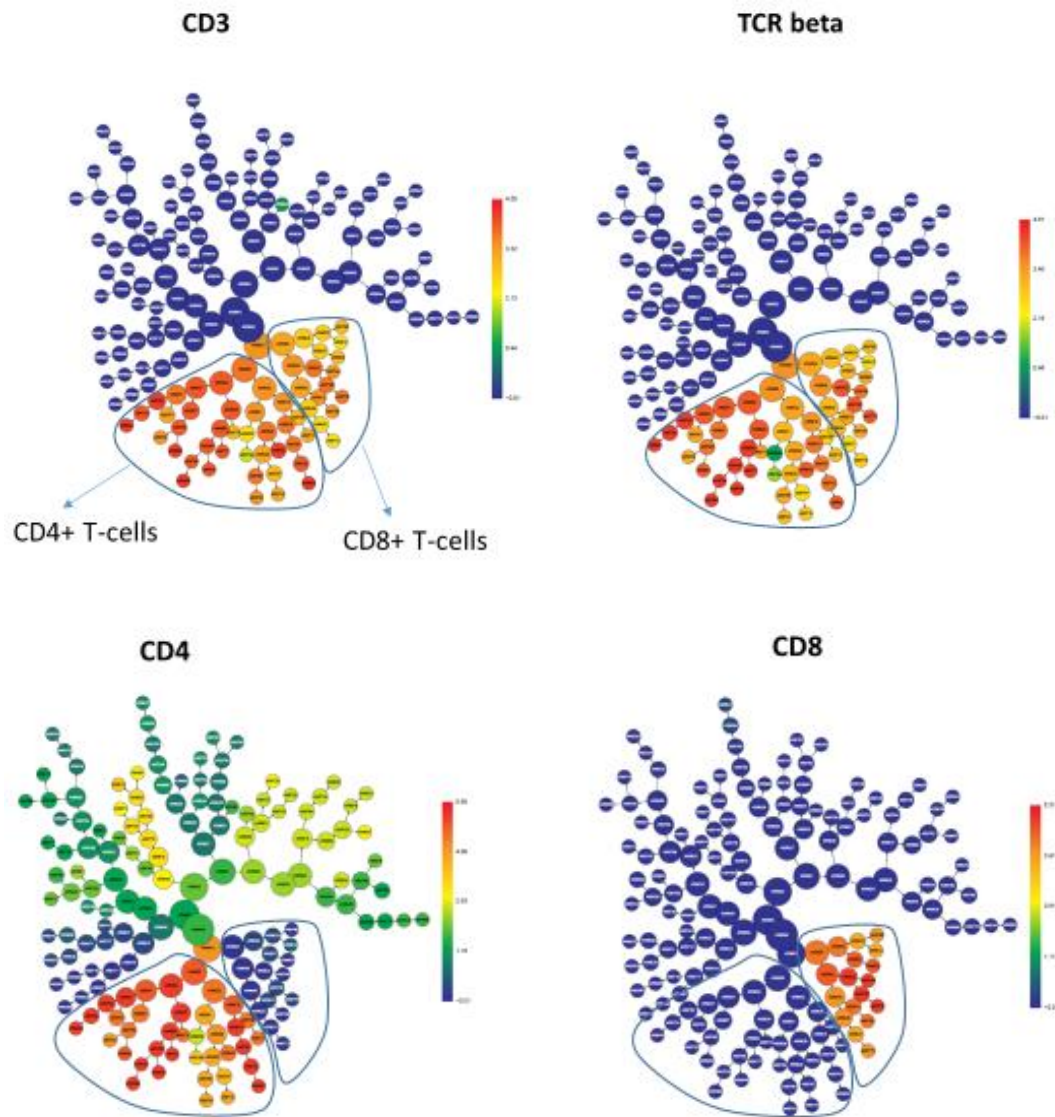
Figure 32: *CITRUS cluster tree and identification of CD4+ and CD8+ T-cells.* Size of the circles denotes the abundance of cells in the cluster, colour scale the median marker intensity (red-high expression, blue-low expression). The tree structure is redundant with proximal clusters containing all distal events.
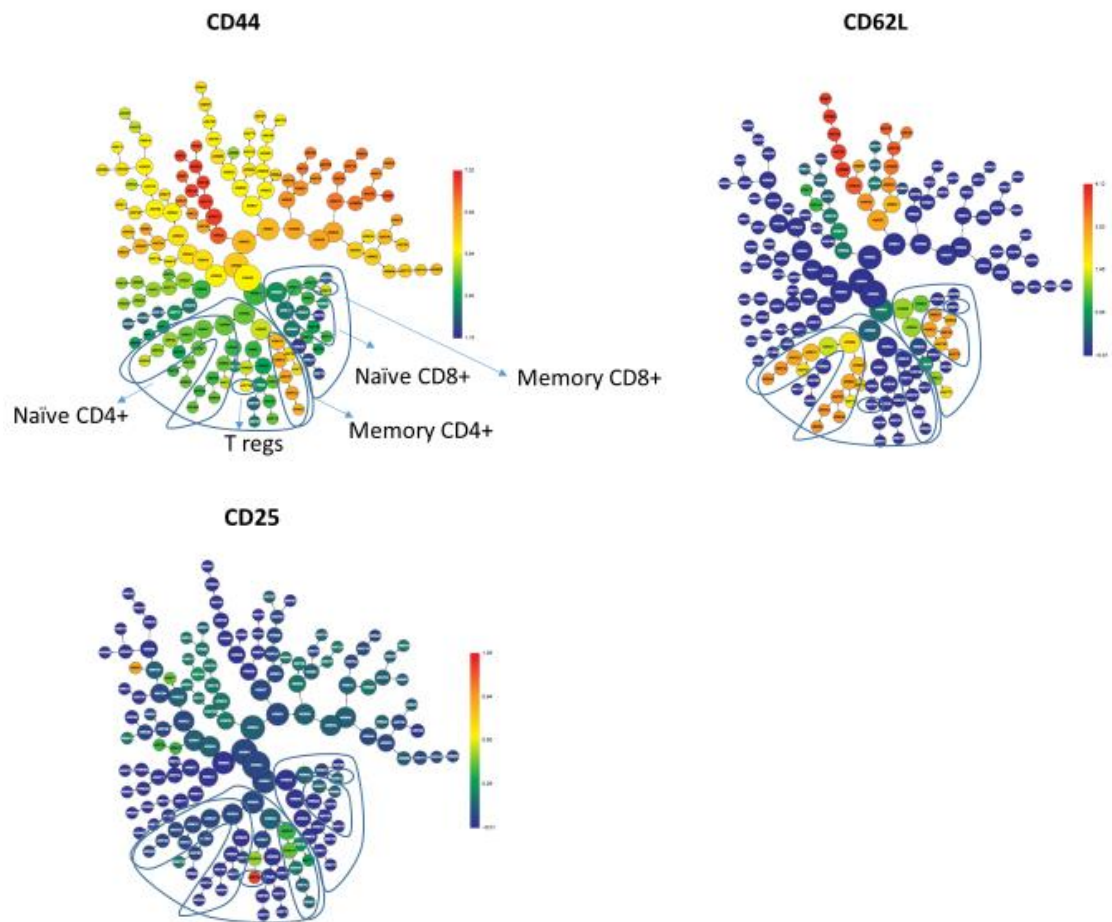
Figure 33: CITRUS cluster tree and identification of memory and naïve T-cells, regulatory T-cells. Size of the circles denotes the abundance of cells in the cluster, colour scale the median marker intensity (red-high expression, blue-low expression). The tree structure is redundant with proximal clusters containing all distal events.
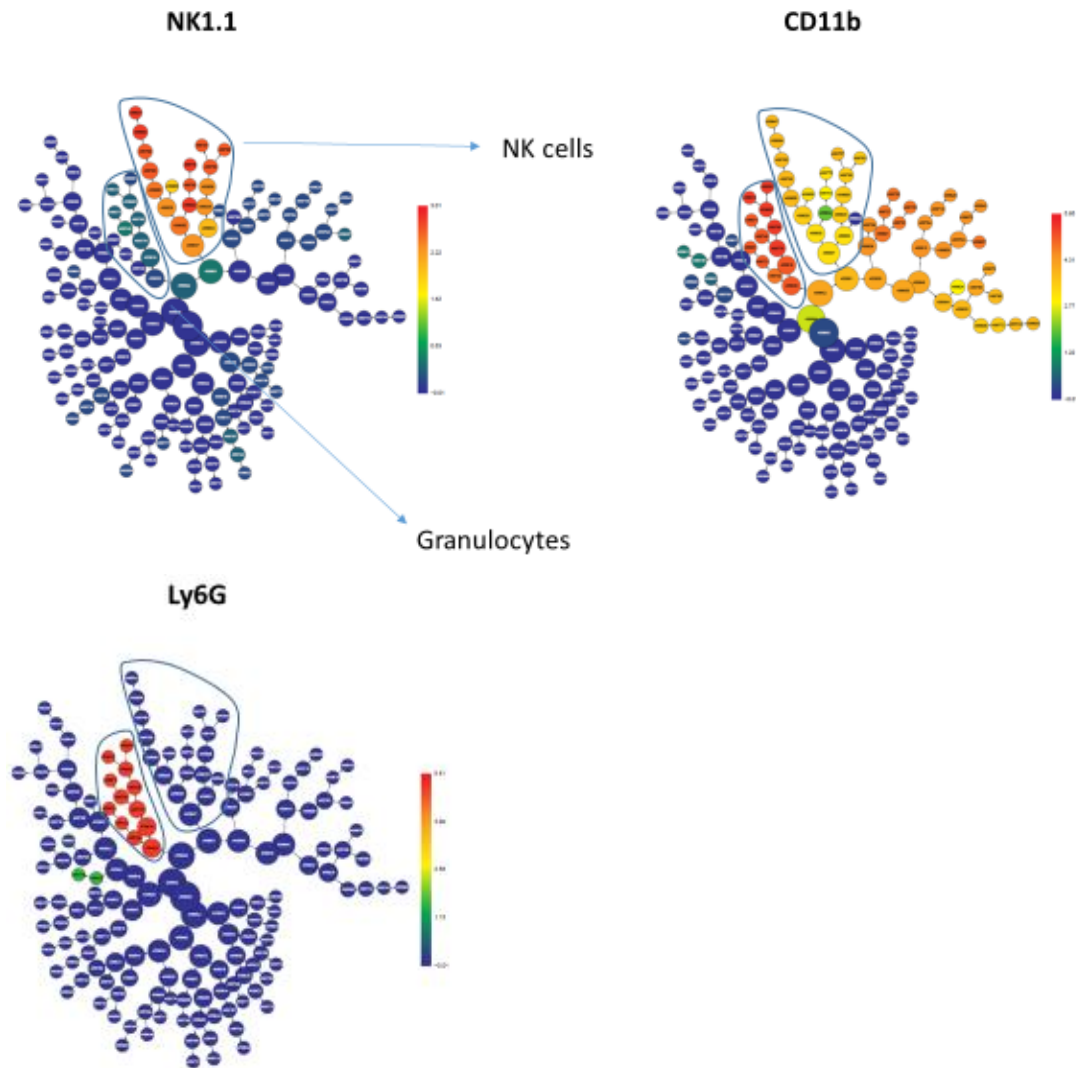
Figure 34: CITRUS cluster tree and identification of Granulocytes and NK-cells. Size of the circles denotes the abundance of cells in the cluster, colour scale the median marker intensity (red-high expression, blue-low expression). The tree structure is redundant with proximal clusters containing all distal events.
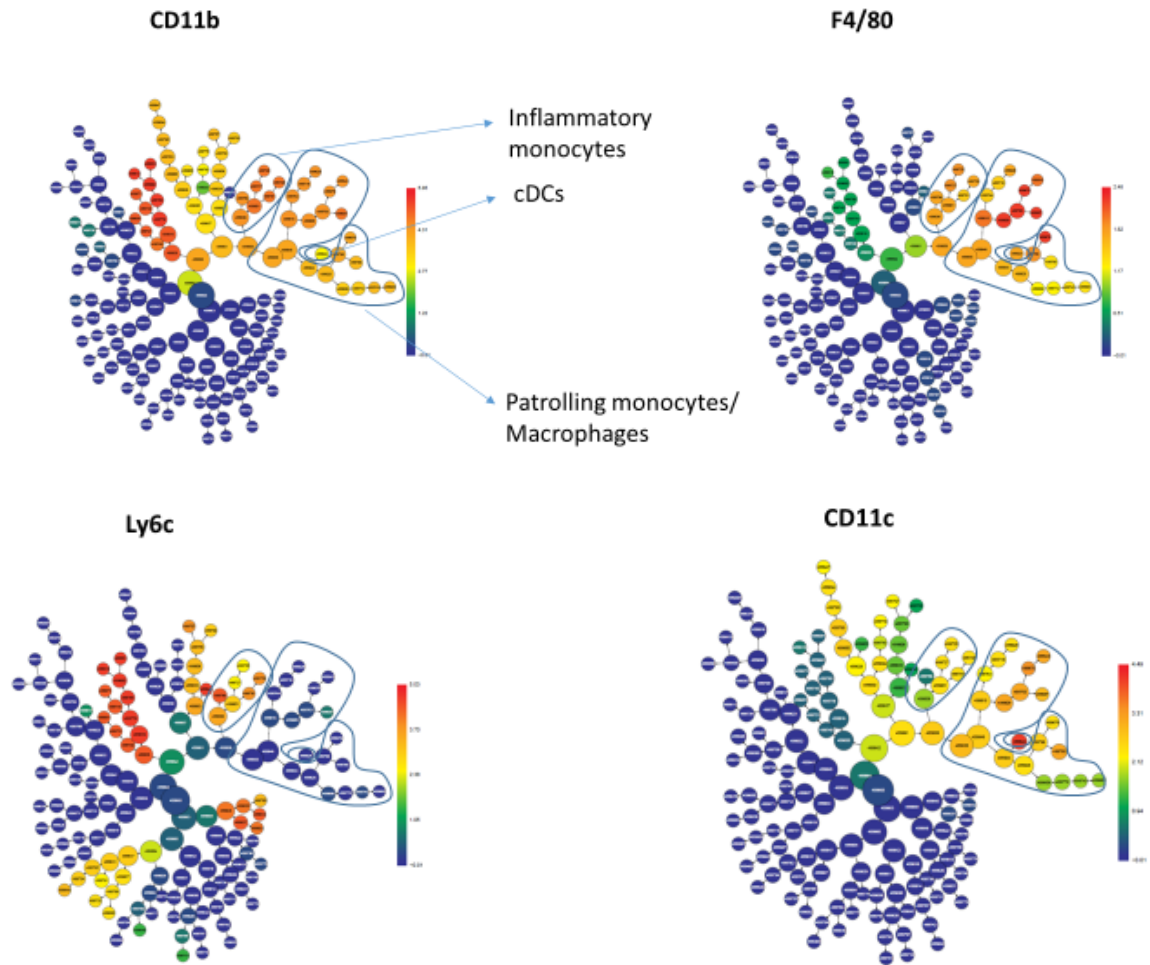
Figure 35: CITRUS cluster tree and identification of dendritic cells and myelomonocytic cells. Size of the circles denotes the abundance of cells in the cluster, colour scale the median marker intensity (red-high expression, blue-low expression). The tree structure is redundant with proximal clusters containing all distal events.

Figure 36 illustrates the comparison of median PD-L1 expression on splenocyte subsets from spleens of both vehicle and BTKi treated animals. We found a statistically significant increase in PD-L1 expression on residual B-cells with BTKi treatment comparable to our findings above. However, the effect on other immune cell subsets was differential with a statistically significant decrease in expression with BTKi treatment on inflammatory monocytes, patrolling monocytes and macrophages. Moreover, we detected a statistically significant but rather modest decrease on overall CD4+ T-cells. Figure 37 demonstrates CD69 expression in the splenic microenvironment. Comparing the expression on immune cell subsets from spleens of BTKi and vehicle treated animals we found a decrease in CD69 expression with BTKi treatment on memory T-cells and on two separate subsets of NK cells. Figure 38 shows expression of PD-1 among splenocyte subsets. We detected a statistically significant decrease of PD-1 expression

on memory CD4+ T-cells and T regulatory cells with BTK inhibitor treatment. Figure 38 illustrates differences in surface LAG-3 expression on immune cell subsets from splenocytes of vehicle and BTK inhibitor treated animals. We found a statistically significant decrease in LAG-3 expression on memory CD4+ T-cells and regulatory T-cells. Figure 40 demonstrates expression of KLRG-1 on immune cell subsets of spleen samples from vehicle and BTK inhibitor treated animals. We showed a decrease in KLRG-1 expression with Ibrutinib treatment on NK cells, memory CD4+ T-cells and regulatory T-cells.

In conclusion we have discovered a differential effect on PD-L1 expression with BTK inhibitor treatment. While the expression on CLL B-cells seems to be increased expression on myeloid cells subsets is decreased. On T-cells we found that the exhaustion phenotype is ameliorate, especially on memory CD4+ T-cells and regulatory T-cells with a decrease in expression of PD-1, LAG-3 and KLRG-1. Interestingly we also found evidence of modulation of NK-cell phenotype with a decrease in expression KLRG-1. CD69 expression was decreased among both CD4+ T-cells and NK-cells.
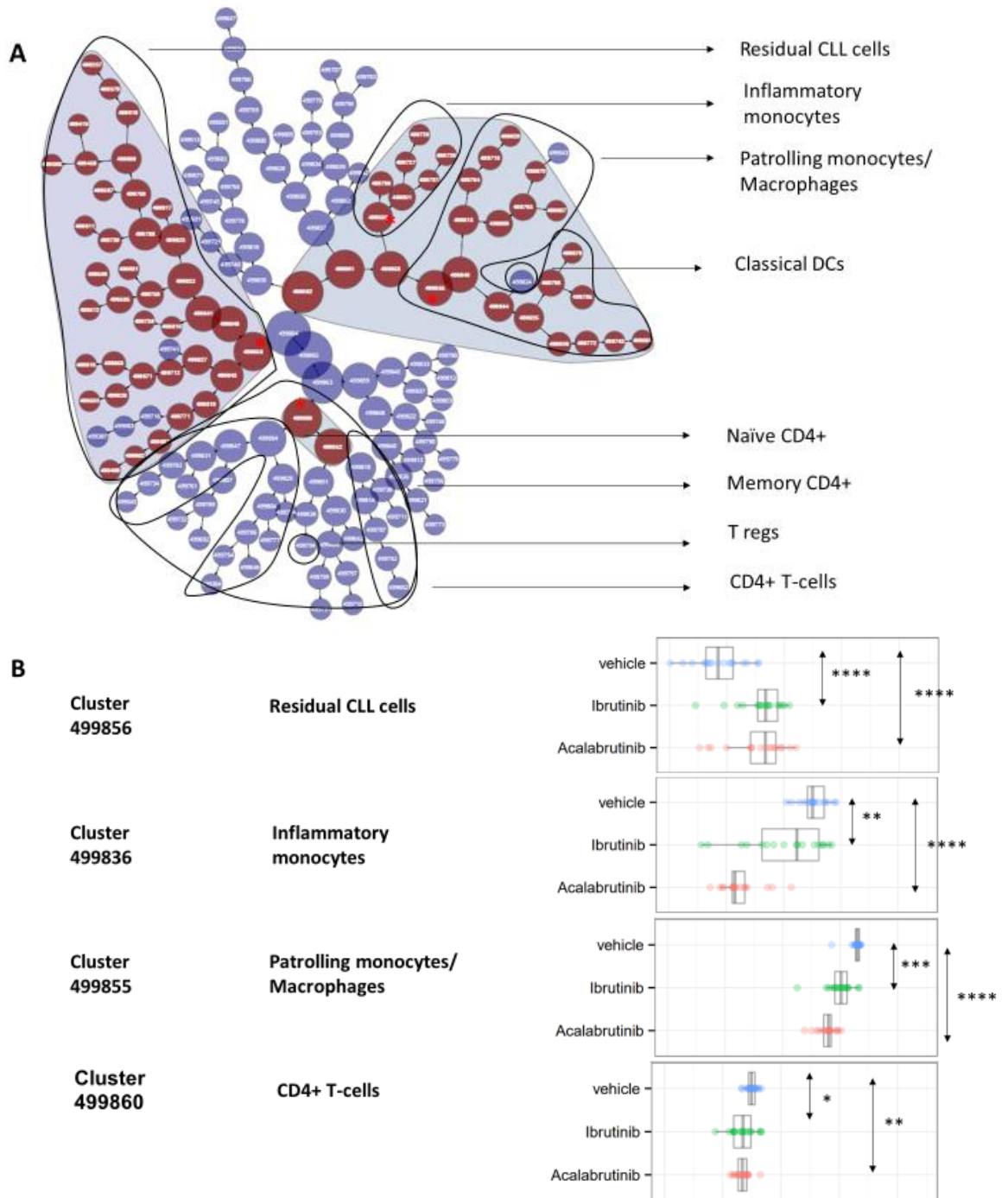
Figure 36: *CITRUS cluster tree, comparison of median PD-L1 expression on splenocyte subsets from BTK inhibitor and vehicle treated animals. (A) CITRUS cluster tree, statistical analysis by "statistical analysis of microarrays", clusters with statistically significant differences in marker expression highlighted in red, false discovery <1%. * denotes cluster displayed in B. (B) Median signal intensity of selected clusters compared in BTK inhibitor and vehicle treated animals. Statistical anaylsis by Kruskal-Wallis test, 3 groups n=17 each, Abbreviations; * - p ≤ 0.05; ** - p ≤ 0.01; *** - p ≤ 0.001; **** - p≤ 0.0001.*
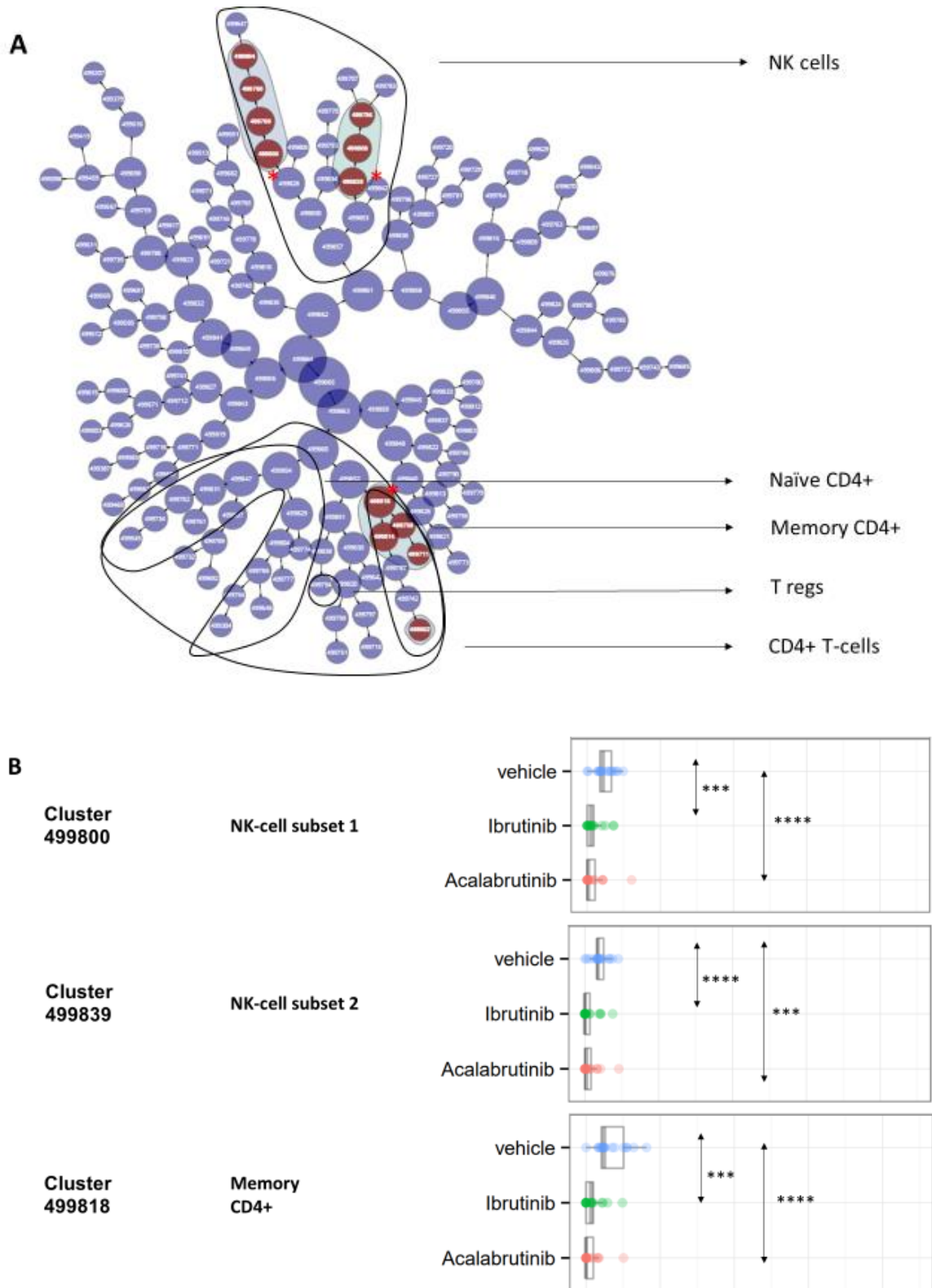
Figure 37: *CITRUS cluster tree, comparison of median CD69 expression on splenocyte subsets from BTK inhibitor and vehicle treated animals. (A) CITRUS cluster tree, statistical analysis by "statistical analysis of microarrays", clusters with statistically significant differences in marker expression highlighted in red, false discovery <1%. * denotes cluster displayed in B. (B) Median signal intensity of selected clusters compared in BTK inhibitor and vehicle treated animals. Statistical anaylsis by Kruskal-Wallis test, 3 groups n=17 each, Abbreviations; * - p ≤ 0.05; ** - p ≤ 0.01; *** - p ≤ 0.001; **** - p ≤ 0.0001.*
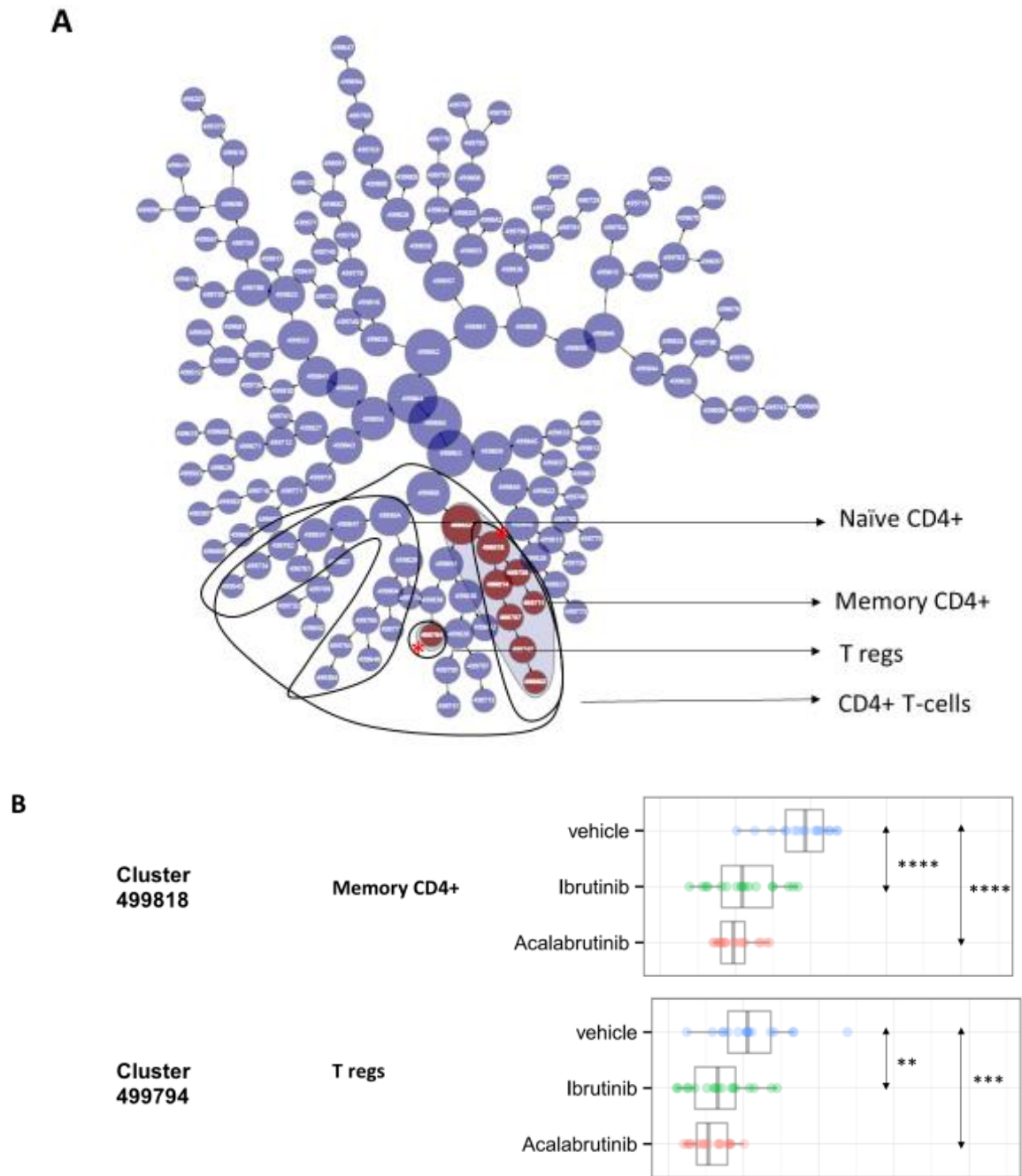
Figure 38: *CITRUS cluster tree, comparison of median PD-1 expression on splenocyte subsets from BTK inhibitor and vehicle treated animals. (A) CITRUS cluster tree, statistical analysis by "statistical analysis of microarrays", clusters with statistically significant differences in marker expression highlighted in red, false discovery <1%. * denotes cluster displayed in B. (B) Median signal intensity of selected clusters compared in BTK inhibitor and vehicle treated animals. Statistical anaylsis by Kruskal-Wallis test, 3 groups n=17 each, Abbreviations: * - p ≤ 0.05; ** - p ≤ 0.01; *** - p ≤ 0.001; **** - p≤ 0.0001.*
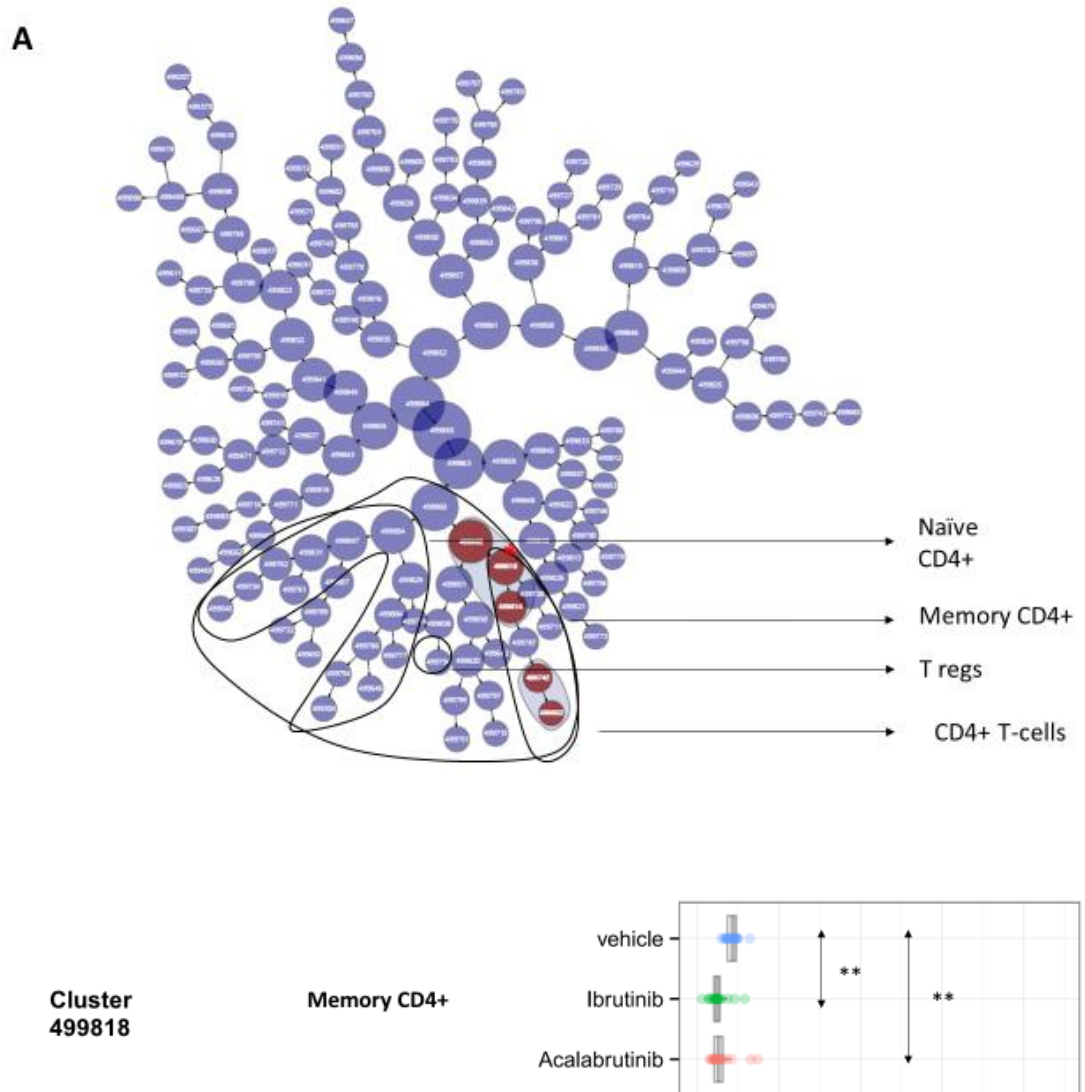
Figure 39: *CITRUS cluster tree, comparison of median LAG-3 expression on splenocyte subsets from BTK inhibitor and vehicle treated animals*. *(A) CITRUS cluster tree, statistical analysis by "statistical analysis of microarrays", clusters with statistically significant differences in marker expression highlighted in red, false discovery <1%. * denotes cluster displayed in B. (B) Median signal intensity of selected clusters compared in BTK inhibitor and vehicle treated animals. Statistical anaylsis by Kruskal-Wallis test, 3 groups n=17 each, Abbreviations; * - p ≤ 0.05; ** - p ≤ 0.01; *** - p ≤ 0.001; **** - p≤ 0.0001.*
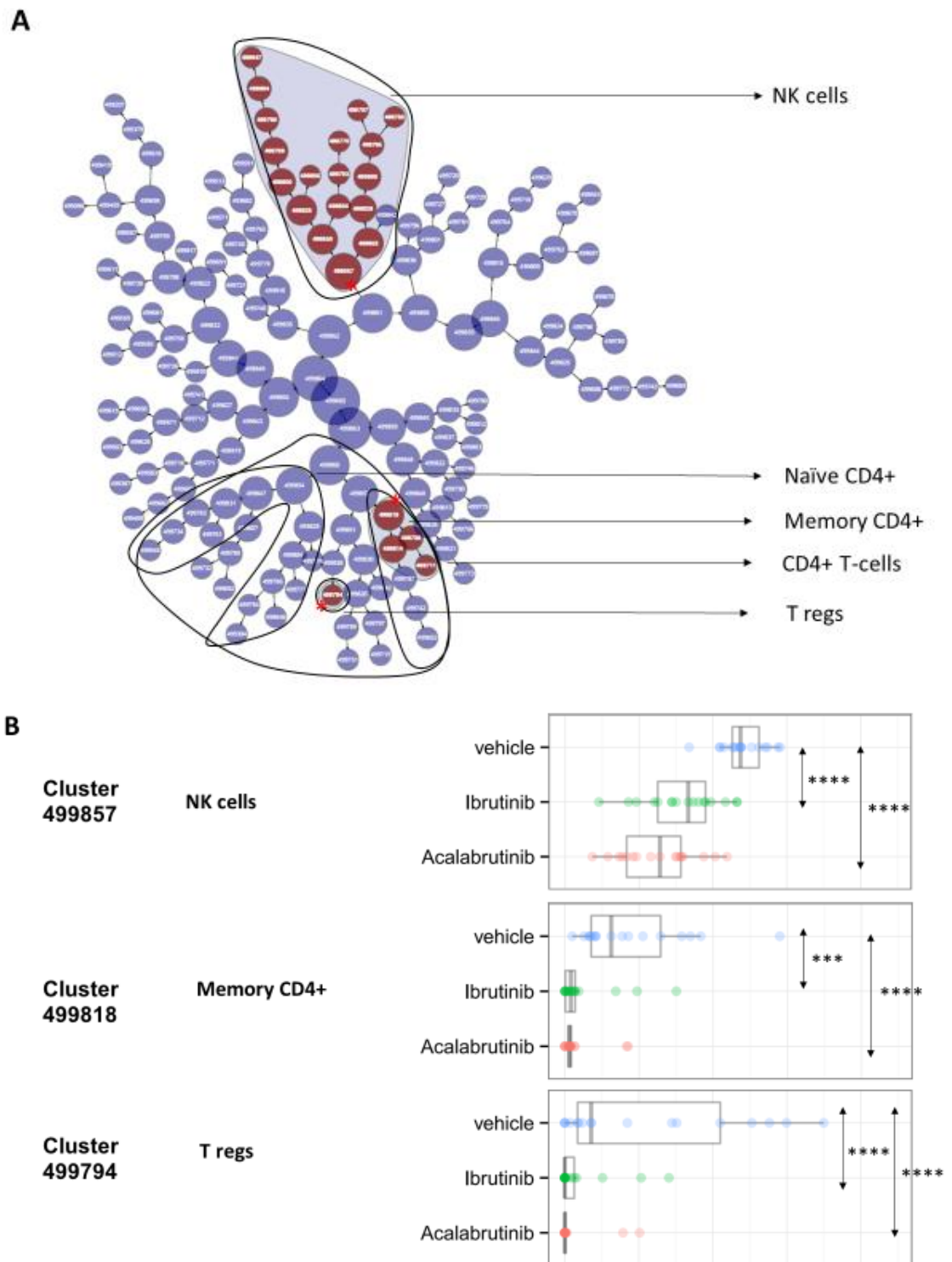
Figure 40: *CITRUS cluster tree, comparison of median KLRG-1 expression on splenocyte subsets from BTK inhibitor and vehicle treated animals*. *(A) CITRUS cluster tree, statistical analysis by "statistical analysis of microarrays", clusters with statistically significant differences in marker expression highlighted in red, false discovery <1%. * denotes cluster displayed in B. (B) Median signal intensity of selected clusters compared in BTK inhibitor and vehicle treated animals. Statistical anaylsis by Kruskal-Wallis test, 3 groups n=17 each, Abbreviation; * - p ≤ 0.05; ** - p ≤ 0.01; *** - p ≤ 0.001; **** - p≤ 0.0001.*

5.5 Discussion

We have here described a differential effect on PD-L1 expression with BTK inhibitor treatment among various immune cell subsets in the splenic microenvironment of CLL bearing animals. While the expression on CLL B-cells seems to be increased modestly with both Ibrutinib and Acalabrutinib treatment, expression on myeloid cells subsets is decreased. The increase of PD-L1 on CLL B-cells in the splenic microenvironment with BTK inhibitor treatment comes as a surprise given their inhibitory effect towards BCR signalling, especially in the light of recent reports suggesting that PD-L1 expression is driven by BCR signalling in the setting of DLBCL (984). A recent publication by Wierz et al. (985) has suggested that PD-L1 high CLL B-cells express higher levels of adhesion molecules. We therefore speculate that these cells are more readily retained in the microenvironment while PD-L1 low CLL B-cells will be mobilized to the peripheral blood by Ibrutinib. We are planning to analyse the levels of PD-L1 expression on peripheral blood B-cells from these animals in a next step – the respective PBMC samples have been cryopreserved. Analysis of dynamics of expression over time and analysis of PD-L1 expression on peripheral blood B-cells may be warranted. PD-L1 expression on infiltrating myeloid derived cells has also been implicated in CLL associated immunosuppression (835). Indeed, we do find a decrease in expression with both Ibrutinib and Acalabrutinib treatment among white pulp inflammatory monocytes as well as white pulp patrolling monocytes and macrophages like cells. Myeloid cells may thus be the driving force in induction of CLL associated T-cell deficiency and the major target for BTK inhibitor mediated T-cell modulation, comparable to the situation in PDAC (881). On T-cells we find, that the exhaustion phenotype is ameliorated, especially on memory CD4+ T-cells and regulatory T-cells, with a decrease in expression of PD-1, LAG-3 and KLRG-1. Interestingly we also find evidence of modulation of NK-cell phenotype with a decrease in expression KLRG-1. The influence of BTK inhibitor treatment on phenotype and function of NK cells in the CLL microenvironment has so far been explored little. Especially in the light of reduced cytolytic activity of NK cells towards CLL B-cells (278, 279) and reports of an influence of NK cells numbers on clinical outcomes in CLL patients (289, 290) a further investigations of these effects of BTK inhibitors seems warranted. CD69 expression, an early activation marker in lymphocytes, was found to be decreased among both CD4+ T-cells and NK-cells. However, in this experiment we did not detect an influence on immunophenotype of CD8+ cytotoxic T-cells. Still, the combination of decreased CD4+ T-cell exhaustion phenotype and decreased expression of inhibitory NK-cell receptors in the setting of a more permissive myeloid cell immune phenotype

could potentially translate into improved immunosurveillance and elimination of CLL B-cells.

6 Influence of BTK inhibition on T-cell function and immune synapse formation

6.1 Specific introduction

The absolute number of T-cells is expanded in the setting of CLL (340-342). T-cells derived from CLL patients have been observed to be shifted away from naïve subsets towards more antigen experienced subsets (348, 350-355). CLL associated T-cells appear to be enriched for a select few clones with identical TCRBV gene usage and CDR3 size distribution, possibly as a result of chronic activation of T-cells (358, 360-362). Analysis of the T-cell receptor repertoire in CLL patients demonstrated the use of shared clonotypes between patients that appear to be CLL-specific, suggesting that antigen drive by CLL B-cells themselves may underlie the CLL-associated T-cell expansion (368). The onset of CLL is associated with severe functional defects of both T helper and cytotoxic T-cell function (298, 397-401). Moreover, CLL associated T helper cells have been shown to be critical in promoting growth and survival of CLL B-cells in vivo (402). With the onset of CLL, T helper cell polarity has been demonstrated to shift away from a Th1 phenotype towards a more humoral immunity and B-cell growth promoting Th2 phenotype (334, 403) with a decreased production of classical Th1 cytokines such as IL2 (353, 404) and increased expression of Th2 cytokines such as IL4, IL5 and IL10 (334, 353, 405, 406). Th2 cytokines such as IL4 and IL10 have been shown to promote proliferation of leukemic cells and keep CLL B-cells safe from apoptosis (407-409). Secretion of classical Th1 cytokines IFN-γ and TNF-α on the other hand has been observed to be increased rather than decreased in CLL T cells and this has been shown to correlate with disease stage (405, 406, 413-415). Both cytokines have also been demonstrated to promote survival and proliferation of CLL B-cells (416, 417). In addition, continuous endogenous tumour specific immune responses have been described to lead to a secondary T-cell deficiency and tumour immune escape via upregulation of PD-L1 expression in the tumour microenvironment through IFN-γ secreted by tumour associated T-cells themselves – a process dubbed "adaptive immune resistance" (842). Moreover, the formation of immunological synapses between both CD4+ and CD8+ CLL patient derived T-cells and superantigen pulsed CLL B-cells has been shown to be severely impaired due to a dysregulation of actin remodelling and recruitment of important signaling molecules of the cytoskeleton like LcK, Cdc42, WASp, filamin-A and dynamin-2 (215). Gene expression profiling of CLL patient derived T-cells has demonstrated dysregulation of proteins involved in T-cell proliferation and differentiation, T-cell activation, vesicle trafficking and actin cytoskeleton remodelling (420, 421). The

functional defects in actin remodelling and synapse formation of CLL associated T-cells have been shown to be directly induced by CLL B-cells via inhibitory surface receptors CD200, PD-L1, B7-H3 and CD270 (216). We have previously been able to demonstrate that T-cell dysfunction in the setting of CLL shares many functional similarities to chronic activation induced T-cell exhaustion in the setting of chronic viral infections such as impaired capacity for proliferation and cytotoxic activity of CD8+ T-cells but also differs significantly in some regards such as increased rather than decreased production of cytokines TNF-α and INF-γ. This functional state has therefore been dubbed "pseudo T-cell exhaustion" (424).

Various studies have suggested that the BTK inhibitor Ibrutinib has the ability to modulate T-cell and myeloid cell function and this contributes to the clinical efficacy of the agent. Stiff et al. demonstrated expression of BTK in both human and murine MDSCs and showed that Ibrutinib treatment has the ability to suppress BTK phosphorylation in MDSCs resulting in impaired nitrous oxide production, cell migration, expression of IDO as well as impaired in vitro generation of human MDSCs. Ibrutinib treatment resulted in reduced numbers of MDSCs in both spleen and tumours of mouse models of mammary cancer and melanoma (879). Ping et al. demonstrated decreased production of CXCL12, CXCL13, CCL19 and VEGF by human macrophages after Ibrutinib treatment. Moreover, adhesion, migration and invasion of co-cultured lymphoid cells was significantly impaired (880). Gunderson et al. reported that tumour growth in a model of PDAC was dependent on a cross-talk between B-cells and FcRY+ tumour associated macrophages resulting in a Th2-permissive macrophage phenotype via BTK activation in a PI3KY dependent manner. Ibrutinib treatment resulted in a shift towards a more Th1-permissive macrophage phenotype and fostered CD8+ T-cell cytotoxicity (881). Dubovsky et al. were able to demonstrate that Ibrutinib has the potential to shift T-helper cell polarity away from Th2 towards Th1 by targeting ITK and could thereby correct malignancy associated T-cell defects (877). Moreover, Kondo et al. have reported downregulation of PD-L1 on the surface of CLL B-cells in the peripheral blood of Ibrutinib treated CLL patients as well as downregulation of expression of PD-1 on the surface of CD4+ and CD8+ T-cells, both in a STAT3 dependent manner (878). Importantly, as Acalabrutinib does not have inhibitory activity towards ITK there is a potential for differential effects on T-cell function between the two BTK inhibitors (986).

6.2   Goals and objectives

Based on the available literature and preliminary data of our group we hypothesize that the clinical efficacy of BTK-inhibitors is based on a synergism between direct anti-tumour

effects and correction of CLL-associated functional T-cell defects. Using the Eµ-TCL1 mouse model we sought to demonstrate that BTK inhibitors have the potential to correct CLL associated T-cell defects. It has been suggested that the major mechanism of T-cell modulation by Ibrutinib is via targeting of ITK. Acalabrutinib does not have inhibitory capacity toward ITK. We therefore sought to investigate whether a differential effect on T-cell function in the setting of CLL can be detected between Ibrutinib and Acalabrutinib.

6.3 Specific methods and materials

6.3.1 Manipulation of mouse splenocyte single cell suspensions

6.3.1.1 Cell thawing procedure

Thawing of cryopreserved splenocyte samples was performed in a water bath at 37°C. To avoid contamination the vials were disinfected using 70% IMS (Fisher Scientific, UK) and subsequently opend in a class II biosafety cabinet. The cell suspension was pipetted into 10ml RPMI 1640 (Gibco, UK) supplemented with 10% FCS (Gibco, UK), 1% Penicillin-Streptomycin (Sigma, UK) at 37°C. Subsequently the suspension was centrifuged at 300 x g for 10 minutes at room temperature and resuspended in a volume suitable for number of cells contained in the pellet. Automated cell counting was conducted on a Luna fl automated cell counter (Logos bioystems, USA) after dilution of a 10µl aliquot with an equal amount of 0.4% Tryphan blue (Sigma, UK).

6.3.1.2 Negative selection of CLL and B cells

CLL and B cells where isolated from splenocytes suspensions using the pan-B-cell isolation kit (Miltenyi, UK) which uses *magnetic activated cell sorting* (MACS). The suspension were centrifuged at 300 x g for 10 minutes at 4°C, the supernatant completely aspirated and the pellet resuspendend in 40 µL of ice-cold MACS buffer (PBS (Sigma, UK) pH 7.2, 0.5% *bovine serum albumin* (BSA) (Sigma, UK), 2mM EDTA (Sigma, UK)) per 10^7 total cells. 10 µL of Pan B Cell Biotin-Antibody Cocktail (Miltenyi, UK) per 10^7 total cells were added. The cells were well mixed and incubated for 5 minutes at 4°C. A further 30 µL of ice-cold MACS buffer per 10^7 total cells and 20 µL of Anti-Biotin MicroBeads (Miltenyi, UK) per 10^7 cells were added. Cells were mixed well and incubated for another 10 minutes at 4°C. Finally, the volume was adjusted to 500µl per 10^8 cells (minimum 500µl). For separation, a LD column (Miltenyi, UK) was placed in the magnetic field of a MACS separator (Miltenyi, UK) and primed with 2 ml of MACS buffer. The cell suspension was applied to the column and flushed through by applying 1ml MACS buffer

twice. The effluent, which was collected in a 15 ml centrifuge tube (VWR, UK), contained the unlabelled pan-B-cell fraction.

6.3.1.3 Negative selection of T cells

T-cells where isolated from splenocytes suspensions using the pan-T-cell isolation kit II (Miltenyi, UK) which uses MACS. The suspension were centrifuged at 300 x g for 10 minutes at 4°C, the supernatant completely aspirated and the pellet resuspendend in 40 µL of ice-cold MACS buffer (PBS (Sigma, UK) pH 7.2, 0.5% BSA (Sigma, UK), 2mM EDTA (Sigma, UK)) per 10^7 total cells. 10 µL of Pan T Cell Biotin-Antibody Cocktail (Miltenyi, UK) per 10^7 total cells were added. The cells were well mixed and incubated for 5 minutes at 4°C. A further 30 µL of ice-cold MACS buffer per 10^7 total cells and 20 µL of Anti-Biotin MicroBeads (Miltenyi, UK) per 10^7 cells were added. Cells were mixed well and incubated for another 10 minutes at 4°C. Finally, the volume was adjusted to 500µl per 10^8 (minimum 500µl). For separation, a LD column (Miltenyi, UK) was placed in the magnetic field of a MACS separator (Miltenyi, UK) and primed with 2 ml of MACS buffer. The cell suspension was applied to the column and flushed through by applying 1ml MACS buffer twice. The effluent, which was collected in a 15 ml centrifuge tube (VWR, UK), contained the unlabelled pan-T-cell fraction..

6.3.2   Flow cytometry based functional T-cell assays

6.3.2.1 EdU incorporation

EdU was used for assessment of in vivo proliferation of T-cells subsets. The substance is utilized during DNA synthesis in lieu of physiological nucleosides. It can subsequently be visualized by convalent binding to an azide coupled to a flurochrome via an alkyne moiety. The reaction is catalysed by copper (953, 954). The EdU assay can be used alongside traditional flow cytometry staining for both surface and intracellular markers. EdU (Life Technologies, UK) was applied to experimental annimals by i.p. injection at a dose of 100µg/g body weight 20 hours before being culled. Priot to the injection an EDU stock solution was prepared by dissolving the substance in sterile PBS (Sigma, UK) under sterile conditions.

6.3.2.2 Cell stimulation

$1x10^6$ splenocytes were incubated in 250µl RPMI 1640 with 10% FCS (Gibco, UK), 1% Penicillin/Streptomycin (Life Technologies, UK) in round-bottom 96-well-plates (VWR, UK). 5µg/ml CD107a per well (Clone 1D4B biolegend, UK) was added. The splenocytes

were stimulated with PMA/ionomycin/brefeldin A/monensin cell stimulation cocktail (eBioscience, UK) for 6 hours at 37ºC/5% CO2. Controls were treated with transport inhibitor cocktail brefeldin A/monensin (eBioscience), but no cell stimulation cocktail.

6.3.2.3 Surface, intracellular and intranuclear flow cytometry staining

1×10^6 PMA/ionomycin/brefeldin A/monensin stimulated splenocytes, 1×10^6 unstimulated splenocytes and their corresponding controls were used per animal and transferred into 5ml polystyrene round-bottom tubes (Corning, UK). All staining steps were performed at a temperature of 2-8°C to avoid internalisation or capping of the antibodies. Unstimulated cells were split for intracellular EDU stain and intranuclear ki67 stains. Cells were resuspended in 100 µl of FACS buffer containing viability stain (fixable viability efluor 506, ebioscience, UK) at a concentration of 1:1000. Surface antibodies (CD3e APC/CY 7, clone 145-2C11, biolegend, UK; CD8a BV605, clone 53-6.7, biolegend, UK; CD44 AF700, clone IM7, ebioscience, UK) were added at a dilution of 1:100 and cells incubated at 4 ºC for 30 minutes. Fixation using IC fixation buffer (ebioscience,UK) and permeabilisation using permeabilisation buffer (ebioscience,UK) for intracellular stains or FOXP3 fixation/permeabilisation buffer (ebioscience,UK) and permeabilisation buffer (ebioscience,UK) for intranuclear stains were performed according to the manufacturer's recommendations. Cells were stained with intracellular antibodies (Interferon gamma AF488, clone XMG1.2, biolegend, UK; IL2 PE/Cy7, clone JES6-5H4, biolegend, UK; IL4 PerCPefluor 710, clone 11B11, ebioscience, UK) and intranuclear antibodies (Ki67 PE/Cy7, clone 16A8, biolegend, UK) for 1h at 4ºC at a 1:100 dilution. Compensation controls consisted of ABC total compensation beads (Thermo fisher scientific, UK). In order to obtain compensation controls one drop each of both negative control beads and positive antibody binding beads were added to 80µl FACS buffer in a 5ml polystyrene round-bottom tube (Corning, UK). One tube per flurochrome included in the panel was prepared. Subsequently a dose appropriate for one test of pre-conjugated flow cytometry antibody was added and the sample incubated at 4°C for 30 minutes in the dark. The solution was then washed in 2ml FACS buffer twice and resuspended in 300µl PBS ready for acquisition. Beads could not be used for compensation control of the viability stain-here single-stained cells were used. For EDU staining, cells were fixed in 100µl of "Click it" fixative (life technologies,UK) for 15 minutes at room temperature in the dark. After 2 washes with FACS buffer cells were resuspended in 100µl of 1x "Click it" permeabilization buffer (life technologies,UK) and incubated for an additional 15 minutes at room temperature in the dark. 500 µl of reaction cocktail (2% CUSO4, 0.5% Alexa Fluor 488 azide, 10% 1x "Click it" reaction buffer additive in PBS, all life technologies,

UK) were added and cells thoroughly mixed. For the *fluorescence minus one* (FMO) control the cocktail was prepared without fluorescent dye azide. After incubation for 30 minutes at room temperature in the dark cells were washed twice in permeabilization buffer and carried forward for acquisition. Acquisiton was performed on a BD LSR Fortessa flow cytometer (BD, UK). The recorded .FCS files were analysed using Cytobank (Cytobank Inc., USA).

6.3.3   Immune synapse formation assay

6.3.3.1 Synapse formation and actin staining

$1 \times 10E^{6}$ B-cells are resuspended in serum free RPMI 1640 (Gibco, UK) with 1% Penicillin/Streptomycin (Life Technologies, UK), and labelled using *7-Amino-4-Chlormethylcumarin* (CMAC) (Thermofisher, UK) at a concentration of 2µg/ml for 30 minutes at 37 ºC 5%CO_2. B-cells were activated using 2ug/ml SEA/SEB (Sigma, UK) for 30 minutes at 37 ºC 5%CO_2 in RPMI 1640 (Gibco, UK) with 10% FCS (Gibco, UK), 1% Penicillin/Streptomycin (Life Technologies). $1 \times 10E^{6}$ T-cells were added in serum free medium and allowed to conjugate to B-cells pelleted for 20 minutes at 37 ºC 5%CO_2. Cells were transferred into a 3 well-cell concentrator and plated on a Poly-l-lysine coated microscope slide (VWR, UK) using a Cytofuge (Beckman Coulter, UK) at 1000 rpm for 6 minutes. Cells were fixed in 3% methanol-free formaldehyde/PBS (TAAB laboratories, UK) for 15 minutes, permeabilized in 0.3% Tritonx100/PBS (Sigma, UK) for 5 minutes and stained using Rhodamine phalloidin (Thermo Fisher, UK) in 5% Goat Serum Buffer (Sigma, UK) at a dilution of 1:40. Slides were mounted using H-1500 Hard set mounting medium for fluorescence (Vectashield, UK).

6.3.3.2 Confocal microscopy and image analysis

A Zeiss 710 confocal laser-scanning microscope with a 63x/1.40 oil objective and Version 2.6 Zen imaging software (Zeiss, UK) was used in order to record confocal microscopy images. Per condition assessed al least 10 images were recorded. The resulting .LSM files were analysed using Zen lite analysis software (Zeiss, UK). The synapse area was defined using the Zen outline tool by marking the edges of the actin accumulation between T cells and B cells. The area of T-cell F-actin immune synapse (µm^2) was used as the readout. A minimum of 100 randomly chosen synapses per condition were analysed.

6.4   Results

6.4.1   Effects of Ibrutinib and Acalabrutinib on T-cell cytokine profile and propensity of CD8+ T-cells to degranulate in the setting of CLL

We were interested in investigating whether BTK inhibitors could be demonstrated to improve T-cell function in the setting of CLL hand in hand with the observed amelioration of the exhaustion phenotype above. Splenocytes of Ibrutinib and Acalabrutinib treated samples were obtained from experiment 4.4.3. Cells were stimulated with PMA/Ionomycin for 6 hours and differences in cytokine profile and ability to degranulate have been recorded. Figure 41 and 42 illustrate the gating strategy. Single cells were identified by gating on FSC-H/FSC-A. Viable cells were identified by focusing on viability dye ef506 low events. Cells were enriched for mononuclear cells by gating FSC-A vs. SSC-A, and T-cells an CD3+CD8+ T-cells by expression of then respective markers (Figure 40). Figure 41 illustrates the gating strategy for assessment of IL2. IL4 and INFγ. The markers of interest we plotted against CD8.The unstimulated control defines the cut-off point.
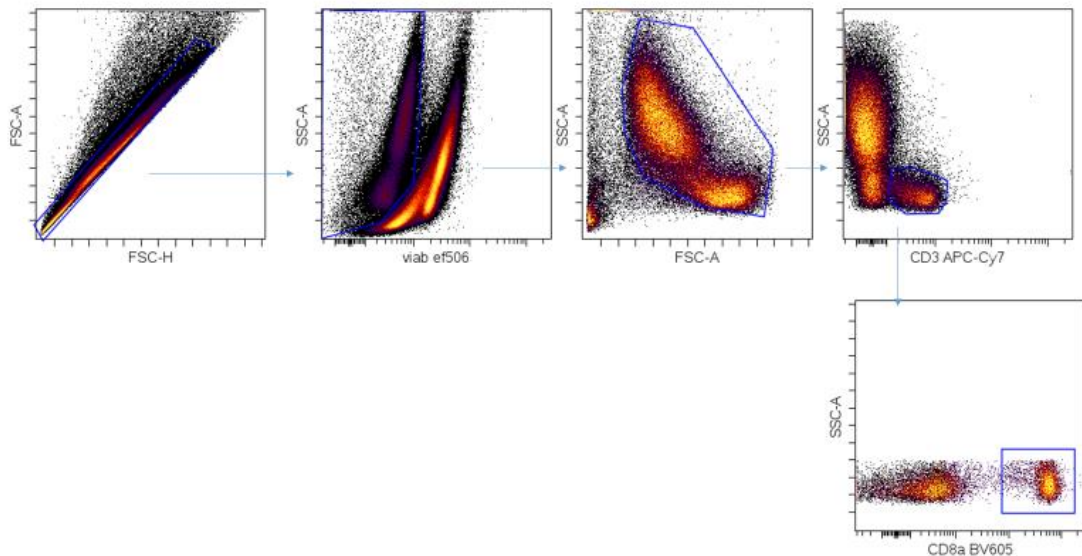
Figure 41: Gating strategy for identification of single cell T-cell population and single cell CD8+ T-cell population: Single cell were identified by gating on FSC-H and FCS-A, viable cells by gating on viability dye efluor506 low cells. Cells were further enriched from the mononuclear cell population and CD3 andn subsequent CD8 staining used to identify overall T-cells and CD8+CD3+ T-cells
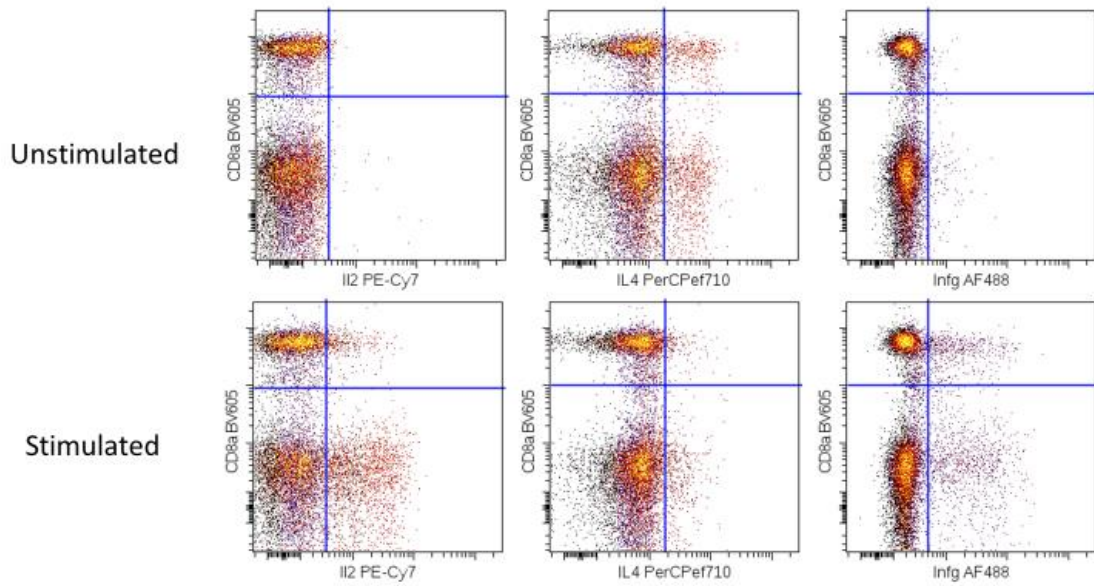
Figure 42: Gating strategy for assessment of IL2, IL4 and INFγ production: In total T-cell population IL2, IL4 and IFNγ are plotted against CD8. Unstimulated samples are used to define the cut-off.

Figure 43 illustrated the gating strategy for assessment of degranulation of cytotoxic T-cells. Among CD3+CD8+ cells events were gated for CD107a and CD44. The unstimulated samples were used to define the cut-off.
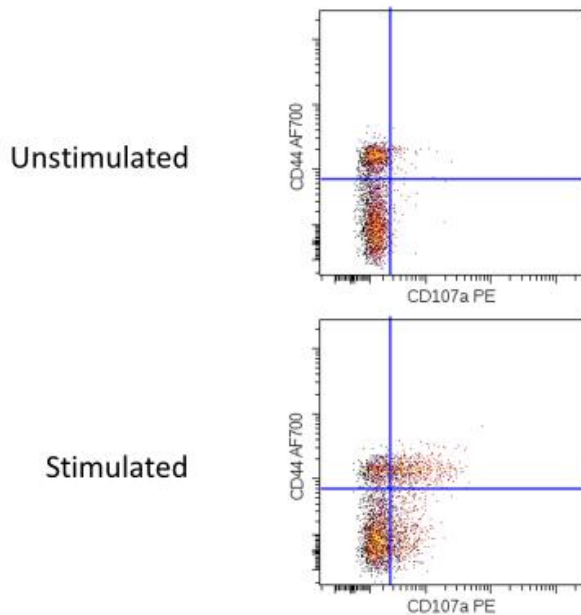
Figure 43: Gating strategy for assessment of CD170a accumulation as a surrogate marker for degranulation: Among CD3+CD8+ T-cells CD107a was platted against CD44 to assess the proponesity to degranuloate compared to the antigen experienced phenotype of these cells.

Figure 44 illustrates the production of IL2 following stimulation of PMA/Ionomycin for 6 hours in various T-cell subsets. IL2 production is statistically significantly increased with both Ibrutinib and Acalabrutinib treatment in overall CD3+ T-cells over vehicle treatment. (p=0.0002). No difference was detected between Ibrutinib and Acalabrutinib treated individuals. In CD3+CD8- helper cells an even stronger statistically significant increase in IL2 production with both Ibrutinib and Acalabrutinib was detected (p<0.0001) while no difference between Ibrutinib and Acalabrutinib treated animals was apparent. In CD3+CD8+ no statistically significant difference in IL2 production could be observed between groups.

Figure 45 demonstrates IL4 production in T-cell subsets following stimulation. We found a statistically significant decrease with both Ibrutinib and Acalabrutinib treatment over vehicle treatment (p<0.0001) while the difference between Ibrutinib and Acalabrutinib was not statistically significant. The situation was the same among CD3+CD8- cells where both Ibrutinib and Acalabrutinib led to a statistically significant decrease in IL4 production (p=0.0043) over vehicle treatment but no detectable difference between Ibrutinib and Acalabrutinib treatment. Among CD3+ CD8+ only Ibrutinib treatment led to a statistically significant suppression of IL4 production while in Acalabrutinib treated animals this remained unaltered compared to wildtype animals (p<0.00001).
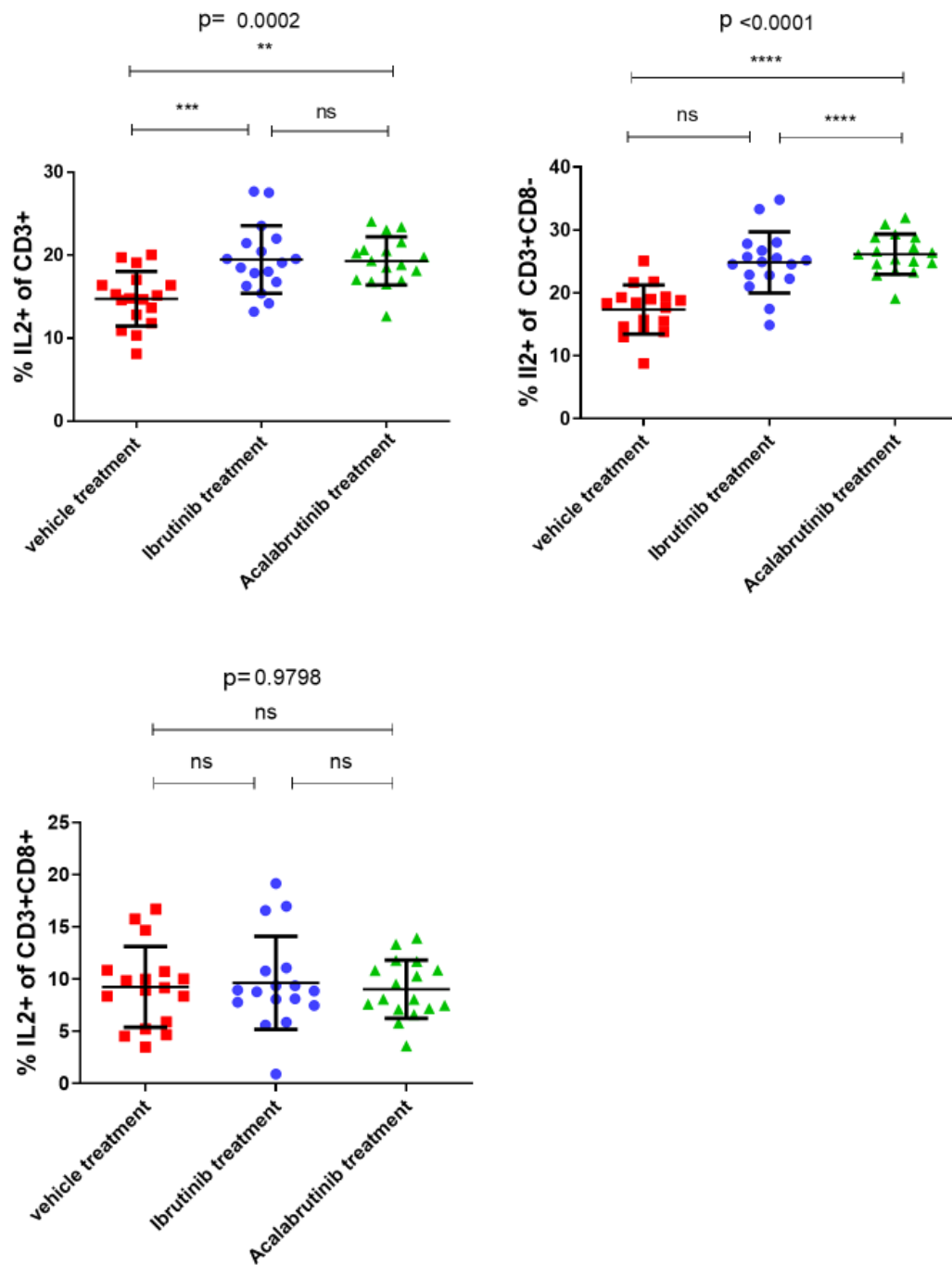
Figure 44: Illustration of IL2 production in overall CD3+, CD3+ CD8+ amd CD3+CD8- following stimulation with PMA/Ionomycin for 6 hrs in Ibrutinib/Acalabrutinib and vehicle treated animals. Statistical analysis by 1way Anova .3 groups, n=17 each Abbreviations: Ns p > 0.05; *p ≤ 0.05; ** p ≤ 0.01; *** p ≤ 0.001; **** p≤ 0.0001.
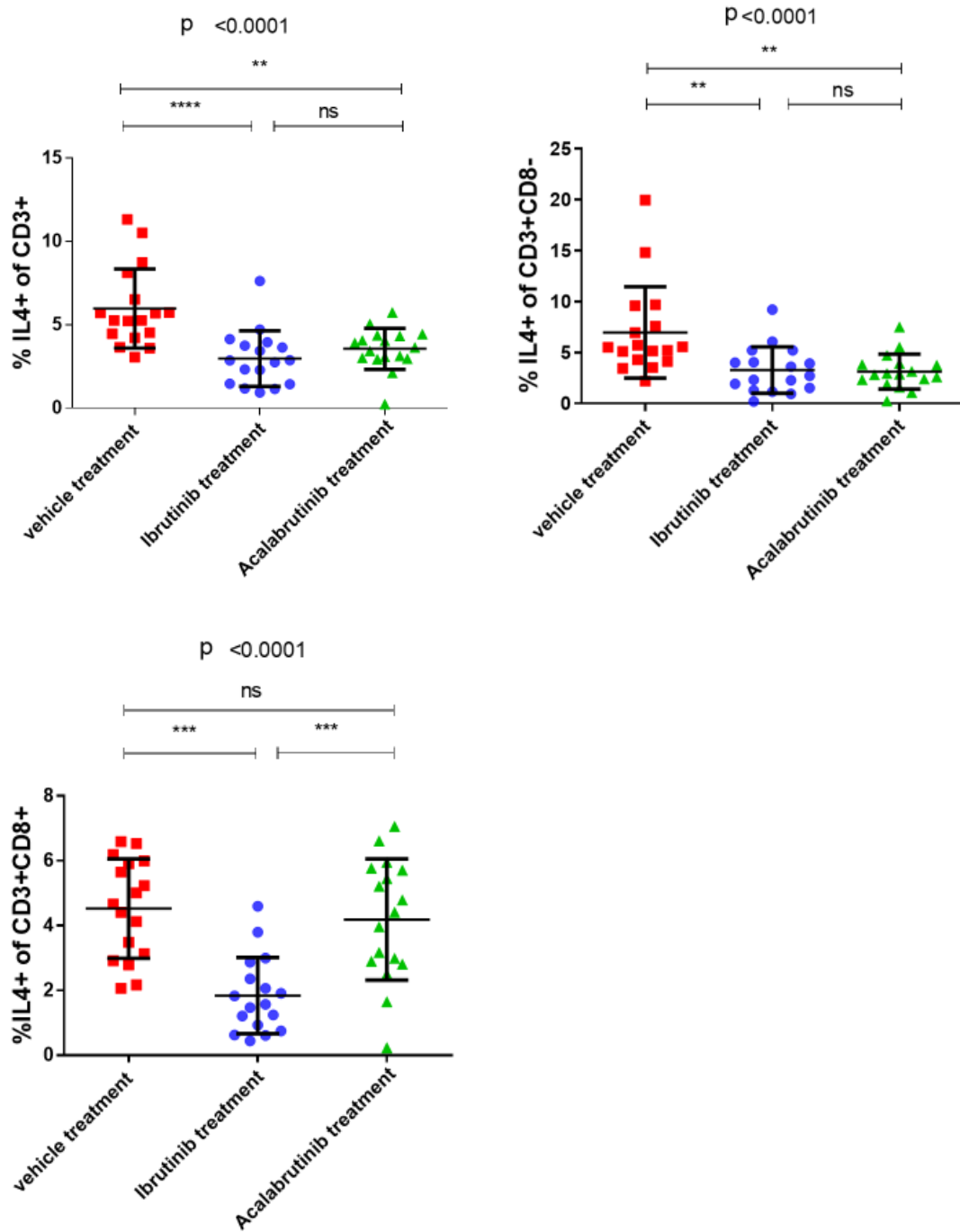
Figure 45: Illustration of IL4 production in overall CD3+, CD3+ CD8+ amd CD3+CD8-following stimulation with PMA/Ionomycin for 6 hrs in Ibrutinib/Acalabrutinib and vehicle treated animals. Statistical analysis by 1way Anova. 3 groups n=17 each. Abbreviations: Ns p > 0.05; *p ≤ 0.05; ** p ≤ 0.01; *** p ≤ 0.001; **** p≤ 0.0001.

Figure 46 illustrates INF-γ production among Ibrutinib/Acalabrutinib and vehicle treated animals. We found that INF-γ production was decreased in overall CD3+ T-cells by both Ibrutinib and Acalabrutinib treatment to a similar extent over vehicle treatment (p=0.0023). The situation was similar in CD3+CD8- helper cells (p=0.0043). In CD3+CD8+ cytotoxic T-cells there was a trend towards decreased IFN-γ with both Ibrutinib and Acalabrutinib treatment. However, a statistically significant decrease was reached only with Ibrutinib (p=0.0042).

Figure 76 illustrates the ratio of CD107a+/CD107a- CD3+CD8+ T-cells, both in the antigen experience CD44+ and less antigen experience CD44- compartments. The ratio of CD107a+/CD017a- cells is a surrogate for degranulation of cytotoxic T-cells and hence their cytolytic function. We found a statistically significant increase of CD107a+/CD107a- with Ibrutinib treatment and even stronger so with Acalabrutinib treatment (p<0.0001) in the antigen experience CD44+ compartment. In the less antigen experience CD44- compartment there was also a trend towards increased CD107a+/CD107a- ratio with Ibrutinib and Acalabrutinib treatment. However, only the increase observed with Acalabrutinib treatment was found to be statistically significant. (p=0.0006).
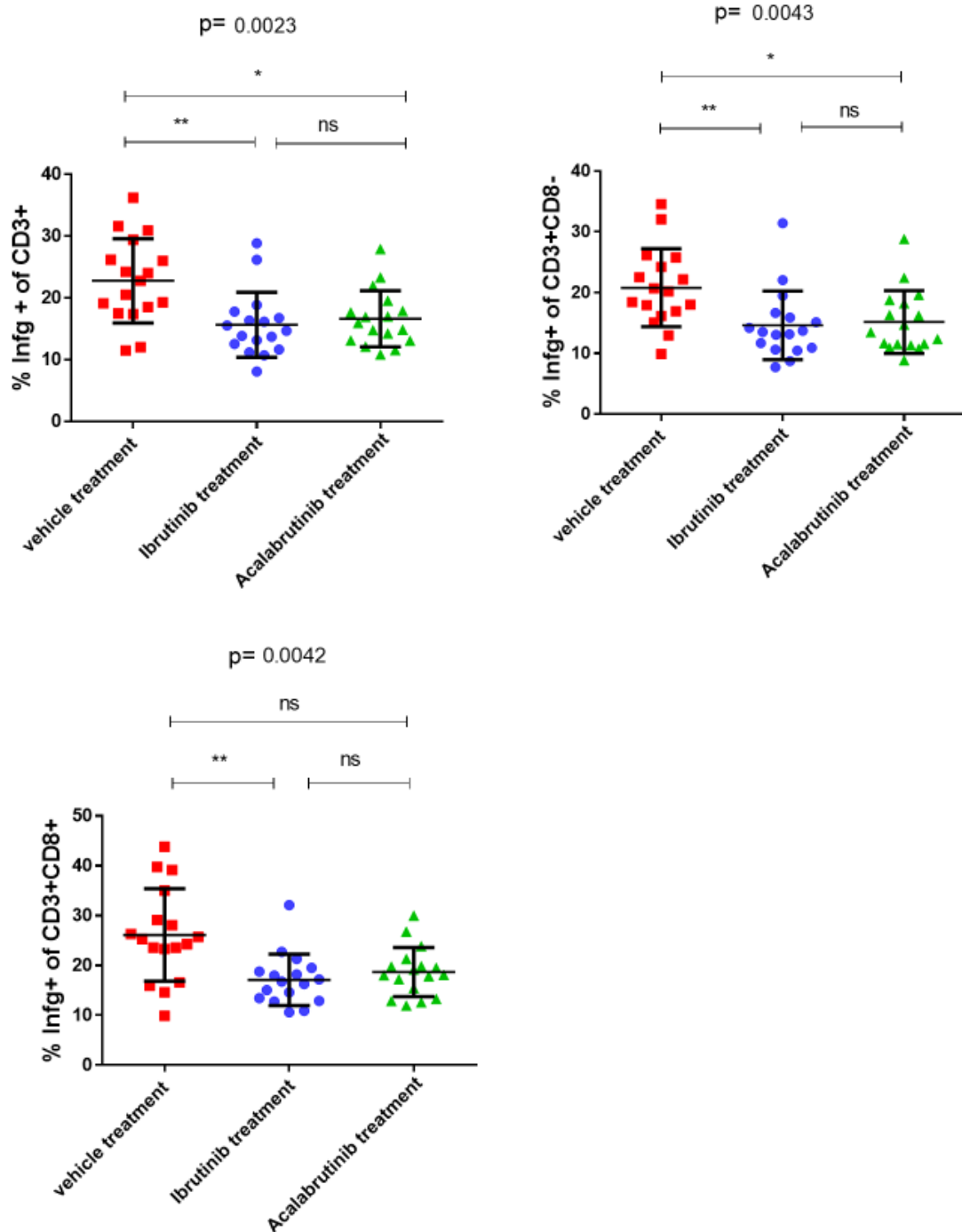
Figure 46: Illustration of IFN-γ production in overall CD3+, CD3+ CD8+ amd CD3+CD8- following stimulation with PMA/Ionomycin for 6 hrs in Ibrutinib/Acalabrutinib and vehicle treated animals. Statistical analysis by 1way Anova. 3 groups n=17 each. Abbreviations: Ns p > 0.05; *p ≤ 0.05; ** p ≤ 0.01; *** p ≤ 0.001; **** p≤ 0.0001.
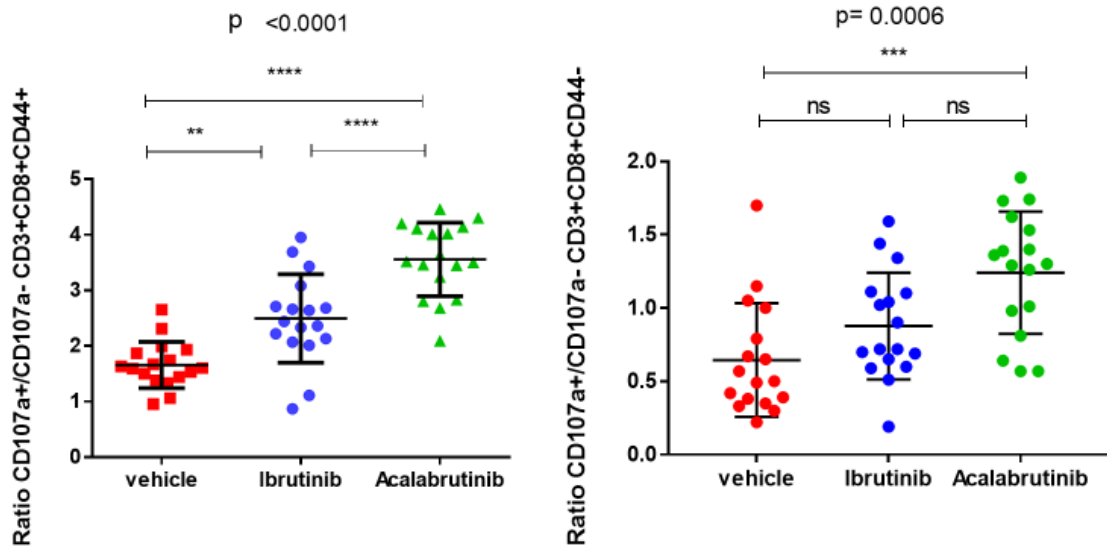
Figure 47: Illustration of CD107a+/CD107- ratio in CD3+CD8+CD44+ and CD3+CD8+CD44-T-cells following stimulation with PMA/Ionomycin for 6 hrs in Ibrutinib/Acalabrutinib and vehicle treated animals. Statistical test: CD3+CD8+CD44+ 1way Anova, CD3+CD8+CD44+ Kruskal wallis test. 3 groups n=17 each. Abbreviations: Ns p > 0.05; *p ≤ 0.05; ** p ≤ 0.01; *** p ≤ 0.001; **** p≤ 0.0001.

6.4.2 Effects of Ibrutinib and Acalabrutinib on T-cell proliferation in the CLL microenvironment

Given the expansion of the overall T-cell compartment with the onset of CLL we were interested whether treatment with Ibrutinib or Acalabrutinib had any effect on proliferation of T cells in the CLL microenvironment. For this purpose, experimental animals were injected with EDU 100µg/kg bodyweight 24 hours prior to sacrificing the animals. EDU incorporation was then made visible using AF488 in the "click it" reactions. In addition, intranuclear Ki67 staining was performed on unstimulated splenocytes to identify proliferating T-cells. Figure 48 illustrates the gating strategy for assessment of ki67 staining or EDU incorporation.
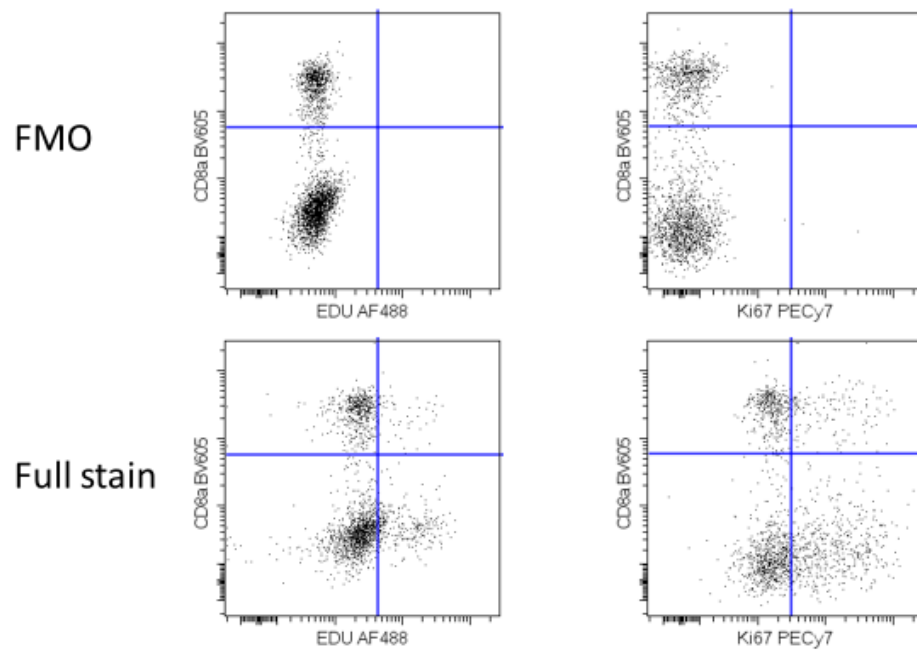
Figure 48: Gating strategy for assessment of ki67 staining and EDU incorportation compared to FMO. CD3+ T-cell were gated with CD8 and EDU AF488 or Ki67 PECY7 against FMO control.

Figure 49 illustrates staining of T-cell subsets for ki67. Ibrutinib treatment reduced proliferation of overall CD3+ T-cells at a statistically significant level and Acalabrutinib did even more so. The trends were similar among CD8- helper cells, however the difference between Ibrutinib and Acalabrutinib treated animals was not statistically significant here. Among CD8+ cytotoxic T-cells only Acalabrutinib treatment suppressed proliferation significantly while among Ibrutinib treated animals the level of intranuclear Ki67 remained largely constant compared to vehicle treated animals.
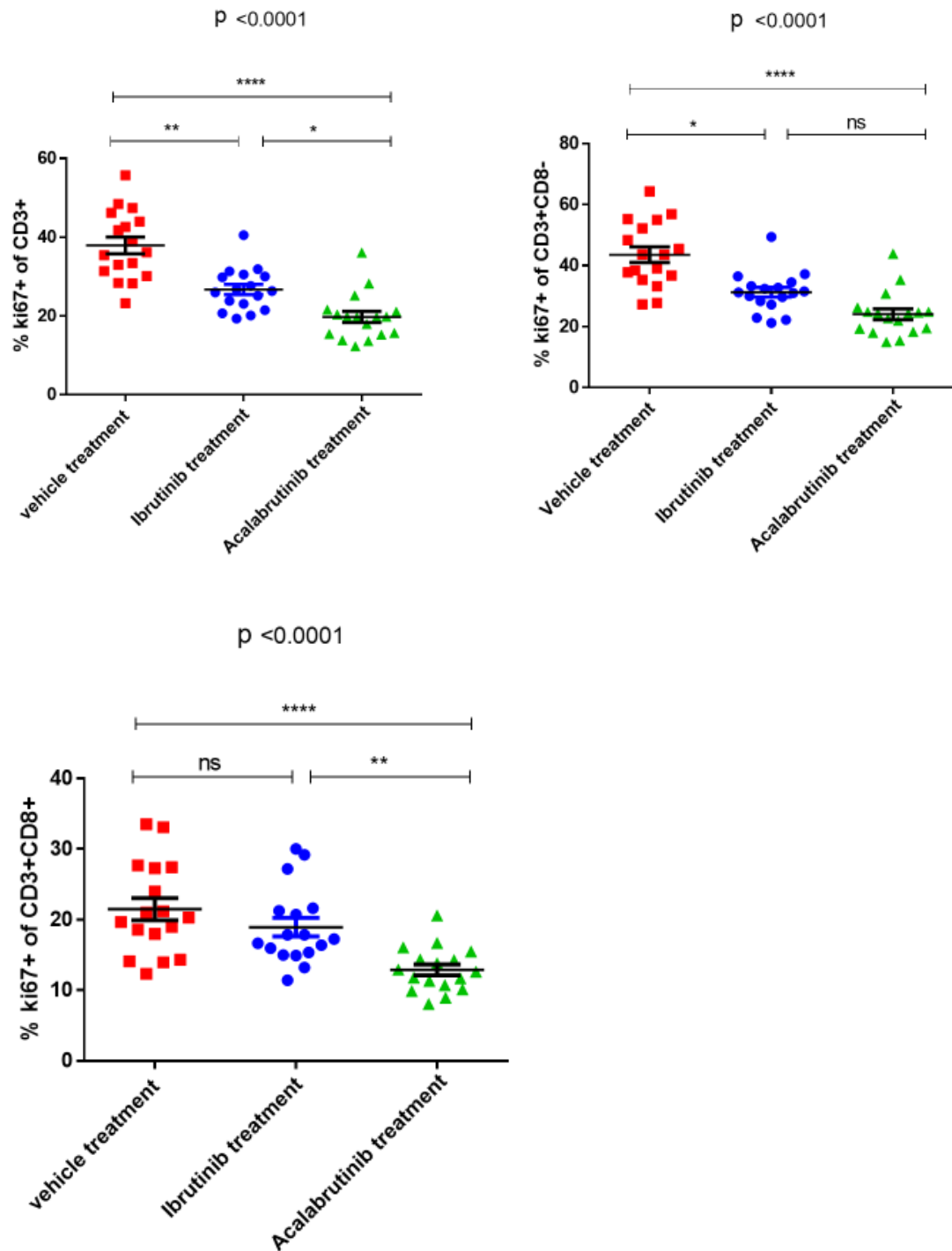
Figure 49: Illustration if intranuclear ki67 staining in T-cells from CLL bearing mice receiving Ibrutinib. Acalabrutinib or vehicle treatment. Statistical analysis by 1way Anova. 3 groups n=17 each. Ns p > 0.05; *p ≤ 0.05; ** p ≤ 0.01; *** p ≤ 0.001; **** p≤ 0.0001.

The analysis of in vivo EDU incorporation in T-cells from Ibrutinib/Acalabrutinib or vehicle treated CLL bearing animals is illustrated in Figure 50. The findings were similar to those obtained by staining for Ki67. Among overall CD3+ T-cell the EDU-incorporation was reduced by Ibrutinib and even more so by Acalabrutinib. Among CD8- helper cells both Ibrutinib and Acalabrutinib treatment reduced EDU incorporation compared to vehicle treatment at a statistically significant level but no statistically significance was detected between Ibrutinib and Acalabrutinib treatment. Among CD8+ cytotoxic T-cells there was a trend to reduction with both agents but only Acalabrutinib treatment leads to statistically significant reduction of EDU incorporation.
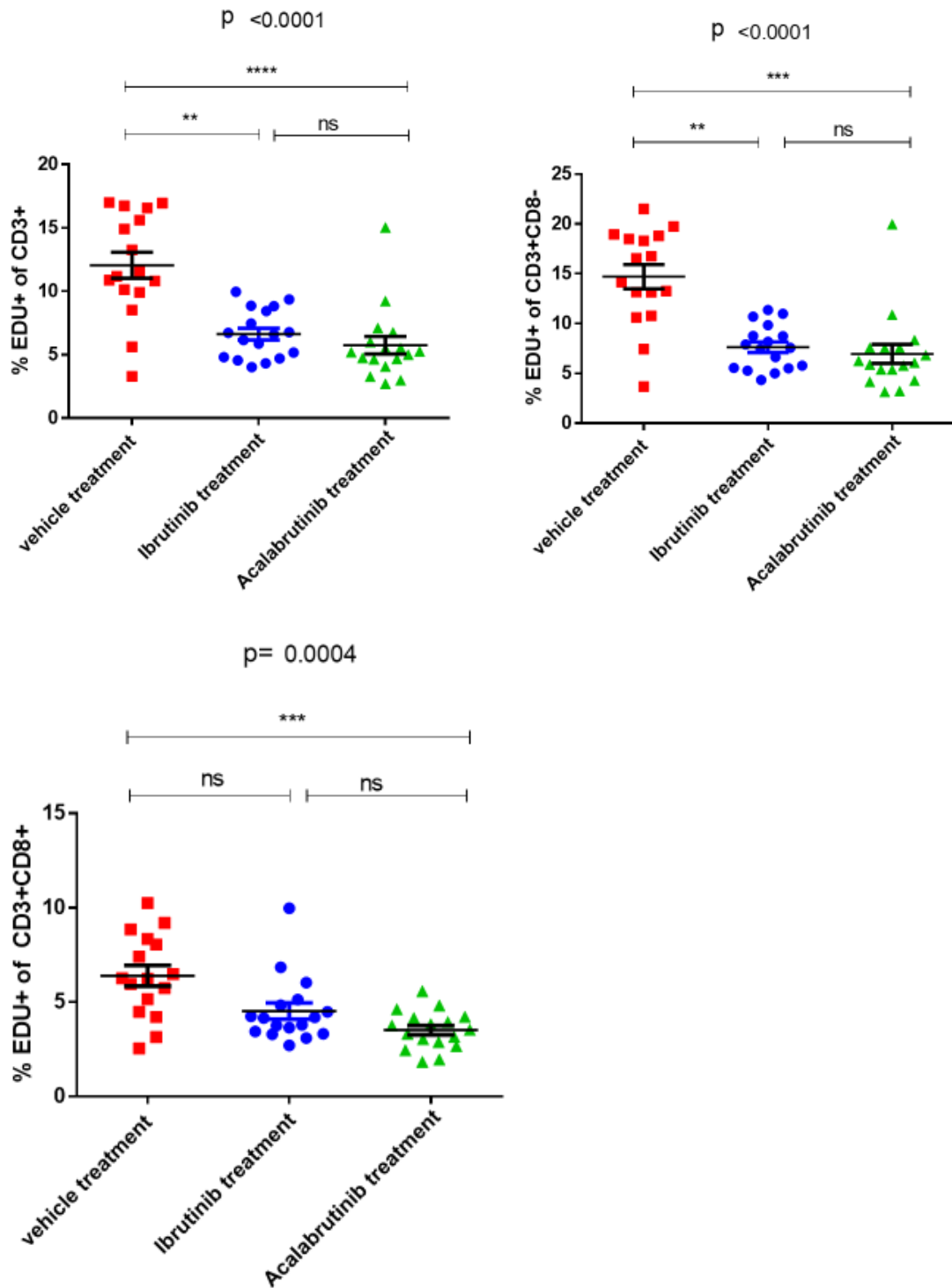
Figure 50: Illustratiion of in vivo EDU incorporaration in T-cells derived from cll bearing animals treared with Ibrutinib, Acalabutinib or vehicle treatment. Statistical analysis by 1way Anova, 3 groups n=17 each. Abbreviations Ns p > 0.05; *p ≤ 0.05; ** p ≤ 0.01; *** p ≤ 0.001; **** p≤ 0.0001.

6.4.3   Effects of Ibrutinib and Acalabrutinib on T-cell synapse fromation

The splenocyte samples obtained in 4.4.3 were subjugated to a T-cell synapse formation assay as described above. 100 synapse per animal were analysed and medians calculated. Figure 51 demonstrates the results of this experiment. Both Ibrutinib and Acalabrutinib treatment seemed to boost immune synapse formation between T-cells and B-cells isolated from spleens of these animals to a comparable level.
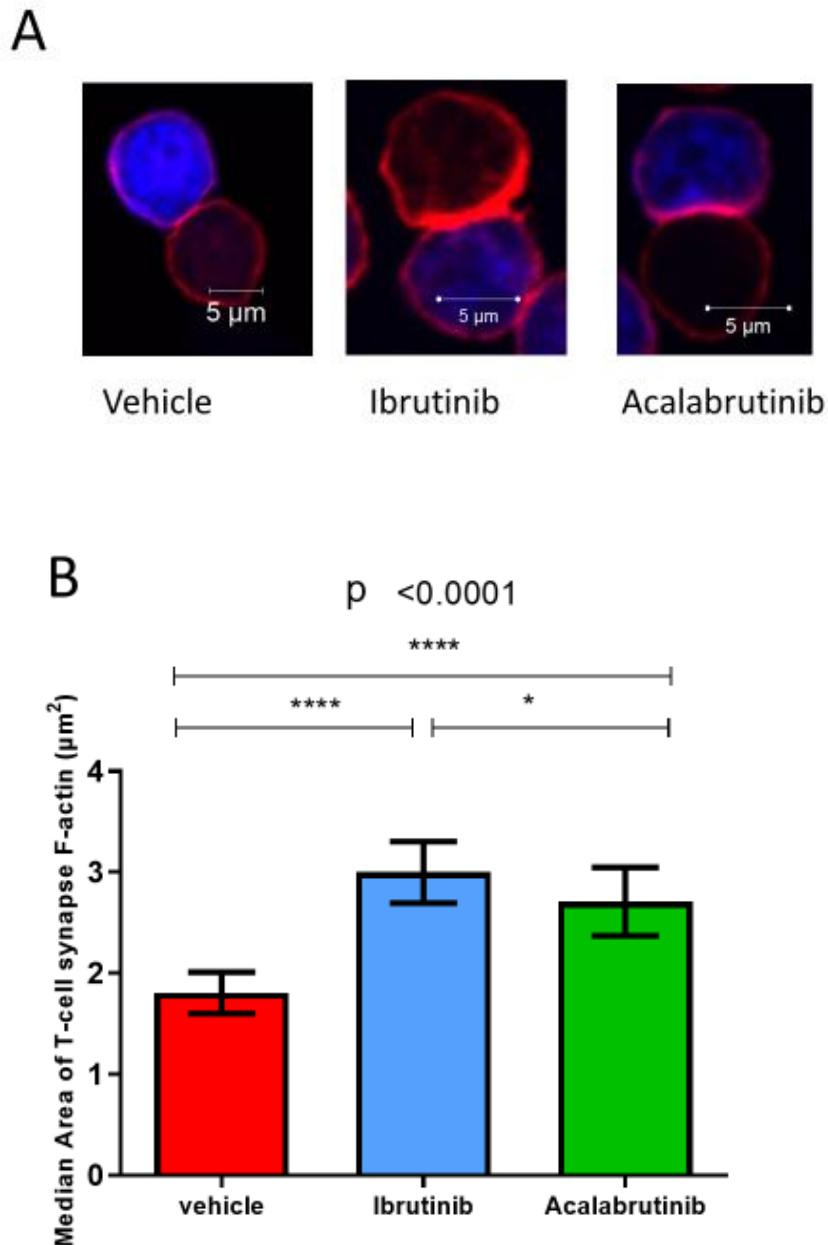
Figure 51: Influence of Ibrutinib and Acalabrutinib treatment on immune synapse formation. (A): Example of T-cell synapse area as measured by confocal microscopy. Red: Rhodamine-Phalloidin staining polymerized F-actin, Blue: CMAC staining B-cells. (B): Median Area of T-cell synapse F-action in μm^2 measured by confocal microscopy in vehicle treated, Ibrutinib treated and Acalabrutinib treated animals. Statistical analysis by 1way Anova. 3 groups n=17 each. Abbreviations Ns $p > 0.05$; *$p \le 0.05$; ** $p \le 0.01$; *** $p \le 0.001$; **** $p \le 0.0001$.

6.5   Discussion

Our goal in this part of the project was to investigate whether the BTK-inhibitors Ibrutinib and Acalabrutinib have the same or different ability to modulate and improve T-cell function in the setting of CLL. Our group has recently demonstrated that the Eμ-TCL1 mouse model recapitulates the T-cell defects observed in human CLL patients such as decreased mitogen induced proliferation of T-cells and reduced capacity to induce idiotype-specific CD8 T-cell with the ability of killing CLL cells. Moreover, T-cell from leukemic mice had dysfunctional cytokine production and CLL bearing animals revealed alterations in gene expression that became more pronounced with increasing tumour load and correlated with findings in human CLL patients. When adoptively transferring CLL B-cells from leukemic mice into young transgenic animals without disease, gene-expression profiles comparable to those from ageing CLL bearing Eμ-TCL1 animals developed within 8 days (907). Several studies have addressed the question of modulation of T-cell function by BTK inhibitors.

Most prominently, Dubosvky et al. have suggested that Ibrutinib has the potential to shift T-helper cell polarity by targeting ITK. As demonstrated above, ITK has a pivotal role in mediating downstream T-cell receptor signalling. When inhibited, however, it's function can be rescued by the redundant enzyme "resting lymphocyte kinase" (RLK) which is expressed in Th1 cells but not Th2 cells thus effectively resulting in a preferential inhibition of Th2 cells (877). As Acalabrutinib does not have inhibitory activity towards ITK it should affect T-cell function in the setting of CLL differentially (986). To our surprise, we did not find evidence of such an effect in the experiments at hand: both Ibrutinib and Acalabrutinib appeared to improve T-cell function in the microenvironment of CLL bearing Eμ-TCL1 animals in almost identical ways. Both substances increased the production of IL2 by overall CD3+ T-cell and CD3+CD8- helper cells to the same extent as well as decreased IL4 production by overall CD3+ T-cells and CD3+CD8- helper cell to a similar extent. The only detectable difference was a reduction of IL4 production in CD3+CD8+ cytotoxic T-cells with Ibrutinib that could not be observed with Acalabrutinib treatment. Moreover, both substances were shown to reduce INFγ secretion by T-cell subsets in quite a similar fashion. A reduction of IFNγ by BTK inhibitor treatment may seem counterintuitive at first, as the substance is an important Th1 cytokine and mediator of cancer immunosurveillance. On the other hand, one should keep in mind that continuous T-cell stimulation has been described to lead to a secondary T-cell dysfunction via IFNγ driven overexpression of PD-L1 (adaptive immune resistance) (842). Moreover, IFNγ is also known to promote survival and proliferation of

CLL B-cells (417). As such, the observed reduction of IFNγ secretion is a step toward normalization of the immune microenvironment. We observed an increase of the ratio of CD107a+/CD107a- among antigen-experienced CD44+CD8+ T-cells with Ibrutinib treatment. This effect is even more pronounced with Acalabrutinib treatment. Among less antigen experienced CD44- CD8 T-cells we have noted a similar trend, however, only the effect of Acalabrutinib treatment compared to vehicle treatment reached statistical significance. It should be noted that surface accumulation of CD107a is merely a surrogate marker for the cytolytic capacity of CD8+ T-cells. Still, it is known that surface CD107a accumulation directly correlates with the ability of cytotoxic T-cells to lyse target cells as measured in chromium release assays (987). CD107a accumulation is thus an adequate tool to assess T-cell cytolytic capacity. Last but not least we have quantified the ability of T-cell and B-cells from splenocytes of CLL bearing animals by analysing the area of F-Actin polymerization at the contact zone via a well established assay originally developed at our lab (216). We found an increased ability for T-cell synapse formation that was similar after both Ibrutinib and Acalabrutinib treatment.

In conclusion, we find that both BTK inhibitors have the ability to normalize T-cell cytokine profile with increased T-helper cell IL2 production and decreased IL4 production. INF-γ production is decreased to a similar extent in line with a decreased pro-survival signal to CLL B-cells and reduce adaptive immune resistance. Effector functions in the form of CD8+ T-cell degranulation and synapse formation between spleen derived T- and B-cells are increased with both Ibrutinib and Acalabrutinib treatment. We thus have little evidence that direct modulation of T-cells via ITK/RLK is the leading mechanism in improved T-cell function in the splenic microenvironment of CLL bearing animals as effects are similar between Ibrutinib and Acalabrutinib, which is known not to have inhibitory capacity towards ITK (986). While this mechanism may contribute in part to Ibrutinib-mediated correction of CLL-associated T-cell function it does not seem to be of central importance. We speculate that an indirect mechanism may play a greater role. A downregulation of PD-L1 expression on the surface of CLL B-cells in the peripheral blood of Ibrutinib treated patients has been reported in one study, suggesting a potential role in direct cell contact mediated suppression of T-cells by CLL B-cells themselves and modulation therefore as a potential mechanism of correction of T-cells function by BTK inhibitors (878). Moreover, myeloid cells are well known to express BTK and modulation of myeloid cell function, especially of MDSCs in the setting of malignancy has been suggested. Ibrutinib has been reported to be able to decrease production of important B-cell attracting chemokines such as CXCL12, CXCL13, CCL19 in human macrophages and thus directly influence the composition of the microenvironment of CLL

manifestations (880). Ibrutinib treatment of MDSCs has been reported to result in reduction of T-cell suppressive mechanisms such as IDO expression and impairment of generation of MDSCs (879). Other authors have suggested enhanced myeloid dendritic cell maturation and co-stimulatory capacity following Ibrutinib treatment (988). Modulation of myeloid cell function in the immunosuppressive microenvironment of CLL may thus be a possible mechanism of improved CLL-associated T-cell function as well. This notion is also supported by findings of Gunderson who reported a skewed immunophenptype of macrophages in the microenvironment of PDAC resulting in a more Th2-permissive environment which was correctable by Ibrutinib administration resulting in impoved CD8+ T-cell cytotoxicity (881).

Based on the data presented above, both Ibrutinib and Acalabrutinib appear to be promising combination partners for a combined BTK inhibition/immune checkpoint blockade strategy.

7   Influence of BTK inhibitor/anti-PD-L1 combinations on immune phenotype in the splenic microenvironment

7.1   Specific introduction

The PD-1/PD-L1 axis is a pathway that is commonly utilized in the microenvironment of malignant diseases to mediate tumour immune escape. We have been able to demonstrate that the functional T-cell impairment induced by CLL is associated with an overexpression of immune checkpoint molecules including PD-1 (401). Aberrant PD-L1 expression has been reported to be used as a means of immune escape by various hematologic malignancies. Our group has previously shown upregulation in primary tumour cells of CLL, FL and DLBCL patients (216). Aberrant expression has also been described in MCL (826), PMBL (827), HL (828) and MM (829) as well as on CD34+ blasts from patients with *MDS* (830), CMML and AML (831). PD-L1 is not only found on tumour cells but also frequently expressed on myeloid derived cells in the tumour microenvironment of various malignancies including CLL (832-835). Various studies have demonstrated the functional relevance of the PD1/PD-L1 axis in mediating malignancy associated immune dysfunction in the setting of hematologic malignancies. Overexpression of both wild type PD-L1 as well as a fusion protein of CIITA and PD-L1 was able to suppress Jurkat T-cell activation in a PMBL cell line (827). In MCL cell lines both anti-PD-L1 antibody blockade and knockdown of PD-L1 by sh-RNA was shown to increase the proliferation of cocultured allogeneic T-cells (826). Our own group has been able to demonstrate that PD-L1 is pivotal in mediating CLL associated T-cell dysfunction (216). In the Eµ-TCL1 adoptive transfer mouse model we have shown that PD-L1 blockade results in prevention of T-cell dysfunction and leukemia growth when given from the day of adoptive transfer (836).

Despite these findings and a clearly demonstrable clinical activity in other hematologic malignancies, attempts to utilize blockade of the PD-1/PD-L1 axis in patients with CLL have largely been disappointing (108). The BTK inhibitor Ibrutinib has been reported to be able to modulate function of T-cell and myeloid cell subsets (877-881). It has been suggested that the clinical efficacy of the agent is due to a combination of direct effects on CLL B-cells via the BCR pathway as well as correction of CLL associated immune defects. Above we have demonstrated that both Ibrutinib and the second generation BTK inhibitor Acalabrutinib have the ability to correct CLL associated T-cell defects. Moreover, we have shown the ability of both agents to modulate expression of PD-1 and its ligand PD-L1. We speculate that combinations of the BTK-inhibitors and PD-L1 immune checkpoint blockade may have synergistic effects in overcoming CLL associated

immune dysfunction and may help to induce durable remissions in the clinical setting. Results in the A20 mouse model of lymphoma support this hypothesis (872). Given our above findings we believe that both Ibrutinib and Acalabrutinib are promising candidates for a combination approach with PD-L1 immune checkpoint blockade in the setting of CLL. A phase I/IIa study of Nivolumab/Ibrutinib in patients with relapse NHL and CLL/SLL has recently reported a promising ORR of 61% of high risk CLL/SLL further advocating for the use of combination approaches (873).

7.2   Goals and objectives

We aimed to develop a combination strategy of BTK inhibitors and anti-PD-L1 immune checkpoint blockade using the Eµ-TCL1 mouse model of CLL. Our goal in this section was to analyse the effect of combinations of Ibrutinib or Acalabrutinib and anti-PD-L1 immune checkpoint blockade on the immune phenotype and expression of immune checkpoint molecules in the splenic microenvironment of CLL bearing animals.

7.3   Specific methods

7.3.1   Cell thawing procedure

Thawing of cryopreserved splenocyte samples was performed in a water bath at 37°C. To avoid contamination the vials were disinfected using 70% IMS (Fisher Scientific, UK) and subsequently opend in a class II biosafety cabinet. The cell suspension was pipetted into 10ml RPMI 1640 (Gibco, UK) supplemented with 10% FCS (Gibco, UK), 1% Penicillin-Streptomycin (Sigma, UK) at 37°C. Subsequently the suspension was centrifuged at 300 x g for 10 minutes at room temperature and resuspended in a volume suitable for number of cells contained in the pellet. Automated cell counting was conducted on a Luna fl automated cell counter (Logos bioystems, USA) after dilution of a 10µl aliquot with an equal amount of 0.4% Tryphan blue (Sigma, UK).

7.3.2   Mass cytometry staining

$3x10^6$ splenocytes from single cell preparations were carried forward for staining. All staining steps are performed in 5 ml polypropylene round bottom tubes (Corning, UK). Cell were resuspended in "Cell-ID" Cisplatin (Fluidigm, UK) in PBS (Sigma, UK) at a concentration of 5µM and incubate for 5 minutes at room temperature. The reaction was quenched with 5x the volume of "Maxpar" cell staining buffer (Fluidigm, UK) and the samples centrifuged. Cells are resuspended in 50µl of "Maxpar" cell staining buffer containing 1 µl of anti-mouse CD16/CD32 monoclonal antibody (clone 93, ebioscience,

UK) and incubated for 10 minutes. The volume was then filled up to 100 µl with "Maxpar" cell staining buffer (Fluidigm, UK) containing mass cytometry antibodies for a final concentration of 1:100. Cells were incubated for 30 minutes at room temperature and then washed 2x in "Maxpar" cell staining buffer (Fluidigm, UK). The samples were then resuspended in 1ml of "Maxpar" Fix and Perm buffer (Fluidigm, UK) containing "Cell-ID" Intercalator-Ir (Fluidigm, UK) at a concentration of 125 nM and incubated over night at 4°C. Cells were washed 2x in "Maxpar" Cell staining buffer (Fluidigim, UK) and 1x in "Maxpar" water (Fluidigm, UK). Cells were left dry-pelleted at 4°C until immediately prior to acquisition on a "cytof 2" mass cytometer (Fluidigm, UK). For a list of mass cytometry antibodies used please refer to table 4.

7.3.3   Acquisition and analysis of mass cytometry data

A "cytof 2" mass cytometer (Fluidigm, UK) was used for acquisition of mass cytometry data. The suspension of stained cells was nebulized in order to create single cell droplets and was subsequently exposed to a high temperature plasma. This breaks the molecular bonds and ionizes the atoms. The resulting charged atomic ion clouds are transferred into the mass spectrometer. The mass cytometer is configured as a qTOF instrument. The two radiofrequency quadrupoles are tuned to filter out naturally occuring low mass ions. The enriched higher mass reporter ions are quantitated by TOF mass analysis. Normalization of the recorded data is achieved via a standardized bead solution containing known concentrations of the metal isotopes 140/142Ce, 151/153Eu, 165Ho, and 175/176Lu. A correction algorithm in the software of the mass cytometer normalizes the recorded data to correct for signal variation that may occur over protracted periods of use.

7.3.4   Citrus analysis of high dimensional single cell immune phenotypic data

For analysis of mass cytometry data, the algorithm *cluster identification, characterization, and regression* (CITRUS) was used. The algorithm was designed to detect statistically significant differences between experimental groups in highly dimensional data sets. CITRUS performs multiple sequential steps in order to achieve this. First, unsupervised hierarchical clustering of cellular events across multiple samples by phenotypic similarity along the lines of a defined set of markers is performed. Then biologically relevant features within these clusters of cellular events are calculated on a per file basis and the resulting tree of clusters annotated with this information. CITRUS then interrogates this dataset as to whether these clusters differ on a statistically significant level in terms of median expression of a defined set of markers different from the subset used to create

the tree of clusters. This is achieved by the use of a correlative linearized regression model, significance analysis of microarrays. The analysis uses non-parametric statistics to test differences along the lines of user defined experimental groups. Repeated permutations of the data are used to determine whether the expression of any of these markers is significantly related to any of the experimental groups (955). The result is reported not by use of classical p-values but by utilizing false discovery rate. This approach is chosen because due to the multiple testing problem an adjustment of p-values is necessary. The use of more traditional techniques such as Bonferroni-correction reduces the number of false positives at the cost of also reducing the number of correctly identified true positive differences. The calculation of a false discovery rate thus has a higher power to detect truly significant differences. After excluding debris and B-cell subsets by manual gating 10000 events per individual were clustered. A minimum cluster size of 1% was chosen. To avoid the detection of false positives only differences with a false discovery rate <1% were reported. The medians were subsequently exported and analysed with the more classical Kruskal-Wallis test with Dunn's post test and correction for multiplicity.

7.4   Results

We have here aimed to develop a combination strategy of BTK inhibitors and anti-PD-L1 immune checkpoint blockade. Animal experiments conducted to derive splenocyte samples are described under 3.4.4. We have used our 27-marker mass cytometry panel to investigate the influence of combinations of Ibrutinib or Acalabrutinib with anti-PD-L1 in comparison to single agent BTK inhibitor or anti-PD-L1 treatment on the immune phenotype of the splenic microenvironment in CLL bearing animals. As detailed in chapter 5.4 manual gating was used to separate CLL B-cell, physiological B-cells and non-B-cells. The gating strategy is illustrated in figure 28. Figure 52 demonstrates expression of PD-L1 in B-cell subsets across single agent treated, combination treated and vehicle treated animals. Unfortunately, application of anti-PD-L1 immune checkpoint blockade masked staining for PD-L1 and thus expression could not be assessed in the PD-L1 treatment arms. Assessing the expression of PD-L1 in the remaining treatment groups, we confirmed the statistically significant increase in PD-L1 expression with BTK inhibitor treatment described in chapter 5. Interestingly, as opposed to the previous experiment, treatment with both Ibrutinib and Acalabrutinib resulted in a reduced expression of PD-L1 among physiological B-cells.

Non-B-cell events where subsequently analysed using the CITRUS clustering algorithm. Compared to the earlier animal experiment described in chapter 5, a better overall

disease control was achieved with both single agent and combination treatments (compare 3.4.3 and 3.4.4). This led to a better separation of CLL B-cells and non-B-cells with only minute residual CD19 low infiltrating B-cells in the non- B-cells population. Figures 53 – 56 illustrate the resulting CITRUS clustering tree and identification of major immune cell subsets.
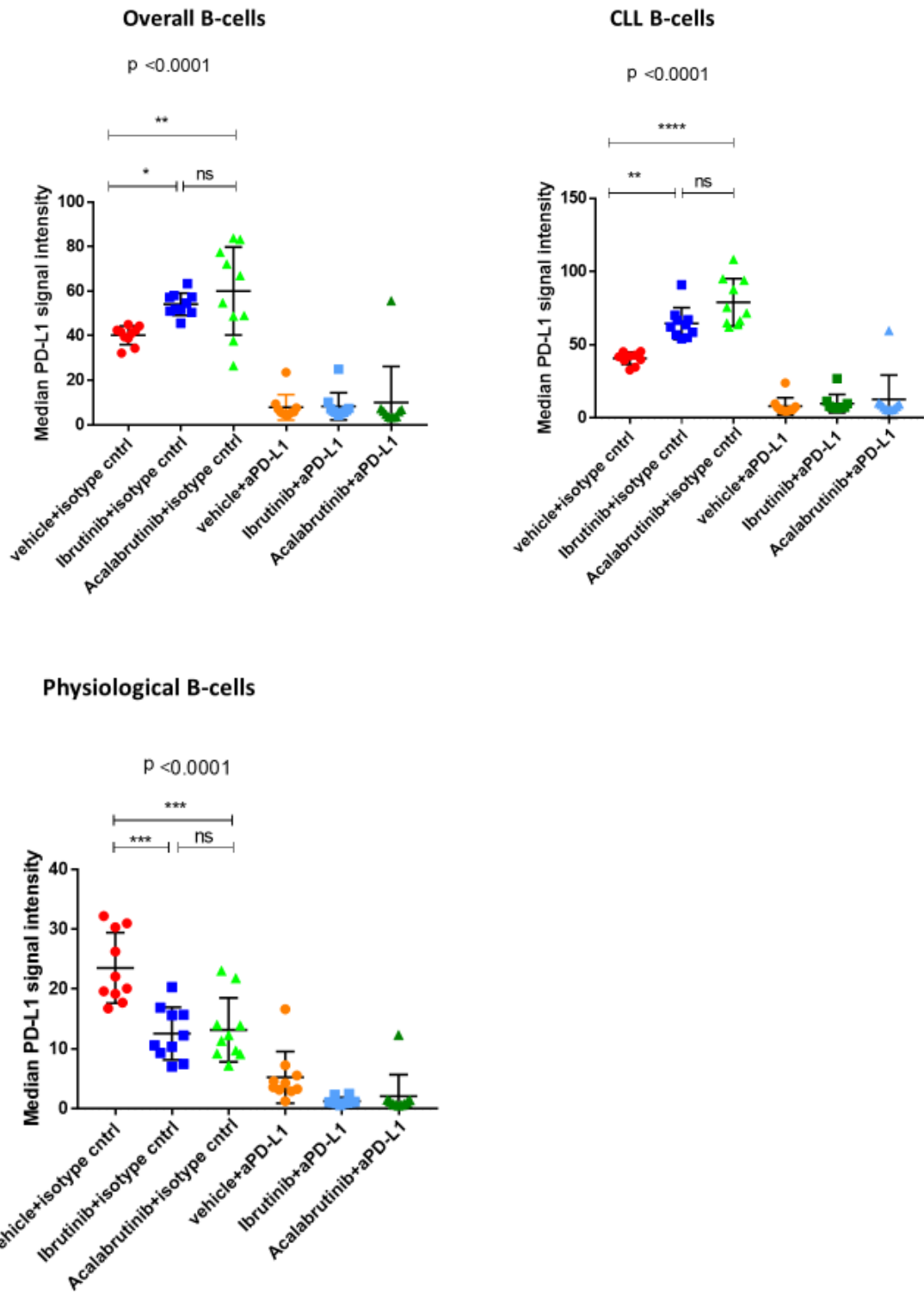
Figure 52: Median PD-L1 153Eu signal intensity on overall B-cells, CLL-B-cells and physiological B-cells of the splenic microenvironment with BTK inhibitor, anti-PD-L1 and BTK inhibitor/anti-PD-L1 combination treatment. Statistical analysis by Kruskal Wallis test. 3 groups, n=10 each. Abbreviations Ns p > 0.05; *p ≤ 0.05; ** p ≤ 0.01; *** p ≤ 0.001; **** p≤ 0.0001.
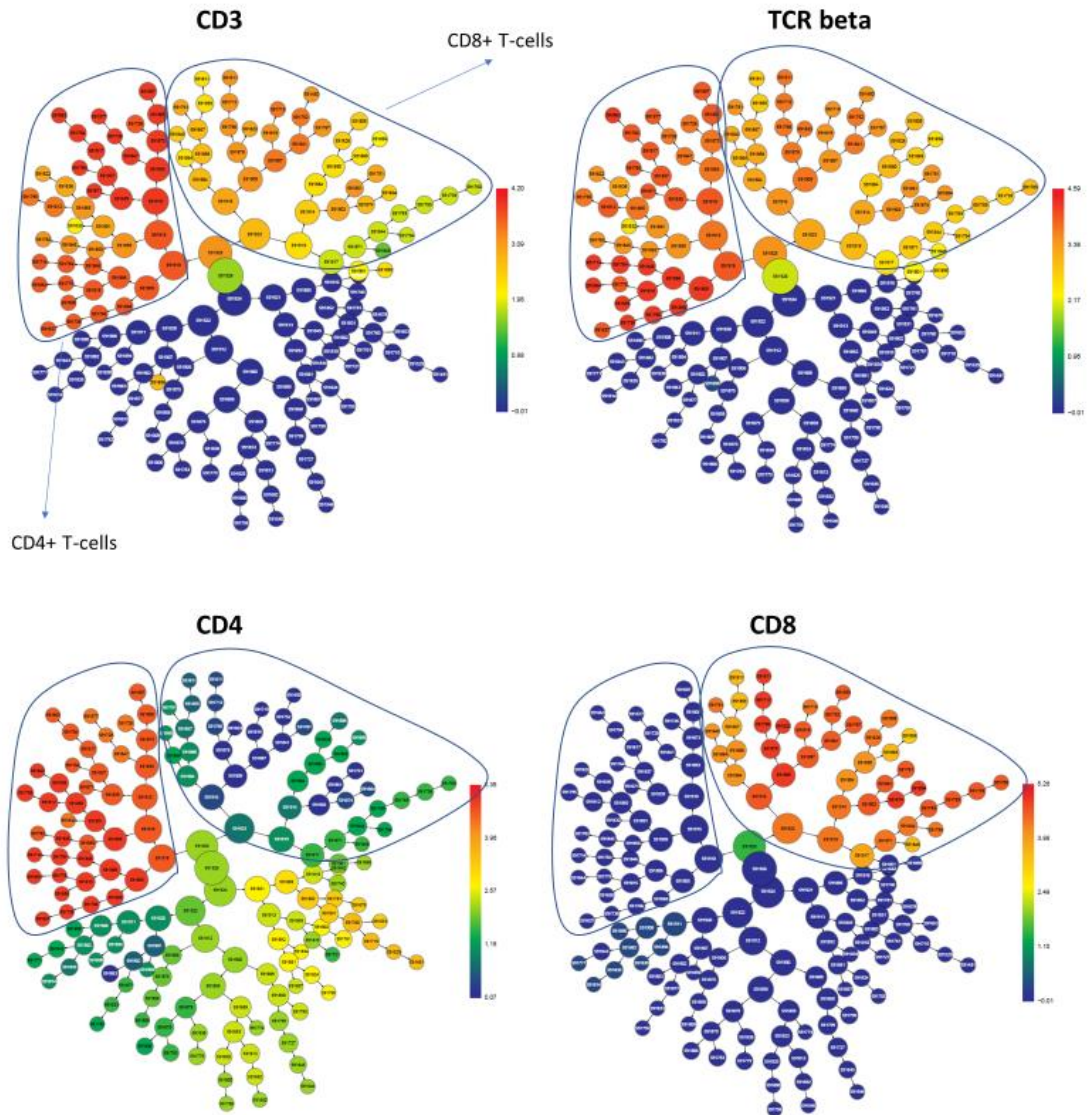
Figure 53: *CITRUS cluster tree and identification of CD4+ and CD8+ T-cells.* Phenotypically similar events are grouped together in clusters. The distance of clusters is thus a measure of their similarity. The Size of the circles denotes the abundance of cells in the cluster, the colour scale the median marker intensity (red-high expression, blue-low expression). The tree structure is redundant with proximal parent clusters in the centre of the plot containing all events of distal children clusters.
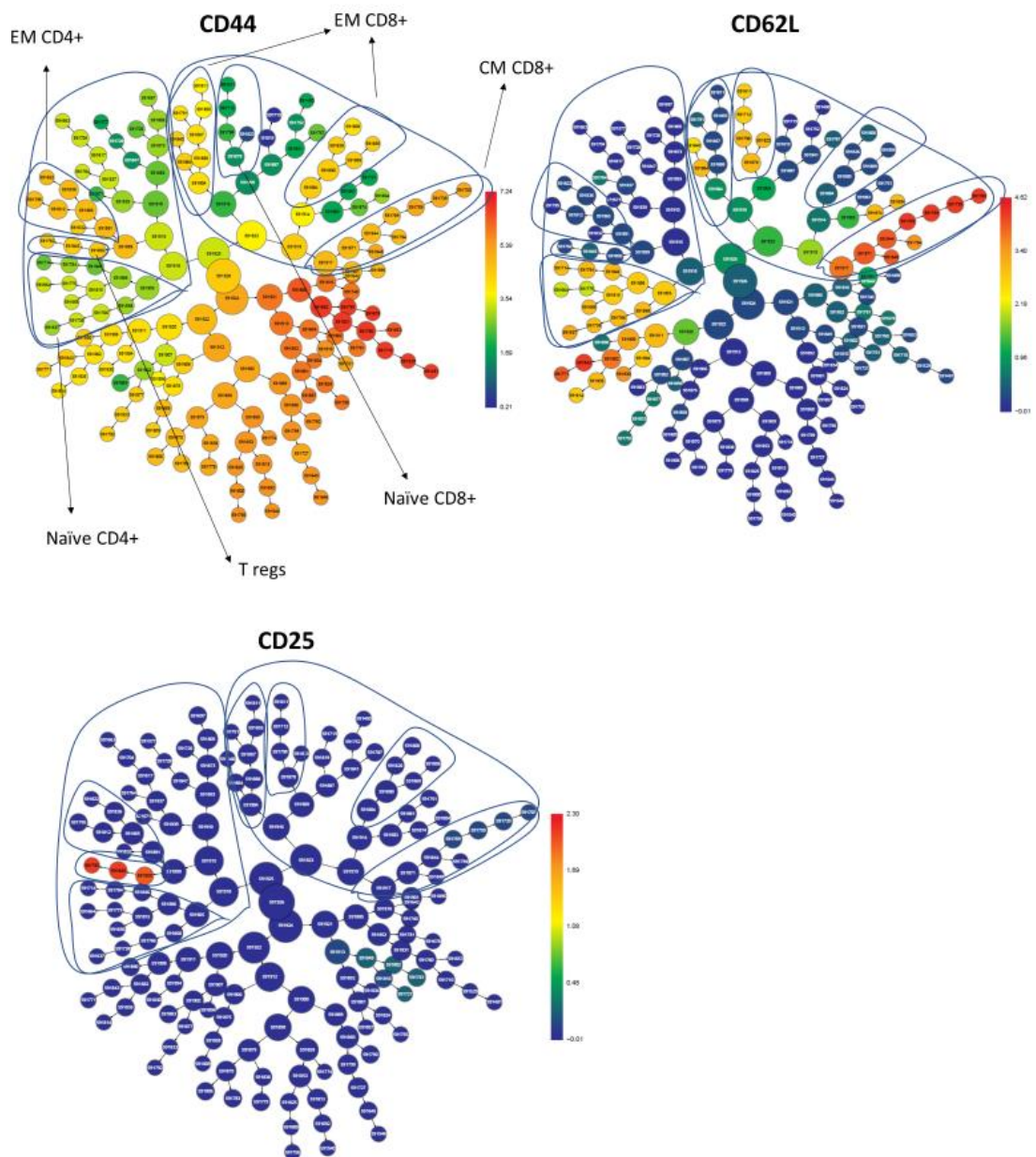
Figure 54: CITRUS cluster tree and identification of memory and naïve T-cells, regulatory T-cells. Size of the circles denotes the abundance of cells in the cluster, colour scale the median marker intensity (red-high expression, blue-low expression). The tree structure is redundant with proximal parent clusters containing all events of distal children clusters. *Abbreviations: CM – central memory, EM – effector memory.*
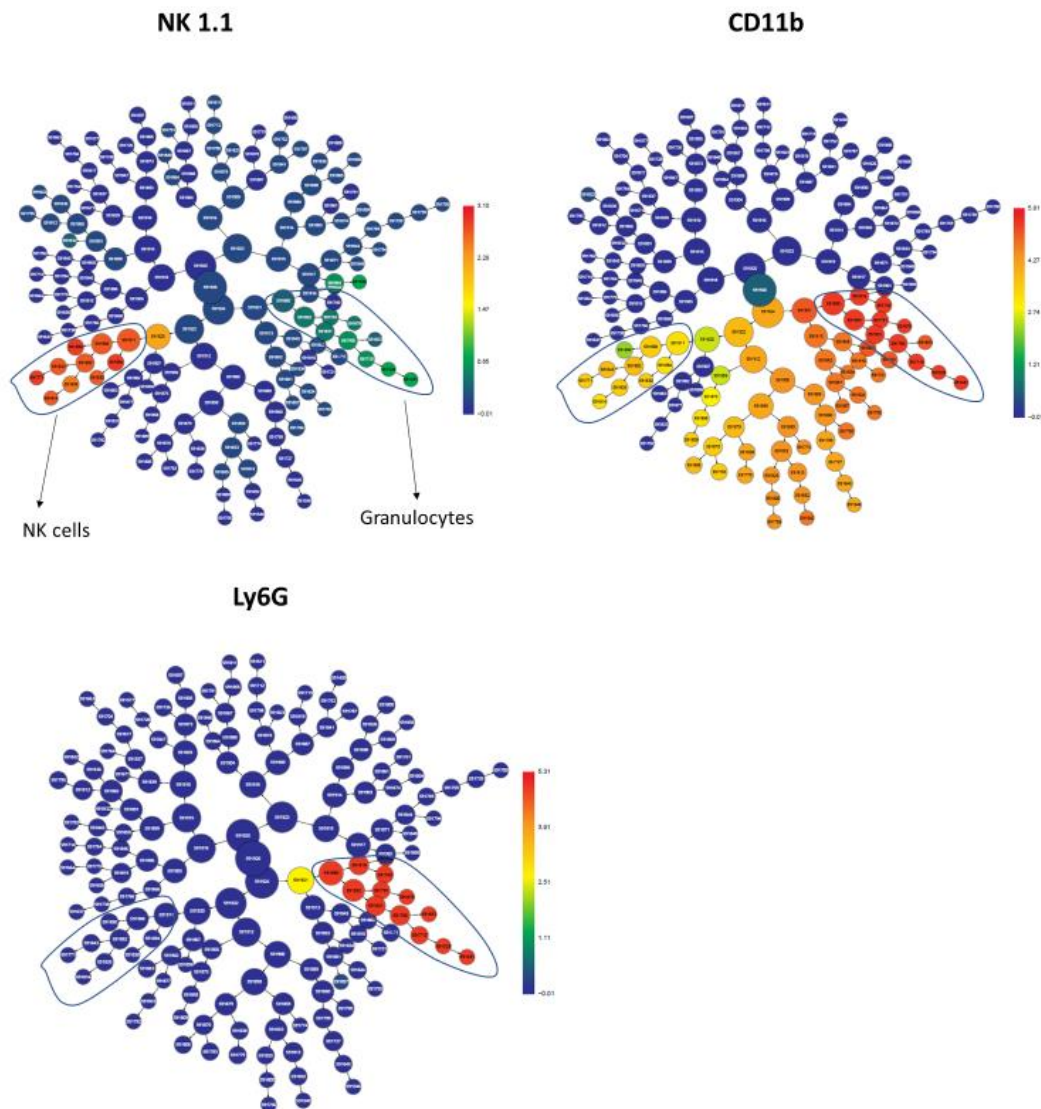
Figure 55: CITRUS cluster tree and identification of Granulocytes and NK-cells. Size of the circles denotes the abundance of cells in the cluster, colour scale the median marker intensity (red-high expression, blue-low expression). The tree structure is redundant with proximal parent clusters containing all events of distal children clusters.
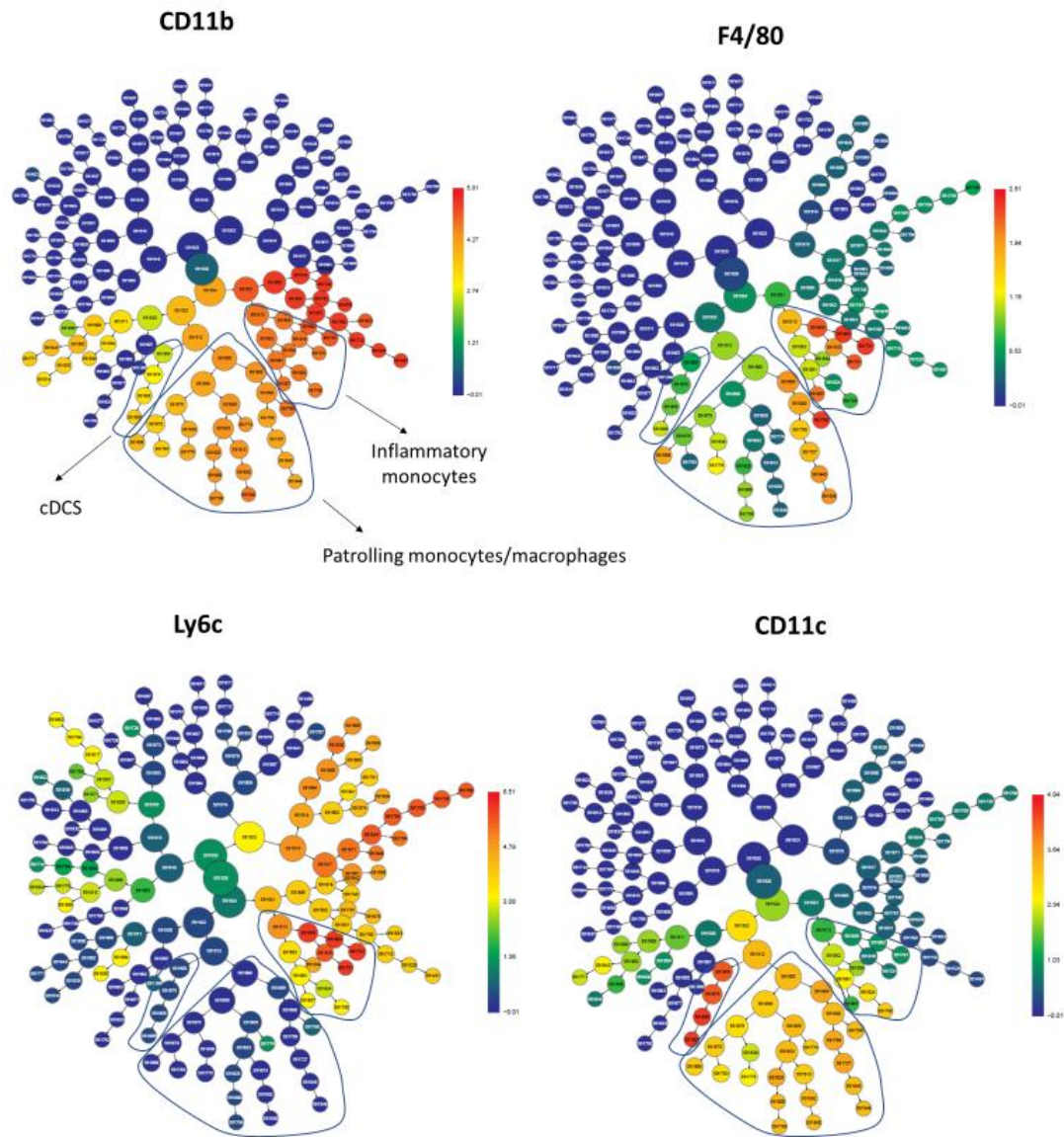
Figure 56: CITRUS cluster tree and identification of dendritic cells and myelomonocytic cells. Size of the circles denotes the abundance of cells in the cluster, colour scale the median marker intensity (red-high expression, blue-low expression). The tree structure is redundant with proximal parent clusters containing all events of distal children clusters.

Figures 57 and 58 illustrate differences in median CD69 expression among cell subsets as analysed using the CITRUS algorithm. We found a decrease in expression with both BTK inhibitor single agent treatments as well as BTK inhibitor/anti-PD-L1 immune checkpoint blockade combinations over vehicle treatment and single agent anti-PD-L1 treatment among NK cells, regulatory T-cells and a subset of effector CD8+ T-cells .A similar trend was observed among naïve and effector CD4+ with statistical signifance reached only for a limited subset of comparisons in those groups.. The effect was similar with single agent BTK inhibitor treatment and both BTK inhibitor/anti-PD-L1 combinations.

Figure 57: *CITRUS cluster tree, comparison of median CD69 expression on splenocyte subsets from BTK inhibitor and BTK inhibitor/anti-PD-L1 combination treated animals. CITRUS cluster tree, statistical analysis by "statistical analysis of microarrays", clusters with statistically significant differences in marker expression highlighted in red, false discovery <1%. * denotes cluster displayed in figures 58. Abbreviations: CM – central memory, EM – effector memory.*

Figure 58: *Comparison of median CD69 expression on lymphocyte and NK cell subsets from spleens of BTK inhibitor and BTK inhibitor/anti-PD-L1 combination treated animals.* *Median signal intensity of selected clusters marked to contain statistically significant differences of expression by "statistical analysis of microarrays, false discovery <1%. For clusters displayed please refer to figure 57. Statistical anaylsis by Kruskal-Wallis test, 6 groups n=10 each, Abbreviations; * - p ≤ 0.05; ** - p ≤ 0.01; *** - p ≤ 0.001; **** - p≤ 0.0001.*

Figures 59-61 demonstrate differences in PD-1 expression among splenocyte subsets in the microenvironment of CLL bearing animals following various modes of treatment. We observed a decrease of PD-1 expression among naïve CD4+ T-cells, regulatory T-cells, effector memory CD4+ T-cells, effector CD4+ T-cells, a subset of effector CD8+ T-cells with both single agent BTK inhibitor treatment and BTK inhibitor/anti-PD-L1 combinations but not with single agent anti-PD-L1 immune checkpoint blockade. Among effector memory CD8+ T-cells a similar trend was observed with only the comparison between single agent PD-L1 inhibitor and single agent Acalabrutinib reaching statiscal significance. Interestingly there was a trnd towards slightly higher expression in animals treated with BTK inhibitor/anti-PD-L1 immune checkpoint inhibitor combinations compared to single agent BTK inhibitor treatment.

Among myeloid cell subsets we found a similar decrease in PD-1 expression. In inflammatory monocytes and classical dendritic cells this effect was similar with both single agent BTK inhibitor treatment and combination treatments. The observed effect in dendritic cells was only very modest albeit statiscally significant. In patrolling monocytes/macrophages expression levels were reduced with both single agent BTK inhibitor and combination treatments over vehicle treatment and single agent anti-PD-L1 immune checkpoint blockade. However, there was trend towards slightly higher expression in single agent BTK treated animals compared to combination treated animals.

Figure 59: *CITRUS cluster tree, comparison of median PD-1 expression on splenocyte subsets from BTK inhibitor and BTK inhibitor/anti-PD-L1 combination treated animals. CITRUS cluster tree, statistical analysis by "statistical analysis of microarrays", clusters with statistically significant differences in marker expression highlighted in red, false discovery <1%. * denotes cluster displayed in figures 60 and 61. Abbreviations: CM – central memory, EM – effector memory.*

Figure 60: C*omparison of median PD-1 expression on lymphocyte subsets from spleens of BTK inhibitor and BTK inhibitor/anti-PD-L1 combination treated animals*. *Median signal intensity of selected clusters marked to contain statistically significant differences of expression by "statistical analysis of microarrays, false discovery <1%. For clusters displayed please refer to figure 59. Statistical anaylsis by Kruskal-Wallis test, 6 groups n=10 each, Abbreviations; * - p ≤ 0.05; ** - p ≤ 0.01; *** - p ≤ 0.001; **** - p≤ 0.0001.*
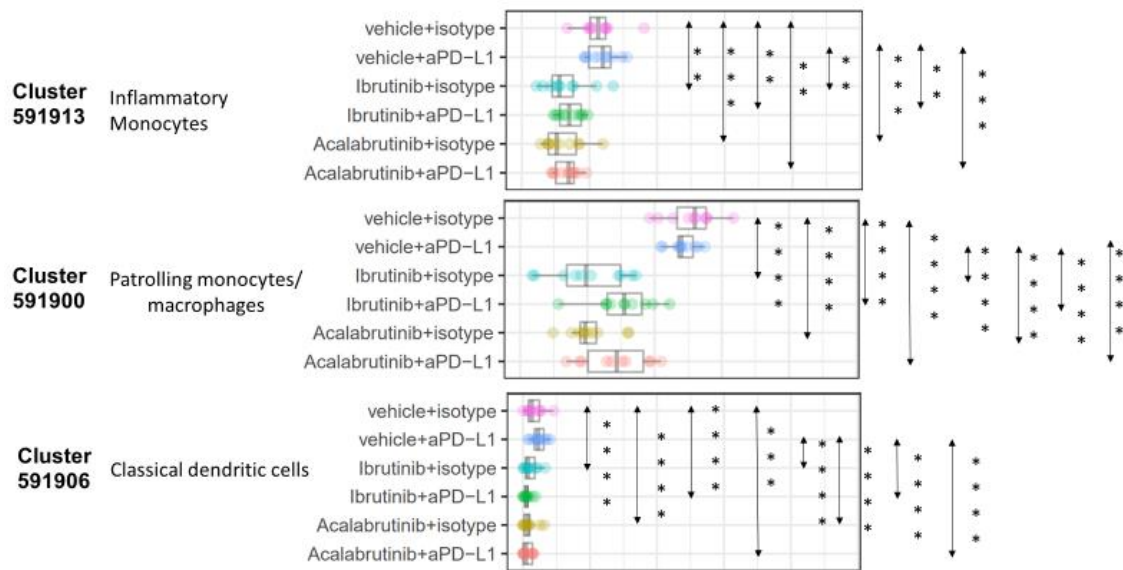
Figure 61: C*omparison of median PD-1 expression on myeloid cell subsets from spleens of animals treated with BTK inhibitor and BTK inhibitor/anti-PD-L1 combination*. *Median signal intensity of selected clusters marked to contain statistically significant differences of expression by "statistical analysis of microarrays, false discovery <1%. For clusters displayed please refer to figure 59. Statistical anaylsis by Kruskal-Wallis test, 6 groups n=10 each, Abbreviations; * - p ≤ 0.05; ** - p ≤ 0.01; *** - p ≤ 0.001; **** - p≤ 0.0001.*

Figures 62 and 63 demonstrate differences in median expression of KLRG-1. We found a very pronounced decrease of expression single agent Acalabrutinib, Acalabrutininib/anti-PD-L1 and Ibrutinib/anti-PD-L1 treatment while a trend towards decreased expression in single agent anti-PD-L1 treatment did not reach statiscal significance. Moreover, a similar but only slight reduction was observed among regulator T-cells. In central memory CD8+ T-cells a statistically significant difference in expression was suggested by the algorithm. However, on inspection of the expression levels no relevant alterations in strength of expression could be appreciated. Only the comparisons between vehicle treatment and anti-PD-L1 treatment as well as anti-PD-L1 treatment and single agent Acalabrutinib treatment reached statiscal significance. This feature, while deemed statistically significant by the algorithm is likely not of functional relevance.
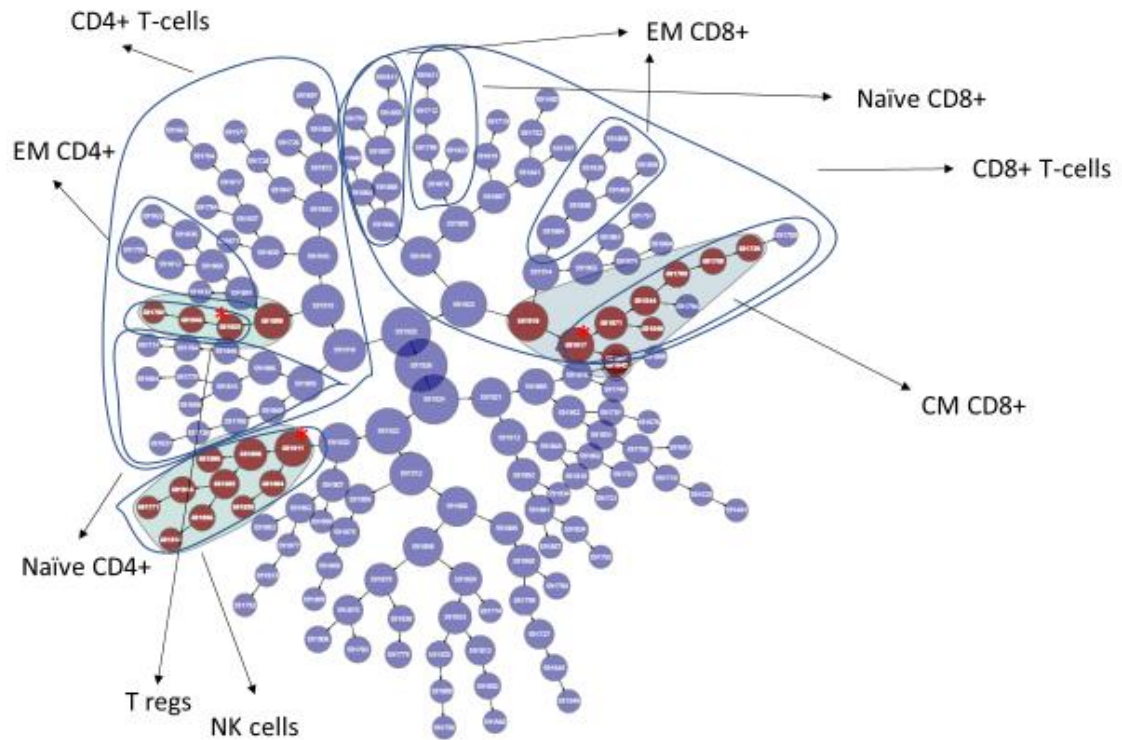
Figure 62: *CITRUS cluster tree, comparison of median KLRG-1 expression on splenocyte subsets from BTK inhibitor and BTK inhibitor/anti-PD-L1 combination treated animals. CITRUS cluster tree, statistical analysis by "statistical analysis of microarrays", clusters with statistically significant differences in marker expression highlighted in red, false discovery <1%. * denotes cluster displayed in figures 63. Abbreviations: CM – central memory, EM – effector memory.*
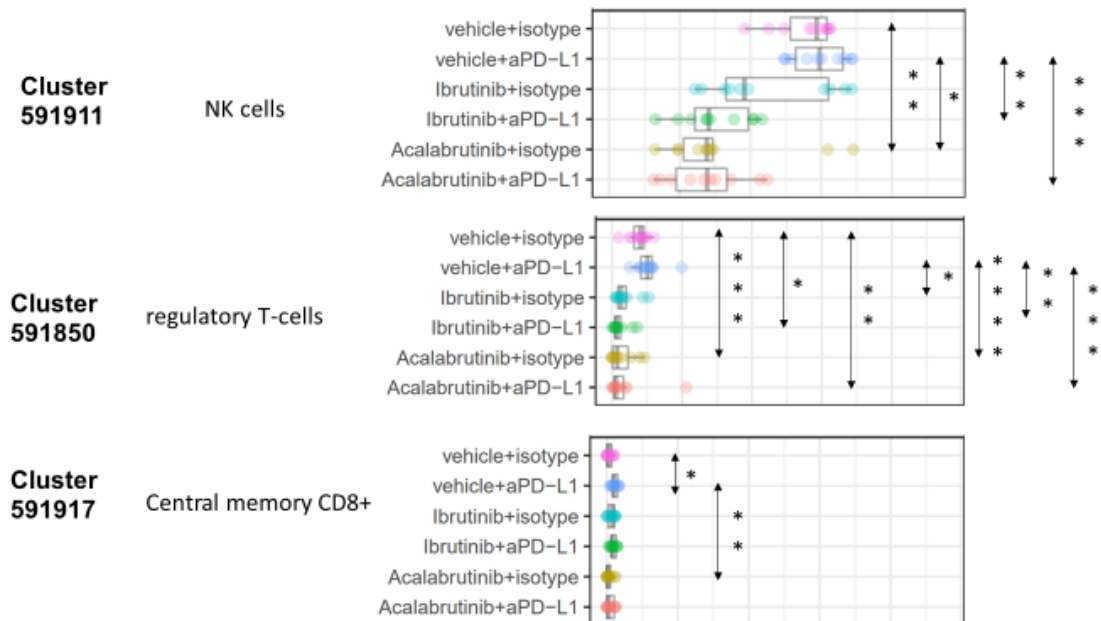
Figure 63: C*omparison of median KLRG-1 expression on NK cell and T-cell subsets from spleens of animals treated with BTK inhibitor and BTK inhibitor/anti-PD-L1 combination*. *Median signal intensity of selected clusters marked to contain statistically significant differences of expression by "statistical analysis of microarrays, false discovery <1%. For clusters displayed please refer to figure 62. Statistical anaylsis by Kruskal-Wallis test, 6 groups n=10 each, Abbreviations; * - p ≤ 0.05; ** - p ≤ 0.01; *** - p ≤ 0.001; **** - p≤ 0.0001.*

Figures 64-66 show median expression of 2B4 among splenocyte subsets of CLL bearing animals following treatment with single agent BTK inhibitor or anti-PD-L1 immune checkpoint blockade as well as BTK inhibitor/anti-PD-L1 combinations. The CITRUS algorithm detected a statistically significant decrease in expression among NK cells following treatment with single agent BTK inhibitor or BTK inhibitor/anti-PD-L1 combinations. Differences highlighted among a subset of effector and effector memory CD8+ T-cells show a very modest increase in expression following single agent anti-PD-L1 treatment only starting from a very low baseline and only very few of these comparisons reached statistical significance.

Other highlighted alterations concern myeloid cell subsets. We have found statistically significant reductions in 2B4 expression among granulocytes, both inflammatory and patrolling monocyte/macrophages subsets as well as among classical dendritic cells among BTK inhibitor treated and combination treated animals.
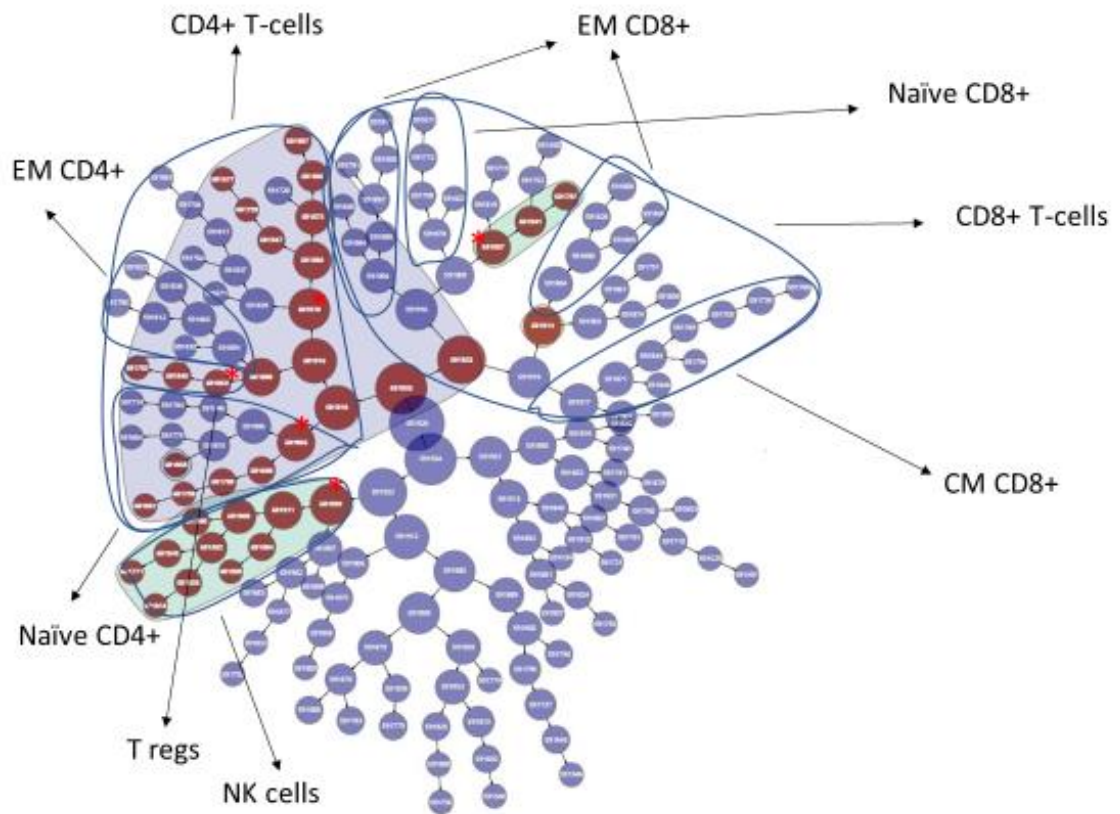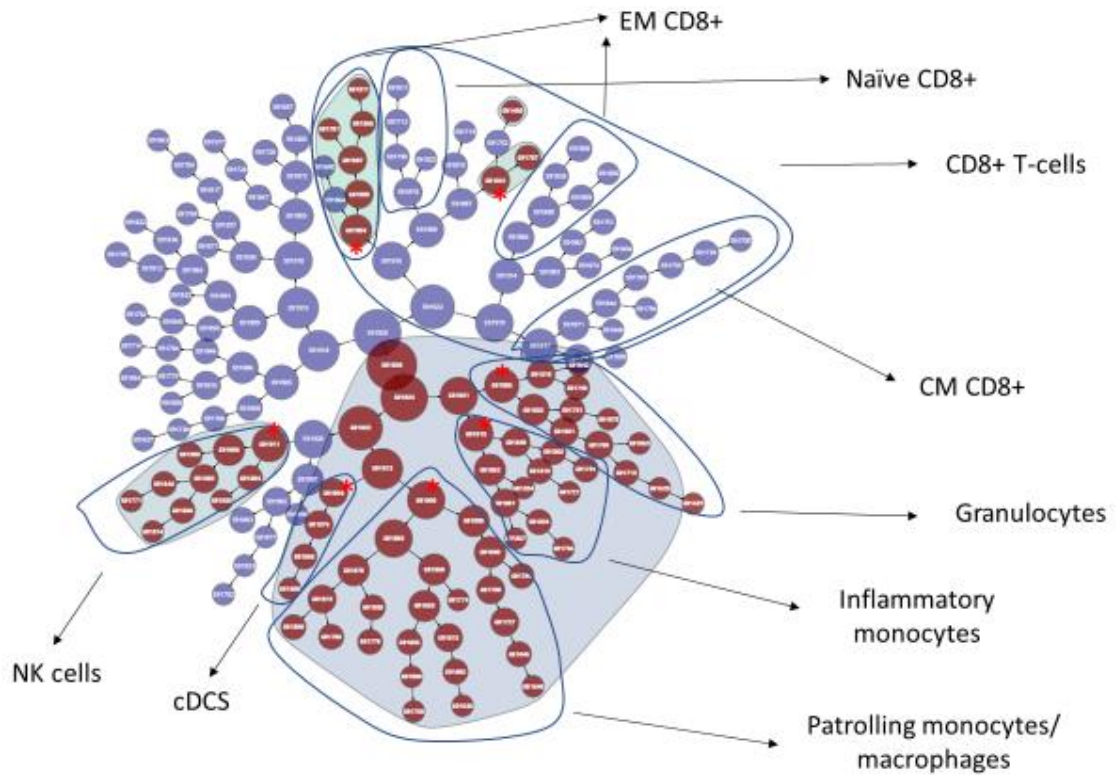
Figure 64: *CITRUS cluster tree, comparison of median 2B4 expression on splenocyte subsets from BTK inhibitor and BTK inhibitor/anti-PD-L1 combination treated animals. CITRUS cluster tree, statistical analysis by "statistical analysis of microarrays", clusters with statistically significant differences in marker expression highlighted in red, false discovery <1%. * denotes cluster displayed in figures 65 and 66. Abbreviations: CM – central memory, EM – effector memory.*
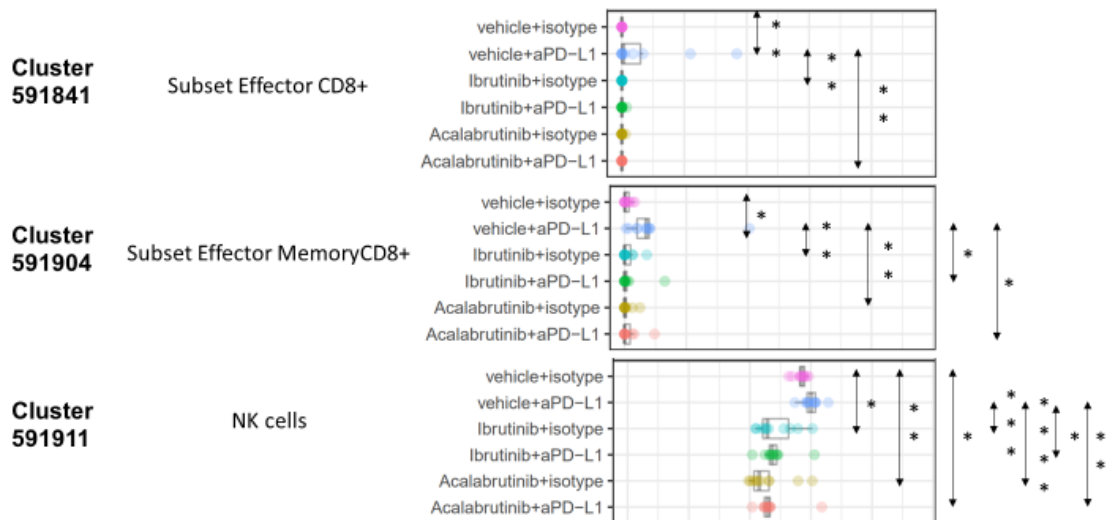
Figure 65: C*omparison of median 2B4 expression on NK cell and T-cell subsets from spleens of animals treated with BTK inhibitor and BTK inhibitor/anti-PD-L1 combination. Median signal intensity of selected clusters marked to contain statistically significant differences of expression by "statistical analysis of microarrays, false discovery <1%. For clusters displayed please refer to figure 64. Statistical anaylsis by Kruskal-Wallis test, 6 groups n=10 each, Abbreviations; * - p ≤ 0.05; ** - p ≤ 0.01; *** - p ≤ 0.001; **** - p≤ 0.0001.*
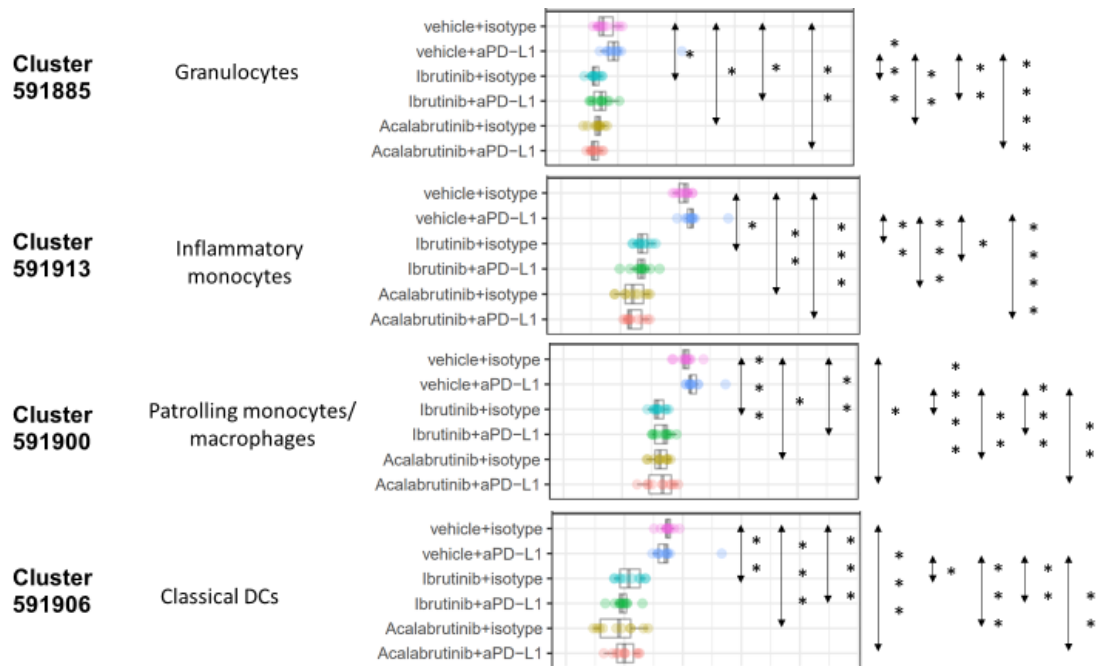
Figure 66: C*omparison of median 2B4 expression on myeloid cell subsets from spleens of animals treated with BTK inhibitor and BTK inhibitor/anti-PD-L1 combination treated*. *Median signal intensity of selected clusters marked to contain statistically significant differences of expression by "statistical analysis of microarrays, false discovery <1%. For clusters displayed please refer to figure 64. Statistical anaylsis by Kruskal-Wallis test, 6 groups n=10 each, Abbreviations; * - p ≤ 0.05; ** - p ≤ 0.01; *** - p ≤ 0.001; **** - p≤ 0.0001.*

Figures 67 and 68 illustrate alterations in TIM-3 expression among splenocyte subsets of treated and untreated CLL bearing animals as detected by the CITRUS algorithm. Interestingly, we did not observe statistically significant differences across treatment groups in lymphocyte subsets but rather in myeloid cell subsets. Expression was found to be increased with BTK inhibitor treatment and combinations of BTK inhibitor and anti-PD-L1 immune checkpoint blockade but not with single agent anti-PD-L1 among patrolling monocytes/macrophag. A similar trend was observed among a subset of inflammatory monocytes. However, statiscal significance was not reached for all comparisons. Among classical dendritic cells only a proximal cluster but not more distal clusters were highlighted as statistically significant. Here, the observed change was inverse with decreased TIM-3 expression with single agent BTK inhibitor and treatment combinations but not single agent anti-PD-L1. Only the comparisons between vehicle treatment and Acalabrutinib containing regimens and single agent anti-PD-L1 treatment and Acalabrutinib containing regimens reached statistical significance.
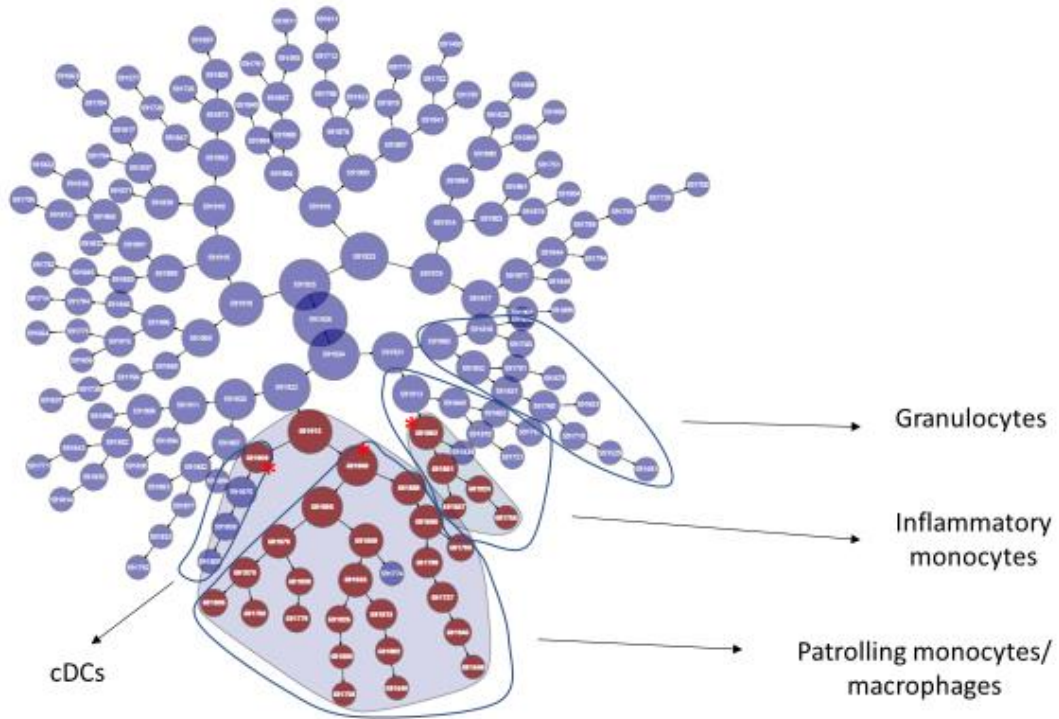
Figure 67: *CITRUS cluster tree, comparison of median TIM-3 expression on splenocyte subsets from animals treated with BTK inhibitor and BTK inhibitor/anti-PD-L1 combination treated*. *CITRUS cluster tree, statistical analysis by "statistical analysis of microarrays", clusters with statistically significant differences in marker expression highlighted in red, false discovery <1%. * denotes cluster displayed in figure 68. Abbreviations: CM – central memory, EM – effector memory.*
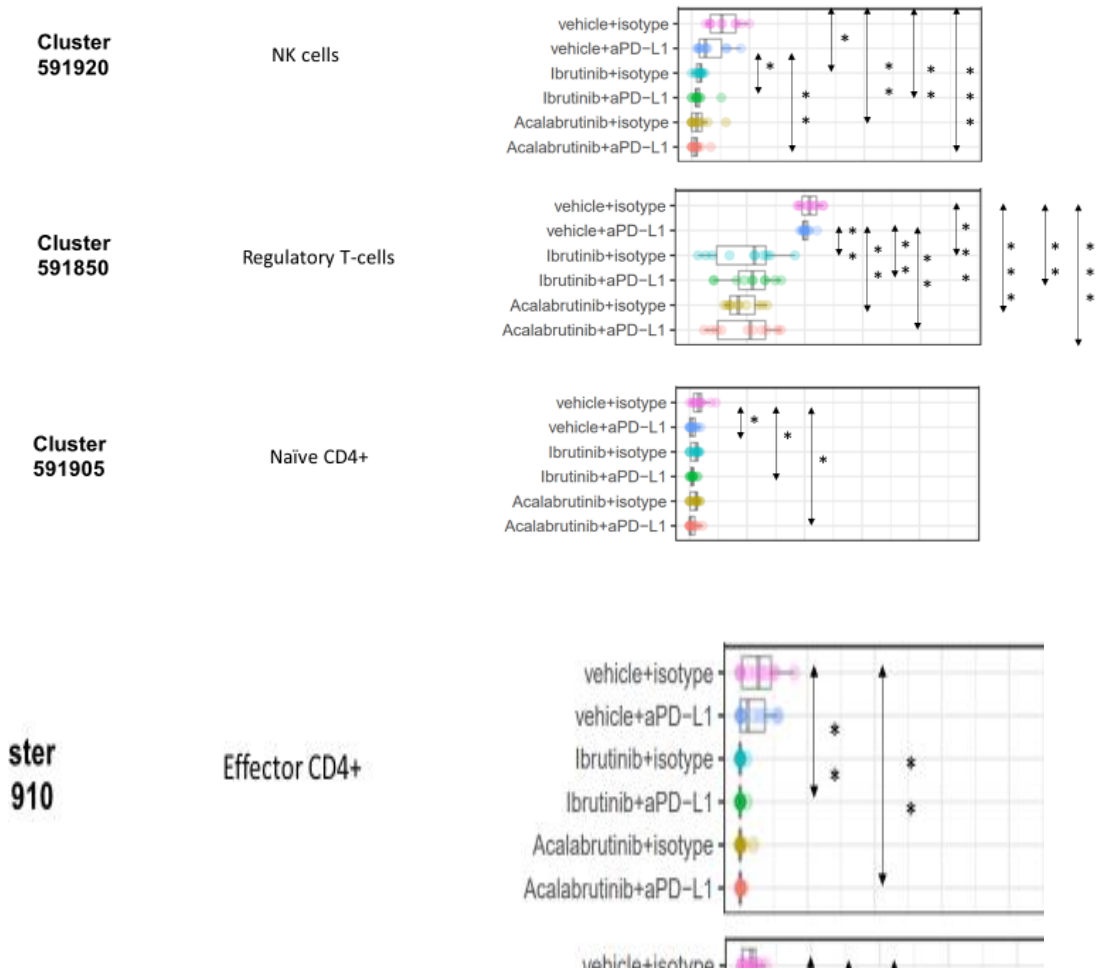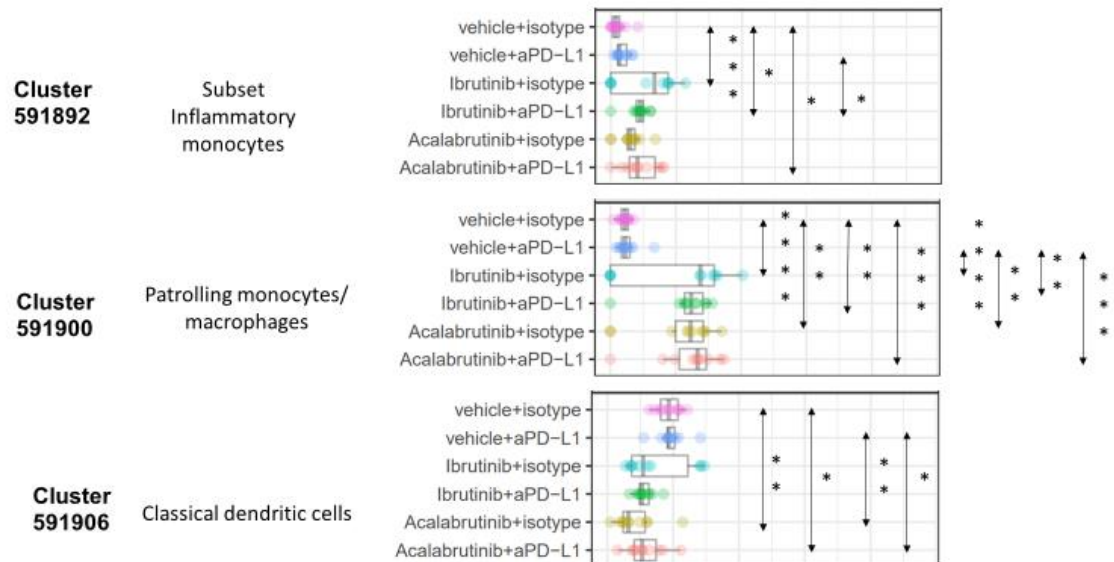

Figure 68: C*omparison of median TIM-3 expression on myeloid cell subsets from spleens of animls treated with BTK inhibitor and BTK inhibitor/anti-PD-L1 combination*. *Median signal intensity of selected clusters marked to contain statistically significant differences of expression by "statistical analysis of microarrays, false discovery <1%. For clusters displayed please refer to figure 67. Statistical anaylsis by Kruskal-Wallis test, 6 groups n=10 each, Abbreviations; * - p ≤ 0.05; ** - p ≤ 0.01; *** - p ≤ 0.001; **** - p≤ 0.0001.*

Figures 68 and 69 illustrate changes observed in median LAG-3 expression in the splenic microenvironment of CLL bearing animals across treatment groups. We observed a decrease in expression of LAG3 with BTK inhibitor treatment and BTK inhibitor/anti-PD-L1 combinations compared with levels seen in vehicle treated and single agent anti-PD-L1 treated animals among a subset of naïve. effector CD4+ T-cells and effector memory CD4+ T-cells. Similarly, slight reductions could be appreciated among a subset of effector and effector memory CD8+ T-cells. Similar trends were observed among NK-cells and central memeory CD8+ T-cells- However, statistically significant reductions were only achieved with Acalabrutinib cointaing regimens or the Acalabrutinib/anti-PD-L1 combination, respectively.
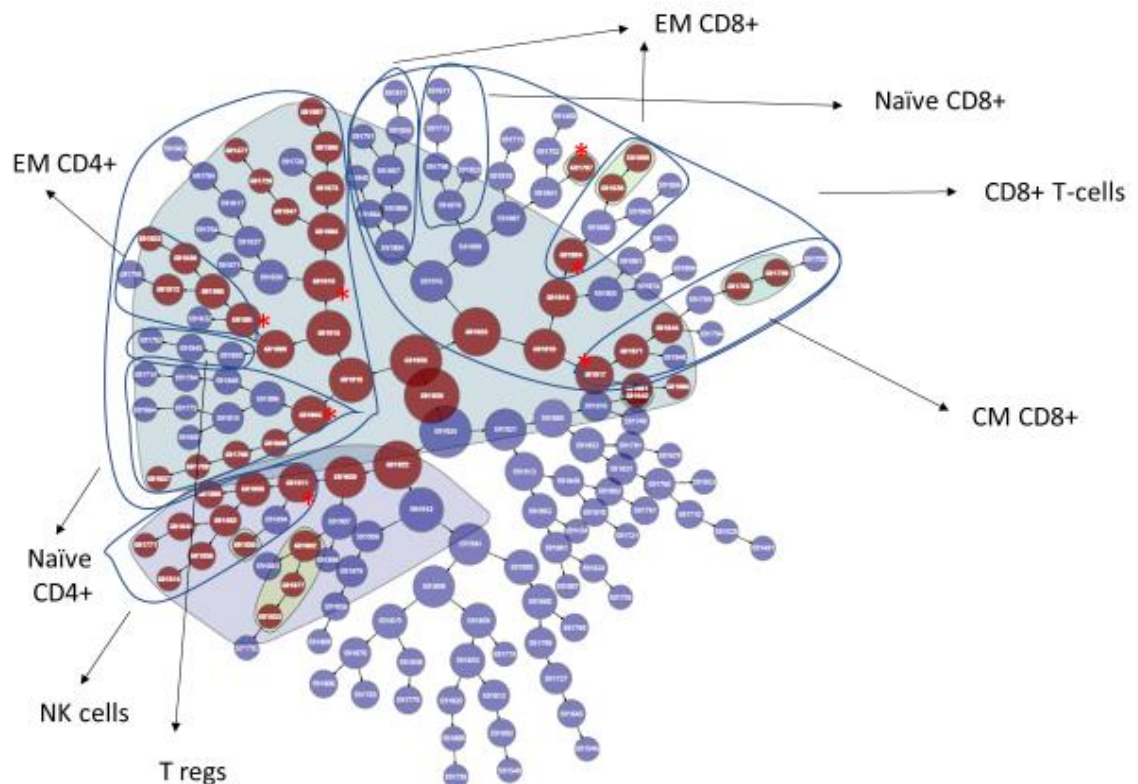
Figure 69: *CITRUS cluster tree, comparison of median LAG-3 expression on splenocyte subsets in anoimals treated with from BTK inhibitor and BTK inhibitor/anti-PD-L1 combination. CITRUS cluster tree, statistical analysis by "statistical analysis of microarrays", clusters with statistically significant differences in marker expression highlighted in red, false discovery <1%. * denotes cluster displayed in figures70. Abbreviations: CM – central memory, EM – effector memory.*
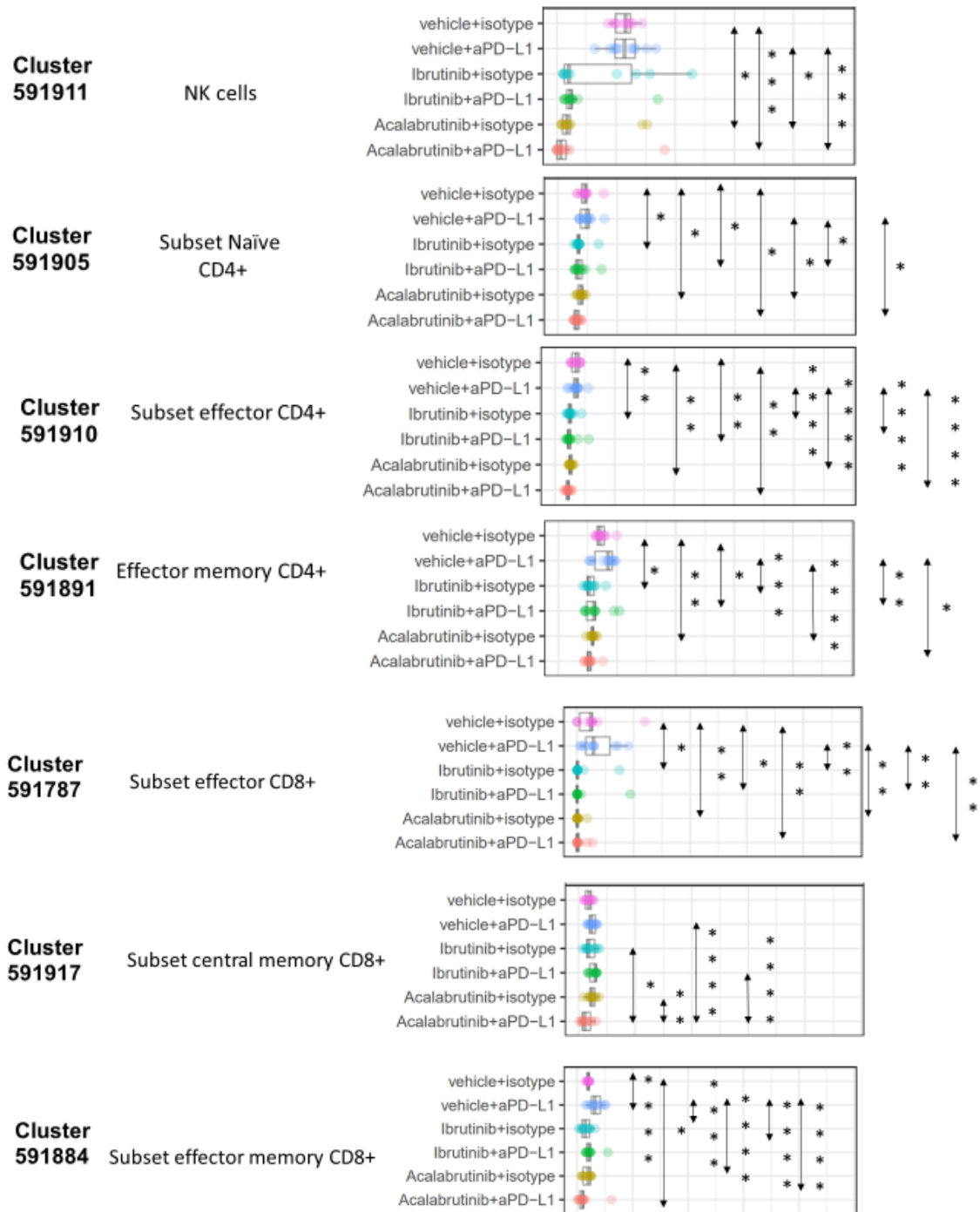
Figure 70: C*omparison of median LAG-3 expression on lymphocyte and NK-cell subsets from spleens animals treated with BTK inhibitor and BTK inhibitor/anti-PD-L1 combination*. *Median signal intensity of selected clusters marked to contain statistically significant differences of expression by "statistical analysis of microarrays, false discovery <1%. For clusters displayed please refer to figure 69. Statistical anaylsis by Kruskal-Wallis test, 6 groups n=10 each, Abbreviations; * - p ≤ 0.05; ** - p ≤ 0.01; *** - p ≤ 0.001; **** - p≤ 0.0001*

In summary we found various effects of BTK inhibitors and BTK inhibitor anti-PD-L1 combinations in this experiment. While PD-L1 staining could not be assessed in anti-PD-L1 treated animals due to masking of staining by the anti-PD-L1 immune checkpoint blockade in BTK inhibitor only treated animals we have confirmed the upregulation of

PD-L1 among CLL B-cells reported in chapter 5. Among T-cells we report a correction of the exhaustion phenotype with downregulation of CD69, PD-1 and LAG-3. These alterations where very similar between BTK-inhibitor only treated and combination treated animals. We did, however, observe a trend towards slightly higher expression levels of PD-1 among anti-PD-L1 treated animals. Compared to the experiment reported in chapter 5 we found more extensive alterations of the immunophenotype of NK cells. These include a downregulation of KLRG-1 and 2B4. We have also observed extensive alterations of the immunophenotype of myelomonocytic cell subsets with downregulation of PD-1 and 2B4 and upregulation of TIM-3. The changes were similar between single agent BTK inhibitor treated and combination treated animals.

7.5   Discussion

We have here sought to investigate the effects of BTK inhibitor/anti-PD-L1 immune checkpoint blockade combinations compared to single agent BTK inhibitor or anti-PD-L1 on the immune phenotype in the splenic microenvironment of CLL bearing animals.

Similar to the findings reported above in chapter 5, we found a downregulation of CD69 expression among T-cell and NK-cell subsets. This effect was similar comparing BTK inhibitor treated and BTK inhibitor/anti-PD-L1 combination treated animals. In the T-cell subsets the observed changes are more centered around less antigen experienced effector cell subsets compared to the experiment reported above in chapter 5. In this regard it is important to note that in comparison to this experiment, animals had a slower initial onset of disease and better overall disease control. This has resulted in a lower overall abundance of memory T-cells and possibly a stronger focus of the observable effects on the effector cell subsets.

On the other hand, we do find comparable alterations in PD-1 expression with a marked downregulation primarily among regulatory T-cells, effector memory CD4+ and CD8+ T-cells but also extending to naïve CD4+ T-cells and effector CD4+ and CD8+ T-cells. A striking difference is, that this downregulation of PD-1 did also affect CD8+ T-cell subsets compared to the earlier experiment where the effect appeared to be focused on CD4+ T-cells. Again, a better overall disease control in the experiment at hand may explain the observed differences. Interestingly, we found that the expression levels of PD-1 were decreased at statistically significant levels in BTK inhibitor/anti-PD-L1 treated animals compared to vehicle and single agent anti-PD-L1 treated animals but there was a trend towards slightly higher expression compared to single-agent BTK inhibitor treated animals. This potentially points to a counterregulatory mechanism of upregulation of PD-

1 in the anti-PD-L1 treatment groups. Moreover, we observed a similar pattern among both inflammatory monocyte and patrolling monocyte/macrophage subsets. Indeed, PD-1 expression has been reported on monocyte and macrophage subsets. In renal cell carcinoma, higher levels of PD-1 expression among classical monocytes in the peripheral blood have been shown to have an association with inferior outcome (989). Higher levels of PD-1 expressing monocytes have been linked to the immunosuppressive phase of sepsis and higher mortality from sepsis in preterm neonates (990). In samples from patients with colorectal cancer and mouse models of the disease increased levels of PD-1 expressing TAMs could be observed. The PD-1 expression increased over time in the research animals and correlates with the stage of the disease in patient samples. TAM PD-1 expression negatively correlated with phagocytic capacity of macrophages against tumour cells and blockade of the PD-1/PD-L1 axis increased phagocytic activity of macrophages, reduced tumour growth and increased survival in mouse models (991). A very modest downregulation of PD-1 expression was observed among classical dendritic cells. Here no differential effect between single agent BTK inhibitor and combination treated animals could be appreciated. Inducible PD-1 expression on splenic dendritic cells has been described in mouse models of bacterial infection and has been reported to impede innate immunity (992). The existence of PD-1 expressing dendritic cells has been demonstrated in both patient samples and mouse models of hepatocellular carcinoma. Intratumoural transfer of DCs lacking PD-1 led to resistance against tumour growth in recipient animals via activation of CD8+ effector T-cells suggesting that PD-1+ dendritic cells may contribute to suppression of CD8+ T-cell function and cancer immune evasion in this disease (993). We believe that similar to the above studies the downregulation of PD-1 among myeloid cell subsets in the splenic microenvironment of CLL bearing animals treated with BTK inhibitor and BTK inhibitor/anti-PD-L1 combinations may contribute to an improved immunosurveillance.

In terms of KLRG-1 expression we find a downregulation with single agent BTK inhibitors and combination treatment centred around NK cells and regulatory T-cells. The changes were very similar in both single agent BTK inhibitor treated and combination treated animals. A further statistically significant feature among central memory CD8+ T-cells did not yield a relevant alteration in expression levels upon closer inspection and is, despite being statistically significant, likely not of functional relevance.

We found 2B4 expression to be decreased both with combinations of BTK inhibitors and anti-PD-L1 immune checkpoint blockade and single agent BTK inhibitor treatment in NK

cells, granulocytes, inflammatory monocytes, patrolling monocytes/macrophages and classical dendritic cells. Highlighted features among subsets of effector and effector memory CD8+ T-cells appeared to be limited to a slightly higher expression among single agent anti-PD-L1 treated animals. As 2B4 expression among lymphocytes has been linked to their activation this may point to an increased CD8+ T-cell activation with anti-PD-L1 treatment. Expression of 2B4 among NK cells is well known and has been reported to have both activating and inhibitory functions. While 2B4 expression is required for optimal activation of CD8+ T-cells and NK cells via interaction with CD48 on neighbouring lymphocytes the interaction of 2B4 on NK cells with CD48 on target cells has been reported to inhibit cytolytic activity of NK cells (994). As high levels of CD48 expression have been described on CLL B-cells the observed downregulation in NK-cell subsets with BTK inhibitor containing treatments could thus also signal an improved NK-cell effector function with these treatments in the splenic microenvironment (995). While CD244 expression has not been reported on the surface of neutrophilic granulocytes, its expression has been suggested to be a hallmark characteristic of granulocytic MDSCs. Its expression on granulocytic cells in the splenic microenvironment of CLL bearing animals and its downregulation with BTK inhibitor containing treatments could point to a reversal of the granulocytic MDSCs phenotype among these animals (996). In dendritic cells expression of 2B4 has been linked to suppression of their pro-inflammatory functions. Dendritic cells derived from the spleens of CD244 -/- animals produced higher levels of pro-inflammatory cytokines and when stimulated with lipopolysaccharide or CpG and DCs from CD244 -/- mice elicited higher NK cell activation in vitro. The downregulation found with BTK inhibitor containing treatment regimens in the splenic microenvironment could thus also contribute to improved immunosurveillance in these animals (997). Expression of 2B4 among monocytes has been described extensively. However, little is known about its function in this cell type (655). Decreased expression has been noted on monocytes derived from the peripheral blood of SLE patients thus suggesting a role in immune tolerance (998). We speculate that the observed downregulation in myelomonocytic cell subsets with BTK inhibitor containing treatment regimens may signal an immunophenotype more permissive of adaptive immune responses.

TIM-3 has been described to act as an immune checkpoint molecule on the surface of T-lymphocytes as well as a marker of T-cell exhaustion (615-617). Surprisingly, we did not find alterations of expression among T-cells with treatment strategies using BTK inhibitors, anti-PD-L1 immune checkpoint blockade or combinations thereof but rather among myeloid cell subsets. Expression was increased among inflammatory monocytes

as well as among patrolling monocyte/macrophage subsets using Ibrutinib, Acalabrutinib or combinations of these BTK inhibitors with anti-PD-L1 immune checkpoint blockade. Among classical dendritic cells, expression was decreased using these regimens. Expression of the surface molecule has previously been described among these cell subsets (613, 614). The functional role of TIM-3 in myeloid cells is still poorly understood. Expression in macrophages has been suggested to help limit the expansion of intracellular pathogens such as Mycobacterium tuberculosis by activation of macrophages (999, 1000). Moreover, evidence suggests that TIM-3 can act as a receptor for PtdSer by phagocytic cells and thus facilitating the clearance of apoptotic cells and cross-presentation of antigens by phagocytic cells (619). Experiments with the monocyte cell line THP-1 as well as CD14+ cells from the peripheral blood of healthy donors have shown that monocyte/macrophages in a quiescent state express high levels of TIM-3 and show low cytokine production while after activation in vitro with LPS or R848 results in reduced TIM-3 expression and increased IL12 production (1001). Antibody mediated blockade of TIM-3 resulted in increased production of IL12 but decreased expression of PD-1. Similarly, silencing of TIM-3 expression in THP-1 cells using si-RNA resulted in increased production of IL12 (1001, 1002). In murine models of hepatocellular carcinoma an increased expression on peripheral blood monocytes and TAMs correlating with disease progression has been noted (1003). As such, the increased expression in myelomonocytic cell subsets following BTK inhibitor containing treatments may signal either improved phagocytosis and cross-presenting capacity of these cells, a decreased activation of monocyte/macrophages or even be detrimental to innate immunity directed against CLL. In tumour infiltrating dendritic cells, TIM-3 has been shown to suppress nucleic-acid-mediated innate immune responses through interaction with the alarmin HMGB-1 (620). The downregulation observed in classical dendritic cells from the splenic microenvironment of CLL bearing animals following treatment with BTK inhibitor containing regimens may thus be a sign of a more innate immunity permissive phenotype. The varied functions of the molecule across these various myeloid cell subsets may also explain the differential effect on the expression profile observed.

With regards to LAG-3 expression, we found a downregulation of median marker expression with both single agent BTK inhibitor treatment and BTK inhibitor/anti-PD-L1 combinations on NK cells, effector memory CD4+ T-cells, effector memory CD8+ T-cells and a subset of effector CD8+ T-cells. In addition, we found a modest downregulation among subsets of effector CD4+ T-cells, and naïve CD4+ T-cells. A feature highlighted among central memory CD8+T-cells did not show relevant alterations in expression levels and is likely not of functional relevance.

In conclusion, we have here demonstrated an amelioration of the exhaustion phenotype among CD4+ and CD8+ T-cells with both single agent BTK-inhibitor treatment and BTK inhibitor/anti-PD-L1 combinations. This is demonstrated by downregulation of CD69, PD-1, LAG-3 and KLRG-1 expression. In addition, we found downregulation of inhibitory receptor 2B4, LAG-3 and KLRG-1 on the surface of NK cells. We also found evidence of a phenotype more permissive of myeloid cell effector function with downregulation of PD-1 and 2B4. We reported differential effects on expression of TIM-3 among myeloid cell subsets with upregulation among myelomonocytic cells and downregulation among classical dendritic cells. While the decreased expression among DCs is in line with reports suggesting a suppressive effect on innate immune responses of TIM-3 in this context the increased expression among myelomonocytic cells is less clear with both positive and negative effects on innate immune response being described in the literature. Marker expression was very similar when directly comparing single agent BTK inhibitor treated and combination treated animals. The most pronounced difference a trend towards a slightly higher expression level of PD-1 among animals treated with BTK inhibitor/anti-PD-L1 combinations compared to single agent BTK inhibitor, possibly signalling a compensatory mechanism in the splenic microenvironment of CLL bearing animals. Differences observed between the experiment reported in chapter 5 and this experiment could potentially be explained with an improved overall disease control and lower levels of infiltrating CLL B-cells achieved in the experiment at hand.

Despite our earlier experiments suggesting a potential for correction of the T-cell exhaustion phenotype with anti-PD-L1 treatment (836) in the present experiments we neither find evidence of an improved T-cell phenotype with single-agent anti-PD-L1 treatment nor evidence of a synergistic effect of combined BTK-Inhibitor and anti-PD-L1 treatment. The current set of experiments and our earlier findings mainly differ in the time-point of anti-PD-L1 application. The treatment seemed to be effective at controlling the disease only when applied from the day of adoptive transfer while application in the setting of already established disease seemed to have little effect clinically and in terms of T-cell exhaustion phenotype. In clinical practice the often initially indolent disease is usually discovered at more advanced stages and an efficacious use of PD-L1 blockade in CLL may thus meet a difficult to surmount obstacles in clinical reality. This notion is also supported by earlier failed attempts to appy PD-1 blockade in CLL patients (108). Of note the anti-PD-L1 antibody applied in our earlier study (836) also had higher capability to directly stimulate ADCC against target cells while the antibody used in the current set of experiments was chosen to include the D265A alteration of the Fc region to more closely model the mode of action of clinically applied PD-L1 inhibitors. It thus

seems possible that clinical success in the earlier study may have at least in part been due to a Rituximab-like direct FCγ-receptor mediated cytotoxicity against PD-L1 bearing CLL B-cells rather than due to modulation of CLL-induced T-cell exhaustion.

8 Influence of BTK inhibitor/anti-PD-L1 combinations on T-cell function

8.1 Specific introduction

According to the cancer immunoediting hypothesis, correction of malignancy associated immune deficiency and development of tools to help counter mechanism of cancer immune escape should provide improved disease control and produce more durable remissions (792). Immune checkpoints pathways are of pivotal importance in limiting T-cell responses under physiological conditions and ensuring tolerance to self. Overexpression of immune checkpoint molecules such as CTLA-4 and PD-1/PD-L1 is frequently utilised in the microenvironment of malignancies to mediate cancer immune evasion (1004). Blockade of immune checkpoint molecules has been successfully used as a means of cancer immunotherapy not only in numerous solid malignancies (846-852) but also, to some extent, in hematologic malignancies such as HL (858, 859).

CLL is a malignant disease that is highly dependent on its supportive microenvironment and the immunosuppressive niche provided by it. Specialized myeloid cells in the CLL microenvironment, so called nurse like cells (NLCs), have been shown to retain CLL B-cells in their supportive microenvironment and confer important stimuli in promoting B-cell proliferation and preventing apoptosis of CLL cells (254-261). Ablation of NLC by either liposomal clodronate or monoclonal antibody mediated inhibition CSF1R signalling reduced leukaemia load in a mouse model of CLL (262). NLCs have been demonstrated to suppress T-cell proliferation and promote Treg expansion which can be prevented by anti-IL10 or anti-TGF-β antibodies as well as IDO inhibitors (268). The development of CLL is associated with severe global defects of both T-helper and cytotoxic T-cell function (298, 397-401). The T-helper cell polarity has been reported to be shifted away from a cellular immunity promoting Th1 phenotype towards a more humoral immunity and B-cell growth promoting Th2 phenotype in CLL (334, 403). Moreover CD4+ T-cells appear to be critical in promoting growth and survival of CLL B-cells in vivo (402).

The high dependency on microenvironmental interactions and marked associated T-cell dysfunction makes CLL an ideal candidate for cancer immunotherapy. Immunotherapeutic strategies are of particularly appeal in this setting, as they may provide a tolerable and potentially even curative treatment approach in a disease that continues to be incurable using standard treatment strategies. Moreover, the disease mainly affects an elderly patient population frequently suffering from relevant comorbidities, thereby limiting treatment options. We have previously shown that CD4 and CD8 T cells from CLL patients show phenotypic and functional similarities to T-cell

in the setting of exhaustion, a chronic activation induced T-cell dysfunction found in chronic viral infections, but retain the ability to produce cytokines such as INF-γ and TNF-α. CLL T cells showed an increased expression of exhaustion markers such as CD244, CD160, and PD1, and these markers were most prominently found in a population of expanded effector T cells (401). PD-1/PD-L1 interaction has been shown to be of pivotal role in CLL associated T-cell defects. In a functional si-RNA screening we could demonstrate a dominant role of PD-L1 in induction of impaired actin-dynamics in CLL (216). This is of particular clinical importance given the role of PD-1/PD-L1 interaction in tumour induced T-cell exhaustion (422). Despite clear evidence of efficacy in other haematologic malignancies and promising pre-clinical studies (836) attempts to utilize PD-1/PD-L1 immune checkpoint blockade in CLL have so far been disappointing (108).

Recent evidence has suggested that the BTK inhibitor Ibrutinib has the ability to modulate T-cell and myeloid cell function (877-881). It has been suggested that the clinical efficacy of the agent is due to a combination of direct effects on CLL B-cells via the BCR pathway as well as correction of CLL associated immune defects. Traditionally modulation of T-cell function by Ibrutinib has been linked to differential suppression of tyrosine kinases ITK and RLK leading to selective pressure favouring Th1 helper cell polarity (877). As the second generation BTK inhibitor Acalabrutinib does not have inhibitory activity towards ITK the agent should theoretically differ in its potential to correct CLL associated T-cell defects (986). In the experiments previously described we have confirmed correction of T-helper cell cytokine profile as well as cytotoxic T-cell effector function using Ibrutinib in the Eµ-TCL1 adoptive transfer model of CLL. Interestingly, we have confirmed very similar effects using Acalabrutinib. We speculate that, rather as by direct modulation of T-cell function via ITK, the effects of BTK-inhibitors are mediated largely via an indirect effect, possibly through modulation of myeloid cell in the CLL microenvironment. Above we have confirmed the potential of both BTK inhibitors to alleviate the exhaustion phenotype of CLL associated T-cell and decrease expression of immune checkpoint molecules such as PD-1, LAG-3 and KLRG-1. We therefore speculate that combinations of the BTK-inhibitors and PD-L1 immune checkpoint blockade may have a synergistic effect. Results in the A20 mouse model of lymphoma support this hypothesis (872). Given our above findings we believe that both Ibrutinib and Acalabrutinib are promising candidates for a combination approach with PD-L1 immune checkpoint blockade in the setting of CLL. A phase I/IIa study of Nivolumab/Ibrutinib in patients with relapse NHL and CLL/SLL has recently reported a promising ORR of 61% of high risk CLL/SLL further advocating for the use of combination strategies (873).

8.2 Goals and objectives

Our goal was to establish a combination strategy of BTK inhibitors and PD-L1 immune checkpoint blockade. We sought to demonstrate improved T-cell function with Ibrutinib or Acalabrutinib in combination with PD-L1 immune checkpoint blockade in the Eµ-TCL1 adoptive transfer model of CLL. The best combination of agents could then be subsequently be carried forward in survival experiments to demonstrate superior efficacy in a pre-clinical model.

8.3 Specific methods and materials

8.3.1 Cell thawing procedure

Thawing of cryopreserved splenocyte samples was performed in a water bath at 37°C. To avoid contamination the vials were disinfected using 70% IMS (Fisher Scientific, UK) and subsequently opend in a class II biosafety cabinet. The cell suspension was pipetted into 10ml RPMI 1640 (Gibco, UK) supplemented with 10% FCS (Gibco, UK), 1% Penicillin-Streptomycin (Sigma, UK) at 37°C. Subsequently the suspension was centrifuged at 300 x g for 10 minutes at room temperature and resuspended in a volume suitable for number of cells contained in the pellet. Automated cell counting was conducted on a Luna fl automated cell counter (Logos bioystems, USA) after dilution of a 10µl aliquot with an equal amount of 0.4% Tryphan blue (Sigma, UK).

8.3.2 Flow cytometry based functional T-cell assays

8.3.2.1 Cell stimulation

1×10^6 splenocytes were incubated in 250µl RPMI 1640 with 10% FCS (Gibco, UK), 1% Penicillin/Streptomycin (Life Technologies, UK) in round-bottom 96-well-plates (VWR, UK). 5µg/ml CD107a per well (Clone 1D4B biolegend, UK) was added. The splenocytes were stimulated with PMA/ionomycin/brefeldin A/monensin cell stimulation cocktail (eBioscience, UK) for 6 hours at 37°C/5% CO2. Controls were treated with transport inhibitor cocktail brefeldin A/monensin (eBioscience), but no cell stimulation cocktail.

8.3.2.2 Surface and intracellular flow cytometry staining

1×10^6 PMA/ionomycin/brefeldin A/monensin stimulated splenocytes, 1×10^6 unstimulated splenocytes and their corresponding controls were used per animal and transferred into 5ml polystyrene round-bottom tubes (Corning, UK). All staining steps were performed at a temperature of 2-8°C to avoid internalisation or capping of the antibodies. Cells were

resuspended in 100 µl of FACS buffer containing viability stain (fixable viability efluor 506, ebioscience, UK) at a concentration of 1:1000. Surface antibodies (CD3e APC/CY 7, clone 145-2C11, biolegend, UK; CD8a BV605, clone 53-6.7, biolegend, UK; CD44 AF700, clone IM7, ebioscience, UK) were added at a dilution of 1:100 and cells incubated at 4 ºC for 30 minutes. Fixation using IC fixation buffer (ebioscience,UK) and permeabilisation using permeabilisation buffer (ebioscience,UK) were performed according to the manufacturer's recommendations. Cells were stained with intracellular antibodies (Interferon gamma AF488, clone XMG1.2, biolegend, UK; IL2 PE/Cy7, clone JES6-5H4, biolegend, UK; IL4 PerCPefluor 710, clone 11B11, ebioscience, UK) for 1h at 4ºC at a 1:100 dilution. Compensation controls consisted of ABC total compensation beads (Thermo fisher scientific, UK). In order to obtain compensation controls one drop each of both negative control beads and positive antibody binding beads were added to 80µl FACS buffer in a 5ml polystyrene round-bottom tube (Corning, UK). One tube per flurochrome included in the panel was prepared. Subsequently a dose appropriate for one test of pre-conjugated flow cytometry antibody was added and the sample incubated at 4°C for 30 minutes in the dark. The solution was then washed in 2ml FACS buffer twice and resuspended in 300µl PBS ready for acquisition. Beads could not be used for compensation control of the viability stain- here single-stained cells were used. Acquisiton was performed on a BD LSR Fortessa flow cytometer (BD, UK). The recorded .FCS files were analysed using Cytobank (Cytobank Inc., USA).

8.4   Results

We analysed cytokine production and degranulation of T-cells as described above in the splenic microenvironment of CLL bearing animals treated with either single agent Ibrutinib, Acalabrutinib, PD-L1 immune checkpoint blockade or combinations of BTK inhibitors and PD-L1 immune checkpoint blockade. Animal experiments conducted to derive splenocyte samples are described under 3.4.4. Figures 71 and 72 illustrate IL2 production among T-cell subsets following stimulation with PMA/Ionomycin. Among overall CD3+ T-cells a statistically significant increase in IL2 production is detected with Acalabrutinib treatment, single agent anti PD-L1 and Ibrutinib/anti-PD-L1 combination to a similar extent. The combination of Acalabrutinib/anti-PD-L1 was observed to lead to a strong decrease in IL2 production.
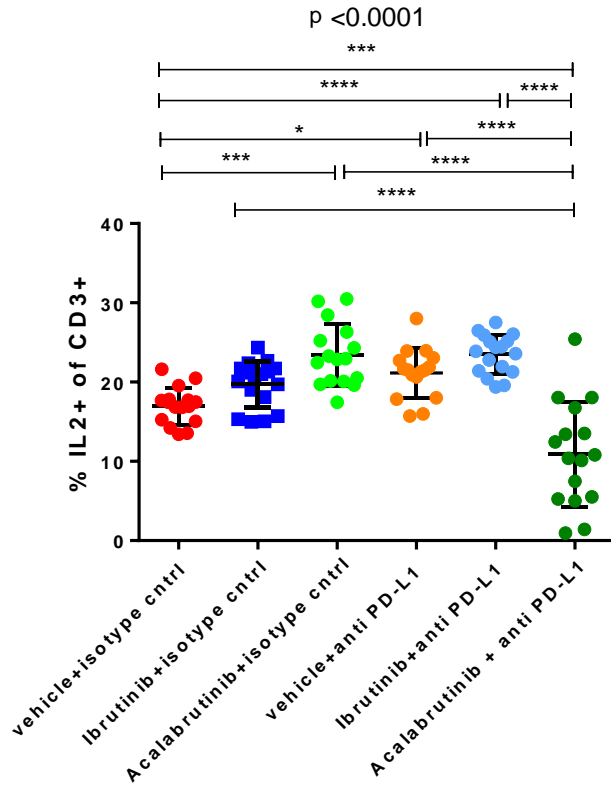
Figure 71: Illustration of *IL2 production in CD3+ T- cells in single agent and BTKi/anti-PD-L1 combination treated CLL bearing animals.* Statistical analysis by 1way Anova. 6 groups n=17 each. *Abbreviations: * $p \leq 0.05$; ** $p \leq 0.01$; *** $p \leq 0.001$; **** $p \leq 0.0001$.*

IL2 production among T-helper cells was increased with BTKi and anti-PD-L1 single agent treatment and slightly more with Ibrutinib/anti-PD-L1 combination treatment. However, Acalabrutinib/anti-PD-L1 decreased IL 2 production. Among cytotoxic T-cells only single agent anti-PD-L1 increased IL2 production at a statistically significant level while Acalabrutinib/anti-PD-L1 decreased production (Figure 72).
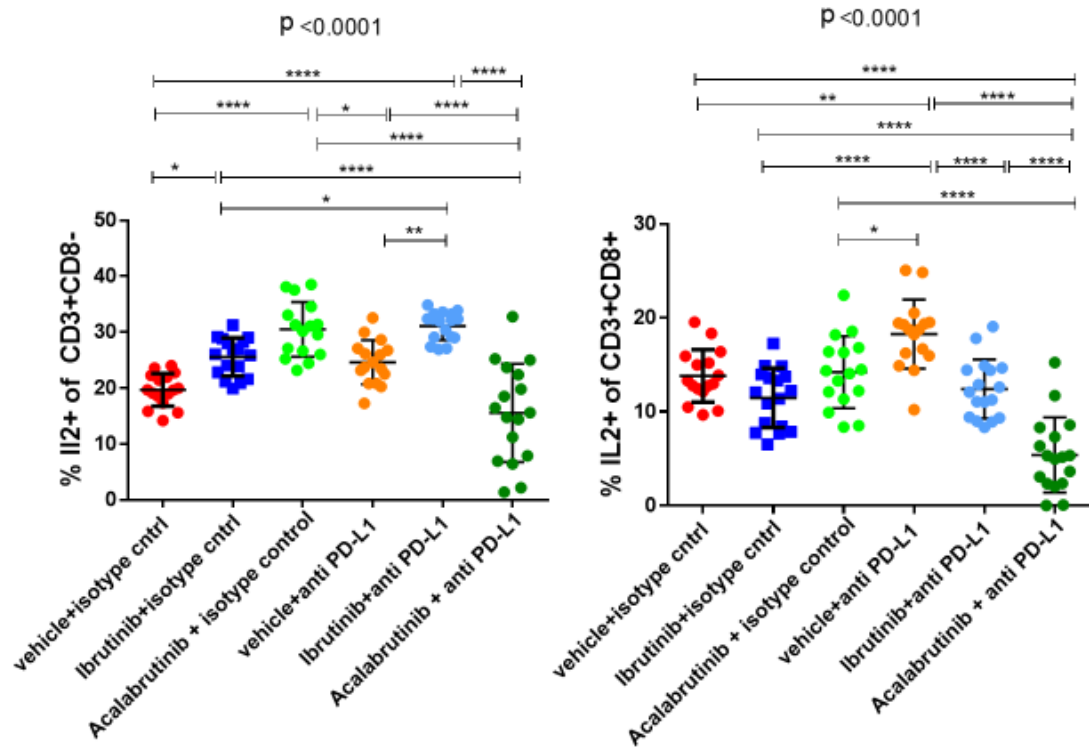
Figure 72: Illustration of *IL2 production in CD8+ and CD8- T- cell subsets in single agent and BTKi/anti-PD-L1 combination treated CLL bearing animals*. Statistical analysis by 1way Anova. 6 groups n=17 each. *Abbreviations: * $p \leq 0.05$; ** $p \leq 0.01$; *** $p \leq 0.001$; **** $p \leq 0.0001$*

Figures 73 and 74 illustrate IL4 production among T-cell subsets. In overall CD3+ T-cells the IL4 production is reduced to a similar extent and at a statistically significant level with both single agent Ibrutinib or Acalabrutinib as well as with Ibrutinib/anti-PD-L1 and Acalabrutinib/anti-PD-L1 combinations. Both single agent BTK inhibitor and BTK inhibitor/anti-PD-L1 combinations decreased IL4 production among helper T-cells while only BTK inhibitor/anti-PD-L1 combinations decreases IL4 production among cytotoxic T-cells at a statistically significant level.
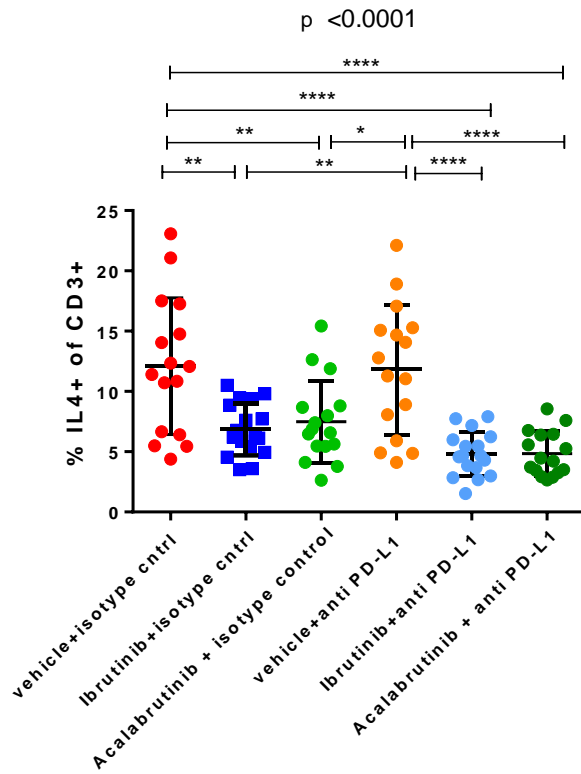
Figure 73: Illustration of *IL4 production in CD3+ T- cells in single agent and BTKi/anti-PD-L1 combination treated CLL bearing animals.* Statistical analysis by 1way Anova. 6 groups n=17 each. *Abbreviations: * p ≤ 0.05; ** p ≤ 0.01; *** p ≤ 0.001; **** p≤ 0.0001.*
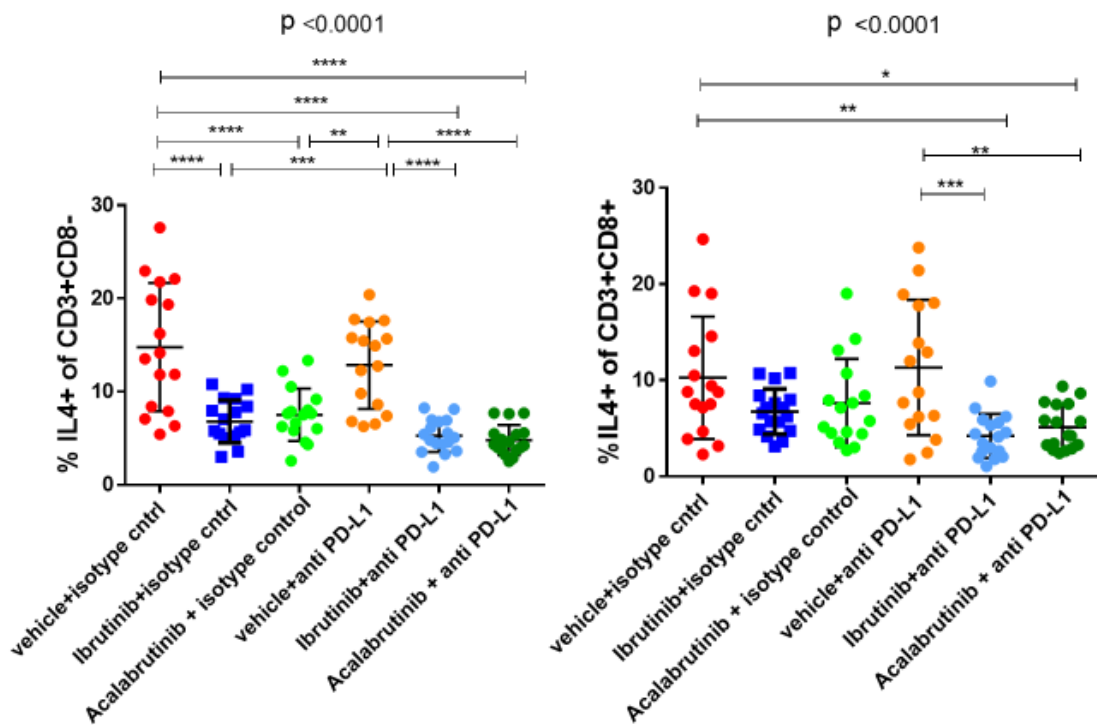
Figure 74: Illustration of *IL4 production in CD8+ and CD8- T- cell subsets in single agent and BTKi/anti-PD-L1 combination treated CLL bearing animals*. Statistical analysis by 1way Anova. 6 groups n=17 each. *Abbreviations: * p ≤ 0.05; ** p ≤ 0.01; *** p ≤ 0.001; **** p≤ 0.0001.*

Figures 75 and 76 illustrate IFNγ production among T-cell subsets derived from the spleens of treated CLL bearing animals following PMA/Ionomycin simulation. Among the overall CD3+ T-cells both single agent BTK inhibitor as well as BTK inhibitor/anti-PD-L1 combinations but not single agent anti-PD-L1 were observed to lead to decreased IFNγ secretion. This is reflected by the situation in cytotoxic T-cells where the same pattern was observed. In the helper cell compartment only Ibrutinib but not Acalabrutinib treatment resulted in a statistically significant decrease of IFNγ production. Both Ibrutinib and Acalabrutinib in combination with anti-PD-L1 resulted in reduced intracellular IFNγ staining in helper cells compared to single agent anti-PD-L1 but not in comparison to vehicle treatment.
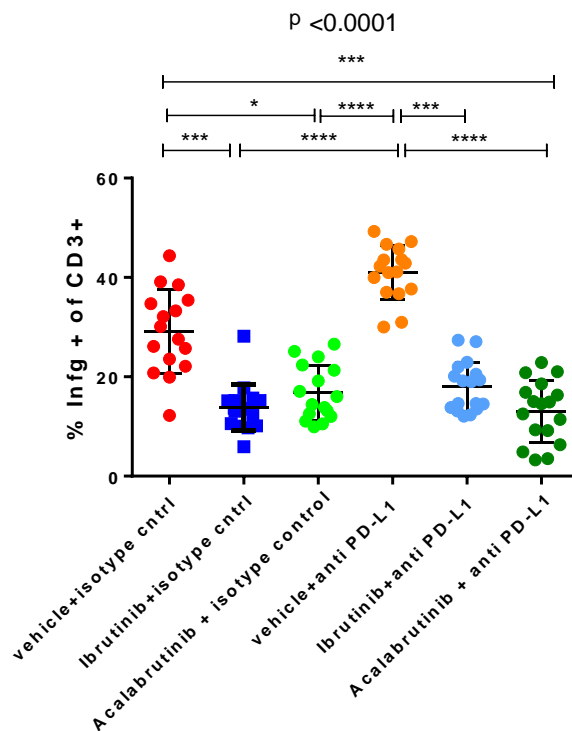
Figure 75: Illustration of *IFN-γ production in CD3+ T- cells in single agent and BTKi/anti-PD-L1 combination treated CLL bearing animals*. Statistical analysis by Kruskal Wallis test. 6 groups n=17 each. *Abbreviations: * p ≤ 0.05; ** p ≤ 0.01; *** p ≤ 0.001; **** p≤ 0.0001.*
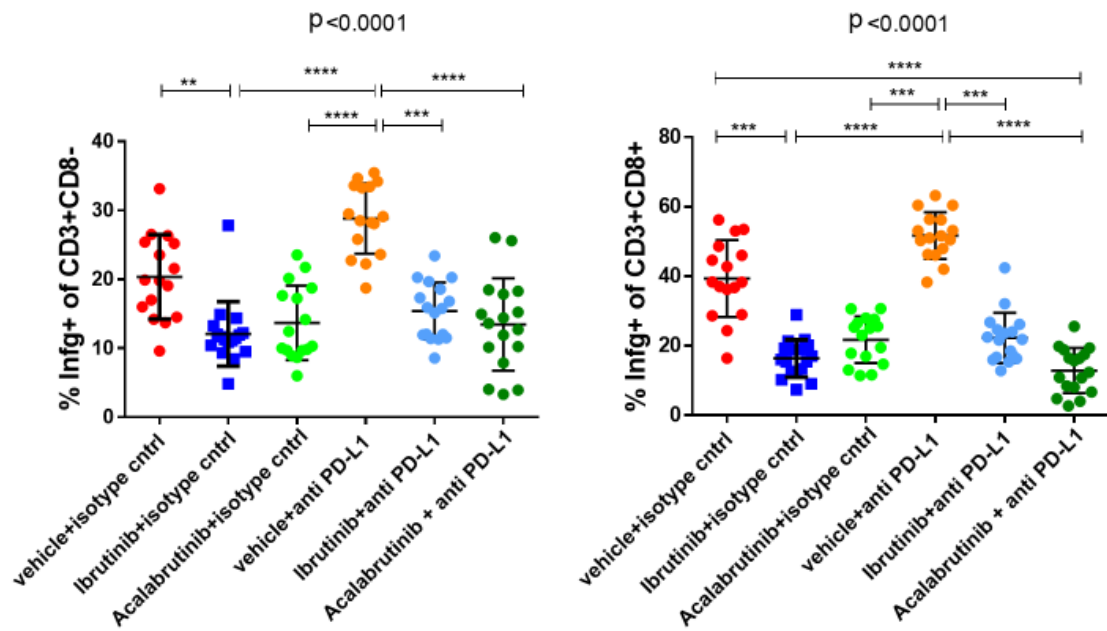
Figure 76: Illustration of *IFN-γ production in CD8+ and CD8- T- cell subsets in single agent and BTKi/anti-PD-L1 combination treated CLL bearing animals*. Statistical analysis by Kruskal Wallis test. 6 groups n=17 each. *Abbreviations: * p ≤ 0.05; ** p ≤ 0.01; *** p ≤ 0.001; **** p≤ 0.0001.*

Figure 77 shows the CD107a+/CD107a- ratio among CD44+ antigen experienced T-cells as well as naïve CD44- T-cells. The CD107a+/CD107a- ratio in CD3+CD8+CD44+ T-cells is increased further over BTKi single treated animals with the Ibrutinib/anti-PD-L1 combination but not with the Acalabrutinib/anti-PD-L1 combination which fairs worse than single agent treatment. Only single agent anti-PD-L1 increased CD107a+/CD107a-ration in CD3+CD8+CD44- T-cells while the ratio is even decreased in Acalabrutinib/anti-PD-L1 combination treated animals.
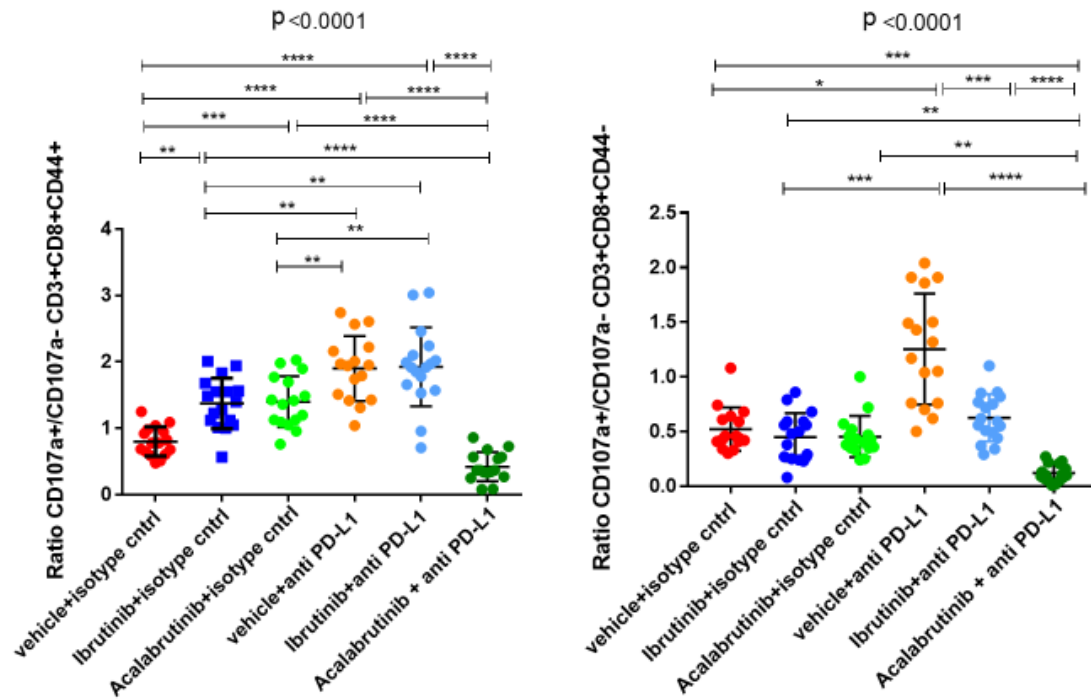
Figure 77: Comparison of the ratio of CD107a+/CD107a- in CD3+CD8+CD44+ and CD3CD8+CD44- T-cells in BTKi and BTKi/anti-PD-L1 combination treated CLL bearing animals. Statistical analysis: CD3+CD8+CD44+ 1way Anova, CD3+CD8+CD44- Kruskal Wallis test. 6 groups n=17 each. *Abbreviations: * $p \leq 0.05$; ** $p \leq 0.01$; *** $p \leq 0.001$; **** $p \leq 0.0001$.*

8.5 Discussion

Here we aimed to assess the impact of a combination approach of BTK inhibitor treatment and anti-PD-L1 immune checkpoint blockade. Based on our findings in previous chapters we speculated that a combination of these two classes of agents may act synergistically in repairing CLL associated functional defects of T-helper cells and cytotoxic T-cells in the CLL microenvironment. Our findings confirm the correction of helper cell cytokine profile and cytotoxic T-cell degranulation observed with Ibrutinib and Acalabrutinib treatment as reported in chapter 6. Single agent anti-PD-L1 immune checkpoint blockade on the other hand had no statistically significant effect on helper cell IL4 and IL2 production but increased IL2 production among cytotoxic T-cells. Moreover, there was a trend towards increased rather than decreased INFγ production with single agent anti PD-L1. The combination of Ibrutinib and anti PD-L1 seemed to result in a slight but very modest improvement of overall T-cell function compared to single agent BTK inhibitor treatment. IL2 production among T helper cells was increased further above the levels observed with single agent Ibrutinib and anti-PD-L1 and on the same level as single agent Acalabrutinib. A similar degree of IL4 suppression compared to single agent BTK inhibitor treatment was achieved. INFγ production was normalized

to an extent similar to that observed with wither BTK inhibitor. Cytotoxic T-cell degranulation among CD3+CD8+CD44+ was increased to the same extent as with single agent anti-PD-L1 treatment while there was no effect on degranulation of CD3+CD8+CD44-.

In conclusion, we find evidence of only very limited additional improvement of T-cell function with combination treatment using Ibrutinib and anti-PD-L1 immune checkpoint blockade over single agent Ibrutinib treatment. A study assessing the impact on survival would be a necessary next step in order to investigate the influence of the combination on the clinical course of the disease. However, given the data presented here and in chapter 7 above, improved CLL disease control with combination treatment even over an extended time course seems unlikely.

Interestingly, while single agent Acalabrutinib was shown to improve T-cell function, the combination of Acalabrutinib and anti-PD-L1 immune checkpoint blockade was detrimental in terms of both helper cell and cytotoxic T-cell function. The drug combination resulted in a similar degree of IL4 suppression among helper cells and IFNγ suppression among cytotoxic T-cells but was found to lead to dramatically decreased capacity of both T-cell subsets to produce IL2 and reduced degranulation upon stimulation among CD44+ and CD44- cytotoxic T-cells. This finding is in spite of a similar immune phenotype and immune checkpoint expression of T-cells in the microenvironment as shown in chapter 7. The mechanism of this phenomenon remains obscure. We speculate that an unforeseen interaction of intracellular signalling mechanisms may underlie this process and propose further investigations into cell signalling in these samples. Complementary pathways could potentially be aberrantly activated or repressed by this combination. This also comes in light of a recent report on a pre-clinical study at the MD Anderson Cancer Centre using a combination of Acalabrutinib and anti-PD-1 immune checkpoint blockade in the Eμ-TCL1 mouse model. Here the occurrence of a CLL clone with a hyperproliferative phenotype among the animals treated with the combination was described. Similar to our own findings, unforeseen interactions of intracellular signalling events have been suggested to contribute to this deleterious effect (1005).

The results presented above would caution against the use of Acalabrutinib/anti-PD1 or anti-PD-L1 combinations in the clinical setting. Suppressive effects on T-cell function could potentially negatively affect treatment results and the findings of our colleagues at the MD Anderson Cancer Centre foster fears of causing or unmasking of hyperproliferative CLL phenotypes. Ongoing trials evaluating such combinations should

be evaluated carefully to ensure no such detrimental effect on T-cell function and CLL B-cell proliferation occurs.

9 Overall Discussion

CLL is a very prevalent form of hematologic malignancy primarily affecting an elderly patient population often suffering from relevant comorbidities. The disease remains incurable using standard chemoimmunotherapy as well as new treatment approaches suppressing the B-cell receptor pathway or anti-apoptotic pathways. As a result, there is an unmet need for truly curative and tolerable treatment approaches. The onset of CLL is associated with the development of a pronounced immunodeficiency of both humoral and cell mediated systems resulting in infections as a major source of morbidity and mortality in the setting of the disease. CLL associated immunodeficiency also contributes to evasion of CLL B-cells from mechanisms of cancer immunosurveillance (228, 298, 397-401). In addition, CLL cells have been shown to depend on their surrounding microenvironment to provide signals that promote B-cell survival and for protection from elimination by the host immune system (254-261, 402). Correction of immune evasion mechanisms could, according to the cancer immunoediting hypothesis, provide a viable treatment strategy (792). The high dependency on microenvironment interaction and marked associated T-cell dysfunction makes CLL an ideal candidate for cancer immunotherapy. Immunotherapeutic strategies are of particularly appeal in this setting as they may provide a tolerable and potentially even curative treatment approach. Overexpression of immune checkpoint molecules has been established as a major mechanism of cancer immune evasion in recent years. Our group has previously shown that PD-1/PD-L1 is pivotal in mediating CLL-associated T-cell dysfunction (216). Despite promising pre-clinical data (836) and successful application in other hematologic malignancies, attempts at establishing PD-1/PD-L1 immune checkpoint blockade as a treatment modality in CLL have been disappointing so far (108). BTK inhibitors such as Ibrutinib have been shown to have the ability to modulate T-cell function and myeloid cell and partially correct CLL associated immune defects (877-881). Recent pre-clinical data suggests a potential synergistic effect in combining BTK inhibition and immune checkpoint blockade (872). Based on the available literature and preliminary data of our group we hypothesized that the clinical efficacy of BTK-inhibitors is based on a synergism between direct anti-tumour effects and correction of CLL-associated functional T-cell defects. We speculated that the correction of CLL associated T-cell dysfunction using Ibrutinib is in part achieved by modulation of the expression of PD-1 or it's ligand PD-L1. We aimed to assess the effect of Ibrutinib and Acalabrutinib on T-cell function, expression of PD-1, PD-L1, PD-L2 and other important immune checkpoint molecules as well as the immunophenotype Combinations of PD-L1 immune checkpoint blockade and BTK inhibition may have synergistic effects in correcting CLL mediated T-

cell defects and may provide improved disease control. We thus sought to develop a combination strategy of such treatment strategies.

Today the Eμ-TCL1 mouse model is the most commonly used animal model of human CLL. Its hallmark characteristics are a high penetrance (901), and a faithful replication of phenotype and biology of human CLL including remodelling of the microenvironment ,CLL induced immune defects, the role of PD1/PD-L1 in mediating CLL associated T-cell defects and the effects of BTK inhibitor treatment. (903-905, 907, 908). Moreover, Eμ-TCL1 mice have been shown to be a suitable platform to study the effects of BTK-inhibitors such as Ibrutinib and Acalabrutinib in the setting of CLL (910, 911). The model is thus suitable to assess the effects of BTK-inhibition on T-cell function and as a platform to develop combination approaches of immune checkpoint blockade and BTK inhibition. We have previously established optimized and standardized adoptive transfer procedures that reliably replicate the CLL disease phenotype in previously disease-free syngeneic wildtype animals. Using a cell dose of 4×10^7 CLL B-cells injected intravenously via the tail vein we have achieved a latency of disease development of approximately 2 weeks. Fully developed leukaemia is observed at approximately 7 weeks after adoptive transfer. This leaves a suitable window to study the influence of new treatment approaches on the immune microenvironment. Animals 2.5 months of age were chosen to avoid ageing related changes of T-cell phenotype and function which could interfere with the outcome of the subsequent functional and phenotypic assessment.

Before the initiation of pre-clinical experiments assessing the effect of single agent BTK inhibitor treatment and combinations of BTK inhibitors and anti-PD-L1 immune checkpoint blockade we sought to confirm that oral administration of Ibrutinib and Acalabrutinib by water bottle would lead to sufficient BTK blockade in vivo. BTK occupancy experiments in C57BL/6 wildtype animal showed a BTK occupancy of 95.9% and 90% respectively for water bottle treatment with Ibrutinib and Acalabrutinib at a concentration of 0.15 mg/ml. The average occupancy measured was thus slightly higher for Acalabrutinib compared to Ibrutinib treatment. The available literature describes a higher first past metabolism and lower oral bioavailability for Ibrutinib compared to Acalabrutinib (959, 960). This may explain the slightly lower BTK occupancy observed for Ibrutinib treatment in these experiments. Still, as ≥90% of occupancy of available target is generally considered full occupancy of the receptor, we have confirmed adequate BTK blockade for oral administration of both substances by water bottle at the reported dose (958).

In an initial adoptive transfer experiment, animals were given vehicle treatment or either Ibrutinib or Acalabrutinib at a concentration of 0.15 mg/ml via water bottle. Both BTK inhibitors showed similar potential to control peripheral blood as well as spleen CLL load in these experiments. Subsequently we conduct further in vivo experiments to assess the effect of BTK inhibitor/anti-PD-L1 combinations on immunophenotype of the splenic microenvironment and T-cell function. Animals were treated with single agent Ibrutinib, Acalabrutinib or anti-PD-L1 immune checkpoint blockade as well as combinations of the BTK inhibitors and anti-PD-L1 antibodies. Similar to the initial experiment, both Ibrutinib and Acalabrutinib showed efficacy in controlling the peripheral blood and spleen CLL load. Single agent anti-PD-L1 antibody demonstrated no effects on spleen sizes and weights and only a modest effect on peripheral blood CLL B-cell load. These findings are contrasted by a previous study conducted by our group which showed a complete blockade of CLL development in the Eµ-TCL1 adoptive transfer model with anti-PD-L1 immune checkpoint blockade (836). In this study, however, anti-PD-L1 immune checkpoint blockade was applied from the day of adoptive transfer. It thus seems likely, that the complete prevention of CLL development in this study was due to disruption of CLL implantation following adoptive transfer rather than treatment of an established disease. As such, these results are difficult to apply to the situation in human CLL patients where disease is usually discovered in more advanced stages and treatment is only initiated in symptomatic patients. As a matter of fact, the modest effect in the current experiments, where treatment was initiated only after established disease could be detected, much more closely resemble the results from early clinical studies assessing the efficacy of single agent Pembrolizumab in CLL patients (108). Combinations of either Ibrutinib or Acalabrutinib and anti-PD-L1 immune checkpoint blockade have failed to show improved CLL clearance in the adoptive transfer experiments at hand. However, it should be noted the current study was powered to detect a difference of at least 10% in PD-1 expression of T-cells and not of clinical outcomes. A prolonged treatment period may help to unmask more nuaced differences in clinical course. Moreover, disease control with single agent Ibrutinib or Acalabrutinib was already quite far reaching with spleen weight and size approaching those of wild type animals in this experiment. A further clinically appreciable effect may thus be difficult to obtain with the treatment combinations. Generally, in this second set of animal experiments the initial increase of CLL load was slower and the overall disease control achieved in all treatment groups more pronounced compared to the initial set of animal experiments despite the same dose of CLL B-cell applied. This may be due to biological differences of CLL-B-cell clones in two separate pools of CLL B-cells applied across these experiments.

We have designed a 27-marker mass cytometry panel to analyse the expression of PD-1, PD-L1, PD-L2 and the immunophenotype of the splenic microenvironment of CLL bearing animals receiving various forms of treatment. The calculated signal overlap was well below the expected tolerance threshold for the markers included with the exception of NKp46 167Er where the maximum tolerance as reached. We have subsequently confirmed the suitability of our panel to identify changes in immunophenotype in the splenic microenvironment as well as changes in expression of immune checkpoint receptors and NK-cell receptors in the setting of CLL. In contrast to human beings, where only a fraction of CD4+CD25+ T-cells with the highest level of CD25 expression show suppressive function (973-975), in mice CD4+CD25+ T-cells are a homogenous population of cells with regulatory function and FOXP3 staining us thus not strictly necessary for identification of Tregs (976, 977). However, moderate suppressive function has been shown for some subsets of CD4+CD25- T-cells (978, 979). The panel at hand thus is limited in its ability to completely identify the mouse regulatory T-cell subsets. Nevertheless, we chose to use the panel in its present form as CD4+CD25+ is a good approximate for identification of the regulatory T-cell subset and a more complete identification would have made the use of intranuclear marker and thus permeabilization of the splenocyte samples necessary. We were reluctant to utilize permeabilization as this is known to disrupt surface staining and thus interfere with staining for immune checkpoint molecules which is major objective of this study. Another limitation of our panel is its inability to fully distinguish white pulp monocyte and macrophages in the splenic microenvironment. Neither strategies of subsequential Ly6C/G and F4/80 staining based on reports of a steric hindrance between these markers (980) nor attempts of additional CD115 or MHC type II staining were able to improve separation of monocyte and macrophage populations. In depth literature search revealed that the findings of our mass cytometry panel are in line with the natural heterogeneity of spleen myelomonocytic cells: CD11b-/F4/80++ red pulp macrophages, CD11b+ F4/80 intermediate monocytes, monocyte derived white pulp macrophages and marginal zone macrophages that cannot be separate based on staining with these markers, calling into question the findings of previous flow cytometry based studies that have claimed to accurately delineate these populations based on the staining of these markers (982, 983). As above, we were reluctant to apply permeabilization to allow for staining of intracellular markers such as CD68 as to not disrupt staining of surface markers. A validation of the mass cytometry panel at hand using flow cytometry in necessary and currently ongoing.

By applying our mass cytometry panel to splenocyte samples of vehicle, Ibrutinib or Acalabrutinib treated animals we have identified a differential effect on PD-L1 expression among various immune cell subsets in the splenic microenvironment. We detected a modest increase in PD-L1 expression among CLL B-cells with both Ibrutinib and Acalabrutinib treatment while its expression among myelomonocytic cells was decreased. The observed increase in PD-L1 expression following BTK inhibitor treatment among CLL B-cells was unexpected as some authors have suggested that PD-L1 expression in driven by B-cell receptor signalling in B-cell malignancies (984). A recent study has shown that PD-L1 high CLL B-cells express higher levels of adhesion molecules (985). We therefore speculate that these cells are more readily retained in the microenvironment while PD-L1 low CLL B-cells will be mobilized to the peripheral blood by BTK inhibitors. The decreased expression of PD-L1 on myelomonocytic cells following BTK inhibitor treatment is in line with studies suggesting a role of PD-L1 expression on infiltrating myeloid derived cells in mediating CLL associated immunosuppression (835). Myeloid cells may thus be the driving force in induction of CLL associated T-cell deficiency and the major target for BTK inhibitor mediated T-cell modulation, comparable to the situation in PDAC (881). Among T-cells we found an amelioration of the exhaustion phenotype, primarily among memory CD4+ T-cells and regulatory T-cells with a downregulation of expression PD-1, LAG-3 and KLRG-1. In addition, we have detected a modulation of the NK-cell phenotype with a downregulation of KLRG-1 expression. The expression of CD69, an early marker for activation of lymphocytes which is also known to be increased in the setting of T-cell exhaustion, was found to be decreased among CD4+ T-cells and NK-cells. The combination of decreased CD4+ T-cell exhaustion phenotype and decreased expression of inhibitory NK-cell receptors in the setting of a more permissive myeloid cell immune phenotype could potentially translate into improved immunosurveillance and elimination of CLL B-cells.

Several studies have addressed the question of modulation of T-cell function by BTK inhibitor Ibrutinib. Most prominently, Dubosvky et al. have suggested that Ibrutinib has the potential to shift T-helper cell polarity by targeting ITK, an enzyme that has a pivotal role in mediating downstream T-cell receptor signalling. When inhibited, it's function can be rescued by the redundant enzyme "resting lymphocyte kinase" (RLK) which is expressed in Th1 cells but not Th2 cells thus effectively resulting in a preferential inhibition of Th2 cells (877). As Acalabrutinib does not have inhibitory activity towards ITK it should affect T-cell function in the setting of CLL differentially (986). However, when analysing cytokine profile and function of T-cells derived from the spleens of the above animals treated with vehicle, Ibrutinib or Acalabrutinib we found very similar

alterations with both BTK inhibitors. Both substances increased the production of IL2 by overall CD3+ T-cell and CD3+CD8- helper cells and decreased IL4 production by overall CD3+ T-cells and CD3+CD8- helper cell to a similar extent. The only detectable difference was a reduction of IL4 production in CD3+CD8+ cytotoxic T-cells with Ibrutinib that could not be observed with Acalabrutinib treatment. Moreover, both substances were shown to reduce INFγ secretion by T-cell subsets in quite a similar fashion. A reduction of IFNγ by BTK inhibitor treatment may seem counterintuitive at first, as the substance is an important Th1 cytokine and mediator of cancer immunosurveillance. On the other hand, one should keep in mind that continuous T-cell stimulation has been described to lead to a secondary T-cell dysfunction via IFNγ driven overexpression of PD-L1 (adaptive immune resistance) (842). IFNγ is also known to increase survival and proliferation of CLL B-cells (417). As such, the observed reduction of IFNγ secretion is a step toward normalization of the immune microenvironment. We also noticed an increase in the ratio of CD107a+/CD107a- antigen experienced CD44+CD8+ T-cells with both Ibrutinib and Acalabrutinib treatment. Among less antigen experienced CD44- CD8 T-cells we have observed a similar trend. However, only the effect of Acalabrutinib treatment compared to vehicle treatment reached statistical significance in this cell subset. It should be noted that surface accumulation of CD107a is merely a surrogate marker for the cytolytic capacity of CD8+ T-cells. Still, it is known that surface CD107a accumulation directly correlates with the ability of cytotoxic T-cells to lyse target cells as measured in chromium release assays (987). CD107a accumulation is thus an adequate tool to assess T-cell cytolytic capacity. Lastly, we have quantified the ability of T-cell and B-cells isolated from the spleens of CLL bearing animals to form immune synapses by analysing the area of F-Actin polymerization at the contact zone via a well-established assay originally developed at our lab (216). We found an increased ability for T-cell synapse formation that was similar after both Ibrutinib and Acalabrutinib treatment. In summary, we find no evidence that direct modulation of T-cells via ITK/RLK is the leading mechanism in improved T-cell function in the splenic microenvironment of CLL bearing animals as effects are similar between Ibrutinib and Acalabrutinib, which is known not to have inhibitory capacity towards ITK (986). Rather, we speculate that an indirect mechanism, possibly via modulation BTK expressing myeloid cells in the CLL microenvironment may be underlying the improved T-cell function following BTK inhibitor treatment.

We have also applied our mass cytometry panel to splenocyte samples of animals treated with single agent BTK inhibitor or BTK inhibitor/anti-PD-L1 combinations in the setting of the second animal experiment. Unfortunately, anti-PD-L1 antibodies masked

staining for PD-L1. Expression of the marker could therefore not be assessed in these animals. Analysis of expression among B-cells derived from the single agent BTK-inhibitor treated and vehicle treated animals confirmed the increase in PD-L1 expression reported with both Ibrutinib and Acalabrutinib treatment reported above. Similar to the findings reported above, we found a downregulation of CD69 expression among T-cell and NK-cell subsets. This effect was similar in single agent BTK-inhibitor treated and combination treated animals. In contrast to the above experiment the alterations among T-cells were more centered around effector cell subsets. We have also observed a downregulation of PD-1 expression among T-cell subsets with both single agent BTK inhibitor and combination treatment. In contrast to the initial animal experiment these changes extended beyond memory CD4+ and regulatory T-cells and could also be found in memory CD8+ T-cells, naïve and effector CD4+ and CD8+ T-cells. Interestingly, we found that the expression levels of PD-1 were decreased in BTK inhibitor/anti-PD-L1 treated animals compared to vehicle and single agent anti-PD-L1 treated animals but slightly higher compared to single-agent BTK inhibitor treated animals. This potentially points to a counterregulatory mechanism of upregulation of PD-1 in the anti-PD-L1 treatment groups. Moreover, we observed a similar pattern among both inflammatory monocyte and patrolling monocyte/macrophage subsets and a modest decrease of expression among classical dendritic cells. High levels of PD-1 expression among myelomonocytic cells has been linked to inferior outcome in renal cell carcinoma (989) and colorectal carcinoma (991). High expression levels in myelomonocytic cells have also been found in the immunosuppressive phase of sepsis (990). In dendritic cells high levels of expression have been reported to impede innate immunity (992). In hepatocellular carcinoma PD-1 expression dendritic cells have been linked to suppression of CD8+ T-cell function and cancer immune evasion (993). We believe that similar to the above studies the downregulation of PD-1 among myeloid cell subsets in the splenic microenvironment of CLL bearing animals treated with BTK inhibitor and BTK inhibitor/anti-PD-L1 combinations may contribute to an improved immunosurveillance. In terms of KLRG-1 expression we find a downregulation with single agent BTK inhibitors and combination treatment centred around NK cells and regulatory T-cells. The changes were very similar in both single agent BTK inhibitor treated and combination treated animals. We found 2B4 expression to be decreased to a similar extent with both combinations of BTK inhibitors and anti-PD-L1 immune checkpoint blockade and single agent BTK inhibitor treatment in NK cells, granulocytes, inflammatory monocytes, patrolling monocytes/macrophages and classical dendritic cells. Highlighted features among subsets of effector and effector memory CD8+ T-cells appeared to be limited to a slightly higher expression among single agent anti-PD-L1 treated animals. As 2B4

expression among lymphocytes has been linked to their activation this may point to an increased CD8+ T-cell activation with single agent anti-PD-L1 treatment. Among NK-cells 2B4 expression has been reported to have both positive and negative functions with 2B4/CD48 interaction between neighbouring NK-cells being required for optimal activation while the interaction of 2B4 on NK cells with CD48 on target cells has been reported to inhibit cytolytic activity of NK cells (994). As high levels of CD48 expression have been described on CLL B-cells the observed downregulation in NK-cell subsets with BTK inhibitor containing treatments could thus also signal an improved NK-cell effector function with these treatments in the splenic microenvironment (995). 2B4 expression has not been reported on the surface of neutrophilic granulocytes, but its expression is a characteristic of granulocytic MDSCs. Its expression on granulocytic cells in the splenic microenvironment of CLL bearing animals and its downregulation with BTK inhibitor containing treatments could point to a reversal of the granulocytic MDSCs phenotype among these animals (996). In dendritic cells expression of 2B4 has been linked to suppression of their pro-inflammatory functions. Dendritic cells derived from the spleens of CD244 -/- animals produced higher levels of pro-inflammatory cytokines and when stimulated with lipopolysaccharide or CpG and DCs from CD244 -/- mice elicited higher NK cell activation in vitro. The downregulation found with BTK inhibitor containing treatment regimens in the splenic microenvironment could thus also contribute to improved immunosurveillance in these animals (997). Expression of 2B4 among monocytes has been described extensively. However, little is known about its function in this cell type (655). Decreased expression has been noted on monocytes derived from the peripheral blood of SLE patients thus suggesting a role in immune tolerance (998). We speculate that the observed downregulation in myelomonocytic cell subsets with BTK inhibitor-containing treatment regimens may signal an immunophenotype more permissive of adaptive immune responses. Surprisingly, we did not find alterations of expression of TIM-3 among T-cells with single agent BTK inhibitor or combination treatment. Expression was increased among inflammatory monocytes as well as among patrolling monocyte/macrophage subsets to a similar extent using Ibrutinib, Acalabrutinib or combinations of these BTK inhibitors with anti-PD-L1 immune checkpoint blockade. Among classical dendritic cells, expression was decreased using these regimens. The functional role of TIM-3 in myeloid cells is still poorly understood. In macrophages TIM-3 has been described to act as a receptor for PtdSer by phagocytic cells and thus facilitating the removal of cells which have undergone apoptosis and cross-presentation of antigens by phagocytic cells (619). Experiments with the monocyte cell line THP-1 as well as CD14+ cells from the peripheral blood of healthy donors have shown that monocyte/macrophages in a quiescent state express high levels of TIM-3 and show low

cytokine production while after activation in vitro with LPS or R848 results in reduced TIM-3 expression and increased IL12 production (1001). Antibody mediated blockade of TIM-3 resulted in increased production of IL12 but decreased expression of PD-1. Similarly, silencing of TIM-3 expression in THP-1 cells using si-RNA resulted in increased production of IL12 (1001, 1002). In murine models of hepatocellular carcinoma an increased expression on peripheral blood monocytes and TAMs correlating with disease progression has been noted (1003). As such, the increased expression in myelomonocytic cell subsets following BTK inhibitor containing treatments may signal either improved phagocytosis and cross-presenting capacity of these cells, a decreased activation of monocyte/macrophages or could even be detrimental to innate immunity directed against CLL. In tumour infiltrating dendritic cells, TIM-3 has been shown to inhibt nucleic-acid-mediated innate immune responses through interaction with the alarmin HMGB-1 (620). The downregulation observed in classical dendritic cells from the splenic microenvironment of CLL bearing animals following treatment with BTK inhibitor containing regimens may thus be a sign of a more innate immunity permissive phenotype. The varied functions of the molecule across these various myeloid cell subsets may also explain the differential effect on the expression profile observed. With regards to LAG-3 expression we found statistically significant downregulation of median marker expression with both single agent BTK inhibitor treatment and BTK inhibitor/anti-PD-L1 combinations on NK cells, effector memory CD4+ T-cells, effector memory CD8+ T-cells and a subset of effector CD8+ T-cells. In addition, we found a modest downregulation among subsets of effector CD4+ T-cells, and naïve CD4+ T-cells. In conclusion we have here demonstrated an amelioration of the exhaustion phenotype among CD4+ and CD8+ T-cells with both single agent BTK-inhibitor treatment and BTK inhibitor/anti-PD-L1 combinations. This is demonstrated downregulation of CD69, PD-1, LAG-3 and KLRG-1 expression. In addition, we found downregulation of inhibitory receptor 2B4, LAG-3 and KLRG-1 on the surface of NK cells. We also found evidence of a phenotype more permissive of myeloid cell effector function with downregulation of PD-1 and 2B4. We reported differential effects on expression of TIM-3 among myeloid cell subsets with upregulation among myelomonocytic cells and downregulation among classical dendritic cells. While the decreased expression among DCs is in line with reports suggested a suppressive effect on innate immune responses of TIM-3 in this context the increased expression among myelomonocytic cells is less clear with both positive and negative effects on innate immune response being described in the literature. Marker expression was very similar when directly comparing single agent BTK inhibitor treated and combination treated animals. The most pronounced difference was a slightly higher expression level of PD-1 among animals treated with BTK inhibitor/anti-

PD-L1 combinations compared to single agent BTK inhibitor, possibly signalling a compensatory mechanism in the splenic microenvironment of CLL bearing animals. Differences observed between this and the earlier animal experiment could potentially be explained with an improved overall disease control and lower levels of infiltrating CLL B-cells achieved in the experiment at hand.

Despite our earlier experiments suggesting a potential for correction of the T-cell exhaustion phenotype with anti-PD-L1 treatment (836) in the present experiments we neither find evidence of an improved T-cell phenotype with single-agent anti-PD-L1 treatment nor evidence of a synergistic effect of combined BTK-Inhibitor and anti-PD-L1 treatment. The current set of experiments and our earlier findings mainly differ in the time-point of anti-PD-L1 application. The treatment seemed to be effective at controlling the disease only when applied from the day of adoptive transfer while application in the setting of already established disease seemed to have little effect clinically and in terms of T-cell exhaustion phenotype. In clinical practice the often initially indolent disease is usually discovered at more advanced stages and an efficacious use of PD-L1 blockade in CLL may thus meet a difficult to surmount obstacles in clinical reality. This notion is also supported by earlier failed attempts to appy PD-1 blockade in CLL patients (108). Of note the anti-PD-L1 antibody applied in our earlier study (836) also had higher capability to directly stimulate ADCC against target cells while the antibody used in the current set of experiments was chosen to include the D265A alteration of the Fc region to more closely model the mode of action of clinically applied PD-L1 inhibitors. It thus seems possible that clinical success in the earlier study may have at least in part been due to a Rituximab-like direct FCγ-receptor mediated cytotoxicity against PD-L1 bearing CLL B-cells rather than due to modulation of CLL-induced T-cell exhaustion.

Functional assessment of T-cells derived from the spleens of animals treated with single agent Ibrutinib, Acalabrutinib, anti-PD-L1 or combinations of BTK inhibitor and anti-PD-L1 immune checkpoint blockade confirmed the correction of helper cell cytokine profile and cytotoxic T-cell degranulation observed with Ibrutinib and Acalabrutinib treatment reported above. Single agent anti-PD-L1 immune checkpoint blockade, however, had no statistically significant effect on helper cell IL4 and IL2 production but increased IL2 production among cytotoxic T-cells. There was a trend towards increased rather than decreased INFγ production with single agent anti PD-L1. The combination of Ibrutinib and anti PD-L1 resulted only in a very modest increase in T-cell function over single agent Ibrutinib treatment. IL2 production among T helper cells was increased futher above the levels observed with single agent Ibrutinib and anti-PD-L1 and on the same

level as single agent Acalabrutinib. A similar degree of IL4 suppression compared to single agent BTK inhibitor treatment was achieved. INFγ production was normalized to an extent similar to that observed with either BTK inhibitor. Cytotoxic T-cell degranulation among CD3+CD8+CD44+ was increased to the same extent as with single agent anti-PD-L1 treatment while there was no effect on degranulation of CD3+CD8+CD44-. To our surprise the combination of Acalabrutinib and anti-PD-L1 immune checkpoint blockade was detrimental in terms of both helper cell and cytotoxic T-cell function. The drug combination resulted in a similar degree of IL4 suppression among helper cells and IFNγ suppression among cytotoxic T-cells but was found to lead to dramatically decreased capacity of both T-cell subsets to produce IL2 and reduced degranulation upon stimulation among CD44+ and CD44- cytotoxic T-cells. This finding is in spite of a similar immune phenotype and immune checkpoint expression of T-cells in the microenvironment as discussed above. The mechanism of this phenomenon remains obscure. We speculate that an unforeseen interaction of intracellular signaling mechanisms may underly this process and propose further investigations into cell signaling in these samples. Complementary pathways could potentially be aberrantly activated or repressed by this combination. This also comes in light of a recent report on a pre-clinical study at the MD Anderson Cancer Centre using a combination of Acalabrutinib and anti-PD-1 immune checkpoint blockade in the Eµ-TCL1 mouse model. Here the occurrence of a CLL clone with a hyperproliferative phenotype among the animals treated with the combination was described. Similar to our own findings, unforeseen interactions of intracellular signaling events have been suggested to contribute to this deleterious effect (1005).

In conclusion we have found evidence of only very modestly improved T-cell function with Ibrutinib/anti-PD-L1 treatment over single agent Ibrutinib treatment. Moreover, no evidence of a further improvement of T-cell exhaustion phenotype with BTK inhibitor/anti-PD-L1 combinations over single agents BTK inhibitor treatment could be detected. A study assessing the impact on survival would be a necessary next step in order to investigate the influence of the combination on the clinical course of the disease. However, given the data presented here improved CLL disease control with combination treatment even over an extended time course seems unlikely. The results presented above would caution against the use of Acalabrutinib/anti-PD1 or anti-PD-L1 combinations in the clinical setting. Suppressive effects on T-cell function could potentially negatively affect treatment results and the findings of our colleagues at the MD Anderson Cancer Centre foster fears of causing or unmasking of hyperproliferative CLL phenotypes. Ongoing trials evaluating such combinations should be evaluated

carefully to ensure no such detrimental effect on T-cell function and CLL B-cell proliferation occurs. We are also planning to assess the reasons for the suprising increase rather than decrease in PD-L1 expression among CLL B-cells following BTK inhibitor treatment. A recent publication by Wierz et al. (985) has suggested that PD-L1 high CLL B-cells express higher levels of adhesion molecules. We therefore speculate that these cells are more readily retained in the microenvironment while PD-L1 low CLL B-cells will be mobilized to the peripheral blood by BT&K inhibitors. We are planning to analyse the levels of PD-L1 expression on peripheral blood B-cells from these animals in a next step – the respective PBMC samples have been cryopreserved. Analysis of dynamics of expression over time may be warranted in a further step.

10   References

1.   Howlader N, Noone A, Krapcho M, Miller D, Brest A, Yu M, et al. SEER Cancer Statistics Review, 1975-2016, National Cancer Institute. Bethesda, MD,   https://seer.cancer.gov/csr/1975_2016/ , based on November 2018 SEER data submission, posted to the SEER web site, April 2019.

2.   Sant M, Allemani C, Tereanu C, De Angelis R, Capocaccia R, Visser O, et al. Incidence of hematologic malignancies in Europe by morphologic subtype: results of the HAEMACARE project. Blood. 2010;116(19):3724-34.

3.   Siegel RL, Miller KD, Jemal A. Cancer statistics, 2019. CA Cancer J Clin. 2019;69(1):7-34.

4.   Chihara D, Ito H, Matsuda T, Shibata A, Katsumi A, Nakamura S, et al. Differences in incidence and trends of haematological malignancies in Japan and the United States. Br J Haematol. 2014;164(4):536-45.

5.   Yang C, Zhang X. Incidence survey of leukemia in China. Chin Med Sci J. 1991;6(2):65-70.

6.   Gale RP, Cozen W, Goodman MT, Wang FF, Bernstein L. Decreased chronic lymphocytic leukemia incidence in Asians in Los Angeles County. Leuk Res. 2000;24(8):665-9.

7.   Cartwright RA, Gurney KA, Moorman AV. Sex ratios and the risks of haematological malignancies. Br J Haematol. 2002;118(4):1071-7.

8.   Fitzmaurice C, Allen C, Barber RM, Barregard L, Bhutta ZA, Brenner H, et al. Global, Regional, and National Cancer Incidence, Mortality, Years of Life Lost, Years Lived With Disability, and Disability-Adjusted Life-years for 32 Cancer Groups, 1990 to 2015: A Systematic Analysis for the Global Burden of Disease Study. JAMA Oncol. 2017;3(4):524-48.

9.   Hodgson K, Ferrer G, Montserrat E, Moreno C. Chronic lymphocytic leukemia and autoimmunity: a systematic review. Haematologica. 2011;96(5):752-61.

10.   Hallek M, Cheson BD, Catovsky D, Caligaris-Cappio F, Dighiero G, Döhner H, et al. iwCLL guidelines for diagnosis, indications for treatment, response assessment, and supportive management of CLL. Blood. 2018;131(25):2745-60.

11.   Oscier D, Else M, Matutes E, Morilla R, Strefford JC, Catovsky D. The morphology of CLL revisited: the clinical significance of prolymphocytes and correlations with prognostic/molecular markers in the LRF CLL4 trial. Br J Haematol. 2016;174(5):767-75.

12.   Rawstron AC, Kreuzer KA, Soosapilla A, Spacek M, Stehlikova O, Gambell P, et al. Reproducible diagnosis of chronic lymphocytic leukemia by flow cytometry: An European Research Initiative on CLL (ERIC) & European Society for Clinical Cell Analysis (ESCCA) Harmonisation project. Cytometry B Clin Cytom. 2018;94(1):121-8.

13.   Marti GE, Rawstron AC, Ghia P, Hillmen P, Houlston RS, Kay N, et al. Diagnostic criteria for monoclonal B-cell lymphocytosis. Br J Haematol. 2005;130(3):325-32.

14.   Rawstron AC, Bennett FL, O'Connor SJM, Kwok M, Fenton JAL, Plummer M, et al. Monoclonal B-Cell Lymphocytosis and Chronic Lymphocytic Leukemia. New England Journal of Medicine. 2008;359(6):575-83.

15.   Strati P, Shanafelt TD. Monoclonal B-cell lymphocytosis and early-stage chronic lymphocytic leukemia: diagnosis, natural history, and risk stratification. Blood. 2015;126(4):454-62.

16.   Fazi C, Scarfo L, Pecciarini L, Cottini F, Dagklis A, Janus A, et al. General population low-count CLL-like MBL persists over time without clinical progression, although carrying the same cytogenetic abnormalities of CLL. Blood. 2011;118(25):6618-25.

17.   Binet JL, Auquier A, Dighiero G, Chastang C, Piguet H, Goasguen J, et al. A new prognostic classification of chronic lymphocytic leukemia derived from a multivariate survival analysis. Cancer. 1981;48(1):198-206.

18.   Rai KR, Sawitsky A, Cronkite EP, Chanana AD, Levy RN, Pasternack BS. Clinical staging of chronic lymphocytic leukemia. Blood. 1975;46(2):219-34.

19.   Damle RN, Wasil T, Fais F, Ghiotto F, Valetto A, Allen SL, et al. Ig V gene mutation status and CD38 expression as novel prognostic indicators in chronic lymphocytic leukemia. Blood. 1999;94(6):1840-7.

20.   Hamblin TJ, Davis Z, Gardiner A, Oscier DG, Stevenson FK. Unmutated Ig V(H) genes are associated with a more aggressive form of chronic lymphocytic leukemia. Blood. 1999;94(6):1848-54.

21.   Crespo M, Bosch F, Villamor N, Bellosillo B, Colomer D, Rozman M, et al. ZAP-70 expression as a surrogate for immunoglobulin-variable-region mutations in chronic lymphocytic leukemia. N Engl J Med. 2003;348(18):1764-75.

22.   Gentile M, Cutrona G, Neri A, Molica S, Ferrarini M, Morabito F. Predictive value of beta2-microglobulin (beta2-m) levels in chronic lymphocytic leukemia since Binet A stages. Haematologica. 2009;94(6):887-8.

23.   Wierda WG, O'Brien S, Wang X, Faderl S, Ferrajoli A, Do KA, et al. Prognostic nomogram and index for overall survival in previously untreated patients with chronic lymphocytic leukemia. Blood. 2007;109(11):4679-85.

24.   Dohner H, Stilgenbauer S, Benner A, Leupolt E, Krober A, Bullinger L, et al. Genomic aberrations and survival in chronic lymphocytic leukemia. N Engl J Med. 2000;343(26):1910-6.

25.   Schroeder HW, Dighiero G. The pathogenesis of chronic lymphocytic leukemia: analysis of the antibody repertoire. Immunol Today. 1994;15(6):288-94.

26.   Fais F, Ghiotto F, Hashimoto S, Sellars B, Valetto A, Allen SL, et al. Chronic lymphocytic leukemia B cells express restricted sets of mutated and unmutated antigen receptors. J Clin Invest. 1998;102(8):1515-25.

27.   Hashimoto S, Dono M, Wakai M, Allen SL, Lichtman SM, Schulman P, et al. Somatic diversification and selection of immunoglobulin heavy and light chain variable region genes in IgG+ CD5+ chronic lymphocytic leukemia B cells. J Exp Med. 1995;181(4):1507-17.

28.   Rossi D, Terzi-di-Bergamo L, De Paoli L, Cerri M, Ghilardi G, Chiarenza A, et al. Molecular prediction of durable remission after first-line fludarabine-cyclophosphamide-rituximab in chronic lymphocytic leukemia. Blood. 2015;126(16):1921-4.

29.   Fischer K, Bahlo J, Fink AM, Goede V, Herling CD, Cramer P, et al. Long-term remissions after FCR chemoimmunotherapy in previously untreated patients with CLL: updated results of the CLL8 trial. Blood. 2016;127(2):208-15.

30.   Thompson PA, Tam CS, O'Brien SM, Wierda WG, Stingo F, Plunkett W, et al. Fludarabine, cyclophosphamide, and rituximab treatment achieves long-term disease-free survival in IGHV-mutated chronic lymphocytic leukemia. Blood. 2016;127(3):303-9.

31.   Rassenti LZ, Huynh L, Toy TL, Chen L, Keating MJ, Gribben JG, et al. ZAP-70 compared with immunoglobulin heavy-chain gene mutation status as a predictor of disease progression in chronic lymphocytic leukemia. N Engl J Med. 2004;351(9):893-901.

32.   Ibrahim S, Keating M, Do KA, O'Brien S, Huh YO, Jilani I, et al. CD38 expression as an important prognostic factor in B-cell chronic lymphocytic leukemia. Blood. 2001;98(1):181-6.

33.   Ghia P, Guida G, Stella S, Gottardi D, Geuna M, Strola G, et al. The pattern of CD38 expression defines a distinct subset of chronic lymphocytic leukemia (CLL) patients at risk of disease progression. Blood. 2003;101(4):1262-9.

34.   Byrd JC, Gribben JG, Peterson BL, Grever MR, Lozanski G, Lucas DM, et al. Select high-risk genetic features predict earlier progression following chemoimmunotherapy with fludarabine and rituximab in chronic lymphocytic leukemia: justification for risk-adapted therapy. J Clin Oncol. 2006;24(3):437-43.

35.   Kröber A, Bloehdorn J, Hafner S, Bühler A, Seiler T, Kienle D, et al. Additional genetic high-risk features such as 11q deletion, 17p deletion, and V3-21 usage characterize discordance of ZAP-70 and VH mutation status in chronic lymphocytic leukemia. J Clin Oncol. 2006;24(6):969-75.

36.   Pflug N, Bahlo J, Shanafelt TD, Eichhorst BF, Bergmann MA, Elter T, et al. Development of a comprehensive prognostic index for patients with chronic lymphocytic leukemia. Blood. 2014;124(1):49-62.

37.   Reinisch W, Willheim M, Hilgarth M, Gasché C, Mader R, Szepfalusi S, et al. Soluble CD23 reliably reflects disease activity in B-cell chronic lymphocytic leukemia. J Clin Oncol. 1994;12(10):2146-52.

38.   Magnac C, Porcher R, Davi F, Nataf J, Payelle-Brogard B, Tang RP, et al. Predictive value of serum thymidine kinase level for Ig-V mutational status in B-CLL. Leukemia. 2003;17(1):133-7.

39.   Matthews C, Catherwood MA, Morris TC, Kettle PJ, Drake MB, Gilmore WS, et al. Serum TK levels in CLL identify Binet stage A patients within biologically defined prognostic subgroups most likely to undergo disease progression. Eur J Haematol. 2006;77(4):309-17.

40.   group IC-Iw. An international prognostic index for patients with chronic lymphocytic leukaemia (CLL-IPI): a meta-analysis of individual patient data. Lancet Oncol. 2016;17(6):779-90.

41.   Tam CS, Shanafelt TD, Wierda WG, Abruzzo LV, Van Dyke DL, O'Brien S, et al. De novo deletion 17p13.1 chronic lymphocytic leukemia shows significant clinical heterogeneity: the M. D. Anderson and Mayo Clinic experience. Blood. 2009;114(5):957-64.

42.   Isobe M, Emanuel BS, Givol D, Oren M, Croce CM. Localization of gene for human p53 tumour antigen to band 17p13. Nature. 1986;320(6057):84-5.

43.   Zenz T, Krober A, Scherer K, Habe S, Buhler A, Benner A, et al. Monoallelic TP53 inactivation is associated with poor prognosis in chronic lymphocytic leukemia: results from a detailed genetic characterization with long-term follow-up. Blood. 2008;112(8):3322-9.

44.   Dicker F, Herholz H, Schnittger S, Nakao A, Patten N, Wu L, et al. The detection of TP53 mutations in chronic lymphocytic leukemia independently predicts rapid disease progression and is highly correlated with a complex aberrant karyotype. Leukemia. 2008;23(1):117-24.

45.   Balatti V, Bottoni A, Palamarchuk A, Alder H, Rassenti LZ, Kipps TJ, et al. NOTCH1 mutations in CLL associated with trisomy 12. Blood. 2012;119(2):329-31.

46.   Stilgenbauer S, Liebisch P, James MR, Schroder M, Schlegelberger B, Fischer K, et al. Molecular cytogenetic delineation of a novel critical genomic region in chromosome bands 11q22.3-923.1 in lymphoproliferative disorders. Proc Natl Acad Sci U S A. 1996;93(21):11837-41.

47.   Calin GA, Dumitru CD, Shimizu M, Bichi R, Zupo S, Noch E, et al. Frequent deletions and down-regulation of micro- RNA genes miR15 and miR16 at 13q14 in chronic lymphocytic leukemia. Proceedings of the National Academy of Sciences. 2002;99(24):15524-9.

48.   Wang L, Lawrence MS, Wan Y, Stojanov P, Sougnez C, Stevenson K, et al. SF3B1 and Other Novel Cancer Genes in Chronic Lymphocytic Leukemia. New England Journal of Medicine. 2011;365(26):2497-506.

49.   Quesada V, Conde L, Villamor N, Ordonez GR, Jares P, Bassaganyas L, et al. Exome sequencing identifies recurrent mutations of the splicing factor SF3B1 gene in chronic lymphocytic leukemia. Nat Genet. 2012;44(1):47-52.

50.   Baliakas P, Hadzidimitriou A, Sutton LA, Rossi D, Minga E, Villamor N, et al. Recurrent mutations refine prognosis in chronic lymphocytic leukemia. Leukemia. 2014:doi: 10.1038/leu.2014.196.

51.   Dreger P, Schnaiter A, Zenz T, Bottcher S, Rossi M, Paschka P, et al. TP53, SF3B1, and NOTCH1 mutations and outcome of allotransplantation for chronic lymphocytic leukemia: six-year follow-up of the GCLLSG CLL3X trial. Blood. 2013;121(16):3284-8.
52.   Schnaiter A, Paschka P, Rossi M, Zenz T, Buhler A, Winkler D, et al. NOTCH1, SF3B1, and TP53 mutations in fludarabine-refractory CLL patients treated with alemtuzumab: results from the CLL2H trial of the GCLLSG. Blood. 2013;122(7):1266-70.
53.   Stilgenbauer S, Schnaiter A, Paschka P, Zenz T, Rossi M, Döhner K, et al. Gene mutations and treatment outcome in chronic lymphocytic leukemia: results from the CLL8 trial. Blood. 2014;123(21):3247-54.
54.   Rossi D, Gaidano G. Richter syndrome: pathogenesis and management. Semin Oncol. 2016;43(2):311-9.
55.   Fabbri G, Khiabanian H, Holmes AB, Wang J, Messina M, Mullighan CG, et al. Genetic lesions associated with chronic lymphocytic leukemia transformation to Richter syndrome. J Exp Med. 2013;210(11):2273-88.
56.   Rossi D, Rasi S, Spina V, Fangazio M, Monti S, Greco M, et al. Different impact of NOTCH1 and SF3B1 mutations on the risk of chronic lymphocytic leukemia transformation to Richter syndrome. Br J Haematol. 2012;158(3):426-9.
57.   Villamor N, Conde L, Martínez-Trillos A, Cazorla M, Navarro A, Beà S, et al. NOTCH1 mutations identify a genetic subgroup of chronic lymphocytic leukemia patients with high risk of transformation and poor outcome. Leukemia. 2013;27(5):1100-6.
58.   Rossi D, Spina V, Cerri M, Rasi S, Deambrogi C, De Paoli L, et al. Stereotyped B-cell receptor is an independent risk factor of chronic lymphocytic leukemia transformation to Richter syndrome. Clin Cancer Res. 2009;15(13):4415-22.
59.   Tsimberidou AM, O'Brien S, Khouri I, Giles FJ, Kantarjian HM, Champlin R, et al. Clinical outcomes and prognostic factors in patients with Richter's syndrome treated with chemotherapy or chemoimmunotherapy with or without stem-cell transplantation. J Clin Oncol. 2006;24(15):2343-51.
60.   Parikh SA, Kay NE, Shanafelt TD. How we treat Richter syndrome. Blood. 2014;123(11):1647-57.
61.   Dreger P, Ghia P, Schetelig J, van Gelder M, Kimby E, Michallet M, et al. High-risk chronic lymphocytic leukemia in the era of pathway inhibitors: integrating molecular and cellular therapies. Blood. 2018;132(9):892-902.
62.   Dighiero G, Maloum K, Desablens B, Cazin B, Navarro M, Leblay R, et al. Chlorambucil in indolent chronic lymphocytic leukemia. French Cooperative Group on Chronic Lymphocytic Leukemia. N Engl J Med. 1998;338(21):1506-14.
63.   Shustik C, Mick R, Silver R, Sawitsky A, Rai K, Shapiro L. Treatment of early chronic lymphocytic leukemia: intermittent chlorambucil versus observation. Hematol Oncol. 1988;6(1):7-12.
64.   Chemotherapeutic options in chronic lymphocytic leukemia: a meta-analysis of the randomized trials. CLL Trialists' Collaborative Group. J Natl Cancer Inst. 1999;91(10):861-8.
65.   Tam CS, O'Brien S, Wierda W, Kantarjian H, Wen S, Do K-A, et al. Long-term results of the fludarabine, cyclophosphamide, and rituximab regimen as initial therapy of chronic lymphocytic leukemia. Blood. 2008;112(4):975-80.
66.   Hallek M, Fischer K, Fingerle-Rowson G, Fink AM, Busch R, Mayer J, et al. Addition of rituximab to fludarabine and cyclophosphamide in patients with chronic lymphocytic leukaemia: a randomised, open-label, phase 3 trial. Lancet. 2010;376(9747):1164-74.
67.   Shanafelt TD, Wang V, Kay NE, Hanson CA, O'Brien SM, Barrientos JC, et al. A Randomized Phase III Study of Ibrutinib (PCI-32765)-Based Therapy Vs. Standard Fludarabine, Cyclophosphamide, and Rituximab (FCR) Chemoimmunotherapy in Untreated Younger Patients with Chronic Lymphocytic Leukemia (CLL): A Trial of the ECOG-ACRIN Cancer Research Group (E1912). Blood. 2018;132(Suppl 1):LBA-4-LBA-.
68.   Shanafelt T. Treatment of older patients with chronic lymphocytic leukemia: key questions and current answers. ASH Education Program Book. 2014;2013(1):158-67.
69.   Teeling JL, Mackus WJ, Wiegman LJ, van den Brakel JH, Beers SA, French RR, et al. The biological activity of human CD20 monoclonal antibodies is linked to unique epitopes on CD20. J Immunol. 2006;177(1):362-71.
70.   Wierda WG, Kipps TJ, Mayer J, Stilgenbauer S, Williams CD, Hellmann A, et al. Ofatumumab as single-agent CD20 immunotherapy in fludarabine-refractory chronic lymphocytic leukemia. J Clin Oncol. 2010;28(10):1749-55.
71.   Wierda WG, Kipps TJ, Durig J, Griskevicius L, Stilgenbauer S, Mayer J, et al. Chemoimmunotherapy with O-FC in previously untreated patients with chronic lymphocytic leukemia. Blood. 2011;117(24):6450-8.
72.   Wierda WG, Padmanabhan S, Chan GW, Gupta IV, Lisby S, Osterborg A, et al. Ofatumumab is active in patients with fludarabine-refractory CLL irrespective of prior rituximab: results from the phase 2 international study. Blood. 2011;118(19):5126-9.
73.   Herter S, Herting F, Mundigl O, Waldhauer I, Weinzierl T, Fauti T, et al. Preclinical Activity of the Type II CD20 Antibody GA101 (Obinutuzumab) Compared with Rituximab and Ofatumumab In Vitro and in Xenograft Models. Molecular Cancer Therapeutics. 2013;12(10):2031-42.

74.   de Romeuf C, Dutertre CA, Le Garff-Tavernier M, Fournier N, Gaucher C, Glacet A, et al. Chronic lymphocytic leukaemia cells are efficiently killed by an anti-CD20 monoclonal antibody selected for improved engagement of FcgammaRIIIA/CD16. Br J Haematol. 2008;140(6):635-43.

75.   Goede V, Fischer K, Busch R, Engelke A, Eichhorst B, Wendtner CM, et al. Obinutuzumab plus chlorambucil in patients with CLL and coexisting conditions. N Engl J Med. 2014;370(12):1101-10.

76.   Hillmen P, Robak T, Janssens A, Babu KG, Kloczko J, Grosicki S, et al. Chlorambucil plus ofatumumab versus chlorambucil alone in previously untreated patients with chronic lymphocytic leukaemia (COMPLEMENT 1): a randomised, multicentre, open-label phase 3 trial. Lancet. 2015;385(9980):1873-83.

77.   Fischer K, Cramer P, Busch R, Böttcher S, Bahlo J, Schubert J, et al. Bendamustine in Combination With Rituximab for Previously Untreated Patients With Chronic Lymphocytic Leukemia: A Multicenter Phase II Trial of the German Chronic Lymphocytic Leukemia Study Group. Journal of Clinical Oncology. 2012;30(26):3209-16.

78.   Brown JR, O'Brien S, Kingsley CD, Eradat H, Pagel JM, Lymp J, et al. Obinutuzumab plus fludarabine/cyclophosphamide or bendamustine in the initial therapy of CLL patients: the phase 1b GALTON trial. Blood. 2015;125(18):2779-85.

79.   Eichhorst B, Fink AM, Bahlo J, Busch R, Kovacs G, Maurer C, et al. First-line chemoimmunotherapy with bendamustine and rituximab versus fludarabine, cyclophosphamide, and rituximab in patients with advanced chronic lymphocytic leukaemia (CLL10): an international, open-label, randomised, phase 3, non-inferiority trial. Lancet Oncol. 2016;17(7):928-42.

80.   Michallet AS, Aktan M, Hiddemann W, Ilhan O, Johansson P, Laribi K, et al. Rituximab plus bendamustine or chlorambucil for chronic lymphocytic leukemia: primary analysis of the randomized, open-label MABLE study. Haematologica. 2018;103(4):698-706.

81.   Woyach JA, Ruppert AS, Heerema NA, Zhao W, Booth AM, Ding W, et al. Ibrutinib Regimens versus Chemoimmunotherapy in Older Patients with Untreated CLL. N Engl J Med. 2018;379(26):2517-28.

82.   Moreno C, Greil R, Demirkan F, Tedeschi A, Anz B, Larratt L, et al. Ibrutinib plus obinutuzumab versus chlorambucil plus obinutuzumab in first-line treatment of chronic lymphocytic leukaemia (iLLUMINATE): a multicentre, randomised, open-label, phase 3 trial. Lancet Oncol. 2019;20(1):43-56.

83.   Döhner H, Stilgenbauer S, Benner A, Leupolt E, Kröber A, Bullinger L, et al. Genomic Aberrations and Survival in Chronic Lymphocytic Leukemia. New England Journal of Medicine. 2000;343(26):1910-6.

84.   Zenz T, Eichhorst B, Busch R, Denzel T, Häbe S, Winkler D, et al. TP53 Mutation and Survival in Chronic Lymphocytic Leukemia. Journal of Clinical Oncology. 2010;28(29):4473-9.

85.   Fink AM, Bottcher S, Ritgen M, Fischer K, Pflug N, Eichhorst B, et al. Prediction of poor outcome in CLL patients following first-line treatment with fludarabine, cyclophosphamide and rituximab. Leukemia. 2013;27(9):1949-52.

86.   Pettitt AR, Sherrington PD, Cawley JC. The effect of p53 dysfunction on purine analogue cytotoxicity in chronic lymphocytic leukaemia. Br J Haematol. 1999;106(4):1049-51.

87.   Hillmen P, Skotnicki AB, Robak T, Jaksic B, Dmoszynska A, Wu J, et al. Alemtuzumab Compared With Chlorambucil As First-Line Therapy for Chronic Lymphocytic Leukemia. Journal of Clinical Oncology. 2007;25(35):5616-23.

88.   Zent CS, Call TG, Shanafelt TD, Tschumper RC, Jelinek DF, Bowen DA, et al. Early treatment of high-risk chronic lymphocytic leukemia with alemtuzumab and rituximab. Cancer. 2008;113(8):2110-8.

89.   Parikh SA, Keating MJ, O'Brien S, Wang X, Ferrajoli A, Faderl S, et al. Frontline chemoimmunotherapy with fludarabine, cyclophosphamide, alemtuzumab, and rituximab for high-risk chronic lymphocytic leukemia. Blood. 2011;118(8):2062-8.

90.   Pettitt AR, Jackson R, Carruthers S, Dodd J, Dodd S, Oates M, et al. Alemtuzumab in Combination With Methylprednisolone Is a Highly Effective Induction Regimen for Patients With Chronic Lymphocytic Leukemia and Deletion of TP53: Final Results of the National Cancer Research Institute CLL206 Trial. Journal of Clinical Oncology. 2012;30(14):1647-55.

91.   Farooqui MZ, Valdez J, Martyr S, Aue G, Saba N, Niemann CU, et al. Ibrutinib for previously untreated and relapsed or refractory chronic lymphocytic leukaemia with TP53 aberrations: a phase 2, single-arm trial. Lancet Oncol. 2015;16(2):169-76.

92.   O'Brien S, Jones JA, Coutre SE, Mato AR, Hillmen P, Tam C, et al. Ibrutinib for patients with relapsed or refractory chronic lymphocytic leukaemia with 17p deletion (RESONATE-17): a phase 2, open-label, multicentre study. The Lancet Oncology. 2016;17(10):1409-18.

93.   Zenz T, Gribben JG, Hallek M, Döhner H, Keating MJ, Stilgenbauer S. Risk categories and refractory CLL in the era of chemoimmunotherapy. Blood. 2012;119(18):4101-7.

94.   Byrd JC, Brown JR, O'Brien S, Barrientos JC, Kay NE, Reddy NM, et al. Ibrutinib versus Ofatumumab in Previously Treated Chronic Lymphoid Leukemia. New England Journal of Medicine. 2014;371(3):213-23.

95.   Chanan-Khan A, Cramer P, Demirkan F, Fraser G, Silva RS, Grosicki S, et al. Ibrutinib combined with bendamustine and rituximab compared with placebo, bendamustine, and rituximab for previously treated chronic lymphocytic leukaemia or small lymphocytic lymphoma (HELIOS): a randomised, double-blind, phase 3 study. Lancet Oncol. 2016;17(2):200-11.

96.   Seymour JF, Kipps TJ, Eichhorst B, Hillmen P, D'Rozario J, Assouline S, et al. Venetoclax-Rituximab in Relapsed or Refractory Chronic Lymphocytic Leukemia. N Engl J Med. 2018;378(12):1107-20.

97.   Stilgenbauer S, Eichhorst B, Schetelig J, Hillmen P, Seymour JF, Coutre S, et al. Venetoclax for Patients With Chronic Lymphocytic Leukemia With 17p Deletion: Results From the Full Population of a Phase II Pivotal Trial. J Clin Oncol. 2018;36(19):1973-80.
98.   Furman RR, Sharman JP, Coutre SE, Cheson BD, Pagel JM, Hillmen P, et al. Idelalisib and rituximab in relapsed chronic lymphocytic leukemia. N Engl J Med. 2014;370(11):997-1007.
99.   Jones JA, Robak T, Brown JR, Awan FT, Badoux X, Coutre S, et al. Efficacy and safety of idelalisib in combination with ofatumumab for previously treated chronic lymphocytic leukaemia: an open-label, randomised phase 3 trial. Lancet Haematol. 2017;4(3):e114-e26.
100.   Zelenetz AD, Barrientos JC, Brown JR, Coiffier B, Delgado J, Egyed M, et al. Idelalisib or placebo in combination with bendamustine and rituximab in patients with relapsed or refractory chronic lymphocytic leukaemia: interim results from a phase 3, randomised, double-blind, placebo-controlled trial. Lancet Oncol. 2017;18(3):297-311.
101.   Smith SM, Pitcher BN, Jung SH, Bartlett NL, Wagner-Johnston N, Park SI, et al. Safety and tolerability of idelalisib, lenalidomide, and rituximab in relapsed and refractory lymphoma: the Alliance for Clinical Trials in Oncology A051201 and A051202 phase 1 trials. Lancet Haematol. 2017;4(4):e176-e82.
102.   Lampson BL, Kasar SN, Matos TR, Morgan EA, Rassenti L, Davids MS, et al. Idelalisib given front-line for treatment of chronic lymphocytic leukemia causes frequent immune-mediated hepatotoxicity. Blood. 2016;128(2):195-203.
103.   Rossi D, Spina V, Deambrogi C, Rasi S, Laurenti L, Stamatopoulos K, et al. The genetics of Richter syndrome reveals disease heterogeneity and predicts survival after transformation. Blood. 2011;117(12):3391-401.
104.   Rossi D, Spina V, Gaidano G. Biology and treatment of Richter syndrome. Blood. 2018;131(25):2761-72.
105.   Cwynarski K, van Biezen A, de Wreede L, Stilgenbauer S, Bunjes D, Metzner B, et al. Autologous and allogeneic stem-cell transplantation for transformed chronic lymphocytic leukemia (Richter's syndrome): A retrospective analysis from the chronic lymphocytic leukemia subcommittee of the chronic leukemia working party and lymphoma working party of the European Group for Blood and Marrow Transplantation. J Clin Oncol. 2012;30(18):2211-7.
106.   Tsang M, Shanafelt TD, Call TG, Ding W, Chanan-Khan A, Leis JF, et al. The efficacy of ibrutinib in the treatment of Richter syndrome. Blood. 2015;125(10):1676-8.
107.   Hillmen P, Schuh A, Eyre TA, Pagel JM, Brown JR, Ghia P, et al. Acalabrutinib Monotherapy in Patients with Richter Transformation from the Phase 1/2 ACE-CL-001 Clinical Study. Blood. 2016;128(22):60-.
108.   Ding W, LaPlant BR, Call TG, Parikh SA, Leis JF, He R, et al. Pembrolizumab in patients with CLL and Richter transformation or with relapsed CLL. Blood. 2017;129(26):3419-27.
109.   Jain N, Basu S, Thompson PA, Ohanian M, Ferrajoli A, Pemmaraju N, et al. Nivolumab Combined with Ibrutinib for CLL and Richter Transformation: A Phase II Trial. Blood. 2016;128(22):59-.
110.   Parikh SA, Habermann TM, Chaffee KG, Call TG, Ding W, Leis JF, et al. Hodgkin transformation of chronic lymphocytic leukemia: Incidence, outcomes, and comparison to de novo Hodgkin lymphoma. Am J Hematol. 2015;90(4):334-8.
111.   Tsimberidou AM, O'Brien S, Kantarjian HM, Koller C, Hagemeister FB, Fayad L, et al. Hodgkin transformation of chronic lymphocytic leukemia: the M. D. Anderson Cancer Center experience. Cancer. 2006;107(6):1294-302.
112.   Bockorny B, Codreanu I, Dasanu CA. Hodgkin lymphoma as Richter transformation in chronic lymphocytic leukaemia: a retrospective analysis of world literature. Br J Haematol. 2012;156(1):50-66.
113.   Kolb H-J. Graft-versus-leukemia effects of transplantation and donor lymphocytes. Blood. 2008;112(12):4371-83.
114.   Dreger P, Döhner H, Ritgen M, Böttcher S, Busch R, Dietrich S, et al. Allogeneic stem cell transplantation provides durable disease control in poor-risk chronic lymphocytic leukemia: long-term clinical and MRD results of the German CLL Study Group CLL3X trial. Blood. 2010;116(14):2438-47.
115.   Krämer I, Stilgenbauer S, Dietrich S, Böttcher S, Zeis M, Stadler M, et al. Allogeneic hematopoietic cell transplantation for high-risk CLL: 10-year follow-up of the GCLLSG CLL3X trial. Blood. 2017;130(12):1477-80.
116.   Sorror ML, Storer BE, Sandmaier BM, Maris M, Shizuru J, Maziarz R, et al. Five-year follow-up of patients with advanced chronic lymphocytic leukemia treated with allogeneic hematopoietic cell transplantation after nonmyeloablative conditioning. J Clin Oncol. 2008;26(30):4912-20.
117.   Schwarzbich MA, McClanahan F, JG DS. Allogeneic Transplantation for Chronic Lymphocytic Leukemia in the Age of Novel Treatment Strategies. Oncology (Williston Park). 2016;30(6):526-33, 40.
118.   Chiorazzi N, Rai KR, Ferrarini M. Chronic lymphocytic leukemia. N Engl J Med. 2005;352(8):804-15.
119.   Woyach JA, Johnson AJ, Byrd JC. The B-cell receptor signaling pathway as a therapeutic target in CLL. Blood. 2012;120(6):1175-84.
120.   Hendriks RW, Yuvaraj S, Kil LP. Targeting Bruton's tyrosine kinase in B cell malignancies. Nature reviews Cancer. 2014;14(4):219-32.
121.   Seda V, Mraz M. B-cell receptor signalling and its crosstalk with other pathways in normal and malignant cells. European Journal of Haematology. 2015;94(3):193-205.

122.   Scharenberg AM, Humphries LA, Rawlings DJ. Calcium signalling and cell-fate choice in B cells. Nature reviews Immunology. 2007;7(10):778-89.

123.   Satterthwaite AB, Witte ON. The role of Bruton's tyrosine kinase in B-cell development and function: a genetic perspective. Immunological reviews. 2000;175:120-7.

124.   Dan HC, Cooper MJ, Cogswell PC, Duncan JA, Ting JP, Baldwin AS. Akt-dependent regulation of NF-{kappa}B is controlled by mTOR and Raptor in association with IKK. Genes Dev. 2008;22(11):1490-500.

125.   Mlinaric-Rascan I, Yamamoto T. B cell receptor signaling involves physical and functional association of FAK with Lyn and IgM. FEBS Lett. 2001;498(1):26-31.

126.   Messmer D, Fecteau JF, O'Hayre M, Bharati IS, Handel TM, Kipps TJ. Chronic lymphocytic leukemia cells receive RAF-dependent survival signals in response to CXCL12 that are sensitive to inhibition by sorafenib. Blood. 2011;117(3):882-9.

127.   de Gorter DJ, Beuling EA, Kersseboom R, Middendorp S, van Gils JM, Hendriks RW, et al. Bruton's tyrosine kinase and phospholipase Cgamma2 mediate chemokine-controlled B cell migration and homing. Immunity. 2007;26(1):93-104.

128.   Stevenson FK, Forconi F, Packham G. The Meaning and Relevance of B-Cell Receptor Structure and Function in Chronic Lymphocytic Leukemia. Seminars in Hematology. 2014;51(3):158-67.

129.   Zhong Y, Byrd JC, Dubovsky JA. The B-Cell Receptor Pathway: A Critical Component of Healthy and Malignant Immune Biology. Seminars in Hematology. 2014;51(3):206-18.

130.   Honigberg LA, Smith AM, Sirisawad M, Verner E, Loury D, Chang B, et al. The Bruton tyrosine kinase inhibitor PCI-32765 blocks B-cell activation and is efficacious in models of autoimmune disease and B-cell malignancy. Proc Natl Acad Sci U S A. 2010;107(29):13075-80.

131.   O'Brien S, Furman RR, Coutre SE, Sharman JP, Burger JA, Blum KA, et al. Ibrutinib as initial therapy for elderly patients with chronic lymphocytic leukaemia or small lymphocytic lymphoma: an open-label, multicentre, phase 1b/2 trial. Lancet Oncol. 2014;15(1):48-58.

132.   Byrd JC, Furman RR, Coutre SE, Burger JA, Blum KA, Coleman M, et al. Three-year follow-up of treatment-naïve and previously treated patients with CLL and SLL receiving single-agent ibrutinib. Blood. 2015;125(16):2497-506.

133.   Brown JR, Hillmen P, O'Brien S, Barrientos JC, Reddy N, Coutre S, et al. Updated Efficacy Including Genetic and Clinical Subgroup Analysis and Overall Safety in the Phase 3 RESONATE Trial of Ibrutinib Versus Ofatumumab in Previously Treated Chronic Lymphocytic Leukemia/Small Lymphocytic Lymphoma. Blood. 2014;124(21):3331-.

134.   Burger JA, Tedeschi A, Barr PM, Robak T, Owen C, Ghia P, et al. Ibrutinib as Initial Therapy for Patients with Chronic Lymphocytic Leukemia. New England Journal of Medicine. 2015;373(25):2425-37.

135.   Barr P, Robak T, Owen CJ, Tedeschi A, Bairey O, Bartlett NL, et al. Updated Efficacy and Safety from the Phase 3 Resonate-2 Study: Ibrutinib As First-Line Treatment Option in Patients 65 Years and Older with Chronic Lymphocytic Leukemia/Small Lymphocytic Leukemia. Blood. 2016;128(22):234-.

136.   Farooqui M, Valdez J, Soto S, Stetler-Stevenson M, Yuan CM, Thomas F, et al. Single Agent Ibrutinib in CLL/SLL Patients with and without Deletion 17p. Blood. 2015;126(23):2937-.

137.   Woyach JA, Smucker K, Smith LL, Lozanski A, Zhong Y, Ruppert AS, et al. Prolonged lymphocytosis during ibrutinib therapy is associated with distinct molecular characteristics and does not indicate a suboptimal response to therapy. Blood. 2014;123(12):1810-7.

138.   de Rooij MFM, Kuil A, Geest CR, Eldering E, Chang BY, Buggy JJ, et al. The clinically active BTK inhibitor PCI-32765 targets B-cell receptor– and chemokine-controlled adhesion and migration in chronic lymphocytic leukemia. Blood. 2012;119(11):2590-4.

139.   Ponader S, Chen S-S, Buggy JJ, Balakrishnan K, Gandhi V, Wierda WG, et al. The Bruton tyrosine kinase inhibitor PCI-32765 thwarts chronic lymphocytic leukemia cell survival and tissue homing in vitro and in vivo. Blood. 2012;119(5):1182-9.

140.   Herman SE, Mustafa RZ, Jones J, Wong DH, Farooqui M, Wiestner A. Treatment with Ibrutinib Inhibits BTK- and VLA-4-Dependent Adhesion of Chronic Lymphocytic Leukemia Cells In Vivo. Clinical cancer research : an official journal of the American Association for Cancer Research. 2015;21(20):4642-51.

141.   Chen SS, Chang BY, Chang S, Tong T, Ham S, Sherry B, et al. BTK inhibition results in impaired CXCR4 chemokine receptor surface expression, signaling and function in chronic lymphocytic leukemia. Leukemia. 2016;30(4):833-43.

142.   Herman SEM, Gordon AL, Hertlein E, Ramanunni A, Zhang X, Jaglowski S, et al. Bruton tyrosine kinase represents a promising therapeutic target for treatment of chronic lymphocytic leukemia and is effectively targeted by PCI-32765. Blood. 2011;117(23):6287-96.

143.   Wodarz D, Garg N, Komarova NL, Benjamini O, Keating MJ, Wierda WG, et al. Kinetics of CLL cells in tissues and blood during therapy with the BTK inhibitor ibrutinib. Blood. 2014;123(26):4132-5.

144.   Burger JA, Li KW, Keating MJ, Sivina M, Amer AM, Garg N, et al. Leukemia cell proliferation and death in chronic lymphocytic leukemia patients on therapy with the BTK inhibitor ibrutinib. JCI insight. 2017;2(2):e89904.

145.   Byrd JC, Furman RR, Coutre SE, Burger JA, Blum KA, Coleman M, et al. Three-year follow-up of treatment-naïve and previously treated patients with CLL and SLL receiving single-agent ibrutinib. Blood. 2015;125(16):2497-506.

146.   Burger JA, Tedeschi A, Barr PM, Robak T, Owen C, Ghia P, et al. Ibrutinib as Initial Therapy for Patients with Chronic Lymphocytic Leukemia. N Engl J Med. 2015;373(25):2425-37.

147.   Leong DP, Caron F, Hillis C, Duan A, Healey JS, Fraser G, et al. The risk of atrial fibrillation with ibrutinib use: a systematic review and meta-analysis. Blood. 2016.

148.   Barbosa CC, DeAngelis LM, Grommes C. Ibrutinib associated infections: A retrospective study. Journal of Clinical Oncology. 2017;35(15_suppl):e19020-e.

149.   Burger JA, Keating MJ, Wierda WG, Hartmann E, Hoellenriegel J, Rosin NY, et al. Safety and activity of ibrutinib plus rituximab for patients with high-risk chronic lymphocytic leukaemia: a single-arm, phase 2 study. The Lancet Oncology. 2014;15(10):1090-9.

150.   Byrd JC, Furman RR, Coutre SE, Flinn IW, Burger JA, Blum KA, et al. Targeting BTK with Ibrutinib in Relapsed Chronic Lymphocytic Leukemia. New England Journal of Medicine. 2013;369(1):32-42.

151.   O'Brien S, Furman RR, Coutre SE, Sharman JP, Burger JA, Blum KA, et al. Ibrutinib as initial therapy for elderly patients with chronic lymphocytic leukaemia or small lymphocytic lymphoma: an open-label, multicentre, phase 1b/2 trial. The Lancet Oncology. 2014;15.

152.   Brown JR, Barrientos JC, Barr PM, Flinn IW, Burger JA, Tran A, et al. The Bruton tyrosine kinase inhibitor ibrutinib with chemoimmunotherapy in patients with chronic lymphocytic leukemia. Blood. 2015;125(19):2915-22.

153.   Arthurs B, Wunderle K, Hsu M, Kim S. Invasive aspergillosis related to ibrutinib therapy for chronic lymphocytic leukemia. Respiratory medicine case reports. 2017;21:27-9.

154.   Okamoto K, Proia LA, Demarais PL. Disseminated Cryptococcal Disease in a Patient with Chronic Lymphocytic Leukemia on Ibrutinib. Case reports in infectious diseases. 2016;2016:4642831.

155.   Jaglowski SM, Jones JA, Nagar V, Flynn JM, Andritsos LA, Maddocks KJ, et al. Safety and activity of BTK inhibitor ibrutinib combined with ofatumumab in chronic lymphocytic leukemia: a phase 1b/2 study. Blood. 2015;126(7):842-50.

156.   Oda A, Ikeda Y, Ochs HD, Druker BJ, Ozaki K, Handa M, et al. Rapid tyrosine phosphorylation and activation of Bruton's tyrosine/Tec kinases in platelets induced by collagen binding or CD32 cross-linking. Blood. 2000;95(5):1663-70.

157.   Levade M, David E, Garcia C, Laurent PA, Cadot S, Michallet AS, et al. Ibrutinib treatment affects collagen and von Willebrand factor-dependent platelet functions. Blood. 2014;124(26):3991-5.

158.   Kamel S, Horton L, Ysebaert L, Levade M, Burbury K, Tan S, et al. Ibrutinib inhibits collagen-mediated but not ADP-mediated platelet aggregation. Leukemia. 2015;29(4):783-7.

159.   Byrd JC, Harrington B, O'Brien S, Jones JA, Schuh A, Devereux S, et al. Acalabrutinib (ACP-196) in Relapsed Chronic Lymphocytic Leukemia. N Engl J Med. 2016;374(4):323-32.

160.   Byrd JC, Wierda WG, Schuh A, Devereux S, Chaves JM, Brown JR, et al. Acalabrutinib Monotherapy in Patients with Relapsed/Refractory Chronic Lymphocytic Leukemia: Updated Results from the Phase 1/2 ACE-CL-001 Study. Blood. 2017;130(Suppl 1):498-.

161.   Walter HS, Rule SA, Dyer MJ, Karlin L, Jones C, Cazin B, et al. A phase 1 clinical trial of the selective BTK inhibitor ONO/GS-4059 in relapsed and refractory mature B-cell malignancies. Blood. 2016;127(4):411-9.

162.   Tam CS, Opat S, Cull G, Trotman J, Gottlieb D, Simpson D, et al. Twice Daily Dosing with the Highly Specific BTK Inhibitor, Bgb-3111, Achieves Complete and Continuous BTK Occupancy in Lymph Nodes, and Is Associated with Durable Responses in Patients (pts) with Chronic Lymphocytic Leukemia (CLL)/Small Lymphocytic Lymphoma (SLL). Blood. 2016;128(22):642-.

163.   Woyach JA, Furman RR, Liu TM, Ozer HG, Zapatka M, Ruppert AS, et al. Resistance mechanisms for the Bruton's tyrosine kinase inhibitor ibrutinib. N Engl J Med. 2014;370(24):2286-94.

164.   Binnerts ME, Otipoby KL, Hopkins BT, Bohnert T, Hansen S, Jamieson G, et al. Abstract C186: SNS-062 is a potent noncovalent BTK inhibitor with comparable activity against wild type BTK and BTK with an acquired resistance mutation. Molecular Cancer Therapeutics. 2015;14(12 Supplement 2):C186-C.

165.   Neuman LL, Ward R, Arnold D, Combs DL, Gruver D, Hill W, et al. First-in-Human Phase 1a Study of the Safety, Pharmacokinetics, and Pharmacodynamics of the Noncovalent Bruton Tyrosine Kinase (BTK) Inhibitor SNS-062 in Healthy Subjects. Blood. 2016;128(22):2032-.

166.   Woyach JA, Flinn IW, Stephens DM, Awan FT, Rogers KA, Reiff SD, et al. A Phase 1 Dose Escalation Study of ARQ 531 in Selected Patients with Relapsed or Refractory Hematologic Malignancies. Blood. 2018;132(Suppl 1):3136-.

167.   Hoellenriegel J, Meadows SA, Sivina M, Wierda WG, Kantarjian H, Keating MJ, et al. The phosphoinositide 3'-kinase delta inhibitor, CAL-101, inhibits B-cell receptor signaling and chemokine networks in chronic lymphocytic leukemia. Blood. 2011;118(13):3603-12.

168.   Herman SE, Lapalombella R, Gordon AL, Ramanunni A, Blum KA, Jones J, et al. The role of phosphatidylinositol 3-kinase-delta in the immunomodulatory effects of lenalidomide in chronic lymphocytic leukemia. Blood. 2011;117(16):4323-7.

169.   Brown JR, Byrd JC, Coutre SE, Benson DM, Flinn IW, Wagner-Johnston ND, et al. Idelalisib, an inhibitor of phosphatidylinositol 3-kinase p110delta, for relapsed/refractory chronic lymphocytic leukemia. Blood. 2014;123(22):3390-7.

170.   O'Brien SM, Lamanna N, Kipps TJ, Flinn I, Zelenetz AD, Burger JA, et al. A phase 2 study of idelalisib plus rituximab in treatment-naïve older patients with chronic lymphocytic leukemia. Blood. 2015;126(25):2686-94.

171.   Ali K, Soond DR, Pineiro R, Hagemann T, Pearce W, Lim EL, et al. Inactivation of PI(3)K p110δ breaks regulatory T-cell-mediated immune tolerance to cancer. Nature. 2014;510(7505):407-11.

172.   Flinn IW, Hillmen P, Montillo M, Nagy Z, Illés Á, Etienne G, et al. The phase 3 DUO trial: duvelisib vs ofatumumab in relapsed and refractory CLL/SLL. Blood. 2018;132(23):2446-55.
173.   Flinn IW, Cherry M, Maris M, Matous JV, Berdeja JG, Patel MR. Combination Trial of Duvelisib (IPI-145) with Bendamustine, Rituximab, or Bendamustine/Rituximab in Patients with Lymphoma or Chronic Lymphocytic Leukemia. Blood. 2015;126(23):3928-.
174.   Davids MS, Kim HT, Gilbert E, Cowen L, Francoeur K, Hellman J, et al. Preliminary Results of a Phase Ib Study of Duvelisib in Combination with FCR (dFCR) in Previously Untreated, Younger Patients with CLL. Blood. 2015;126(23):4158-.
175.   Burris HA, Flinn IW, Patel MR, Fenske TS, Deng C, Brander DM, et al. Umbralisib, a novel PI3Kδ and casein kinase-1ε inhibitor, in relapsed or refractory chronic lymphocytic leukaemia and lymphoma: an open-label, phase 1, dose-escalation, first-in-human study. Lancet Oncol. 2018;19(4):486-96.
176.   Kater AP, Tonino SH, Spiering M, Chamuleau MED, Liu R, Adewoye AH, et al. Final results of a phase 1b study of the safety and efficacy of the PI3Kδ inhibitor acalisib (GS-9820) in relapsed/refractory lymphoid malignancies. Blood Cancer J. 2018;8(2):16.
177.   Brown JR, Davids MS, Rodon J, Abrisqueta P, Kasar SN, Lager J, et al. Phase I Trial of the Pan-PI3K Inhibitor Pilaralisib (SAR245408/XL147) in Patients with Chronic Lymphocytic Leukemia (CLL) or Relapsed/Refractory Lymphoma. Clin Cancer Res. 2015;21(14):3160-9.
178.   Chen L, Chen G, Fecteau J-F, Coffey G, Prussak C, Carson DA, et al. Highly Specific Inhibitor for Syk Induces Chronic Lymphocytic Leukemia Cell Apoptosis. Blood. 2011;118(21):3875-.
179.   Friedberg JW, Sharman J, Sweetenham J, Johnston PB, Vose JM, Lacasce A, et al. Inhibition of Syk with fostamatinib disodium has significant clinical activity in non-Hodgkin lymphoma and chronic lymphocytic leukemia. Blood. 2010;115(13):2578-85.
180.   Currie KS, Kropf JE, Lee T, Blomgren P, Xu J, Zhao Z, et al. Discovery of GS-9973, a selective and orally efficacious inhibitor of spleen tyrosine kinase. J Med Chem. 2014;57(9):3856-73.
181.   Youle RJ, Strasser A. The BCL-2 protein family: opposing activities that mediate cell death. Nat Rev Mol Cell Biol. 2008;9(1):47-59.
182.   Del Gaizo Moore V, Brown JR, Certo M, Love TM, Novina CD, Letai A. Chronic lymphocytic leukemia requires BCL2 to sequester prodeath BIM, explaining sensitivity to BCL2 antagonist ABT-737. J Clin Invest. 2007;117(1):112-21.
183.   Kuwana T, Olson NH, Kiosses WB, Peters B, Newmeyer DD. Pro-apoptotic Bax molecules densely populate the edges of membrane pores. Sci Rep. 2016;6:27299.
184.   Faderl S, Keating MJ, Do KA, Liang SY, Kantarjian HM, O'Brien S, et al. Expression profile of 11 proteins and their prognostic significance in patients with chronic lymphocytic leukemia (CLL). Leukemia. 2002;16(6):1045-52.
185.   Roberts AW, Seymour JF, Brown JR, Wierda WG, Kipps TJ, Khaw SL, et al. Substantial Susceptibility of Chronic Lymphocytic Leukemia to BCL2 Inhibition: Results of a Phase I Study of Navitoclax in Patients With Relapsed or Refractory Disease. Journal of Clinical Oncology. 2012;30(5):488-96.
186.   Mason KD, Carpinelli MR, Fletcher JI, Collinge JE, Hilton AA, Ellis S, et al. Programmed anuclear cell death delimits platelet life span. Cell. 2007;128(6):1173-86.
187.   Roberts AW, Davids MS, Pagel JM, Kahl BS, Puvvada SD, Gerecitano JF, et al. Targeting BCL2 with Venetoclax in Relapsed Chronic Lymphocytic Leukemia. N Engl J Med. 2016;374(4):311-22.
188.   Ma S, Brander DM, Seymour JF, Kipps TJ, Barrientos JC, Davids MS, et al. Deep and Durable Responses Following Venetoclax (ABT-199 / GDC-0199) Combined with Rituximab in Patients with Relapsed/Refractory Chronic Lymphocytic Leukemia: Results from a Phase 1b Study. Blood. 2015;126(23):830-.
189.   Jones JA, Mato AR, Wierda WG, Davids MS, Choi M, Cheson BD, et al. Venetoclax for chronic lymphocytic leukaemia progressing after ibrutinib: an interim analysis of a multicentre, open-label, phase 2 trial. Lancet Oncol. 2018;19(1):65-75.
190.   Rosenwald A, Alizadeh AA, Widhopf G, Simon R, Davis RE, Yu X, et al. Relation of gene expression phenotype to immunoglobulin mutation genotype in B cell chronic lymphocytic leukemia. J Exp Med. 2001;194(11):1639-47.
191.   Fukuda T, Chen L, Endo T, Tang L, Lu D, Castro JE, et al. Antisera induced by infusions of autologous Ad-CD154-leukemia B cells identify ROR1 as an oncofetal antigen and receptor for Wnt5a. Proc Natl Acad Sci U S A. 2008;105(8):3047-52.
192.   Yu J, Chen L, Cui B, Wu C, Choi MY, Chen Y, et al. Cirmtuzumab inhibits Wnt5a-induced Rac1 activation in chronic lymphocytic leukemia treated with ibrutinib. Leukemia. 2017;31(6):1333-9.
193.   Choi MY, Widhopf GF, Ghia EM, Kidwell RL, Hasan MK, Yu J, et al. Phase I Trial: Cirmtuzumab Inhibits ROR1 Signaling and Stemness Signatures in Patients with Chronic Lymphocytic Leukemia. Cell Stem Cell. 2018;22(6):951-9.e3.
194.   Woyach JA, Awan F, Flinn IW, Berdeja JG, Wiley E, Mansoor S, et al. A phase 1 trial of the Fc-engineered CD19 antibody XmAb5574 (MOR00208) demonstrates safety and preliminary efficacy in relapsed CLL. Blood. 2014;124(24):3553-60.
195.   Byrd JC, Pagel JM, Awan FT, Forero A, Flinn IW, Deauna-Limayo DP, et al. A phase 1 study evaluating the safety and tolerability of otlertuzumab, an anti-CD37 mono-specific ADAPTIR therapeutic protein in chronic lymphocytic leukemia. Blood. 2014;123(9):1302-8.

196.   Robak T, Hellmann A, Kloczko J, Loscertales J, Lech-Maranda E, Pagel JM, et al. Randomized phase 2 study of otlertuzumab and bendamustine versus bendamustine in patients with relapsed chronic lymphocytic leukaemia. Br J Haematol. 2017;176(4):618-28.

197.   Lokhorst HM, Plesner T, Laubach JP, Nahi H, Gimsing P, Hansson M, et al. Targeting CD38 with Daratumumab Monotherapy in Multiple Myeloma. N Engl J Med. 2015;373(13):1207-19.

198.   Zhang S, Wu CCN, Fecteau J-F, Cui B, Chen L, Zhang L, et al. Targeting chronic lymphocytic leukemia cells with a humanized monoclonal antibody specific for CD44. Proceedings of the National Academy of Sciences. 2013;110(15):6127-32.

199.   Bannerji R, Brown JR, Advani RH, Arnason J, O'Brien SM, Allan JN, et al. Phase 1 Study of REGN1979, an Anti-CD20 x Anti-CD3 Bispecific Monoclonal Antibody, in Patients with CD20+ B-Cell Malignancies Previously Treated with CD20-Directed Antibody Therapy. Blood. 2016;128(22):621-.

200.   Morgan DO. Principles of CDK regulation. Nature. 1995;374(6518):131-4.

201.   Chen R, Keating MJ, Gandhi V, Plunkett W. Transcription inhibition by flavopiridol: mechanism of chronic lymphocytic leukemia cell death. Blood. 2005;106(7):2513-9.

202.   Byrd JC, Lin TS, Dalton JT, Wu D, Phelps MA, Fischer B, et al. Flavopiridol administered using a pharmacologically derived schedule is associated with marked clinical efficacy in refractory, genetically high-risk chronic lymphocytic leukemia. Blood. 2007;109(2):399-404.

203.   Lin TS, Ruppert AS, Johnson AJ, Fischer B, Heerema NA, Andritsos LA, et al. Phase II Study of Flavopiridol in Relapsed Chronic Lymphocytic Leukemia Demonstrating High Response Rates in Genetically High-Risk Disease. Journal of Clinical Oncology. 2009;27(35):6012-8.

204.   Blum KA, Ruppert AS, Woyach JA, Jones JA, Andritsos L, Flynn JM, et al. Risk factors for tumor lysis syndrome in patients with chronic lymphocytic leukemia treated with the cyclin-dependent kinase inhibitor, flavopiridol. Leukemia. 2011;25(9):1444-51.

205.   Stephens DM, Ruppert AS, Maddocks K, Andritsos L, Baiocchi R, Jones J, et al. Cyclophosphamide, alvocidib (flavopiridol), and rituximab, a novel feasible chemoimmunotherapy regimen for patients with high-risk chronic lymphocytic leukemia. Leuk Res. 2013;37(10):1195-9.

206.   Chen R, Chen Y, Frame S, Blake D, Wierda WG, Zheleva D, et al. Abstract 3905: Strategic combination of the cyclin-dependent kinase inhibitor CYC065 with venetoclax to target anti-apoptotic proteins in chronic lymphocytic leukemia. Cancer Research. 2018;78(13 Supplement):3905-.

207.   Paiva C, Godbersen JC, Soderquist RS, Rowland T, Kilmarx S, Spurgeon SE, et al. Cyclin-Dependent Kinase Inhibitor P1446A Induces Apoptosis in a JNK/p38 MAPK-Dependent Manner in Chronic Lymphocytic Leukemia B-Cells. PLoS One. 2015;10(11):e0143685.

208.   Calin GA, Liu CG, Sevignani C, Ferracin M, Felli N, Dumitru CD, et al. MicroRNA profiling reveals distinct signatures in B cell chronic lymphocytic leukemias. Proc Natl Acad Sci U S A. 2004;101(32):11755-60.

209.   Cui B, Chen L, Zhang S, Mraz M, Fecteau JF, Yu J, et al. MicroRNA-155 influences B-cell receptor signaling and associates with aggressive disease in chronic lymphocytic leukemia. Blood. 2014;124(4):546-54.

210.   Krönke J, Udeshi ND, Narla A, Grauman P, Hurst SN, McConkey M, et al. Lenalidomide Causes Selective Degradation of IKZF1 and IKZF3 in Multiple Myeloma Cells. Science. 2014;343(6168):301-5.

211.   Lu G, Middleton RE, Sun H, Naniong M, Ott CJ, Mitsiades CS, et al. The Myeloma Drug Lenalidomide Promotes the Cereblon-Dependent Destruction of Ikaros Proteins. Science. 2014;343(6168):305-9.

212.   Fecteau JF, Corral LG, Ghia EM, Gaidarova S, Futalan D, Bharati IS, et al. Lenalidomide inhibits the proliferation of CLL cells via a cereblon/p21(WAF1/Cip1)-dependent mechanism independent of functional p53. Blood. 2014;124(10):1637-44.

213.   Gandhi AK, Kang J, Havens CG, Conklin T, Ning Y, Wu L, et al. Immunomodulatory agents lenalidomide and pomalidomide co-stimulate T cells by inducing degradation of T cell repressors Ikaros and Aiolos via modulation of the E3 ubiquitin ligase complex CRL4(CRBN.). Br J Haematol. 2014;164(6):811-21.

214.   Henry JY, Labarthe MC, Meyer B, Dasgupta P, Dalgleish AG, Galustian C. Enhanced cross-priming of naive CD8+ T cells by dendritic cells treated by the IMiDs® immunomodulatory compounds lenalidomide and pomalidomide. Immunology. 2013;139(3):377-85.

215.   Ramsay AG, Johnson AJ, Lee AM, Gorgun G, Le Dieu R, Blum W, et al. Chronic lymphocytic leukemia T cells show impaired immunological synapse formation that can be reversed with an immunomodulating drug. J Clin Invest. 2008;118(7):2427-37.

216.   Ramsay AG, Clear AJ, Fatah R, Gribben JG. Multiple inhibitory ligands induce impaired T-cell immunologic synapse function in chronic lymphocytic leukemia that can be blocked with lenalidomide: establishing a reversible immune evasion mechanism in human cancer. Blood. 2012;120(7):1412-21.

217.   Ramsay AG, Evans R, Kiaii S, Svensson L, Hogg N, Gribben JG. Chronic lymphocytic leukemia cells induce defective LFA-1-directed T-cell motility by altering Rho GTPase signaling that is reversible with lenalidomide. Blood. 2013;121(14):2704-14.

218.   Chanan-Khan A, Miller KC, Musial L, Lawrence D, Padmanabhan S, Takeshita K, et al. Clinical efficacy of lenalidomide in patients with relapsed or refractory chronic lymphocytic leukemia: results of a phase II study. J Clin Oncol. 2006;24(34):5343-9.

219.   Ferrajoli A, Lee BN, Schlette EJ, O'Brien SM, Gao H, Wen S, et al. Lenalidomide induces complete and partial remissions in patients with relapsed and refractory chronic lymphocytic leukemia. Blood. 2008;111(11):5291-7.
220.   Chen CI, Bergsagel PL, Paul H, Xu W, Lau A, Dave N, et al. Single-agent lenalidomide in the treatment of previously untreated chronic lymphocytic leukemia. Journal of clinical oncology : official journal of the American Society of Clinical Oncology. 2011;29(9):1175-81.
221.   Badoux XC, Keating MJ, Wen S, Lee BN, Sivina M, Reuben J, et al. Lenalidomide as initial therapy of elderly patients with chronic lymphocytic leukemia. Blood. 2011;118(13):3489-98.
222.   Wendtner CM, Hillmen P, Mahadevan D, Buhler A, Uharek L, Coutre S, et al. Final results of a multicenter phase 1 study of lenalidomide in patients with relapsed or refractory chronic lymphocytic leukemia. Leuk Lymphoma. 2012;53(3):417-23.
223.   Badoux XC, Keating MJ, Wen S, Wierda WG, O'Brien SM, Faderl S, et al. Phase II study of lenalidomide and rituximab as salvage therapy for patients with relapsed or refractory chronic lymphocytic leukemia. J Clin Oncol. 2013;31(5):584-91.
224.   Strati P, Keating MJ, Wierda WG, Badoux XC, Calin S, Reuben JM, et al. Lenalidomide induces long-lasting responses in elderly patients with chronic lymphocytic leukemia. Blood. 2013;122(5):734-7.
225.   James DF, Werner L, Brown JR, Wierda WG, Barrientos JC, Castro JE, et al. Lenalidomide and rituximab for the initial treatment of patients with chronic lymphocytic leukemia: a multicenter clinical-translational study from the chronic lymphocytic leukemia research consortium. J Clin Oncol. 2014;32(19):2067-73.
226.   Andritsos LA, Johnson AJ, Lozanski G, Blum W, Kefauver C, Awan F, et al. Higher doses of lenalidomide are associated with unacceptable toxicity including life-threatening tumor flare in patients with chronic lymphocytic leukemia. J Clin Oncol. 2008;26(15):2519-25.
227.   Moreira J, Rabe KG, Cerhan JR, Kay NE, Wilson JW, Call TG, et al. Infectious complications among individuals with clinical monoclonal B-cell lymphocytosis (MBL): a cohort study of newly diagnosed cases compared to controls. Leukemia. 2013;27(1):136-41.
228.   Nosari A. Infectious complications in chronic lymphocytic leukemia. Mediterranean journal of hematology and infectious diseases. 2012;4(1):e2012070.
229.   Molica S, Levato D, Levato L. Infections in chronic lymphocytic leukemia. Analysis of incidence as a function of length of follow-up. Haematologica. 1993;78(6):374-7.
230.   Itala M, Helenius H, Nikoskelainen J, Remes K. Infections and serum IgG levels in patients with chronic lymphocytic leukemia. Eur J Haematol. 1992;48(5):266-70.
231.   Francis S, Karanth M, Pratt G, Starczynski J, Hooper L, Fegan C, et al. The effect of immunoglobulin VH gene mutation status and other prognostic factors on the incidence of major infections in patients with chronic lymphocytic leukemia. Cancer. 2006;107(5):1023-33.
232.   Hensel M, Kornacker M, Yammeni S, Egerer G, Ho AD. Disease activity and pretreatment, rather than hypogammaglobulinaemia, are major risk factors for infectious complications in patients with chronic lymphocytic leukaemia. Br J Haematol. 2003;122(4):600-6.
233.   Molteni A, Nosari A, Montillo M, Cafro A, Klersy C, Morra E. Multiple lines of chemotherapy are the main risk factor for severe infections in patients with chronic lymphocytic leukemia with febrile episodes. Haematologica. 2005;90(8):1145-7.
234.   Zent CS, Kay NE. Autoimmune complications in chronic lymphocytic leukaemia (CLL). Best Pract Res Clin Haematol. 2010;23(1):47-59.
235.   Schlesinger M, Broman I, Lugassy G. The complement system is defective in chronic lymphatic leukemia patients and in their healthy relatives. Leukemia. 1996;10(9):1509-13.
236.   Füst G, Miszlay Z, Czink E, Varga L, Pálóczi K, Szegedi G, et al. C1 and C4 abnormalities in chronic lymphocytic leukaemia and their significance. Immunol Lett. 1987;14(3):255-9.
237.   Miszlai Z, Czink E, Varga L, Pálóczi K, Szegedi G, Füst G, et al. Repressed classical complement pathway activities and clinical correlations in chronic lymphocytic leukaemia. Acta Med Hung. 1986;43(4):389-95.
238.   Varga L, Czink E, Miszlai Z, Paloczi K, Banyai A, Szegedi G, et al. Low activity of the classical complement pathway predicts short survival of patients with chronic lymphocytic leukaemia. Clin Exp Immunol. 1995;99(1):112-6.
239.   Michelis R, Tadmor T, Barhoum M, Shehadeh M, Shvidel L, Aviv A, et al. A C5a-Immunoglobulin complex in chronic lymphocytic leukemia patients is associated with decreased complement activity. PLoS One. 2019;14(1):e0209024.
240.   Kontoyiannis DP, Georgiadou SP, Wierda WG, Wright S, Albert ND, Ferrajoli A, et al. Impaired bactericidal but not fungicidal activity of polymorphonuclear neutrophils in patients with chronic lymphocytic leukemia. Leuk Lymphoma. 2013;54(8):1730-3.
241.   Itala M, Vainio O, Remes K. Functional abnormalities in granulocytes predict susceptibility to bacterial infections in chronic lymphocytic leukaemia. Eur J Haematol. 1996;57(1):46-53.
242.   Zeya HI, Keku E, Richards F, Spurr CL. Monocyte and granulocyte defect in chronic lymphocytic leukemia. Am J Pathol. 1979;95(1):43-54.
243.   Podaza E, Risnik D, Colado A, Elías E, Almejún MB, Fernandez Grecco H, et al. Chronic lymphocytic leukemia cells increase neutrophils survival and promote their differentiation into CD16. Int J Cancer. 2019;144(5):1128-34.

244.   Gätjen M, Brand F, Grau M, Gerlach K, Kettritz R, Westermann J, et al. Splenic Marginal Zone Granulocytes Acquire an Accentuated Neutrophil B-Cell Helper Phenotype in Chronic Lymphocytic Leukemia. Cancer Res. 2016;76(18):5253-65.

245.   Herishanu Y, Kay S, Sarid N, Kohan P, Braunstein R, Rotman R, et al. Absolute monocyte count trichotomizes chronic lymphocytic leukemia into high risk patients with immune dysregulation, disease progression and poor survival. Leuk Res. 2013;37(10):1222-8.

246.   Friedman DR, Sibley AB, Owzar K, Chaffee KG, Slager S, Kay NE, et al. Relationship of blood monocytes with chronic lymphocytic leukemia aggressiveness and outcomes: a multi-institutional study. Am J Hematol. 2016;91(7):687-91.

247.   Maffei R, Bulgarelli J, Fiorcari S, Bertoncelli L, Martinelli S, Guarnotta C, et al. The monocytic population in chronic lymphocytic leukemia shows altered composition and deregulation of genes involved in phagocytosis and inflammation. Haematologica. 2013;98(7):1115-23.

248.   Gustafson MP, Abraham RS, Lin Y, Wu W, Gastineau DA, Zent CS, et al. Association of an increased frequency of CD14+ HLA-DR lo/neg monocytes with decreased time to progression in chronic lymphocytic leukaemia (CLL). Br J Haematol. 2012;156(5):674-6.

249.   Lapuc I, Bolkun L, Eljaszewicz A, Rusak M, Luksza E, Singh P, et al. Circulating classical CD14++CD16- monocytes predict shorter time to initial treatment in chronic lymphocytic leukemia patients: Differential effects of immune chemotherapy on monocyte-related membrane and soluble forms of CD163. Oncol Rep. 2015;34(3):1269-78.

250.   Jurado-Camino T, Córdoba R, Esteban-Burgos L, Hernández-Jiménez E, Toledano V, Hernandez-Rivas JA, et al. Chronic lymphocytic leukemia: a paradigm of innate immune cross-tolerance. J Immunol. 2015;194(2):719-27.

251.   Jitschin R, Braun M, Buettner M, Dettmer-Wilde K, Bricks J, Berger J, et al. CLL-cells induce IDOhi CD14+HLA-DRlo myeloid-derived suppressor cells that inhibit T-cell responses and promote TRegs. Blood. 2014;124(5):750-60.

252.   Bruns H, Böttcher M, Qorraj M, Fabri M, Jitschin S, Dindorf J, et al. CLL-cell-mediated MDSC induction by exosomal miR-155 transfer is disrupted by vitamin D. Leukemia. 2017;31(4):985-8.

253.   Haderk F, Schulz R, Iskar M, Cid LL, Worst T, Willmund KV, et al. Tumor-derived exosomes modulate PD-L1 expression in monocytes. Sci Immunol. 2017;2(13).

254.   Burger JA, Tsukada N, Burger M, Zvaifler NJ, Dell'Aquila M, Kipps TJ. Blood-derived nurse-like cells protect chronic lymphocytic leukemia B cells from spontaneous apoptosis through stromal cell-derived factor-1. Blood. 2000;96(8):2655-63.

255.   Bürkle A, Niedermeier M, Schmitt-Gräff A, Wierda WG, Keating MJ, Burger JA. Overexpression of the CXCR5 chemokine receptor, and its ligand, CXCL13 in B-cell chronic lymphocytic leukemia. Blood. 2007;110(9):3316-25.

256.   Boissard F, Tosolini M, Ligat L, Quillet-Mary A, Lopez F, Fournié JJ, et al. Nurse-like cells promote CLL survival through LFA-3/CD2 interactions. Oncotarget. 2017;8(32):52225-36.

257.   Deaglio S, Vaisitti T, Bergui L, Bonello L, Horenstein AL, Tamagnone L, et al. CD38 and CD100 lead a network of surface receptors relaying positive signals for B-CLL growth and survival. Blood. 2005;105(8):3042-50.

258.   Nishio M, Endo T, Tsukada N, Ohata J, Kitada S, Reed JC, et al. Nurselike cells express BAFF and APRIL, which can promote survival of chronic lymphocytic leukemia cells via a paracrine pathway distinct from that of SDF-1alpha. Blood. 2005;106(3):1012-20.

259.   Burger JA, Quiroga MP, Hartmann E, Bürkle A, Wierda WG, Keating MJ, et al. High-level expression of the T-cell chemokines CCL3 and CCL4 by chronic lymphocytic leukemia B cells in nurselike cell cocultures and after BCR stimulation. Blood. 2009;113(13):3050-8.

260.   Burgess M, Cheung C, Chambers L, Ravindranath K, Minhas G, Knop L, et al. CCL2 and CXCL2 enhance survival of primary chronic lymphocytic leukemia cells in vitro. Leuk Lymphoma. 2012;53(10):1988-98.

261.   van Attekum MHA, Terpstra S, Slinger E, von Lindern M, Moerland PD, Jongejan A, et al. Macrophages confer survival signals via CCR1-dependent translational MCL-1 induction in chronic lymphocytic leukemia. Oncogene. 2017;36(26):3651-60.

262.   Galletti G, Scielzo C, Barbaglio F, Rodriguez TV, Riba M, Lazarevic D, et al. Targeting Macrophages Sensitizes Chronic Lymphocytic Leukemia to Apoptosis and Inhibits Disease Progression. Cell Rep. 2016;14(7):1748-60.

263.   Filip AA, Cisel B, Wąsik-Szczepanek E. Guilty bystanders: nurse-like cells as a model of microenvironmental support for leukemic lymphocytes. Clin Exp Med. 2015;15(1):73-83.

264.   Ysebaert L, Fournié JJ. Genomic and phenotypic characterization of nurse-like cells that promote drug resistance in chronic lymphocytic leukemia. Leuk Lymphoma. 2011;52(7):1404-6.

265.   Boissard F, Fournié JJ, Laurent C, Poupot M, Ysebaert L. Nurse like cells: chronic lymphocytic leukemia associated macrophages. Leuk Lymphoma. 2015;56(5):1570-2.

266.   Tsukada N, Burger JA, Zvaifler NJ, Kipps TJ. Distinctive features of "nurselike" cells that differentiate in the context of chronic lymphocytic leukemia. Blood. 2002;99(3):1030-7.

267.   Filip AA, Cisel B, Koczkodaj D, Wasik-Szczepanek E, Piersiak T, Dmoszynska A. Circulating microenvironment of CLL: are nurse-like cells related to tumor-associated macrophages? Blood Cells Mol Dis. 2013;50(4):263-70.

268.   Giannoni P, Pietra G, Travaini G, Quarto R, Shyti G, Benelli R, et al. Chronic lymphocytic leukemia nurse-like cells express hepatocyte growth factor receptor (c-MET) and indoleamine 2,3-dioxygenase and display features of immunosuppressive type 2 skewed macrophages. Haematologica. 2014;99(6):1078-87.
269.   Reinart N, Nguyen P-H, Boucas J, Rosen N, Kvasnicka H-M, Heukamp L, et al. Delayed development of chronic lymphocytic leukemia in the absence of macrophage migration inhibitory factor. Blood. 2013;121(5):812-21.
270.   Polk A, Lu Y, Wang T, Seymour E, Bailey NG, Singer JW, et al. Colony-Stimulating Factor-1 Receptor Is Required for Nurse-like Cell Survival in Chronic Lymphocytic Leukemia. Clin Cancer Res. 2016;22(24):6118-28.
271.   Audrito V, Serra S, Brusa D, Mazzola F, Arruga F, Vaisitti T, et al. Extracellular nicotinamide phosphoribosyltransferase (NAMPT) promotes M2 macrophage polarization in chronic lymphocytic leukemia. Blood. 2014;ePub ahead of print.
272.   Banchereau J, Steinman RM. Dendritic cells and the control of immunity. Nature. 1998;392(6673):245-52.
273.   Orsini E, Guarini A, Chiaretti S, Mauro FR, Foa R. The circulating dendritic cell compartment in patients with chronic lymphocytic leukemia is severely defective and unable to stimulate an effective T-cell response. Cancer Res. 2003;63(15):4497-506.
274.   Orsini E, Pasquale A, Maggio R, Calabrese E, Mauro FR, Giammartini E, et al. Phenotypic and functional characterization of monocyte-derived dendritic cells in chronic lymphocytic leukaemia patients: influence of neoplastic CD19 cells in vivo and in vitro. Br J Haematol. 2004;125(6):720-8.
275.   Rezvany MR, Jeddi-Tehrani M, Biberfeld P, Söderlund J, Mellstedt H, Osterborg A, et al. Dendritic cells in patients with non-progressive B-chronic lymphocytic leukaemia have a normal functional capability but abnormal cytokine pattern. Br J Haematol. 2001;115(2):263-71.
276.   Vuillier F, Maloum K, Thomas EK, Jouanne C, Dighiero G, Scott-Algara D. Functional monocyte-derived dendritic cells can be generated in chronic lymphocytic leukaemia. Br J Haematol. 2001;115(4):831-44.
277.   Saulep-Easton D, Vincent FB, Le Page M, Wei A, Ting SB, Croce CM, et al. Cytokine-driven loss of plasmacytoid dendritic cell function in chronic lymphocytic leukemia. Leukemia. 2014;28(10):2005-15.
278.   Ziegler HW, Kay NE, Zarling JM. Deficiency of natural killer cell activity in patients with chronic lymphocytic leukemia. International journal of cancer Journal international du cancer. 1981;27(3):321-7.
279.   Kay NE, Zarling JM. Impaired natural killer activity in patients with chronic lymphocytic leukemia is associated with a deficiency of azurophilic cytoplasmic granules in putative NK cells. Blood. 1984;63(2):305-9.
280.   Kay NE, Zarling J. Restoration of impaired natural killer cell activity of B-chronic lymphocytic leukemia patients by recombinant interleukin-2. Am J Hematol. 1987;24(2):161-7.
281.   MacFarlane AW, Jillab M, Smith MR, Alpaugh RK, Cole ME, Litwin S, et al. NK cell dysfunction in chronic lymphocytic leukemia is associated with loss of the mature cells expressing inhibitory killer cell Ig-like receptors. Oncoimmunology. 2017;6(7):e1330235.
282.   Huergo-Zapico L, Acebes-Huerta A, Gonzalez-Rodriguez AP, Contesti J, Gonzalez-García E, Payer AR, et al. Expansion of NK cells and reduction of NKG2D expression in chronic lymphocytic leukemia. Correlation with progressive disease. PLoS One. 2014;9(10):e108326.
283.   Hadadi L, Hafezi M, Amirzargar AA, Sharifian RA, Abediankenari S, Asgarian-Omran H. Dysregulated Expression of Tim-3 and NKp30 Receptors on NK Cells of Patients with Chronic Lymphocytic Leukemia. Oncol Res Treat. 2019;42(4):202-8.
284.   Parry HM, Stevens T, Oldreive C, Zadran B, McSkeane T, Rudzki Z, et al. NK cell function is markedly impaired in patients with chronic lymphocytic leukaemia but is preserved in patients with small lymphocytic lymphoma. Oncotarget. 2016;7(42):68513-26.
285.   Reiners KS, Topolar D, Henke A, Simhadri VR, Kessler J, Sauer M, et al. Soluble ligands for NK cell receptors promote evasion of chronic lymphocytic leukemia cells from NK cell anti-tumor activity. Blood. 2013;121(18):3658-65.
286.   Maki G, Hayes GM, Naji A, Tyler T, Carosella ED, Rouas-Freiss N, et al. NK resistance of tumor cells from multiple myeloma and chronic lymphocytic leukemia patients: implication of HLA-G. Leukemia. 2008;22(5):998-1006.
287.   Buechele C, Baessler T, Schmiedel BJ, Schumacher CE, Grosse-Hovest L, Rittig K, et al. 4-1BB ligand modulates direct and Rituximab-induced NK-cell reactivity in chronic lymphocytic leukemia. Eur J Immunol. 2012;42(3):737-48.
288.   Buechele C, Baessler T, Wirths S, Schmohl JU, Schmiedel BJ, Salih HR. Glucocorticoid-induced TNFR-related protein (GITR) ligand modulates cytokine release and NK cell reactivity in chronic lymphocytic leukemia (CLL). Leukemia. 2012;26(5):991-1000.
289.   Palmer S, Hanson CA, Zent CS, Porrata LF, Laplant B, Geyer SM, et al. Prognostic importance of T and NK-cells in a consecutive series of newly diagnosed patients with chronic lymphocytic leukaemia. Br J Haematol. 2008;141(5):607-14.
290.   Wang WT, Zhu HY, Wu YJ, Xia Y, Wu JZ, Wu W, et al. Elevated absolute NK cell counts in peripheral blood predict good prognosis in chronic lymphocytic leukemia. J Cancer Res Clin Oncol. 2018;144(3):449-57.
291.   Foa R, Catovsky D, Brozovic M, Marsh G, Ooyirilangkumaran T, Cherchi M, et al. Clinical staging and immunological findings in chronic lymphocytic leukemia. Cancer. 1979;44(2):483-7.

292.   Rozman C, Montserrat E, Viñolas N. Serum immunoglobulins in B-chronic lymphocytic leukemia. Natural history and prognostic significance. Cancer. 1988;61(2):279-83.

293.   Jurlander J, Geisler CH, Hansen MM. Treatment of hypogammaglobulinaemia in chronic lymphocytic leukaemia by low-dose intravenous gammaglobulin. Eur J Haematol. 1994;53(2):114-8.

294.   Parikh SA, Leis JF, Chaffee KG, Call TG, Hanson CA, Ding W, et al. Hypogammaglobulinemia in newly diagnosed chronic lymphocytic leukemia: Natural history, clinical correlates, and outcomes. Cancer. 2015;121(17):2883-91.

295.   Aittoniemi J, Miettinen A, Laine S, Sinisalo M, Laippala P, Vilpo L, et al. Opsonising immunoglobulins and mannan-binding lectin in chronic lymphocytic leukemia. Leuk Lymphoma. 1999;34(3-4):381-5.

296.   Copson ER, Ellis BA, Westwood NB, Majumdar G. IgG subclass levels in patients with B cell chronic lymphocytic leukaemia. Leuk Lymphoma. 1994;14(5-6):471-3.

297.   Griffiths H, Lea J, Bunch C, Lee M, Chapel H. Predictors of infection in chronic lymphocytic leukaemia (CLL). Clin Exp Immunol. 1992;89(3):374-7.

298.   Chiorazzi N, Fu SM, Montazeri G, Kunkel HG, Rai K, Gee T. T cell helper defect in patients with chronic lymphocytic leukemia. J Immunol. 1979;122(3):1087-90.

299.   Cantwell M, Hua T, Pappas J, Kipps TJ. Acquired CD40-ligand deficiency in chronic lymphocytic leukemia. Nat Med. 1997;3(9):984-9.

300.   Cerutti A, Kim EC, Shah S, Schattner EJ, Zan H, Schaffer A, et al. Dysregulation of CD30+ T cells by leukemia impairs isotype switching in normal B cells. Nat Immunol. 2001;2(2):150-6.

301.   Arens R, Nolte MA, Tesselaar K, Heemskerk B, Reedquist KA, van Lier RA, et al. Signaling through CD70 regulates B cell activation and IgG production. J Immunol. 2004;173(6):3901-8.

302.   Sampalo A, Navas G, Medina F, Segundo C, Cámara C, Brieva JA. Chronic lymphocytic leukemia B cells inhibit spontaneous Ig production by autologous bone marrow cells: role of CD95-CD95L interaction. Blood. 2000;96(9):3168-74.

303.   Sinisalo M, Aittoniemi J, Käyhty H, Vilpo J. Vaccination against infections in chronic lymphocytic leukemia. Leuk Lymphoma. 2003;44(4):649-52.

304.   Hartkamp A, Mulder AH, Rijkers GT, van Velzen-Blad H, Biesma DH. Antibody responses to pneumococcal and haemophilus vaccinations in patients with B-cell chronic lymphocytic leukaemia. Vaccine. 2001;19(13-14):1671-7.

305.   Sinisalo M, Vilpo J, Itälä M, Väkeväinen M, Taurio J, Aittoniemi J. Antibody response to 7-valent conjugated pneumococcal vaccine in patients with chronic lymphocytic leukaemia. Vaccine. 2007;26(1):82-7.

306.   Pasiarski M, Rolinski J, Grywalska E, Stelmach-Goldys A, Korona-Glowniak I, Gozdz S, et al. Antibody and plasmablast response to 13-valent pneumococcal conjugate vaccine in chronic lymphocytic leukemia patients--preliminary report. PLoS One. 2014;9(12):e114966.

307.   Sánchez-Ramón S, Dhalla F, Chapel H. Challenges in the Role of Gammaglobulin Replacement Therapy and Vaccination Strategies for Hematological Malignancy. Front Immunol. 2016;7:317.

308.   Raanani P, Gafter-Gvili A, Paul M, Ben-Bassat I, Leibovici L, Shpilberg O. Immunoglobulin prophylaxis in hematological malignancies and hematopoietic stem cell transplantation. Cochrane Database Syst Rev. 2008(4):CD006501.

309.   Wolos JA, Davey FR. B lymphocyte function in B cell chronic lymphocytic leukaemia. British Journal of Haematology. 1981;49(3):395-403.

310.   Han T, Bloom M, Dadey B, Bennett G, Minowada J, Sandberg A, et al. Lack of autologous mixed lymphocyte reaction in patients with chronic lymphocytic leukemia: evidence for autoreactive T-cell dysfunction not correlated with phenotype, karyotype, or clinical status. Blood. 1982;60(5):1075-81.

311.   Dazzi F, D'Andrea E, Biasi G, De Silvestro G, Gaidano G, Schena M, et al. Failure of B cells of chronic lymphocytic leukemia in presenting soluble and alloantigens. Clin Immunol Immunopathol. 1995;75(1):26-32.

312.   Kretz-Rommel A, Qin F, Dakappagari N, Ravey EP, McWhirter J, Oltean D, et al. CD200 expression on tumor cells suppresses antitumor immunity: new approaches to cancer immunotherapy. J Immunol. 2007;178(9):5595-605.

313.   Pallasch CP, Ulbrich S, Brinker R, Hallek M, Uger RA, Wendtner C-M. Disruption of T cell suppression in chronic lymphocytic leukemia by CD200 blockade. Leukemia Research. 2009;33(3):460-4.

314.   Do P, Beckwith KA, Cheney C, Tran M, Beaver L, Griffin BG, et al. Leukemic B Cell CTLA-4 Suppresses Costimulation of T Cells. J Immunol. 2019;202(9):2806-16.

315.   DiLillo DJ, Weinberg JB, Yoshizaki A, Horikawa M, Bryant JM, Iwata Y, et al. Chronic lymphocytic leukemia and regulatory B cells share IL-10 competence and immunosuppressive function. Leukemia. 2013;27(1):170-82.

316.   Mauri C, Bosma A. Immune regulatory function of B cells. Annu Rev Immunol. 2012;30:221-41.

317.   de Waal Malefyt R, Abrams J, Bennett B, Figdor CG, de Vries JE. Interleukin 10(IL-10) inhibits cytokine synthesis by human monocytes: an autoregulatory role of IL-10 produced by monocytes. J Exp Med. 1991;174(5):1209-20.

318.   Fiorentino DF, Zlotnik A, Mosmann TR, Howard M, O'Garra A. IL-10 inhibits cytokine production by activated macrophages. J Immunol. 1991;147(11):3815-22.

319.   de Waal Malefyt R, Haanen J, Spits H, Roncarolo MG, te Velde A, Figdor C, et al. Interleukin 10 (IL-10) and viral IL-10 strongly reduce antigen-specific human T cell proliferation by diminishing the antigen-

presenting capacity of monocytes via downregulation of class II major histocompatibility complex expression. J Exp Med. 1991;174(4):915-24.

320.		Ding L, Linsley PS, Huang LY, Germain RN, Shevach EM. IL-10 inhibits macrophage costimulatory activity by selectively inhibiting the up-regulation of B7 expression. J Immunol. 1993;151(3):1224-34.

321.		Willems F, Marchant A, Delville JP, Gérard C, Delvaux A, Velu T, et al. Interleukin-10 inhibits B7 and intercellular adhesion molecule-1 expression on human monocytes. Eur J Immunol. 1994;24(4):1007-9.

322.		Del Prete G, De Carli M, Almerigogna F, Giudizi MG, Biagiotti R, Romagnani S. Human IL-10 is produced by both type 1 helper (Th1) and type 2 helper (Th2) T cell clones and inhibits their antigen-specific proliferation and cytokine production. J Immunol. 1993;150(2):353-60.

323.		Groux H, Bigler M, de Vries JE, Roncarolo MG. Interleukin-10 induces a long-term antigen-specific anergic state in human CD4+ T cells. J Exp Med. 1996;184(1):19-29.

324.		Wolf SD, Dittel BN, Hardardottir F, Janeway CA. Experimental autoimmune encephalomyelitis induction in genetically B cell-deficient mice. J Exp Med. 1996;184(6):2271-8.

325.		Evans JG, Chavez-Rueda KA, Eddaoudi A, Meyer-Bahlburg A, Rawlings DJ, Ehrenstein MR, et al. Novel suppressive function of transitional 2 B cells in experimental arthritis. J Immunol. 2007;178(12):7868-78.

326.		Blair PA, Chavez-Rueda KA, Evans JG, Shlomchik MJ, Eddaoudi A, Isenberg DA, et al. Selective targeting of B cells with agonistic anti-CD40 is an efficacious strategy for the generation of induced regulatory T2-like B cells and for the suppression of lupus in MRL/lpr mice. J Immunol. 2009;182(6):3492-502.

327.		Inoue S, Leitner WW, Golding B, Scott D. Inhibitory effects of B cells on antitumor immunity. Cancer Res. 2006;66(15):7741-7.

328.		Olkhanud PB, Damdinsuren B, Bodogai M, Gress RE, Sen R, Wejksza K, et al. Tumor-evoked regulatory B cells promote breast cancer metastasis by converting resting CD4+ T cells to T-regulatory cells. Cancer Res. 2011;71(10):3505-15.

329.		Lindner S, Dahlke K, Sontheimer K, Hagn M, Kaltenmeier C, Barth TF, et al. Interleukin 21-induced granzyme B-expressing B cells infiltrate tumors and regulate T cells. Cancer Res. 2013;73(8):2468-79.

330.		Deaglio S, Capobianco A, Bergui L, Dürig J, Morabito F, Dührsen U, et al. CD38 is a signaling molecule in B-cell chronic lymphocytic leukemia cells. Blood. 2003;102(6):2146-55.

331.		Gondek DC, Lu LF, Quezada SA, Sakaguchi S, Noelle RJ. Cutting edge: contact-mediated suppression by CD4+CD25+ regulatory cells involves a granzyme B-dependent, perforin-independent mechanism. J Immunol. 2005;174(4):1783-6.

332.		Jahrsdörfer B, Vollmer A, Blackwell SE, Maier J, Sontheimer K, Beyer T, et al. Granzyme B produced by human plasmacytoid dendritic cells suppresses T-cell expansion. Blood. 2010;115(6):1156-65.

333.		Jahrsdörfer B, Blackwell SE, Wooldridge JE, Huang J, Andreski MW, Jacobus LS, et al. B-chronic lymphocytic leukemia cells and other B cells can produce granzyme B and gain cytotoxic potential after interleukin-21-based activation. Blood. 2006;108(8):2712-9.

334.		Karmali R, Paganessi LA, Frank RR, Jagan S, Larson ML, Venugopal P, et al. Aggressive disease defined by cytogenetics is associated with cytokine dysregulation in CLL/SLL patients. J Leukoc Biol. 2013;93(1):161-70.

335.		Garaud S, Morva A, Lemoine S, Hillion S, Bordron A, Pers JO, et al. CD5 promotes IL-10 production in chronic lymphocytic leukemia B cells through STAT3 and NFAT2 activation. J Immunol. 2011;186(8):4835-44.

336.		Saulep-Easton D, Vincent FB, Quah PS, Wei A, Ting SB, Croce CM, et al. The BAFF receptor TACI controls IL-10 production by regulatory B cells and CLL B cells. Leukemia. 2016;30(1):163-72.

337.		Hagn M, Blackwell SE, Beyer T, Ebel V, Fabricius D, Lindner S, et al. B-CLL cells acquire APC- and CTL-like phenotypic characteristics after stimulation with CpG ODN and IL-21. Int Immunol. 2014;26(7):383-95.

338.		Ringelstein-Harlev S, Avivi I, Fanadka M, Horowitz NA, Katz T. Chronic lymphocytic leukemia cells acquire regulatory B-cell properties in response to TLR9 and CD40 activation. Cancer Immunol Immunother. 2018;67(5):739-48.

339.		Alhakeem SS, McKenna MK, Oben KZ, Noothi SK, Rivas JR, Hildebrandt GC, et al. Chronic Lymphocytic Leukemia-Derived IL-10 Suppresses Antitumor Immunity. J Immunol. 2018;200(12):4180-9.

340.		Catovsky D, Miliani E, Okos A, Galton DA. Clinical significance of T-cells in chronic lymphocytic leukaemia. Lancet. 1974;2(7883):751-2.

341.		Platsoucas CD, Galinski M, Kempin S, Reich L, Clarkson B, Good RA. Abnormal T lymphocyte subpopulations in patients with B cell chronic lymphocytic leukemia: an analysis by monoclonal antibodies. J Immunol. 1982;129(5):2305-12.

342.		Röth A, de Beer D, Nückel H, Sellmann L, Dührsen U, Dürig J, et al. Significantly shorter telomeres in T-cells of patients with ZAP-70+/CD38+ chronic lymphocytic leukaemia. Br J Haematol. 2008;143(3):383-6.

343.		Herrmann F, Lochner A, Philippen H, Jauer B, Ruhl H. Imbalance of T cell subpopulations in patients with chronic lymphocytic leukaemia of the B cell type. Clin Exp Immunol. 1982;49(1):157-62.

344.		Mills KH, Cawley JC. Suppressor T cells in B-cell chronic lymphocytic leukaemia: relationship to clinical stage. Leuk Res. 1982;6(5):653-7.

345.		Pizzolo G, Chilosi M, Ambrosetti A, Semenzato G, Fiore-Donati L, Perona G. Immunohistologic study of bone marrow involvement in B-chronic lymphocytic leukemia. Blood. 1983;62(6):1289-96.

346.   Ghia P, Strola G, Granziero L, Geuna M, Guida G, Sallusto F, et al. Chronic lymphocytic leukemia B cells are endowed with the capacity to attract CD4+, CD40L+ T cells by producing CCL22. Eur J Immunol. 2002;32(5):1403-13.

347.   Guarini A, Gaidano G, Mauro FR, Capello D, Mancini F, De Propris MS, et al. Chronic lymphocytic leukemia patients with highly stable and indolent disease show distinctive phenotypic and genotypic features. Blood. 2003;102(3):1035-41.

348.   Nunes C, Wong R, Mason M, Fegan C, Man S, Pepper C. Expansion of a CD8(+)PD-1(+) replicative senescence phenotype in early stage CLL patients is associated with inverted CD4:CD8 ratios and disease progression. Clin Cancer Res. 2012;18(3):678-87.

349.   Wu J, Xu X, Lee EJ, Shull AY, Pei L, Awan F, et al. Phenotypic alteration of CD8+ T cells in chronic lymphocytic leukemia is associated with epigenetic reprogramming. Oncotarget. 2016;7(26):40558-70.

350.   Tinhofer I, Weiss L, Gassner F, Rubenzer G, Holler C, Greil R. Difference in the relative distribution of CD4+ T-cell subsets in B-CLL with mutated and unmutated immunoglobulin (Ig) VH genes: implication for the course of disease. J Immunother. 2009;32(3):302-9.

351.   Brusa D, Serra S, Coscia M, Rossi D, D'Arena G, Laurenti L, et al. The PD-1/PD-L1 axis contributes to T-cell dysfunction in chronic lymphocytic leukemia. Haematologica. 2013;98(6):953-63.

352.   Göthert JR, Eisele L, Klein-Hitpass L, Weber S, Zesewitz ML, Sellmann L, et al. Expanded CD8+ T cells of murine and human CLL are driven into a senescent KLRG1+ effector memory phenotype. Cancer Immunol Immunother. 2013;62(11):1697-709.

353.   Monserrat J, Sánchez M, de Paz R, Díaz D, Mur S, Reyes E, et al. Distinctive patterns of naïve/memory subset distribution and cytokine expression in CD4 T lymphocytes in ZAP-70 B-chronic lymphocytic patients. Cytometry B Clin Cytom. 2014;86(1):32-43.

354.   Palma M, Gentilcore G, Heimersson K, Mozaffari F, Nasman-Glaser B, Young E, et al. T cells in chronic lymphocytic leukemia display dysregulated expression of immune checkpoints and activation markers. Haematologica. 2017;102(3):562-72.

355.   Gonnord P, Costa M, Abreu A, Peres M, Ysebaert L, Gadat S, et al. Multiparametric analysis of CD8. Oncoimmunology. 2019;8(4):e1570774.

356.   Wikby A, Månsson IA, Johansson B, Strindhall J, Nilsson SE. The immune risk profile is associated with age and gender: findings from three Swedish population studies of individuals 20-100 years of age. Biogerontology. 2008;9(5):299-308.

357.   Velardi A, Prchal JT, Prasthofer EF, Grossi CE. Expression of NK-lineage markers on peripheral blood lymphocytes with T-helper (Leu3+/T4+) phenotype in B cell chronic lymphocytic leukemia. Blood. 1985;65(1):149-55.

358.   Serrano D, Monteiro J, Allen SL, Kolitz J, Schulman P, Lichtman SM, et al. Clonal expansion within the CD4+CD57+ and CD8+CD57+ T cell subsets in chronic lymphocytic leukemia. J Immunol. 1997;158(3):1482-9.

359.   Van den Hove LE, Van Gool SW, Vandenberghe P, Boogaerts MA, Ceuppens JL. CD57+/CD28- T cells in untreated hemato-oncological patients are expanded and display a Th1-type cytokine secretion profile, ex vivo cytolytic activity and enhanced tendency to apoptosis. Leukemia. 1998;12(10):1573-82.

360.   Rezvany MR, Jeddi-Tehrani M, Osterborg A, Kimby E, Wigzell H, Mellstedt H. Oligoclonal TCRBV gene usage in B-cell chronic lymphocytic leukemia: major perturbations are preferentially seen within the CD4 T-cell subset. Blood. 1999;94(3):1063-9.

361.   Lanasa MC, Allgood SD, Bond KM, Gockerman JP, Levesque MC, Weinberg JB. Oligoclonal TRBV gene usage among CD8(+) T cells in monoclonal B lymphocytosis and CLL. Br J Haematol. 2009;145(4):535-7.

362.   Blanco G, Vardi A, Puiggros A, Gómez-Llonín A, Muro M, Rodríguez-Rivera M, et al. Restricted T cell receptor repertoire in CLL-like monoclonal B cell lymphocytosis and early stage CLL. Oncoimmunology. 2018;7(6):e1432328.

363.   O'Hara GA, Welten SP, Klenerman P, Arens R. Memory T cell inflation: understanding cause and effect. Trends Immunol. 2012;33(2):84-90.

364.   Pourgheysari B, Bruton R, Parry H, Billingham L, Fegan C, Murray J, et al. The number of cytomegalovirus-specific CD4+ T cells is markedly expanded in patients with B-cell chronic lymphocytic leukemia and determines the total CD4+ T-cell repertoire. Blood. 2010;116(16):2968-74.

365.   Mackus WJ, Frakking FN, Grummels A, Gamadia LE, De Bree GJ, Hamann D, et al. Expansion of CMV-specific CD8+CD45RA+CD27- T cells in B-cell chronic lymphocytic leukemia. Blood. 2003;102(3):1057-63.

366.   Walton JA, Lydyard PM, Nathwani A, Emery V, Akbar A, Glennie MJ, et al. Patients with B cell chronic lymphocytic leukaemia have an expanded population of CD4 perforin expressing T cells enriched for human cytomegalovirus specificity and an effector-memory phenotype. Br J Haematol. 2010;148(2):274-84.

367.   Parry HM, Damery S, Hudson C, Maurer MJ, Cerhan JR, Pachnio A, et al. Cytomegalovirus infection does not impact on survival or time to first treatment in patients with chronic lymphocytic leukemia. Am J Hematol. 2016;91(8):776-81.

368.   Vardi A, Vlachonikola E, Karypidou M, Stalika E, Bikos V, Gemenetzi K, et al. Restrictions in the T-cell repertoire of chronic lymphocytic leukemia: high-throughput immunoprofiling supports selection by shared antigenic elements. Leukemia. 2017;31(7):1555-61.

369.   Sakaguchi S, Miyara M, Costantino CM, Hafler DA. FOXP3+ regulatory T cells in the human immune system. Nat Rev Immunol. 2010;10(7):490-500.

370.   Oleinika K, Nibbs RJ, Graham GJ, Fraser AR. Suppression, subversion and escape: the role of regulatory T cells in cancer progression. Clin Exp Immunol. 2013;171(1):36-45.

371.   Beyer M, Kochanek M, Darabi K, Popov A, Jensen M, Endl E, et al. Reduced frequencies and suppressive function of CD4+CD25hi regulatory T cells in patients with chronic lymphocytic leukemia after therapy with fludarabine. Blood. 2005;106(6):2018-25.

372.   Motta M, Rassenti L, Shelvin BJ, Lerner S, Kipps TJ, Keating MJ, et al. Increased expression of CD152 (CTLA-4) by normal T lymphocytes in untreated patients with B-cell chronic lymphocytic leukemia. Leukemia. 2005;19(10):1788-93.

373.   D'Arena G, Laurenti L, Minervini MM, Deaglio S, Bonello L, De Martino L, et al. Regulatory T-cell number is increased in chronic lymphocytic leukemia patients and correlates with progressive disease. Leuk Res. 2011;35(3):363-8.

374.   Piper KP, Karanth M, McLarnon A, Kalk E, Khan N, Murray J, et al. Chronic lymphocytic leukaemia cells drive the global CD4+ T cell repertoire towards a regulatory phenotype and leads to the accumulation of CD4+ forkhead box P3+ T cells. Clin Exp Immunol. 2011;166(2):154-63.

375.   Lad DP, Varma S, Varma N, Sachdeva MU, Bose P, Malhotra P. Regulatory T-cell and T-helper 17 balance in chronic lymphocytic leukemia progression and autoimmune cytopenias. Leuk Lymphoma. 2015;56(8):2424-8.

376.   Rissiek A, Schulze C, Bacher U, Schieferdecker A, Thiele B, Jacholkowski A, et al. Multidimensional scaling analysis identifies pathological and prognostically relevant profiles of circulating T-cells in chronic lymphocytic leukemia. International journal of cancer Journal international du cancer. 2014;135(10):2370-9.

377.   Mpakou VE, Ioannidou HD, Konsta E, Vikentiou M, Spathis A, Kontsioti F, et al. Quantitative and qualitative analysis of regulatory T cells in B cell chronic lymphocytic leukemia. Leuk Res. 2017;60:74-81.

378.   De Matteis S, Molinari C, Abbati G, Rossi T, Napolitano R, Ghetti M, et al. Immunosuppressive Treg cells acquire the phenotype of effector-T cells in chronic lymphocytic leukemia patients. J Transl Med. 2018;16(1):172.

379.   D'Arena G, Laurenti L, Minervini MM, Deaglio S, Bonello L, De Martino L, et al. Regulatory T-cell number is increased in chronic lymphocytic leukemia patients and correlates with progressive disease. Leukemia Research. 2011;35(3):363-8.

380.   Jadidi-Niaragh F, Yousefi M, Memarian A, Hojjat-Farsangi M, Khoshnoodi J, Razavi SM, et al. Increased frequency of CD8+ and CD4+ regulatory T cells in chronic lymphocytic leukemia: association with disease progression. Cancer Invest. 2013;31(2):121-31.

381.   de Weerdt I, Hofland T, Dobber J, Dubois J, Eldering E, Mobasher M, et al. First Evidence of Restoration of T and NK Cell Compartment after Venetoclax Treatment. Blood. 2018;132(Suppl 1):1860-.

382.   Bailey SR, Nelson MH, Himes RA, Li Z, Mehrotra S, Paulos CM. Th17 cells in cancer: the ultimate identity crisis. Front Immunol. 2014;5:276.

383.   Jadidi-Niaragh F, Ghalamfarsa G, Memarian A, Asgarian-Omran H, Razavi SM, Sarrafnejad A, et al. Downregulation of IL-17-producing T cells is associated with regulatory T cell expansion and disease progression in chronic lymphocytic leukemia. Tumour biology : the journal of the International Society for Oncodevelopmental Biology and Medicine. 2013;34(2):929-40.

384.   Hus I, Bojarska-Junak A, Chocholska S, Tomczak W, Wos J, Dmoszynska A, et al. Th17/IL-17A might play a protective role in chronic lymphocytic leukemia immunity. PLoS One. 2013;8(11):e78091.

385.   Bendelac A, Savage PB, Teyton L. The biology of NKT cells. Annu Rev Immunol. 2007;25:297-336.

386.   Fais F, Morabito F, Stelitano C, Callea V, Zanardi S, Scudeletti M, et al. CD1d is expressed on B-chronic lymphocytic leukemia cells and mediates alpha-galactosylceramide presentation to natural killer T lymphocytes. Int J Cancer. 2004;109(3):402-11.

387.   Zaborsky N, Gassner FJ, Asslaber D, Reinthaler P, Denk U, Flenady S, et al. CD1d expression on chronic lymphocytic leukemia B cells affects disease progression and induces T cell skewing in CD8 positive and CD4CD8 double negative T cells. Oncotarget. 2016;7(31):49459-69.

388.   Bojarska-Junak A, Hus I, Sieklucka M, Wasik-Szczepanek E, Mazurkiewicz T, Polak P, et al. Natural killer-like T CD3+/CD16+CD56+ cells in chronic lymphocytic leukemia: intracellular cytokine expression and relationship with clinical outcome. Oncol Rep. 2010;24(3):803-10.

389.   Jadidi-Niaragh F, Jeddi-Tehrani M, Ansaripour B, Razavi SM, Sharifian RA, Shokri F. Reduced frequency of NKT-like cells in patients with progressive chronic lymphocytic leukemia. Med Oncol. 2012;29(5):3561-9.

390.   Gorini F, Azzimonti L, Delfanti G, Scarfò L, Scielzo C, Bertilaccio MT, et al. Invariant NKT cells contribute to chronic lymphocytic leukemia surveillance and prognosis. Blood. 2017;129(26):3440-51.

391.   Bojarska-Junak A, Waldowska M, Woś J, Chocholska S, Hus I, Tomczak W, et al. Intracellular IL-4 and IFN-γ expression in iNKT cells from patients with chronic lymphocytic leukemia. Oncol Lett. 2018;15(2):1580-90.

392.   Lafont V, Sanchez F, Laprevotte E, Michaud HA, Gros L, Eliaou JF, et al. Plasticity of γδ T Cells: Impact on the Anti-Tumor Response. Front Immunol. 2014;5:622.

393.   Bartkowiak J, Kulczyck-Wojdala D, Blonski JZ, Robak T. Molecular diversity of gammadelta T cells in peripheral blood from patients with B-cell chronic lymphocytic leukaemia. Neoplasma. 2002;49(2):86-90.

394.   Simões C, Silva I, Carvalho A, Silva S, Santos S, Marques G, et al. Quantification and phenotypic characterization of peripheral blood Vδ1 + T cells in chronic lymphocytic leukemia and monoclonal B cell lymphocytosis. Cytometry B Clin Cytom. 2019;96(2):164-8.

395.   Poggi A, Venturino C, Catellani S, Clavio M, Miglino M, Gobbi M, et al. Vdelta1 T lymphocytes from B-CLL patients recognize ULBP3 expressed on leukemic B cells and up-regulated by trans-retinoic acid. Cancer Res. 2004;64(24):9172-9.

396.   Coscia M, Vitale C, Peola S, Foglietta M, Rigoni M, Griggio V, et al. Dysfunctional Vγ9Vδ2 T cells are negative prognosticators and markers of dysregulated mevalonate pathway activity in chronic lymphocytic leukemia cells. Blood. 2012;120(16):3271-9.

397.   Lauria F, Foa R, Mantovani V, Fierro MT, Catovsky D, Tura S. T-cell functional abnormality in B-chronic lymphocytic leukaemia: evidence of a defect of the T-helper subset. Br J Haematol. 1983;54(2):277-83.

398.   Taghiloo S, Allahmoradi E, Tehrani M, Hossein-Nataj H, Shekarriz R, Janbabaei G, et al. Frequency and functional characterization of exhausted CD8+ T cells in chronic lymphocytic leukemia. Eur J Haematol. 2017.

399.   Krackhardt AM, Harig S, Witzens M, Broderick R, Barrett P, Gribben JG. T-cell responses against chronic lymphocytic leukemia cells: implications for immunotherapy. Blood. 2002;100(1):167-73.

400.   Kabanova A, Sanseviero F, Candi V, Gamberucci A, Gozzetti A, Campoccia G, et al. Human Cytotoxic T Lymphocytes Form Dysfunctional Immune Synapses with B Cells Characterized by Non-Polarized Lytic Granule Release. Cell Rep. 2016;15(10):2313.

401.   Riches JC, Davies JK, McClanahan F, Fatah R, Iqbal S, Agrawal S, et al. T cells from CLL patients exhibit features of T-cell exhaustion but retain capacity for cytokine production. Blood. 2013;121(9):1612-21.

402.   Bagnara D, Kaufman MS, Calissano C, Marsilio S, Patten PE, Simone R, et al. A novel adoptive transfer model of chronic lymphocytic leukemia suggests a key role for T lymphocytes in the disease. Blood. 2011;117(20):5463-72.

403.   Podhorecka M, Dmoszynska A, Rolinski J, Wasik E. T type 1/type 2 subsets balance in B-cell chronic lymphocytic leukemia--the three-color flow cytometry analysis. Leuk Res. 2002;26(7):657-60.

404.   Gallego A, Vargas JA, Castejon R, Citores MJ, Romero Y, Millan I, et al. Production of intracellular IL-2, TNF-alpha, and IFN-gamma by T cells in B-CLL. Cytometry B Clin Cytom. 2003;56(1):23-9.

405.   Kiaii S, Choudhury A, Mozaffari F, Kimby E, Osterborg A, Mellstedt H. Signaling molecules and cytokine production in T cells of patients with B-cell chronic lymphocytic leukemia (B-CLL): comparison of indolent and progressive disease. Med Oncol. 2005;22(3):291-302.

406.   Mainou-Fowler T, Miller S, Proctor SJ, Dickinson AM. The levels of TNF alpha, IL4 and IL10 production by T-cells in B-cell chronic lymphocytic leukaemia (B-CLL). Leuk Res. 2001;25(2):157-63.

407.   Dancescu M, Rubio-Trujillo M, Biron G, Bron D, Delespesse G, Sarfati M. Interleukin 4 protects chronic lymphocytic leukemic B cells from death by apoptosis and upregulates Bcl-2 expression. The Journal of Experimental Medicine. 1992;176(5):1319-26.

408.   Bhattacharya N, Reichenzeller M, Caudron-Herger M, Haebe S, Brady N, Diener S, et al. Loss of cooperativity of secreted CD40L and increased dose–response to IL4 on CLL cell viability correlates with enhanced activation of NF-kB and STAT6. International Journal of Cancer. 2014:n/a-n/a.

409.   Kitabayashi A, Hirokawa M, Miura A. The role of interleukin-10 (IL-10) in chronic B-lymphocytic leukemia: IL-10 prevents leukemic cells from apoptotic cell death. Int J Hematol. 1995;62(2):99.

410.   Buggins AG, Patten PE, Richards J, Thomas NS, Mufti GJ, Devereux S. Tumor-derived IL-6 may contribute to the immunological defect in CLL. Leukemia. 2008;22(5):1084-7.

411.   Fayad L, Keating MJ, Reuben JM, O'Brien S, Lee B-N, Lerner S, et al. Interleukin-6 and interleukin-10 levels in chronic lymphocytic leukemia: correlation with phenotypic characteristics and outcome. Blood. 2001;97(1):256-63.

412.   Lai R, O'Brien S, Maushouri T, Rogers A, Kantarjian H, Keating M, et al. Prognostic value of plasma interleukin-6 levels in patients with chronic lymphocytic leukemia. Cancer. 2002;95(5):1071-5.

413.   Zaki M, Douglas R, Patten N, Bachinsky M, Lamb R, Nowell P, et al. Disruption of the IFN-gamma cytokine network in chronic lymphocytic leukemia contributes to resistance of leukemic B cells to apoptosis. Leuk Res. 2000;24(7):611-21.

414.   Bojarska-Junak A, Rolinski J, Wasik-Szczepaneko E, Kaluzny Z, Dmoszynska A. Intracellular tumor necrosis factor production by T- and B-cells in B-cell chronic lymphocytic leukemia. Haematologica. 2002;87(5):490-9.

415.   Podhorecka M, Dmoszynska A, Rolinski J. Intracellular IFN-gamma expression by CD3+/CD8+ cell subset in B-CLL patients correlates with stage of the disease. Eur J Haematol. 2004;73(1):29-35.

416.   Digel W, Stefanic M, Schoniger W, Buck C, Raghavachar A, Frickhofen N, et al. Tumor necrosis factor induces proliferation of neoplastic B cells from chronic lymphocytic leukemia. Blood. 1989;73(5):1242-6.

417.   Buschle M, Campana D, Carding SR, Richard C, Hoffbrand AV, Brenner MK. Interferon gamma inhibits apoptotic cell death in B cell chronic lymphocytic leukemia. J Exp Med. 1993;177(1):213-8.

418.   Ferrajoli A, Keating MJ, Manshouri T, Giles FJ, Dey A, Estrov Z, et al. The clinical significance of tumor necrosis factor-alpha plasma level in patients having chronic lymphocytic leukemia. Blood. 2002;100(4):1215-9.

419.   Yan XJ, Dozmorov I, Li W, Yancopoulos S, Sison C, Centola M, et al. Identification of outcome-correlated cytokine clusters in chronic lymphocytic leukemia. Blood. 2011;118(19):5201-10.
420.   Gorgun G, Holderried TAW, Zahrieh D, Neuberg D, Gribben JG. Chronic lymphocytic leukemia cells induce changes in gene expression of CD4 and CD8 T cells. The Journal of Clinical Investigation. 2005;115(7):1797-805.
421.   Di Ianni M, Moretti L, Terenzi A, Bazzucchi F, Ciurnelli R, Lucchesi A, et al. Activated autologous T cells exert an anti-B-cell chronic lymphatic leukemia effect in vitro and in vivo. Cytotherapy. 2009;11(1):86-96.
422.   Wherry EJ, Kurachi M. Molecular and cellular insights into T cell exhaustion. Nat Rev Immunol. 2015;15(8):486-99.
423.   Crawford A, Angelosanto JM, Kao C, Doering TA, Odorizzi PM, Barnett BE, et al. Molecular and transcriptional basis of CD4^{+} T cell dysfunction during chronic infection. Immunity. 2014;40(2):289-302.
424.   Riches JC, Davies JK, McClanahan F, Fatah R, Iqbal S, Agrawal S, et al. T cells from CLL patients exhibit features of T-cell exhaustion but retain capacity for cytokine production. Blood. 2013;121(9):1612-21.
425.   Gassner FJ, Zaborsky N, Catakovic K, Rebhandl S, Huemer M, Egle A, et al. Chronic lymphocytic leukaemia induces an exhausted T cell phenotype in the TCL1 transgenic mouse model. Br J Haematol. 2015;170(4):515-22.
426.   Allahmoradi E, Taghiloo S, Tehrani M, Hossein-Nattaj H, Janbabaei G, Shekarriz R, et al. CD4+ T Cells are Exhausted and Show Functional Defects in Chronic Lymphocytic Leukemia. Iran J Immunol. 2017;14(4):257-69.
427.   Catakovic K, Gassner FJ, Ratswohl C, Zaborsky N, Rebhandl S, Schubert M, et al. TIGIT expressing CD4+T cells represent a tumor-supportive T cell subset in chronic lymphocytic leukemia. Oncoimmunology. 2017;7(1):e1371399.
428.   Lewinsky H, Barak AF, Huber V, Kramer MP, Radomir L, Sever L, et al. CD84 regulates PD-1/PD-L1 expression and function in chronic lymphocytic leukemia. J Clin Invest. 2018;128(12):5465-78.
429.   Ashwell JD, Klusner RD. Genetic and mutational analysis of the T-cell antigen receptor. Annu Rev Immunol. 1990;8:139-67.
430.   Kieke MC, Shusta EV, Boder ET, Teyton L, Wittrup KD, Kranz DM. Selection of functional T cell receptor mutants from a yeast surface-display library. Proc Natl Acad Sci U S A. 1999;96(10):5651-6.
431.   Call ME, Pyrdol J, Wiedmann M, Wucherpfennig KW. The organizing principle in the formation of the T cell receptor-CD3 complex. Cell. 2002;111(7):967-79.
432.   Samelson LE, Patel MD, Weissman AM, Harford JB, Klausner RD. Antigen activation of murine T cells induces tyrosine phosphorylation of a polypeptide associated with the T cell antigen receptor. Cell. 1986;46(7):1083-90.
433.   Janeway CA. The T cell receptor as a multicomponent signalling machine: CD4/CD8 coreceptors and CD45 in T cell activation. Annu Rev Immunol. 1992;10:645-74.
434.   Veillette A, Bookman MA, Horak EM, Bolen JB. The CD4 and CD8 T cell surface antigens are associated with the internal membrane tyrosine-protein kinase p56lck. Cell. 1988;55(2):301-8.
435.   Samelson LE, Phillips AF, Luong ET, Klausner RD. Association of the fyn protein-tyrosine kinase with the T-cell antigen receptor. Proc Natl Acad Sci U S A. 1990;87(11):4358-62.
436.   McNeill L, Salmond RJ, Cooper JC, Carret CK, Cassady-Cain RL, Roche-Molina M, et al. The differential regulation of Lck kinase phosphorylation sites by CD45 is critical for T cell receptor signaling responses. Immunity. 2007;27(3):425-37.
437.   Chan AC, Iwashima M, Turck CW, Weiss A. ZAP-70: a 70 kd protein-tyrosine kinase that associates with the TCR zeta chain. Cell. 1992;71(4):649-62.
438.   Irving BA, Chan AC, Weiss A. Functional characterization of a signal transducing motif present in the T cell antigen receptor zeta chain. J Exp Med. 1993;177(4):1093-103.
439.   Sommers CL, Samelson LE, Love PE. LAT: a T lymphocyte adapter protein that couples the antigen receptor to downstream signaling pathways. Bioessays. 2004;26(1):61-7.
440.   Koretzky GA, Abtahian F, Silverman MA. SLP76 and SLP65: complex regulation of signalling in lymphocytes and beyond. Nat Rev Immunol. 2006;6(1):67-78.
441.   Bustelo XR. Vav family exchange factors: an integrated regulatory and functional view. Small GTPases. 2014;5(2):9.
442.   Zhang W, Trible RP, Zhu M, Liu SK, McGlade CJ, Samelson LE. Association of Grb2, Gads, and phospholipase C-gamma 1 with phosphorylated LAT tyrosine residues. Effect of LAT tyrosine mutations on T cell angigen receptor-mediated signaling. J Biol Chem. 2000;275(30):23355-61.
443.   Chardin P, Camonis JH, Gale NW, van Aelst L, Schlessinger J, Wigler MH, et al. Human Sos1: a guanine nucleotide exchange factor for Ras that binds to GRB2. Science. 1993;260(5112):1338-43.
444.   Egan SE, Giddings BW, Brooks MW, Buday L, Sizeland AM, Weinberg RA. Association of Sos Ras exchange protein with Grb2 is implicated in tyrosine kinase signal transduction and transformation. Nature. 1993;363(6424):45-51.
445.   Ye ZS, Baltimore D. Binding of Vav to Grb2 through dimerization of Src homology 3 domains. Proc Natl Acad Sci U S A. 1994;91(26):12629-33.
446.   Beach D, Gonen R, Bogin Y, Reischl IG, Yablonski D. Dual role of SLP-76 in mediating T cell receptor-induced activation of phospholipase C-gamma1. J Biol Chem. 2007;282(5):2937-46.

447. Sommers CL, Lee J, Steiner KL, Gurson JM, Depersis CL, El-Khoury D, et al. Mutation of the phospholipase C-gamma1-binding site of LAT affects both positive and negative thymocyte selection. J Exp Med. 2005;201(7):1125-34.

448. Dombroski D, Houghtling RA, Labno CM, Precht P, Takesono A, Caplen NJ, et al. Kinase-independent functions for Itk in TCR-induced regulation of Vav and the actin cytoskeleton. J Immunol. 2005;174(3):1385-92.

449. Qi Q, August A. Keeping the (kinase) party going: SLP-76 and ITK dance to the beat. Sci STKE. 2007;2007(396):pe39.

450. Grasis JA, Browne CD, Tsoukas CD. Inducible T cell tyrosine kinase regulates actin-dependent cytoskeletal events induced by the T cell antigen receptor. J Immunol. 2003;170(8):3971-6.

451. Vig M, Peinelt C, Beck A, Koomoa DL, Rabah D, Koblan-Huberson M, et al. CRACM1 is a plasma membrane protein essential for store-operated Ca2+ entry. Science. 2006;312(5777):1220-3.

452. Penna A, Demuro A, Yeromin AV, Zhang SL, Safrina O, Parker I, et al. The CRAC channel consists of a tetramer formed by Stim-induced dimerization of Orai dimers. Nature. 2008;456(7218):116-20.

453. Oh-hora M, Rao A. Calcium signaling in lymphocytes. Curr Opin Immunol. 2008;20(3):250-8.

454. Hoffmann A, Natoli G, Ghosh G. Transcriptional regulation via the NF-kappaB signaling module. Oncogene. 2006;25(51):6706-16.

455. Ebinu JO, Bottorff DA, Chan EY, Stang SL, Dunn RJ, Stone JC. RasGRP, a Ras guanyl nucleotide-releasing protein with calcium- and diacylglycerol-binding motifs. Science. 1998;280(5366):1082-6.

456. Ebinu JO, Stang SL, Teixeira C, Bottorff DA, Hooton J, Blumberg PM, et al. RasGRP links T-cell receptor signaling to Ras. Blood. 2000;95(10):3199-203.

457. Genot E, Cantrell DA. Ras regulation and function in lymphocytes. Curr Opin Immunol. 2000;12(3):289-94.

458. Burnet FM, Fenner F. The *Production of Antibodies* (2nd ed.) Melbourne: Macmillan; 1949

459. Janeway CA. Approaching the asymptote? Evolution and revolution in immunology. Cold Spring Harb Symp Quant Biol. 1989;54 Pt 1:1-13.

460. Matzinger P. Tolerance, danger, and the extended family. Annu Rev Immunol. 1994;12:991-1045.

461. Rubartelli A, Lotze MT. Inside, outside, upside down: damage-associated molecular-pattern molecules (DAMPs) and redox. Trends Immunol. 2007;28(10):429-36.

462. Beutler B, Jiang Z, Georgel P, Crozat K, Croker B, Rutschmann S, et al. Genetic analysis of host resistance: Toll-like receptor signaling and immunity at large. Annu Rev Immunol. 2006;24:353-89.

463. Caruso R, Warner N, Inohara N, Núñez G. NOD1 and NOD2: signaling, host defense, and inflammatory disease. Immunity. 2014;41(6):898-908.

464. Kumar H, Kawai T, Akira S. Pathogen recognition by the innate immune system. Int Rev Immunol. 2011;30(1):16-34.

465. Geijtenbeek TB, Gringhuis SI. Signalling through C-type lectin receptors: shaping immune responses. Nat Rev Immunol. 2009;9(7):465-79.

466. Lenschow DJ, Walunas TL, Bluestone JA. CD28/B7 system of T cell costimulation. Annu Rev Immunol. 1996;14:233-58.

467. Wang S, Zhu G, Chapoval AI, Dong H, Tamada K, Ni J, et al. Costimulation of T cells by B7-H2, a B7-like molecule that binds ICOS. Blood. 2000;96(8):2808-13.

468. Kobata T, Agematsu K, Kameoka J, Schlossman SF, Morimoto C. CD27 is a signal-transducing molecule involved in CD45RA+ naive T cell costimulation. J Immunol. 1994;153(12):5422-32.

469. Croft M. Costimulation of T cells by OX40, 4-1BB, and CD27. Cytokine Growth Factor Rev. 2003;14(3-4):265-73.

470. Pagès F, Ragueneau M, Rottapel R, Truneh A, Nunes J, Imbert J, et al. Binding of phosphatidylinositol-3-OH kinase to CD28 is required for T-cell signalling. Nature. 1994;369(6478):327-9.

471. Cross DA, Alessi DR, Cohen P, Andjelkovich M, Hemmings BA. Inhibition of glycogen synthase kinase-3 by insulin mediated by protein kinase B. Nature. 1995;378(6559):785-9.

472. Crabtree GR, Olson EN. NFAT signaling: choreographing the social lives of cells. Cell. 2002;109 Suppl:S67-79.

473. Schneider H, Cai YC, Prasad KV, Shoelson SE, Rudd CE. T cell antigen CD28 binds to the GRB-2/SOS complex, regulators of p21ras. Eur J Immunol. 1995;25(4):1044-50.

474. Raab M, Pfister S, Rudd CE. CD28 signaling via VAV/SLP-76 adaptors: regulation of cytokine transcription independent of TCR ligation. Immunity. 2001;15(6):921-33.

475. Holdorf AD, Green JM, Levin SD, Denny MF, Straus DB, Link V, et al. Proline residues in CD28 and the Src homology (SH)3 domain of Lck are required for T cell costimulation. J Exp Med. 1999;190(3):375-84.

476. Coudronniere N, Villalba M, Englund N, Altman A. NF-kappa B activation induced by T cell receptor/CD28 costimulation is mediated by protein kinase C-theta. Proc Natl Acad Sci U S A. 2000;97(7):3394-9.

477. Monks CR, Freiberg BA, Kupfer H, Sciaky N, Kupfer A. Three-dimensional segregation of supramolecular activation clusters in T cells. Nature. 1998;395(6697):82-6.

478. Grakoui A, Bromley SK, Sumen C, Davis MM, Shaw AS, Allen PM, et al. The immunological synapse: a molecular machine controlling T cell activation. Science. 1999;285(5425):221-7.

479. Lee KH, Holdorf AD, Dustin ML, Chan AC, Allen PM, Shaw AS. T cell receptor signaling precedes immunological synapse formation. Science. 2002;295(5559):1539-42.

480.   Monks CR, Kupfer H, Tamir I, Barlow A, Kupfer A. Selective modulation of protein kinase C-theta during T-cell activation. Nature. 1997;385(6611):83-6.

481.   Dustin ML, Olszowy MW, Holdorf AD, Li J, Bromley S, Desai N, et al. A novel adaptor protein orchestrates receptor patterning and cytoskeletal polarity in T-cell contacts. Cell. 1998;94(5):667-77.

482.   Delon J, Kaibuchi K, Germain RN. Exclusion of CD43 from the immunological synapse is mediated by phosphorylation-regulated relocation of the cytoskeletal adaptor moesin. Immunity. 2001;15(5):691-701.

483.   Freiberg BA, Kupfer H, Maslanik W, Delli J, Kappler J, Zaller DM, et al. Staging and resetting T cell activation in SMACs. Nat Immunol. 2002;3(10):911-7.

484.   Sims TN, Soos TJ, Xenias HS, Dubin-Thaler B, Hofman JM, Waite JC, et al. Opposing effects of PKCtheta and WASp on symmetry breaking and relocation of the immunological synapse. Cell. 2007;129(4):773-85.

485.   Tseng SY, Waite JC, Liu M, Vardhana S, Dustin ML. T cell-dendritic cell immunological synapses contain TCR-dependent CD28-CD80 clusters that recruit protein kinase C theta. J Immunol. 2008;181(7):4852-63.

486.   Brossard C, Feuillet V, Schmitt A, Randriamampita C, Romao M, Raposo G, et al. Multifocal structure of the T cell - dendritic cell synapse. Eur J Immunol. 2005;35(6):1741-53.

487.   Yokosuka T, Sakata-Sogawa K, Kobayashi W, Hiroshima M, Hashimoto-Tane A, Tokunaga M, et al. Newly generated T cell receptor microclusters initiate and sustain T cell activation by recruitment of Zap70 and SLP-76. Nat Immunol. 2005;6(12):1253-62.

488.   Montoya MC, Sancho D, Bonello G, Collette Y, Langlet C, He HT, et al. Role of ICAM-3 in the initial interaction of T lymphocytes and APCs. Nat Immunol. 2002;3(2):159-68.

489.   Dustin ML, Ferguson LM, Chan PY, Springer TA, Golan DE. Visualization of CD2 interaction with LFA-3 and determination of the two-dimensional dissociation constant for adhesion receptors in a contact area. J Cell Biol. 1996;132(3):465-74.

490.   Dustin ML, Depoil D. New insights into the T cell synapse from single molecule techniques. Nat Rev Immunol. 2011;11(10):672-84.

491.   Grigorian A, Torossian S, Demetriou M. T-cell growth, cell surface organization, and the galectin-glycoprotein lattice. Immunol Rev. 2009;230(1):232-46.

492.   Dustin ML, Bromley SK, Kan Z, Peterson DA, Unanue ER. Antigen receptor engagement delivers a stop signal to migrating T lymphocytes. Proc Natl Acad Sci U S A. 1997;94(8):3909-13.

493.   Sanderson CJ, Glauert AM. The mechanism of T-cell mediated cytotoxicity. VI. T-cell projections and their role in target cell killing. Immunology. 1979;36(1):119-29.

494.   Ueda H, Morphew MK, McIntosh JR, Davis MM. CD4+ T-cell synapses involve multiple distinct stages. Proc Natl Acad Sci U S A. 2011;108(41):17099-104.

495.   Sanderson CJ, Glauert AM. The mechanism of T cell mediated cytotoxicity. V. Morphological studies by electron microscopy. Proc R Soc Lond B Biol Sci. 1977;198(1132):315-23.

496.   Bunnell SC, Kapoor V, Trible RP, Zhang W, Samelson LE. Dynamic actin polymerization drives T cell receptor-induced spreading: a role for the signal transduction adaptor LAT. Immunity. 2001;14(3):315-29.

497.   Hashimoto-Tane A, Yokosuka T, Sakata-Sogawa K, Sakuma M, Ishihara C, Tokunaga M, et al. Dynein-driven transport of T cell receptor microclusters regulates immune synapse formation and T cell activation. Immunity. 2011;34(6):919-31.

498.   Higashida C, Miyoshi T, Fujita A, Oceguera-Yanez F, Monypenny J, Andou Y, et al. Actin polymerization-driven molecular movement of mDia1 in living cells. Science. 2004;303(5666):2007-10.

499.   Campellone KG, Welch MD. A nucleator arms race: cellular control of actin assembly. Nat Rev Mol Cell Biol. 2010;11(4):237-51.

500.   Abdul-Manan N, Aghazadeh B, Liu GA, Majumdar A, Ouerfelli O, Siminovitch KA, et al. Structure of Cdc42 in complex with the GTPase-binding domain of the 'Wiskott-Aldrich syndrome' protein. Nature. 1999;399(6734):379-83.

501.   Eden S, Rohatgi R, Podtelejnikov AV, Mann M, Kirschner MW. Mechanism of regulation of WAVE1-induced actin nucleation by Rac1 and Nck. Nature. 2002;418(6899):790-3.

502.   Tavano R, Contento RL, Baranda SJ, Soligo M, Tuosto L, Manes S, et al. CD28 interaction with filamin-A controls lipid raft accumulation at the T-cell immunological synapse. Nat Cell Biol. 2006;8(11):1270-6.

503.   Gomez TS, Hamann MJ, McCarney S, Savoy DN, Lubking CM, Heldebrant MP, et al. Dynamin 2 regulates T cell activation by controlling actin polymerization at the immunological synapse. Nat Immunol. 2005;6(3):261-70.

504.   Kruchten AE, McNiven MA. Dynamin as a mover and pincher during cell migration and invasion. J Cell Sci. 2006;119(Pt 9):1683-90.

505.   Hotulainen P, Paunola E, Vartiainen MK, Lappalainen P. Actin-depolymerizing factor and cofilin-1 play overlapping roles in promoting rapid F-actin depolymerization in mammalian nonmuscle cells. Mol Biol Cell. 2005;16(2):649-64.

506.   Lee KH, Meuer SC, Samstag Y. Cofilin: a missing link between T cell co-stimulation and rearrangement of the actin cytoskeleton. Eur J Immunol. 2000;30(3):892-9.

507.   Shattil SJ, Kim C, Ginsberg MH. The final steps of integrin activation: the end game. Nat Rev Mol Cell Biol. 2010;11(4):288-300.

508. Lee HS, Lim CJ, Puzon-McLaughlin W, Shattil SJ, Ginsberg MH. RIAM activates integrins by linking talin to ras GTPase membrane-targeting sequences. J Biol Chem. 2009;284(8):5119-27.
509. Ménasché G, Kliche S, Chen EJ, Stradal TE, Schraven B, Koretzky G. RIAM links the ADAP/SKAP-55 signaling module to Rap1, facilitating T-cell-receptor-mediated integrin activation. Mol Cell Biol. 2007;27(11):4070-81.
510. Fagerholm SC, Lek HS, Morrison VL. Kindlin-3 in the immune system. Am J Clin Exp Immunol. 2014;3(1):37-42.
511. Stinchcombe JC, Griffiths GM. Communication, the centrosome and the immunological synapse. Philos Trans R Soc Lond B Biol Sci. 2014;369(1650).
512. Choudhuri K, Llodrá J, Roth EW, Tsai J, Gordo S, Wucherpfennig KW, et al. Polarized release of T-cell-receptor-enriched microvesicles at the immunological synapse. Nature. 2014;507(7490):118-23.
513. Tsun A, Qureshi I, Stinchcombe JC, Jenkins MR, de la Roche M, Kleczkowska J, et al. Centrosome docking at the immunological synapse is controlled by Lck signaling. J Cell Biol. 2011;192(4):663-74.
514. Kuhné MR, Lin J, Yablonski D, Mollenauer MN, Ehrlich LI, Huppa J, et al. Linker for activation of T cells, zeta-associated protein-70, and Src homology 2 domain-containing leukocyte protein-76 are required for TCR-induced microtubule-organizing center polarization. J Immunol. 2003;171(2):860-6.
515. Quann EJ, Merino E, Furuta T, Huse M. Localized diacylglycerol drives the polarization of the microtubule-organizing center in T cells. Nat Immunol. 2009;10(6):627-35.
516. Quann EJ, Liu X, Altan-Bonnet G, Huse M. A cascade of protein kinase C isozymes promotes cytoskeletal polarization in T cells. Nat Immunol. 2011;12(7):647-54.
517. Liu X, Kapoor TM, Chen JK, Huse M. Diacylglycerol promotes centrosome polarization in T cells via reciprocal localization of dynein and myosin II. Proc Natl Acad Sci U S A. 2013;110(29):11976-81.
518. Bertrand F, Esquerré M, Petit AE, Rodrigues M, Duchez S, Delon J, et al. Activation of the ancestral polarity regulator protein kinase C zeta at the immunological synapse drives polarization of Th cell secretory machinery toward APCs. J Immunol. 2010;185(5):2887-94.
519. Gomez TS, Kumar K, Medeiros RB, Shimizu Y, Leibson PJ, Billadeau DD. Formins regulate the actin-related protein 2/3 complex-independent polarization of the centrosome to the immunological synapse. Immunity. 2007;26(2):177-90.
520. Tsukita S, Yonemura S. ERM proteins: head-to-tail regulation of actin-plasma membrane interaction. Trends Biochem Sci. 1997;22(2):53-8.
521. Lasserre R, Charrin S, Cuche C, Danckaert A, Thoulouze MI, de Chaumont F, et al. Ezrin tunes T-cell activation by controlling Dlg1 and microtubule positioning at the immunological synapse. EMBO J. 2010;29(14):2301-14.
522. Stinchcombe JC, Bossi G, Booth S, Griffiths GM. The immunological synapse of CTL contains a secretory domain and membrane bridges. Immunity. 2001;15(5):751-61.
523. Fife BT, Bluestone JA. Control of peripheral T-cell tolerance and autoimmunity via the CTLA-4 and PD-1 pathways. Immunol Rev. 2008;224:166-82.
524. Waterhouse P, Penninger JM, Timms E, Wakeham A, Shahinian A, Lee KP, et al. Lymphoproliferative disorders with early lethality in mice deficient in Ctla-4. Science. 1995;270(5238):985-8.
525. Tivol EA, Borriello F, Schweitzer AN, Lynch WP, Bluestone JA, Sharpe AH. Loss of CTLA-4 leads to massive lymphoproliferation and fatal multiorgan tissue destruction, revealing a critical negative regulatory role of CTLA-4. Immunity. 1995;3(5):541-7.
526. Chambers CA, Sullivan TJ, Allison JP. Lymphoproliferation in CTLA-4-deficient mice is mediated by costimulation-dependent activation of CD4+ T cells. Immunity. 1997;7(6):885-95.
527. Nishimura H, Nose M, Hiai H, Minato N, Honjo T. Development of lupus-like autoimmune diseases by disruption of the PD-1 gene encoding an ITIM motif-carrying immunoreceptor. Immunity. 1999;11:141-51.
528. Nishimura H. Autoimmune dilated cardiomyopathy in PD-1 receptor-deficient mice. Science. 2001;291:319-22.
529. Brunet JF, Denizot F, Luciani MF, Roux-Dosseto M, Suzan M, Mattei MG, et al. A new member of the immunoglobulin superfamily--CTLA-4. Nature. 1987;328(6127):267-70.
530. Perkins D, Wang Z, Donovan C, He H, Mark D, Guan G, et al. Regulation of CTLA-4 expression during T cell activation. J Immunol. 1996;156(11):4154-9.
531. Jago CB, Yates J, Câmara NO, Lechler RI, Lombardi G. Differential expression of CTLA-4 among T cell subsets. Clin Exp Immunol. 2004;136(3):463-71.
532. Takahashi T, Tagami T, Yamazaki S, Uede T, Shimizu J, Sakaguchi N, et al. Immunologic self-tolerance maintained by CD25(+)CD4(+) regulatory T cells constitutively expressing cytotoxic T lymphocyte-associated antigen 4. J Exp Med. 2000;192(2):303-10.
533. Walunas TL, Lenschow DJ, Bakker CY, Linsley PS, Freeman GJ, Green JM, et al. CTLA-4 can function as a negative regulator of T cell activation. Immunity. 1994;1(5):405-13.
534. Krummel MF, Allison JP. CD28 and CTLA-4 have opposing effects on the response of T cells to stimulation. J Exp Med. 1995;182(2):459-65.
535. Walunas TL, Bakker CY, Bluestone JA. CTLA-4 ligation blocks CD28-dependent T cell activation. J Exp Med. 1996;183(6):2541-50.
536. Schneider H, Downey J, Smith A, Zinselmeyer BH, Rush C, Brewer JM, et al. Reversal of the TCR stop signal by CTLA-4. Science. 2006;313(5795):1972-5.

537.   Wei B, da Rocha Dias S, Wang H, Rudd CE. CTL-associated antigen-4 ligation induces rapid T cell polarization that depends on phosphatidylinositol 3-kinase, Vav-1, Cdc42, and myosin light chain kinase. J Immunol. 2007;179(1):400-8.

538.   Lu Y, Schneider H, Rudd CE. Murine regulatory T cells differ from conventional T cells in resisting the CTLA-4 reversal of TCR stop-signal. Blood. 2012;120(23):4560-70.

539.   Knieke K, Hoff H, Maszyna F, Kolar P, Schrage A, Hamann A, et al. CD152 (CTLA-4) determines CD4 T cell migration in vitro and in vivo. PLoS One. 2009;4(5):e5702.

540.   Balzano C, Buonavista N, Rouvier E, Golstein P. CTLA-4 and CD28: similar proteins, neighbouring genes. Int J Cancer Suppl. 1992;7:28-32.

541.   Qureshi OS, Zheng Y, Nakamura K, Attridge K, Manzotti C, Schmidt EM, et al. Trans-endocytosis of CD80 and CD86: a molecular basis for the cell-extrinsic function of CTLA-4. Science. 2011;332(6029):600-3.

542.   Parry RV, Chemnitz JM, Frauwirth KA, Lanfranco AR, Braunstein I, Kobayashi SV, et al. CTLA-4 and PD-1 receptors inhibit T-cell activation by distinct mechanisms. Mol Cell Biol. 2005;25(21):9543-53.

543.   Guntermann C, Alexander DR. CTLA-4 suppresses proximal TCR signaling in resting human CD4(+) T cells by inhibiting ZAP-70 Tyr(319) phosphorylation: a potential role for tyrosine phosphatases. J Immunol. 2002;168(9):4420-9.

544.   Marengère LE, Waterhouse P, Duncan GS, Mittrücker HW, Feng GS, Mak TW. Regulation of T cell receptor signaling by tyrosine phosphatase SYP association with CTLA-4. Science. 1996;272(5265):1170-3.

545.   Schneider H, Rudd CE. Tyrosine phosphatase SHP-2 binding to CTLA-4: absence of direct YVKM/YFIP motif recognition. Biochem Biophys Res Commun. 2000;269(1):279-83.

546.   Yokosuka T, Kobayashi W, Takamatsu M, Sakata-Sogawa K, Zeng H, Hashimoto-Tane A, et al. Spatiotemporal basis of CTLA-4 costimulatory molecule-mediated negative regulation of T cell activation. Immunity. 2010;33(3):326-39.

547.   Ishida Y, Agata Y, Shibahara K, Honjo T. Induced expression of PD-1, a novel member of the immunoglobulin gene superfamily, upon programmed cell death. EMBO J. 1992;11:3887-95.

548.   Shinohara T, Taniwaki M, Ishida Y, Kawaichi M, Honjo T. Structure and Chromosomal Localization of the Human PD-1 Gene (PDCD1). Genomics. 1994;23(3):704-6.

549.   Finger LR, Pu J, Wasserman R, Vibhakar R, Louie E, Hardy RR, et al. The human PD-1 gene: complete cDNA, genomic organization, and developmentally regulated expression in B cell progenitors. Gene. 1997;197(1-2):177-87.

550.   Keir ME, Butte MJ, Freeman GJ, Sharpe AH. PD-1 and its ligands in tolerance and immunity. Annu Rev Immunol. 2008;26:677-704.

551.   Dong H, Zhu G, Tamada K, Chen L. B7-H1, a third member of the B7 family, co-stimulates T-cell proliferation and interleukin-10 secretion. Nat Med. 1999;5(12):1365-9.

552.   Freeman GJ, Long AJ, Iwai Y, Bourque K, Chernova T, Nishimura H, et al. Engagement of the PD-1 immunoinhibitory receptor by a novel B7 family member leads to negative regulation of lymphocyte activation. J Exp Med. 2000;192(7):1027-34.

553.   Carter L, Fouser LA, Jussif J, Fitz L, Deng B, Wood CR, et al. PD-1:PD-L inhibitory pathway affects both CD4(+) and CD8(+) T cells and is overcome by IL-2. Eur J Immunol. 2002;32(3):634-43.

554.   Fife BT, Pauken KE, Eagar TN, Obu T, Wu J, Tang Q, et al. Interactions between PD-1 and PD-L1 promote tolerance by blocking the TCR-induced stop signal. Nat Immunol. 2009;10(11):1185-92.

555.   Ishida M, Iwai Y, Tanaka Y, Okazaki T, Freeman GJ, Minato N, et al. Differential expression of PD-L1 and PD-L2, ligands for an inhibitory receptor PD-1, in the cells of lymphohematopoietic tissues. Immunology Letters. 2002;84(1):57-62.

556.   Lee SJ, Jang BC, Lee SW, Yang YI, Suh SI, Park YM, et al. Interferon regulatory factor-1 is prerequisite to the constitutive expression and IFN-gamma-induced upregulation of B7-H1 (CD274). FEBS Lett. 2006;580(3):755-62.

557.   Garcia-Diaz A, Shin DS, Moreno BH, Saco J, Escuin-Ordinas H, Rodriguez GA, et al. Interferon Receptor Signaling Pathways Regulating PD-L1 and PD-L2 Expression. Cell Rep. 2017;19(6):1189-201.

558.   Yamazaki T, Akiba H, Iwai H, Matsuda H, Aoki M, Tanno Y, et al. Expression of programmed death 1 ligands by murine T cells and APC. J Immunol. 2002;169(10):5538-45.

559.   Dong H, Zhu G, Tamada K, Flies DB, van Deursen JMA, Chen L. B7-H1 Determines Accumulation and Deletion of Intrahepatic CD8+ T Lymphocytes. Immunity. 2004;20(3):327-36.

560.   Latchman YE, Liang SC, Wu Y, Chernova T, Sobel RA, Klemm M, et al. PD-L1-deficient mice show that PD-L1 on T cells, antigen-presenting cells, and host tissues negatively regulates T cells. Proc Natl Acad Sci U S A. 2004;101(29):10691-6.

561.   Latchman Y, Wood CR, Chernova T, Chaudhary D, Borde M, Chernova I, et al. PD-L2 is a second ligand for PD-1 and inhibits T cell activation. Nat Immunol. 2001;2(3):261-8.

562.   Tseng SY, Otsuji M, Gorski K, Huang X, Slansky JE, Pai SI, et al. B7-DC, a new dendritic cell molecule with potent costimulatory properties for T cells. J Exp Med. 2001;193(7):839-46.

563.   Latchman Y, Wood CR, Chernova T, Chaudhary D, Borde M, Chernova I, et al. PD-L2 is a second ligand for PD-1 and inhibits T cell activation. Nat Immunol. 2001;2(3):261-8.

564.   Messal N, Serriari NE, Pastor S, Nunès JA, Olive D. PD-L2 is expressed on activated human T cells and regulates their function. Mol Immunol. 2011;48(15-16):2214-9.

565.   Keir ME. Tissue expression of PD-L1 mediates peripheral T cell tolerance. J Exp Med. 2006;203:883-95.

566.   Dong H, Zhu G, Tamada K, Chen L. B7-H1, a third member of the B7 family, co-stimulates T-cell proliferation and interleukin-10 secretion. Nat Med. 1999;5(12):1365-9.

567.   Tamura H, Dong H, Zhu G, Sica GL, Flies DB, Tamada K, et al. B7-H1 costimulation preferentially enhances CD28-independent T-helper cell function. Blood. 2001;97(6):1809-16.

568.   Shin T, Yoshimura K, Crafton EB, Tsuchiya H, Housseau F, Koseki H, et al. In vivo costimulatory role of B7-DC in tuning T helper cell 1 and cytotoxic T lymphocyte responses. J Exp Med. 2005;201(10):1531-41.

569.   Wang S, Bajorath J, Flies DB, Dong H, Honjo T, Chen L. Molecular modeling and functional mapping of B7-H1 and B7-DC uncouple costimulatory function from PD-1 interaction. J Exp Med. 2003;197(9):1083-91.

570.   Shin T, Kennedy G, Gorski K, Tsuchiya H, Koseki H, Azuma M, et al. Cooperative B7-1/2 (CD80/CD86) and B7-DC costimulation of CD4+ T cells independent of the PD-1 receptor. J Exp Med. 2003;198(1):31-8.

571.   Butte MJ, Keir ME, Phamduy TB, Sharpe AH, Freeman GJ. Programmed death-1 ligand 1 interacts specifically with the B7–1 costimulatory molecule to inhibit T cell responses. Immunity. 2007;27:111-22.

572.   Park JJ, Omiya R, Matsumura Y, Sakoda Y, Kuramasu A, Augustine MM, et al. B7-H1/CD80 interaction is required for the induction and maintenance of peripheral T-cell tolerance. Blood. 2010;116(8):1291-8.

573.   Butte MJ, Keir ME, Phamduy TB, Sharpe AH, Freeman GJ. Programmed death-1 ligand 1 interacts specifically with the B7-1 costimulatory molecule to inhibit T cell responses. Immunity. 2007;27(1):111-22.

574.   Chaudhri A, Xiao Y, Klee AN, Wang X, Zhu B, Freeman GJ. PD-L1 Binds to B7-1 Only. Cancer Immunol Res. 2018;6(8):921-9.

575.   Sugiura D, Maruhashi T, Okazaki IM, Shimizu K, Maeda TK, Takemoto T, et al. Restriction of PD-1 function by. Science. 2019;364(6440):558-66.

576.   Mazzarella G, Bianco A, Catena E, De Palma R, Abbate GF. Th1/Th2 lymphocyte polarization in asthma. Allergy. 2000;55 Suppl 61:6-9.

577.   Akbari O, Stock P, Singh AK, Lombardi V, Lee WL, Freeman GJ, et al. PD-L1 and PD-L2 modulate airway inflammation and iNKT-cell-dependent airway hyperreactivity in opposing directions. Mucosal Immunol. 2009;3(1):81-91.

578.   Nie X, Chen W, Zhu Y, Huang B, Yu W, Wu Z, et al. B7-DC (PD-L2) costimulation of CD4$^+$ T-helper 1 response via RGMb. Cell Mol Immunol. 2018;15(10):888-97.

579.   Chemnitz JM, Parry RV, Nichols KE, June CH, Riley JL. SHP-1 and SHP-2 associate with immunoreceptor tyrosine-based switch motif of programmed death 1 upon primary human T cell stimulation, but only receptor ligation prevents T cell activation. J Immunol. 2004;173(2):945-54.

580.   Yokosuka T, Takamatsu M, Kobayashi-Imanishi W, Hashimoto-Tane A, Azuma M, Saito T. Programmed cell death 1 forms negative costimulatory microclusters that directly inhibit T cell receptor signaling by recruiting phosphatase SHP2. J Exp Med. 2012;209(6):1201-17.

581.   Sheppard KA, Fitz LJ, Lee JM, Benander C, George JA, Wooters J, et al. PD-1 inhibits T-cell receptor induced phosphorylation of the ZAP70/CD3zeta signalosome and downstream signaling to PKCtheta. FEBS Lett. 2004;574(1-3):37-41.

582.   Bardhan K, Patsoukis N, Sari D, Anagnostou T, Chatterjee P, Freeman GJ, et al. PD-1 Inhibits TCR Proximal Signaling By Sequestering SHP-2 Phosphatase and Facilitating Csk-Mediated Inhibitory Phosphorylation of Lck. Blood. 2015;126(23):283-.

583.   Patsoukis N, Li L, Sari D, Petkova V, Boussiotis VA. PD-1 increases PTEN phosphatase activity while decreasing PTEN protein stability by inhibiting casein kinase 2. Mol Cell Biol. 2013;33(16):3091-8.

584.   Patsoukis N, Brown J, Petkova V, Liu F, Li L, Boussiotis VA. Selective effects of PD-1 on Akt and Ras pathways regulate molecular components of the cell cycle and inhibit T cell proliferation. Sci Signal. 2012;5(230):ra46.

585.   Parry RV, Chemnitz JM, Frauwirth KA, Lanfranco AR, Braunstein I, Kobayashi SV, et al. CTLA-4 and PD-1 receptors inhibit T-cell activation by distinct mechanisms. Mol Cell Biol. 2005;25:9543-53.

586.   Gibbons RM, Liu X, Pulko V, Harrington SM, Krco CJ, Kwon ED, et al. B7-H1 limits the entry of effector CD8(+) T cells to the memory pool by upregulating Bim. OncoImmunology. 2012;1(7):1061-73.

587.   Karwacz K, Bricogne C, MacDonald D, Arce F, Bennett CL, Collins M, et al. PD-L1 co-stimulation contributes to ligand-induced T cell receptor down-modulation on CD8+ T cells. EMBO Mol Med. 2011;3(10):581-92.

588.   Francisco LM, Salinas VH, Brown KE, Vanguri VK, Freeman GJ, Kuchroo VK, et al. PD-L1 regulates the development, maintenance, and function of induced regulatory T cells. J Exp Med. 2009;206(13):3015-29.

589.   Triebel F, Jitsukawa S, Baixeras E, Roman-Roman S, Genevee C, Viegas-Pequignot E, et al. LAG-3, a novel lymphocyte activation gene closely related to CD4. J Exp Med. 1990;171(5):1393-405.

590.   Workman CJ, Vignali DA. The CD4-related molecule, LAG-3 (CD223), regulates the expansion of activated T cells. Eur J Immunol. 2003;33(4):970-9.

591.   Kisielow M, Kisielow J, Capoferri-Sollami G, Karjalainen K. Expression of lymphocyte activation gene 3 (LAG-3) on B cells is induced by T cells. Eur J Immunol. 2005;35(7):2081-8.

592.   Workman CJ, Wang Y, El Kasmi KC, Pardoll DM, Murray PJ, Drake CG, et al. LAG-3 regulates plasmacytoid dendritic cell homeostasis. J Immunol. 2009;182(4):1885-91.

593.   Huard B, Prigent P, Tournier M, Bruniquel D, Triebel F. CD4/major histocompatibility complex class II interaction analyzed with CD4- and lymphocyte activation gene-3 (LAG-3)-Ig fusion proteins. Eur J Immunol. 1995;25(9):2718-21.

594.   Xu F, Liu J, Liu D, Liu B, Wang M, Hu Z, et al. LSECtin expressed on melanoma cells promotes tumor progression by inhibiting antitumor T-cell responses. Cancer Res. 2014;74(13):3418-28.

595.   Wang J, Sanmamed MF, Datar I, Su TT, Ji L, Sun J, et al. Fibrinogen-like Protein 1 Is a Major Immune Inhibitory Ligand of LAG-3. Cell. 2019;176(1-2):334-47.e12.

596.   Huard B, Tournier M, Hercend T, Triebel F, Faure F. Lymphocyte-activation gene 3/major histocompatibility complex class II interaction modulates the antigenic response of CD4+ T lymphocytes. Eur J Immunol. 1994;24(12):3216-21.

597.   Workman CJ, Dugger KJ, Vignali DA. Cutting edge: molecular analysis of the negative regulatory function of lymphocyte activation gene-3. J Immunol. 2002;169(10):5392-5.

598.   Workman CJ, Rice DS, Dugger KJ, Kurschner C, Vignali DA. Phenotypic analysis of the murine CD4-related glycoprotein, CD223 (LAG-3). Eur J Immunol. 2002;32(8):2255-63.

599.   Workman CJ, Cauley LS, Kim IJ, Blackman MA, Woodland DL, Vignali DA. Lymphocyte activation gene-3 (CD223) regulates the size of the expanding T cell population following antigen activation in vivo. J Immunol. 2004;172(9):5450-5.

600.   Workman CJ, Vignali DA. Negative regulation of T cell homeostasis by lymphocyte activation gene-3 (CD223). J Immunol. 2005;174(2):688-95.

601.   Camisaschi C, Casati C, Rini F, Perego M, De Filippo A, Triebel F, et al. LAG-3 expression defines a subset of CD4(+)CD25(high)Foxp3(+) regulatory T cells that are expanded at tumor sites. J Immunol. 2010;184(11):6545-51.

602.   Gagliani N, Magnani CF, Huber S, Gianolini ME, Pala M, Licona-Limon P, et al. Coexpression of CD49b and LAG-3 identifies human and mouse T regulatory type 1 cells. Nat Med. 2013;19(6):739-46.

603.   Huang CT, Workman CJ, Flies D, Pan X, Marson AL, Zhou G, et al. Role of LAG-3 in regulatory T cells. Immunity. 2004;21(4):503-13.

604.   Andreae S, Piras F, Burdin N, Triebel F. Maturation and activation of dendritic cells induced by lymphocyte activation gene-3 (CD223). J Immunol. 2002;168(8):3874-80.

605.   Woo SR, Turnis ME, Goldberg MV, Bankoti J, Selby M, Nirschl CJ, et al. Immune inhibitory molecules LAG-3 and PD-1 synergistically regulate T-cell function to promote tumoral immune escape. Cancer Res. 2012;72(4):917-27.

606.   Matsuzaki J, Gnjatic S, Mhawech-Fauceglia P, Beck A, Miller A, Tsuji T, et al. Tumor-infiltrating NY-ESO-1-specific CD8+ T cells are negatively regulated by LAG-3 and PD-1 in human ovarian cancer. Proc Natl Acad Sci U S A. 2010;107(17):7875-80.

607.   Monney L, Sabatos CA, Gaglia JL, Ryu A, Waldner H, Chernova T, et al. Th1-specific cell surface protein Tim-3 regulates macrophage activation and severity of an autoimmune disease. Nature. 2002;415(6871):536-41.

608.   Lee J, Su EW, Zhu C, Hainline S, Phuah J, Moroco JA, et al. Phosphotyrosine-dependent coupling of Tim-3 to T-cell receptor signaling pathways. Mol Cell Biol. 2011;31(19):3963-74.

609.   van de Weyer PS, Muehlfeit M, Klose C, Bonventre JV, Walz G, Kuehn EW. A highly conserved tyrosine of Tim-3 is phosphorylated upon stimulation by its ligand galectin-9. Biochem Biophys Res Commun. 2006;351(2):571-6.

610.   Hastings WD, Anderson DE, Kassam N, Koguchi K, Greenfield EA, Kent SC, et al. TIM-3 is expressed on activated human CD4+ T cells and regulates Th1 and Th17 cytokines. Eur J Immunol. 2009;39(9):2492-501.

611.   Gao X, Zhu Y, Li G, Huang H, Zhang G, Wang F, et al. TIM-3 expression characterizes regulatory T cells in tumor tissues and is associated with lung cancer progression. PLoS One. 2012;7(2):e30676.

612.   Gleason MK, Lenvik TR, McCullar V, Felices M, O'Brien MS, Cooley SA, et al. Tim-3 is an inducible human natural killer cell receptor that enhances interferon gamma production in response to galectin-9. Blood. 2012;119(13):3064-72.

613.   Anderson AC, Anderson DE, Bregoli L, Hastings WD, Kassam N, Lei C, et al. Promotion of tissue inflammation by the immune receptor Tim-3 expressed on innate immune cells. Science. 2007;318(5853):1141-3.

614.   Ocaña-Guzman R, Torre-Bouscoulet L, Sada-Ovalle I. TIM-3 Regulates Distinct Functions in Macrophages. Front Immunol. 2016;7:229.

615.   Jin HT, Anderson AC, Tan WG, West EE, Ha SJ, Araki K, et al. Cooperation of Tim-3 and PD-1 in CD8 T-cell exhaustion during chronic viral infection. Proc Natl Acad Sci U S A. 2010;107(33):14733-8.

616.   Yang ZZ, Grote DM, Ziesmer SC, Niki T, Hirashima M, Novak AJ, et al. IL-12 upregulates TIM-3 expression and induces T cell exhaustion in patients with follicular B cell non-Hodgkin lymphoma. J Clin Invest. 2012;122(4):1271-82.

617.   Fourcade J, Sun Z, Benallaoua M, Guillaume P, Luescher IF, Sander C, et al. Upregulation of Tim-3 and PD-1 expression is associated with tumor antigen-specific CD8+ T cell dysfunction in melanoma patients. J Exp Med. 2010;207(10):2175-86.

618.   Sakuishi K, Apetoh L, Sullivan JM, Blazar BR, Kuchroo VK, Anderson AC. Targeting Tim-3 and PD-1 pathways to reverse T cell exhaustion and restore anti-tumor immunity. J Exp Med. 2010;207(10):2187-94.

619.   Nakayama M, Akiba H, Takeda K, Kojima Y, Hashiguchi M, Azuma M, et al. Tim-3 mediates phagocytosis of apoptotic cells and cross-presentation. Blood. 2009;113(16):3821-30.

620.   Chiba S, Baghdadi M, Akiba H, Yoshiyama H, Kinoshita I, Dosaka-Akita H, et al. Tumor-infiltrating DCs suppress nucleic acid-mediated innate immune responses through interactions between the receptor TIM-3 and the alarmin HMGB1. Nat Immunol. 2012;13(9):832-42.

621.   Zhu C, Anderson AC, Schubart A, Xiong H, Imitola J, Khoury SJ, et al. The Tim-3 ligand galectin-9 negatively regulates T helper type 1 immunity. Nat Immunol. 2005;6(12):1245-52.

622.   Tomkowicz B, Walsh E, Cotty A, Verona R, Sabins N, Kaplan F, et al. TIM-3 Suppresses Anti-CD3/CD28-Induced TCR Activation and IL-2 Expression through the NFAT Signaling Pathway. PLoS One. 2015;10(10):e0140694.

623.   Clayton KL, Haaland MS, Douglas-Vail MB, Mujib S, Chew GM, Ndhlovu LC, et al. T cell Ig and mucin domain-containing protein 3 is recruited to the immune synapse, disrupts stable synapse formation, and associates with receptor phosphatases. J Immunol. 2014;192(2):782-91.

624.   Sabatos CA, Chakravarti S, Cha E, Schubart A, Sánchez-Fueyo A, Zheng XX, et al. Interaction of Tim-3 and Tim-3 ligand regulates T helper type 1 responses and induction of peripheral tolerance. Nat Immunol. 2003;4(11):1102-10.

625.   Sánchez-Fueyo A, Tian J, Picarella D, Domenig C, Zheng XX, Sabatos CA, et al. Tim-3 inhibits T helper type 1-mediated auto- and alloimmune responses and promotes immunological tolerance. Nat Immunol. 2003;4(11):1093-101.

626.   Boenisch O, D'Addio F, Watanabe T, Elyaman W, Magee CN, Yeung MY, et al. TIM-3: a novel regulatory molecule of alloimmune activation. J Immunol. 2010;185(10):5806-19.

627.   Veenstra RG, Taylor PA, Zhou Q, Panoskaltsis-Mortari A, Hirashima M, Flynn R, et al. Contrasting acute graft-versus-host disease effects of Tim-3/galectin-9 pathway blockade dependent upon the presence of donor regulatory T cells. Blood. 2012;120(3):682-90.

628.   Huang YH, Zhu C, Kondo Y, Anderson AC, Gandhi A, Russell A, et al. CEACAM1 regulates TIM-3-mediated tolerance and exhaustion. Nature. 2015;517(7534):386-90.

629.   Rangachari M, Zhu C, Sakuishi K, Xiao S, Karman J, Chen A, et al. Bat3 promotes T cell responses and autoimmunity by repressing Tim-3–mediated cell death and exhaustion. Nat Med. 2012;18(9):1394-400.

630.   Guthmann MD, Tal M, Pecht I. A secretion inhibitory signal transduction molecule on mast cells is another C-type lectin. Proc Natl Acad Sci U S A. 1995;92(20):9397-401.

631.   Blaser C, Kaufmann M, Pircher H. Virus-activated CD8 T cells and lymphokine-activated NK cells express the mast cell function-associated antigen, an inhibitory C-type lectin. J Immunol. 1998;161(12):6451-4.

632.   Voehringer D, Koschella M, Pircher H. Lack of proliferative capacity of human effector and memory T cells expressing killer cell lectinlike receptor G1 (KLRG1). Blood. 2002;100(10):3698-702.

633.   Eberl M, Engel R, Aberle S, Fisch P, Jomaa H, Pircher H. Human Vgamma9/Vdelta2 effector memory T cells express the killer cell lectin-like receptor G1 (KLRG1). J Leukoc Biol. 2005;77(1):67-70.

634.   Henson SM, Akbar AN. KLRG1--more than a marker for T cell senescence. Age (Dordr). 2009;31(4):285-91.

635.   Greenberg SA, Kong SW, Thompson E, Gulla SV. Co-inhibitory T cell receptor KLRG1: human cancer expression and efficacy of neutralization in murine cancer models. Oncotarget. 2019;10(14):1399-406.

636.   Bengsch B, Seigel B, Ruhl M, Timm J, Kuntz M, Blum HE, et al. Coexpression of PD-1, 2B4, CD160 and KLRG1 on exhausted HCV-specific CD8+ T cells is linked to antigen recognition and T cell differentiation. PLoS Pathog. 2010;6(6):e1000947.

637.   Gründemann C, Bauer M, Schweier O, von Oppen N, Lässing U, Saudan P, et al. Cutting edge: identification of E-cadherin as a ligand for the murine killer cell lectin-like receptor G1. J Immunol. 2006;176(3):1311-5.

638.   Ito M, Maruyama T, Saito N, Koganei S, Yamamoto K, Matsumoto N. Killer cell lectin-like receptor G1 binds three members of the classical cadherin family to inhibit NK cell cytotoxicity. J Exp Med. 2006;203(2):289-95.

639.   Schwartzkopff S, Gründemann C, Schweier O, Rosshart S, Karjalainen KE, Becker KF, et al. Tumor-associated E-cadherin mutations affect binding to the killer cell lectin-like receptor G1 in humans. J Immunol. 2007;179(2):1022-9.

640.   Gloushankova NA, Rubtsova SN, Zhitnyak IY. Cadherin-mediated cell-cell interactions in normal and cancer cells. Tissue Barriers. 2017;5(3):e1356900.

641.   Van den Bossche J, Malissen B, Mantovani A, De Baetselier P, Van Ginderachter JA. Regulation and function of the E-cadherin/catenin complex in cells of the monocyte-macrophage lineage and DCs. Blood. 2012;119(7):1623-33.

642.   Rosshart S, Hofmann M, Schweier O, Pfaff AK, Yoshimoto K, Takeuchi T, et al. Interaction of KLRG1 with E-cadherin: new functional and structural insights. Eur J Immunol. 2008;38(12):3354-64.

643.   Robbins SH, Nguyen KB, Takahashi N, Mikayama T, Biron CA, Brossay L. Cutting edge: inhibitory functions of the killer cell lectin-like receptor G1 molecule during the activation of mouse NK cells. J Immunol. 2002;168(6):2585-9.

644.	Müller-Durovic B, Lanna A, Covre LP, Mills RS, Henson SM, Akbar AN. Killer Cell Lectin-like Receptor G1 Inhibits NK Cell Function through Activation of Adenosine 5'-Monophosphate-Activated Protein Kinase. J Immunol. 2016;197(7):2891-9.
645.	Beyersdorf NB, Ding X, Karp K, Hanke T. Expression of inhibitory "killer cell lectin-like receptor G1" identifies unique subpopulations of effector and memory CD8 T cells. Eur J Immunol. 2001;31(12):3443-52.
646.	Tessmer MS, Fugere C, Stevenaert F, Naidenko OV, Chong HJ, Leclercq G, et al. KLRG1 binds cadherins and preferentially associates with SHIP-1. Int Immunol. 2007;19(4):391-400.
647.	Henson SM, Franzese O, Macaulay R, Libri V, Azevedo RI, Kiani-Alikhan S, et al. KLRG1 signaling induces defective Akt (ser473) phosphorylation and proliferative dysfunction of highly differentiated CD8+ T cells. Blood. 2009;113(26):6619-28.
648.	Li L, Wan S, Tao K, Wang G, Zhao E. KLRG1 restricts memory T cell antitumor immunity. Oncotarget. 2016;7(38):61670-8.
649.	Xu R, Abramson J, Fridkin M, Pecht I. SH2 domain-containing inositol polyphosphate 5'-phosphatase is the main mediator of the inhibitory action of the mast cell function-associated antigen. J Immunol. 2001;167(11):6394-402.
650.	Nakajima H, Cella M, Langen H, Friedlein A, Colonna M. Activating interactions in human NK cell recognition: the role of 2B4-CD48. Eur J Immunol. 1999;29(5):1676-83.
651.	Valiante NM, Trinchieri G. Identification of a novel signal transduction surface molecule on human cytotoxic lymphocytes. J Exp Med. 1993;178(4):1397-406.
652.	Boles KS, Nakajima H, Colonna M, Chuang SS, Stepp SE, Bennett M, et al. Molecular characterization of a novel human natural killer cell receptor homologous to mouse 2B4. Tissue Antigens. 1999;54(1):27-34.
653.	Romero X, Benítez D, March S, Vilella R, Miralpeix M, Engel P. Differential expression of SAP and EAT-2-binding leukocyte cell-surface molecules CD84, CD150 (SLAM), CD229 (Ly9) and CD244 (2B4). Tissue Antigens. 2004;64(2):132-44.
654.	Munitz A, Bachelet I, Fraenkel S, Katz G, Mandelboim O, Simon HU, et al. 2B4 (CD244) is expressed and functional on human eosinophils. J Immunol. 2005;174(1):110-8.
655.	Boles KS, Stepp SE, Bennett M, Kumar V, Mathew PA. 2B4 (CD244) and CS1: novel members of the CD2 subset of the immunoglobulin superfamily molecules expressed on natural killer cells and other leukocytes. Immunol Rev. 2001;181:234-49.
656.	Kubota K. A structurally variant form of the 2B4 antigen is expressed on the cell surface of mouse mast cells. Microbiol Immunol. 2002;46(8):589-92.
657.	Kambayashi T, Assarsson E, Chambers BJ, Ljunggren HG. Cutting edge: Regulation of CD8(+) T cell proliferation by 2B4/CD48 interactions. J Immunol. 2001;167(12):6706-10.
658.	van Driel BJ, Liao G, Engel P, Terhorst C. Responses to Microbial Challenges by SLAMF Receptors. Front Immunol. 2016;7:4.
659.	Latchman Y, McKay PF, Reiser H. Identification of the 2B4 molecule as a counter-receptor for CD48. J Immunol. 1998;161(11):5809-12.
660.	Brown MH, Boles K, van der Merwe PA, Kumar V, Mathew PA, Barclay AN. 2B4, the natural killer and T cell immunoglobulin superfamily surface protein, is a ligand for CD48. J Exp Med. 1998;188(11):2083-90.
661.	Kato K, Koyanagi M, Okada H, Takanashi T, Wong YW, Williams AF, et al. CD48 is a counter-receptor for mouse CD2 and is involved in T cell activation. J Exp Med. 1992;176(5):1241-9.
662.	Thorley-Lawson DA, Schooley RT, Bhan AK, Nadler LM. Epstein-Barr virus superinduces a new human B cell differentiation antigen (B-LAST 1) expressed on transformed lymphoblasts. Cell. 1982;30(2):415-25.
663.	Yokoyama S, Staunton D, Fisher R, Amiot M, Fortin JJ, Thorley-Lawson DA. Expression of the Blast-1 activation/adhesion molecule and its identification as CD48. J Immunol. 1991;146(7):2192-200.
664.	Kubin MZ, Parshley DL, Din W, Waugh JY, Davis-Smith T, Smith CA, et al. Molecular cloning and biological characterization of NK cell activation-inducing ligand, a counterstructure for CD48. Eur J Immunol. 1999;29(11):3466-77.
665.	Claus M, Meinke S, Bhat R, Watzl C. Regulation of NK cell activity by 2B4, NTB-A and CRACC. Front Biosci. 2008;13:956-65.
666.	Lee KM, Bhawan S, Majima T, Wei H, Nishimura MI, Yagita H, et al. Cutting edge: the NK cell receptor 2B4 augments antigen-specific T cell cytotoxicity through CD48 ligation on neighboring T cells. J Immunol. 2003;170(10):4881-5.
667.	Mooney JM, Klem J, Wülfing C, Mijares LA, Schwartzberg PL, Bennett M, et al. The murine NK receptor 2B4 (CD244) exhibits inhibitory function independent of signaling lymphocytic activation molecule-associated protein expression. J Immunol. 2004;173(6):3953-61.
668.	Lee KM, McNerney ME, Stepp SE, Mathew PA, Schatzle JD, Bennett M, et al. 2B4 acts as a non-major histocompatibility complex binding inhibitory receptor on mouse natural killer cells. J Exp Med. 2004;199(9):1245-54.
669.	Vaidya SV, Stepp SE, McNerney ME, Lee JK, Bennett M, Lee KM, et al. Targeted disruption of the 2B4 gene in mice reveals an in vivo role of 2B4 (CD244) in the rejection of B16 melanoma cells. J Immunol. 2005;174(2):800-7.
670.	Assarsson E, Kambayashi T, Schatzle JD, Cramer SO, von Bonin A, Jensen PE, et al. NK cells stimulate proliferation of T and NK cells through 2B4/CD48 interactions. J Immunol. 2004;173(1):174-80.

671.   Laurie SJ, Liu D, Wagener ME, Stark PC, Terhorst C, Ford ML. 2B4 Mediates Inhibition of CD8 +T Cell Responses via Attenuation of Glycolysis and Cell Division. J Immunol. 2018;201(5):1536-48.

672.   Liu D, Suchard SJ, Nadler SG, Ford ML. Inhibition of Donor-Reactive CD8+ T Cell Responses by Selective CD28 Blockade Is Independent of Reduced ICOS Expression. PLoS One. 2015;10(6):e0130490.

673.   Stepp SE, Schatzle JD, Bennett M, Kumar V, Mathew PA. Gene structure of the murine NK cell receptor 2B4: presence of two alternatively spliced isoforms with distinct cytoplasmic domains. Eur J Immunol. 1999;29(8):2392-9.

674.   Schatzle JD, Sheu S, Stepp SE, Mathew PA, Bennett M, Kumar V. Characterization of inhibitory and stimulatory forms of the murine natural killer cell receptor 2B4. Proc Natl Acad Sci U S A. 1999;96(7):3870-5.

675.   Chen R, Relouzat F, Roncagalli R, Aoukaty A, Tan R, Latour S, et al. Molecular dissection of 2B4 signaling: implications for signal transduction by SLAM-related receptors. Mol Cell Biol. 2004;24(12):5144-56.

676.   Eissmann P, Beauchamp L, Wooters J, Tilton JC, Long EO, Watzl C. Molecular basis for positive and negative signaling by the natural killer cell receptor 2B4 (CD244). Blood. 2005;105(12):4722-9.

677.   Parolini S, Bottino C, Falco M, Augugliaro R, Giliani S, Franceschini R, et al. X-linked lymphoproliferative disease. 2B4 molecules displaying inhibitory rather than activating function are responsible for the inability of natural killer cells to kill Epstein-Barr virus-infected cells. J Exp Med. 2000;192(3):337-46.

678.   Cannons JL, Tangye SG, Schwartzberg PL. SLAM family receptors and SAP adaptors in immunity. Annu Rev Immunol. 2011;29:665-705.

679.   Watzl C, Long EO. Natural killer cell inhibitory receptors block actin cytoskeleton-dependent recruitment of 2B4 (CD244) to lipid rafts. J Exp Med. 2003;197(1):77-85.

680.   Klem J, Verrett PC, Kumar V, Schatzle JD. 2B4 is constitutively associated with linker for the activation of T cells in glycolipid-enriched microdomains: properties required for 2B4 lytic function. J Immunol. 2002;169(1):55-62.

681.   West EE, Youngblood B, Tan WG, Jin HT, Araki K, Alexe G, et al. Tight regulation of memory CD8(+) T cells limits their effectiveness during sustained high viral load. Immunity. 2011;35(2):285-98.

682.   Hilmenyuk T, Ruckstuhl CA, Hayoz M, Berchtold C, Nuoffer JM, Solanki S, et al. T cell inhibitory mechanisms in a model of aggressive Non-Hodgkin's Lymphoma. Oncoimmunology. 2017;7(1):e1365997.

683.   Yu X, Harden K, Gonzalez LC, Francesco M, Chiang E, Irving B, et al. The surface protein TIGIT suppresses T cell activation by promoting the generation of mature immunoregulatory dendritic cells. Nat Immunol. 2009;10(1):48-57.

684.   Levin SD, Taft DW, Brandt CS, Bucher C, Howard ED, Chadwick EM, et al. Vstm3 is a member of the CD28 family and an important modulator of T-cell function. Eur J Immunol. 2011;41(4):902-15.

685.   Wang PL, O'Farrell S, Clayberger C, Krensky AM. Identification and molecular cloning of tactile. A novel human T cell activation antigen that is a member of the Ig gene superfamily. J Immunol. 1992;148(8):2600-8.

686.   Meyer D, Seth S, Albrecht J, Maier MK, du Pasquier L, Ravens I, et al. CD96 interaction with CD155 via its first Ig-like domain is modulated by alternative splicing or mutations in distal Ig-like domains. J Biol Chem. 2009;284(4):2235-44.

687.   Shibuya K, Shirakawa J, Kameyama T, Honda S, Tahara-Hanaoka S, Miyamoto A, et al. CD226 (DNAM-1) is involved in lymphocyte function-associated antigen 1 costimulatory signal for naive T cell differentiation and proliferation. J Exp Med. 2003;198(12):1829-39.

688.   Tahara-Hanaoka S, Shibuya K, Onoda Y, Zhang H, Yamazaki S, Miyamoto A, et al. Functional characterization of DNAM-1 (CD226) interaction with its ligands PVR (CD155) and nectin-2 (PRR-2/CD112). Int Immunol. 2004;16(4):533-8.

689.   Seth S, Maier MK, Qiu Q, Ravens I, Kremmer E, Förster R, et al. The murine pan T cell marker CD96 is an adhesion receptor for CD155 and nectin-1. Biochem Biophys Res Commun. 2007;364(4):959-65.

690.   Boles KS, Vermi W, Facchetti F, Fuchs A, Wilson TJ, Diacovo TG, et al. A novel molecular interaction for the adhesion of follicular CD4 T cells to follicular DC. Eur J Immunol. 2009;39(3):695-703.

691.   Stanietsky N, Simic H, Arapovic J, Toporik A, Levy O, Novik A, et al. The interaction of TIGIT with PVR and PVRL2 inhibits human NK cell cytotoxicity. Proc Natl Acad Sci U S A. 2009;106(42):17858-63.

692.   Wu H, Chen Y, Liu H, Xu LL, Teuscher P, Wang S, et al. Follicular regulatory T cells repress cytokine production by follicular helper T cells and optimize IgG responses in mice. Eur J Immunol. 2016;46(5):1152-61.

693.   Pende D, Castriconi R, Romagnani P, Spaggiari GM, Marcenaro S, Dondero A, et al. Expression of the DNAM-1 ligands, Nectin-2 (CD112) and poliovirus receptor (CD155), on dendritic cells: relevance for natural killer-dendritic cell interaction. Blood. 2006;107(5):2030-6.

694.   Chauvin JM, Pagliano O, Fourcade J, Sun Z, Wang H, Sander C, et al. TIGIT and PD-1 impair tumor antigen-specific CD8^{+} T cells in melanoma patients. J Clin Invest. 2015;125(5):2046-58.

695.   Chan CJ, Martinet L, Gilfillan S, Souza-Fonseca-Guimaraes F, Chow MT, Town L, et al. The receptors CD96 and CD226 oppose each other in the regulation of natural killer cell functions. Nat Immunol. 2014;15(5):431-8.

696.   Stanietsky N, Rovis TL, Glasner A, Seidel E, Tsukerman P, Yamin R, et al. Mouse TIGIT inhibits NK-cell cytotoxicity upon interaction with PVR. Eur J Immunol. 2013;43(8):2138-50.

697.   Wang F, Hou H, Wu S, Tang Q, Liu W, Huang M, et al. TIGIT expression levels on human NK cells correlate with functional heterogeneity among healthy individuals. Eur J Immunol. 2015;45(10):2886-97.

698.   Fuchs A, Cella M, Giurisato E, Shaw AS, Colonna M. Cutting edge: CD96 (tactile) promotes NK cell-target cell adhesion by interacting with the poliovirus receptor (CD155). J Immunol. 2004;172(7):3994-8.

699.   Johnston RJ, Comps-Agrar L, Hackney J, Yu X, Huseni M, Yang Y, et al. The immunoreceptor TIGIT regulates antitumor and antiviral CD8(+) T cell effector function. Cancer Cell. 2014;26(6):923-37.

700.   Kurtulus S, Sakuishi K, Ngiow SF, Joller N, Tan DJ, Teng MW, et al. TIGIT predominantly regulates the immune response via regulatory T cells. J Clin Invest. 2015;125(11):4053-62.

701.   Kong Y, Zhu L, Schell TD, Zhang J, Claxton DF, Ehmann WC, et al. T-Cell Immunoglobulin and ITIM Domain (TIGIT) Associates with CD8+ T-Cell Exhaustion and Poor Clinical Outcome in AML Patients. Clin Cancer Res. 2016;22(12):3057-66.

702.   Liu S, Zhang H, Li M, Hu D, Li C, Ge B, et al. Recruitment of Grb2 and SHIP1 by the ITT-like motif of TIGIT suppresses granule polarization and cytotoxicity of NK cells. Cell Death Differ. 2013;20(3):456-64.

703.   Li M, Xia P, Du Y, Liu S, Huang G, Chen J, et al. T-cell immunoglobulin and ITIM domain (TIGIT) receptor/poliovirus receptor (PVR) ligand engagement suppresses interferon-γ production of natural killer cells via β-arrestin 2-mediated negative signaling. J Biol Chem. 2014;289(25):17647-57.

704.   Montgomery RI, Warner MS, Lum BJ, Spear PG. Herpes simplex virus-1 entry into cells mediated by a novel member of the TNF/NGF receptor family. Cell. 1996;87(3):427-36.

705.   Granger SW, Ware CF. Turning on LIGHT. J Clin Invest. 2001;108(12):1741-2.

706.   Morel Y, Truneh A, Sweet RW, Olive D, Costello RT. The TNF superfamily members LIGHT and CD154 (CD40 ligand) costimulate induction of dendritic cell maturation and elicit specific CTL activity. J Immunol. 2001;167(5):2479-86.

707.   Duhen T, Pasero C, Mallet F, Barbarat B, Olive D, Costello RT. LIGHT costimulates CD40 triggering and induces immunoglobulin secretion; a novel key partner in T cell-dependent B cell terminal differentiation. Eur J Immunol. 2004;34(12):3534-41.

708.   Harrop JA, Reddy M, Dede K, Brigham-Burke M, Lyn S, Tan KB, et al. Antibodies to TR2 (herpesvirus entry mediator), a new member of the TNF receptor superfamily, block T cell proliferation, expression of activation markers, and production of cytokines. J Immunol. 1998;161(4):1786-94.

709.   Harrop JA, McDonnell PC, Brigham-Burke M, Lyn SD, Minton J, Tan KB, et al. Herpesvirus entry mediator ligand (HVEM-L), a novel ligand for HVEM/TR2, stimulates proliferation of T cells and inhibits HT29 cell growth. J Biol Chem. 1998;273(42):27548-56.

710.   Tamada K, Shimozaki K, Chapoval AI, Zhai Y, Su J, Chen SF, et al. LIGHT, a TNF-like molecule, costimulates T cell proliferation and is required for dendritic cell-mediated allogeneic T cell response. J Immunol. 2000;164(8):4105-10.

711.   Mauri DN, Ebner R, Montgomery RI, Kochel KD, Cheung TC, Yu GL, et al. LIGHT, a new member of the TNF superfamily, and lymphotoxin alpha are ligands for herpesvirus entry mediator. Immunity. 1998;8(1):21-30.

712.   Nelson CA, Fremont MD, Sedy JR, Norris PS, Ware CF, Murphy KM, et al. Structural determinants of herpesvirus entry mediator recognition by murine B and T lymphocyte attenuator. J Immunol. 2008;180(2):940-7.

713.   Gavrieli M, Watanabe N, Loftin SK, Murphy TL, Murphy KM. Characterization of phosphotyrosine binding motifs in the cytoplasmic domain of B and T lymphocyte attenuator required for association with protein tyrosine phosphatases SHP-1 and SHP-2. Biochem Biophys Res Commun. 2003;312(4):1236-43.

714.   Watanabe N, Gavrieli M, Sedy JR, Yang J, Fallarino F, Loftin SK, et al. BTLA is a lymphocyte inhibitory receptor with similarities to CTLA-4 and PD-1. Nat Immunol. 2003;4(7):670-9.

715.   Han P, Goularte OD, Rufner K, Wilkinson B, Kaye J. An inhibitory Ig superfamily protein expressed by lymphocytes and APCs is also an early marker of thymocyte positive selection. J Immunol. 2004;172(10):5931-9.

716.   Otsuki N, Kamimura Y, Hashiguchi M, Azuma M. Expression and function of the B and T lymphocyte attenuator (BTLA/CD272) on human T cells. Biochem Biophys Res Commun. 2006;344(4):1121-7.

717.   Krieg C, Han P, Stone R, Goularte OD, Kaye J. Functional analysis of B and T lymphocyte attenuator engagement on CD4+ and CD8+ T cells. J Immunol. 2005;175(10):6420-7.

718.   Wang XF, Chen YJ, Wang Q, Ge Y, Dai Q, Yang KF, et al. Distinct expression and inhibitory function of B and T lymphocyte attenuator on human T cells. Tissue Antigens. 2007;69(2):145-53.

719.   Chemnitz JM, Lanfranco AR, Braunstein I, Riley JL. B and T lymphocyte attenuator-mediated signal transduction provides a potent inhibitory signal to primary human CD4 T cells that can be initiated by multiple phosphotyrosine motifs. J Immunol. 2006;176(11):6603-14.

720.   Anumanthan A, Bensussan A, Boumsell L, Christ AD, Blumberg RS, Voss SD, et al. Cloning of BY55, a novel Ig superfamily member expressed on NK cells, CTL, and intestinal intraepithelial lymphocytes. J Immunol. 1998;161(6):2780-90.

721.   Cheung TC, Steinberg MW, Oborne LM, Macauley MG, Fukuyama S, Sanjo H, et al. Unconventional ligand activation of herpesvirus entry mediator signals cell survival. Proc Natl Acad Sci U S A. 2009;106(15):6244-9.

722.	Maïza H, Leca G, Mansur IG, Schiavon V, Boumsell L, Bensussan A. A novel 80-kD cell surface structure identifies human circulating lymphocytes with natural killer activity. J Exp Med. 1993;178(3):1121-6.

723.	Tsujimura K, Obata Y, Matsudaira Y, Nishida K, Akatsuka Y, Ito Y, et al. Characterization of murine CD160+ CD8+ T lymphocytes. Immunol Lett. 2006;106(1):48-56.

724.	Cai G, Anumanthan A, Brown JA, Greenfield EA, Zhu B, Freeman GJ. CD160 inhibits activation of human CD4+ T cells through interaction with herpesvirus entry mediator. Nat Immunol. 2008;9(2):176-85.

725.	Giustiniani J, Marie-Cardine A, Bensussan A. A soluble form of the MHC class I-specific CD160 receptor is released from human activated NK lymphocytes and inhibits cell-mediated cytotoxicity. J Immunol. 2007;178(3):1293-300.

726.	Murphy KM, Nelson CA, Sedý JR. Balancing co-stimulation and inhibition with BTLA and HVEM. Nat Rev Immunol. 2006;6(9):671-81.

727.	Wherry EJ, Ha SJ, Kaech SM, Haining WN, Sarkar S, Kalia V, et al. Molecular signature of CD8+ T cell exhaustion during chronic viral infection. Immunity. 2007;27(4):670-84.

728.	Farren TW, Giustiniani J, Liu FT, Tsitsikas DA, Macey MG, Cavenagh JD, et al. Differential and tumor-specific expression of CD160 in B-cell malignancies. Blood. 2011;118(8):2174-83.

729.	Ehrlich P. Über den jetzigen Stand der Chemotherapie. Berichte der deutschen chemischen Gesellschaft. 1909;42(1):17-47.

730.	Burnet FM. The concept of immunological surveillance. Prog Exp Tumor Res. 1970;13:1-27.

731.	Thomas L. On immunosurveillance in human cancer. Yale J Biol Med. 1982;55(3-4):329-33.

732.	Stutman O. Tumor development after 3-methylcholanthrene in immunologically deficient athymic-nude mice. Science. 1974;183(4124):534-6.

733.	Stutman O. Chemical carcinogenesis in nude mice: comparison between nude mice from homozygous matings and heterozygous matings and effect of age and carcinogen dose. J Natl Cancer Inst. 1979;62(2):353-8.

734.	Rygaard J, Povlsen CO. The mouse mutant nude does not develop spontaneous tumours. An argument against immunological surveillance. Acta Pathol Microbiol Scand B Microbiol Immunol. 1974;82(1):99-106.

735.	Ikehara S, Pahwa RN, Fernandes G, Hansen CT, Good RA. Functional T cells in athymic nude mice. Proc Natl Acad Sci U S A. 1984;81(3):886-8.

736.	Klein AS, Plata F, Jackson MJ, Shin S. Cellular tumorigenicity in nude mice. Role of susceptibility to natural killer cells. Exp Cell Biol. 1979;47(6):430-45.

737.	Heidelberger C. Chemical carcinogenesis. Cancer. 1977;40(1 Suppl):430-3.

738.	Dighe AS, Richards E, Old LJ, Schreiber RD. Enhanced in vivo growth and resistance to rejection of tumor cells expressing dominant negative IFN gamma receptors. Immunity. 1994;1(6):447-56.

739.	Kaplan DH, Shankaran V, Dighe AS, Stockert E, Aguet M, Old LJ, et al. Demonstration of an interferon gamma-dependent tumor surveillance system in immunocompetent mice. Proc Natl Acad Sci U S A. 1998;95(13):7556-61.

740.	Street SE, Cretney E, Smyth MJ. Perforin and interferon-gamma activities independently control tumor initiation, growth, and metastasis. Blood. 2001;97(1):192-7.

741.	Street SE, Trapani JA, MacGregor D, Smyth MJ. Suppression of lymphoma and epithelial malignancies effected by interferon gamma. J Exp Med. 2002;196(1):129-34.

742.	van den Broek ME, Kägi D, Ossendorp F, Toes R, Vamvakas S, Lutz WK, et al. Decreased tumor surveillance in perforin-deficient mice. J Exp Med. 1996;184(5):1781-90.

743.	Smyth MJ, Thia KY, Street SE, MacGregor D, Godfrey DI, Trapani JA. Perforin-mediated cytotoxicity is critical for surveillance of spontaneous lymphoma. J Exp Med. 2000;192(5):755-60.

744.	Bolitho P, Street SE, Westwood JA, Edelmann W, Macgregor D, Waring P, et al. Perforin-mediated suppression of B-cell lymphoma. Proc Natl Acad Sci U S A. 2009;106(8):2723-8.

745.	Shinkai Y, Rathbun G, Lam KP, Oltz EM, Stewart V, Mendelsohn M, et al. RAG-2-deficient mice lack mature lymphocytes owing to inability to initiate V(D)J rearrangement. Cell. 1992;68(5):855-67.

746.	Shankaran V, Ikeda H, Bruce AT, White JM, Swanson PE, Old LJ, et al. IFNgamma and lymphocytes prevent primary tumour development and shape tumour immunogenicity. Nature. 2001;410(6832):1107-11.

747.	Smyth MJ, Crowe NY, Godfrey DI. NK cells and NKT cells collaborate in host protection from methylcholanthrene-induced fibrosarcoma. Int Immunol. 2001;13(4):459-63.

748.	Dunn GP, Bruce AT, Sheehan KC, Shankaran V, Uppaluri R, Bui JD, et al. A critical function for type I interferons in cancer immunoediting. Nat Immunol. 2005;6(7):722-9.

749.	Swann JB, Hayakawa Y, Zerafa N, Sheehan KC, Scott B, Schreiber RD, et al. Type I IFN contributes to NK cell homeostasis, activation, and antitumor function. J Immunol. 2007;178(12):7540-9.

750.	Cretney E, Takeda K, Yagita H, Glaccum M, Peschon JJ, Smyth MJ. Increased susceptibility to tumor initiation and metastasis in TNF-related apoptosis-inducing ligand-deficient mice. J Immunol. 2002;168(3):1356-61.

751.	Takeda K, Smyth MJ, Cretney E, Hayakawa Y, Kayagaki N, Yagita H, et al. Critical role for tumor necrosis factor-related apoptosis-inducing ligand in immune surveillance against tumor development. J Exp Med. 2002;195(2):161-9.

752.	Zerafa N, Westwood JA, Cretney E, Mitchell S, Waring P, Iezzi M, et al. Cutting edge: TRAIL deficiency accelerates hematological malignancies. J Immunol. 2005;175(9):5586-90.

753.   Smyth MJ, Taniguchi M, Street SE. The anti-tumor activity of IL-12: mechanisms of innate immunity that are model and dose dependent. J Immunol. 2000;165(5):2665-70.
754.   Swann JB, Vesely MD, Silva A, Sharkey J, Akira S, Schreiber RD, et al. Demonstration of inflammation-induced cancer and cancer immunoediting during primary tumorigenesis. Proc Natl Acad Sci U S A. 2008;105(2):652-6.
755.   Davidson WF, Giese T, Fredrickson TN. Spontaneous development of plasmacytoid tumors in mice with defective Fas-Fas ligand interactions. J Exp Med. 1998;187(11):1825-38.
756.   Iguchi-Manaka A, Kai H, Yamashita Y, Shibata K, Tahara-Hanaoka S, Honda S, et al. Accelerated tumor growth in mice deficient in DNAM-1 receptor. J Exp Med. 2008;205(13):2959-64.
757.   Guerra N, Tan YX, Joncker NT, Choy A, Gallardo F, Xiong N, et al. NKG2D-deficient mice are defective in tumor surveillance in models of spontaneous malignancy. Immunity. 2008;28(4):571-80.
758.   Girardi M, Oppenheim DE, Steele CR, Lewis JM, Glusac E, Filler R, et al. Regulation of cutaneous malignancy by gammadelta T cells. Science. 2001;294(5542):605-9.
759.   Girardi M, Glusac E, Filler RB, Roberts SJ, Propperova I, Lewis J, et al. The distinct contributions of murine T cell receptor (TCR)gammadelta+ and TCRalphabeta+ T cells to different stages of chemically induced skin cancer. J Exp Med. 2003;198(5):747-55.
760.   Swann JB, Uldrich AP, van Dommelen S, Sharkey J, Murray WK, Godfrey DI, et al. Type I natural killer T cells suppress tumors caused by p53 loss in mice. Blood. 2009;113(25):6382-5.
761.   Smyth MJ, Thia KY, Street SE, Cretney E, Trapani JA, Taniguchi M, et al. Differential tumor surveillance by natural killer (NK) and NKT cells. J Exp Med. 2000;191(4):661-8.
762.   Iannello A, Thompson TW, Ardolino M, Lowe SW, Raulet DH. p53-dependent chemokine production by senescent tumor cells supports NKG2D-dependent tumor elimination by natural killer cells. J Exp Med. 2013;210(10):2057-69.
763.   Gatti RA, Good RA. Occurrence of malignancy in immunodeficiency diseases. A literature review. Cancer. 1971;28(1):89-98.
764.   Boshoff C, Weiss R. AIDS-related malignancies. Nat Rev Cancer. 2002;2(5):373-82.
765.   Frisch M, Biggar RJ, Engels EA, Goedert JJ, Group A-CMRS. Association of cancer with AIDS-related immunosuppression in adults. JAMA. 2001;285(13):1736-45.
766.   Birkeland SA, Storm HH, Lamm LU, Barlow L, Blohmé I, Forsberg B, et al. Cancer risk after renal transplantation in the Nordic countries, 1964-1986. Int J Cancer. 1995;60(2):183-9.
767.   Pham SM, Kormos RL, Landreneau RJ, Kawai A, Gonzalez-Cancel I, Hardesty RL, et al. Solid tumors after heart transplantation: lethality of lung cancer. Ann Thorac Surg. 1995;60(6):1623-6.
768.   Penn I. Malignant melanoma in organ allograft recipients. Transplantation. 1996;61(2):274-8.
769.   Penn I. Sarcomas in organ allograft recipients. Transplantation. 1995;60(12):1485-91.
770.   Ueda R, Shiku H, Pfreundschuh M, Takahashi T, Li LT, Whitmore WF, et al. Cell surface antigens of human renal cancer defined by autologous typing. J Exp Med. 1979;150(3):564-79.
771.   Knuth A, Danowski B, Oettgen HF, Old LJ. T-cell-mediated cytotoxicity against autologous malignant melanoma: analysis with interleukin 2-dependent T-cell cultures. Proc Natl Acad Sci U S A. 1984;81(11):3511-5.
772.   Traversari C, van der Bruggen P, Van den Eynde B, Hainaut P, Lemoine C, Ohta N, et al. Transfection and expression of a gene coding for a human melanoma antigen recognized by autologous cytolytic T lymphocytes. Immunogenetics. 1992;35(3):145-52.
773.   Sahin U, Türeci O, Schmitt H, Cochlovius B, Johannes T, Schmits R, et al. Human neoplasms elicit multiple specific immune responses in the autologous host. Proc Natl Acad Sci U S A. 1995;92(25):11810-3.
774.   Boon T, van der Bruggen P. Human tumor antigens recognized by T lymphocytes. J Exp Med. 1996;183(3):725-9.
775.   Old LJ, Chen YT. New paths in human cancer serology. J Exp Med. 1998;187(8):1163-7.
776.   Rosenberg SA. A new era for cancer immunotherapy based on the genes that encode cancer antigens. Immunity. 1999;10(3):281-7.
777.   Scanlan MJ, Gure AO, Jungbluth AA, Old LJ, Chen YT. Cancer/testis antigens: an expanding family of targets for cancer immunotherapy. Immunol Rev. 2002;188:22-32.
778.   Darnell RB. Onconeural antigens and the paraneoplastic neurologic disorders: at the intersection of cancer, immunity, and the brain. Proc Natl Acad Sci U S A. 1996;93(10):4529-36.
779.   Albert ML, Austin LM, Darnell RB. Detection and treatment of activated T cells in the cerebrospinal fluid of patients with paraneoplastic cerebellar degeneration. Ann Neurol. 2000;47(1):9-17.
780.   Ferradini L, Mackensen A, Genevée C, Bosq J, Duvillard P, Avril MF, et al. Analysis of T cell receptor variability in tumor-infiltrating lymphocytes from a human regressive melanoma. Evidence for in situ T cell clonal expansion. J Clin Invest. 1993;91(3):1183-90.
781.   Zorn E, Hercend T. A natural cytotoxic T cell response in a spontaneously regressing human melanoma targets a neoantigen resulting from a somatic point mutation. Eur J Immunol. 1999;29(2):592-601.
782.   Mihm MC, Clemente CG, Cascinelli N. Tumor infiltrating lymphocytes in lymph node melanoma metastases: a histopathologic prognostic indicator and an expression of local immune response. Lab Invest. 1996;74(1):43-7.

783.   Clemente CG, Mihm MC, Bufalino R, Zurrida S, Collini P, Cascinelli N. Prognostic value of tumor infiltrating lymphocytes in the vertical growth phase of primary cutaneous melanoma. Cancer. 1996;77(7):1303-10.

784.   Zhang L, Conejo-Garcia JR, Katsaros D, Gimotty PA, Massobrio M, Regnani G, et al. Intratumoral T cells, recurrence, and survival in epithelial ovarian cancer. N Engl J Med. 2003;348(3):203-13.

785.   Naito Y, Saito K, Shiiba K, Ohuchi A, Saigenji K, Nagura H, et al. CD8+ T cells infiltrated within cancer cell nests as a prognostic factor in human colorectal cancer. Cancer Res. 1998;58(16):3491-4.

786.   Schumacher K, Haensch W, Röefzaad C, Schlag PM. Prognostic significance of activated CD8(+) T cell infiltrations within esophageal carcinomas. Cancer Res. 2001;61(10):3932-6.

787.   Ishigami S, Natsugoe S, Tokuda K, Nakajo A, Che X, Iwashige H, et al. Prognostic value of intratumoral natural killer cells in gastric carcinoma. Cancer. 2000;88(3):577-83.

788.   Villegas FR, Coca S, Villarrubia VG, Jiménez R, Chillón MJ, Jareño J, et al. Prognostic significance of tumor infiltrating natural killer cells subset CD57 in patients with squamous cell lung cancer. Lung Cancer. 2002;35(1):23-8.

789.   Coca S, Perez-Piqueras J, Martinez D, Colmenarejo A, Saez MA, Vallejo C, et al. The prognostic significance of intratumoral natural killer cells in patients with colorectal carcinoma. Cancer. 1997;79(12):2320-8.

790.   Matsushita H, Vesely MD, Koboldt DC, Rickert CG, Uppaluri R, Magrini VJ, et al. Cancer exome analysis reveals a T-cell-dependent mechanism of cancer immunoediting. Nature. 2012;482(7385):400-4.

791.   DuPage M, Mazumdar C, Schmidt LM, Cheung AF, Jacks T. Expression of tumour-specific antigens underlies cancer immunoediting. Nature. 2012;482(7385):405-9.

792.   Dunn GP, Old LJ, Schreiber RD. The three Es of cancer immunoediting. Annu Rev Immunol. 2004;22:329-60.

793.   Hanahan D, Weinberg RA. The hallmarks of cancer. Cell. 2000;100(1):57-70.

794.   Hodge-Dufour J, Noble PW, Horton MR, Bao C, Wysoka M, Burdick MD, et al. Induction of IL-12 and chemokines by hyaluronan requires adhesion-dependent priming of resident but not elicited macrophages. J Immunol. 1997;159(5):2492-500.

795.   D'Andrea A, Rengaraju M, Valiante NM, Chehimi J, Kubin M, Aste M, et al. Production of natural killer cell stimulatory factor (interleukin 12) by peripheral blood mononuclear cells. J Exp Med. 1992;176(5):1387-98.

796.   Atochina O, Harn D. LNFPIII/LeX-stimulated macrophages activate natural killer cells via CD40-CD40L interaction. Clin Diagn Lab Immunol. 2005;12(9):1041-9.

797.   Kitamura H, Iwakabe K, Yahata T, Nishimura S, Ohta A, Ohmi Y, et al. The natural killer T (NKT) cell ligand alpha-galactosylceramide demonstrates its immunopotentiating effect by inducing interleukin (IL)-12 production by dendritic cells and IL-12 receptor expression on NKT cells. J Exp Med. 1999;189(7):1121-8.

798.   Borg C, Jalil A, Laderach D, Maruyama K, Wakasugi H, Charrier S, et al. NK cell activation by dendritic cells (DCs) requires the formation of a synapse leading to IL-12 polarization in DCs. Blood. 2004;104(10):3267-75.

799.   Fujii S, Liu K, Smith C, Bonito AJ, Steinman RM. The linkage of innate to adaptive immunity via maturing dendritic cells in vivo requires CD40 ligation in addition to antigen presentation and CD80/86 costimulation. J Exp Med. 2004;199(12):1607-18.

800.   Michel T, Hentges F, Zimmer J. Consequences of the crosstalk between monocytes/macrophages and natural killer cells. Front Immunol. 2012;3:403.

801.   Diefenbach A, Jamieson AM, Liu SD, Shastri N, Raulet DH. Ligands for the murine NKG2D receptor: expression by tumor cells and activation of NK cells and macrophages. Nat Immunol. 2000;1(2):119-26.

802.   Bromberg JF, Horvath CM, Wen Z, Schreiber RD, Darnell JE. Transcriptionally active Stat1 is required for the antiproliferative effects of both interferon alpha and interferon gamma. Proc Natl Acad Sci U S A. 1996;93(15):7673-8.

803.   Qin Z, Blankenstein T. CD4+ T cell--mediated tumor rejection involves inhibition of angiogenesis that is dependent on IFN gamma receptor expression by nonhematopoietic cells. Immunity. 2000;12(6):677-86.

804.   Kotredes KP, Gamero AM. Interferons as inducers of apoptosis in malignant cells. J Interferon Cytokine Res. 2013;33(4):162-70.

805.   Nathan CF, Murray HW, Wiebe ME, Rubin BY. Identification of interferon-gamma as the lymphokine that activates human macrophage oxidative metabolism and antimicrobial activity. J Exp Med. 1983;158(3):670-89.

806.   Smyth MJ, Cretney E, Takeda K, Wiltrout RH, Sedger LM, Kayagaki N, et al. Tumor necrosis factor-related apoptosis-inducing ligand (TRAIL) contributes to interferon gamma-dependent natural killer cell protection from tumor metastasis. J Exp Med. 2001;193(6):661-70.

807.   Hayakawa Y, Kelly JM, Westwood JA, Darcy PK, Diefenbach A, Raulet D, et al. Cutting edge: tumor rejection mediated by NKG2D receptor-ligand interaction is dependent upon perforin. J Immunol. 2002;169(10):5377-81.

808.   Reis e Sousa C. Activation of dendritic cells: translating innate into adaptive immunity. Curr Opin Immunol. 2004;16(1):21-5.

809.   Sallusto F, Mackay CR, Lanzavecchia A. The role of chemokine receptors in primary, effector, and memory immune responses. Annu Rev Immunol. 2000;18:593-620.
810.   Albert ML, Sauter B, Bhardwaj N. Dendritic cells acquire antigen from apoptotic cells and induce class I-restricted CTLs. Nature. 1998;392(6671):86-9.
811.   Yu P, Spiotto MT, Lee Y, Schreiber H, Fu YX. Complementary role of CD4+ T cells and secondary lymphoid tissues for cross-presentation of tumor antigen to CD8+ T cells. J Exp Med. 2003;197(8):985-95.
812.   Zhu J, Paul WE. CD4 T cells: fates, functions, and faults. Blood. 2008;112(5):1557-69.
813.   Zhang N, Bevan MJ. CD8(+) T cells: foot soldiers of the immune system. Immunity. 2011;35(2):161-8.
814.   Lengauer C, Kinzler KW, Vogelstein B. Genetic instabilities in human cancers. Nature. 1998;396(6712):643-9.
815.   Farrar JD, Katz KH, Windsor J, Thrush G, Scheuermann RH, Uhr JW, et al. Cancer dormancy. VII. A regulatory role for CD8+ T cells and IFN-gamma in establishing and maintaining the tumor-dormant state. J Immunol. 1999;162(5):2842-9.
816.   Teng MW, Vesely MD, Duret H, McLaughlin N, Towne JE, Schreiber RD, et al. Opposing roles for IL-23 and IL-12 in maintaining occult cancer in an equilibrium state. Cancer Res. 2012;72(16):3987-96.
817.   Wu X, Peng M, Huang B, Zhang H, Wang H, Xue Z, et al. Immune microenvironment profiles of tumor immune equilibrium and immune escape states of mouse sarcoma. Cancer Lett. 2013;340(1):124-33.
818.   Müller-Hermelink N, Braumüller H, Pichler B, Wieder T, Mailhammer R, Schaak K, et al. TNFR1 signaling and IFN-gamma signaling determine whether T cells induce tumor dormancy or promote multistage carcinogenesis. Cancer Cell. 2008;13(6):507-18.
819.   Braumüller H, Wieder T, Brenner E, Aßmann S, Hahn M, Alkhaled M, et al. T-helper-1-cell cytokines drive cancer into senescence. Nature. 2013;494(7437):361-5.
820.   Penn I. Donor transmitted disease: cancer. Transplant Proc. 1991;23(5):2629-31.
821.   Vinay DS, Ryan EP, Pawelec G, Talib WH, Stagg J, Elkord E, et al. Immune evasion in cancer: Mechanistic basis and therapeutic strategies. Semin Cancer Biol. 2015;35 Suppl:S185-S98.
822.   Nomi T, Sho M, Akahori T, Hamada K, Kubo A, Kanehiro H, et al. Clinical Significance and Therapeutic Potential of the Programmed Death-1 Ligand/Programmed Death-1 Pathway in Human Pancreatic Cancer. Clinical Cancer Research. 2007;13(7):2151-7.
823.   Dong H. Tumor-associated B7-H1 promotes T-cell apoptosis: a potential mechanism of immune evasion. Nature Med. 2002;8:793-800.
824.   Ohigashi Y, Sho M, Yamada Y, Tsurui Y, Hamada K, Ikeda N, et al. Clinical Significance of Programmed Death-1 Ligand-1 and Programmed Death-1 Ligand-2 Expression in Human Esophageal Cancer. Clinical Cancer Research. 2005;11(8):2947-53.
825.   Hamanishi J, Mandai M, Iwasaki M, Okazaki T, Tanaka Y, Yamaguchi K, et al. Programmed cell death 1 ligand 1 and tumor-infiltrating CD8+ T lymphocytes are prognostic factors of human ovarian cancer. Proc Natl Acad Sci U S A. 2007;104(9):3360-5.
826.   Wang L, Qian J, Lu Y, Li H, Bao H, He D, et al. Immune evasion of mantle cell lymphoma: expression of B7-H1 leads to inhibited T-cell response to and killing of tumor cells. Haematologica. 2013;98(9):1458-66.
827.   Steidl C, Shah SP, Woolcock BW, Rui L, Kawahara M, Farinha P, et al. MHC class II transactivator CIITA is a recurrent gene fusion partner in lymphoid cancers. Nature. 2011;471:377-81.
828.   Yamamoto R, Nishikori M, Kitawaki T, Sakai T, Hishizawa M, Tashima M, et al. PD-1/PD-1 ligand interaction contributes to immunosuppressive microenvironment of Hodgkin lymphoma. Blood. 2008;111:3220-4.
829.   Liu J, Hamrouni A, Wolowiec D, Coiteux V, Kuliczkowski K, Hetuin D, et al. Plasma cells from multiple myeloma patients express B7-H1 (PD-L1) and increase expression after stimulation with IFN-γ and TLR ligands via a MyD88-, TRAF6-, and MEK-dependent pathway. Blood. 2007;110(1):296-304.
830.   Kondo A, Yamashita T, Tamura H, Zhao W, Tsuji T, Shimizu M, et al. Interferon-γ and tumor necrosis factor-α induce an immunoinhibitory molecule, B7-H1, via nuclear factor-kB activation in blasts in myelodysplastic syndromes. Blood. 2010;116(7):1124-31.
831.   Yang H, Bueso-Ramos C, DiNardo C, Estecio MR, Davanlou M, Geng QR, et al. Expression of PD-L1, PD-L2, PD-1 and CTLA4 in myelodysplastic syndromes is enhanced by treatment with hypomethylating agents. Leukemia. 2014;28(6):1280-8.
832.   Curiel TJ, Wei S, Dong H, Alvarez X, Cheng P, Mottram P, et al. Blockade of B7-H1 improves myeloid dendritic cell-mediated antitumor immunity. Nat Med. 2003;9(5):562-7.
833.   Kuang DM, Zhao Q, Peng C, Xu J, Zhang JP, Wu C, et al. Activated monocytes in peritumoral stroma of hepatocellular carcinoma foster immune privilege and disease progression through PD-L1. J Exp Med. 2009;206(6):1327-37.
834.   Liu Y, Zeng B, Zhang Z, Zhang Y, Yang R. B7-H1 on myeloid-derived suppressor cells in immune suppression by a mouse model of ovarian cancer. Clin Immunol. 2008;129(3):471-81.
835.   Jitschin R, Braun M, Buttner M, Dettmer-Wilde K, Bricks J, Berger J, et al. CLL-cells induce IDOhi CD14+HLA-DRlo myeloid-derived suppressor cells that inhibit T-cell responses and promote TRegs. Blood. 2014;124(5):750-60.
836.   McClanahan F, Hanna B, Miller S, Clear AJ, Lichter P, Gribben JG, et al. PD-L1 checkpoint blockade prevents immune dysfunction and leukemia development in a mouse model of chronic lymphocytic leukemia. Blood. 2015;126(2):203-11.

837.   Parsa AT. Loss of tumor suppressor PTEN function increases B7-H1 expression and immunoresistance in glioma. Nature Med. 2007;13:84-8.
838.   Rosenwald A, Wright G, Leroy K, Yu X, Gaulard P, Gascoyne RD, et al. Molecular diagnosis of primary mediastinal B cell lymphoma identifies a clinically favorable subgroup of diffuse large B cell lymphoma related to Hodgkin lymphoma. J Exp Med. 2003;198:851-62.
839.   Green MR, Monti S, Rodig SJ, Juszczynski P, Currie T, O'Donnell E, et al. Integrative analysis reveals selective 9p24.1 amplification, increased PD-1 ligand expression, and further induction via JAK2 in nodular sclerosing Hodgkin lymphoma and primary mediastinal large B-cell lymphoma. Blood. 2010;116(17):3268-77.
840.   Marzec M. Oncogenic kinase NPM/ALK induces through STAT3 expression of immunosuppressive protein CD274 (PD-L1, B7-H1). Proc Natl Acad Sci USA. 2008;105:20852-7.
841.   Kataoka K, Shiraishi Y, Takeda Y, Sakata S, Matsumoto M, Nagano S, et al. Aberrant PD-L1 expression through 3'-UTR disruption in multiple cancers. Nature. 2016;534(7607):402-6.
842.   Taube JM, Anders RA, Young GD, Xu H, Sharma R, McMiller TL, et al. Colocalization of inflammatory response with B7-h1 expression in human melanocytic lesions supports an adaptive resistance mechanism of immune escape. Sci Transl Med. 2012;4(127):127ra37.
843.   Berthon C, Driss V, Liu J, Kuranda K, Leleu X, Jouy N, et al. In acute myeloid leukemia, B7-H1 (PD-L1) protection of blasts from cytotoxic T cells is induced by TLR ligands and interferon-gamma and can be reversed using MEK inhibitors. Cancer Immunology, Immunotherapy. 2010;59(12):1839-49.
844.   O'Day SJ, Hamid O, Urba WJ. Targeting cytotoxic T-lymphocyte antigen-4 (CTLA-4): a novel strategy for the treatment of melanoma and other malignancies. Cancer. 2007;110(12):2614-27.
845.   Hodi FS, O'Day SJ, McDermott DF, Weber RW, Sosman JA, Haanen JB, et al. Improved survival with ipilimumab in patients with metastatic melanoma. N Engl J Med. 2010;363(8):711-23.
846.   Topalian SL, Hodi FS, Brahmer JR, Gettinger SN, Smith DC, McDermott DF, et al. Safety, activity, and immune correlates of anti-PD-1 antibody in cancer. N Engl J Med. 2012;366(26):2443-54.
847.   Robert C, Ribas A, Wolchok JD, Hodi FS, Hamid O, Kefford R, et al. Anti-programmed-death-receptor-1 treatment with pembrolizumab in ipilimumab-refractory advanced melanoma: a randomised dose-comparison cohort of a phase 1 trial. Lancet. 2014;384(9948):1109-17.
848.   Topalian SL, Sznol M, McDermott DF, Kluger HM, Carvajal RD, Sharfman WH, et al. Survival, durable tumor remission, and long-term safety in patients with advanced melanoma receiving nivolumab. J Clin Oncol. 2014;32(10):1020-30.
849.   Brahmer JR, Tykodi SS, Chow LQ, Hwu WJ, Topalian SL, Hwu P, et al. Safety and activity of anti-PD-L1 antibody in patients with advanced cancer. N Engl J Med. 2012;366(26):2455-65.
850.   Garassino MC, Cho BC, Kim JH, Mazières J, Vansteenkiste J, Lena H, et al. Durvalumab as third-line or later treatment for advanced non-small-cell lung cancer (ATLANTIC): an open-label, single-arm, phase 2 study. Lancet Oncol. 2018;19(4):521-36.
851.   Harshman LC, Drake CG, Choueiri TK. PD-1 blockade in renal cell carcinoma: to equilibrium and beyond. Cancer Immunol Res. 2014;2(12):1132-41.
852.   Fehrenbacher L, Spira A, Ballinger M, Kowanetz M, Vansteenkiste J, Mazieres J, et al. Atezolizumab versus docetaxel for patients with previously treated non-small-cell lung cancer (POPLAR): a multicentre, open-label, phase 2 randomised controlled trial. Lancet. 2016;387(10030):1837-46.
853.   Ansell SM, Hurvitz SA, Koenig PA, LaPlant BR, Kabat BF, Fernando D, et al. Phase I study of ipilimumab, an anti-CTLA-4 monoclonal antibody, in patients with relapsed and refractory B-cell non-Hodgkin lymphoma. Clin Cancer Res. 2009;15(20):6446-53.
854.   Davids MS, Kim HT, Bachireddy P, Costello C, Liguori R, Savell A, et al. Ipilimumab for Patients with Relapse after Allogeneic Transplantation. N Engl J Med. 2016;375(2):143-53.
855.   Ansell S, Gutierrez ME, Shipp MA, Gladstone D, Moskowitz A, Borello I, et al. A Phase 1 Study of Nivolumab in Combination with Ipilimumab for Relapsed or Refractory Hematologic Malignancies (CheckMate 039). Blood. 2016;128(22):183-.
856.   Zeidan AM, Knaus HA, Robinson TM, Towlerton AMH, Warren EH, Zeidner JF, et al. A Multi-center Phase I Trial of Ipilimumab in Patients with Myelodysplastic Syndromes following Hypomethylating Agent Failure. Clinical Cancer Research. 2018;24(15):3519-27.
857.   Ansell SM, Lesokhin AM, Borrello I, Halwani A, Scott EC, Gutierrez M, et al. PD-1 blockade with nivolumab in relapsed or refractory Hodgkin's lymphoma. N Engl J Med. 2015;372(4):311-9.
858.   Younes A, Santoro A, Shipp M, Zinzani PL, Timmerman JM, Ansell S, et al. Nivolumab for classical Hodgkin's lymphoma after failure of both autologous stem-cell transplantation and brentuximab vedotin: a multicentre, multicohort, single-arm phase 2 trial. Lancet Oncol. 2016;17(9):1283-94.
859.   Armand P, Engert A, Younes A, Fanale M, Santoro A, Zinzani PL, et al. Nivolumab for Relapsed/Refractory Classic Hodgkin Lymphoma After Failure of Autologous Hematopoietic Cell Transplantation: Extended Follow-Up of the Multicohort Single-Arm Phase II CheckMate 205 Trial. J Clin Oncol. 2018;36(14):1428-39.
860.   Lesokhin AM, Ansell SM, Armand P, Scott EC, Halwani A, Gutierrez M, et al. Nivolumab in Patients With Relapsed or Refractory Hematologic Malignancy: Preliminary Results of a Phase Ib Study. J Clin Oncol. 2016;34(23):2698-704.
861.   Nayak L, Iwamoto FM, LaCasce A, Mukundan S, Roemer MGM, Chapuy B, et al. PD-1 blockade with nivolumab in relapsed/refractory primary central nervous system and testicular lymphoma. Blood. 2017;129(23):3071-3.

862.   Daver N, Basu S, Garcia-Manero G, Cortes JE, Ravandi F, Jabbour EJ, et al. Phase IB/II Study of Nivolumab in Combination with Azacytidine (AZA) in Patients (pts) with Relapsed Acute Myeloid Leukemia (AML). Blood. 2016;128(22):763-.

863.   Garcia-Manero G, Daver NG, Montalban-Bravo G, Jabbour EJ, DiNardo CD, Kornblau SM, et al. A Phase II Study Evaluating the Combination of Nivolumab (Nivo) or Ipilimumab (Ipi) with Azacitidine in Pts with Previously Treated or Untreated Myelodysplastic Syndromes (MDS). Blood. 2016;128(22):344-.

864.   Armand P, Shipp MA, Ribrag V, Michot J-M, Zinzani PL, Kuruvilla J, et al. Pembrolizumab in Patients with Classical Hodgkin Lymphoma after Brentuximab Vedotin Failure: Long-Term Efficacy from the Phase 1b Keynote-013 Study. Blood. 2016;128(22):1108-.

865.   Chen R, Zinzani PL, Fanale MA, Armand P, Johnson NA, Brice P, et al. Phase II Study of the Efficacy and Safety of Pembrolizumab for Relapsed/Refractory Classic Hodgkin Lymphoma. J Clin Oncol. 2017;35(19):2125-32.

866.   Zinzani P, Ribrag V, Moskowitz CH, Michot J, Kuruvilla J, Bartlett N, et al. PHASE 1B STUDY OF PEMBROLIZUMAB IN PATIENTS WITH RELAPSED/REFRACTORY PRIMARY MEDIASTINAL LARGE B-CELL LYMPHOMA (RRPMBCL): UPDATED RESULTS FROM THE KEYNOTE-013 TRIAL. Hematological Oncology. 2017;35(S2):189-90.

867.   Garcia-Manero G, Tallman MS, Martinelli G, Ribrag V, Yang H, Balakumaran A, et al. Pembrolizumab, a PD-1 Inhibitor, in Patients with Myelodysplastic Syndrome (MDS) after Failure of Hypomethylating Agent Treatment. Blood. 2016;128(22):345-.

868.   San Miguel J, Mateos M-V, Shah JJ, Ocio EM, Rodriguez-Otero P, Reece D, et al. Pembrolizumab in Combination with Lenalidomide and Low-Dose Dexamethasone for Relapsed/Refractory Multiple Myeloma (RRMM): Keynote-023. Blood. 2015;126(23):505-.

869.   Badros AZ, Hyjek E, Ma N, Lesokhin AM, Rapoport AP, Kocoglu MH, et al. Pembrolizumab in Combination with Pomalidomide and Dexamethasone for Relapsed/Refractory Multiple Myeloma (RRMM). Blood. 2016;128(22):490-.

870.   Wilson L, Cohen AD, Weiss BM, Vogl DT, Garfall AL, Capozzi DL, et al. Pembrolizumab in Combination with Pomalidomide and Dexamethasone (PEMBRO/POM/DEX) for Pomalidomide Exposed Relapsed or Refractory Multiple Myeloma. Blood. 2016;128(22):2119-.

871.   Till BG, Park SI, Popplewell LL, Goy A, Penuel E, Venstrom JM, et al. Safety and Clinical Activity of Atezolizumab (Anti-PDL1) in Combination with Obinutuzumab in Patients with Relapsed or Refractory Non-Hodgkin Lymphoma. Blood. 2015;126(23):5104-.

872.   Sagiv-Barfi I, Kohrt HE, Czerwinski DK, Ng PP, Chang BY, Levy R. Therapeutic antitumor immunity by checkpoint blockade is enhanced by ibrutinib, an inhibitor of both BTK and ITK. Proc Natl Acad Sci U S A. 2015;112(9):E966-72.

873.   Younes A, Brody J, Carpio C, Lopez-Guillermo A, Ben-Yehuda D, Ferhanoglu B, et al. Safety and activity of ibrutinib in combination with nivolumab in patients with relapsed non-Hodgkin lymphoma or chronic lymphocytic leukaemia: a phase 1/2a study. Lancet Haematol. 2019;6(2):e67-e78.

874.   Kumar V, Chaudhary N, Garg M, Floudas CS, Soni P, Chandra AB. Current Diagnosis and Management of Immune Related Adverse Events (irAEs) Induced by Immune Checkpoint Inhibitor Therapy. Front Pharmacol. 2017;8:49.

875.   Horvat TZ, Adel NG, Dang TO, Momtaz P, Postow MA, Callahan MK, et al. Immune-Related Adverse Events, Need for Systemic Immunosuppression, and Effects on Survival and Time to Treatment Failure in Patients With Melanoma Treated With Ipilimumab at Memorial Sloan Kettering Cancer Center. J Clin Oncol. 2015;33(28):3193-8.

876.   Weber JS, Hodi FS, Wolchok JD, Topalian SL, Schadendorf D, Larkin J, et al. Safety Profile of Nivolumab Monotherapy: A Pooled Analysis of Patients With Advanced Melanoma. J Clin Oncol. 2017;35(7):785-92.

877.   Dubovsky JA, Beckwith KA, Natarajan G, Woyach JA, Jaglowski S, Zhong Y, et al. Ibrutinib is an irreversible molecular inhibitor of ITK driving a Th1-selective pressure in T lymphocytes. Blood. 2013;122(15):2539-49.

878.   Kondo K, Shaim H, Thompson PA, Burger JA, Keating M, Estrov Z, et al. Ibrutinib modulates the immunosuppressive CLL microenvironment through STAT3-mediated suppression of regulatory B-cell function and inhibition of the PD-1/PD-L1 pathway. Leukemia. 2017.

879.   Stiff A, Trikha P, Wesolowski R, Kendra K, Hsu V, Uppati S, et al. Myeloid-Derived Suppressor Cells Express Bruton's Tyrosine Kinase and Can Be Depleted in Tumor-Bearing Hosts by Ibrutinib Treatment. Cancer research. 2016;76(8):2125-36.

880.   Ping L, Ding N, Shi Y, Feng L, Li J, Liu Y, et al. The Bruton's tyrosine kinase inhibitor ibrutinib exerts immunomodulatory effects through regulation of tumor-infiltrating macrophages. Oncotarget. 2017;8(24):39218-29.

881.   Gunderson AJ, Kaneda MM, Tsujikawa T, Nguyen AV, Affara NI, Ruffell B, et al. Bruton Tyrosine Kinase–Dependent Immune Cell Cross-talk Drives Pancreas Cancer. Cancer discovery. 2016;6(3):270-85.

882.   Herman SE, Gordon AL, Wagner AJ, Heerema NA, Zhao W, Flynn JM, et al. Phosphatidylinositol 3-kinase-δ inhibitor CAL-101 shows promising preclinical activity in chronic lymphocytic leukemia by antagonizing intrinsic and extrinsic cellular survival signals. Blood. 2010;116(12):2078-88.

883.   Patton DT, Garden OA, Pearce WP, Clough LE, Monk CR, Leung E, et al. Cutting edge: the phosphoinositide 3-kinase p110 delta is critical for the function of CD4+CD25+Foxp3+ regulatory T cells. J Immunol. 2006;177(10):6598-602.

884.   Lim EL, Cugliandolo FM, Rosner DR, Gyori D, Roychoudhuri R, Okkenhaug K. Phosphoinositide 3-kinase δ inhibition promotes antitumor responses but antagonizes checkpoint inhibitors. JCI Insight. 2018;3(11).

885.   Dong S, Harrington BK, Hu EY, Greene JT, Lehman AM, Tran M, et al. PI3K p110δ inactivation antagonizes chronic lymphocytic leukemia and reverses T cell immune suppression. J Clin Invest. 2019;129(1):122-36.

886.   Chellappa S, Kushekhar K, Munthe LA, Tjønnfjord GE, Aandahl EM, Okkenhaug K, et al. The PI3K p110δ Isoform Inhibitor Idelalisib Preferentially Inhibits Human Regulatory T Cell Function. J Immunol. 2019;202(5):1397-405.

887.   Bowers JS, Majchrzak K, Nelson MH, Aksoy BA, Wyatt MM, Smith AS, et al. PI3Kδ Inhibition Enhances the Antitumor Fitness of Adoptively Transferred CD8. Front Immunol. 2017;8:1221.

888.   Hanna BS, Roessner PM, Scheffold A, Jebaraj BMC, Demerdash Y, Öztürk S, et al. PI3Kδ inhibition modulates regulatory and effector T-cell differentiation and function in chronic lymphocytic leukemia. Leukemia. 2019;33(6):1427-38.

889.   Pekarsky Y, Hallas C, Isobe M, Russo G, Croce CM. Abnormalities at 14q32.1 in T cell malignancies involve two oncogenes. Proceedings of the National Academy of Sciences. 1999;96(6):2949-51.

890.   Sugimoto J, Hatakeyama T, Narducci MG, Russo G, Isobe M. Identification of the TCL1/MTCP1-like 1 (TML1) Gene from the Region Next to the TCL1 Locus. Cancer Research. 1999;59(10):2313-7.

891.   Virgilio L, Narducci MG, Isobe M, Billips LG, Cooper MD, Croce CM, et al. Identification of the TCL1 gene involved in T-cell malignancies. Proc Natl Acad Sci U S A. 1994;91(26):12530-4.

892.   Narducci MG, Fiorenza MT, Kang SM, Bevilacqua A, Di Giacomo M, Remotti D, et al. TCL1 participates in early embryonic development and is overexpressed in human seminomas. Proc Natl Acad Sci U S A. 2002;99(18):11712-7.

893.   Narducci MG, Pescarmona E, Lazzeri C, Signoretti S, Lavinia AM, Remotti D, et al. Regulation of TCL1 expression in B- and T-cell lymphomas and reactive lymphoid tissues. Cancer Res. 2000;60(8):2095-100.

894.   Ragone G, Bresin A, Piermarini F, Lazzeri C, Picchio MC, Remotti D, et al. The Tcl1 oncogene defines secondary hair germ cells differentiation at catagen-telogen transition and affects stem-cell marker CD34 expression. Oncogene. 2009;28(10):1329-38.

895.   Pekarsky Y, Santanam U, Cimmino A, Palamarchuk A, Efanov A, Maximov V, et al. Tcl1 expression in chronic lymphocytic leukemia is regulated by miR-29 and miR-181. Cancer Res. 2006;66(24):11590-3.

896.   Pekarsky Y, Koval A, Hallas C, Bichi R, Tresini M, Malstrom S, et al. Tcl1 enhances Akt kinase activity and mediates its nuclear translocation. Proc Natl Acad Sci U S A. 2000;97(7):3028-33.

897.   Widhopf GF, 2nd, Cui B, Ghia EM, Chen L, Messer K, Shen Z, et al. ROR1 can interact with TCL1 and enhance leukemogenesis in Emu-TCL1 transgenic mice. Proc Natl Acad Sci U S A. 2014;111(2):793-8.

898.   Pekarsky Y, Palamarchuk A, Maximov V, Efanov A, Nazaryan N, Santanam U, et al. Tcl1 functions as a transcriptional regulator and is directly involved in the pathogenesis of CLL. Proc Natl Acad Sci U S A. 2008;105(50):19643-8.

899.   Gaudio E, Spizzo R, Paduano F, Luo Z, Efanov A, Palamarchuk A, et al. Tcl1 interacts with Atm and enhances NF-κB activation in hematologic malignancies. Blood. 2012;119(1):180-7.

900.   Kriss CL, Pinilla-Ibarz JA, Mailloux AW, Powers JJ, Tang CH, Kang CW, et al. Overexpression of TCL1 activates the endoplasmic reticulum stress response: a novel mechanism of leukemic progression in mice. Blood. 2012;120(5):1027-38.

901.   Bichi R, Shinton SA, Martin ES, Koval A, Calin GA, Cesari R, et al. Human chronic lymphocytic leukemia modeled in mouse by targeted TCL1 expression. Proceedings of the National Academy of Sciences. 2002;99(10):6955-60.

902.   Zanesi N, Aqeilan R, Drusco A, Kaou M, Sevignani C, Costinean S, et al. Effect of rapamycin on mouse chronic lymphocytic leukemia and the development of nonhematopoietic malignancies in Emu-TCL1 transgenic mice. Cancer Res. 2006;66(2):915-20.

903.   Hofbauer JP, Heyder C, Denk U, Kocher T, Holler C, Trapin D, et al. Development of CLL in the TCL1 transgenic mouse model is associated with severe skewing of the T-cell compartment homologous to human CLL. Leukemia. 2011;25(9):1452-8.

904.   McClanahan F, Riches JC, Miller S, Day WP, Kotsiou E, Neuberg D, et al. Mechanisms of PD-L1/PD-1-mediated CD8 T-cell dysfunction in the context of aging-related immune defects in the Eμ-TCL1 CLL mouse model. Blood. 2015;126(2):212-21.

905.   Yan X-j, Albesiano E, Zanesi N, Yancopoulos S, Sawyer A, Romano E, et al. B cell receptors in TCL1 transgenic mice resemble those of aggressive, treatment-resistant human chronic lymphocytic leukemia. Proceedings of the National Academy of Sciences. 2006;103(31):11713-8.

906.   Chen SS, Raval A, Johnson AJ, Hertlein E, Liu TH, Jin VX. Epigenetic changes during disease progression in a murine model of human chronic lymphocytic leukemia. Proc Natl Acad Sci USA. 2009;106:13433-8.

907.   Gorgun G, Ramsay AG, Holderried TAW, Zahrieh D, Le Dieu R, Liu F, et al. Eu-TCL1 mice represent a model for immunotherapeutic reversal of chronic lymphocytic leukemia-induced T-cell dysfunction. Proceedings of the National Academy of Sciences. 2009;106(15):6250-5.

908.   Hanna BS, McClanahan F, Yazdanparast H, Zaborsky N, Kalter V, Rossner PM, et al. Depletion of CLL-associated patrolling monocytes and macrophages controls disease development and repairs immune dysfunction in vivo. Leukemia. 2015.

909.   Johnson AJ, Lucas DM, Muthusamy N, Smith LL, Edwards RB, De Lay MD, et al. Characterization of the TCL-1 transgenic mouse as a preclinical drug development tool for human chronic lymphocytic leukemia. Blood. 2006;108(4):1334-8.

910.   Ponader S, Chen SS, Buggy JJ, Balakrishnan K, Gandhi V, Wierda WG, et al. The Bruton tyrosine kinase inhibitor PCI-32765 thwarts chronic lymphocytic leukemia cell survival and tissue homing in vitro and in vivo. Blood. 2012;119(5):1182-9.

911.   Herman SE, Montraveta A, Niemann CU, Mora-Jensen H, Gulrajani M, Krantz F, et al. The Bruton Tyrosine Kinase (BTK) Inhibitor Acalabrutinib Demonstrates Potent On-Target Effects and Efficacy in Two Mouse Models of Chronic Lymphocytic Leukemia. Clin Cancer Res. 2016.

912.   Merkel O, Wacht N, Sifft E, Melchardt T, Hamacher F, Kocher T, et al. Actinomycin D induces p53-independent cell death and prolongs survival in high-risk chronic lymphocytic leukemia. Leukemia. 2012;26(12):2508-16.

913.   Lucas DM, Edwards RB, Lozanski G, West DA, Shin JD, Vargo MA, et al. The novel plant-derived agent silvestrol has B-cell selective activity in chronic lymphocytic leukemia and acute lymphoblastic leukemia in vitro and in vivo. Blood. 2009;113(19):4656-66.

914.   Lapalombella R, Sun Q, Williams K, Tangeman L, Jha S, Zhong Y, et al. Selective inhibitors of nuclear export show that CRM1/XPO1 is a target in chronic lymphocytic leukemia. Blood. 2012;120(23):4621-34.

915.   Hertlein E, Wagner AJ, Jones J, Lin TS, Maddocks KJ, Towns WH, et al. 17-DMAG targets the nuclear factor-kappa B family of proteins to induce apoptosis in chronic lymphocytic leukemia: clinical implications of HSP90 inhibition. Blood. 2010;116(1):45-53.

916.   Klein U, Lia M, Crespo M, Siegel R, Shen Q, Mo T, et al. The DLEU2/miR-15a/16-1 Cluster Controls B Cell Proliferation and Its Deletion Leads to Chronic Lymphocytic Leukemia. Cancer Cell. 2010;17(1):28-40.

917.   Lia M, Carette A, Tang H, Shen Q, Mo T, Bhagat G, et al. Functional dissection of the chromosome 13q14 tumor-suppressor locus using transgenic mouse lines. Blood. 2012;119(13):2981-90.

918.   Phillips JA, Mehta K, Fernandez C, Raveche ES. The NZB Mouse as a Model for Chronic Lymphocytic Leukemia. Cancer Research. 1992;52(2):437-43.

919.   Salerno E, Yuan Y, Scaglione BJ, Marti G, Jankovic A, Mazzella F, et al. The New Zealand black mouse as a model for the development and progression of chronic lymphocytic leukemia. Cytometry Part B: Clinical Cytometry. 2010;78B(S1):S98-S109.

920.   Raveche ES, Salerno E, Scaglione BJ, Manohar V, Abbasi F, Lin Y-C, et al. Abnormal microRNA-16 locus with synteny to human 13q14 linked to CLL in NZB mice. Blood. 2007;109(12):5079-86.

921.   Santanam U, Zanesi N, Efanov A, Costinean S, Palamarchuk A, Hagan JP, et al. Chronic lymphocytic leukemia modeled in mouse by targeted miR-29 expression. Proceedings of the National Academy of Sciences. 2010;107(27):12210-5.

922.   Zapata JM, Krajewska M, Morse HC, Choi Y, Reed JC. TNF receptor-associated factor (TRAF) domain and Bcl-2 cooperate to induce small B cell lymphoma/chronic lymphocytic leukemia in transgenic mice. Proceedings of the National Academy of Sciences of the United States of America. 2004;101(47):16600-5.

923.   Planelles L, Carvalho-Pinto CE, Hardenberg G, Smaniotto S, Savino W, Gomez-Caro R, et al. APRIL promotes B-1 cell-associated neoplasm. Cancer Cell. 2004;6(4):399-408.

924.   Zhang W, Kater AP, Widhopf GF, Chuang H-Y, Enzler T, James DF, et al. B-cell activating factor and v-Myc myelocytomatosis viral oncogene homolog (c-Myc) influence progression of chronic lymphocytic leukemia. Proceedings of the National Academy of Sciences. 2010;107(44):18956-60.

925.   Shukla V, Ma S, Hardy RR, Joshi SS, Lu R. A role for IRF4 in the development of CLL. 2013. 2013;122:2848-55.

926.   ter Brugge PJ, Ta VBT, de Bruijn MJW, Keijzers G, Maas A, van Gent DC, et al. A mouse model for chronic lymphocytic leukemia based on expression of the SV40 large T antigen. Blood. 2009;114:119-27.

927.   Tang CH, Ranatunga S, Kriss CL, Cubitt CL, Tao J, Pinilla-Ibarz JA, et al. Inhibition of ER stress-associated IRE-1/XBP-1 pathway reduces leukemic cell survival. J Clin Invest. 2014;124(6):2585-98.

928.   Bertilaccio MTS, Simonetti G, Dagklis A, Rocchi M, Rodriguez TV, Apollonio B, et al. Lack of TIR8/SIGIRR triggers progression of chronic lymphocytic leukemia in mouse models. Blood. 2011;118(3):660-9.

929.   Holler C, Pinon JD, Denk U, Heyder C, Hofbauer S, Greil R. PKCbeta is essential for the development of chronic lymphocytic leukemia in the TCL1 transgenic mouse model: validation of PKCbeta as a therapeutic target in chronic lymphocytic leukemia. Blood. 2009;113:2791-4.

930.   Woyach JA, Bojnik E, Ruppert AS, Stefanovski MR, Goettl VM, Smucker KA, et al. Bruton's tyrosine kinase (BTK) function is important to the development and expansion of chronic lymphocytic leukemia (CLL). Blood. 2014;123(8):1207-13.

931.   Nganga VK, Palmer VL, Naushad H, Kassmeier MD, Anderson DK, Perry GA, et al. Accelerated progression of chronic lymphocytic leukemia in Emu-TCL1 mice expressing catalytically inactive RAG1. Blood. 2013;121(19):3855-66, S1-16.

932.   Scielzo C, Bertilaccio MT, Simonetti G, Dagklis A, ten Hacken E, Fazi C, et al. HS1 has a central role in the trafficking and homing of leukemic B cells. Blood. 2010;116(18):3537-46.

933.   Troeger A, Johnson A, Wood J, Blum W, Andritsos L, Byrd J, et al. RhoH is critical for cell-microenvironment interactions in chronic lymphocytic leukemia in mice and humans. Blood. 2012.

934.   Chen SS, Claus R, Lucas DM, Yu L, Qian J, Ruppert AS, et al. Silencing of the inhibitor of DNA binding protein 4 (ID4) contributes to the pathogenesis of mouse and human CLL. Blood. 2011;117(3):862-71.

935.   Liu J, Chen G, Feng L, Zhang W, Pelicano H, Wang F, et al. Loss of p53 and altered miR15-a/16-1short right arrowMCL-1 pathway in CLL: insights from TCL1-Tg:p53(-/-) mouse model and primary human leukemia cells. Leukemia. 2014;28(1):118-28.

936.   Wu Q-L, Zierold C, Ranheim EA. Dysregulation of Frizzled 6 is a critical component of B-cell leukemogenesis in a mouse model of chronic lymphocytic leukemia. Blood. 2009;113(13):3031-9.

937.   Fedorchenko O, Stiefelhagen M, Peer-Zada AA, Barthel R, Mayer P, Eckei L, et al. CD44 regulates the apoptotic response and promotes disease development in chronic lymphocytic leukemia. Blood. 2013;121(20):4126-36.

938.   Lascano V, Guadagnoli M, Schot JG, Luijks DM, Guikema JE, Cameron K, et al. Chronic lymphocytic leukemia disease progression is accelerated by APRIL-TACI interaction in the TCL1 transgenic mouse model. Blood. 2013;122(24):3960-3.

939.   Enzler T, Kater AP, Zhang W, Widhopf GF, Chuang HY, Lee J. Chronic lymphocytic leukemia of Emu-TCL1 transgenic mice undergoes rapid cell turnover that can be offset by extrinsic CD257 to accelerate disease progression. Blood. 2009;114:4469-76.

940.   Simonetti G, Bertilaccio MTS, Ghia P, Klein U. Mouse models in the study of chronic lymphocytic leukemia pathogenesis and therapy. Blood. 2014.

941.   Bertilaccio MT, Scielzo C, Simonetti G, Ten Hacken E, Apollonio B, Ghia P, et al. Xenograft models of chronic lymphocytic leukemia: problems, pitfalls and future directions. Leukemia.27(3):534-40.

942.   Kobayashi R, Picchio G, Kirven M, Meisenholder G, Baird S, Carson DA, et al. Transfer of human chronic lymphocytic leukemia to mice with severe combined immune deficiency. Leukemia Research. 1992;16(10):1013-23.

943.   Hummel JL, Lichty BD, Reis M, Dube I, Kamel-Reid S. Engraftment of human chronic lymphocytic leukemia cells in SCID mice: in vivo and in vitro studies. Leukemia. 1996;10(8):1370-6.

944.   Shimoni A, Marcus H, Canaan A, Ergas D, David M, Berrebi A, et al. A model for human B-chronic lymphocytic leukemia in human/mouse radiation chimera: evidence for tumor-mediated suppression of antibody production in low-stage disease. Blood. 1997;89(6):2210-8.

945.   Shimoni A, Shvidel L, Klepfish A, Shtalrid M, Sigler E, Berrebi A. Refractory pure red cell aplasia associated with B-CLL: successful treatment with a combination of fludarabine, cyclosporin A and erythropoietin. Leukemia. 1999;13(1):142-3.

946.   Durig J, Ebeling P, Grabellus F, Sorg UR, Mollmann M, Schutt P. A novel nonobese diabetic/severe combined immunodeficient xenograft model for chronic lymphocytic leukemia reflects important clinical characteristics of the disease. Cancer Res. 2007;67:8653-61.

947.   Aydin S, Grabellus F, Eisele L, Möllmann M, Hanoun M, Ebeling P, et al. Investigating the role of CD38 and functionally related molecular risk factors in the CLL NOD/SCID xenograft model. European Journal of Haematology. 2011;87(1):10-9.

948.   Bagnara D, Kaufman MS, Calissano C, Marsilio S, Patten PEM, Simone R, et al. A novel adoptive transfer model of chronic lymphocytic leukemia suggests a key role for T lymphocytes in the disease. Blood. 2011;117(20):5463-72.

949.   Kikushige Y, Ishikawa F, Miyamoto T, Shima T, Urata S, Yoshimoto G, et al. Self-renewing hematopoietic stem cell is the primary target in pathogenesis of human chronic lymphocytic leukemia. Cancer Cell.20(2):246-59.

950.   Herman SE, Sun X, McAuley EM, Hsieh MM, Pittaluga S, Raffeld M, et al. Modeling tumor-host interactions of chronic lymphocytic leukemia in xenografted mice to study tumor biology and evaluate targeted therapy. Leukemia. 2013;27(12):2311-21.

951.   Russell WMS, Burch RL. The principles of humane experimental technique: Methuen; 1959.

952.   Lundberg P, Skoda R. Hematology Testing in Mice. Current Protocols in Mouse Biology: John Wiley & Sons, Inc.; 2011.

953.   Buck SB, Bradford J, Gee KR, Agnew BJ, Clarke ST, Salic A. Detection of S-phase cell cycle progression using 5-ethynyl-2′-deoxyuridine incorporation with click chemistry, an alternative to using 5-bromo-2′-deoxyuridine antibodies. BioTechniques. 2008;44(7):927-9.

954.   Cappella P, Gasparri F, Pulici M, Moll J. Cell Proliferation Method: Click Chemistry Based on BrdU Coupling for Multiplex Antibody Staining. Current Protocols in Cytometry. 2008;Chapter 7(Unit7.34).

955.   Bruggner RV, Bodenmiller B, Dill DL, Tibshirani RJ, Nolan GP. Automated identification of stratifying signatures in cellular subpopulations. Proc Natl Acad Sci U S A. 2014;111(26):E2770-7.

956.   Zanesi N, Aqeilan R, Drusco A, Kaou M, Sevignani C, Costinean S, et al. Effect of Rapamycin on Mouse Chronic Lymphocytic Leukemia and the Development of Nonhematopoietic Malignancies in Eu-TCL1 Transgenic Mice. Cancer Research. 2006;66(2):915-20.

957.   Linder CC. Mouse Nomenclature and Maintenance of Genetically Engineered Mice. Comparative Medicine. 2003;53(2):119-25.

958.   Harrington BK, Gardner HL, Izumi R, Hamdy A, Rothbaum W, Coombes KR, et al. Preclinical Evaluation of the Novel BTK Inhibitor Acalabrutinib in Canine Models of B-Cell Non-Hodgkin Lymphoma. PloS one. 2016;11(7):e0159607.

959.   Scheers E, Leclercq L, de Jong J, Bode N, Bockx M, Laenen A, et al. Absorption, metabolism, and excretion of oral ¹⁴C radiolabeled ibrutinib: an open-label, phase I, single-dose study in healthy men. Drug Metab Dispos. 2015;43(2):289-97.

960.   Podoll T, Pearson PG, Evarts J, Ingallinera T, Bibikova E, Sun H, et al. Bioavailability, Biotransformation, and Excretion of the Covalent Bruton Tyrosine Kinase Inhibitor Acalabrutinib in Rats, Dogs, and Humans. Drug Metab Dispos. 2019;47(2):145-54.

961.   Mahnke Y, Chattopadhyay P, Roederer M. Publication of optimized multicolor immunofluorescence panels. Cytometry A. 2010;77(9):814-8.

962.   Bandura DR, Baranov VI, Ornatsky OI, Antonov A, Kinach R, Lou X, et al. Mass cytometry: technique for real time single cell multitarget immunoassay based on inductively coupled plasma time-of-flight mass spectrometry. Anal Chem. 2009;81(16):6813-22.

963.   Lou X, Zhang G, Herrera I, Kinach R, Ornatsky O, Baranov V, et al. Polymer-based elemental tags for sensitive bioassays. Angew Chem Int Ed Engl. 2007;46(32):6111-4.

964.   Majonis D, Herrera I, Ornatsky O, Schulze M, Lou X, Soleimani M, et al. Synthesis of a functional metal-chelating polymer and steps toward quantitative mass cytometry bioassays. Anal Chem. 2010;82(21):8961-9.

965.   Ornatsky OI, Lou X, Nitz M, Schafer S, Sheldrick WS, Baranov VI, et al. Study of cell antigens and intracellular DNA by identification of element-containing labels and metallointercalators using inductively coupled plasma mass spectrometry. Anal Chem. 2008;80(7):2539-47.

966.   Newell EW, Sigal N, Bendall SC, Nolan GP, Davis MM. Cytometry by time-of-flight shows combinatorial cytokine expression and virus-specific cell niches within a continuum of CD8+ T cell phenotypes. Immunity. 2012;36(1):142-52.

967.   Bendall SC, Simonds EF, Qiu P, Amir el AD, Krutzik PO, Finck R, et al. Single-cell mass cytometry of differential immune and drug responses across a human hematopoietic continuum. Science. 2011;332(6030):687-96.

968.   Fienberg HG, Simonds EF, Fantl WJ, Nolan GP, Bodenmiller B. A platinum-based covalent viability reagent for single-cell mass cytometry. Cytometry Part A. 2012;81A(6):467-75.

969.   Finehout EJ, Lee KH. An introduction to mass spectrometry applications in biological research. Biochem Mol Biol Educ. 2004;32(2):93-100.

970.   Ornatsky OI, Kinach R, Bandura DR, Lou X, Tanner SD, Baranov VI, et al. Development of analytical methods for multiplex bio-assay with inductively coupled plasma mass spectrometry. J Anal At Spectrom. 2008;23(4):463-9.

971.   Takahashi C, Au-Yeung A, Fuh F, Ramirez-Montagut T, Bolen C, Mathews W, et al. Mass cytometry panel optimization through the designed distribution of signal interference. Cytometry A. 2017;91(1):39-47.

972.   Bendall SC, Nolan GP, Roederer M, Chattopadhyay PK. A deep profiler's guide to cytometry. Trends Immunol. 2012;33(7):323-32.

973.   Baecher-Allan C, Brown JA, Freeman GJ, Hafler DA. CD4+CD25high regulatory cells in human peripheral blood. J Immunol. 2001;167(3):1245-53.

974.   Baecher-Allan C, Viglietta V, Hafler DA. Inhibition of human CD4(+)CD25(+high) regulatory T cell function. J Immunol. 2002;169(11):6210-7.

975.   Miyara M, Yoshioka Y, Kitoh A, Shima T, Wing K, Niwa A, et al. Functional delineation and differentiation dynamics of human CD4+ T cells expressing the FoxP3 transcription factor. Immunity. 2009;30(6):899-911.

976.   Sakaguchi S, Sakaguchi N, Asano M, Itoh M, Toda M. Immunologic self-tolerance maintained by activated T cells expressing IL-2 receptor alpha-chains (CD25). Breakdown of a single mechanism of self-tolerance causes various autoimmune diseases. J Immunol. 1995;155(3):1151-64.

977.   Thornton AM, Shevach EM. CD4+CD25+ immunoregulatory T cells suppress polyclonal T cell activation in vitro by inhibiting interleukin 2 production. J Exp Med. 1998;188(2):287-96.

978.   Chen X, Subleski JJ, Kopf H, Howard OM, Männel DN, Oppenheim JJ. Cutting edge: expression of TNFR2 defines a maximally suppressive subset of mouse CD4+CD25+FoxP3+ T regulatory cells: applicability to tumor-infiltrating T regulatory cells. J Immunol. 2008;180(10):6467-71.

979.   Chen X, Hamano R, Subleski JJ, Hurwitz AA, Howard OM, Oppenheim JJ. Expression of costimulatory TNFR2 induces resistance of CD4+FoxP3- conventional T cells to suppression by CD4+FoxP3+ regulatory T cells. J Immunol. 2010;185(1):174-82.

980.   Rose S, Misharin A, Perlman H. A novel Ly6C/Ly6G-based strategy to analyze the mouse splenic myeloid compartment. Cytometry A. 2012;81(4):343-50.

981.   Breslin WL, Strohacker K, Carpenter KC, Haviland DL, McFarlin BK. Mouse blood monocytes: standardizing their identification and analysis using CD115. J Immunol Methods. 2013;390(1-2):1-8.

982.   Gordon S, Hamann J, Lin HH, Stacey M. F4/80 and the related adhesion-GPCRs. Eur J Immunol. 2011;41(9):2472-6.

983.   Hey YY, O'Neill HC. Murine spleen contains a diversity of myeloid and dendritic cells distinct in antigen presenting function. J Cell Mol Med. 2012;16(11):2611-9.

984.   Wang WG, Jiang XN, Sheng D, Sun CB, Lee J, Zhou XY, et al. PD-L1 over-expression is driven by B-cell receptor signaling in diffuse large B-cell lymphoma. Lab Invest. 2019.

985.   Wierz M, Janji B, Berchem G, Moussay E, Paggetti J. High-dimensional mass cytometry analysis revealed microenvironment complexity in chronic lymphocytic leukemia. Oncoimmunology. 2018;7(8):e1465167.

986.   Covey T, Barf T, Gulrajani M, Krantz F, van Lith B, Bibikova E, et al. Abstract 2596: ACP-196: a novel covalent Bruton's tyrosine kinase (Btk) inhibitor with improved selectivity and in vivo target coverage in chronic lymphocytic leukemia (CLL) patients. Cancer Research. 2015;75(15 Supplement):2596-.

987.   Rubio V, Stuge TB, Singh N, Betts MR, Weber JS, Roederer M, et al. Ex vivo identification, isolation and analysis of tumor-cytolytic T cells. Nat Med. 2003;9(11):1377-82.

988.   Saljoughian N, Varikuti S, Halsey G, Oghumu S, Satoskar A. Ibrutinib has a novel immunomodulatory effect by enhancing DC maturation both in vivo and in a model of inflammation. The Journal of Immunology. 2018;200(1 Supplement):56.3-.3.

989.   Haseebuddin M, Macfarlane A, Ruth K, Uzzo RG, Plimack ER, Jillab M, et al. PD-1 expression on classical monocytes (CM) as an independent predictor of cancer specific survival in clear cell renal carcinoma (ccRCC). Journal of Clinical Oncology. 2016;34(2_suppl):562-.

990.   Zasada M, Lenart M, Rutkowska-Zapała M, Stec M, Durlak W, Grudzień A, et al. Analysis of PD-1 expression in the monocyte subsets from non-septic and septic preterm neonates. PLoS One. 2017;12(10):e0186819.

991.   Gordon SR, Maute RL, Dulken BW, Hutter G, George BM, McCracken MN, et al. PD-1 expression by tumour-associated macrophages inhibits phagocytosis and tumour immunity. Nature. 2017;545(7655):495-9.

992.   Yao S, Wang S, Zhu Y, Luo L, Zhu G, Flies S, et al. PD-1 on dendritic cells impedes innate immunity against bacterial infection. Blood. 2009;113(23):5811-8.

993.   Lim TS, Chew V, Sieow JL, Goh S, Yeong JP, Soon AL, et al. PD-1 expression on dendritic cells suppresses CD8+ T cell function and antitumor immunity. Oncoimmunology. 2016;5(3):e1085146.

994.   McNerney ME, Lee KM, Kumar V. 2B4 (CD244) is a non-MHC binding receptor with multiple functions on natural killer cells and CD8+ T cells. Mol Immunol. 2005;42(4):489-94.

995.   Henniker AJ, Bradstock KF, Grimsley P, Atkinson MK. A novel non-lineage antigen on human leucocytes: characterization with two CD-48 monoclonal antibodies. Dis Markers. 1990;8(4):179-90.

996.   Youn JI, Collazo M, Shalova IN, Biswas SK, Gabrilovich DI. Characterization of the nature of granulocytic myeloid-derived suppressor cells in tumor-bearing mice. J Leukoc Biol. 2012;91(1):167-81.

997.   Georgoudaki AM, Khodabandeh S, Puiac S, Persson CM, Larsson MK, Lind M, et al. CD244 is expressed on dendritic cells and regulates their functions. Immunol Cell Biol. 2015;93(6):581-90.

998.   Mak A, Thornhill SI, Lee HY, Lee B, Poidinger M, Connolly JE, et al. Brief report: Decreased expression of CD244 (SLAMF4) on monocytes and platelets in patients with systemic lupus erythematosus. Clin Rheumatol. 2018;37(3):811-6.

999.   Sada-Ovalle I, Chávez-Galán L, Torre-Bouscoulet L, Nava-Gamiño L, Barrera L, Jayaraman P, et al. The Tim3-galectin 9 pathway induces antibacterial activity in human macrophages infected with Mycobacterium tuberculosis. J Immunol. 2012;189(12):5896-902.

1000.   Jayaraman P, Sada-Ovalle I, Beladi S, Anderson AC, Dardalhon V, Hotta C, et al. Tim3 binding to galectin-9 stimulates antimicrobial immunity. J Exp Med. 2010;207(11):2343-54.

1001.   Zhang Y, Ma CJ, Wang JM, Ji XJ, Wu XY, Jia ZS, et al. Tim-3 negatively regulates IL-12 expression by monocytes in HCV infection. PLoS One. 2011;6(5):e19664.

1002.   Zhang Y, Ma CJ, Wang JM, Ji XJ, Wu XY, Moorman JP, et al. Tim-3 regulates pro- and anti-inflammatory cytokine expression in human CD14+ monocytes. J Leukoc Biol. 2012;91(2):189-96.

1003.   Yan W, Liu X, Ma H, Zhang H, Song X, Gao L, et al. Tim-3 fosters HCC development by enhancing TGF-β-mediated alternative activation of macrophages. Gut. 2015;64(10):1593-604.

1004.   Ok CY, Young KH. Checkpoint inhibitors in hematological malignancies. J Hematol Oncol. 2017;10(1):103.

1005.   Gu A, Ma H, Zhang X, Malaney P, Gallardo M, Liu J, et al. Combination Therapy with BTK Inhibitor Plus Anti-PD-1 Antibody Results in a Hyperprogressor Phenotype in a Mouse Model of CLL. Blood. 2018;132(Suppl 1):4416-.